



Exploring Ocular Motor Biomarkers in Parkinson's Disease and Atypical Parkinsonian Syndromes

AKILA RAMAMOORTHY SEKAR

Supervisor:

Dr. Diego Kaski

April 2025

A thesis submitted to University College London for the degree of Doctor of Philosophy

SENSE Research Unit

Department of Clinical and Movement Neurosciences

Queen Square Institute of Neurology

University College London

Declaration

I, Akila Ramamoorthy Sekar, confirm that the work presented in this thesis is my own. Where information has been derived from other sources, I confirm that this has been indicated in the thesis.

Abstract

Parkinson's disease and atypical Parkinsonian syndromes—including progressive supranuclear palsy, multiple system atrophy, corticobasal syndrome, and dementia with Lewy bodies—are rising in global prevalence due to an ageing population. These conditions are challenging to diagnose in the early stages, as they share overlapping clinical symptoms and currently rely on subjective clinical assessments, costly imaging techniques, and laboratory tests. Moreover, these assessments often require input from specialists, whose availability may be limited, leading to delays in both diagnosis and the initiation of treatment.

This thesis investigates the potential of eye movements as diagnostic biomarkers for Parkinson's disease and atypical Parkinsonian syndromes. Utilizing a comprehensive ocular motor battery and advanced eye-tracking technologies, the first part of the thesis aims to develop a unique ocular motor profile capable of distinguishing between Parkinson's subtypes and atypical syndromes. Subsequent projects examine the effects of dopaminergic treatment in Parkinson's disease and analyse longitudinal changes in eye movements to understand how these metrics evolve over time and how these changes are affected with short term and long term medication use. This approach seeks to establish the utility of eye movement measures in tracking disease progression. Additionally, studying the short-term effects of dopamine will inform future ocular motor studies by determining whether and how the impact of medication must be accounted for in experimental design and interpretation. Another study within this thesis explores saccadic adaptation in Parkinson's disease and multiple system atrophy, offering key insights into motor learning deficits and neuroplasticity. Investigating such paradigms enhances our understanding of how neural connectivity and functionality are altered in specific pathologies. The final section of the thesis focuses on integrating machine learning, portable eye-tracking devices, and mobile applications into ocular motor research. Portable eye trackers offer a more accessible and scalable alternative to traditional equipment, enabling assessments in both clinical and home settings. When combined with machine learning algorithms, these tools can enhance diagnostic accuracy by detecting subtle, condition-specific eye movement patterns. Furthermore, the development of mobile and tablet-based applications facilitates large-scale, remote assessments—reducing barriers to specialist evaluations and allowing for continuous, real-time disease monitoring.

By combining clinical neuroscience, artificial intelligence, and digital health, this thesis presents evidence

for the use of eye movements in diagnosing Parkinson's disease and atypical Parkinsonian syndromes. With continued advancements, eye-tracking technology has the potential to become a vital tool for early detection, diagnosis, disease monitoring, and possibly the development of personalized treatment strategies.

Impact Statement

Eye movement abnormalities are well-recognized features of Parkinson's disease and atypical Parkinsonian syndromes, including progressive supranuclear palsy, multiple system atrophy, corticobasal syndrome, and dementia with Lewy bodies. Clinical examination of eye movements using simple paradigms such as saccades, fixation, and pursuit can provide valuable information for a differential diagnosis, especially when motor symptoms overlap between Parkinson's disease and atypical Parkinsonian syndromes.

Eye movement assessments offer several advantages: they are non-invasive, easy to perform, and provide objective metrics. Moreover, ocular motor disturbances can offer insight into the specific brain pathways affected with disease pathology. Harnessing the advances in technology, the utility of eye movements in remote diagnosis is growing. However, to establish eye movements as a robust diagnostic tool, several challenges must be addressed. These include: developing standardised ocular motor profiles for each condition through comprehensive ocular motor batteries covering a wide range of assessments; maximising the potential of artificial intelligence to detect subtle patterns critical for diagnosis; and advancing technologies to enable quick, remote eye movement evaluations. This thesis aims to take initial steps toward addressing these challenges.

Studying eye movements—particularly through structured research paradigms—can yield novel insights into the brain regions and pathways affected by both healthy ageing and disease-related neurodegeneration. Correlating ocular motor profiles with neuroimaging and physiological data can deepen our understanding of disease pathology and identify potential targets for diagnostic tools and therapeutic interventions. To obtain concrete evidence of the brain regions involved, post-mortem studies of individuals who have undergone detailed ocular motor assessments would be highly valuable, further strengthening the case for eye movements as a diagnostic tool.

Investigating how eye movements evolve over time can also support the use of ocular motor assessments as progression markers, in addition to diagnostic indicators. Longitudinal studies examining changes in eye movements alongside motor and non-motor symptoms can provide critical insights into disease progression. Furthermore, assessing the impact of medications and interventional therapies on eye movements can help

determine whether ocular motor assessments can be incorporated into clinical trials to monitor therapeutic efficacy.

Coupling technological advancements with scientific evidence opens new opportunities for integrating eye movement assessments into routine clinical examinations for early detection of Parkinson's disease and atypical Parkinsonian syndromes. Given the limited access to specialist consultants in the early stages of these diseases, the development of portable eye trackers and mobile applications for tablets and smartphones can empower physicians to conduct ocular motor assessments with ease. Integrating machine learning algorithms can further streamline this process, producing diagnostic outputs with minimal user input. This not only reduces the training burden for clinicians and non-clinicians alike but also enhances the practicality of implementing simple, scalable diagnostic tools.

In conclusion, ocular motor assessments have the potential to serve as robust diagnostic and progression markers when combined with motor and non-motor symptom assessments in Parkinson's disease and atypical Parkinsonian syndromes. Scientific and technological advancements in this field hold the promise of faster, more accurate diagnoses—ultimately leading to improved patient care and better clinical outcomes.

Acknowledgements

This PhD is dedicated to all the incredible people in my life who have impacted me in one way or another, making it possible for me to reach this milestone. I am truly grateful for your presence and the role you've played in shaping the person I am today. This PhD is also dedicated to all individuals living with neurodegenerative disorders. As a scientific community, we remain committed to discovering novel solutions that can alleviate, prevent, and ultimately cure these illnesses. With continued collaboration and innovation, we hold hope for a brighter future.

I would first like to thank my supervisor, Diego, for nurturing me as a researcher and giving me the opportunity to contribute to the field of movement disorders. You have consistently encouraged me to explore new ideas and opportunities, and taught me how to navigate challenging situations, all while being a constant source of support. Since our first project together in 2018, you have mentored me far beyond the bounds of academia and been a strong advocate for all my endeavours.

I extend my gratitude to the members of my thesis committee—Dr. Muriel Panouilleres, Prof. Tony Schapira, Dr. Rimona Weil, and Prof. Huw Morris—for their guidance and for challenging my scientific thinking, helping me grow as a researcher.

To all the members of the SENSE research unit: thank you for your encouragement and support over the past three years. I am also grateful to all my collaborators—Isaac, Oliver, Antonio, and the PROSPECT team: Marte, Riona, Yoana, Megan, and Prof. Huw Morris; the PD Frontline team: Marco, Nadine, Prof. Tony Schapira; the GENFI team: Rhian, Amelia, Sophie, and Prof. Jonathan Rohrer; as well as Adtee and Emily. Thank you all for your contributions—working with you has been a pleasure, and I've learned so much through our collaborations. The success of the projects within this PhD would not have been possible without your efforts.

To the registrars and nurses who supported recruitment and coordinated participant visits—your help has been instrumental in increasing the output and impact of my work. Thank you also to the staff at 33 Queen Square for your unwavering support throughout this journey.

To my three pillars of strength—my mother, father, and brother—I would not have reached this stage in my life without you. I am truly blessed to have you as my family. You have always pushed me to be the best version of myself and lifted me up during my lowest moments. My father has shown me that there is no substitute for hard work and perseverance, and that self-improvement comes from learning through every opportunity. My mother has taught me the importance of staying true to myself and instilled in me the values that give me confidence to face life's challenges. Your love and constant encouragement have given me the freedom to make mistakes, learn, and grow. To my brother, who was always just a phone call away, you have helped me through the toughest of days and celebrated all my victories with me. Knowing that you have my back gives me the strength to keep going. Through your own incredible journey, you've taught me many lessons, especially the power of critical self-reflection. I've seen what it's done for you, and I hope to carry that with me as I grow. I'm so grateful to celebrate this achievement with you all—you mean the world to me.

To all my friends, who are my family away from home—thank you for your constant support, laughter, and the countless memories. Aakriti & Shubham, Adtee, Akshal, Bhoomika, Henrique, Kenneth, Rishabh, Sameer, Sanjana G, Sanjana S, Shakunt, and Sravani—your unwavering belief in me, even when I doubted myself, has been one of the greatest sources of strength throughout this journey. I'm endlessly grateful for the countless conversations, spontaneous distractions, and emotional check-ins that made all the days enjoyable.

A special thank you to all the mentors and teachers who have guided me throughout my life. Your wisdom and encouragement have left an indelible mark, and I carry your lessons with me every day.

Finally, from the bottom of my heart, I thank every single person who participated in my study. None of this would have been possible without your time and effort. I sincerely hope this research contributes, in some small way, to improving your lives and advancing our understanding of Parkinson's disease and atypical Parkinsonian syndromes.

Contributions

Project	Contributors	Role
Ocular Motor Function in Parkinson's Disease	Dr. Marco Toffoli, Nadine Leofflad, Orla Mitchell, Prof. Antony Schapira	Recruitment
	Isaac Hempsted Wright, Oliver Dennet, Adtee Ketan Janvekar, Emily Navarro-Jones	Data Collection
Ocular Motor Function in Atypical Parkinsonian Syndromes	Marte Theilmann Jensen, Riona Fumi, Megan Hodgson, Yoana Kordovska, Prof. Huw Morris, Dr. Yee Goh, Dr. Viorica Chelban, Prof. Henry Houlden, Dr. Rohan Bhome, Prof. Rimona Weil	Recruitment
	Isaac Hempsted Wright, Oliver Dennet, Adtee Ketan Janvekar, Emily Navarro-Jones	Data Collection
Saccadic Adaptation in Parkinson's Disease and MSA	Isaac Hempsted Wright, Oliver Dennet	Data Collection
Effect of Levodopa on Eye Movements in Parkinson's Disease	Antonio C. Luque Ambrosiani	Data Collection
Comparison of Eyelink and Tobii Eye Trackers	Dr. Rhian Convery, Amelia Blesius, Sophie Farley, Prof. Jonathan Rohrer	Project Coordination
	Adtee Ketan Janvekar, Emily Navarro-Jones	Project Coordination and Recruitment
Detection of Eye Movements in PD with Smartphone Application – Proof of Concept	Adtee Ketan Janvekar, Emily Navarro-Jones	Project Coordination and Recruitment

Contents

List of Figures	19
List of Tables	25
List of Abbreviations	29
1 Introduction	31
1.1 Human Ocular Motor System	33
1.2 Classes of Eye Movements	33
1.2.1 Fixational Eye Movements	34
1.2.2 Saccadic Eye Movements	37
1.2.3 Smooth Pursuit	44
1.2.4 Vestibular Eye Movements	47
1.2.5 Optokinetic Eye Movements	47
1.2.6 Vergence Eye Movements	49
1.3 Evaluating the Study of Eye Movements	49
1.4 Translation Into Clinical Settings	51
1.5 Methods for Studying and Quantifying Eye Movements	53
1.6 Thesis Aims	55
1.7 Chapter Summary	55
2 General Methods	57
2.1 Participant Recruitment	57
2.2 Ethics	59
2.3 Data Collection and Storage	59
2.4 Eye Tracking	60
2.4.1 Comparative Analysis for Eye Tracker Selection	60
2.4.2 Eye Tracker Setup	62
2.4.3 Participant Setup	64
2.5 Quality Control of Data Collection	68

2.6	Ocular Motor Battery	69
2.7	Data Processing and Analysis	75
2.8	Chapter Summary	79
3	Ocular Motor Function in Parkinson's Disease	80
3.1	Introduction	80
3.1.1	Parkinson's Disease Pathology	81
3.1.2	Eye Movements in Parkinson's Disease	82
3.2	Project Aims	86
3.3	Methods	86
3.3.1	Participants	86
3.3.2	Ocular Motor Assessment	87
3.3.3	Data Processing and Analysis	87
3.3.4	Statistical Analyses	88
3.4	Results	89
3.4.1	Participants	89
3.4.2	Ocular Motor Function in Idiopathic Parkinson's Disease	90
3.4.3	Ocular Motor Function in GBA Mutation Parkinson's Disease	92
3.4.4	Ocular Motor Function in LRRK2 Mutation Parkinson's Disease	94
3.4.5	Saccadic Pursuit	95
3.4.6	Timescale Analysis	95
3.4.7	Ocular Motor Composite Score	96
3.5	Discussion	146
3.5.1	Clinical Implications	158
3.5.2	Limitations	159
3.5.3	Future Directions	161
3.6	Chapter Summary	162
4	Ocular Motor Function in Atypical Parkinsonian Syndromes	163
4.1	Introduction	163
4.1.1	Progressive Supranuclear Palsy	164

4.1.2	Eye Movements in Progressive Supranuclear Palsy	164
4.1.3	Multiple System Atrophy	166
4.1.4	Eye Movements in Multiple System Atrophy	167
4.1.5	Corticobasal Syndrome	168
4.1.6	Eye Movements in Corticobasal Syndrome	168
4.1.7	Dementia with Lewy Bodies	170
4.1.8	Eye Movements in Dementia with Lewy Bodies	170
4.2	Project Aims	171
4.3	Methods	171
4.3.1	Participants	171
4.3.2	Ocular Motor Assessment	172
4.3.3	Data Processing and Analysis	173
4.3.4	Statistical Analyses	174
4.4	Results	175
4.4.1	Participants	175
4.4.2	Eye Movements in Progressive Supranuclear Palsy	176
4.4.3	Eye Movements in Corticobasal Syndrome	180
4.4.4	Eye Movements in Multiple System Atrophy	182
4.4.5	Eye Movements in Dementia with Lewy Bodies	184
4.4.6	Eye Movements in Atypical Cases	187
4.4.7	Composite Score	190
4.4.8	Timescale Analysis	190
4.4.9	Saccadic Pursuit	191
4.5	Discussion	240
4.5.1	Clinical Implications	254
4.5.2	Limitations	255
4.5.3	Future Directions	256
4.6	Chapter Summary	256
5	Longitudinal Study of Eye Movements in Parkinson's Disease	258

5.1	Introduction	258
5.2	Project Aims	259
5.3	Methods	259
5.3.1	Participants	259
5.3.2	Ocular Motor Battery	260
5.3.3	Data Processing and Analysis	260
5.3.4	Statistical Analyses	260
5.3.5	Participants	261
5.3.6	Ocular Motor Function	261
5.4	Discussion	296
5.4.1	Clinical Implications	298
5.4.2	Limitations	299
5.4.3	Future Directions	300
5.5	Chapter Summary	301
6	Saccadic Adaptation in Parkinson's Disease and Multiple System Atrophy	302
6.1	Introduction	302
6.1.1	Neural Circuitry of Saccadic Adaptation	303
6.1.2	Saccadic Adaptation in Parkinson's Disease	304
6.1.3	Saccadic Adaptation in Multiple System Atrophy	304
6.2	Project Aims	305
6.3	Methods	305
6.3.1	Participants	305
6.3.2	Experimental Protocol	306
6.3.3	Data Processing and Analysis	306
6.3.4	Statistical Analyses	307
6.4	Results	307
6.4.1	Participants	307
6.5	Results	308
6.5.1	Participants	308

6.5.2	Saccadic Adaptation in Controls	308
6.5.3	Saccadic Adaptation in Parkinson's Disease	309
6.5.4	Saccadic Adaptation in Multiple System Atrophy	309
6.6	Discussion	314
6.6.1	Clinical Implications	316
6.6.2	Limitations	317
6.6.3	Future Directions	317
6.7	Chapter Summary	318
7	Effect of Levodopa on Eye Movements in Parkinson's Disease	319
7.1	Introduction	319
7.2	Project Aims	320
7.3	Methodology	321
7.3.1	Participants	321
7.3.2	Experimental Conditions	321
7.3.3	Ocular Motor Assessment	322
7.3.4	Data Processing	322
7.3.5	Statistical Analyses	322
7.4	Results	323
7.4.1	Participants	323
7.4.2	ON vs. OFF Comparisons	324
7.5	Discussion	337
7.5.1	Clinical Implications	340
7.5.2	Limitations	341
7.5.3	Future Directions	342
7.6	Chapter Summary	342
8	Machine Learning for the Prediction of Parkinson's Disease and Atypical Parkinsonian Syndromes	344
8.1	Introduction	344
8.2	Project Aims	346

8.3	Methods	346
8.3.1	Data Source	346
8.3.2	Data Preparation	347
8.3.3	Model Construction	348
8.3.4	Class Imbalance and Training Strategy	350
8.4	Results	350
8.5	Discussion	362
8.5.1	Clinical Implications	364
8.5.2	Limitations	366
8.5.3	Future Directions	367
8.6	Chapter Summary	367
9	Pilot Test for the Comparison of EyeLink (Desktop-Based) and Tobii (Mobile) Eye Trackers as a Diagnostic Tool for Neurodegenerative Disorders	369
9.1	Introduction	369
9.2	Project Aims	373
9.3	Methods	373
9.3.1	Participants	373
9.3.2	EyeLink 1000 Plus Experimental Procedure	374
9.3.3	Tobii Nano Pro Experimental Procedure	374
9.3.4	Data Processing and Analysis	375
9.4	Statistical Analyses	375
9.5	Results	376
9.5.1	Participants	376
9.5.2	Ocular Motor Metrics Using Tobii	376
9.5.3	Tobii Versus EyeLink 1000 Plus	376
9.6	Discussion	377
9.6.1	Clinical Implications	379
9.6.2	Limitations	380
9.6.3	Future Directions	380

9.7 Chapter Summary	380
10 Detection of Eye Movements in Parkinson's Disease in Laptop/Tablet/Smartphone Application	
– Proof of Concept	382
10.1 Introduction	382
10.2 Project Aims	384
10.3 Methods	384
10.3.1 Experimental Design	384
10.3.2 Hardware and Software Requirements	384
10.3.3 Software Development	385
10.3.4 Ethical Considerations	389
10.3.5 Pilot Testing	389
10.3.6 Statistical Analyses	390
10.4 Results	390
10.4.1 Application Development	390
10.4.2 Participants	390
10.4.3 Application Function	391
10.4.4 Application Usability	394
10.5 Discussion	394
10.5.1 Clinical Implications	396
10.5.2 Limitations	397
10.5.3 Future Directions	397
10.6 Chapter Summary	398
11 General Discussion	399
References	406
Appendices	461
A Ocular Motor Function in Parkinson's Disease	461
B Ocular Motor Function in Atypical Parkinsonian Syndromes	467

C	Longitudinal Study of Eye Movements in Parkinson's Disease	480
D	Effect of Levodopa on Eye Movements in Parkinson's Disease	484

List of Figures

1	Schematic of Fixational Eye Movements	36
2	Traces of Fixational Eye Movements	36
3	Saccadic Waveform	38
4	Main Sequence Effect of Saccades	40
5	Schematic of Saccadic Control	40
6	Neural Pathway of Horizontal Saccades	41
7	Neural Pathway of Vertical Saccades	41
8	Neural Pathway of Reflexive Saccades	42
9	Neural Pathway of Volitional Saccades	42
10	Neural Pathway of Memory Guided Saccades	43
11	Neural Pathway of Antisaccades	43
12	Schematic of Smooth Pursuit Control	45
13	Smooth Pursuit Waveform	46
14	Neural Pathway of Smooth Pursuit	46
15	Classification of Participant Cohorts	57
16	Eye Tracking Systems Evaluated	60
17	EyeLink 1000 Plus in Head-stabilized Mode	63
18	Schematic Illustration of Eye Tracking Setup	63
19	Participant Positioning for Eye Tracking	64
20	EyeLink 1000 Plus Camera Setup Interface for Monocular Eye Tracking.	65
21	Illustration of Pupil and Corneal Reflection Alignment in the EyeLink 1000 Plus System	65
22	Calibration Models in the EyeLink 1000 Plus System.	66
23	Validation Screen from the EyeLink 1000 Plus System.	66
24	Centroid Tracking Mode	67
25	Illustration of Correct and Incorrect Participant Positioning for Optimal Eye Tracking	68
26	Screen Coordinate System	69
27	Central Fixation Paradigm	70
28	Positional Fixation/ Nystagmus Paradigm	71

29	Antisaccades Horizontal Paradigm	72
30	Antisaccades Vertical Paradigm	72
31	Oblique Saccades Paradigm	73
32	Reflexive Saccades Horizontal Paradigm	73
33	Reflexive Saccades Vertical Paradigm	74
34	Volitional and Memory Guided Saccades Horizontal Paradigm	75
35	Volitional and Memory Guided Saccades Vertical Paradigm	75
36	Central Fixation Metrics in Parkinson's Disease	97
37	Central Fixation Metrics in Parkinson's Disease	98
38	Fixation Traces in Parkinson's Disease	99
39	Fixation Traces in Parkinson's Disease	100
40	Positional Fixation/ Nystagmus Metrics in Parkinson's Disease	102
41	Positional Fixation/ Nystagmus Metrics in Parkinson's Disease	103
42	Positional Fixation/ Nystagmus Metrics in Parkinson's Disease	104
43	Positional Fixation/ Nystagmus Metrics in Parkinson's Disease	105
44	Positional Fixation/ Nystagmus Metrics in Parkinson's Disease	106
45	Positional Fixation/ Nystagmus Metrics in Parkinson's Disease	107
46	Smooth Pursuit Metrics in Parkinson's Disease	109
47	Smooth Pursuit Metrics in Parkinson's Disease	110
48	Smooth Pursuit Metrics in Parkinson's Disease	111
49	Saccadic Pursuit Histogram in Parkinson's Disease	113
50	Smooth Pursuit Trace in Parkinson's Disease	114
51	Oblique Saccades Metrics in Parkinson's Disease	115
52	Oblique Saccades Metrics in Parkinson's Disease	116
53	Oblique Saccades Metrics in Parkinson's Disease	117
54	Oblique Saccades Metrics in Parkinson's Disease	118
55	Oblique Saccades Metrics in Parkinson's Disease	119
56	Antisaccades Horizontal Metrics in Parkinson's Disease	121
57	Antisaccades Horizontal Metrics in Parkinson's Disease	122
58	Antisaccades Vertical Metrics in Parkinson's Disease	123

59	Antisaccades Vertical Metrics in Parkinson's Disease	124
60	Reflexive Saccades Horizontal Metrics in Parkinson's Disease	126
61	Reflexive Saccades Horizontal Metrics in Parkinson's Disease	127
62	Reflexive Saccades Vertical Metrics in Parkinson's Disease	128
63	Reflexive Saccades Vertical Metrics in Parkinson's Disease	129
64	Hypometric Saccades in Parkinson's Disease	130
65	Timescale Analysis of Reflexive Saccades in Parkinson's Disease	132
66	Volitional Saccades Horizontal Metrics in Parkinson's Disease	133
67	Volitional Saccades Horizontal Metrics in Parkinson's Disease	134
68	Volitional Saccades Vertical Metrics in Parkinson's Disease	135
69	Volitional Saccades Vertical Metrics in Parkinson's Disease	136
70	Timescale Analysis of Volitional Saccades in Parkinson's Disease	138
71	Memory Guided Saccades Horizontal Metrics in Parkinson's Disease	139
72	Memory Guided Saccades Horizontal Metrics in Parkinson's Disease	140
73	Memory Guided Saccades Vertical Metrics in Parkinson's Disease	141
74	Memory Guided Saccades Vertical Metrics in Parkinson's Disease	142
75	Timescale Analysis of Memory Guided Saccades in Parkinson's Disease	144
76	Spider Plot of Ocular Motor Paradigms in Parkinson's Disease	145
77	Central Fixation Metrics in Atypical Parkinsonian Syndromes	192
78	Central Fixation Metrics in Atypical Parkinsonian Syndromes	193
79	Fixation Traces in Progressive Supranuclear Palsy	194
80	Positional Fixation/ Nystagmus Metrics in Atypical Parkinsonian Syndromes	195
81	Positional Fixation/ Nystagmus Metrics in Atypical Parkinsonian Syndromes	196
82	Positional Fixation/ Nystagmus Metrics in Atypical Parkinsonian Syndromes	197
83	Positional Fixation/ Nystagmus Metrics in Atypical Parkinsonian Syndromes	198
84	Positional Fixation/ Nystagmus Metrics in Atypical Parkinsonian Syndromes	199
85	Positional Fixation/ Nystagmus Metrics in Atypical Parkinsonian Syndromes	200
86	Positional Fixation/ Nystagmus Traces in Multiple System Atrophy	201
87	Smooth Pursuit Metrics in Atypical Parkinsonian Syndromes	202
88	Smooth Pursuit Metrics in Atypical Parkinsonian Syndromes	203

89	Smooth Pursuit Metrics in Atypical Parkinsonian Syndromes	204
90	Saccadic Pursuit Histogram in Atypical Parkinsonian Syndromes	205
91	Saccadic Pursuit Histogram in Atypical Parkinsonian Syndromes	206
92	Smooth Pursuit Trace in Corticobasal Syndrome	207
93	Oblique Saccades Metrics in Atypical Parkinsonian Syndromes	208
94	Oblique Saccades Metrics in Atypical Parkinsonian Syndromes	209
95	Oblique Saccades Metrics in Atypical Parkinsonian Syndromes	210
96	Oblique Saccades Metrics in Atypical Parkinsonian Syndromes	211
97	Oblique Saccades Metrics in Atypical Parkinsonian Syndromes	212
98	Oblique Saccades Trace in Progressive Supranuclear Palsy	213
99	Antisaccades Horizontal Metrics in Atypical Parkinsonian Syndromes	214
100	Antisaccades Horizontal Metrics in Atypical Parkinsonian Syndromes	215
101	Antisaccades Vertical Metrics in Atypical Parkinsonian Syndromes	216
102	Antisaccades Vertical Metrics in Atypical Parkinsonian Syndromes	217
103	Antisaccades Trace in Multiple System Atrophy	218
104	Reflexive Saccades Horizontal Metrics in Atypical Parkinsonian Syndromes	219
105	Reflexive Saccades Horizontal Metrics in Atypical Parkinsonian Syndromes	220
106	Reflexive Saccades Vertical Metrics in Atypical Parkinsonian Syndromes	221
107	Reflexive Saccades Vertical Metrics in Atypical Parkinsonian Syndromes	222
108	Hypometric Saccades in Atypical Parkinsonian Syndromes	223
109	Timescale Analysis of Reflexive Saccades in Atypical Parkinsonian Syndromes	224
110	Timescale Analysis of Reflexive Saccades in Atypical Parkinsonian Syndromes	225
111	Volitional Saccades Horizontal Metrics in Atypical Parkinsonian Syndromes	226
112	Volitional Saccades Horizontal Metrics in Atypical Parkinsonian Syndromes	227
113	Volitional Saccades Vertical Metrics in Atypical Parkinsonian Syndromes	228
114	Volitional Saccades Vertical Metrics in Atypical Parkinsonian Syndromes	229
115	Timescale Analysis of Volitional Saccades in Atypical Parkinsonian Syndromes	230
116	Timescale Analysis of Volitional Saccades in Atypical Parkinsonian Syndromes	231
117	Memory Guided Saccades Horizontal Metrics in Atypical Parkinsonian Syndromes	232
118	Memory Guided Saccades Horizontal Metrics in Atypical Parkinsonian Syndromes	234

119	Memory Guided Saccades Vertical Metrics in Atypical Parkinsonian Syndromes	235
120	Memory Guided Saccades Vertical Metrics in Atypical Parkinsonian Syndromes	236
121	Timescale Analysis of Memory Guided Saccades in Atypical Parkinsonian Syndromes . .	237
122	Timescale Analysis of Memory Guided Saccades in Atypical Parkinsonian Syndromes . .	238
123	Spider Plot of Ocular Motor Paradigms in Atypical Parkinsonian Syndromes	239
124	Longitudinal Change Central Fixation	264
125	Longitudinal Change Central Fixation	265
126	Longitudinal Change Positional Fixation/ Nystagmus	266
127	Longitudinal Change Positional Fixation/ Nystagmus	267
128	Longitudinal Change Positional Fixation/ Nystagmus	268
129	Longitudinal Change Positional Fixation/ Nystagmus	269
130	Longitudinal Change Positional Fixation/ Nystagmus	270
131	Longitudinal Change Pursuit	272
132	Longitudinal Change Pursuit	273
133	Longitudinal Change Pursuit	274
134	Longitudinal Change Oblique Saccades	275
135	Longitudinal Change Oblique Saccades	276
136	Longitudinal Change Oblique Saccades	277
137	Longitudinal Change Oblique Saccades	278
138	Longitudinal Change Oblique Saccades	279
139	Longitudinal Change Antisaccades Horizontal	280
140	Longitudinal Change Antisaccades Horizontal	281
141	Longitudinal Change Antisaccades Vertical	282
142	Longitudinal Change Antisaccades Vertical	283
143	Longitudinal Change Reflexive Saccades Horizontal	284
144	Longitudinal Change Reflexive Saccades Horizontal	285
145	Longitudinal Change Reflexive Saccades Vertical	286
146	Longitudinal Change Reflexive Saccades Vertical	287
147	Longitudinal Change Volitional Saccades Horizontal	288
148	Longitudinal Change Volitional Saccades Vertical	289

149	Longitudinal Change Volitional Saccades Vertical	290
150	Longitudinal Change Memory Guided Saccades Horizontal	291
151	Longitudinal Change Memory Guided Saccades Horizontal	292
152	Longitudinal Change Memory Guided Saccades Horizontal	293
153	Longitudinal Change Memory Guided Saccades Vertical	294
154	Longitudinal Change Memory Guided Saccades Vertical	295
155	Gain in Adaptation and Test Phases	310
156	Metrics in Adaptation Phase	311
157	Metrics in Test Phase	312
158	Metrics in Adaptation and Test Phases	313
159	Central Fixation Metrics ON and OFF States	325
160	Central Fixation Metrics ON and OFF States	326
161	Antisaccades Metrics ON and OFF States	327
162	Antisaccades Metrics ON and OFF States	328
163	Reflexive Saccades Horizontal Metrics ON and OFF States	329
164	Reflexive Saccades Horizontal Metrics ON and OFF States	330
165	Reflexive Saccades Vertical Metrics ON and OFF States	331
166	Reflexive Saccades Vertical Metrics ON and OFF States	332
167	Volitional Saccades Metrics ON and OFF States	333
168	Volitional Saccades Metrics ON and OFF States	334
169	Memory Guided Saccades Metrics ON and OFF States	335
170	Memory Guided Saccades Metrics ON and OFF States	336
171	Machine Learning Pipeline for Classification	348
172	Hierarchical Classification of Participants	349
173	Confusion Matrices for Level 1 Classification (Disease vs. Healthy)	352
174	Performance of Models in Level 1 Classification (Disease vs. Healthy)	353
175	Classification Metrics for Level 1 (Disease vs. Healthy)	354
176	Confusion Matrices for Level 2 Classification (PD vs. Atypical Parkinsonian Syndromes)	355
177	Performance of Models in Level 2 Classification (PD vs. Atypical Parkinsonian Syndromes)	356
178	Classification Metrics for Level 2 (PD vs. Atypical Parkinsonian Syndromes)	357

179	Confusion Matrices for Level 3 Classification (PD and Atypical Subtypes)	358
180	Performance of Models in Level 3 Classification (PD and Atypical Subtypes)	359
181	Classification Metrics for Level 3 (PD and Atypical Subtypes)	359
182	Confusion Matrices for Level 4 Classification (Genetic PD: GBA vs. LRRK2)	360
183	Performance of Models in Level 4 Classification (Genetic PD: GBA vs. LRRK2)	361
184	Classification Metrics for Level 4 (Genetic PD: GBA vs. LRRK2)	362
185	Targets Displayed on Laptop Screen	386
186	Isolated Eye Regions for Tracking	387
187	Sample Results from Application	388
188	Application Results for Saccadic Metrics	392
189	Application Results for Saccadic Metrics	393
190	Ocular Motor Features of Parkinson's Disease and Atypical Parkinsonian Syndromes	400

List of Tables

1	Comparative Analysis of Eye Trackers	61
2	Demographic and clinical characteristics of the study cohort. Values are presented as mean \pm standard deviation (SD). Age is reported for all participants, while disease duration and levodopa equivalent daily dose (LEDD) are reported for Parkinson's disease (PD) groups only. Data are stratified by group and sex. "-" indicates not applicable or unavailable.	90
3	Qualitative Description of Central Fixation Metrics in the LRRK2 Mutation PD Group.	101
4	Qualitative Description of Eye Movement Metrics in the LRRK2 Mutation PD Group (Positional Fixation Paradigm).	108
5	Qualitative Description of Pursuit Metrics in the LRRK2 Mutation PD Group.	112
6	Qualitative Description of Oblique Saccades Metrics in the LRRK2 Mutation PD Group.	120
7	Qualitative Description of Antisaccades Metrics in the LRRK2 Mutation PD Group.	125
8	Qualitative Description of Reflexive Saccades Metrics in the LRRK2 Mutation PD Group.	131
9	Qualitative Description of Volitional Saccades Metrics in the LRRK2 Mutation PD Group.	137
10	Qualitative Description of Memory-Guided Saccades Metrics in the LRRK2 Mutation PD Group.	143

11	Demographic and clinical characteristics of the study cohort. Values are presented as mean \pm standard deviation (SD). Age is reported for all participants, while disease duration is reported for disease groups only. Data are stratified by group and sex. “-” indicates not applicable or unavailable.	176
12	Demographic and clinical characteristics of the study cohort at baseline and one year. Values are presented as mean \pm standard deviation (SD). Age is reported for all participants, while disease duration and LEDD are reported for disease groups only. Data are stratified by group and sex. “-” indicates not applicable or unavailable.	261
13	Demographic and clinical characteristics of the study cohort. Values are presented as mean \pm standard deviation (SD). Age is reported for all participants. Data are stratified by group and sex. “-” indicates not applicable or unavailable.	308
14	Demographic and clinical characteristics of the study cohort. Values are presented as mean \pm standard deviation (SD). Age and disease duration are reported for all participants. Data are stratified by group and sex. “-” indicates not applicable or unavailable.	323
15	Demographic and clinical characteristics of the study cohort. Values are presented as mean \pm standard deviation (SD). Age and disease duration are reported for all participants. Data are stratified by group and sex. “-” indicates not applicable or unavailable.	391
16	GBA-PD Generalised Linear Model Results for Antisaccades Horizontal	461
17	GBA-PD Generalised Linear Model Results for Antisaccades Vertical	461
18	GBA-PD Generalised Linear Model Results for Central Fixation	461
19	GBA-PD Generalised Linear Model Results for Memory Guided Saccades Horizontal . . .	462
20	GBA-PD Generalised Linear Model Results for Memory Guided Saccades Vertical	462
21	GBA-PD Generalised Linear Model Results for Nystagmus/ Positional Fixation	463
22	GBA-PD Generalised Linear Model Results for Oblique Saccades	464
23	GBA-PD Generalised Linear Model Results for Pursuit	464
24	Generalised Linear Model Results for Reflexive Saccades Horizontal	465
25	GBA-PD Generalised Linear Model Results for Reflexive Saccades Vertical	465
26	GBA-PD Generalised Linear Model Results for Volitional Saccades Horizontal	465
27	GBA-PD Generalised Linear Model Results for Volitional Saccades Vertical	466
28	Composite Scores for iPD, GBA-PD, LRRK2-PD	466

29	Atypical Parkinsonian Syndromes Generalised Linear Model Results Memory Guided Saccades Vertical	467
30	Atypical Parkinsonian Syndromes Generalised Linear Model Results Memory Guided Saccades Horizontal	468
31	Atypical Parkinsonian Syndromes Generalised Linear Model Results Volitional Saccades Vertical	469
32	Atypical Parkinsonian Syndromes Generalised Linear Model Results Volitional Saccades Horizontal	470
33	Atypical Parkinsonian Syndromes Generalised Linear Model Results Reflexive Saccades Vertical	471
34	Atypical Parkinsonian Syndromes Generalised Linear Model Results Reflexive Saccades Horizontal	472
35	Atypical Parkinsonian Syndromes Generalised Linear Model Results Oblique Saccades . .	473
36	Atypical Parkinsonian Syndromes Generalised Linear Model Results Antisaccades Vertical	476
37	Atypical Parkinsonian Syndromes Generalised Linear Model Results Antisaccades Horizontal	477
38	Atypical Parkinsonian Syndromes Generalised Linear Model Results Pursuit	478
39	Composite Z-Scores for Atypical Parkinsonian Syndromes	479
40	Longitudinal Study of Eye Movements in Parkinson's Disease Fixation Generalised Linear Model Results	480
41	Longitudinal Study of Eye Movements in Parkinson's Disease Positional Fixation/ Nystagmus Generalised Linear Model Results	480
42	Longitudinal Study of Eye Movements in Parkinson's Disease Pursuit Generalised Linear Model Results	481
43	Longitudinal Study of Eye Movements in Parkinson's Disease Oblique Saccades Generalised Linear Model Results	481
44	Longitudinal Study of Eye Movements in Parkinson's Disease Antisaccades Generalised Linear Model Results with Paradigm	482
45	Longitudinal Study of Eye Movements in Parkinson's Disease Reflexive Saccades Generalised Linear Model Results	482

46	Longitudinal Study of Eye Movements in Parkinson's Disease Volitional Saccades Generalised Linear Model Results	483
47	Longitudinal Study of Eye Movements in Parkinson's Disease Memory Guided Saccades Generalised Linear Model Results	483
48	Effect of Levodopa on Eye Movements in Parkinson's Disease Central Fixation Generalised Linear Model Results	484
49	Effect of Levodopa on Eye Movements in Parkinson's Disease Central Fixation Wilcoxon Signed-Rank Test Results	484
50	Effect of Levodopa on Eye Movements in Parkinson's Disease Antisaccades Generalised Linear Model Results	484
51	Effect of Levodopa on Eye Movements in Parkinson's Disease Antisaccades Wilcoxon Signed-Rank Test Results	485
52	Effect of Levodopa on Eye Movements in Parkinson's Disease Reflexive Saccades Horizontal Generalised Linear Model Results	485
53	Effect of Levodopa on Eye Movements in Parkinson's Disease Reflexive Saccades Horizontal Wilcoxon Signed-Rank Test Results	486
54	Effect of Levodopa on Eye Movements in Parkinson's Disease Reflexive Saccades Vertical Generalised Linear Model Results	486
55	Effect of Levodopa on Eye Movements in Parkinson's Disease Reflexive Saccades Vertical Wilcoxon Signed-Rank Test Results	487
56	Effect of Levodopa on Eye Movements in Parkinson's Disease Volitional Saccades Generalised Linear Model Results	487
57	Effect of Levodopa on Eye Movements in Parkinson's Disease Volitional Saccades Wilcoxon Signed-Rank Test Results	488
58	Effect of Levodopa on Eye Movements in Parkinson's Disease Memory Guided Saccades Generalised Linear Model Results	488
59	Effect of Levodopa on Eye Movements in Parkinson's Disease Memory Guided Saccades Wilcoxon Signed-Rank Test Results	489

List of Abbreviations

AI artificial intelligence.

AIC akaike information criterion.

AOS accessory optic system.

ATP atypical parkinsonism.

BG basal ganglia.

BIC bayesian information criterion.

CBS corticobasal syndrome.

CI confidence interval.

CT computed tomography.

DBS deep brain stimulation.

DLB dementia with Lewy bodies.

DLPFC dorsolateral prefrontal cortex.

DLPN dorsolateral pontine nucleus.

EBN excitatory burst neuron.

ER endoplasmic reticulum.

FEF frontal eye field.

GBA glucocerebrosidase.

GLM generalized linear model.

H&Y hoehn and yahr.

IBN inhibitory burst neuron.

iPD idiopathic-parkinson's disease.

LC locus coeruleus.

LEDD levodopa equivalent daily dose.

LMM linear mixed models.

LRRK2 leucine-rich repeat kinase 2.

MRI magnetic resonance imaging.

MSA multiple system atrophy.

MSA-C multiple system atrophy - cerebellar.

MSA-P multiple system atrophy - parkinsonian.

MST medial superior temporal area.

MT middle temporal area.

MVN medial vestibular nucleus.

NE norepinephrine.

NOT nucleus of the optic tract.

NRTP nucleus reticularis tegmenti pontis.

OKN optokinetic nystagmus.

OPN omnipause neuron.

PC parietal cortex.

PD Parkinson's disease.

PEF parietal eye field.

PPC posterior parietal cortex.

PPRF paramedian pontine reticular formation.

PROSPECT-M-UK progressive supranuclear palsy–corticobasal syndrome–multiple system atrophy study.

PSP progressive supranuclear palsy.

RAPSODI remote assessment of parkinsonism supporting ongoing development of interventions in gaucher disease.

RBD rem behavior disorder.

REM rapid eye movement.

riMLF rostral interstitial nucleus of the medial longitudinal fasciculus.

RMS root mean square.

RMSE root mean squared error.

RN raphe nuclei.

ROS reactive oxygen species.

SC superior colliculus.

SD standard deviation.

SEF supplementary eye field.

SN substantia nigra.

SNpr substantia nigra pars reticulata.

STR striatum.

SWJ square wave jerk.

UCL university college london.

UCLH university college london hospital.

UPDRS unified parkinson’s disease rating scale.

VIF variance inflation factor.

VOR vestibulo-ocular reflex.

1 Introduction

The eye is often regarded as a window into the brain due to its intricate connection with the central nervous system, while remaining accessible and relatively easy to study. The study of eye movements can provide insights into key brain pathways and reflect changes in anatomy and function associated with neurodegenerative diseases. Abnormal eye movements have been observed and studied in Parkinson's disease (PD) and atypical Parkinsonian syndromes, including progressive supranuclear palsy (PSP), multiple system atrophy (MSA), corticobasal syndrome (CBS), and dementia with Lewy bodies (DLB). When motor and non-motor symptoms of PD and atypical Parkinsonian syndromes overlap, clinical examination of eye movements using basic paradigms such as saccades, fixation, and pursuit can aid a differential diagnosis. Eye movements are particularly useful because they provide objective, non-invasive measures, and advancements in technology continue to improve their accuracy and potential for remote diagnosis.

However, several obstacles must be overcome before eye movement assessments can be considered diagnostically reliable. First, due to the significant overlap between PD and atypical Parkinsonian syndromes, a detailed ocular motor profile must be established for each condition. Second, there is currently no standardised protocol for eye movement testing across clinical or research settings, which limits comparability across studies and reduces general utility. Third, eye movements can be influenced by medication, disease duration, and disease severity; therefore, it is essential to study abnormalities across diverse settings. Lastly, the requirement for eye-tracking equipment, advanced analytical techniques, and expert interpretation presents a key challenge in translating research findings into routine clinical practice. Solutions to these challenges include the development of technology that enables quick and remote eye movement assessments, the application of artificial intelligence to detect subtle patterns that may be critical for diagnosis, and the creation of a standardised ocular motor profile for each condition. This profile should be supported by a comprehensive ocular motor battery that incorporates a wide range of assessments.

Research paradigms such as anticipatory eye movements and saccadic adaptation tasks offer new insights into the brain pathways and regions affected by both disease-associated and healthy ageing. By linking ocular motor profiles with neuroimaging and physiological data, we can better understand disease pathophysiology and identify potential targets for diagnosis and treatment. Post-mortem analysis of patients who underwent

comprehensive ocular motor evaluations could provide critical evidence regarding the specific brain regions and pathways impacted. As a diagnostic tool, this would further strengthen the utility of eye movement assessments. Ocular motor assessments can also be developed as markers of disease progression by investigating how eye movements change over time. Longitudinal studies tracking these changes can offer valuable insights into how both motor and non-motor symptoms influence ocular motility across disease stages. Additionally, understanding how medications and other interventions affect eye movements will help determine whether ocular motor assessments can serve as reliable markers for evaluating treatment efficacy in clinical trials.

Combining technological advancements with scientific data may open up new opportunities for integrating eye movement analysis into routine examinations, particularly in the early stages of PD and atypical Parkinsonian syndromes. As access to specialised clinicians can be limited in early disease stages, portable eye trackers, smartphones, and tablet applications could facilitate eye movement assessments by general practitioners. Integrating machine learning techniques to generate diagnostic reports automatically can further reduce processing time. This would enhance the efficiency of basic diagnostic evaluations while reducing the expertise and training required by clinicians and non-clinicians alike.

This thesis builds upon the foundations of ocular motor research by addressing critical knowledge gaps and working towards overcoming major challenges in the clinical application of eye movement assessments. Chapters 3 and 4 examine eye movements in genetic and sporadic forms of PD and atypical Parkinsonian syndromes to establish distinct ocular motor profiles for each condition. Chapter 5 explores the longitudinal changes in eye movements to evaluate their potential as a progression marker. Chapter 6 offers novel insights into the pathophysiology of PD and MSA through the study of saccadic adaptation, while Chapter 7 investigates the short-term effects of levodopa on eye movements in PD. Chapters 9 to 11 focus on technological areas: Chapter 9 explores how machine learning can enhance the predictive power of eye movements; Chapter 10 compares the performance of a portable eye tracker with a desktop-mounted eye tracker; and Chapter 11 tests the viability of an application for remotely recording eye movements. Together, the research projects presented in this thesis aim to advance the field of eye movement science, with the potential to transform the diagnostic approach to PD and atypical Parkinsonian syndromes—enabling earlier interventions, improved patient care, and better outcomes for those affected.

1.1 Human Ocular Motor System

The human ocular motor system is a complex neural network responsible for initiating and controlling eye movements essential for visual perception and interaction with the environment. To achieve a clear and stable view of the surroundings, the object within the field of view must not only be positioned on the central foveal region of the retina but also remain stabilised (Bosman et al. 2002; Gauthier, Vercher and David S. Zee 1994; Martinez-Conde and Macknik 2008). Accordingly, there are different types of eye movements, including fixational, saccadic, and smooth pursuit eye movements, to meet the visual requirements of the human body.

Neuroanatomical studies have shown that the ocular motor system is organised hierarchically, with distinct pathways responsible for different types of eye movements. The motor neurons that innervate the extraocular muscles are located in specific nuclei within the brainstem, including the oculomotor, trochlear, and abducens nuclei. These nuclei receive input from premotor areas such as the frontal eye field (FEF) and the superior colliculus (SC), which coordinate the timing and direction of eye movements (S. F.W. Neggers et al. 2005; MacLean, Klein and Hilchey 2015). The competitive integration model proposes that eye movement programming arises from the integration of information from multiple sources, including the prefrontal cortex, FEF, and the dorsolateral prefrontal cortex (DLPFC), within the SC (Meeter, Van Der Stigchel and Theeuwes 2010). This model highlights the role of both bottom-up sensory input and top-down cognitive processes in determining the timing and direction of eye movements.

1.2 Classes of Eye Movements

Eye movements broadly fall into two groups: those that stabilise the image on the retina—fixational eye movements, pursuit, vestibular eye movements, and optokinetic eye movements—and those that shift the field of vision to bring the area of interest into focus—vergence and saccades (T. J. Anderson and MacAskill 2013; R. John Leigh and David S. Zee 2015a). Within these two categories, there are several functional classes of eye movements, each designed to serve a specific purpose.

1.2.1 Fixational Eye Movements

Fixational eye movements are small, involuntary movements that allow the eye to maintain gaze on a stationary object in the field of view. The visibility of moving objects depends on their spatial frequencies (D. C. Burr and Ross 1982), but for clear vision, the image motion should be less than approximately $5^\circ/\text{second}$ (Demer and Amjadi 1993) and should remain within 0.5° of the fovea (Jacobs 1979). Another component of maintaining fixation is head movement (Grossman et al. 1988; Pozzo, Berthoz and Lefort 1990), along with involuntary eye movements which, in normal individuals, deviate by less than 0.25° and at speeds under 0.5° per second (Cherici et al. 2012; R. M. Schneider et al. 2013). Thus, the eyes are always in subtle motion during fixation attempts. The three main components of fixational eye movements are microsaccades, tremor, and drift (Pansell et al. 2011).

Microsaccades are small involuntary saccades that occur in all directions during fixation, with amplitudes between 0.02° and 2° (Martinez-Conde, Macknik and Hubel 2004; Martinez-Conde, Otero-Millan and Macknik 2013). Microsaccades and saccades share similar neural pathways, primarily involving the SC, which receives input from various cortical and subcortical regions, including the FEF, parietal cortex (PC), and the basal ganglia (BG) (Otero-Millan, Macknik, Serra et al. 2011; Fang et al. 2018). These inputs modulate the activity of SC neurones, creating a complex interplay between excitatory and inhibitory processes (Hafed, Yoshida et al. 2021). Specifically, the rostral SC, which encodes the foveal region of the visual field, contains neurons that fire before and during microsaccades. These neurones are influenced by omnipause neurones in the brainstem raphe nuclei (RN), which inhibit saccade-related activity in the SC and help maintain fixation (Otero-Millan, Macknik, Langston et al. 2013). Although the role of microsaccades in vision is debated, evidence suggests that they contribute to perception in several ways. Firstly, microsaccades reverse the visual fading phenomenon known as Troxler fading to restore peripheral acuity (Martinez-Conde, Macknik, Troncoso et al. 2006; McCamy, Otero-Millan, Macknik et al. 2012). Secondly, they bring the image back to the fovea when drift becomes excessive, such as during blinks (R. John Leigh and David S. Zee 2015a). Thirdly, they enhance information acquisition during visual scanning (McCamy, Otero-Millan, Di Stasi et al. 2014). Lastly, as images on the fovea are not uniform, microsaccades enable the viewing of finer visual details (Optican and David S. Zee 1984).

Ocular tremor is the smallest of the fixation movements, with a frequency of up to 150Hz and an amplitude of

less than 0.01° (Spaushus et al. 1999). Ocular drift occurs when the eyes slowly drift away from the centre of a stationary target at speeds of approximately 0.5/second (Cherici et al. 2012). The neural substrates of ocular tremor and drift include the SC and several cortical and subcortical regions, similar to microsaccades (Fang et al. 2018; Otero-Millan, Macknik, Serra et al. 2011). In addition, the cerebello-thalamo-cortical pathway and the flocculus and paraflocculus regions of the cerebellum are involved in the modulation of ocular tremor and drift via connections with brainstem and cortical areas (Xue et al. 2020; Dalmaso et al. 2017; Siegenthaler et al. 2014). The relationship between ocular tremor and drift and visual processing is complex. On one hand, ocular tremor prevents visual fading by shaking the retinal image and refreshing the activity of visual neurones (Costela et al. 2013; Raffi et al. 2021) and on the other hand, the retinal motion caused by ocular tremor can suppress visual signals in the SC, impacting perception (Hafed and Krauzlis 2010; Rolfs and Ohl 2011).

The functional importance of fixational eye movements extends beyond stabilising the visual field; these movements contribute to the processing of intricate spatial details. Research has shown that fixational eye movements improve the perception of high spatial frequency data, which is critical for tasks requiring visual precision, such as reading and face recognition (Kuang et al. 2012; Inagaki et al. 2020). The interaction between drift and microsaccades maintains the visual system's sensitivity to environmental change, supporting a dynamic representation of the visual world even during seemingly stable gaze. Beyond perceptual functions, fixational eye movements are also influenced by neural mechanisms associated with attention and cognition.

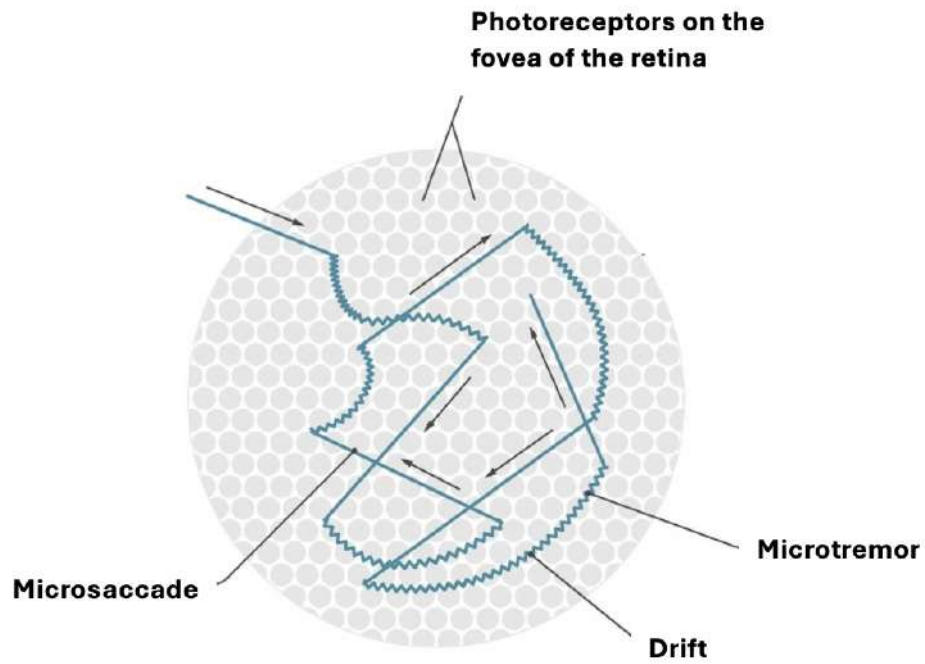


Figure 1: Schematic of Fixational Eye Movements. Diagram of fixational eye movement patterns on the retinal fovea, highlighting microsaccades, drift, and microtremors. Figure by author.

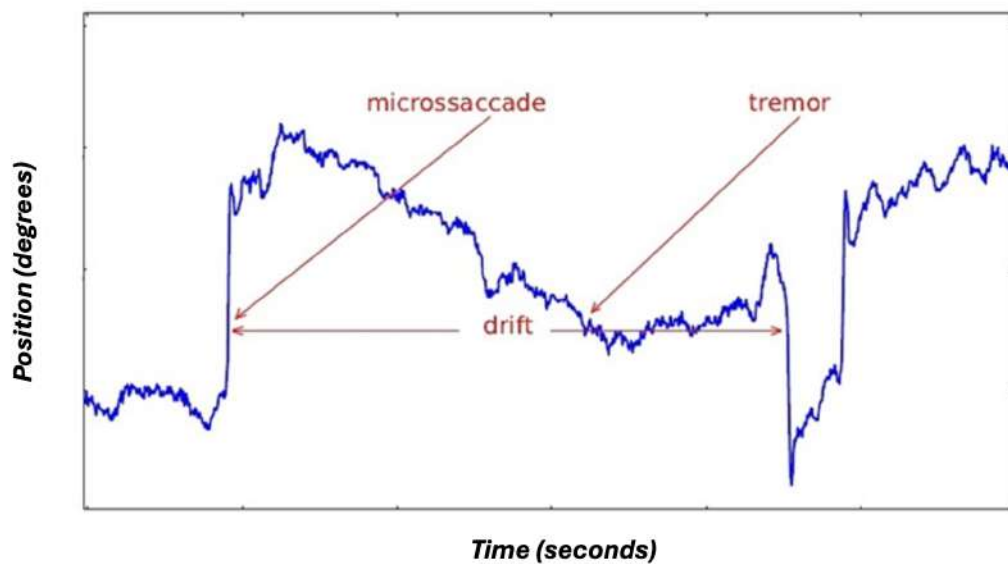


Figure 2: Traces of Fixational Eye Movements. Recording of fixational eye movement components, including microsaccades, drifts, and tremors, during visual fixation. Figure by author.

1.2.2 Saccadic Eye Movements

Saccades are rapid, ballistic eye movements that enable the fovea to shift towards an object of interest. Different types of saccades form the foundation of visual exploration, allowing the eyes to rapidly redirect fixation from one point to another (R. John Leigh and David S. Zee 2015a). Saccades can be volitional (intentionally directed eye movements), memory-guided saccades (made toward a remembered location), antisaccades (executed in the opposite direction of a visual stimulus), or predictive saccades (anticipatory movements made while scanning a visual scene based on expected target motion or position). They can also be reflexive, triggered by novel stimuli; express saccades, which are short-latency movements in response to a gap stimulus; quick phases of nystagmus, which help stabilise vision during head movements or optokinetic stimulation; and rapid eye movements (REM) during sleep (Dodge 1903; Hong et al. 2009; Schütz, Kerzel and Souto 2014; Van Opstal and Van Gisbergen 1987).

Saccades possess several key properties, including velocity, duration, latency, and waveform. Saccadic amplitude and peak velocity scale non-linearly, following a phenomenon known as the main sequence effect. In this relationship, small saccades show a linear increase in peak velocity, whereas larger saccades exhibit a soft saturation effect, with an upper limit of approximately 500°/s (Lebedev, Van Gelder and Wai Hon Tsui 1996; Yarbus 1967; Wyatt 1998). The saccadic waveform is asymmetrical, with the acceleration phase peaking earlier than the deceleration phase. Antisaccades display greater skewness compared to reactive saccades in this waveform (A. N. Kumar et al. 2005; Van Opstal and Van Gisbergen 1987; Wyatt 1998). When there is a mismatch between the pulse (a brief, high-frequency burst of neural activity that generates the rapid eye movement) and step (a sustained level of neural activity that holds the eye in its new position) components of the neural command, post-saccadic drifts known as glissades can occur to make necessary adjustments for refined focus on the target (Van Leeuwen, Collewyn and Casper J. Erkelens 1998; H. Watanabe et al. 2023).

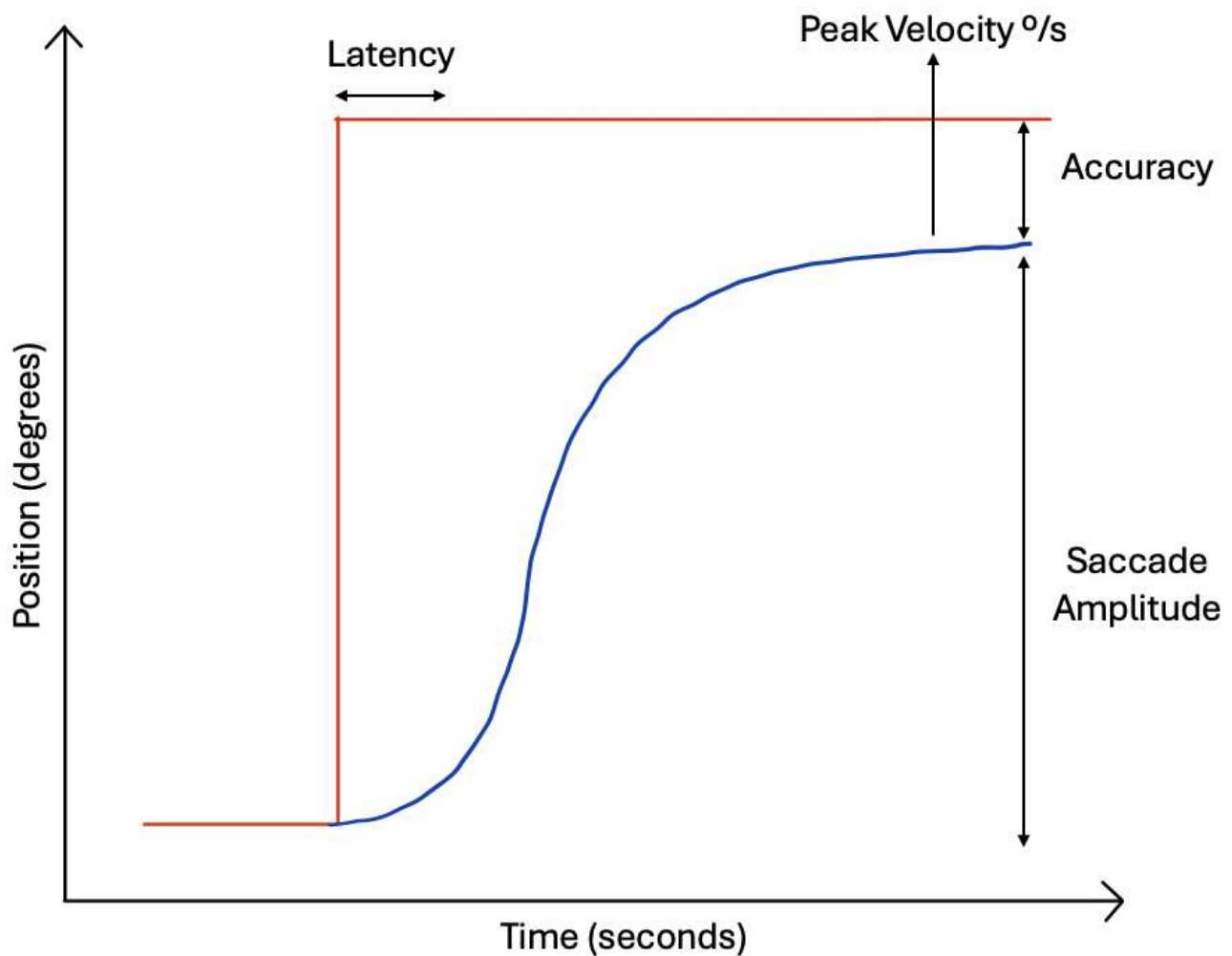


Figure 3: Saccadic Waveform. Typical saccadic eye movement profile, showing key parameters such as latency, peak velocity, accuracy, and amplitude. Figure by author.

Saccades are generated through a complex neural network involving the cortex, subcortex, brainstem, and cerebellum. The FEF and the supplementary eye field (SEF) control the initiation of volitional saccades, with the FEF selecting saccadic targets and providing motor commands for execution, while the SEF is involved in sequencing saccades and mediating anticipatory eye movements. The parietal eye field (PEF) and the posterior parietal cortex (PPC) integrate spatial information and direct reflexive saccades towards the intended target. The DLPFC is responsible for higher-order tasks such as memory-guided saccades and antisaccades, which require suppression of reflexive responses (Karantinos et al. 2014; McDowell, Clementz and Sweeney 2012; Schmid and Ron 1986; Van Leeuwen, Collewyn and Casper J. Erkelens 1998).

The SC serves as a command centre, integrating cortical input with multimodal sensory information—including visual, auditory, and somatosensory stimuli—to compute saccade vectors. The output is sent to the brainstem,

particularly the paramedian pontine reticular formation (PPRF) for horizontal saccades and the rostral interstitial nucleus of the medial longitudinal fasciculus (riMLF) for vertical saccades. Excitatory burst neurons in the brainstem generate the high-frequency pulse required for saccadic velocity; inhibitory burst neurons suppress antagonistic muscles, and omnipause neurones provide tonic inhibition of burst neurons during fixation. When a saccade is initiated, omnipause neurones pause their activity, allowing burst neurons to fire and generate the saccadic movement (Milstein and Dorris 2011; Shelhamer and Joiner 2003; Kanai, Van Der Geest and Frens 2003; Sweeney et al. 2007). The dorsal vermis and fastigial nucleus of the cerebellum ensure the precision and adaptability of saccadic movements by fine-tuning motor commands and recalibrating in response to errors to maintain accuracy (S. Van der Stigchel et al. 2012; David S. Zee 2012). Lesions in any of these regions involved in saccadic control can result in dysmetria, the failure to suppress automatic responses, or impaired initiation of saccades (Zingale and Kowler 1987).

Models of saccadic eye movements provide a theoretical framework for understanding their dynamics. The local feedback model, introduced by D. A. Robinson, suggests that saccades operate as a closed-loop system. In this model, retinal error—the difference between desired and actual eye position—drives motor commands aimed at minimising this error. The model explains key features of saccades, including the main sequence effect and compensatory mechanisms (Rottach et al. 1997; Tu et al. 2006; R. Walker, Deubel et al. 1997). More recent extensions incorporate cerebellar feedback loops to refine saccadic sequences and correct errors in real time. These account for phenomena such as curved trajectories in oblique saccades and adaptive adjustments in response to visual perturbations (Sommer and Robert H. Wurtz 2004; Strassman, Highstein and McCrea 1986; R. Walker, D. G. Walker et al. 2000). Predictive models based on Bayesian principles have further elucidated how sensory inputs, task instructions, and prior experiences are integrated to optimise saccadic performance. This is especially relevant for complex behaviours such as antisaccades. The probabilistic nature of Bayesian models captures the dynamic interplay between sensory uncertainty and motor planning, highlighting the importance of cortical, brainstem, and cerebellar interactions in saccade generation (Vokoun et al. 2014; Wolfe, Palmer and Horowitz 2010; Zingale and Kowler 1987).

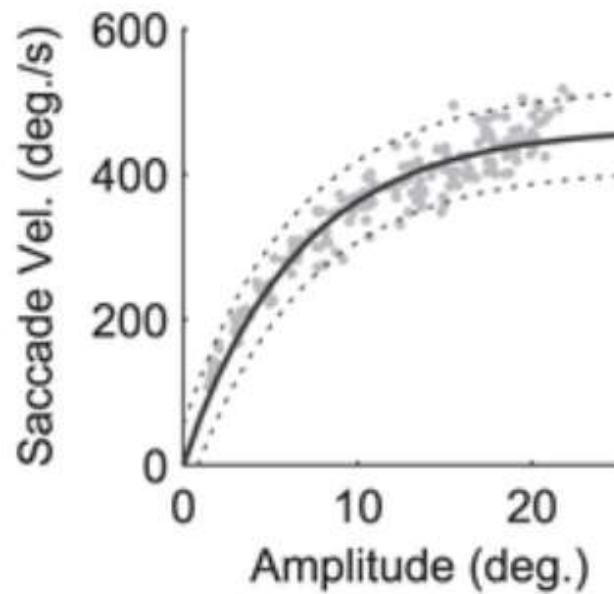


Figure 4: Main Sequence Effect of Saccades. The relationship between saccadic velocity and amplitude, demonstrating the nonlinear increase in velocity with larger saccade amplitudes. Figure by author.

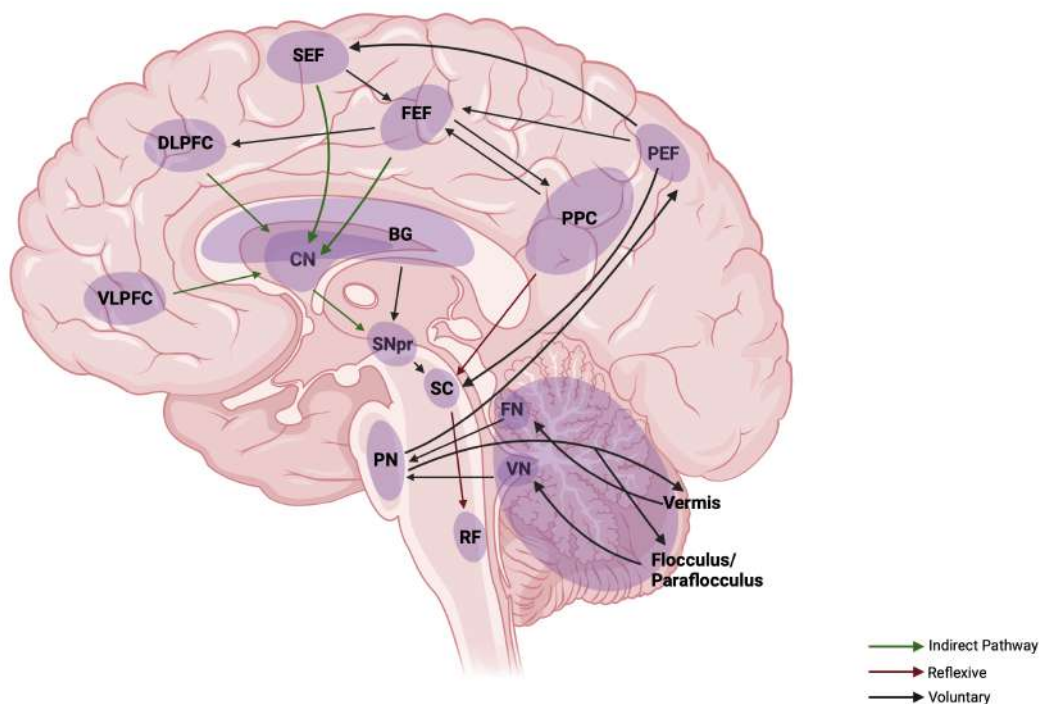


Figure 5: Neural Pathways in Saccadic Control. SEF, supplementary eye field; FEF, frontal eye field; PEF, parietal eye field; PPC, posterior parietal cortex; DLPFC, dorsolateral prefrontal cortex; VLPFC, ventrolateral prefrontal cortex; CN, caudate nucleus; BG, basal ganglia; SNpr, substantia nigra pars reticulata; SC, superior colliculus; PN, pontine nuclei; RF, reticular formation; FN, fastigial nucleus; VN, vestibular nuclei; Vermis, cerebellar vermis; Flocculus/Paraflocculus, cerebellar flocculus and paraflocculus. Figure by author.

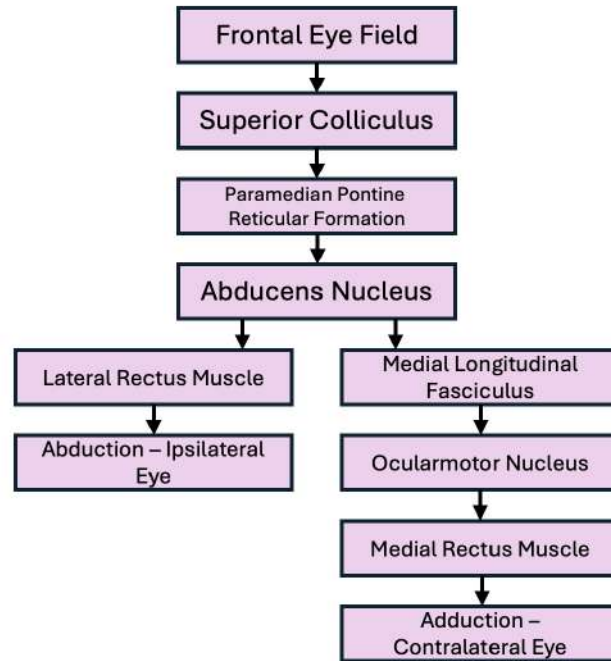


Figure 6: Neural Pathway of Horizontal Saccades. The neural pathways involved in generating horizontal saccades, illustrating the role of the frontal eye fields, superior colliculus, paramedian pontine reticular formation, and oculomotor nuclei. Figure by author.

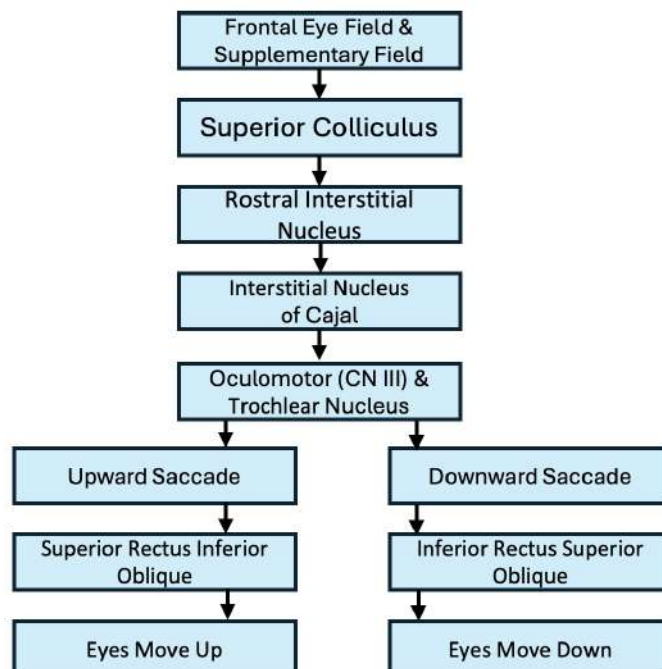
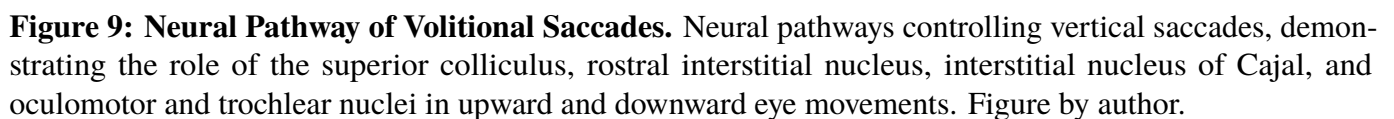
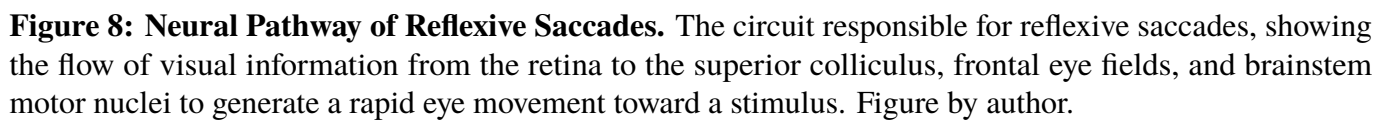


Figure 7: Neural Pathway of Vertical Saccades. Neural pathways controlling vertical saccades, demonstrating the role of the superior colliculus, rostral interstitial nucleus, interstitial nucleus of Cajal, and oculomotor and trochlear nuclei in upward and downward eye movements. Figure by author.



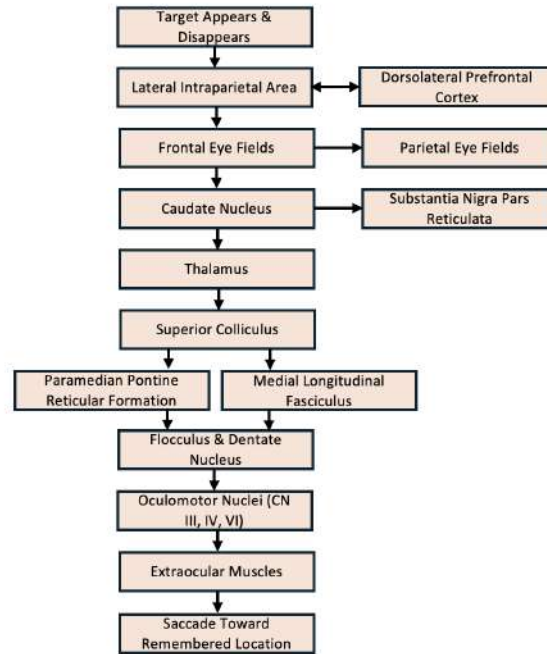


Figure 10: Neural Pathway of Memory Guided Saccades. Neural circuitry underlying memory-guided saccades, highlighting the role of the lateral intraparietal area, frontal eye fields, caudate nucleus, and superior colliculus in generating saccades toward a remembered location. Figure by author.

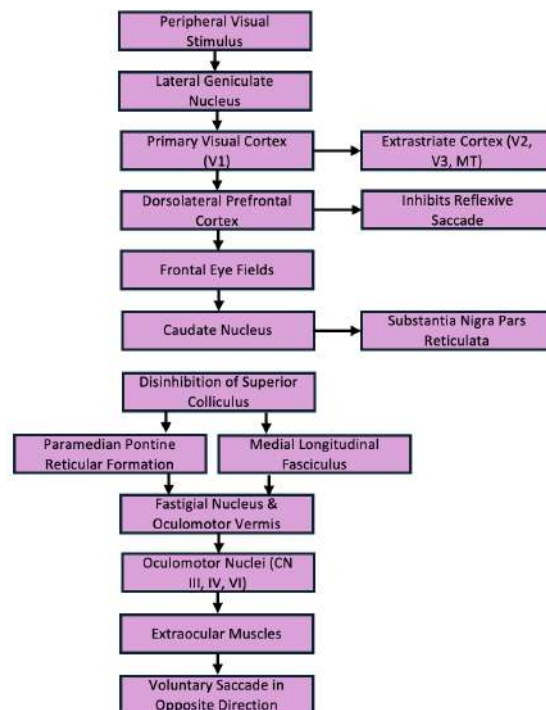


Figure 11: Neural Pathways of Antisaccades. Schematic representation of the neural circuitry involved in generating voluntary antisaccades, showing the inhibition of reflexive saccades and the role of the frontal eye fields, basal ganglia, and superior colliculus. Figure by author.

1.2.3 Smooth Pursuit

Pursuit eye movements allow continuous tracking of a moving object, keeping a stable image of the target on the retina. The neural substrates and pathways for smooth pursuit span cortical, subcortical, and cerebellar regions. Visual information from the retina is processed by the primary visual cortex (V1) via the magnocellular layers of the lateral geniculate nucleus (Blohm, Marcus Missal and Lefèvre 2003). This information is then projected to the middle temporal area (MT) and medial superior temporal area (MST), where visual motion signals are extracted (K. J. Chen et al. 2005; Churchland and Lisberger 2002). The MT and MST send signals to the FEF and SEF, which initiate voluntary and predictive smooth pursuit (Churchland and Lisberger 2002; De Hemptinne, Barnes and M. Missal 2010).

There are two parallel descending pathways for smooth pursuit originating from the cortex. The first originates from the MT and MST and projects to the dorsolateral pontine nucleus (DLPN), supporting sustained pursuit (Blohm, Marcus Missal and Lefèvre 2003; K. J. Chen et al. 2005). The second originates from the FEF and SEF and projects to the nucleus reticularis tegmenti pontis (NRTP) for the initiation and optimisation of pursuit (Churchland and Lisberger 2002; De Hemptinne, Barnes and M. Missal 2010). The first pathway transmits information to the dorsal vermis and fastigial nucleus, while the second connects to the paraflocculus and vestibular nucleus—all within the cerebellum. These regions are essential for fine-tuning motor responses (Dell’Osso and Z. I. Wang 2008). Lastly, the BG and brainstem reticular formation integrate cortical input with motor signals to further modulate pursuit behaviour (Chubb and A. F. Fuchs 1982; K. J. Chen et al. 2005; Blohm, Marcus Missal and Lefèvre 2003).

Smooth pursuit models have been proposed to describe how the brain processes and controls the output of smooth tracking. The earliest model, the negative feedback model, postulates that retinal error velocity—the difference between target velocity and eye velocity—is the stimulus for pursuit. This error is amplified by a central neural gain factor to generate eye velocity that compensates for the target’s movement (Hashiba et al. 1995; Newsome, R. H. Wurtz and Komatsu 1988; Barnes 2008). However, a limitation of this model is that due to inherent processing delays, simple feedback mechanisms cannot account for lag-free pursuit.

Alternatively, models incorporating internal estimates of target velocity, in combination with retinal error and efference copy signals, offer a more accurate explanation for sustained smooth pursuit (Shibata et al. 2005;

Fukushima et al. 2013; J. Yamada and Noda 1987). Predictive and Bayesian models suggest that smooth pursuit integrates memory and current visual input to anticipate target motion, optimising performance based on recent motion patterns and probabilistic expectations (Mustari and Ono 2011; Freeman, Champion and P. A. Warren 2010; Spering et al. 2013). Although no single model fully explains smooth pursuit, it is evident that a complex integration of sensory, motor, predictive signals and learned behaviour is involved. Moreover, the interaction between saccadic movements and smooth pursuit is significant. Saccades can enhance the gain of subsequent pursuit movements, suggesting a synergistic relationship between these two types of eye movements (Pattadkal, Barr and Priebe 2024).

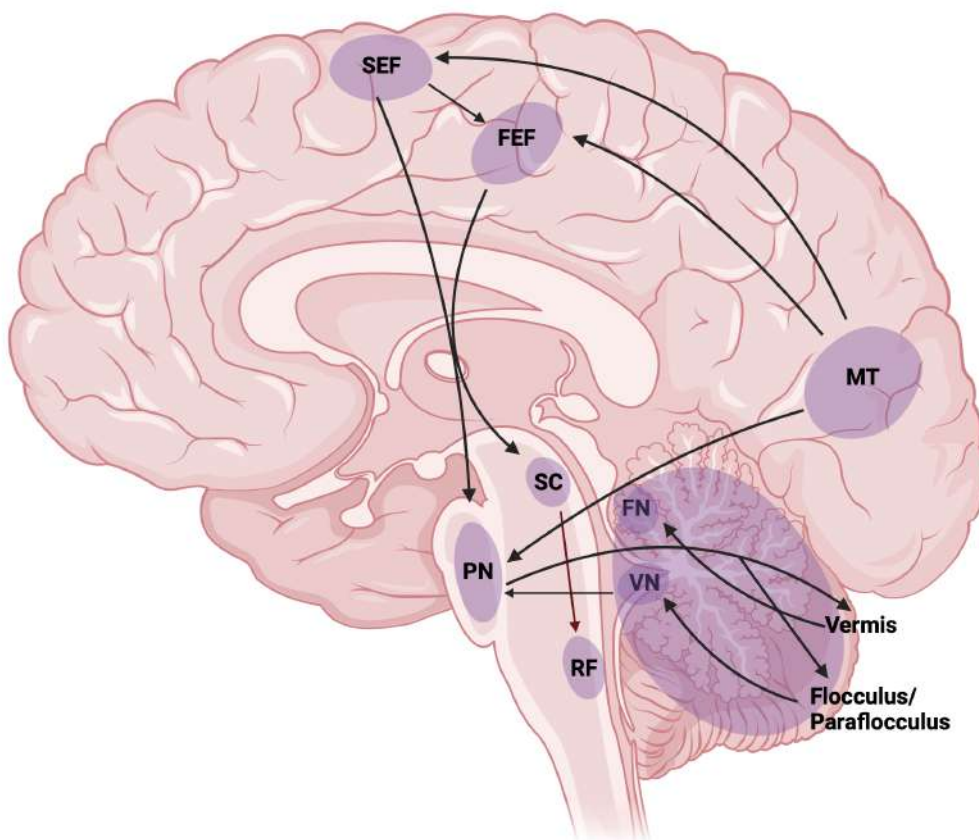


Figure 12: Neural pathways involved in smooth pursuit - SEF, supplementary eye field; FEF, frontal eye field; MT, middle temporal visual area; SC, superior colliculus; PN, pontine nuclei; RF, reticular formation; FN, fastigial nucleus; VN, vestibular nuclei; Vermis, cerebellar vermis; Flocculus/Paraflocculus, cerebellar flocculus and paraflocculus. Figure by author.

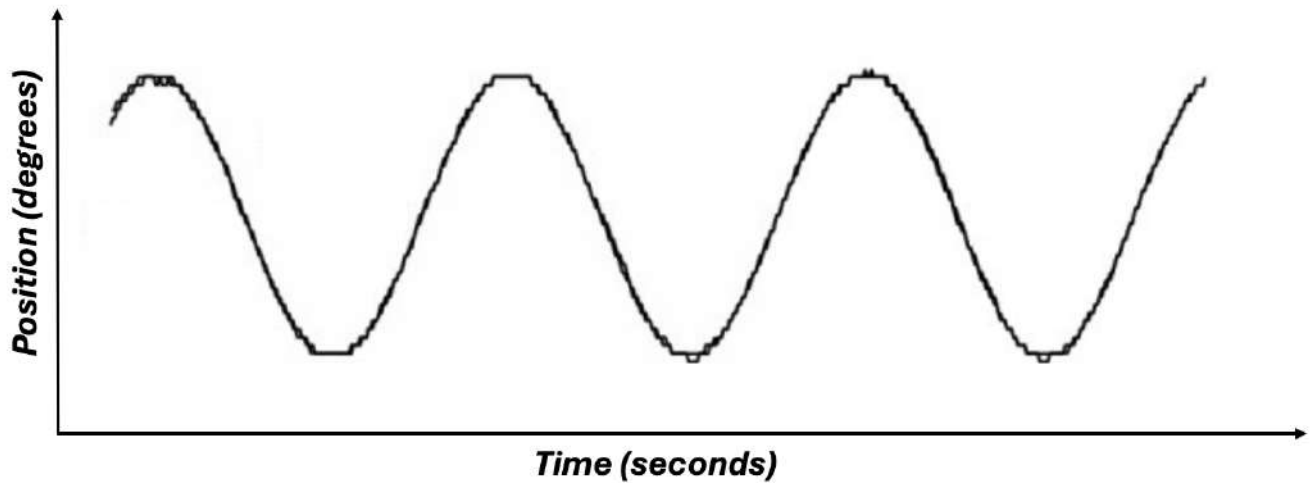


Figure 13: Smooth Pursuit Waveform. Representative eye position trace over time during smooth pursuit eye movements, illustrating the sinusoidal tracking of a moving target. Figure by author.

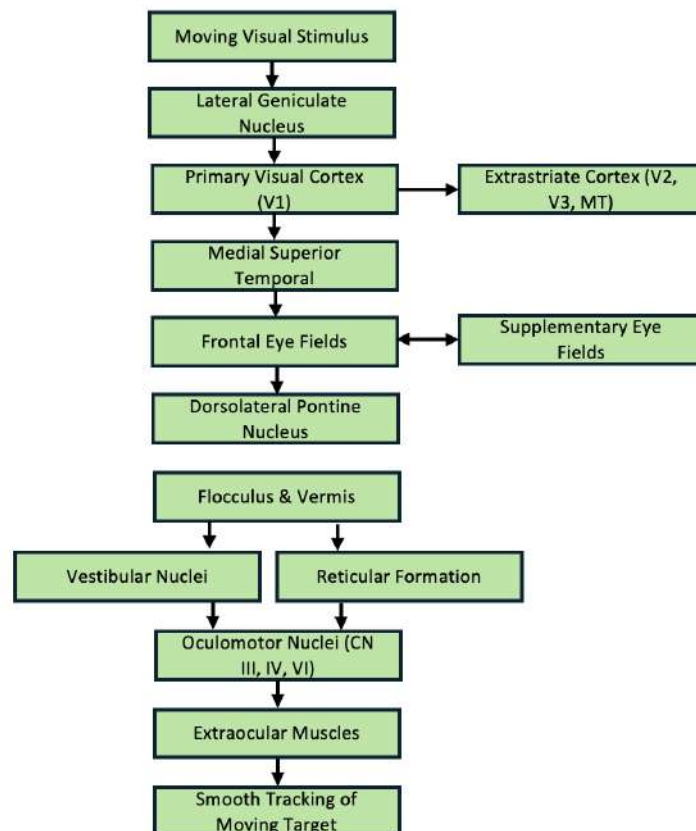


Figure 14: Neural Pathway of Smooth Pursuit. The neural pathways involved in smooth pursuit eye movements, illustrating the processing of a moving visual stimulus through the primary visual cortex, medial superior temporal area, and brainstem structures. Figure by author.

1.2.4 Vestibular Eye Movements

Vestibular eye movements are primarily controlled by the vestibulo-ocular reflex (VOR), which provides stability to visual focus during head movements. The VOR produces compensatory eye movements equal and opposite to the direction of head motion, thereby maintaining visual image stability on the retina. This reflex is critical for preserving clear vision and balance, especially in dynamic situations involving rapid head movements. The VOR originates from signals within the vestibular system, which comprises the semicircular canals (detecting angular acceleration) and the otolith organs (detecting linear acceleration) (Abe et al., 2019; Dai et al., 2011). The neural pathways mediating vestibular eye movements involve key brainstem structures.

The primary processing centres for vestibular information are the vestibular nuclei, located in the medulla and pons. These nuclei integrate sensory input from the vestibular system with visual and proprioceptive data to generate appropriate commands for eye movements (Mendoza et al., 2016; Fridman et al., 2010). In particular, the medial vestibular nucleus (MVN) plays a critical role in the VOR, as it projects to the oculomotor nuclei that innervate the extraocular muscles (Mendoza et al., 2016; Fridman et al., 2010). The VOR demonstrates notable plasticity and can adapt in response to sensory input and motor learning. Several studies have shown that changes in VOR gain can occur due to altered vestibular function, suggesting a sensory substitution mechanism wherein visual input compensates for vestibular deficits (Nelson et al., 2017; Sadeghi et al., 2010).

Additionally, the interaction between vestibular and visual inputs plays a critical role in ocular motor control during complex tasks involving coordinated head and eye movements (Shanidze et al., 2010). This integration relies on feedback systems that continuously calibrate vestibular interneurons and motoneurons based on head position and velocity (Gong et al., 2008; Frens, 2009). Such coordination is essential for maintaining both visual stability and spatial orientation in dynamic environments (Abekawa et al., 2018).

1.2.5 Optokinetic Eye Movements

Optokinetic movements or optokinetic nystagmus (OKN) are reflexive responses that stabilise retinal images during sustained movement of the visual field. This is particularly relevant when either the observer or the environment is in motion. The OKN consists of two phases: a slow phase that follows the visual stimulus

and a fast phase that resets eye position. This reflex counters image slip to prevent motion blur and preserve visual clarity. Anatomical studies have demonstrated that OKN is mediated by both cortical and subcortical pathways (Miura et al. 2019). The slow phase shares neural substrates with smooth pursuit movements, while the fast phase involves saccadic generation circuits (S. Garbutt, Harwood and Harris 2001; Konen et al. 2005).

Overlapping neural regions between smooth pursuit, saccades, and OKN include the FEF, SEF, ventrolateral premotor cortex, and PPC—notably areas ventral intraparietal area, parietal inferior-to-postcentra tract, and posterior superior parietal cortex—as well as areas V1/V2, V4, and the MT and MST (Heide, Kurzidim and Kömpf 1996; Paus 1996; Berman et al. 1999; Petit and Haxby 1999; O’Driscoll et al. 2000; Tanabe et al. 2002). The culmen and declive regions of the cerebellum also contribute to the modulation of OKN (Hayakawa et al. 2002; Nitschke et al. 2004; Krauzlis 2004). Although OKN and smooth pursuit share overlapping pathways, neuroimaging and electrophysiology show distinct activation patterns. OKN elicits stronger responses in primary visual areas due to heightened visual input, whereas smooth pursuit is associated with greater activation of the cerebellum (Konen et al. 2005). Voluntary (look-nystagmus) and reflexive (stare-nystagmus) forms of OKN differ in cortical activation, with the former showing greater cortical engagement (Wyatt 1998; Ilg 1997). Furthermore, OKN and smooth pursuit involve reciprocal inhibitory interactions between visual and vestibular cortices, including deactivation of the parieto-insular vestibular cortex (Brandt et al. 1998).

Initial visual motion processing for OKN begins in the retina and travels via retinal ganglion cells to the accessory optic system (AOS) (Yonehara et al., 2009), which relays horizontal and vertical motion signals to brainstem nuclei such as the DLPN and nucleus of the optic tract (NOT) (Hoffmann et al., 2009). These nuclei contribute to the subcortical control of OKN, working in coordination with vestibular and oculomotor nuclei (Pham et al., 2020; Zupan & Merfeld, 2003). The oculomotor nuclei provide the final motor commands to generate appropriately timed and directed eye movements. The cerebellum also supports adaptive plasticity in the optokinetic reflex by adjusting to repeated image motion over time (Wada et al., 2014).

Studies have shown that the neural circuits underlying OKN are not only reflexive but also capable of adaptation in response to changes in visual input or motor demands (Aasen et al., 2013). This integration of visual, vestibular, and motor signals highlights the complexity and significance of optokinetic eye movements in maintaining perceptual stability.

1.2.6 Vergence Eye Movements

Vergence eye movements are dysconjugate movements where the eyes move in opposite directions to maintain binocular vision at varying depths. They contribute to depth perception through two key mechanisms: retinal disparity and blur cues. Retinal disparity refers to the differences in the images seen by each eye, while blur cues relate to the need for refocusing depending on object distance. Vergence movements are classified into convergence (inward movement) and divergence (outward movement) (Gamlin 2002).

Multiple brain regions are involved in vergence control. The rostral SC contains neurons involved in vergence signal generation (Stuphorn 2015; Upadhyaya and Das 2019). The NRTP plays a major role in encoding vergence velocity and is closely linked with cerebellar structures, supporting the integration of vergence and saccadic commands (Pallus, Walton and Mustari 2018). The FEF and PPC also contribute to vergence control, processing visual information to align the eyes accurately (Alvarez et al. 2014). The pontine nuclei are part of the corticopontocerebellar circuit, integrating vergence signals and coordinating conjugate and dysconjugate eye movements (Rambold, El Baz and Helmchen 2005). The cerebellum also plays a critical role in error correction during vergence, ensuring proper alignment and visual stability.

1.3 Evaluating the Study of Eye Movements

Eye movements are a powerful tool and an objective window into neurological function, providing critical diagnostic and monitoring insights into a wide range of neurological, cognitive, and vestibular disorders. While most other clinical signs may be subjective or variable, all aspects of eye movement analysis are precise and measurable. Eye movements are governed by well-defined neurological pathways involving the brainstem, cerebellum, and cerebral cortex, making them highly reliable for clinical applications (R. John Leigh and David S. Zee 2015a). As a result, abnormalities in eye movements often signal dysfunction in these regions, making them particularly sensitive indicators of early-stage neurological diseases. For example, in Parkinson's disease, there is evidence that saccadic and pursuit eye movements may be impaired before the onset of motor symptoms, potentially serving as early diagnostic markers of the disease (T. J. Anderson and MacAskill 2013).

Eye movement analysis is also economically efficient. While imaging techniques such as magnetic resonance imaging (MRI) or computed tomography (CT) scans are expensive, eye-tracking technology requires minimal setup and is relatively low-cost. This affordability makes it suitable for routine clinical use and regular monitoring, enabling consistent evaluation of patients (Valliappan et al. 2020; Bryan and Reso 2008). Moreover, eye movement testing is highly versatile—the same basic assessments can be applied across neurodegenerative diseases, vestibular disorders, and cognitive impairments—making it favourable compared to specialised tests that address only a single condition.

From the patient's perspective, eye movement testing is non-invasive and simple; very little effort is required, as patients are typically asked to follow targets or focus on a fixed point. This ease of participation makes the test accessible even to those with severe cognitive impairment or physical disability, ensuring wide applicability. This, in turn, benefits clinicians as well, since the tests are not time-consuming and produce quantifiable results, enabling accurate interpretation and effective monitoring of disease progression.

Studies have also highlighted the potential of eye movement analysis as a continuous monitoring tool, particularly with the development of wearable devices. These technologies are useful for tracking disease progression in neurodegenerative conditions such as multiple sclerosis, where changes in saccadic latency or nystagmus can be used to assess disease severity and therapeutic response (Tang, Luk and Y. Zhou 2023; D. Li et al. 2024). The objective and quantifiable nature of eye movements allows for precise longitudinal tracking, providing clinicians with a reliable method to detect changes and adjust treatment strategies.

Contemporary techniques such as video-oculography (VOG) enable detailed recording and analysis of eye movements within just a few minutes. This quick and effective approach significantly reduces diagnostic time, which is crucial for early intervention in progressive neurological conditions (Furman and Wuyts 2012). Traditional imaging methods such as MRI are often time-consuming and focused on structural changes, potentially missing subtle functional abnormalities in the brain's ocular motor system. In contrast, eye movement analysis offers a more sensitive, efficient, and precise diagnostic alternative (Ladd et al. 2018).

1.4 Translation Into Clinical Settings

Eye movement analysis has emerged as an important modality in the diagnosis and monitoring of neurological and vestibular disorders. Despite its advantages, there remain some limitations and challenges that must be addressed to enhance its validity and reliability as a clinical tool (A. Kheradmand, Colpak and D. S. Zee 2016).

A major limitation is that interpreting eye movement data is complex and requires specialised knowledge. Analysis involves understanding nuanced patterns such as saccadic latency, smooth pursuit gain, and features of nystagmus—factors that may be difficult for general physicians to interpret. As such, specialised training is often required, which restricts the widespread adoption of eye movement analysis in general clinical settings (D. Li et al. 2024).

Another challenge lies in the variability of eye movement patterns between individuals. Factors such as age, vision, fatigue, and attentional state can significantly influence the results (Helo et al. 2014; Y. Yamada and Kobayashi 2018; Zargari Marandi et al. 2018). This variability makes it difficult to establish generalised diagnostic criteria based solely on eye movement patterns. Furthermore, patients with ophthalmological pathologies—such as cataracts or retinal disorders—may exhibit abnormal eye movements unrelated to neurological status, potentially confounding diagnostic interpretations (Wan et al. 2020).

Practical and financial barriers also exist. Although eye-tracking is generally more affordable than imaging technologies like MRI, high-end systems—such as those used in VOG—require significant upfront investment (Ivanchenko et al. 2021). These systems also require periodic maintenance and recalibration, adding to operational costs. In resource-limited settings, this can restrict access and implementation.

Another fundamental limitation is the incomplete understanding of the neurological pathways that control eye movements. In contrast to other systems, few autopsy studies have been conducted to fully define these pathways (Mayà et al. 2024). This lack of anatomical and physiological detail limits accurate interpretation and the detection of specific abnormalities. As a result, diagnosing or monitoring disease solely based on eye movement patterns remains challenging in the absence of clearly defined underlying mechanisms.

Additionally, eye movement analysis may lack sensitivity for some conditions. While it is highly effective for

certain neurological and vestibular disorders, it may not be as useful in psychiatric or cognitive conditions such as depression or anxiety, where abnormalities may be subtle or overlap with normal variation (M. Wen et al. 2022). In such cases, complementary diagnostic tools are often required.

External factors can also impact data accuracy, including lighting conditions, screen resolution, and the quality of calibration. These variables can distort results and are not always easy to standardise across clinical environments (Dorr et al. 2010; Friedman et al. 2023). Reliable results also require good patient cooperation. Distractions, limited attention, or cognitive impairments—especially in children or vulnerable populations—can reduce test accuracy (Evans et al. 2012).

Longitudinal monitoring presents additional challenges. Detecting small changes over time is difficult due to confounding variables such as ageing, medication effects, and variations in testing conditions (Pinkhardt, Kassubek et al. 2009; Temel, Visser-Vandewalle and Carpenter 2009; Sophie Rivaud-Péchoux et al. 2000). While consistent protocols are desirable, they are not always feasible, reducing the reliability of long-term tracking (Marandi and Gazerani 2019).

Different clinical sites may also employ different technologies, calibration protocols, and analysis guidelines, leading to inconsistencies in data interpretation. This lack of standardisation complicates comparison between studies or centres and limits the generalisability and reproducibility of findings. Standardised protocols are essential to establish eye movement analysis as a widely accepted diagnostic tool.

Finally, the effectiveness of eye movement analysis is also constrained by technological and software limitations. Some current systems may not differentiate between similar types of eye movements—for instance, smooth pursuits versus small saccades—or may be unable to detect very subtle movements (Komogortsev and Karpov 2013). This can lead to misclassification and imprecise measurements in contexts where high resolution and specificity are required for accurate diagnosis.

1.5 Methods for Studying and Quantifying Eye Movements

The study of ocular movements is a multidisciplinary field that employs a range of methodologies to analyse and interpret visual behaviour. Research in this area has evolved considerably over the years, incorporating advanced technologies and analytical techniques to better understand cognitive processes, visual perception, and clinical disorders. Four commonly used methods for recording eye movements are: electro-oculography (EOG), VOG, scleral search coils, and infrared oculography (IOG) (Eggert 2007). Before selecting a method for clinical or research use, key parameters such as spatial and temporal resolution, setup complexity, cost, data quality, and participant comfort must be carefully considered.

Electro-oculography: EOG measures corneo-retinal potential changes using electrodes placed around the eyes. As the eye moves, electrical dipoles shift, and the resulting deflections are captured as an electro-oculogram (Creel 2019). EOG offers a spatial resolution of approximately 1° and a temporal resolution of around 40 Hz (Timothy 2024). While the temporal resolution is adequate for measuring reaction times and fast eye movements, the low spatial resolution limits its ability to determine precise gaze locations. EOG is relatively non-invasive, cost-effective, and easy to set up, with surface electrodes requiring no head fixation or intrusive hardware (Skoglund et al. 2022). It can also be used in the dark or with eyes closed. However, EOG is prone to artifacts from facial muscle activity, blinking, and head movements, which compromises data quality and makes it unsuitable for analysing microsaccades, fixations, or slow, subtle movements (Issa and Juhasz 2019). EOG is best suited for sleep research, particularly for detecting rapid eye movements during REM sleep, and in clinical contexts where timing and direction of movement are more relevant than spatial precision (I. G. Campbell 2009).

Video-oculography: VOG is a non-invasive method that uses high-speed cameras to record horizontal and vertical eye movements by tracking features like the pupil, iris, and corneal reflections (Larrazabal, García Cena and Martínez 2019). VOG systems can achieve high spatial and temporal resolution, ranging from 20–2000 Hz, making them suitable for both cognitive research and clinical diagnostics (Timothy 2024). However, higher-resolution systems are often expensive, limiting their availability. Modern VOG systems are designed to minimise drift and maximise stability, providing accurate spatial data for analysing fixations, saccades, pursuits, and microsaccades (Mantokoudis, Otero-Millan and Gold 2022). Many systems also come with dedicated software, such as the Eyelink Toolbox, which facilitates experimental design and data

analysis (H. C. O. Li et al. 2002). VOG does have limitations: it does not function well in the dark due to reliance on corneal reflections, often requires head stabilisation (e.g., chin rests), and may be less effective for individuals with ptosis, small pupils, or excessive blinking (Wunderlich et al. 2021). Recent advances in VOG, including 3D tracking and improved tolerance to obstructions like eyelashes and eyelids, are increasing its accuracy and utility in clinical and research settings (S. C. Kim et al. 2006).

Scleral Search Coils: This method represents the gold standard for high-resolution eye tracking. It involves placing miniature coils on the eye, which generate signals through electromagnetic induction as the eye moves within a magnetic field (Robinson 1963). Scleral coils offer exceptional spatial (0.01°) and temporal (up to 2000 Hz) resolution (Timothy 2024). They are particularly suited for detecting small, high-frequency movements such as torsional saccades, and exhibit minimal drift or calibration issues, even with blinking (Stahl, Van Alphen and De Zeeuw 2000). However, the method is invasive, often requiring anaesthetic eye drops, and can sometimes cause corneal abrasions (Newman, Phillips and Cox 2022). Eyelid motion may introduce artifacts during vertical recordings, and participants must remain within a fixed magnetic field, limiting ecological validity (R. John Leigh and David S. Zee 2015a; DiScenna et al. 1995). Additionally, the equipment is costly, and setup requires expert handling and calibration time. Therefore, while ideal for high-precision ocular motor research, it is less suitable for clinical populations or large-scale studies.

Infrared Oculography: IOG uses sensors to detect differences in reflected infrared light from the cornea and sclera during eye rotation (A. Kumar and Krol 1992). Often embedded in goggles or glasses, IOG is especially effective in dark environments and provides high temporal resolution similar to advanced VOG systems (Timothy 2024). IOG is easy to set up, making it accessible for clinical and research settings. However, data quality can be affected by head movement, eyelid drooping, eyelashes, and reflections. The method also performs poorly under variable lighting conditions, requiring environmental control for optimal accuracy (Anders et al. 2004). While less expensive than scleral coils, IOG can still be costly depending on the hardware. It is most commonly used in vestibular and balance assessments (C. Anderson et al. 2013).

Emerging Technologies and Machine Learning: Modern research increasingly incorporates machine learning to classify and interpret complex eye movement data. These approaches can extract subtle features and patterns from large datasets, supporting the development of biomarkers for psychiatric and neurological

disorders such as schizophrenia (Lai et al. 2021; Vabalas et al. 2020). Furthermore, integration with other biometric modalities—such as iris recognition—offers opportunities for secure, robust identification systems in non-cooperative environments.

Each method—EOG, VOG, scleral coils, and IOG—offers distinct advantages and limitations depending on clinical or research objectives. Continued advancement in analytics and machine learning reinforces the growing potential of eye movement tracking as a sensitive and scalable tool for diagnosis and monitoring.

1.6 Thesis Aims

1. To explore ocular motor biomarkers as diagnostic and disease monitoring tools in PD and atypical Parkinsonian syndromes by evaluating eye movement metrics across multiple paradigms, including fixation, saccades, smooth pursuit, and nystagmus.
2. To establish the clinical relevance of ocular motor impairments in PD and atypical Parkinsonian syndromes through a comprehensive analysis of pharmacological and disease progression influences.
3. To explore novel insights into ocular motor control in glspd and atypical Parkinsonian syndromes by studying experimental paradigms.
4. To leverage emerging technologies and machine learning for improving diagnostic accuracy and advancing accessible tools for early detection and monitoring of PD and atypical Parkinsonian syndromes.

1.7 Chapter Summary

This chapter provides an overview of eye movements including the different functional classes, their role in visual perception and the neural substrates for each. It also covers an evaluation of the use of eye movements in clinical and research settings and discusses the different methodologies and technologies used for studying eye movements. The thesis aims to address technological and methodological challenges in using eye movements

as reliable diagnostic and disease monitoring tools by developing standardized ocular motor assessments, leveraging artificial intelligence, and integrating remote tracking technologies.

2 General Methods

This chapter describes the general methods and experimental protocols repeated within the thesis. The details of project-specific methodologies, paradigm-specific analyses, and statistics for individual projects are given within the methods section of each project.

2.1 Participant Recruitment

Participants in the studies included individuals with PD—both sporadic and genetic forms—including glucocerebrosidase (GBA) and leucine-rich repeat kinase 2 (LRRK2) mutation carriers, and individuals with atypical Parkinsonian syndromes: PSP, CBS, MSA, DLB, and unclassified atypical Parkinsonian individuals atypical parkinsonism (ATP) as well as healthy controls.

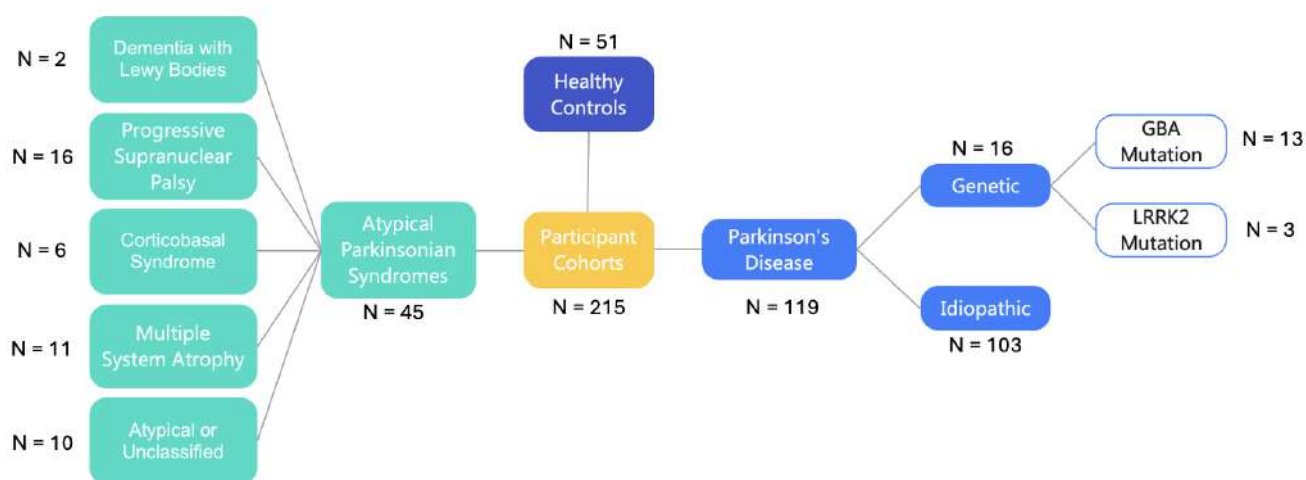


Figure 15: Classification of Participant Cohorts in the Study. Healthy controls, Parkinson’s disease (idiopathic and genetic subtypes), and atypical Parkinsonian syndromes (dementia with Lewy bodies, progressive supranuclear palsy, corticobasal syndrome, multiple system atrophy, and unclassified individuals or atypical cases). Figure by author.

PD participants were recruited through the Clinical and Movement Disorders Registry at 33 Queen Square and via the ongoing PD Frontline and Remote Assessment of Parkinsonism Supporting Ongoing Development of Interventions in Gaucher Disease (remote assessment of parkinsonism supporting ongoing development of interventions in gaucher disease (RAPSODI)) studies at university college london (UCL). The RAPSODI study is a UK-wide initiative for individuals carrying mutations in the GBA gene associated with PD. Individuals

who had previously undergone genetic testing or were suspected GBA carriers were recruited (Toffoli et al. 2023). Upon registration, participants completed an online questionnaire and were sent saliva testing kits. These samples were used for genetic testing for GBA and LRRK2 mutations. Genotyping was conducted at the National Institutes of Health/Laboratory of Neurogenetics and UCL Genomics centres using the Global Diversity Array with NeuroBooster content.

PD Frontline is a sister study to RAPSODI, in which individuals with a confirmed diagnosis of PD register via an online survey. Diagnosis was verified by the RAPSODI team using consultant letters. Individuals enrolled in both studies were contacted via email with information about the ocular motor study and were invited to participate. The initial outreach was conducted by the RAPSODI and PD Frontline teams. Interested participants received a screening questionnaire, participant information sheet, and an image of the eye-tracking setup. The screening was used to filter individuals unable to travel or follow the experimental protocol due to mobility issues.

PSP, CBS, and MSA participants were recruited through the ongoing 'Progressive Supranuclear Palsy–Corticobasal Syndrome–Multiple System Atrophy' (progressive supranuclear palsy–corticobasal syndrome–multiple system atrophy study (PROSPECT-M-UK)) study at UCL. PROSPECT-M-UK was established to assess alternative outcome measures for PSP, CBS, and MSA (Street et al. 2023). It is a multicentre observational cohort study aiming to identify diagnostic markers, monitor disease progression, and understand pathogenesis. The cohort includes defined clinical subtypes as well as indeterminate phenotypes. Recruitment sites included university college london hospital (UCLH), the Universities of Cambridge, Oxford, Manchester, Sussex, Newcastle, and Royal Gwent Hospital. Participants attending the PROSPECT-M-UK UCLH visit were invited to participate. Diagnoses were based on NINDS-SPSP (1996) and revised MDS (2017) criteria for PSP (Ali, Martin et al. 2019; Hoglinger et al. 2017), Armstrong criteria for CBS (Armstrong 2015), and Gilman criteria for MSA (Gilman et al. 2008). Individuals with unclassified phenotypes were categorised as ATP in this thesis.

Participants with DLB were recruited through consultants at the National Hospital for Neurology and Neurosurgery, using the 2017 revised International DLB Consortium criteria (M. Yamada et al. 2020). Some were referred via inpatient admissions or consultants at the National Hospital.

Healthy controls were recruited through PROSPECT-M-UK and convenience sampling. Participants from RAPSODI and PD Frontline were also asked whether family or friends were interested in participating as controls. If so, controls were assessed during the same session as the PD participant.

2.2 Ethics

Informed consent was obtained from all participants. The RAPSODI study was reviewed and approved by an independent ethics committee at Queen Square, London, on July 16th, 2015 (ref: 15/LO/155), fulfilling all legal obligations regarding use of genetic results in the ocular motor study. Participants in the PROSPECT-M-UK study also gave informed consent.

Ethics approval for all ocular motor studies within this thesis was granted by the UCL Research Ethics Committee (ref: 23/PR/1233/AM02). Consent forms adhered to the Declaration of Helsinki, and UCL was the data controller. All information was collected under GDPR and DPA 2018 regulations.

Participants received the information sheet before the study visit. The study protocol was explained beforehand, including confidentiality measures and the right to withdraw consent at any time. Consent was digitally recorded and securely stored. Each participant was assigned a study code under which their data was anonymised and stored.

2.3 Data Collection and Storage

Consent forms were stored on the NHS drive. Demographic data, medical history, and questionnaire responses were recorded in Excel sheets on the UCL drive. Eye-tracking data was stored on the display computer and then transferred to the UCL drive. All data was secured with password protection and two-factor authentication.

2.4 Eye Tracking

2.4.1 Comparative Analysis for Eye Tracker Selection

The EyeLink 1000 Plus was selected as the primary eye tracker for this thesis following a pilot study comparing the usability and reliability of several systems.

Devices tested included the EyeLink 1000 Plus (SR Research n.d.), Cyclops Eye Tracker (Cyclops Medtech Pvt Ltd n.d.), EyeBrain T2[®] Video Eye Tracker (Suricog n.d.), and Tobii Pro Nano (tobii n.d.). Each system was assessed based on hardware (sampling rate, camera, processor, eye-tracking system), software (paradigm design and analysis), output quality (measures, preprocessing needs), participant usability, and overall advantages and limitations.

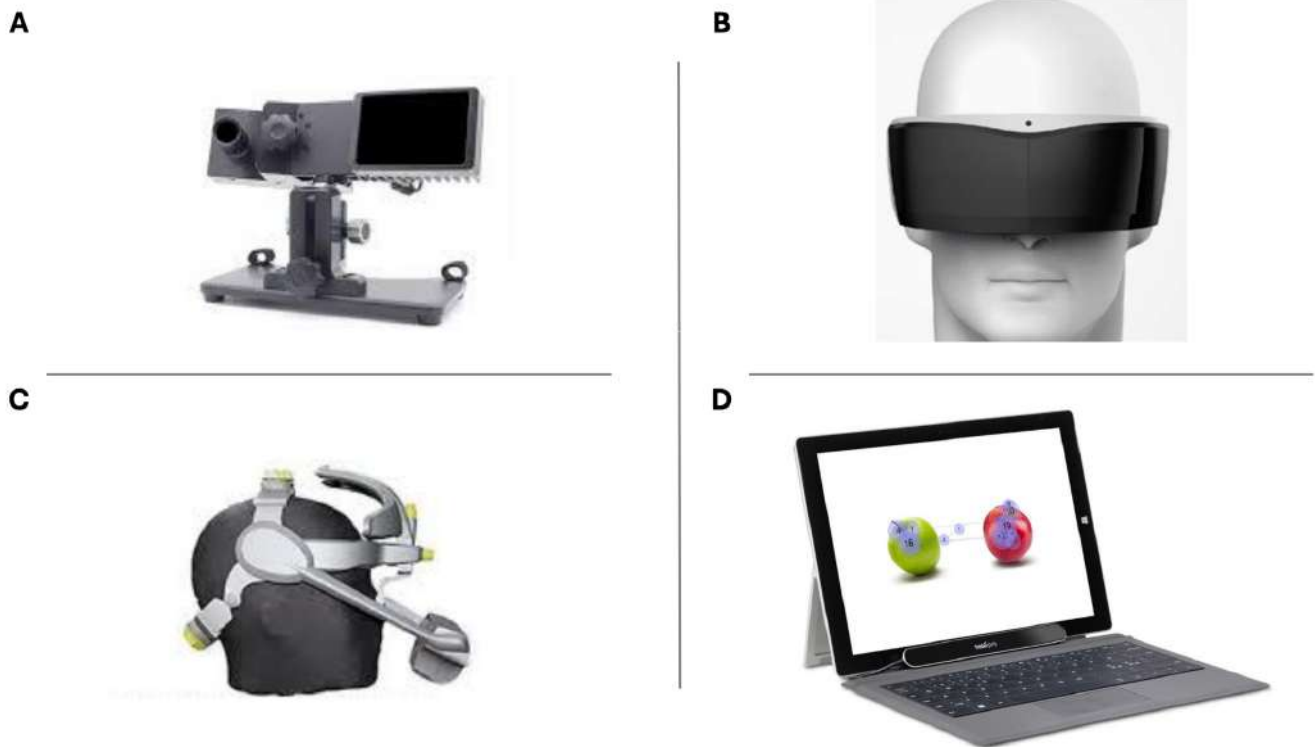


Figure 16: Eye tracking Systems Evaluated. (A) EyeLink 1000 Plus – a high-precision, desktop-mounted system; (B) Cyclops Eye Tracker – a virtual reality (VR) based head-mounted eye tracker; (C) EyeBrain T2 – a head-mounted system used for neurophysiological research; (D) Tobii Pro Nano – a compact, screen-based eye tracker designed for natural viewing conditions. Figure by author.

Evaluation Criteria	Eyelink 1000 Plus	Cyclops Eye Tracker	EyeBrain T2	Tobii Pro Nano
Sampling Rate (Hz)	Up to 2000	Up to 600	Up to 600	Up to 60
Camera Quality	High-resolution infrared camera	Infrared camera with moderate resolution	Infrared camera with moderate resolution	Infrared camera with lower resolution
Processor	Dedicated FPGA-based processing	Built-in processor for real-time tracking	Built-in processor for real-time tracking	No dedicated processor, USB connection
Eye Tracking System	Video-based pupil and corneal reflection tracking	Video-based tracking	Video-based tracking	Video-based tracking
Preprocessing Required	Minimal	Moderate	Moderate	Higher
Ease of Use for Participants	Requires chin rest, can be restrictive	Head-free tracking, relatively comfortable	Head-free tracking, relatively comfortable	Highly portable, least restrictive
Advantages	High sampling rate, precise tracking, widely used in research	Compact design, real-time tracking, cost-effective	Good balance between precision and ease of use	Highly portable, user-friendly, cost-effective
Disadvantages	Requires chin rest, costly, setup complexity	Lower sampling rate than Eyelink, software limitations	Lower sampling rate than Eyelink, software constraints	Lower sampling rate, less precise tracking

Table 1: Comparative analysis of four eye trackers: Eyelink 1000 Plus, Cyclops Eye Tracker, EyeBrain T2, and Tobii Pro Nano based on various technical and usability aspects.

Projects 1-6 utilised the same EyeLink 1000 Plus setup. If the standard ocular motor battery was not used in a given project, the specific paradigms and analyses used are described within the respective project's methods section.

2.4.2 Eye Tracker Setup

The EyeLink 1000 Plus is a desktop-mounted eye tracker that supports both head-stabilised and remote (head-free) modes. As many participants in these studies were unable to hold their head stable throughout testing, the head-stabilised mode was selected. In this mode, the eye tracker has a sampling rate of 2000 Hz for both monocular and binocular recordings and an accuracy of 0.15° – 0.50° . The resolution, calculated through root mean square (RMS), is 0.01° and 0.05° for microsaccades. A 35 mm lens was used.

The EyeLink is connected to a host PC and a display PC via Ethernet cables. The host PC is operated by the researcher for participant setup and monitoring of parameters and performance during testing. It also performs real-time detection of saccades, fixations, and blinks. The display PC presents visual stimuli for all tasks and is used to set parameters prior to recording. All data files generated during each paradigm are stored on the display PC.

A Dell monitor (U2312HMT 23" VGA DVI-D DisplayPort USB 2.0 Hub HDCP) was used as the display screen. It has a display area of 509.2 mm (width) by 286.4 mm (height), with a resolution of 1920 x 1080 pixels and a refresh rate of 60 Hz. The display was positioned 850 mm from the participant's eyes (approximately 1.65 times the screen width), and the eye tracker was placed 550 mm from the chin rest of the headrest. These placements followed SR Research's guidelines for optimising the trackable range of the EyeLink 1000 Plus: 32° horizontally and 25° vertically. The camera of the eye tracker was aligned to the centre of the screen.

Eye tracking was conducted in a dark room with blackout curtains and no background light. The eye tracker was mounted on a custom-built table, which accommodated participants in wheelchairs who could not transfer to the designated seat, allowing them to complete the tasks in their own chairs.



Figure 17: The EyeLink 1000 Plus in Head-stabilized Mode. The system comprises a host PC for participant setup, real-time detection and a display PC for stimulus presentation and data storage. Figure by author.

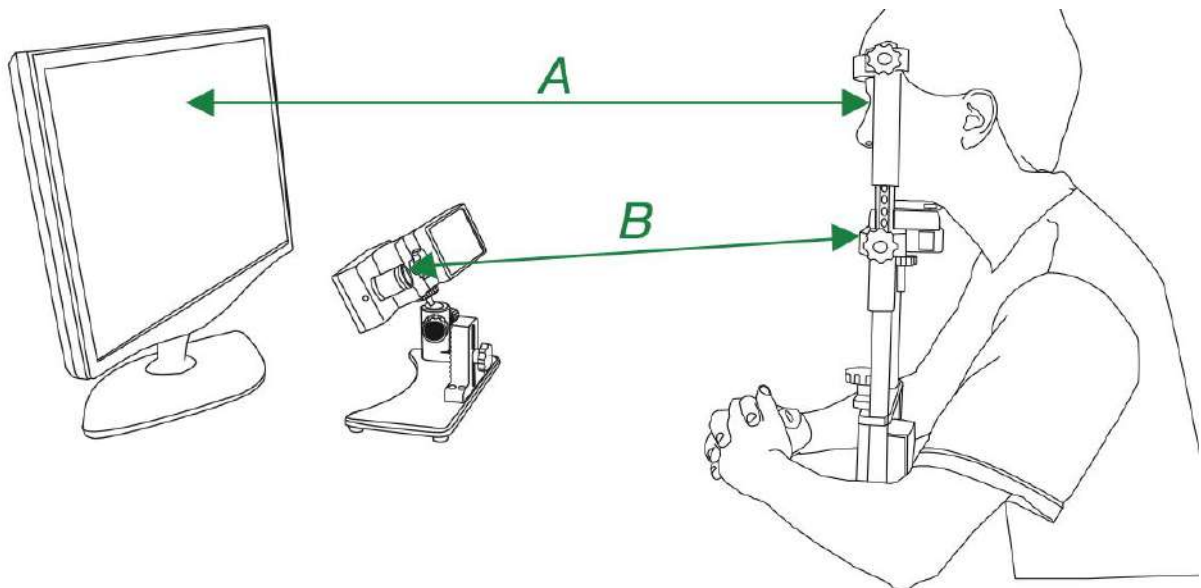


Figure 18: Schematic Illustration of the Eye Tracking Setup. Display PC positioned 850mm (A) from the participant's eyes and EyeLink 1000 Plus eye tracker was placed 550mm (B) from the chin rest, ensuring a trackable range of 32° horizontally and 25° vertically, following SR Research guidelines. Figure by author.

2.4.3 Participant Setup

Participants were seated on a height-adjustable chair, and their chin was positioned on the chin rest. The height was adjusted so that the participants' eyes were aligned with the top 25% of the monitor, and the eye tracker was placed as close as possible to the bottom of the screen—covering the logo but not obstructing the view of the monitor.

The camera position was adjusted so that the participant's head was centred on the host PC screen, with the central symmetry line aligned through the middle of the participant's nose and both eyes positioned roughly equidistant on either side. Red boxes were placed around each eye. The lens focus was adjusted to minimise corneal reflection, indicated by a light blue circle. The pupil threshold was calibrated to cover the maximum area of the pupil without including other parts of the eye, and was maintained above 75. The corneal reflection threshold was further adjusted to reduce the light blue circle near the eyes, with the threshold consistently set between 200 and 240.

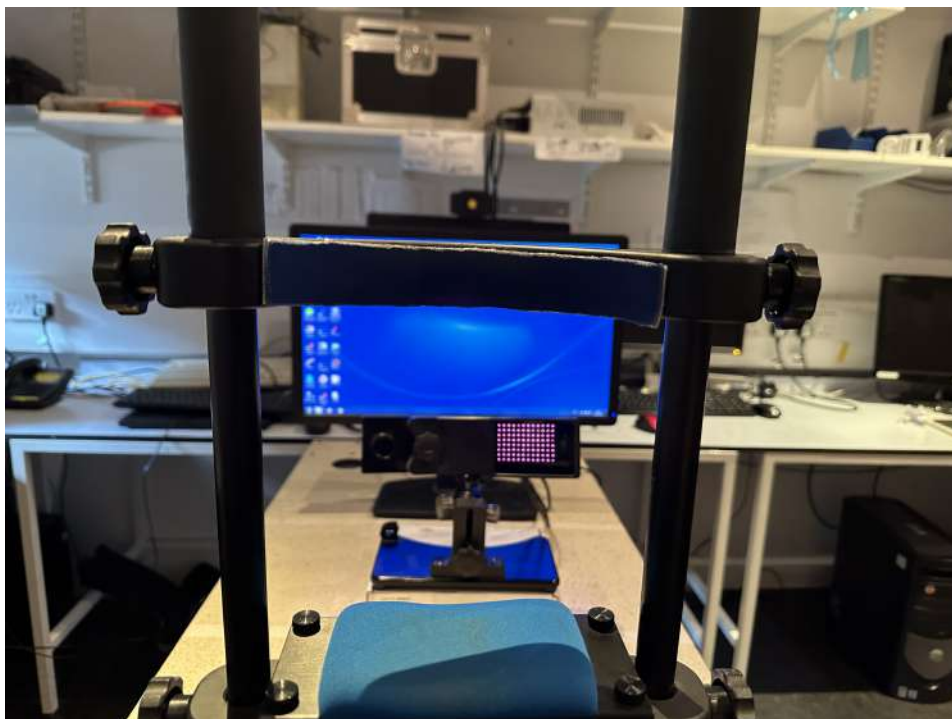


Figure 19: Participant Positioning for Eye Tracking. *The chair height was adjusted to align their eyes with the top 25% of the monitor and the eye tracker was positioned as high as possible beneath the screen, covering the logo but not obstructing the bottom of the display. Figure by author.*

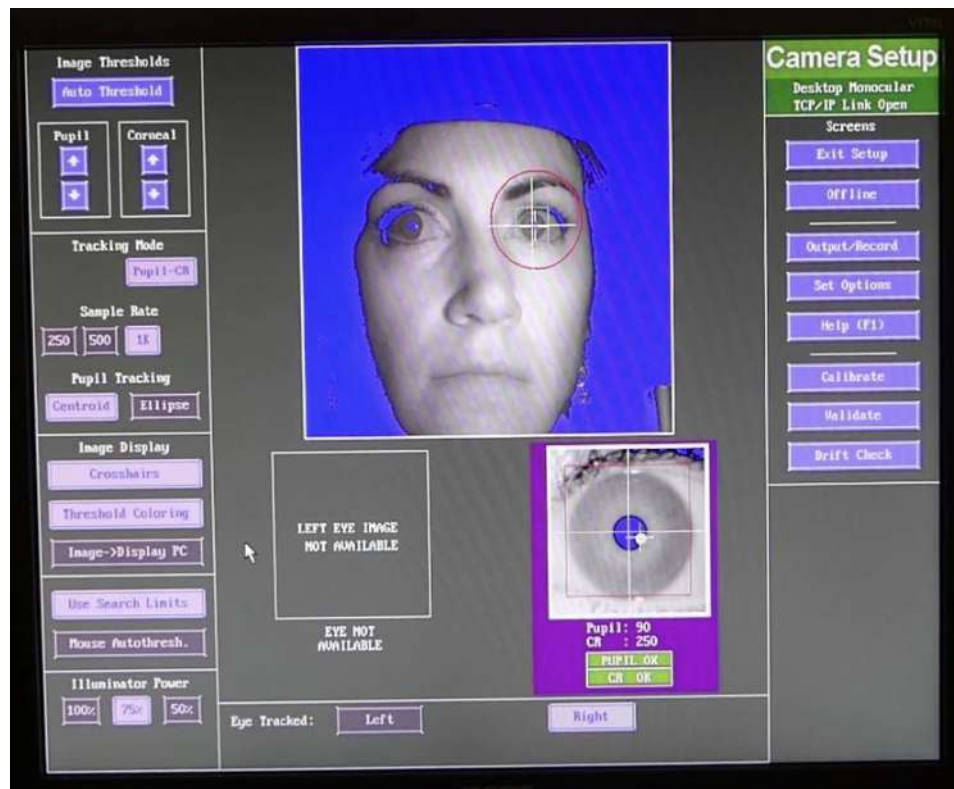


Figure 20: EyeLink 1000 Plus Camera Setup Interface for Monocular Eye Tracking. *The system detects and tracks the pupil using centroid and corneal reflection methods. Figure by author.*

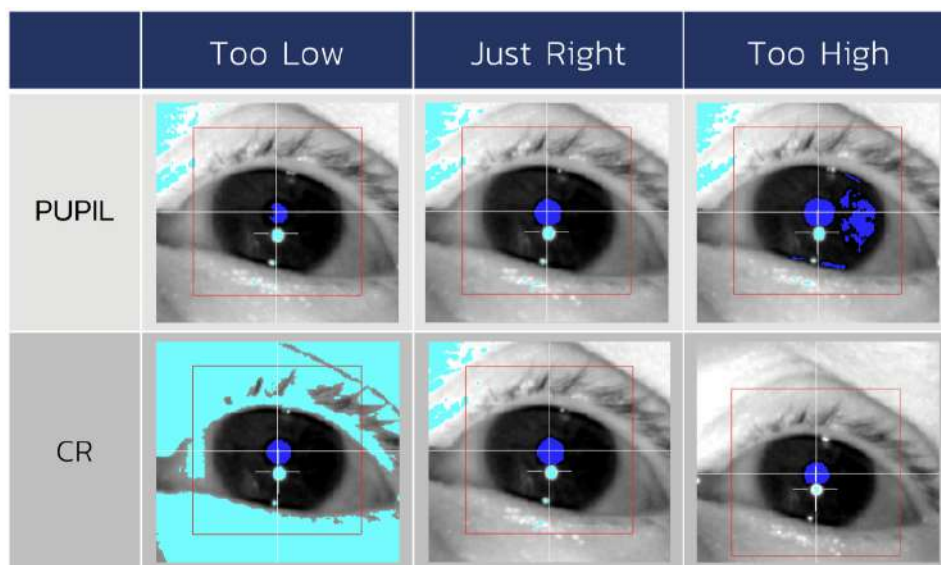


Figure 21: Illustration of Pupil and Corneal Reflection Alignment in the EyeLink 1000 Plus System. The three columns represent incorrect (too low, too high) and correct (just right) eye positioning. Figure by author.

After the setup was completed, a manual 5-point calibration was performed, where participants were instructed to fixate on the centre of a target until it moved position. Calibration was deemed successful if a symmetrical crosshair or grid pattern was achieved. If the grid was asymmetrical or even a single point

deviated, calibration was repeated. Upon successful calibration, a 5-point validation was carried out using the same targets, with the two worst-performing points sampled again. Validation assessed the deviation error from the calibration at each point. It was considered successful if the average error was less than 0.5 and the maximum error was less than 1.0. For participants who, due to their condition, were unable to maintain accurate fixation, the average error threshold was increased to 0.75 while the maximum remained at 1.0. Once both calibration and validation were successfully completed, the paradigm was initiated. Calibration and validation were conducted on a white background with a black target featuring a smaller white circle at its centre—preset settings provided by SR Research.

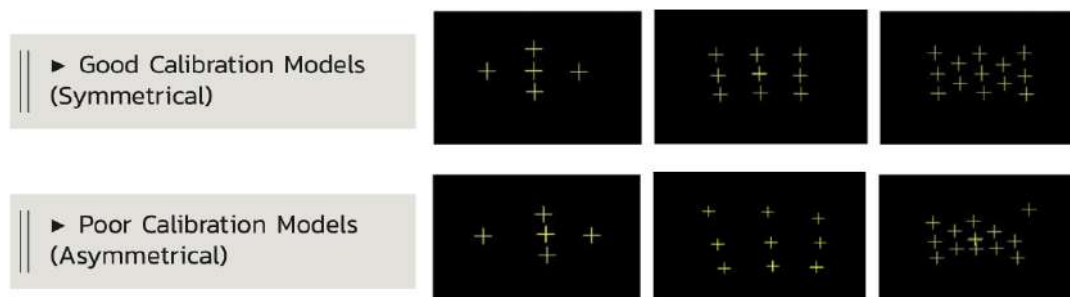


Figure 22: Calibration Models in the EyeLink 1000 Plus System. *Good, symmetrical and poor, asymmetrical calibration models. Figure by author.*



Figure 23: Validation Screen from the EyeLink 1000 Plus System. Recorded gaze positions and error values; the system calculates the average and maximum error, ensuring calibration accuracy before proceeding with data collection. Figure by author.

If the participant wore glasses, their ability to view a central stationary target on the screen was first assessed. If they were able to see the target clearly, they were encouraged to continue the paradigms without glasses, as reflections from the lenses could cause signal loss. However, if the participant could not see the target clearly without glasses, the setup was adjusted accordingly. To minimise reflections, the angle of the head was adjusted so that reflections were reduced when the participant looked at all four corners of the screen. If pupil thresholds were too low, the illuminator power was increased to 100% or the camera was brought closer. Another common issue was with participants who had very large pupils or whose eyelids obstructed the top or bottom of the pupil. In such cases, the pupil tracking mode was switched from centroid to ellipse.

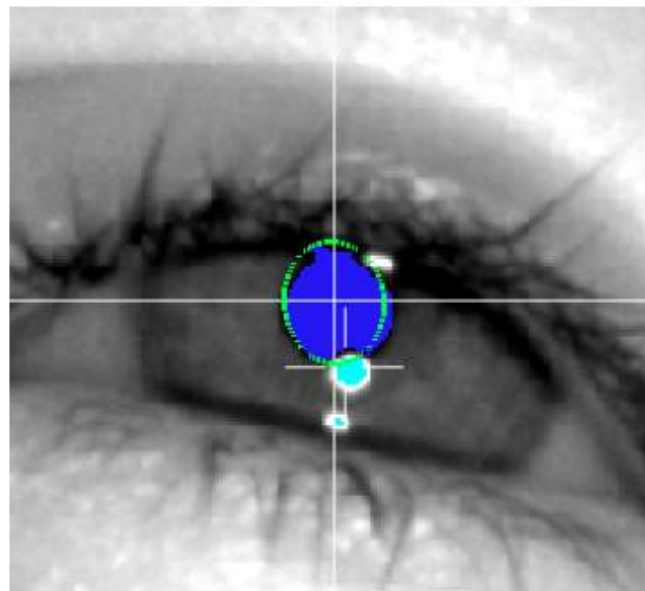


Figure 24: Centroid Tracking Mode. If signal loss occurred due to glasses, participants were advised to remove them unless necessary; adjustments included modifying head position to minimize glare, increasing the illuminator power to 100%, or bringing the camera closer. For large pupils or obstructed eyelids, the tracking mode was switched from centroid to ellipse. Figure by author.

At the start of every paradigm, a drift check was performed using a central fixation point to assess any deviation of the eyes from the calibration. If the deviation was below 2, the drift check was deemed successful and the paradigm started automatically. If the deviation exceeded 2, the drift check failed, and calibration and validation were repeated before proceeding with data collection. In longer paradigms or those with multiple parts, a drift check was also performed before each individual part.

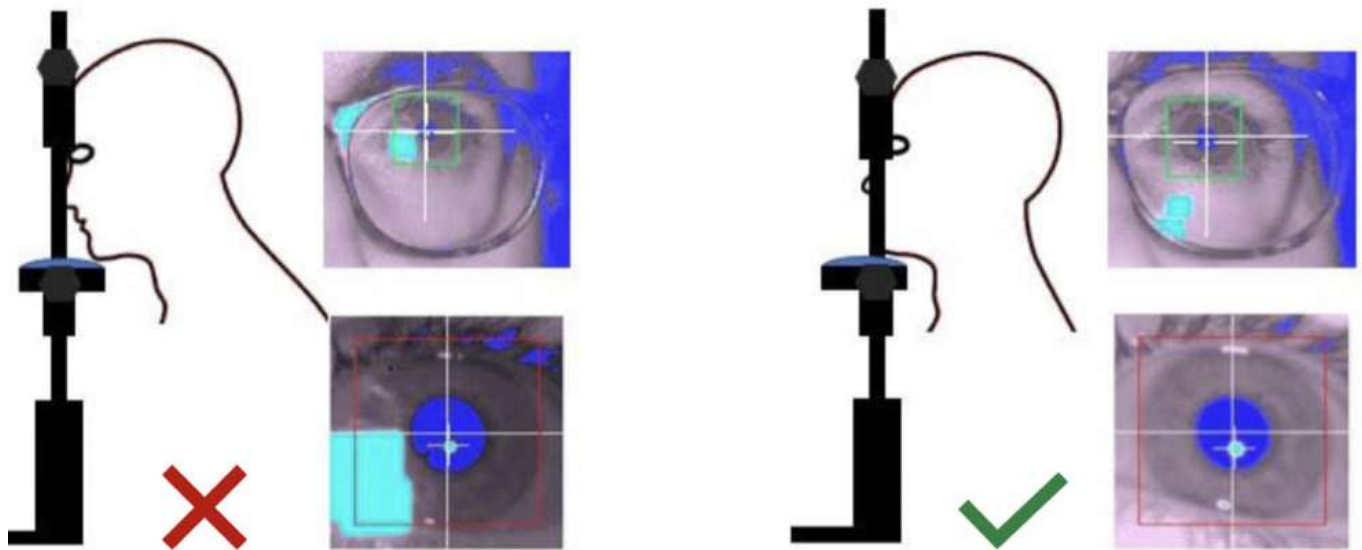


Figure 25: Illustration of Correct and Incorrect Participant Positioning for Optimal Eye Tracking. When glasses were worn, the head angle was adjusted to reduce reflections, ensuring visibility in all four corners of the screen; proper alignment improved signal detection and minimized tracking errors.

Participants were given periodic breaks between paradigms and, when necessary, within paradigms to ensure they remained as attentive as possible during the recordings. Once data collection was complete, the chin rest and equipment were sanitised and prepared for the next participant.

2.5 Quality Control of Data Collection

As eye tracking data is inherently noisy, specific measures were taken during data collection to maximise quality, accuracy, and precision—beyond the technical specifications of the eye tracker.

Data quality was periodically monitored using accuracy and precision metrics. Accuracy was defined as the angular distance between the average x and y location within a fixation and the target's predefined x and y coordinates. Precision was calculated either as the standard deviation of the x and y positions (in degrees of visual angle) or the RMS of the angular distance between samples. Samples with low accuracy or poor precision were either re-recorded or excluded from the analysis. Blinks, while inevitable, were accounted for during analysis.

If participants took a break between paradigms, a drift check was conducted before restarting to ensure the

calibration and validation remained valid. If the drift check failed, calibration and validation were repeated. The EyeLink is designed such that calibration remains valid throughout a session if the setup—including the headrest, camera, and monitor—remains unchanged. However, if adjustments were made due to participant discomfort or accidental movement of the equipment, calibration and validation were repeated.

2.6 Ocular Motor Battery

Paradigms were initially selected and designed to emulate clinical eye movement assessments. As a result, basic forms of all paradigms can also be performed at the bedside. All paradigms used a black background with a green dot target, selected for its high contrast without causing visual discomfort (Baik et al. 2013). The target size was 1° (31 pixels, calculated based on the screen dimensions and participant distance) (Nieboer et al. 2023). Target positions on the screen were determined by converting degrees of visual angle into pixel coordinates. The centre of the screen was defined as 960 (x-axis), 540 (y-axis).

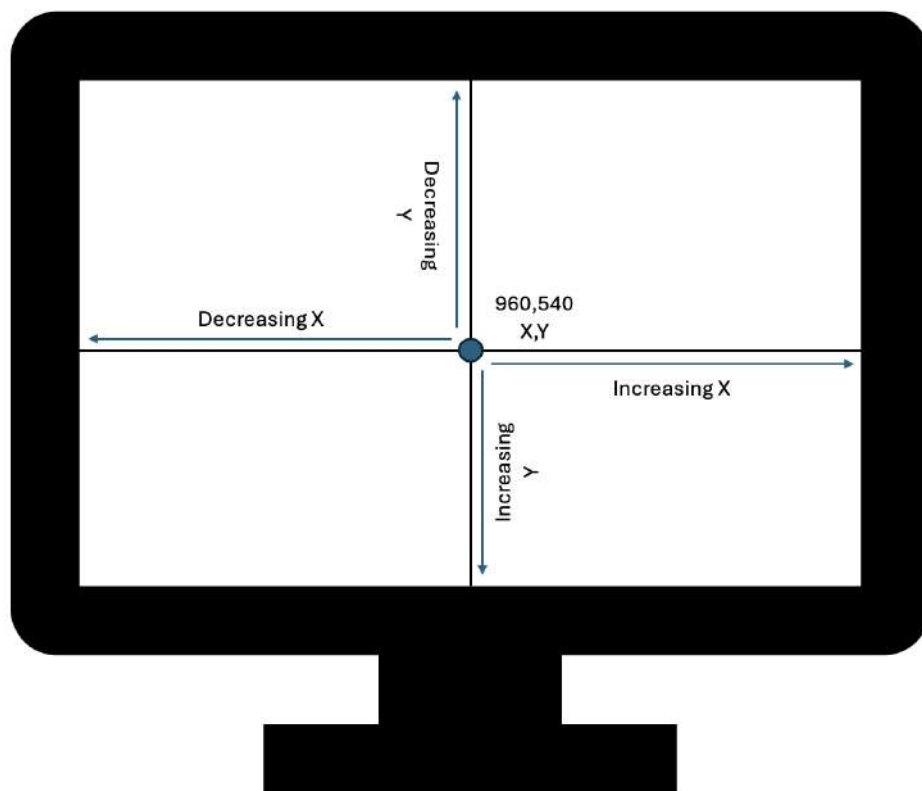


Figure 26: Screen Coordinate System. The centre of the screen is defined at (960, 540) in pixel coordinates; the x-axis increases to the right and decreases to the left, while the y-axis increases downward and decreases upward. Figure by author.

Eight types of paradigms were included in the ocular motor battery, the details of which are given below. A schematic of all paradigms accompanies the descriptions. All paradigms were designed using Experiment Builder, a software developed by SR Research.

Central Fixation: A central stationary target was displayed at the centre of the screen (960, 540) for 30 seconds. Participants were instructed to fixate on the middle of the target with minimal blinking. There was only one trial for this condition (total duration: 30 seconds).



Figure 27: Central Fixation Paradigm. A central stationary target was displayed at the centre of the screen (960, 540) for 30 seconds.

Positional Fixation/ Nystagmus: Four stationary targets were displayed at positions corresponding to $+10^\circ$ (960, 41) and -10° (960, 1039) vertically, and $+15^\circ$ (1718, 540) and -15° (202, 540) horizontally. Each target was presented for 30 seconds. Participants were instructed to fixate on the centre of each target with minimal blinking. There were four trials in total, with a combined duration of 120 seconds.

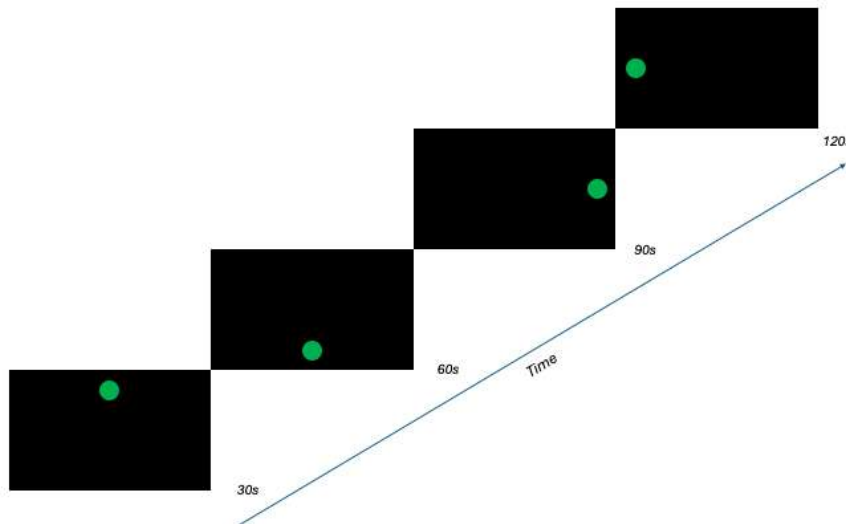


Figure 28: Positional Fixation/ Nystagmus Paradigm. Four stationary targets were displayed at positions corresponding to $+10^\circ$ (960, 41) and -10° (960, 1039) vertically, and $+15^\circ$ (1718, 540) and -15° (202, 540) horizontally. Each target was presented for 30 seconds.

Pursuit: Three types of pursuit were assessed—horizontal, vertical, and elliptical—with 2, 2, and 4 trials respectively. In horizontal pursuit, the target moved between $+15^\circ$ (1718, 540) and -15° (202, 540) at speeds of 0.2 Hz and 0.4 Hz for 20 seconds each. In vertical pursuit, the target moved between $+10^\circ$ (960, 41) and -10° (960, 1039) at the same speeds and durations. For elliptical pursuit, the target moved in a 10° radius from the centre of the screen, in both clockwise and anticlockwise directions, also at 0.2 Hz and 0.4 Hz for 20 seconds each. Participants were instructed to continuously follow the moving target. There were eight trials in total, with a combined duration of 160 seconds.

Antisaccades: Saccades directed in the opposite direction to the target stimulus were tested in both horizontal and vertical directions. In the horizontal condition, 20 trials were presented in a randomised order (10 at $+15^\circ$ and 10 at -15°). In the vertical condition, another 20 randomised trials were presented (10 at $+10^\circ$ and 10 at -10°). Participants were informed that the target would appear either left/right or up/down and were instructed to look in the opposite direction of the target. Each trial lasted 2 seconds, resulting in a total paradigm duration of 80 seconds.

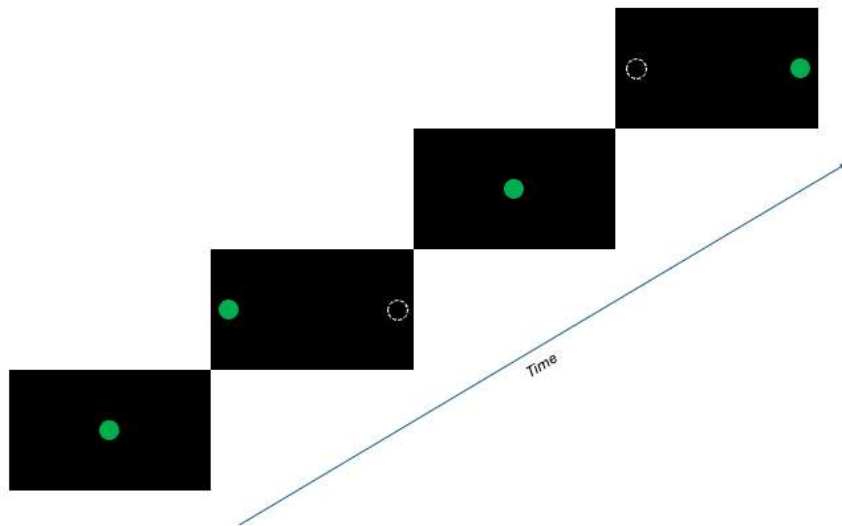


Figure 29: Antisaccades Horizontal Paradigm. In the horizontal condition, 20 trials were presented in a randomised order (10 at $+15^\circ$ and 10 at -15°).

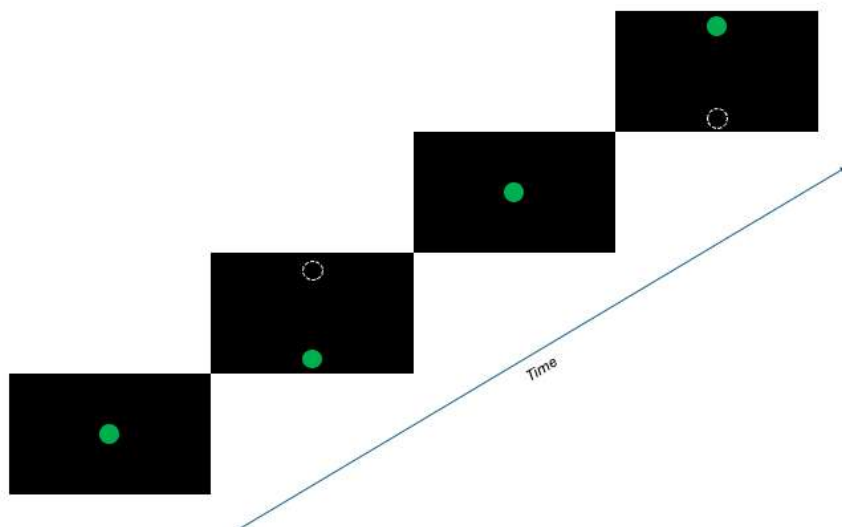


Figure 30: Antisaccades Vertical Paradigm. In the vertical condition, another 20 randomised trials were presented (10 at $+10^\circ$ and 10 at -10°).

Oblique Saccades: There were three blocks of oblique saccades at 4° , 8° , and 10° , each consisting of 30 trials. Within each block, twelve target positions were defined along the circumference of a circle centred on the screen. Targets were presented diagonally from the centre in a randomised order. Participants were instructed to follow the targets. Each trial lasted 2 seconds, resulting in a total paradigm duration of 180 seconds.

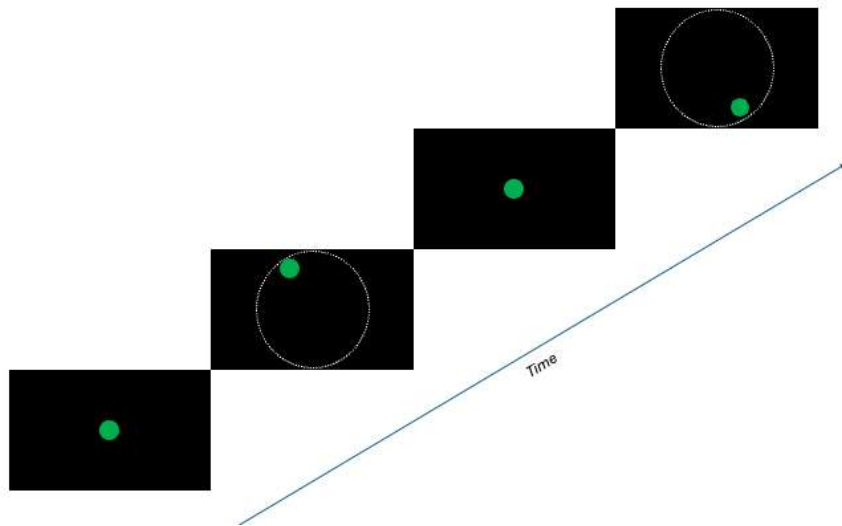


Figure 31: Oblique Saccades Paradigm. There were three blocks of oblique saccades at 4° , 8° , and 10° , each consisting of 30 trials.

Reflexive Saccades: Reflexive saccades to novel stimuli were assessed in both horizontal and vertical directions, with 30 trials in each. In the horizontal condition, targets appeared at $+15^\circ$ and -15° from the centre of the screen; in the vertical condition, targets appeared at $+10^\circ$ and -10° . Target presentation was randomised. Participants were instructed to follow the targets as they appeared. Each trial lasted 2 seconds, resulting in a total paradigm duration of 120 seconds.

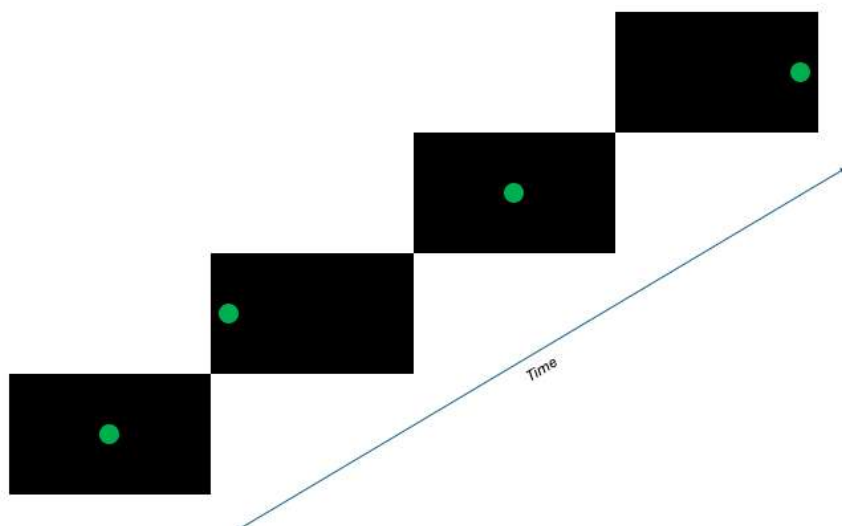


Figure 32: Reflexive Saccades Horizontal Paradigm. In the horizontal condition, targets appeared at $+15^\circ$ and -15° from the centre of the screen.

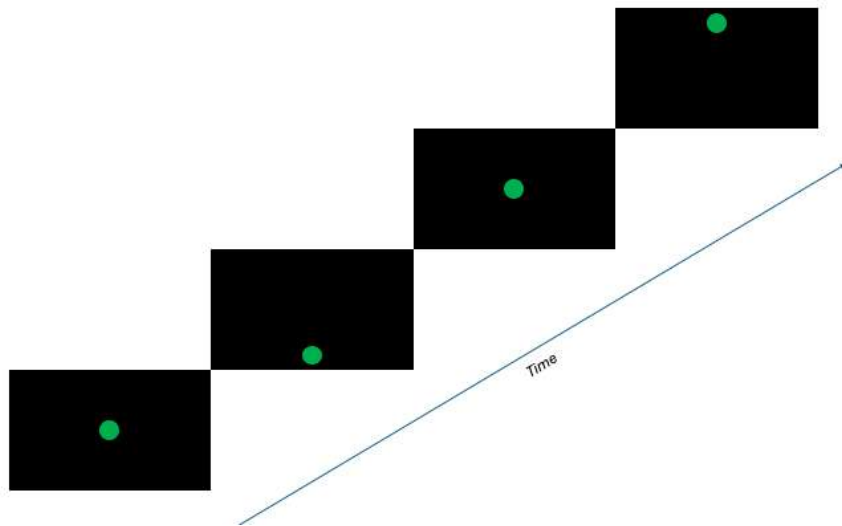


Figure 33: Reflexive Saccades Vertical Paradigm. In the vertical condition, targets appeared at $+10^\circ$ and -10° .

Volitional Saccades: Volitional saccades were tested in both horizontal and vertical directions. In the horizontal condition, two stationary targets were positioned at $+15^\circ$ and -15° from the centre of the screen; in the vertical condition, targets were placed at $+10^\circ$ and -10° . Participants were instructed to move their eyes between the two targets at their own pace. Each condition lasted 60 seconds and consisted of a single trial, resulting in a total duration of 120 seconds.

Memory Guided Saccades: Memory-guided saccades followed the volitional saccades paradigm in both horizontal and vertical directions. A blank black screen was presented, and participants were instructed to remember the positions of the targets from the volitional paradigm and replicate the same movements, shifting their gaze between the remembered target locations. Each condition lasted 60 seconds and consisted of a single trial, resulting in a total duration of 120 seconds.

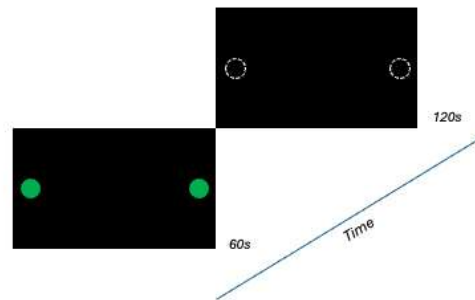


Figure 34: Volitional and Memory Guided Saccades Horizontal Paradigm. In the horizontal condition, two stationary targets were positioned at $+15^\circ$ and -15° from the centre of the screen.

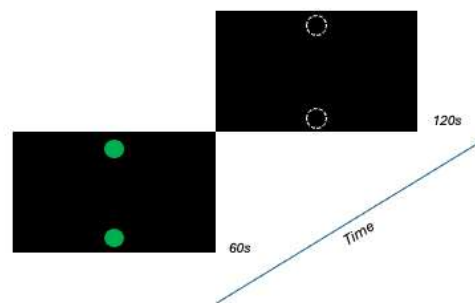


Figure 35: Volitional and Memory Guided Saccades Vertical Paradigm. In the vertical condition, targets were placed at $+10^\circ$ and -10° .

The entire ocular motor battery had a total duration of approximately 16 minutes. Periodic breaks were provided between paradigms and, where needed, within paradigms. Refreshments were also offered to ensure participant comfort and sustained attention.

2.7 Data Processing and Analysis

The saved files from each paradigm (EDF files) were imported into DataViewer, an analysis software from SR Research. Key metrics were extracted in the form of reports for each paradigm, and further analysis was

conducted using Python 3 and RStudio. Detailed analyses for each paradigm are described below.

Fixation: A fixation report was generated in DataViewer for each participant, containing metrics such as pupil size, precision measured using RMS, and precision using standard deviation (SD). It is important to note that an increase in fixation precision values measured by RMS and SD indicates worsened precision or increased deviation in the gaze position. These metrics were calculated for each fixation duration—defined as the period between two blinks—and then a weighted average based on the duration of the fixation was calculated per participant.

Microsaccades: Defined as saccades with an amplitude less than 1° (R. John Leigh and David S. Zee 2015a). Analysis was performed using a modified R script based on Engbert et al. (2015) (Engbert, Trukenbrod et al. 2015; Engbert and Kliegl 2003). The original script used binocular data, but as only monocular data were collected, the script was adapted accordingly. Binocular tracking typically reduces background noise; therefore, an alternative parsing mechanism by applying a low pass Savitzky-Golay filter, was implemented to minimise this in monocular data (Dai et al. 2017). Sample reports containing left and right X/Y gaze data were created in DataViewer and fed into the modified R script, which produced output with the start time, end time, duration, peak velocity, distance, amplitude, and orientation of each microsaccade.

The square wave jerk (SWJ) and saccadic intrusions were analysed using a saccade report generated in DataViewer for each participant, which included amplitude, start time, and direction. A thresholding method was applied to identify the following:

Small Square Wave Jerks: Defined as a saccade moving away from the central fixation point followed by a return saccade of similar amplitude, with less than 0.75° difference, occurring within 300ms (R. John Leigh and David S. Zee 2015a). The amplitude of the initial saccade had to be less than 2° .

Large Square Wave Jerks: Defined as a saccade with amplitudes between $2-6^\circ$, moving away from the central fixation point followed by a return saccade of similar amplitude, than 0.75° difference, occurring within 300 ms (R. John Leigh and David S. Zee 2015a).

Intrusive Saccades: Saccades greater than 2° . Metrics such as count, average amplitude, and start time were computed per participant (R. John Leigh and David S. Zee 2015a; Bylsma et al. 1995).

Nystagmus: The analysis followed the same pipeline as fixation, treating each target position (left, right, up, down) as a distinct fixation point. Fixation, sample, and saccade reports were generated for each trial and analysed individually.

Pursuit: A modified SR Research algorithm was used to compute pursuit gain and root mean squared error (RMSE) gaze—a proxy for pursuit accuracy—for each trial and participant. Pursuit was analysed as a series of fixations. Saccadic components were analysed by generating a saccade report with details on all saccades. Metrics such as count, start time, amplitude, and velocity were computed for each saccade in all pursuit directions (horizontal, vertical, elliptical).

For the analysis of saccades, saccadic latency was defined as the time (in milliseconds) from target appearance to the onset of the first saccade. Peak velocity was the maximum velocity reached during the saccade, and average velocity was the weighted mean velocity. Amplitude referred to the angular distance covered by the saccade.

Antisaccades: A saccade report with metrics including saccade start time, end time, amplitude, average velocity, and peak velocity was generated per participant. If multiple saccades were present within a single trial index, the saccade with the largest amplitude was selected for analysis. One saccade was retained per trial, and excluded saccades were manually reviewed to minimise data loss. Average values were computed per participant. Saccades made in the same direction as the target were considered errors. If a saccade in the target's direction was followed by a corrective saccade in the opposite direction, it was classified as a self-correcting error. Both error types were counted. This analysis was conducted for both horizontal and vertical tasks.

Reflexive Saccades: A saccade report with metrics including start time, end time, amplitude, average velocity, peak velocity, and end position (X or Y) was generated per participant. If multiple saccades were present within a trial, the one with the largest amplitude was retained. One saccade per trial was analysed, with

discarded saccades reviewed to ensure minimal data loss. The difference between the target's position and the saccade end position defined saccade accuracy. It is important to note that an increase in the accuracy measure indicates greater deviation of gaze from the target position and decreased accuracy. A deviation of less than 10% of the intended saccadic amplitude (e.g. 1° for a 10° target) was considered accurate (R. John Leigh and David S. Zee 2015a). Greater deviations were classified as hypometric (undershoot) or hypermetric (overshoot). All analyses were performed for horizontal and vertical directions.

Volitional Saccades: A saccade report with metrics including saccade start time, end time, amplitude, average velocity, peak velocity, and end position (X or Y) was generated per participant. A complete saccade was defined as a movement in one direction (left/right or up/down) followed by a saccade in the opposite direction. Multiple consecutive saccades in the same direction with small amplitudes were counted as one, and a weighted average of the metrics was calculated based on saccade amplitude. The total number of complete saccades and their average metrics were computed for each participant. Saccade accuracy was defined as the difference between the target position and the saccade end position. If this deviation was less than 10% of the intended saccadic amplitude, the saccade was classified as correct (R. John Leigh and David S. Zee 2015a). Deviations greater than 10% were classified as hypometric (undershoot) or hypermetric (overshoot). This analysis was conducted for both horizontal and vertical tasks.

Memory Guided Saccades: This analysis followed the same procedure as for volitional saccades. A complete saccade was counted as a movement in one direction followed by one in the opposite direction. If multiple small-amplitude saccades occurred in the same direction, they were combined and averaged using a weighted approach. Accuracy was assessed using the same criteria: a deviation of less than 10% of the intended saccadic amplitude was classified as correct; otherwise, the saccade was labelled hypometric or hypermetric (R. John Leigh and David S. Zee 2015a). Separate analyses were performed for horizontal and vertical tasks.

Oblique Saccades: A saccade report containing start time, end time, amplitude, average velocity, peak velocity, and both X and Y end positions was generated for each participant. The saccade with the greatest amplitude within each trial index was retained. Accuracy was assessed by constructing a circular boundary around the intended endpoint, with a 10% margin (R. John Leigh and David S. Zee 2015a). Endpoints falling within this boundary were classified as correct. Those outside the boundary were classified as hypometric

(towards the screen centre) or hypermetric (away from the centre). Analyses were performed separately for 4°, 8°, and 10° oblique saccades.

2.8 Chapter Summary

This chapter outlines the general methods and experimental protocols used throughout the thesis. While specific methodologies and analyses for each project are detailed within individual sections, this chapter provides a comprehensive overview of participant recruitment, ethical considerations, data collection, eye tracking methodologies, and data processing approaches.

3 Ocular Motor Function in Parkinson's Disease

3.1 Introduction

Parkinson's disease (PD) is a complex neurodegenerative disorder, primarily characterised by the progressive loss of dopaminergic neurons in the substantia nigra (SN). This degeneration leads to a range of clinical symptoms, including both motor and non-motor features. Motor symptoms comprise bradykinesia, rigidity, and tremors, while non-motor symptoms include neuropsychiatric conditions, autonomic disturbances, and sleep disorders (Jankovic 2008; Blochberger and S. Jones 2011). Multiple molecular pathways contribute to the pathophysiology of PD, reflecting a combination of genetic and sporadic aetiologies.

Genetic forms of PD often involve specific mutations in key genes. Notably, mutations in the *synuclein alpha* (*SNCA*) gene—which encodes the protein alpha-synuclein—are associated with inherited forms of PD, particularly those following an autosomal dominant pattern. Among these, the *A30P*, *A53T*, and *E46K* gene mutations are the most frequently reported in familial cases (Hoffman-Zacharska et al. 2013). Additionally, mutations in the *LRRK2* gene (*PARK8*) represent the most common genetic cause of PD, accounting for approximately 5–6% of hereditary cases and also serving as a major risk factor in sporadic PD (Deyaert et al. 2017). Another significant genetic contributor is the *GBA* gene, which is also implicated in Gaucher disease and is now established as a major risk factor for PD, although it exhibits variable penetrance across different populations (Vieira and Schapira 2022). Furthermore, recessive mutations in genes such as *PINK1* and *parkin* lead to early-onset forms of PD, highlighting the genetic heterogeneity of the disorder (Narendra et al. 2010).

In contrast, sporadic PD, also referred to as idiopathic PD, accounts for approximately 90–95% of all cases and typically presents without an identifiable genetic cause (Chai and Lim 2014). However, recent findings suggest that even sporadic cases may involve genetic predispositions. For instance, genome-wide association studies have identified common genetic variants associated with increased alpha-synuclein expression, thereby implicating genetic contributions in ostensibly non-genetic forms of the disease (Nussbaum 2017). Environmental factors, ageing, and lifestyle further interact with these genetic elements, contributing to the complex aetiology of sporadic PD (Pang et al. 2019).

3.1.1 Parkinson's Disease Pathology

The pathophysiology of PD is driven by the death of dopaminergic neurons within the pars compacta of the SN, which triggers a cascade of neurobiological alterations. This neurodegeneration leads to a reduction in dopaminergic inputs into the striatum (STR). Dopamine is a neurotransmitter crucial for maintaining proper motor function, and its loss underlies the cardinal motor symptoms of PD: bradykinesia, rigidity, tremor, and postural instability (Blesa, Phani et al. 2012; Campos-Acuña, Elgueta and Pacheco 2019; Sackner-Bernstein 2021). The degeneration of dopaminergic neurons is frequently associated with the presence of Lewy bodies—aggregates of alpha-synuclein—a protein considered central to the neurodegenerative mechanism (Elgueta et al. 2022; Limphaibool et al. 2019).

A major contributor to the pathophysiological processes implicated in PD is oxidative stress, characterised by an imbalance between reactive oxygen species (ROS) production and the cellular antioxidant defence system. The deterioration of dopaminergic neurons is strongly associated with heightened oxidative stress, which may arise from factors such as mitochondrial impairment and the accumulation of harmful metabolites generated during dopamine metabolism (Guo et al. 2018; Zhe Zhao et al. 2021; Bose and Beal 2016). Specifically, dopamine oxidation produces neurotoxic compounds like dopamine o-quinone, which provoke additional oxidative damage and neuronal cell death (Segura-Aguilar et al. 2014). Lipid peroxidation has also been identified as a significant mechanism by which α -synuclein aggregates contribute to cellular demise (Angelova, Esteras and Abramov 2021).

Mitochondrial dysfunction is another hallmark of PD pathophysiology. Mitochondria are critical for energy production and cellular homeostasis. Evidence includes impaired mitochondrial function—particularly in the electron transport chain—which enhances ROS production and promotes neuronal damage (Dias, Junn and Mouradian 2013; Chang and C. M. Chen 2020). Genetic alterations linked to familial PD, including mutations in *PINK1* and *Parkin*, exacerbate mitochondrial dysfunction and oxidative stress, highlighting the interconnected nature of these biological pathways (Gaki and Papavassiliou 2014).

Neuroinflammation also plays a central role in PD. Activated microglia release pro-inflammatory cytokines and ROS, which further contribute to neurodegeneration. This inflammatory response may be triggered by environmental toxins or misfolded protein aggregates such as α -synuclein (Angelova, Esteras and Abramov

2021; Chang and C. M. Chen 2020). The interaction between oxidative stress and neuroinflammation forms a vicious cycle that intensifies neuronal damage.

endoplasmic reticulum (ER) stress is increasingly recognised as a key mechanism in neurodegeneration. Prolonged ER stress activates the unfolded protein response, which, if unresolved, can lead to apoptosis of dopaminergic neurons. This mechanism may be particularly relevant in the context of genetic mutations (McNeill et al. 2014). The accumulation of misfolded proteins, such as α -synuclein, overwhelms the ER's capacity to maintain protein homeostasis, ultimately resulting in cellular dysfunction and death (Chang and C. M. Chen 2020).

Lastly, dopamine imbalance is a critical factor in PD pathology. Disruptions in dopamine transport and metabolism may exert cytotoxic effects, promoting the degeneration of dopaminergic neurons (Z. D. Zhou et al. 2023). These disturbances impair vesicular monoamine transporters, increasing cytosolic dopamine concentrations that trigger oxidative stress and neurotoxicity (Bucher et al. 2020). Such interference not only exacerbates motor symptoms but also contributes significantly to non-motor features, including cognitive impairment and mood disorders—manifestations now increasingly recognised in individuals with PD (Blesa and Przedborski 2014).

3.1.2 Eye Movements in Parkinson's Disease

Eye movements have been extensively studied in PD using a variety of techniques and methodologies, providing insights into the pathological changes in the brain associated with neurodegeneration. Some ocular motor abnormalities such as hypometric saccades, increased saccadic latency, and decreased smooth pursuit gain are widely accepted and have been proposed as non-invasive biomarkers for diagnosis (H. Li et al. 2023; Bueno, Sato and Hornberger 2019). Furthermore, ocular motor profiles can aid in providing a differential diagnosis between PD and atypical Parkinsonian syndromes (Terao, Tokushige et al. 2019; Y. Yu et al. 2024). Eye movement deficits seen in PD are also correlated with cognitive dysfunction, particularly within domains of attention, working memory, and visuospatial processing (Stuart et al. 2019).

Fixation instability in PD is characterised by square wave jerks (SWJ), microsaccadic abnormalities, and

impaired gaze holding. Individuals with PD have an increased frequency of SWJs compared to healthy controls, reflecting impairment in the suppression of involuntary saccades driven by BG dysfunction (Weil et al. 2016; Sinem B. Beylergil et al. 2022). Microsaccades seen in PD exhibit increased amplitude and decreased frequency, which can interfere with visual stability required for tasks such as reading (Frei 2021) and reduce visual clarity, disrupting perceptual continuity (Bueno, Sato and Hornberger 2019). This interference also arises from unwanted gaze shifts and fixation drift that require corrective eye movements. Impairments in gaze holding are linked to disruptions in the SC and its interactions with the BG (H. Li et al. 2023). A lack of attentional control can further exacerbate fixation instability, making individuals with PD more prone to visual distractions. This suggests deficits in top-down attentional control (Sinem B. Beylergil et al. 2022). The neurological mechanisms contributing to fixation instability in PD are linked to the overactive inhibitory output from the BG to the SC and impairments in the integration of ocular motor and visual networks involving the FEF and PC (Terao 2022; Weil et al. 2016). The presence of nystagmus in PD is less common compared to other movement disorders; however, when present as either gaze-evoked or positional nystagmus, it may reflect dysfunction in cerebellar, vestibular, or brainstem circuits (Jung and J. S. Kim 2019). Additionally, a lack of consensus on the classification and underlying mechanisms of nystagmus in PD complicates interpretation of findings (Pretegeiani and Optican 2017).

Smooth pursuit impairments in PD primarily manifest as decreased pursuit gain, reduced smooth tracking with saccadic intrusions, and directional and velocity-specific changes. Decreased smooth pursuit gain results in an inability to track moving objects, thus requiring catch-up saccades to compensate for smooth tracking errors (Frei 2021). This reduction has also been shown to correlate with disease severity, suggesting its potential as a marker for disease progression (Shaikh and Ghasia 2019). The jerky appearance of smooth pursuit, referred to as saccadic pursuit, although present in PD, is not as prominent as in atypical Parkinsonian syndromes (Sekar, T N Panouillères and Kaski n.d.). Some studies have also reported increased anticipatory saccades during smooth pursuit, suggesting reduced inhibitory control in the BG (Helmchen, Pohlmann et al. 2012). Unlike in PSP, smooth pursuit is more adversely affected in the horizontal direction than the vertical, indicating subtle differences in the neural circuits responsible for each direction (Shaikh, C. Antoniadis et al. 2018). Pursuit accuracy also decreases as target velocity increases, highlighting reduced capacity to maintain higher pursuit speeds (White et al. 1983). Although the BG and SC contribute to impaired modulation of pursuit-related neurons, the cerebellum also plays a role in fine-tuning pursuit movements, with compensatory mechanisms

becoming insufficient in advanced stages of PD (Gorges, Müller et al. 2016). Lastly, unlike other motor symptoms, smooth pursuit does not consistently improve with dopaminergic medication, suggesting involvement of serotonergic and cholinergic pathways in pursuit control (M. J. Munoz, Reilly et al. 2022; Reilly et al. 2008).

Abnormalities in saccadic control are also observed in PD, depending on the type of saccade performed. Reflexive saccades are relatively preserved, with only mild impairments in latency and saccadic gain (amplitude/target distance ratio), particularly with increased disease severity (Srivastava, Sharma, Sood et al. 2014). Increased latency in later stages of the disease is attributed to disrupted signal transmission through the BG-thalamus-SC pathway (Fridley et al. 2013). Individuals with PD also exhibit higher error rates and increased latency in antisaccade tasks, indicating impaired inhibitory control and reduced frontal cortical function (Helmchen, Pohlmann et al. 2012). Hypometric saccades are observed in volitional saccades, which are more severely affected than reflexive saccades due to reliance on frontal cortical and BG circuits (Hikosaka, Takikawa and Kawagoe 2000; Waldthaler, Tsitsi and Svenningsson 2019). Saccadic hypometria and increased latency also extend to memory-guided saccades, which require working memory and transformation of stored spatial memory into motor commands (Srivastava, Sharma, Sood et al. 2014). Memory-guided saccades in PD often require multiple-step corrections to compensate for hypometria (Srivastava, Sharma, Sood et al. 2014; Pierrot-Deseilligny, R. M. Müri, Ploner, Gaymard and S. Rivaud-Péchoux 2003; Pierrot-Deseilligny, R. M. Müri, Ploner, Gaymard, Demeret et al. 2003). Overall, saccadic impairments result from excessive inhibitory output from the substantia nigra pars reticulata (substantia nigra pars reticulata (SNpr)) to the SC, FEF dysfunction affecting voluntary and memory-guided saccades, and insufficient cerebellar compensation with disease progression (H. Li et al. 2023; Srivastava, Sharma, Goyal et al. 2020). Pharmacological interventions and (deep brain stimulation (DBS)) may have variable effects on these impairments, underscoring the need for more targeted research.

Bradykinesia, a cardinal symptom of PD, encompasses not only the slowness of movement but also a decrease in amplitude and speed, often leading to a decrement or sequence effect during repetitive tasks (Pretegitani and Optican 2017). "Saccadic bradykinesia" has recently been used to describe the decline in speed and amplitude of saccadic movements. In PD, saccades are often hypometric, exhibit increased latency, and slow over repetitive sequences—negatively impacting visual scanning and attentional processes (Koohi et al. 2021). A recent study found that saccade period correlates with bradykinesia, while maximal amplitude

reflects apathy, suggesting that saccadic metrics may reflect broader motor and motivational states in PD (Rey et al. 2025).

Although numerous studies have investigated eye movements in PD, several methodological limitations and knowledge gaps remain. Given the heterogeneity of PD, more research is required to assess population-level differences, including ethnic variations. Most research has focused on early to moderate disease stages, creating a knowledge gap in advanced or presymptomatic stages. Furthermore, many studies use artificial, lab-based tasks that do not fully reflect the complexity of real-world visuomotor behaviour. Incorporating naturalistic environments, such as virtual reality, may improve ecological validity. Translating findings into clinical practice by using clinically applicable paradigms is also essential to establish eye movements as diagnostic biomarkers. Moreover, longitudinal studies on disease progression are scarce, limiting the use of ocular motor features as progression markers (MacAskill and T. J. Anderson 2016). The effects of interventions such as DBS and levodopa remain debated, necessitating controlled studies that account for medication status and neurosurgical interventions (M. J. Munoz, Arora et al. 2023).

Methodological inconsistencies between studies also hinder cross-comparison. Variability in task design, analysis pipelines, and criteria for classifying SWJs, or defining thresholds for hypometric/hypermetric saccades, limit generalisability. Standardisation of ocular motor assessments is needed to build robust conclusions about PD-related eye movement abnormalities. Small sample sizes also reduce statistical power and generalisability. Additionally, many studies rely on subjective cognitive assessments, impeding insights into the link between cognitive decline and eye movements. Over-reliance on dopaminergic hypotheses may also overlook other important contributors to ocular motor dysfunction in PD. Several unexplored questions remain. Oblique saccades in PD are understudied, despite potentially revealing unique dysfunctions. Differences in eye movements across PD subtypes—such as tremor-dominant versus akinetic-rigid, or genetic versus sporadic—are rarely addressed. More comprehensive studies using neuroimaging could clarify the specific neural circuits underlying these dysfunctions and inform the development of targeted interventions.

3.2 Project Aims

1. To characterise ocular motor impairments in idiopathic and genetic forms of PD (GBA and LRRK2 mutations) across multiple eye movement paradigms.
2. To examine the relationship between ocular motor metrics, age, and Levodopa Equivalent Daily Dose (LEDD).

3.3 Methods

3.3.1 Participants

Participants were recruited for the ocular motor study in PD through the procedures outlined in Chapter 2: General Methods. Participants were included in the study if they: (1) had a confirmed diagnosis of PD, either idiopathic or genetic, verified through consultant letters prior to inclusion; (2) were between 40 and 80 years of age; (3) had normal or corrected-to-normal vision; (4) were able to provide informed consent; (5) were capable of following verbal instructions; and (6) could sit comfortably for the duration of testing.

Participants were excluded if they: (1) had other neurological conditions or a history of head trauma or stroke; (2) had visual impairments in both eyes (if impairment was present in one eye, the other eye was used for analysis) or ocular motor impairments such as diplopia (double vision); (3) had severe psychiatric conditions such as psychosis; (4) had systemic health conditions affecting vision, such as diabetes with retinopathy; (5) were pregnant or possibly pregnant (self-declared); and (6) had a history of epilepsy.

Healthy controls were also recruited following the methods described in Chapter 2: General Methods. Controls were included if they: (1) had no history of neurodegenerative diseases, neurological disorders, head trauma, or movement disorders such as dystonia; (2) had normal or corrected vision; (3) had normal cognitive function; and (4) were able to provide informed consent and comply with study protocols.

Controls were excluded if they: (1) had visual impairments in both eyes (if impairment was present in one eye, the other eye was used for analysis) or ocular motor impairments such as diplopia; (2) had severe psychiatric conditions such as psychosis; (3) had systemic health conditions affecting vision, such as diabetes with retinopathy; (4) were pregnant or possibly pregnant (self-declared); and (5) had a history of epilepsy.

Participants were divided into four cohorts: idiopathic PD (idiopathic-parkinson's disease (iPD)), PD with GBA mutation (GBA-PD), PD with LRRK2 mutation (LRRK2-PD), and healthy controls. A total of 170 participants were included: 103 with iPD, 13 with GBA-PD, 3 with LRRK2-PD, and 51 healthy controls. The study was approved by the UCL Research Ethics Committee, and informed consent was obtained from all participants prior to testing.

3.3.2 Ocular Motor Assessment

The standard ocular motor battery described in Chapter 2: General Methods was used for all participants in this study. The experimental setup, including calibration and validation steps, was consistent with the procedures previously outlined.

3.3.3 Data Processing and Analysis

Data processing methods and the metrics extracted followed those described in Chapter 2: General Methods. Additional analyses were conducted to further investigate eye movement patterns.

Saccadic analysis of pursuit was performed by generating a saccade report for each participant, which included the total number of saccades as well as the details of each saccade: amplitude, peak velocity, average velocity, start time, end time, and end position. Saccades were categorised into amplitude bins: less than 1 degree, 1–2 degrees, 2–3 degrees, 3–4 degrees, 4–5 degrees, 5–6 degrees, 6–7 degrees, 7–8 degrees, 8–9 degrees, 9–10 degrees, and greater than 10 degrees. The number of saccades in each bin was calculated across all directions (horizontal, vertical, and elliptical). The total number of saccades and within each amplitude bin were adjusted for the number of participants within each group. Histograms were plotted to visualise saccade distribution. Data normality was assessed using the Shapiro–Wilk test.

The amplitude and peak velocity of saccades are known to follow a non-linear function known as the main sequence effect, where saccades with larger amplitudes have higher peak velocities (R. John Leigh and David S. Zee 2015a). To account for this, saccadic velocities were corrected using the equations described in Koohi et al. 2021. These adjusted residual velocity values were used for further analysis. For reflexive, volitional,

and memory-guided saccades, a time-series analysis was conducted. Residual velocities of consecutive saccades were plotted against time (X-axis) for the duration of each paradigm. Each point represented an individual saccade. A line of best fit was applied, and the slope and coefficient of determination (R^2) were calculated for each group.

To identify which ocular motor measures were most sensitive in detecting PD-related changes, a composite score was computed for each type of eye movement. Hybrid-weighted composite z -scores were calculated by incorporating both statistical significance (p-values) and precision (confidence interval widths) into the weighting process. First, the z -scores for each group's effect size were computed using the formula:

$$z = \frac{x - \mu}{\sigma}$$

where x is the group's effect size, μ is the mean effect size across groups, and σ is the standard deviation. The confidence interval (CI) width for each metric was calculated as:

$$\text{CI Width} = \text{Upper CI} - \text{Lower CI}$$

The hybrid weight for each metric was then computed as:

$$\text{Weight} = \frac{1}{(\text{p-value} \times \text{CI Width}) + \varepsilon'}$$

where ε' is a small constant to prevent division by zero. Each z -score was multiplied by its corresponding hybrid weight, and the weighted z -scores were summed across all metrics for each group. The final composite z -score was obtained by normalising the weighted sum by the total hybrid weight for each group. This approach ensures that the composite scores reflect both the statistical significance and the precision of the effect sizes, providing a robust measure of relative group performance across paradigms.

3.3.4 Statistical Analyses

Demographic data were summarised using descriptive statistics. The dataset was inspected for missing values, and participants with incomplete data were excluded from further analysis. Given the small sample sizes for the GBA and LRRK2 groups, bootstrapping was conducted to generate resampled distributions

for more robust comparisons. Bootstrapping with 1,000 replicates was applied to ensure stable estimates, while data from the control and iPD groups were retained without modification. The bootstrapped values were subsequently used for further analysis. A series of generalized linear model (GLM)s were fitted to evaluate the effects of group, age, sex, levodopa equivalent daily dose (LEDD), and disease duration on each ocular motor metric using the `glm2` function in R. Model estimates included regression coefficients (β estimates), 95% CIs, p-values, akaike information criterion (AIC), and bayesian information criterion (BIC) for model comparison. Multiple comparisons were accounted for using the Bonferroni correction. Following the GLM analysis, post hoc pairwise comparisons were conducted among the three PD subgroups (iPD, GBA, LRRK2) using the estimated marginal means package in R. Multiple comparisons were adjusted using the Bonferroni correction. The significance level for all analyses was set at $\alpha = 0.05$. All analyses were conducted using R (Version 2023.09.1+494, R Core Team, Vienna, Austria). The data tables for all the analyses are provided in the appendix.

3.4 Results

3.4.1 Participants

After accounting for data loss, the final study cohort included 164 participants. The control group comprised 48 individuals (26 females and 22 males) with a mean age of 62.66 years (SD = 13.68, range = 22.25–79.59). The GBA mutation group included 13 participants (9 males and 4 females) with a mean age of 64.30 years (SD = 7.71, range = 48.53–78.33). The iPD group was the largest, consisting of 100 individuals (66 males and 34 females), with a mean age of 66.84 years (SD = 7.69, range = 45.45–87.62). The LRRK2 mutation group was the smallest, comprising 3 males with a mean age of 53.31 years (SD = 3.04, range = 50.56–56.58). The mean disease duration was 5.69 years (SD = 4.47) for the GBA group, 6.25 years (SD = 5.13) for the iPD group, and 9.67 years (SD = 10.69) for the LRRK2 group. The mean LEDD was highest in the iPD group at 433.57 mg (SD = 363.25), followed by 368.33 mg (SD = 510.40) in the GBA group and 330 mg (SD = 571.58) in the LRRK2 group.

Table 2: Demographic and clinical characteristics of the study cohort. Values are presented as mean \pm standard deviation (SD). Age is reported for all participants, while disease duration and levodopa equivalent daily dose (LEDD) are reported for Parkinson’s disease (PD) groups only. Data are stratified by group and sex. “-” indicates not applicable or unavailable.

Group	Age (Mean \pm SD)	Disease Duration (Mean \pm SD)	LEDD (Mean \pm SD)
Healthy Controls (N = 48)	62.66 \pm 13.68	-	-
Males (N = 22)	62.91 \pm 15.11	-	-
Females (N = 26)	62.45 \pm 12.64	-	-
Idiopathic PD (N = 100)	66.99 \pm 7.80	6.26 \pm 5.15	425.58 \pm 364.29
Males (N = 66)	67.32 \pm 8.20	6.04 \pm 5.38	430.03 \pm 358.04
Females (N = 34)	66.35 \pm 7.06	6.70 \pm 4.72	417.06 \pm 381.28
GBA Mutation PD (N = 13)	63.37 \pm 6.18	5.63 \pm 4.36	434.23 \pm 497.33
Males (N = 9)	63.40 \pm 6.24	5.12 \pm 4.45	543.89 \pm 566.18
Females (N = 4)	63.32 \pm 7.00	6.77 \pm 4.55	187.50 \pm 131.50
LRRK2 Mutation PD (N = 3)	53.31 \pm 3.04	9.67 \pm 10.69	330.00 \pm 571.58
Males (N = 3)	53.31 \pm 3.04	9.67 \pm 10.69	330.00 \pm 571.58
Females (N = 0)	-	-	-

3.4.2 Ocular Motor Function in Idiopathic Parkinson’s Disease

In the fixation task, pupil size was significantly larger in individuals with iPD compared to controls ($\beta = 571.305$, 95% CI [196.431, 946.179], $p = 0.003$). The iPD group also had an increased number of small SWJs compared to the control group ($\beta = 20.887$, 95% CI [2.715, 44.489], $p = 0.044$). No significant differences were observed in the number of large SWJs or other fixation-related metrics.

Individuals with iPD exhibited significant alterations in fixation pupil size and small SWJs in the positional fixation/nystagmus task. Pupil size was significantly increased in the up ($\beta = 459.343$, 95% CI [109.578, 809.108], $p = 0.011$), down ($\beta = 479.572$, 95% CI [93.283, 865.861], $p = 0.016$), right ($\beta = 474.891$, 95% CI [114.840, 834.943], $p = 0.011$), and left ($\beta = 429.413$, 95% CI [52.124, 806.703], $p = 0.027$) positions compared to controls. Additionally, an increased number of small SWJs was observed in the right position ($\beta = 21.736$, 95% CI [2.673, 40.798], $p = 0.027$) compared to controls. A higher count of

large SWJs and large intrusive saccades was also found in the right position ($\beta = 5.434$, 95% CI [0.680, 10.188], $p = 0.026$ and $\beta = 0.414$, 95% CI [0.057, 0.771], $p = 0.024$, respectively) in iPD compared to controls.

In the pursuit task, the iPD group showed no differences in pursuit gain in the horizontal and vertical directions at both target speeds, 0.2 Hz and 0.4 Hz. However, notable reduced performance was found in the elliptical directions. Increased pursuit gain was found in the anticlockwise direction at 0.4 Hz ($\beta = 0.085$, 95% CI [0.019, 0.151], $p = 0.011$) and in the clockwise direction at 0.4 Hz ($\beta = 0.170$, 95% CI [0.033, 0.306], $p = 0.015$). No differences were observed between the iPD group and controls for pursuit accuracy.

The iPD group in the oblique saccades task showed some deficits in performance, specifically at 10° target eccentricity. Individuals with iPD had lower saccadic amplitude ($\beta = -0.722$, 95% CI [-1.364, -0.081], $p = 0.028$), decreased X and Y positional accuracy ($\beta = 40.203$, 95% CI [8.469, 71.938], $p = 0.014$ and $\beta = 59.430$, 95% CI [16.003, 102.857], $p = 0.006$, respectively), reduced number of correct saccades ($\beta = -2.664$, 95% CI [-4.593, -0.734], $p = 0.007$), and a higher number of hypermetric saccades ($\beta = 3.009$, 95% CI [0.300, 5.897], $p = 0.031$) compared to controls. At 4° and 8°, no significant differences were found in any of the metrics, and at 10°, saccade velocities, end time, and the number of hypometric saccades also showed no differences.

Antisaccade performance in the horizontal direction was not significantly different in the iPD group compared to controls, with all metrics showing no statistically significant differences. However, in the vertical direction, some differences were found, primarily associated with saccadic speed. Average saccade velocity ($\beta = -19.298$, 95% CI [-31.033, -7.562], $p = 0.001$) and peak saccade velocity ($\beta = -45.571$, 95% CI [-88.391, -2.752], $p = 0.038$) were both lower in iPD compared to healthy controls. Additionally, saccadic amplitude was reduced in the iPD group ($\beta = -0.934$, 95% CI [-1.721, -0.149], $p = 0.02$) compared to controls.

Individuals with iPD showed no differences in saccadic velocities or start and end time for reflexive saccades in the horizontal direction. There was a significant difference in saccadic amplitude ($\beta = -0.880$, 95% CI [-1.579, -0.182], $p = 0.014$), resulting in an increased number of hypometric saccades ($\beta = 2.520$, 95% CI [0.215, 5.256], $p = 0.042$) compared to controls. Similarly, in the vertical direction, saccadic amplitude was reduced in iPD compared to controls ($\beta = -0.473$, 95% CI [-0.933, -0.014], $p = 0.045$), and iPD individuals

made a higher number of hypometric saccades ($\beta = 3.106$, 95% CI [0.090, 6.121], $p = 0.045$) than controls. No differences were noted in measures of saccadic velocity or start and end times.

Volitional saccades in the vertical and horizontal directions showed no significant differences in any of the saccadic measures, including measures of saccadic steps and the total number of saccades, when comparing iPD individuals with healthy controls. The same results were found in the memory-guided saccades in the horizontal and vertical planes, with no notable differences being observed in the iPD group compared to controls.

3.4.3 Ocular Motor Function in GBA Mutation Parkinson's Disease

Individuals with GBA-PD exhibited significantly larger pupil size compared to controls ($\beta = 595.517$, 95% CI [30.795, 1160.239], $p = 0.040$). Additionally, the number of large SWJs was significantly increased in the GBA-PD group ($\beta = 0.576$, 95% CI [0.110, 1.043], $p = 0.017$), compared to controls. No other fixation-related metrics differed significantly. In the positional fixation task, pupil size was significantly greater in the down ($\beta = 753.232$, 95% CI [171.314, 1335.150], $p = 0.012$) and in the right ($\beta = 579.692$, 95% CI [37.299, 1122.084], $p = 0.038$) positions compared to controls. No differences in SWJs or other fixation metrics were found.

No significant group differences were found in pursuit gain or RMSE gaze at either 0.2 Hz or 0.4 Hz across horizontal, vertical, or elliptical directions.

In the oblique saccade task, differences were only observed at 10° eccentricity. The GBA-PD group showed reduced amplitude ($\beta = -1.097$, 95% CI [-1.364, -0.081], $p = 0.027$), average velocity ($\beta = -19.272$, 95% CI [-37.945, -0.601], $p = 0.044$), and peak velocity ($\beta = -55.139$, 95% CI [-108.701, -1.576], $p = 0.045$) compared to controls. X-accuracy ($\beta = 55.192$, 95% CI [7.386, 102.998], $p = 0.025$) and Y-accuracy ($\beta = 92.725$, 95% CI [27.306, 158.145], $p = 0.006$) were both lower in GBA-PD compared to controls. The GBA-PD group also made fewer correct saccades ($\beta = -3.671$, 95% CI [-6.577, -0.764], $p = 0.007$) and more hypermetric saccades ($\beta = 6.561$, 95% CI [2.345, 10.777], $p = 0.002$) compared to controls. Latency, end time, and hypometric saccades were unaffected.

In the horizontal antisaccade task, the GBA group made smaller saccades with smaller saccadic amplitudes compared to controls ($\beta = -0.719$, 95% CI [-3.068, -0.382], $p = 0.012$). the GBA group also had lower average velocity ($\beta = -8.401$, 95% CI [-43.273, -3.534], $p = 0.022$) and peak velocity ($\beta = -55.176$, 95% CI [-108.681, -1.652], $p = 0.045$) compared to controls. In the vertical direction, saccadic amplitude ($\beta = -1.644$, 95% CI [-2.829, -0.458], $p = 0.007$), average velocity ($\beta = -30.982$, 95% CI [-48.661, -13.303], $p < 0.001$), and peak velocity ($\beta = -86.757$, 95% CI [-151.262, -22.252], $p = 0.009$) were also reduced compared to controls.

In the horizontal reflexive task, the GBA group showed reduced average velocity ($\beta = -21.198$, 95% CI [-39.668, -2.708], $p = 0.026$), peak velocity ($\beta = -73.047$, 95% CI [-135.258, -10.837], $p = 0.022$), and smaller amplitude saccades ($\beta = -1.357$, 95% CI [-2.409, -0.306], $p = 0.014$) compared to controls. They made fewer correct saccades ($\beta = -4.787$, 95% CI [-9.070, -0.502], $p = 0.029$) and more hypometric saccades ($\beta = 4.090$, 95% CI [0.030, 8.211], $p = 0.033$) compared to controls. Similar effects were observed in the vertical direction; amplitude ($\beta = -1.386$, 95% CI [-2.609, -0.165], $p = 0.027$), average velocity ($\beta = -25.492$, 95% CI [-45.386, -5.598], $p = 0.013$), and peak velocity ($\beta = -73.761$, 95% CI [-140.124, -7.397], $p = 0.030$) were all lower in the GBA group compared to controls. Correct saccades were reduced ($\beta = -4.768$, 95% CI [-8.831, -0.704], $p = 0.022$), and hypometric saccades increased ($\beta = 6.335$, 95% CI [0.090, 6.121], $p = 0.006$) in the GBA group compared to controls. Saccadic latency was marginally increased ($\beta = 40.551$, 95% CI [0.303, 80.799], $p = 0.043$) in the GBA group compared to controls.

In the volitional saccade task, no differences were found in the horizontal direction. In the vertical direction, hypometric saccades were more frequent in the GBA group ($\beta = 15.564$, 95% CI [3.241, 27.886], $p = 0.014$) compared to controls. Memory-guided saccades showed no group differences in the horizontal direction. In the vertical direction, the GBA group exhibited more hypometric saccades ($\beta = 12.677$, 95% CI [0.116, 25.237], $p = 0.046$) and reduced peak velocity ($\beta = -80.842$, 95% CI [-159.084, -2.599], $p = 0.044$) compared to controls.

3.4.4 Ocular Motor Function in LRRK2 Mutation Parkinson's Disease

Pupil size was significantly larger in individuals with LRRK2-PD compared to controls ($\beta = 2091.930$, 95% CI [1063.174, 3120.687], $p < 0.001$). No significant differences were found in the number of large SWJs or other fixation-related measures.

Individuals with LRRK2-PD exhibited multiple significant differences across positional conditions. Pupil size was significantly larger in the up ($\beta = 1731.166$, 95% CI [771.315, 2691.017], $p = 0.001$), down ($\beta = 1311.136$, 95% CI [251.053, 2371.219], $p = 0.016$), right ($\beta = 1317.765$, 95% CI [329.686, 2305.844], $p = 0.010$), and left ($\beta = 1134.452$, 95% CI [99.066, 2169.839], $p = 0.033$) positions compared to controls. An increased number of microsaccades and small SWJs were observed in the right position ($\beta = 82.919$, 95% CI [31.090, 134.749], $p = 0.002$ and $\beta = 115.518$, 95% CI [63.206, 167.831], $p < 0.001$, respectively) compared to controls. Large intrusive saccades were also increased in the down ($\beta = 17.912$, 95% CI [7.577, 28.246], $p = 0.001$) and right ($\beta = 14.639$, 95% CI [1.593, 27.686], $p = 0.029$) positions compared to controls. Lastly, fixation precision metrics were altered in the right position, with a significant decrease in fixation precision RMS S2S ($\beta = 0.024$, 95% CI [0.004, 0.045], $p = 0.023$) and fixation precision SD Window ($\beta = 0.048$, 95% CI [0.015, 0.080], $p = 0.005$) compared to controls.

In the pursuit task, no significant differences were found in pursuit gain and accuracy when LRRK2 mutation PD was compared to controls for all the different directions of pursuit assessed—horizontal, vertical, and elliptical—and at both speeds, 0.2 Hz and 0.4 Hz. Oblique saccades performance was found to be preserved in individuals with an LRRK2 mutation at all three degrees of eccentricity (4°, 8°, and 10°), with all measures of saccadic performance not being significantly different in LRRK2-PD from healthy controls. Antisaccade performance in the horizontal direction was not significantly different in the group with LRRK2 mutation PD compared to controls, with all metrics showing no statistically significant differences. Similar results were found in the vertical antisaccade task, with no notable differences between individuals with an LRRK2 mutation and healthy controls. The LRRK2 mutation population had normal reflexive saccades in the horizontal and vertical directions, with no pronounced differences in any key metrics compared to controls.

Volitional saccades in both the vertical and horizontal directions showed no significant differences in all the saccadic measures, including measures of saccadic steps and total number of saccades, when comparing

LRRK2 individuals with healthy controls. Although no differences were found in saccadic measures in the memory-guided saccades task, in both the horizontal and vertical directions, the LRRK2 group had an increased number of hypometric saccades compared to healthy controls ($\beta = 33.625$, 95% CI [11.533, 54.997], $p = 0.003$ and $\beta = 25.720$, 95% CI [2.838, 48.601], $p = 0.029$, respectively).

3.4.5 Saccadic Pursuit

Individuals with iPD exhibited the highest total saccade count across all amplitude bins, with an adjusted count of 130.42 in the $<1^\circ$ bin and 142.80 in the $1\text{--}1.99^\circ$ bin. The Shapiro–Wilk normality test revealed significant deviation from normality ($W = 0.774$, $p = 0.004$). Saccades in the GBA-PD group showed an adjusted count of 91.92 in the $<1^\circ$ bin and 128.54 in the $1\text{--}1.99^\circ$ bin. Non-normality was confirmed ($W = 0.766$, $p = 0.003$). The LRRK2-PD group showed an adjusted count of 123.67 in the $<1^\circ$ bin and 115.00 in the $1\text{--}1.99^\circ$ bin. The Shapiro–Wilk test again showed significant non-normality ($W = 0.763$, $p = 0.003$).

3.4.6 Timescale Analysis

In the timescale analysis of peak residual saccadic velocity over time, significant changes were observed in the iPD, GBA-PD, and LRRK2-PD groups compared to controls. For reflexive saccades in the vertical direction, the iPD and GBA groups exhibited a significant decline over time (textitp < 0.0001 for both). The LRRK2 group did not show significant alterations in reflexive saccades over time in either direction. In volitional saccades, horizontal residual velocity declined significantly in all three PD groups—iPD (textitp < 0.0001), GBA (textitp < 0.0001), and LRRK2 (textitp = 0.015). For vertical volitional saccades, only the iPD (textitp < 0.0001) and GBA (textitp = 0.040) groups showed significant changes. In memory-guided saccades, significant reductions in vertical residual velocity were observed in all PD groups—iPD (textitp < 0.0001), GBA (textitp < 0.0001), and LRRK2 (textitp = 0.015). No significant differences were noted in the horizontal direction.

3.4.7 Ocular Motor Composite Score

To evaluate the relative sensitivity of different eye movement paradigms in distinguishing PD subtypes, hybrid-weighted composite z -scores were calculated for each paradigm. The antisaccade paradigms demonstrated the highest sensitivity in the GBA mutation PD group, with the vertical antisaccades ($z = 62.82$) and horizontal antisaccades ($z = 31.97$) showing the largest composite scores. In contrast, the central fixation paradigm exhibited the greatest sensitivity in the LRRK2-PD group ($z = 5.43$), indicating its potential as a distinguishing marker for this genetic subtype. iPD participants showed more moderate composite scores across paradigms, with vertical antisaccades ($z = 6.24$) being the most sensitive, followed by horizontal antisaccades ($z = 1.23$) and pursuit ($z = 0.97$). Other paradigms, such as memory-guided saccades (horizontal: $z = 0.06$, vertical: $z = 0.03$) and reflexive saccades (horizontal: $z = 0.03$, vertical: $z = 0.00$), had relatively lower scores across all groups, suggesting limited sensitivity for differentiating PD subtypes.

Central Fixation Metrics in Parkinson's Disease

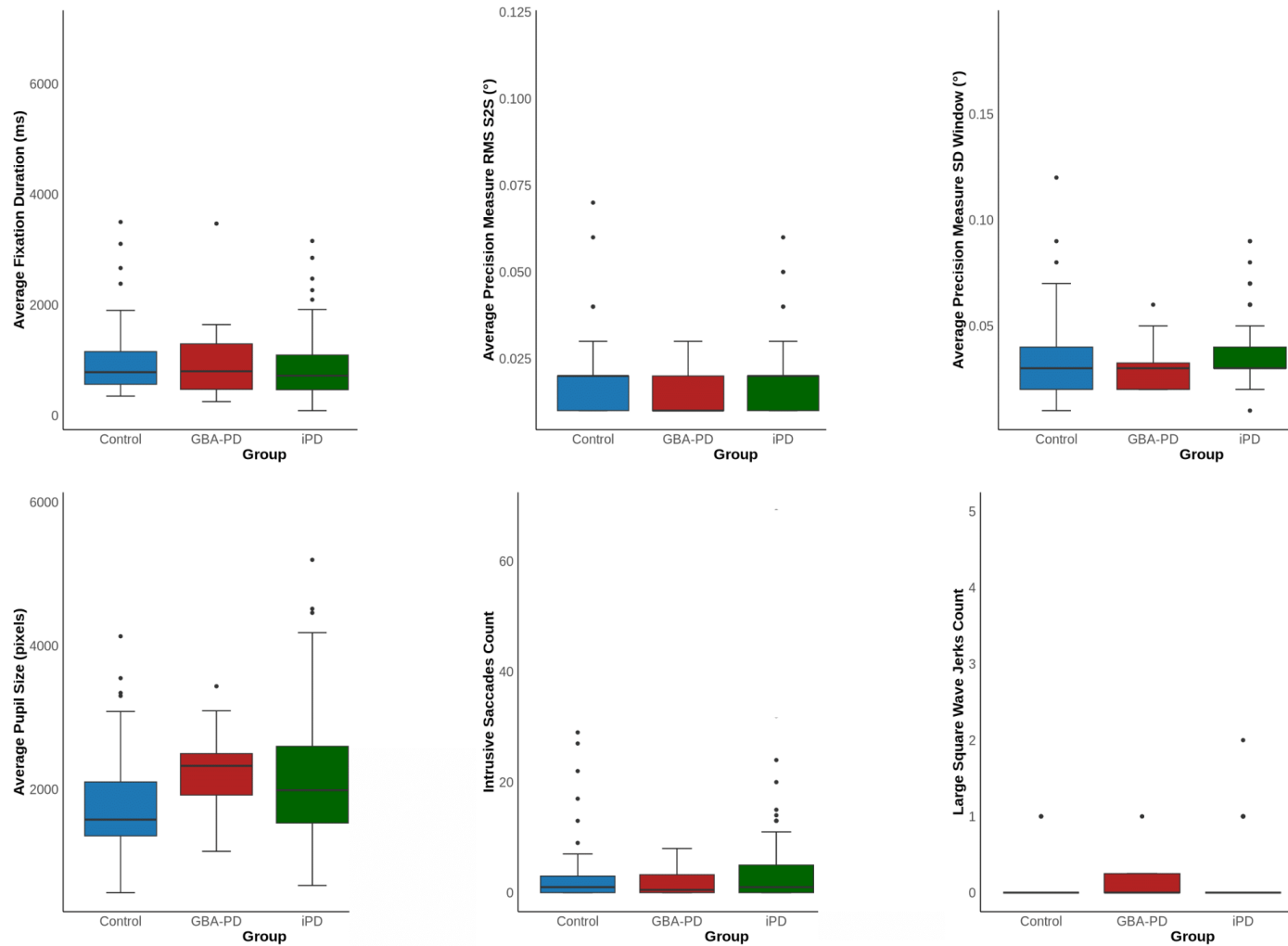


Figure 36: Central Fixation Metrics in Parkinson's Disease. Box plots show the median, interquartile range, and full range. Generalized linear models were used to assess the effects of group, age, sex, LEDD, and disease duration. Statistical significance was set at $p < 0.05$.

Central Fixation Metrics in Parkinson's Disease

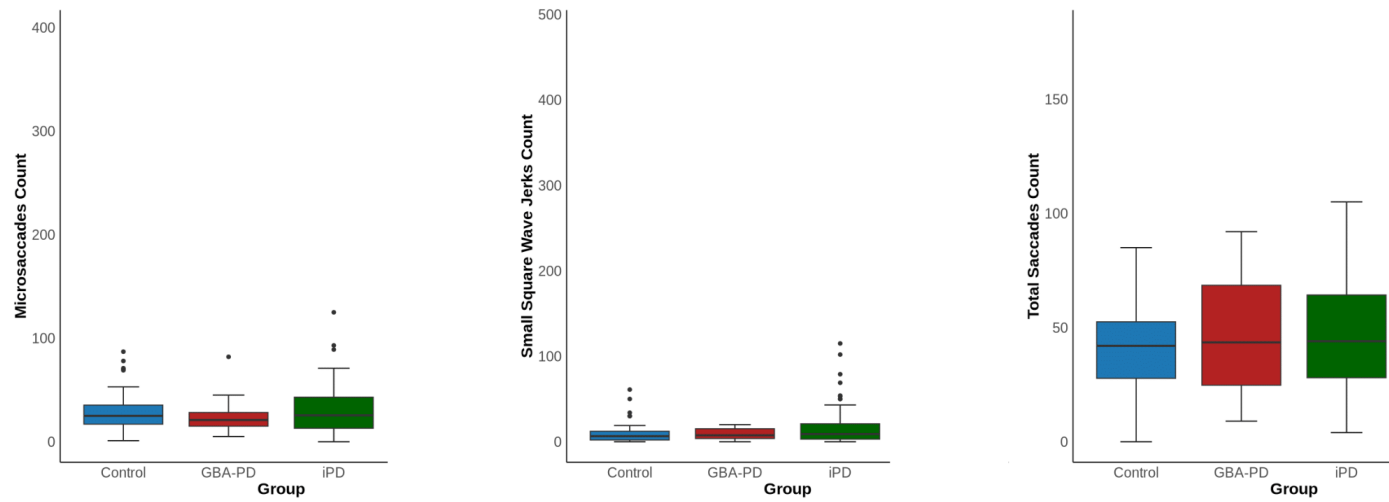


Figure 37: Central Fixation Metrics in Parkinson's Disease. Box plots show the median, interquartile range, and full range. Generalized linear models were used to assess the effects of group, age, sex, LEDD, and disease duration. Statistical significance was set at $p < 0.05$.

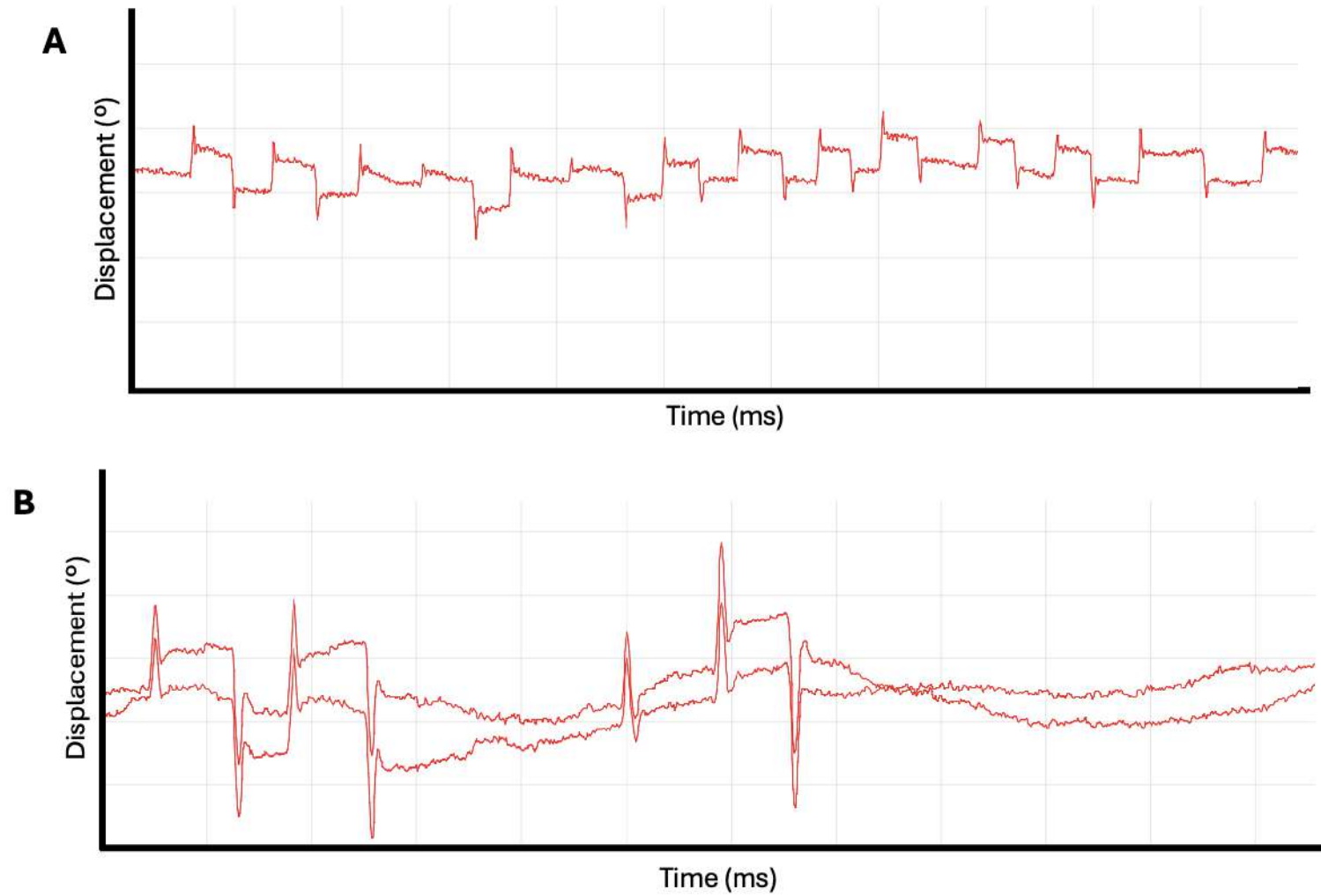


Figure 38: Fixation Traces in Parkinson's Disease. A) Small square wave jerks in idiopathic Parkinson's disease; B) Large square wave jerks in GBA mutation Parkinson's disease.

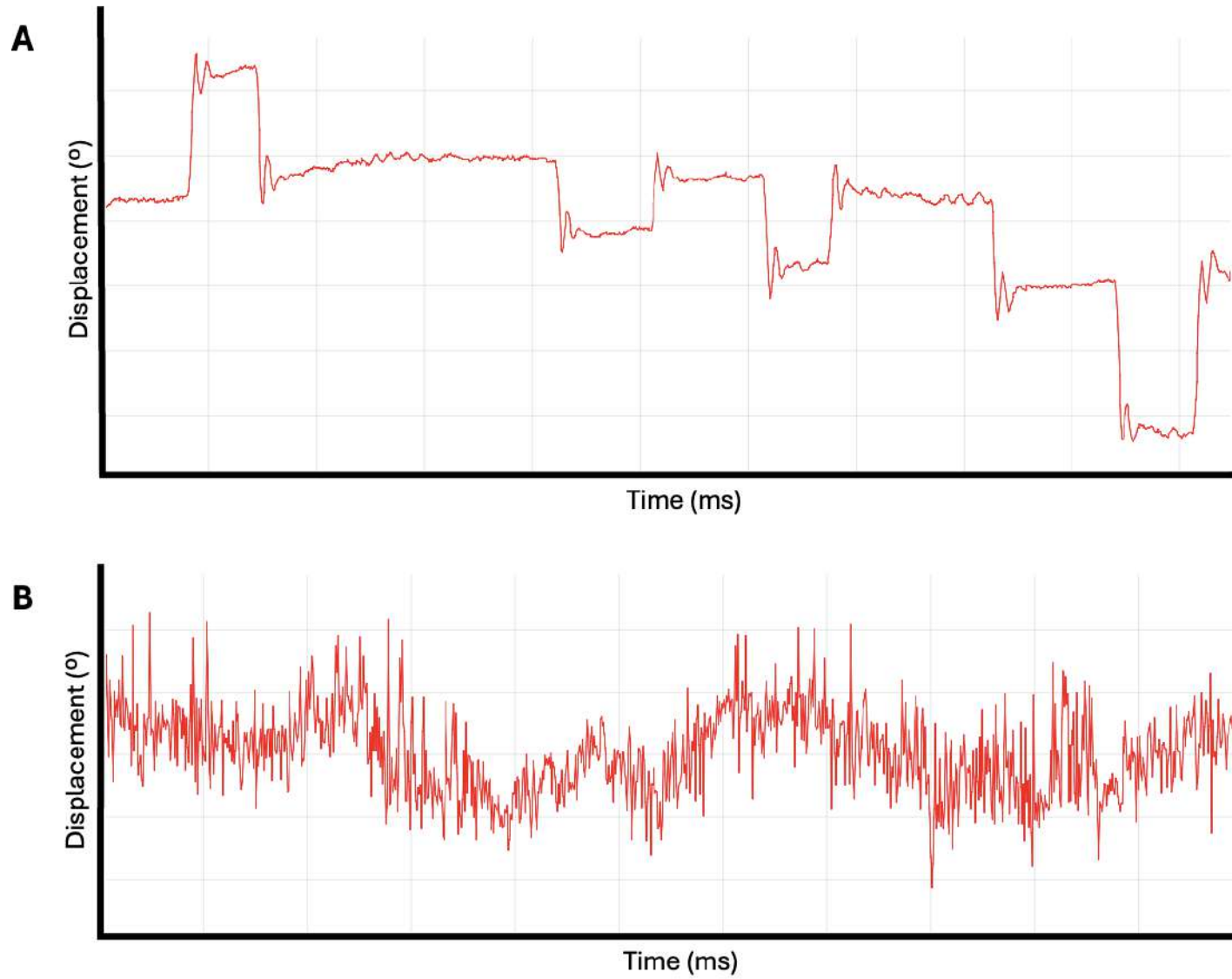


Figure 39: Fixation Traces in Parkinson's Disease. A) Large intrusive saccades in GBA mutation Parkinson's disease B) Microsaccades in idiopathic Parkinson's disease.

Table 3: Qualitative Description of Central Fixation Metrics in the LRRK2 Mutation PD Group.

Metric	LRRK2 Mutation PD Group Characteristics
Saccade Count	Lowest median (40–50); narrow IQR (20–70); range 10–70; no outliers. Suggests reduced spontaneous saccades.
Average Fixation Duration	Higher median (300–350 ms); IQR 250–400 ms; some outliers (500 ms). Indicates prolonged fixation.
Small Square Wave Jerk Count	Very low median (0–5); extremely narrow distribution; no outliers. Suggests minimal jerky eye movements.
Microsaccade Count	Strikingly low median (10–20); narrow IQR and whiskers; no outliers. Indicates suppressed microsaccade generation.
Large Square Wave Jerk Count	Median close to 0; rare outliers (up to 2–3); slightly longer whiskers. Reflects infrequent large jerks.
Large Intrusive Saccade Count	Median = 0; distinct outliers (1–5); slightly extended upper whisker. Suggests rare but present large intrusive movements.
Fixation Precision RMS	Slightly lower median (0.04–0.05); narrow IQR; few minor outliers. Indicates stable fixation.
Average Pupil Size	Prominently higher median (4000–4500); IQR 3500–5000; outliers up to 6000. Greater variability and dilation.
Fixation Precision SD	Median 0.05; narrow IQR; similar to other groups. Fixation stability (SD) is comparable.

Positional Fixation/ Nystagmus Metrics in Parkinson's Disease

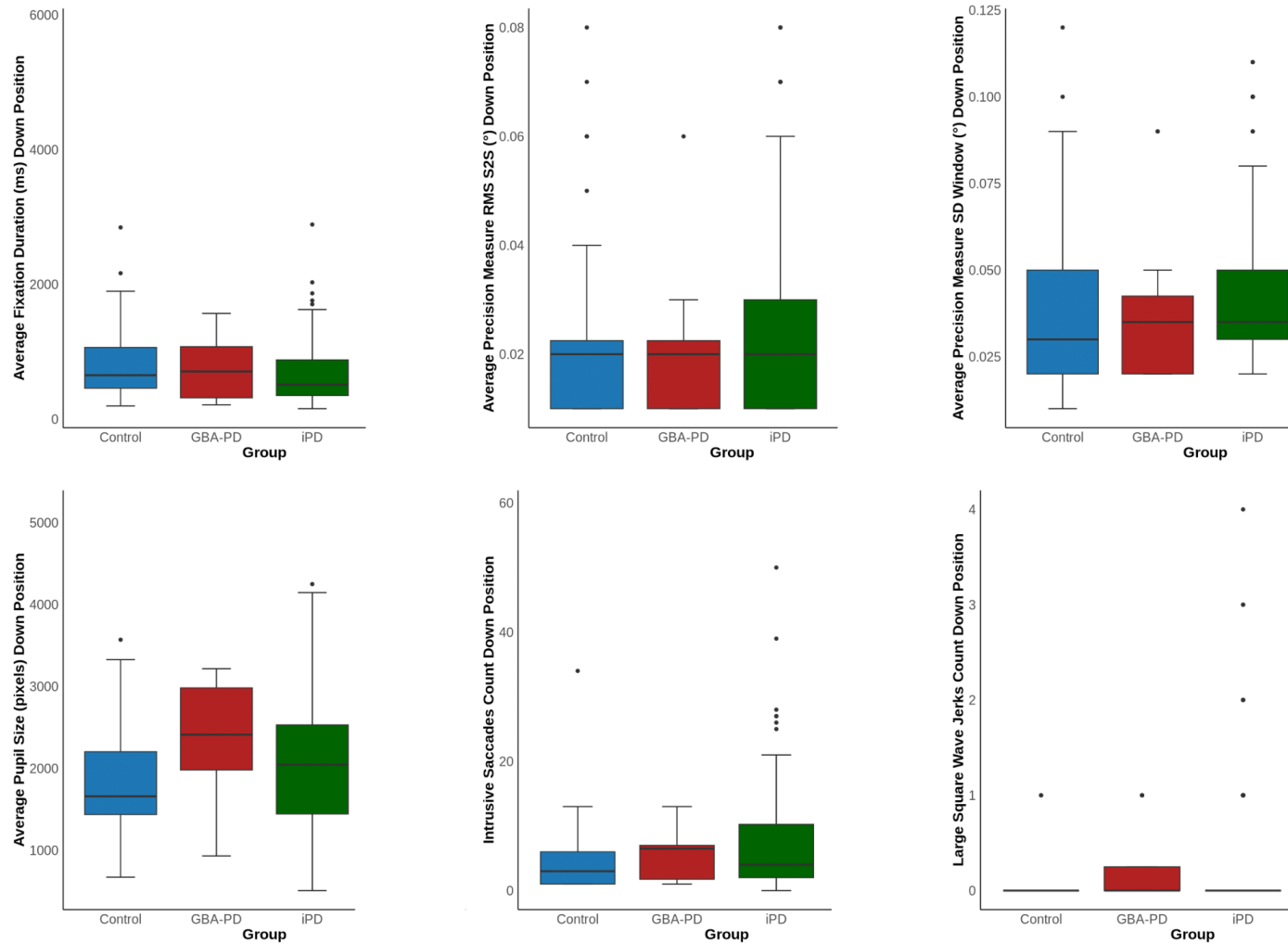


Figure 40: Positional Fixation/ Nystagmus Metrics in Parkinson's Disease. Box plots show the median, interquartile range, and full range. Generalized linear models were used to assess the effects of group, age, sex, LEDD, and disease duration. Statistical significance was set at $p < 0.05$.

Positional Fixation/ Nystagmus Metrics in Parkinson's Disease

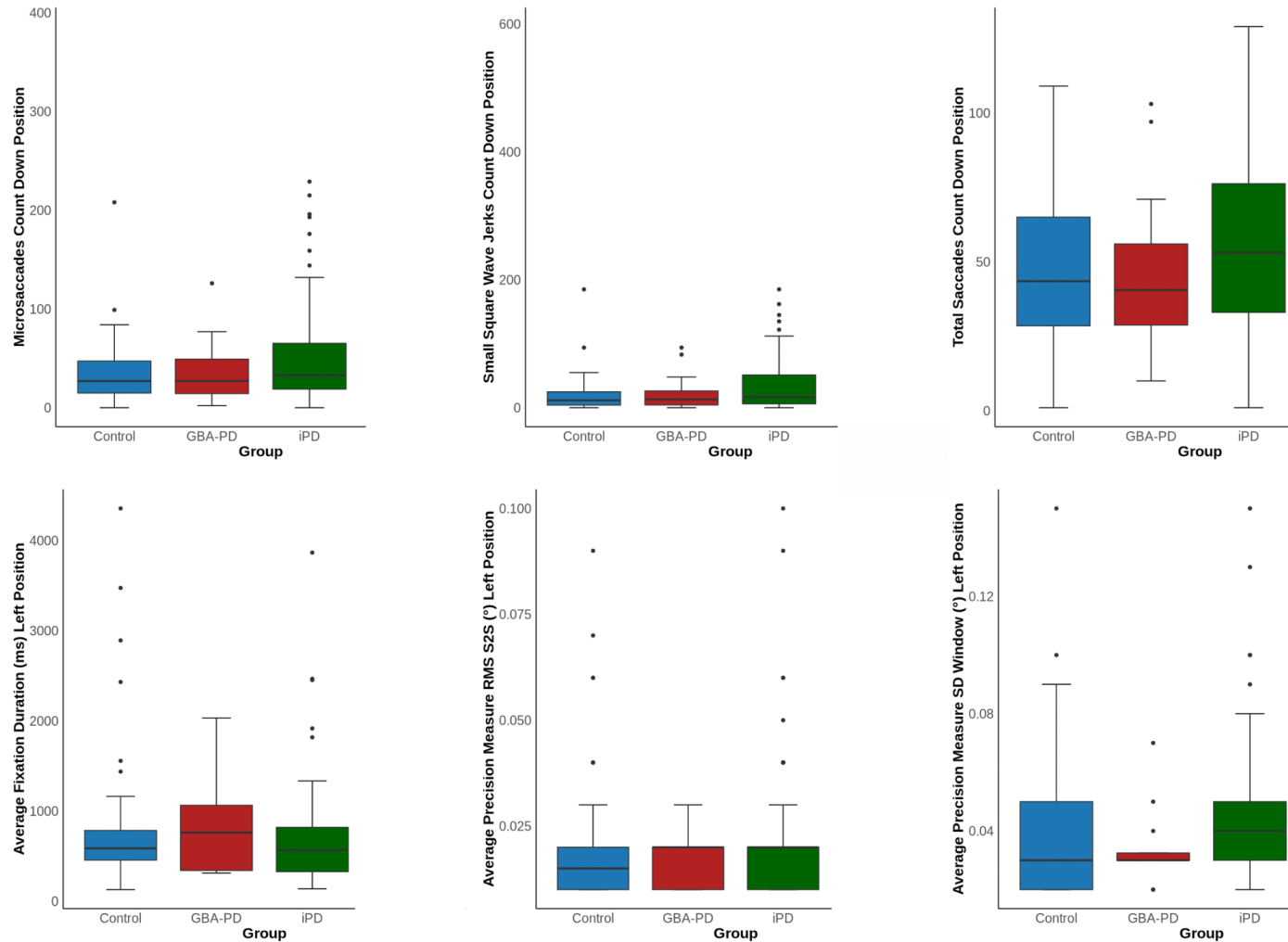


Figure 41: Positional Fixation/ Nystagmus Metrics in Parkinson's Disease. Box plots show the median, interquartile range, and full range. Generalized linear models were used to assess the effects of group, age, sex, LEDD, and disease duration. Statistical significance was set at $p < 0.05$.

Positional Fixation/ Nystagmus Metrics in Parkinson's Disease

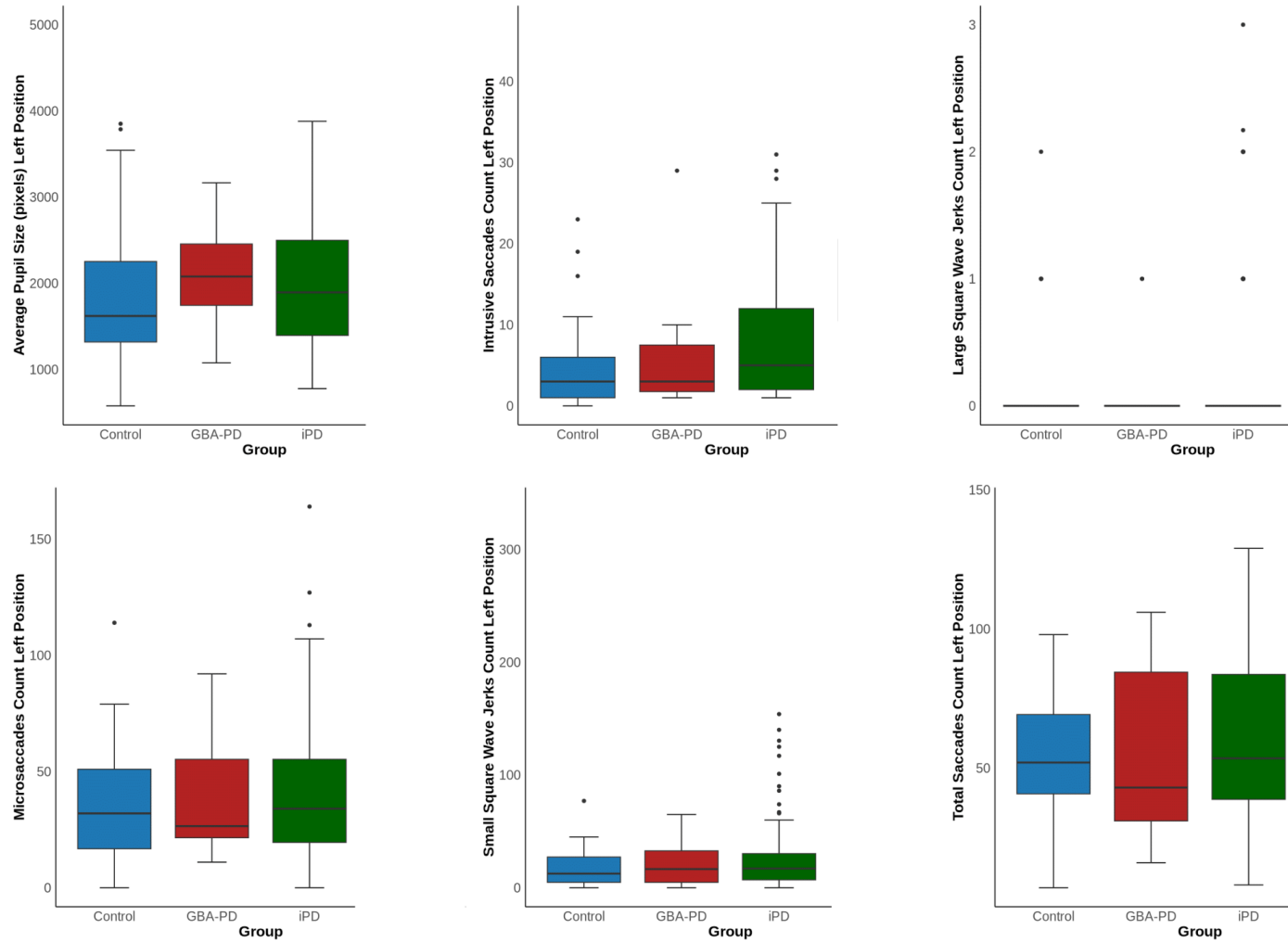


Figure 42: Positional Fixation/ Nystagmus Metrics in Parkinson's Disease. Box plots show the median, interquartile range, and full range. Generalized linear models were used to assess the effects of group, age, sex, LEDD, and disease duration. Statistical significance was set at $p < 0.05$.

Positional Fixation/ Nystagmus Metrics in Parkinson's Disease

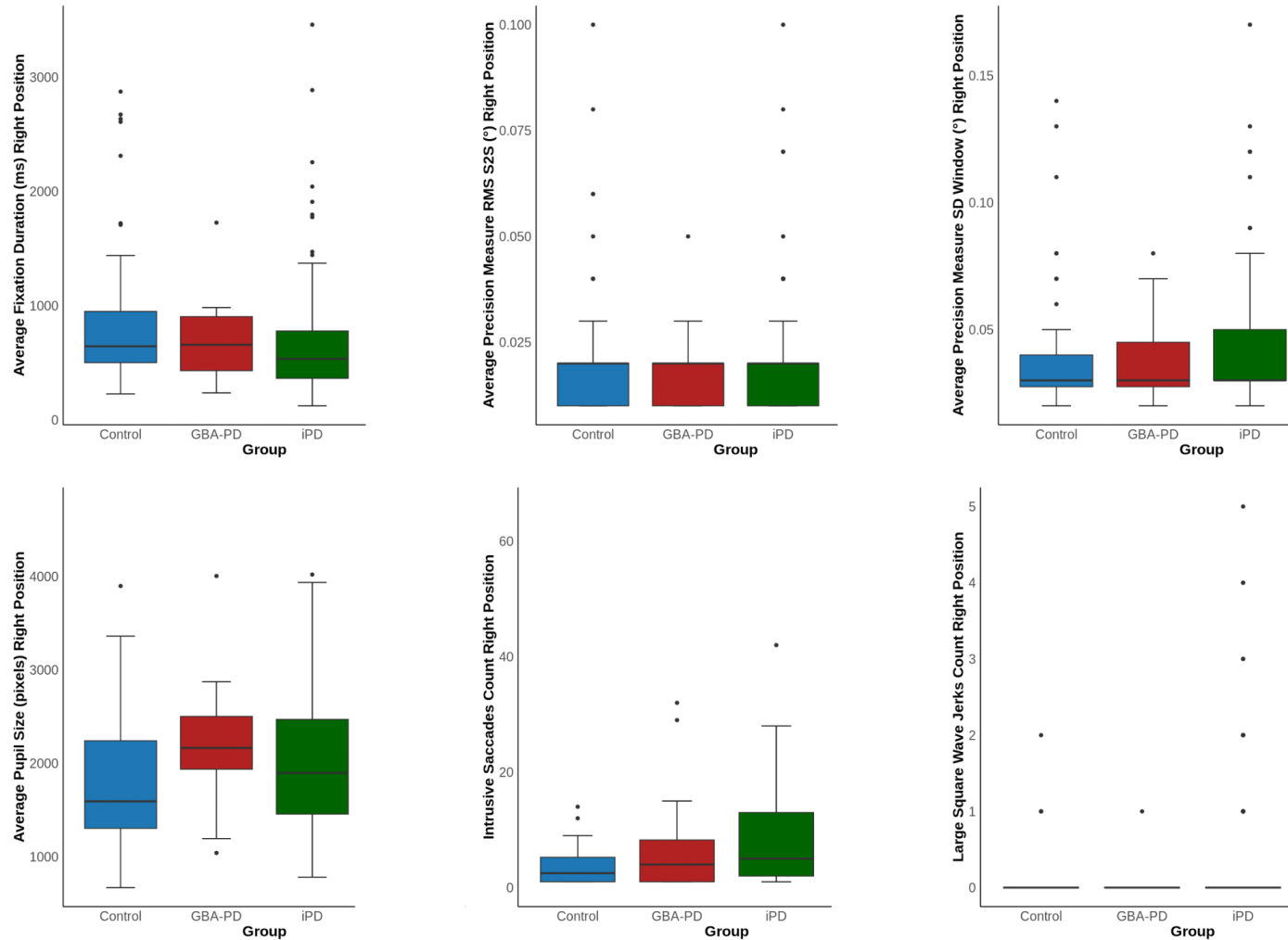


Figure 43: Positional Fixation/ Nystagmus Metrics in Parkinson's Disease. Box plots show the median, interquartile range, and full range. Generalized linear models were used to assess the effects of group, age, sex, LEDD, and disease duration. Statistical significance was set at $p < 0.05$.

Positional Fixation/ Nystagmus Metrics in Parkinson's Disease

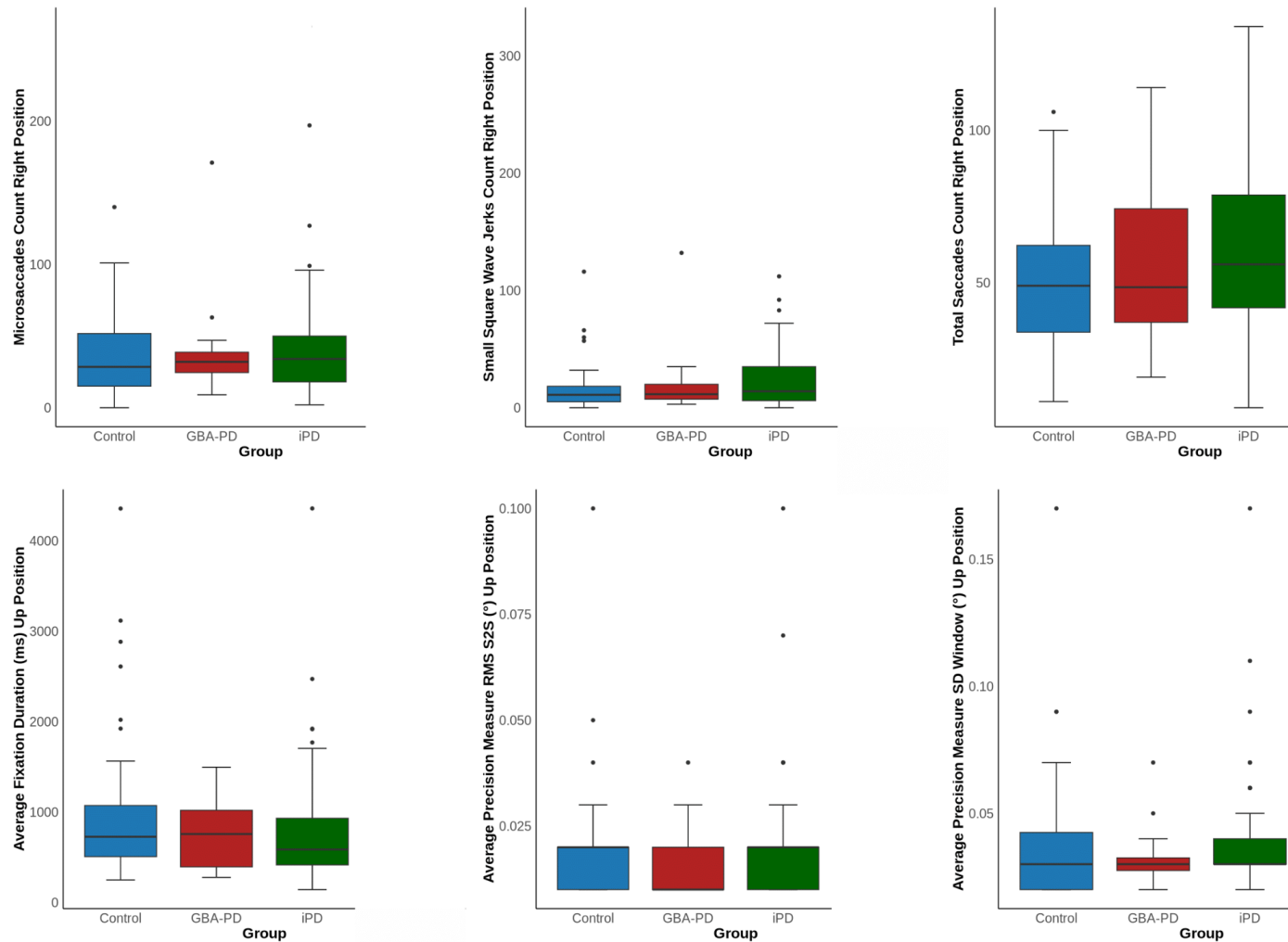


Figure 44: Positional Fixation/ Nystagmus Metrics in Parkinson's Disease. Box plots show the median, interquartile range, and full range. Generalized linear models were used to assess the effects of group, age, sex, LEDD, and disease duration. Statistical significance was set at $p < 0.05$.

Positional Fixation/ Nystagmus Metrics in Parkinson's Disease

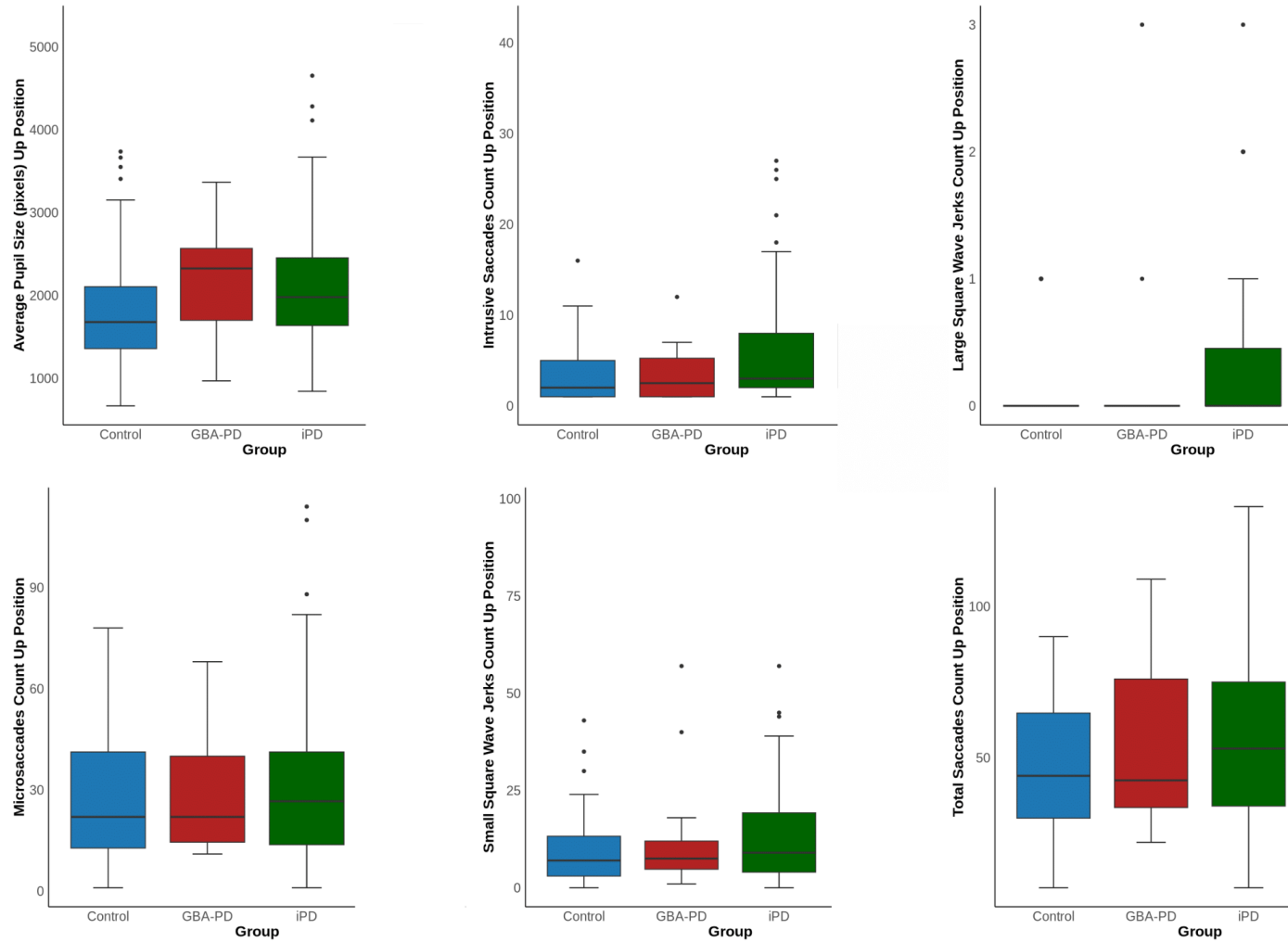


Figure 45: Positional Fixation/ Nystagmus Metrics in Parkinson's Disease. Box plots show the median, interquartile range, and full range. Generalized linear models were used to assess the effects of group, age, sex, LEDD, and disease duration. Statistical significance was set at $p < 0.05$.

Table 4: Qualitative Description of Eye Movement Metrics in the LRRK2 Mutation PD Group (Positional Fixation Paradigm).

Metric	LRRK2 Mutation PD Group Characteristics
Average Pupil Size by Direction	Consistently larger pupil sizes across all directions; largest in Up (3500–4000), followed by Right and Down (3000–3500), elevated compared to other groups.
Average Fixation Duration by Direction	Generally longer fixation durations across all directions; most pronounced increase Up (>2000 ms), with Right also elevated (2000 ms), Down and Left slightly lower (1500–2000 ms).
Microsaccade Count by Direction	Suppressed microsaccade counts in Down, Left, and Up (20–30), but markedly high in Right direction (100–120) with broad distribution.
Saccade Count by Direction	Consistently low saccade counts (30–40) across all directions; narrow interquartile ranges indicating reduced spontaneous saccadic activity.
Fixation Precision SD by Direction	Good fixation precision (low SD 0.04–0.05) in Down, Left, and Up directions; notably reduced precision (higher SD 0.06–0.07) when fixating Right.
Large Intrusive Saccade Count by Direction	Increased presence of large intrusive saccades, especially in Right direction (median 5–10, range up to 30); lower medians and fewer outliers in other directions.
Fixation Precision RMS by Direction	Good (low) fixation precision in Left (0.02) and Up (0.01) directions; higher RMS (0.05–0.06) and wider variability in Right direction; somewhat elevated RMS (0.03–0.04) in Down direction.
Large Square Wave Jerk Count by Direction	Generally low median (0) counts; presence of outliers particularly in Down and Up directions (up to 1); minimal variability in Left and Right directions.
Small Square Wave Jerk Count by Direction	Substantially increased counts in Down (100–120), Left (50–60), and especially Right (150–180) directions; low counts (5–10) in Up direction. Indicates fixation instability with intrusive movements.

Smooth Pursuit Metrics in Parkinson's Disease

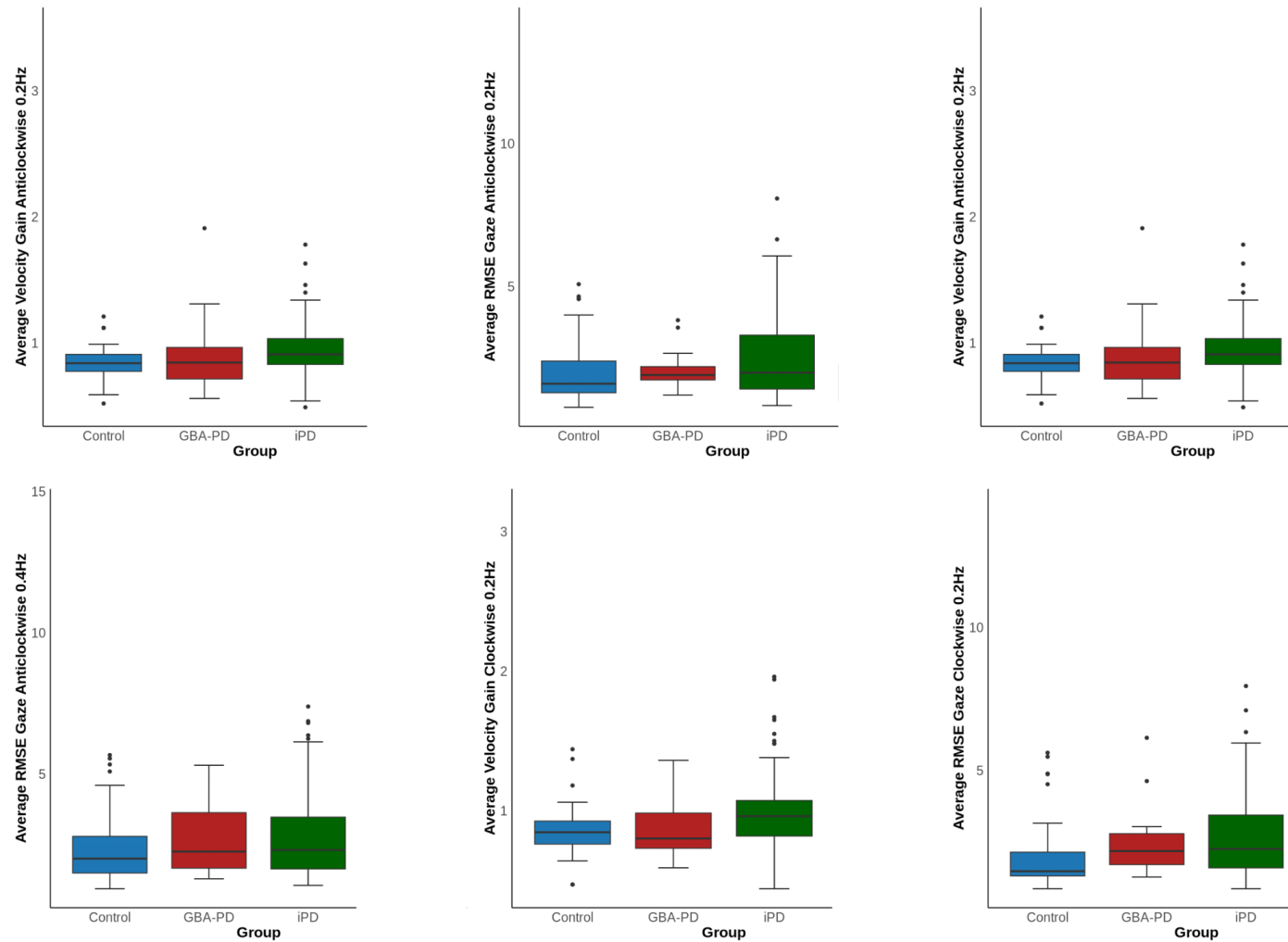


Figure 46: Smooth Pursuit Metrics in Parkinson's Disease. Box plots show the median, interquartile range, and full range. Generalized linear models were used to assess the effects of group, age, sex, LEDD, and disease duration. Statistical significance was set at $p < 0.05$.

Smooth Pursuit Metrics in Parkinson's Disease

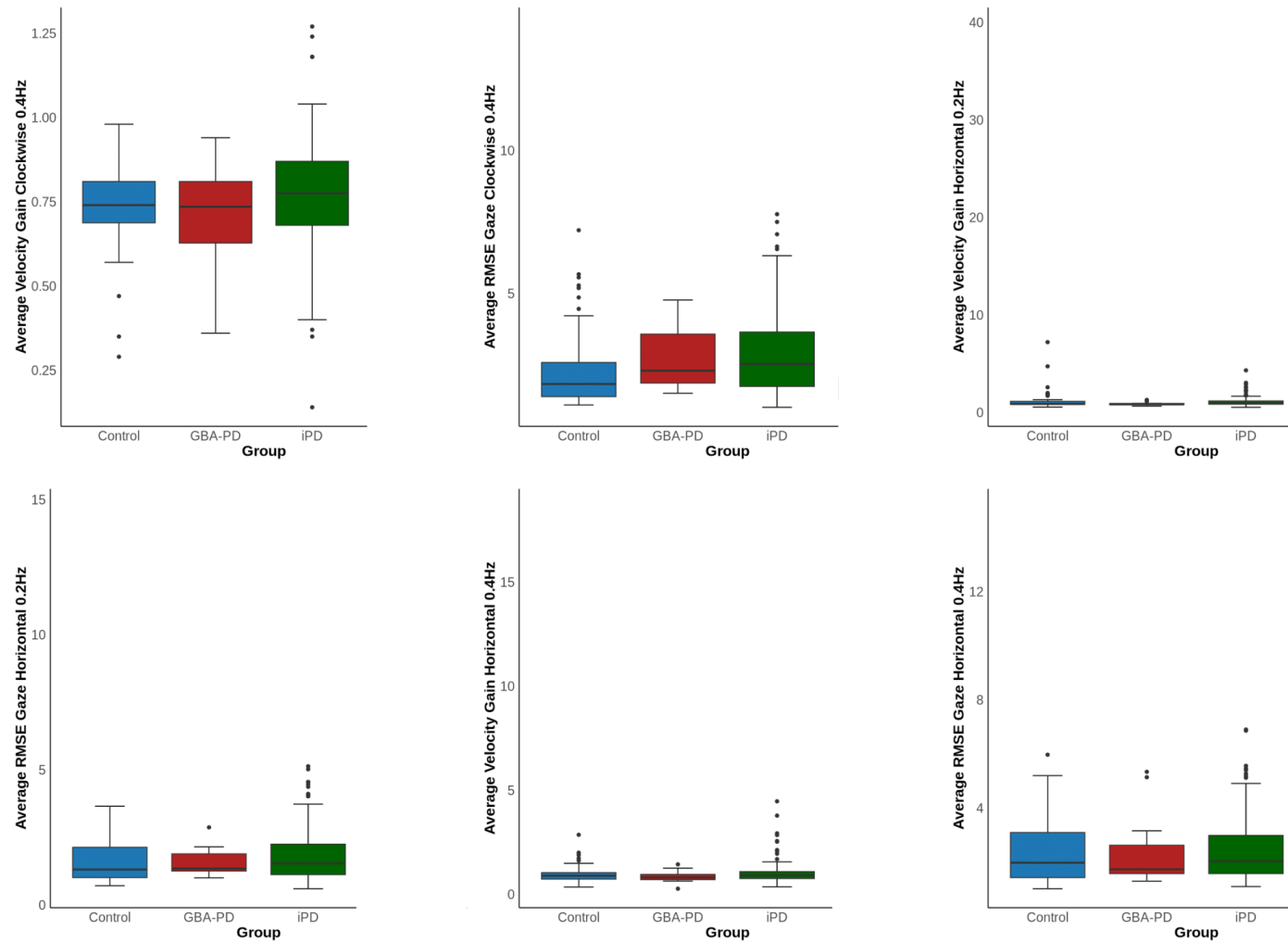


Figure 47: Smooth Pursuit Metrics in Parkinson's Disease. Box plots show the median, interquartile range, and full range. Generalized linear models were used to assess the effects of group, age, sex, LEDD, and disease duration. Statistical significance was set at $p < 0.05$.

Smooth Pursuit Metrics in Parkinson's Disease

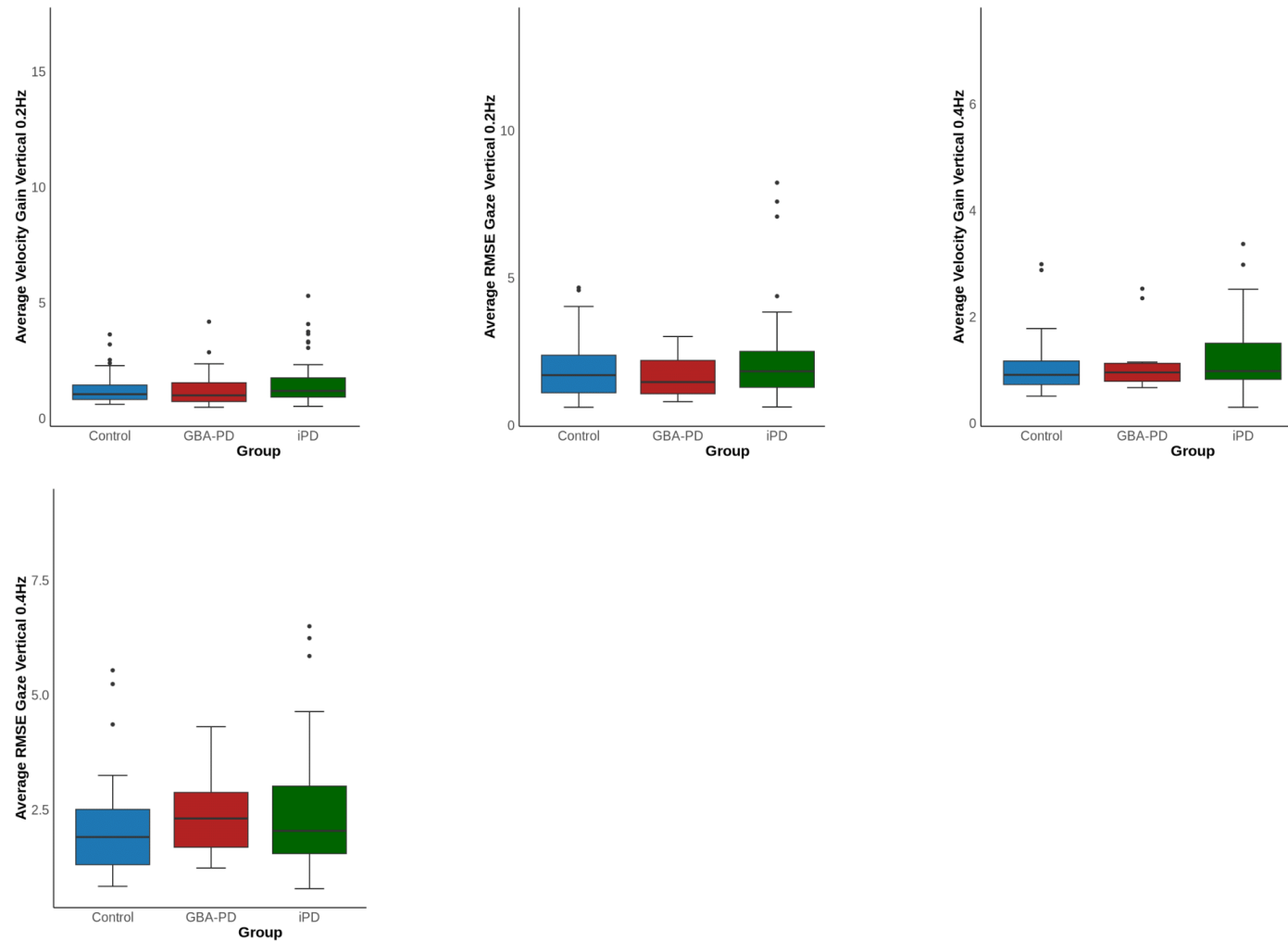


Figure 48: Smooth Pursuit Metrics in Parkinson's Disease. Box plots show the median, interquartile range, and full range. Generalized linear models were used to assess the effects of group, age, sex, LEDD, and disease duration. Statistical significance was set at $p < 0.05$.

Table 5: Qualitative Description of Pursuit Metrics in the LRRK2 Mutation PD Group.

Metric	LRRK2 Mutation PD Group Characteristics
Pursuit Velocity Gain (Anticlockwise - 0.2Hz)	Median 0.9 with tight IQR (0.85–0.95); consistent and good gain, similar to controls and slightly higher than GBA and iPD.
Pursuit Velocity Gain (Anticlockwise - 0.4Hz)	Median 0.9, highest among groups; tight IQR (0.85–0.95); strong and consistent pursuit at higher frequency.
Pursuit Velocity Gain (Clockwise - 0.2Hz)	Median 0.9, tight IQR (0.85–0.95); good and consistent gain, comparable or slightly better than controls, GBA, and iPD.
Pursuit Velocity Gain (Clockwise - 0.4Hz)	Median 0.8 with IQR (0.75–0.85); slightly lower than 0.2Hz clockwise gain, suggesting mild frequency-dependent reduction.
Pursuit Velocity Gain (Horizontal - 0.2Hz)	High median (0.9–1.0) with very tight distribution; excellent and consistent horizontal pursuit.
Pursuit Velocity Gain (Horizontal - 0.4Hz)	Slightly reduced median (0.85–0.9) with narrow IQR; good consistency but slight drop with increased frequency.
Pursuit Velocity Gain (Vertical - 0.2Hz)	High median (0.9–1.0) with tight IQR; excellent and consistent vertical pursuit.
Pursuit Velocity Gain (Vertical - 0.4Hz)	Slightly reduced median (0.8–0.9) with narrow and consistent distribution; similar to horizontal gain at 0.4Hz.
Pursuit RMSE (Horizontal - 0.2Hz)	Low median RMSE (1.5–2.0) with tight IQR and minimal outliers; excellent precision and accuracy.
Pursuit RMSE (Horizontal - 0.4Hz)	Maintained low median RMSE (1.5–2.0) and narrow IQR; good precision at higher horizontal frequency.
Pursuit RMSE (Vertical - 0.2Hz)	Notably higher median RMSE (3.0–3.5) with wider IQR and several outliers; poorer precision in vertical pursuit at this frequency.
Pursuit RMSE (Vertical - 0.4Hz)	Lower median RMSE (2.0–2.5) with narrower IQR; improved precision compared to 0.2Hz but still some outliers.
Pursuit RMSE (Anticlockwise - 0.2Hz)	Low median RMSE (1.5–2.0) with narrow IQR; good precision in anticlockwise circular pursuit.
Pursuit RMSE (Anticlockwise - 0.4Hz)	Sustained low median RMSE (1.5–2.0) with narrow IQR; good precision at higher frequency.
Pursuit RMSE (Clockwise - 0.2Hz)	Very low median RMSE (1.5–2.0) with tight IQR; excellent precision in clockwise circular pursuit.
Pursuit RMSE (Clockwise - 0.4Hz)	Maintained low median RMSE (1.5–2.0) with narrow IQR; good precision at higher clockwise frequency.

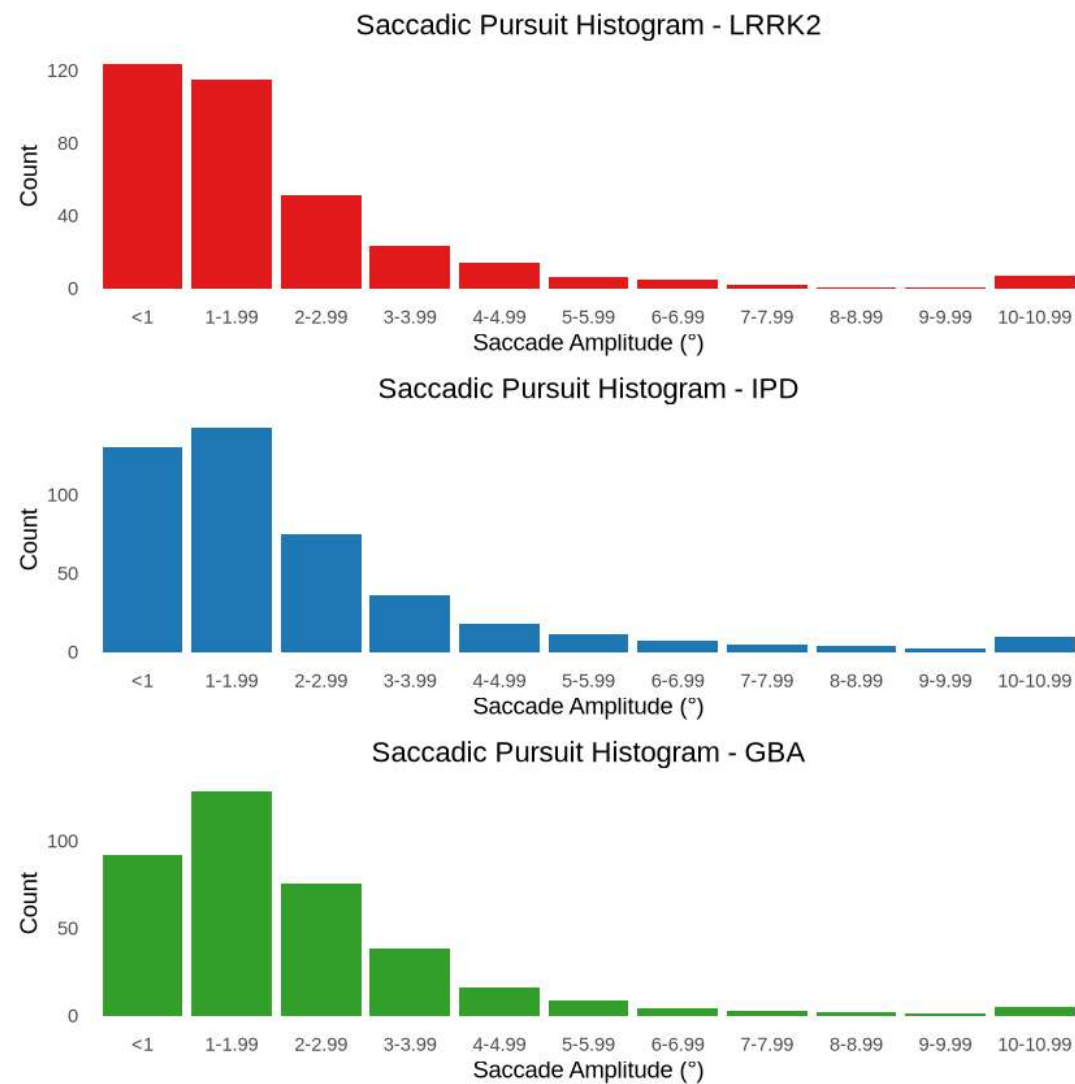


Figure 49: Saccadic Pursuit Histogram in Parkinson's Disease. Saccades grouped by amplitude.

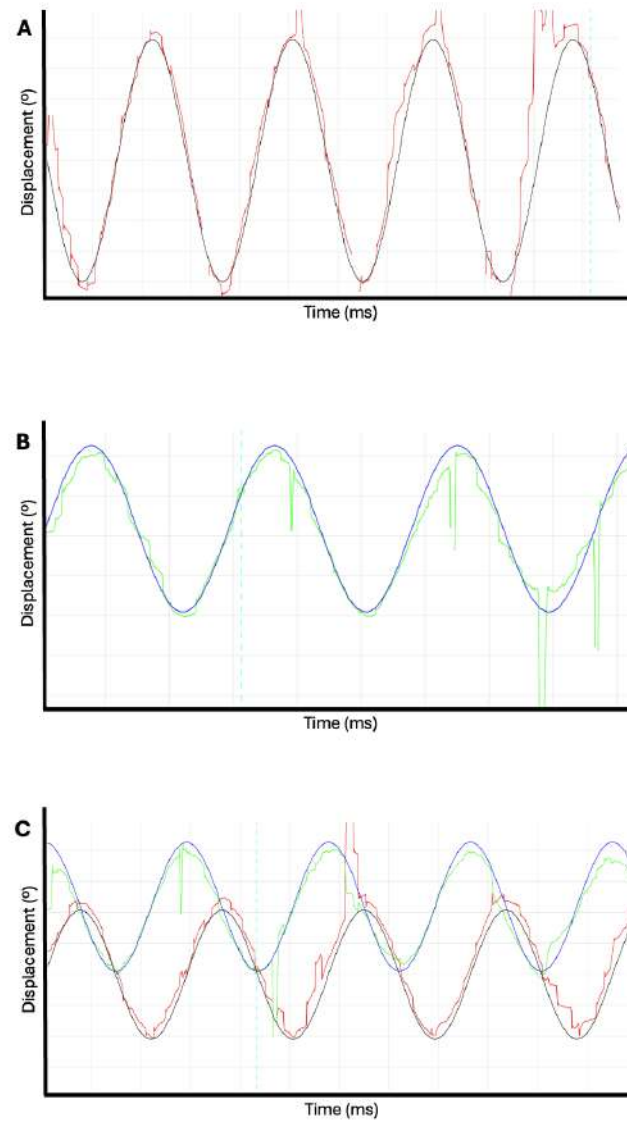


Figure 50: Smooth Pursuit Trace in Parkinson's Disease. A) Horizontal pursuit at 0.4Hz in idiopathic Parkinson's disease; B) Vertical pursuit at 0.4Hz in idiopathic Parkinson's disease;

Oblique Saccades Metrics in Parkinson's Disease

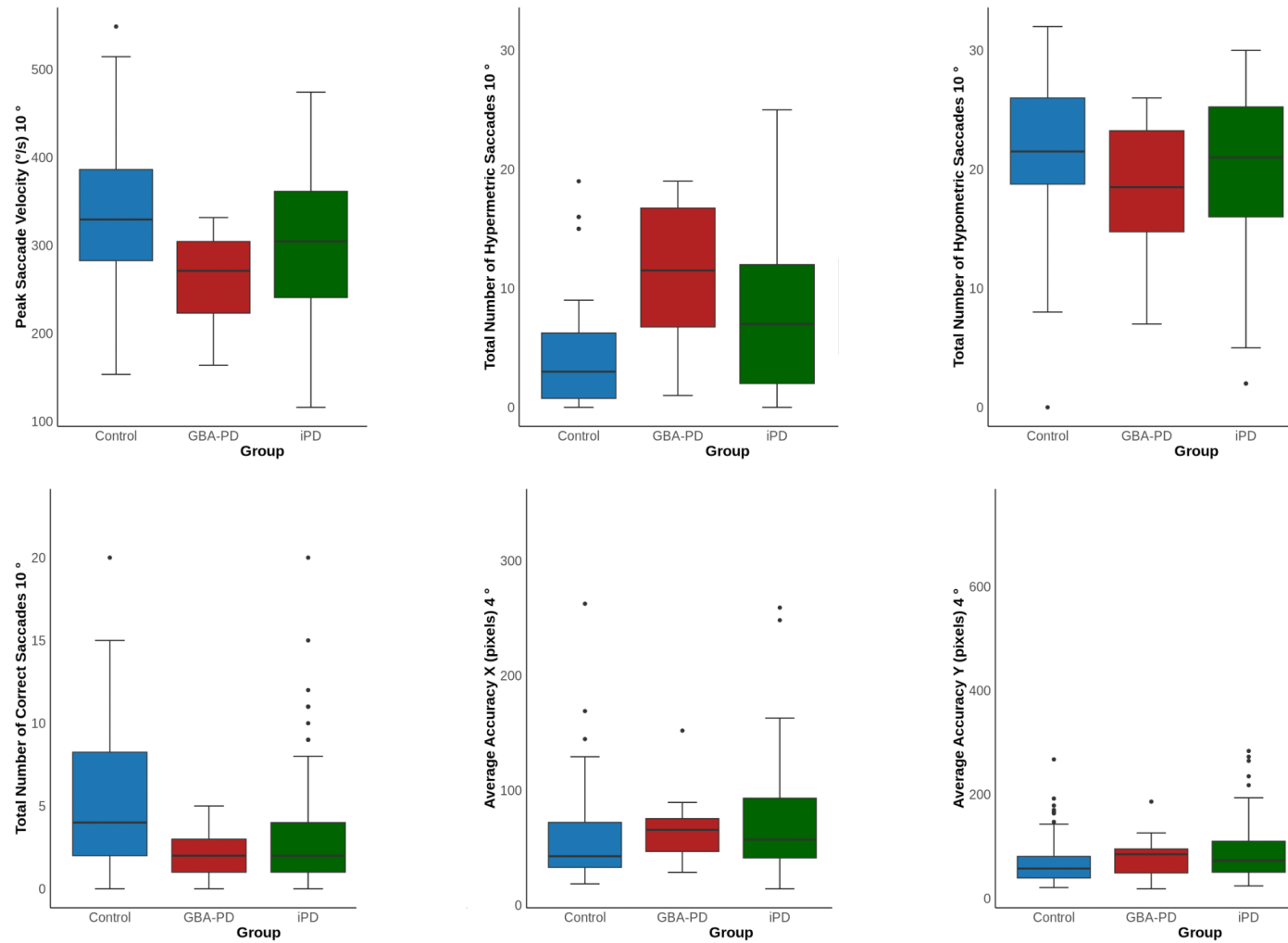


Figure 51: Oblique Saccades Metrics in Parkinson's Disease. Box plots show the median, interquartile range, and full range. Generalized linear models were used to assess the effects of group, age, sex, LEDD, and disease duration. Statistical significance was set at $p < 0.05$.

Oblique Saccades Metrics in Parkinson's Disease

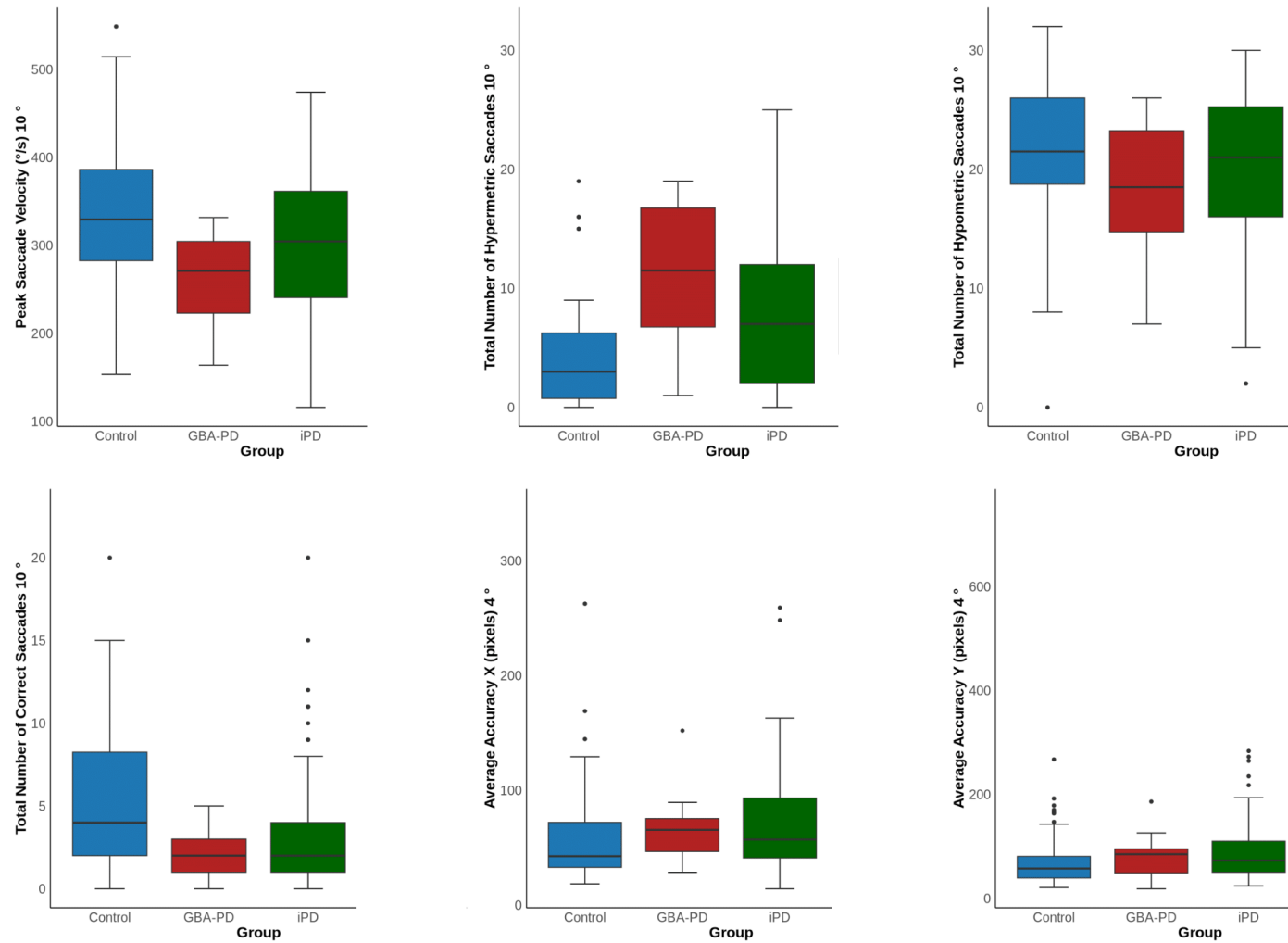


Figure 52: Oblique Saccades Metrics in Parkinson's Disease. Box plots show the median, interquartile range, and full range. Generalized linear models were used to assess the effects of group, age, sex, LEDD, and disease duration. Statistical significance was set at $p < 0.05$.

Oblique Saccades Metrics in Parkinson's Disease

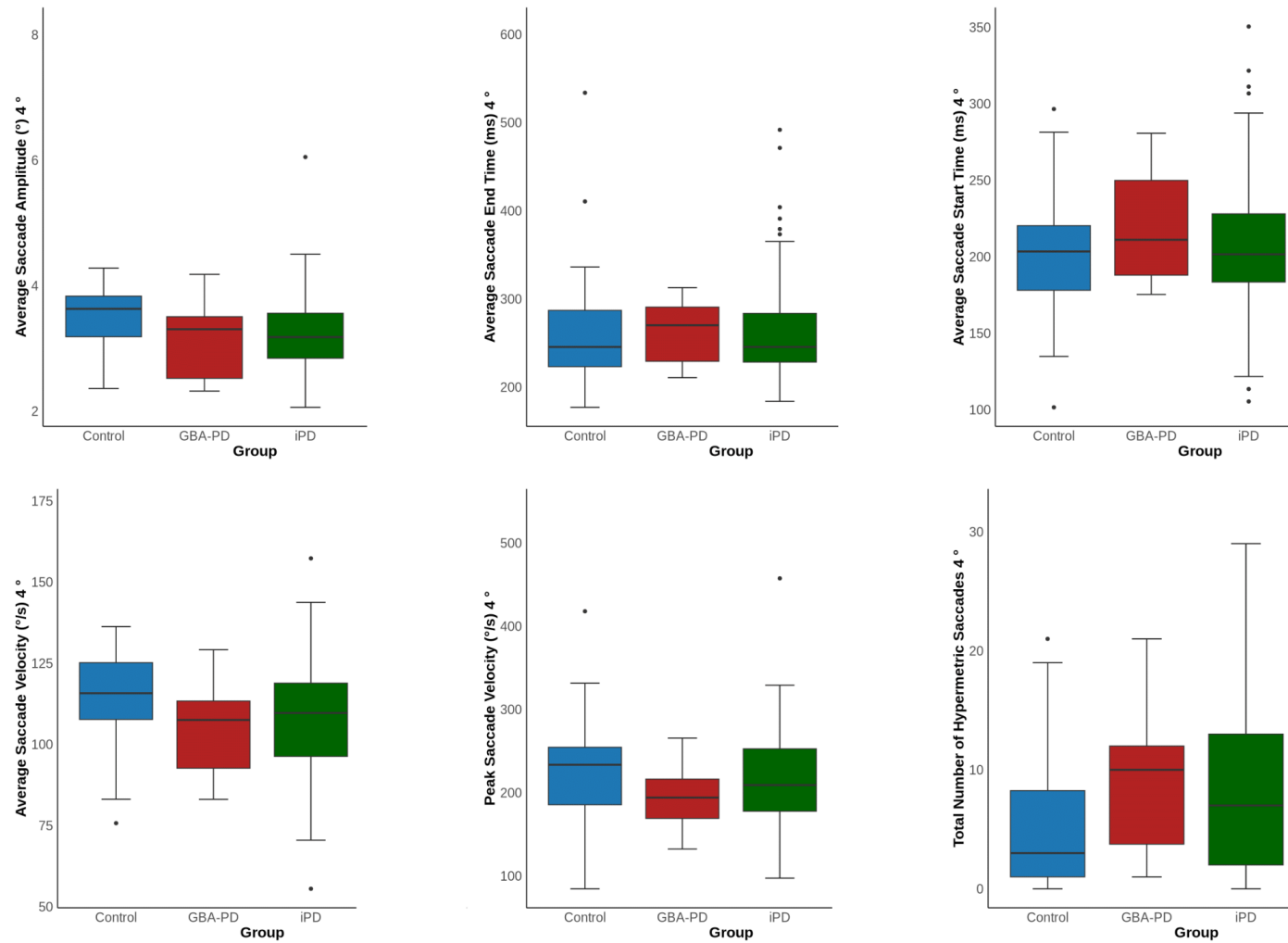


Figure 53: Oblique Saccades Metrics in Parkinson's Disease. Box plots show the median, interquartile range, and full range. Generalized linear models were used to assess the effects of group, age, sex, LEDD, and disease duration. Statistical significance was set at $p < 0.05$.

Oblique Saccades Metrics in Parkinson's Disease

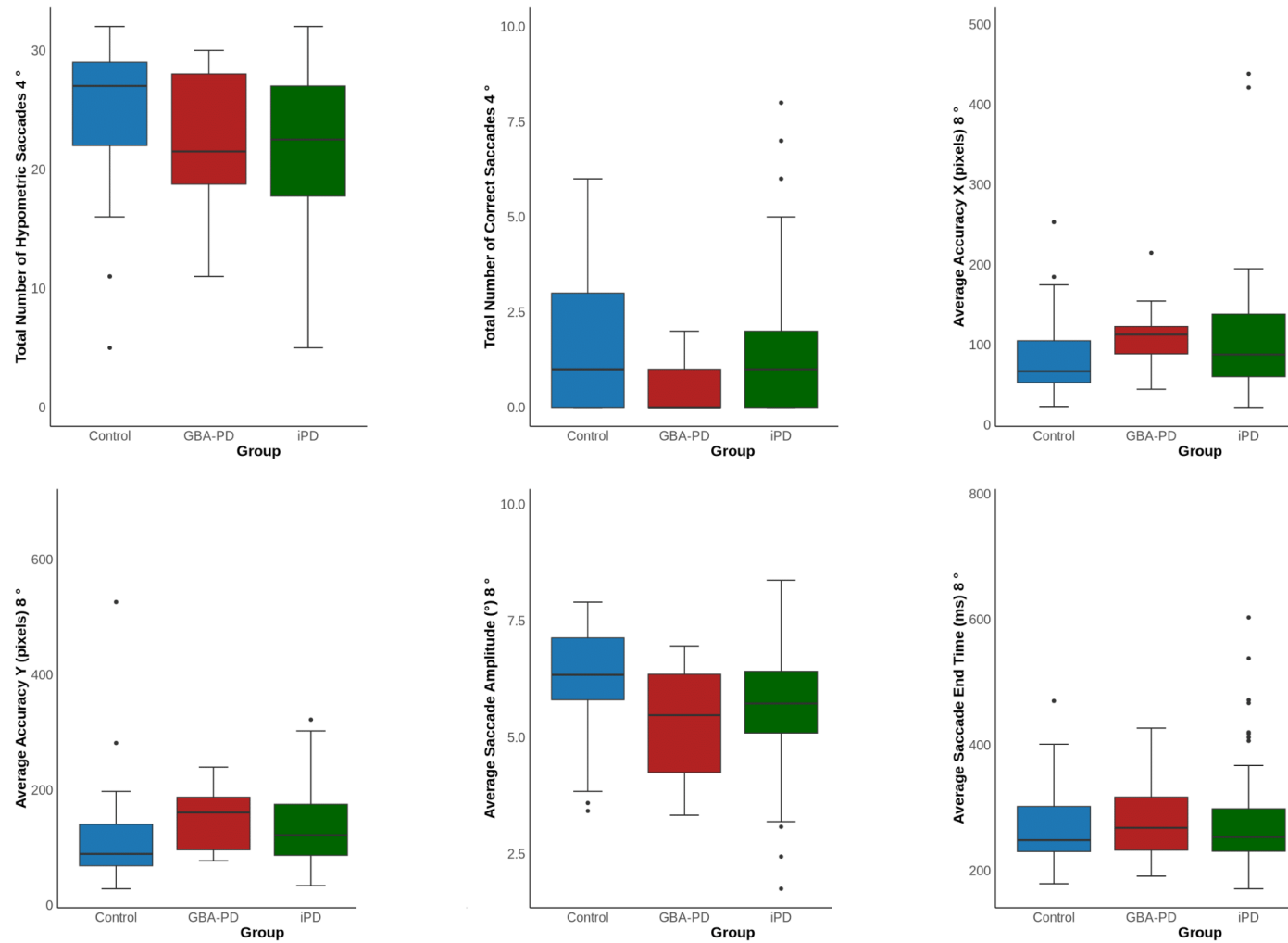


Figure 54: Oblique Saccades Metrics in Parkinson's Disease. Box plots show the median, interquartile range, and full range. Generalized linear models were used to assess the effects of group, age, sex, LEDD, and disease duration. Statistical significance was set at $p < 0.05$.

Oblique Saccades Metrics in Parkinson's Disease

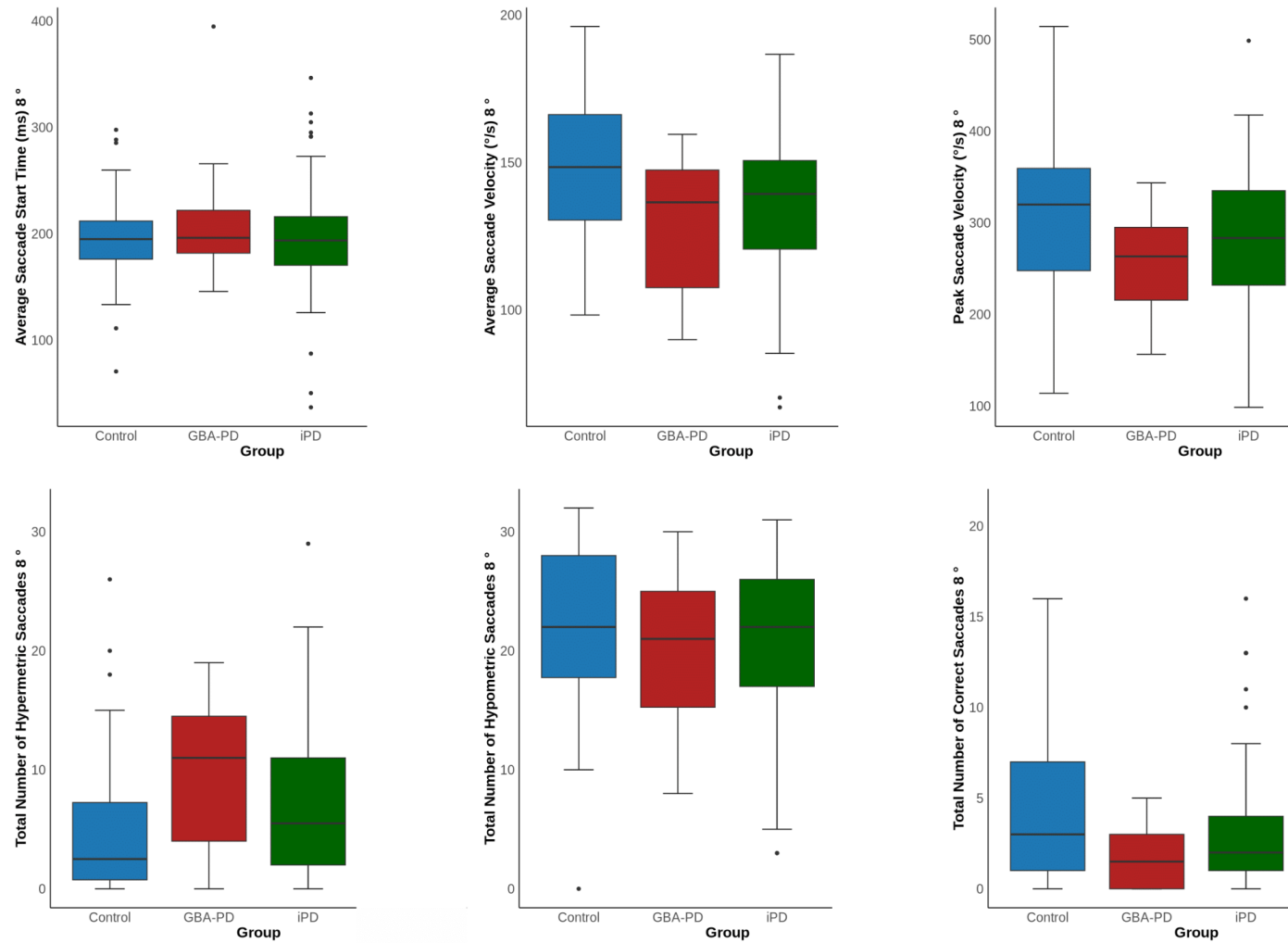


Figure 55: Oblique Saccades Metrics in Parkinson's Disease. Box plots show the median, interquartile range, and full range. Generalized linear models were used to assess the effects of group, age, sex, LEDD, and disease duration. Statistical significance was set at $p < 0.05$.

Table 6: Qualitative Description of Oblique Saccades Metrics in the LRRK2 Mutation PD Group.

Metric	LRRK2 Mutation PD Group Characteristics
Oblique Saccade Average Velocity	Increasing median velocity with eccentricity (140–150 deg/s at 4°, 160–170 deg/s at 8°, 170–180 deg/s at 10°). Generally consistent with controls but slightly slower than iPD at 8°.
Oblique Saccade Start Time	Consistent median start time (220–230 ms) across all eccentricities with narrow IQR, comparable to other groups.
Oblique Saccade Amplitude	Median amplitude increases with eccentricity (3.5–4.0° at 4°, 6.0–6.5° at 8°, 7.5–8.0° at 10°), showing expected scaling and consistent performance.
Oblique Saccade Y Accuracy	Increasing variability and poorer vertical accuracy with eccentricity; median rises from 50–75 units at 4° to 175–200 units at 10°, with many outliers indicating less precise vertical targeting.
Oblique Saccade Correct Count	Relatively stable correct counts (10–12 at 4° and 8°), with a slight decrease (8–10) at 10°, comparable to other groups.
Oblique Saccade End Time	Increasing median end time with eccentricity (250–275 ms at 4°, 300 ms at 8°, 325–350 ms at 10°), reflecting longer completion times for larger saccades.
Oblique Saccade X Accuracy	Median horizontal deviation increases with eccentricity (50–75 units at 4°, 100 units at 8°, 150–175 units at 10°), indicating growing horizontal inaccuracy for larger saccades.
Oblique Saccade Peak Velocity	Median peak velocity rises with eccentricity (200 deg/s at 4°, 250 deg/s at 8°, 275–300 deg/s at 10°), consistent with saccade main sequence.
Oblique Saccade Hypermetric Count	Low median counts (0–5) across eccentricities with occasional higher outliers, indicating infrequent overshooting saccades.
Oblique Saccade Hypometric Count	Increasing median counts with eccentricity (10–15 at 4°, 15–20 at 8°, 20–25 at 10°), suggesting more frequent undershooting of targets for larger saccades.

Antisaccades Horizontal Metrics in Parkinson's Disease

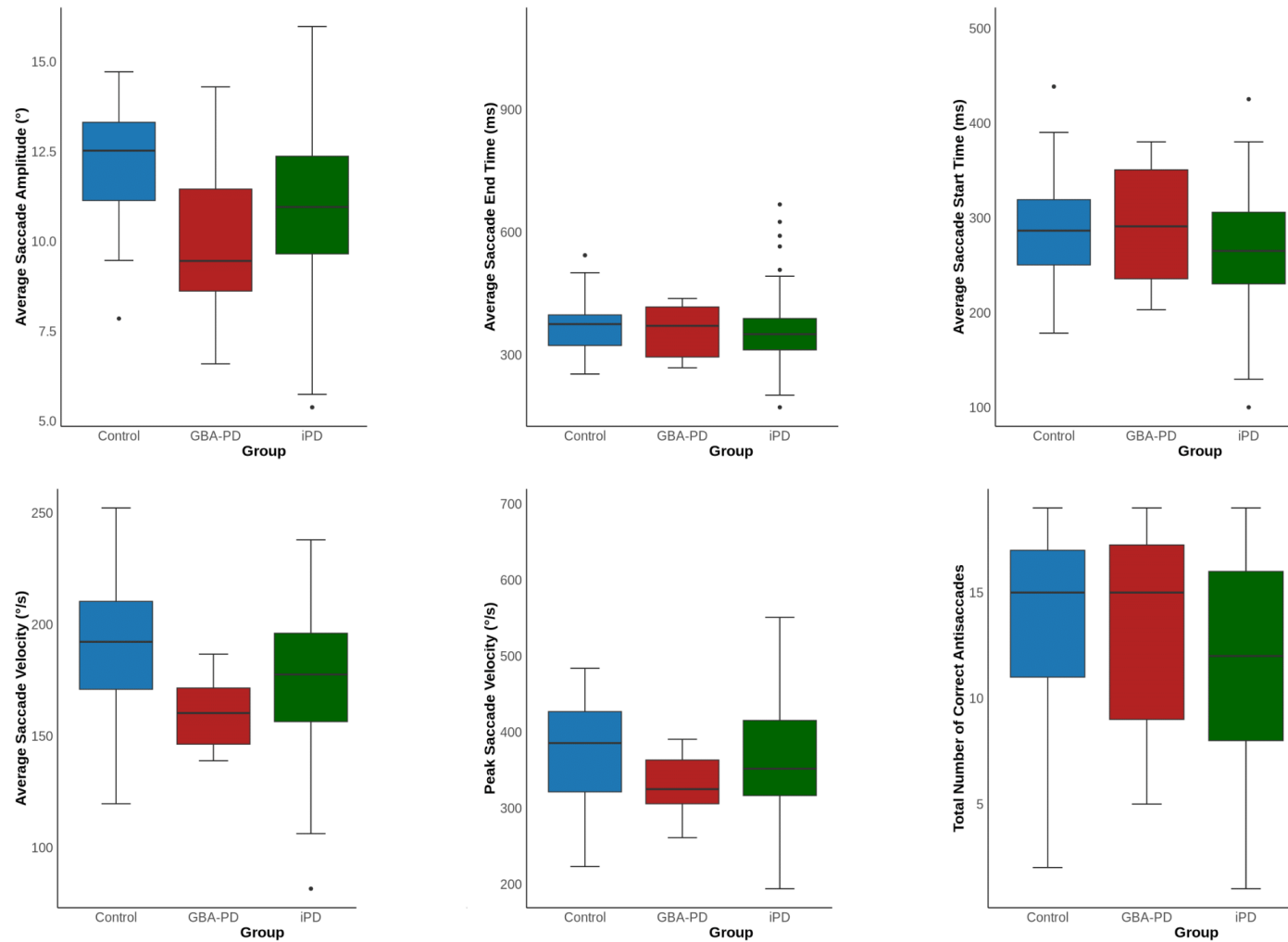


Figure 56: Antisaccades Horizontal Metrics in Parkinson's Disease. Box plots show the median, interquartile range, and full range. Generalized linear models were used to assess the effects of group, age, sex, LEDD, and disease duration. Statistical significance was set at $p < 0.05$.

Antisaccades Horizontal Metrics in Parkinson's Disease

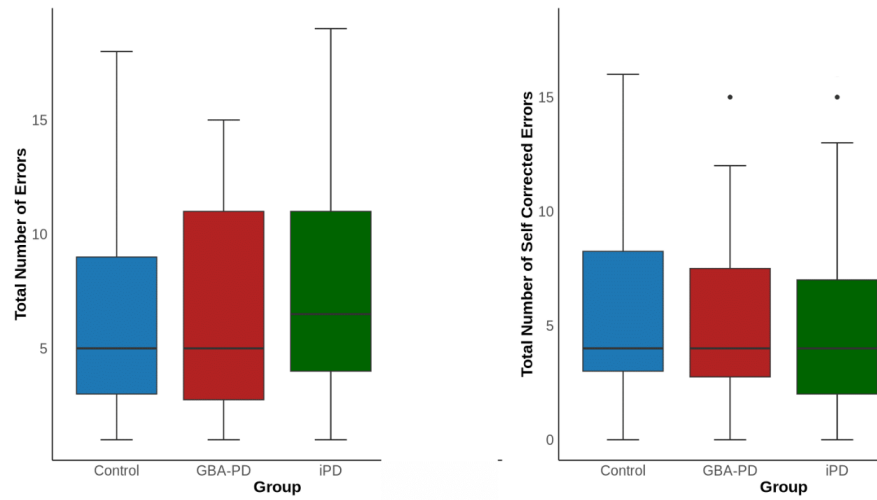


Figure 57: Antisaccades Horizontal Metrics in Parkinson's Disease. Box plots show the median, interquartile range, and full range. Generalized linear models were used to assess the effects of group, age, sex, LEDD, and disease duration. Statistical significance was set at $p < 0.05$.

Antisaccades Vertical Metrics in Parkinson's Disease

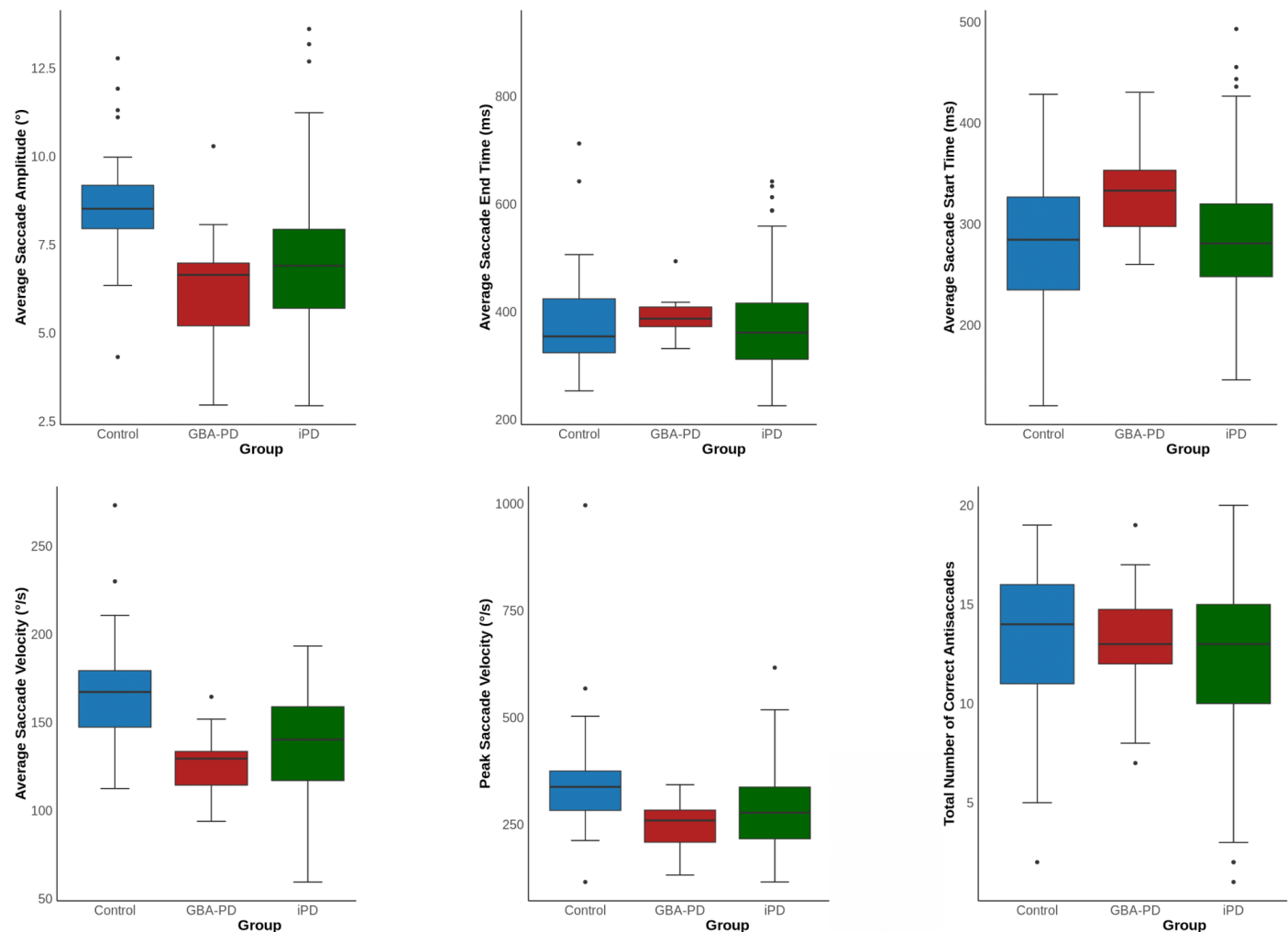


Figure 58: Antisaccades Vertical Metrics in Parkinson's Disease. Box plots show the median, interquartile range, and full range. Generalized linear models were used to assess the effects of group, age, sex, LEDD, and disease duration. Statistical significance was set at $p < 0.05$.

Antisaccades Vertical Metrics in Parkinson's Disease

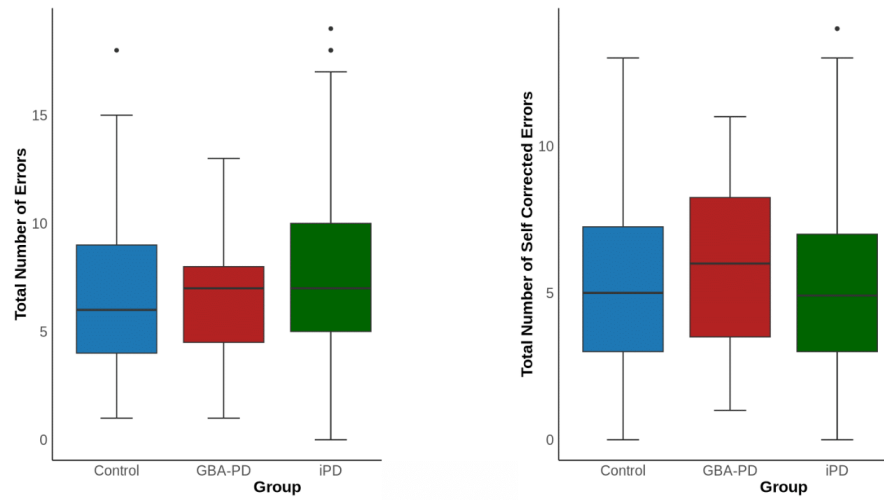


Figure 59: Antisaccades Vertical Metrics in Parkinson's Disease. Box plots show the median, interquartile range, and full range. Generalized linear models were used to assess the effects of group, age, sex, LEDD, and disease duration. Statistical significance was set at $p < 0.05$.

Table 7: Qualitative Description of Antisaccades Metrics in the LRRK2 Mutation PD Group.

Metric		LRRK2 Mutation PD Group Characteristics
Antisaccade Velocity	Average	High median velocity (225-250 deg/s) in Horizontal direction with narrow IQR indicating consistency; lower median (175-200 deg/s) in Vertical direction comparable to other PD groups.
Antisaccade Peak Velocity		High median peak velocity (600-700 deg/s) in Horizontal direction with consistent distribution; lower median (400-450 deg/s) in Vertical direction, comparable to other PD groups.
Antisaccade Count	Correct	High and consistent correct counts: median 17-18 Horizontal, 15 Vertical, indicating strong inhibitory control.
Antisaccade Start Time		Consistent start times in both directions, median around 300-325 ms with tight IQR.
Antisaccade Amplitude		Consistent amplitudes across directions: 10-11 degrees Horizontal, 8-9 degrees Vertical with narrow IQRs.
Antisaccade Corrected Count	Self-	Very low median self-corrected counts (0-1) in both directions with some outliers, indicating high initial accuracy.
Antisaccade Count	Error	Low median error counts (4-5) in both directions; horizontal errors show more variability with some individuals having higher errors.
Antisaccade End Time		Consistent end times around 350-375 ms in both directions with relatively tight IQRs.

Reflexive Saccades Horizontal Metrics in Parkinson's Disease

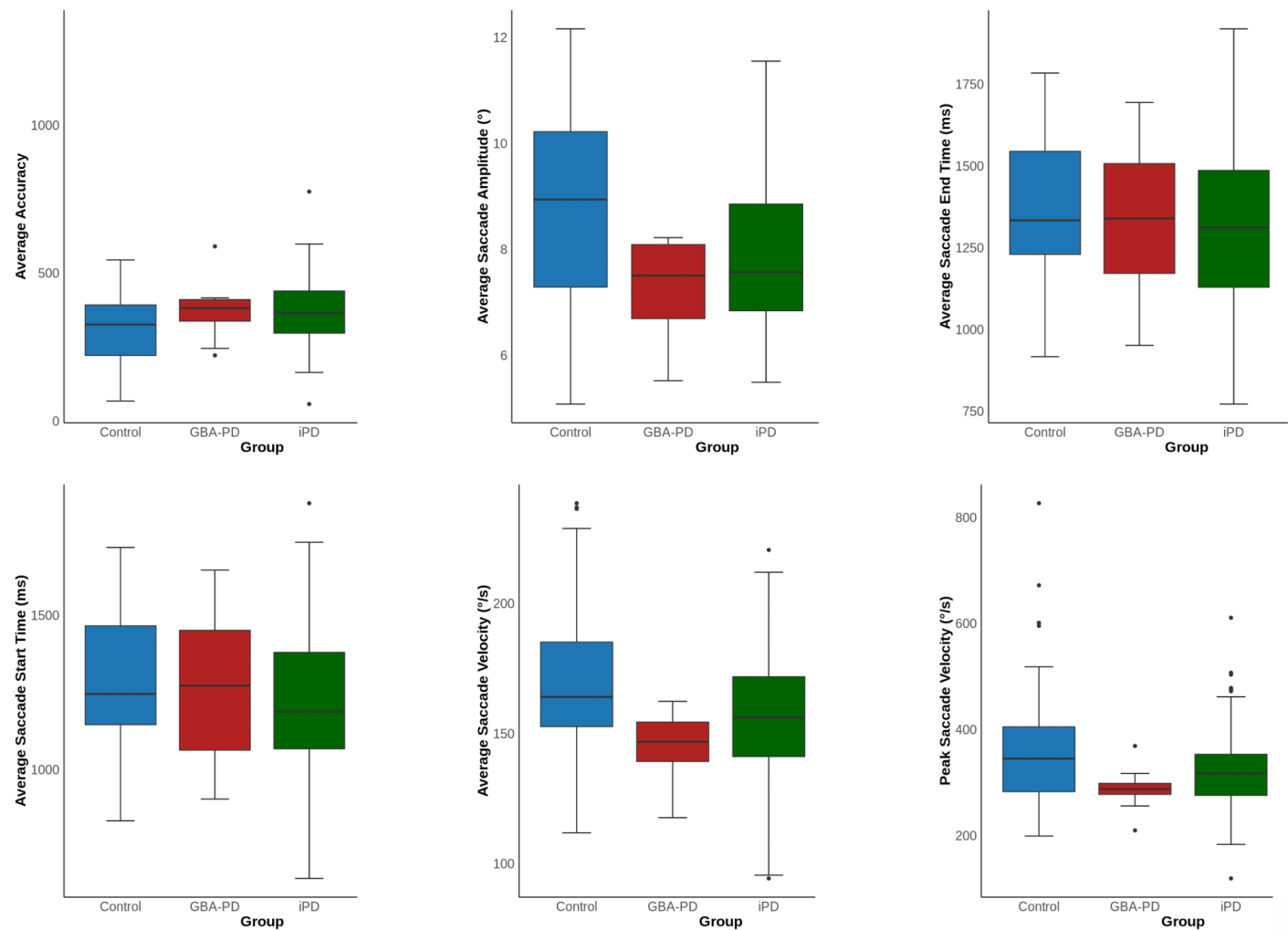


Figure 60: Reflexive Saccades Horizontal Metrics in Parkinson's Disease. Box plots show the median, interquartile range, and full range. Generalized linear models were used to assess the effects of group, age, sex, LEDD, and disease duration. Statistical significance was set at $p < 0.05$.

Reflexive Saccades Horizontal Metrics in Parkinson's Disease

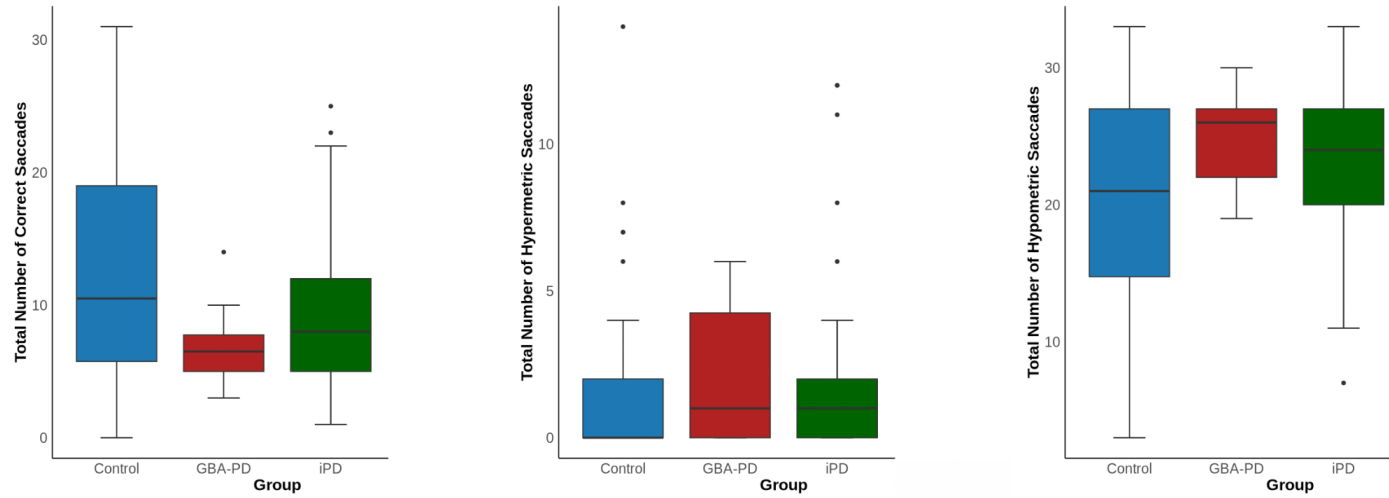


Figure 61: Reflexive Saccades Horizontal Metrics in Parkinson's Disease. Box plots show the median, interquartile range, and full range. Generalized linear models were used to assess the effects of group, age, sex, LEDD, and disease duration. Statistical significance was set at $p < 0.05$.

Reflexive Saccades Vertical Metrics in Parkinson's Disease

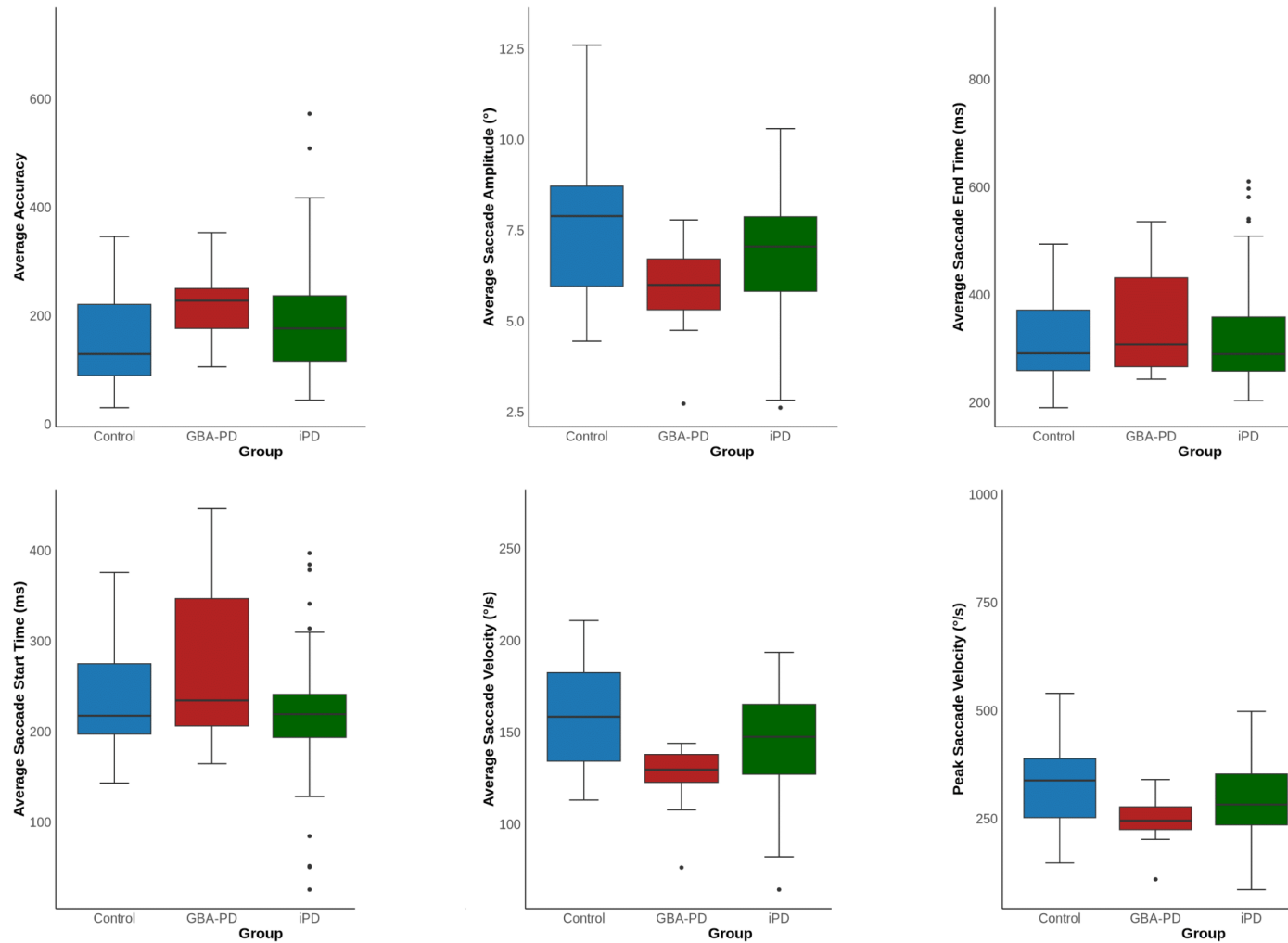


Figure 62: Reflexive Saccades Vertical Metrics in Parkinson's Disease. Box plots show the median, interquartile range, and full range. Generalized linear models were used to assess the effects of group, age, sex, LEDD, and disease duration. Statistical significance was set at $p < 0.05$.

Reflexive Saccades Vertical Metrics in Parkinson's Disease

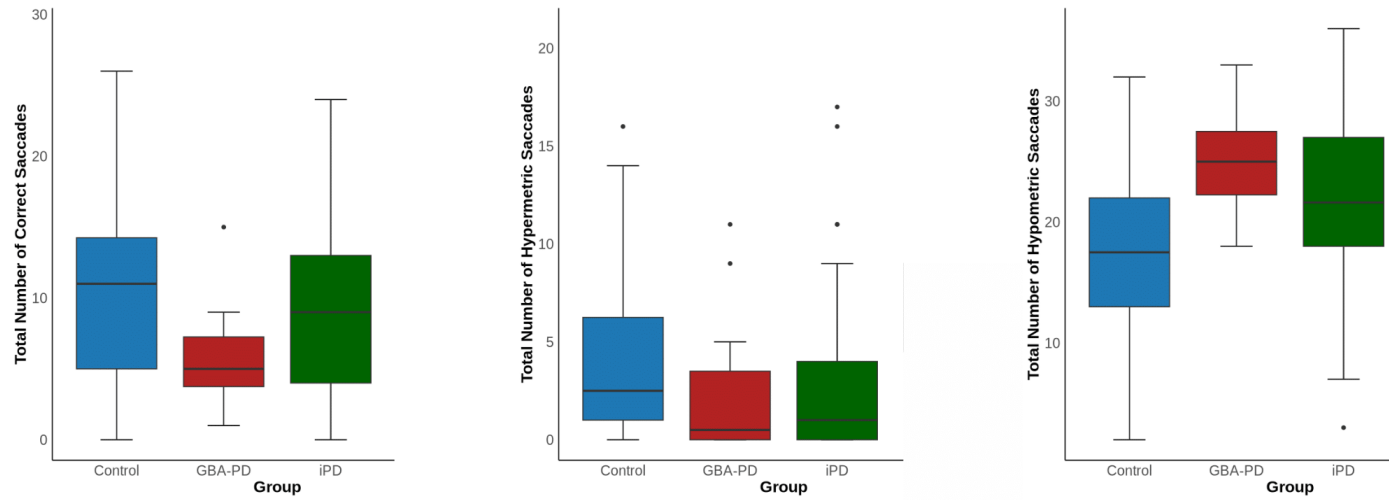


Figure 63: Reflexive Saccades Vertical Metrics in Parkinson's Disease. Box plots show the median, interquartile range, and full range. Generalized linear models were used to assess the effects of group, age, sex, LEDD, and disease duration. Statistical significance was set at $p < 0.05$.

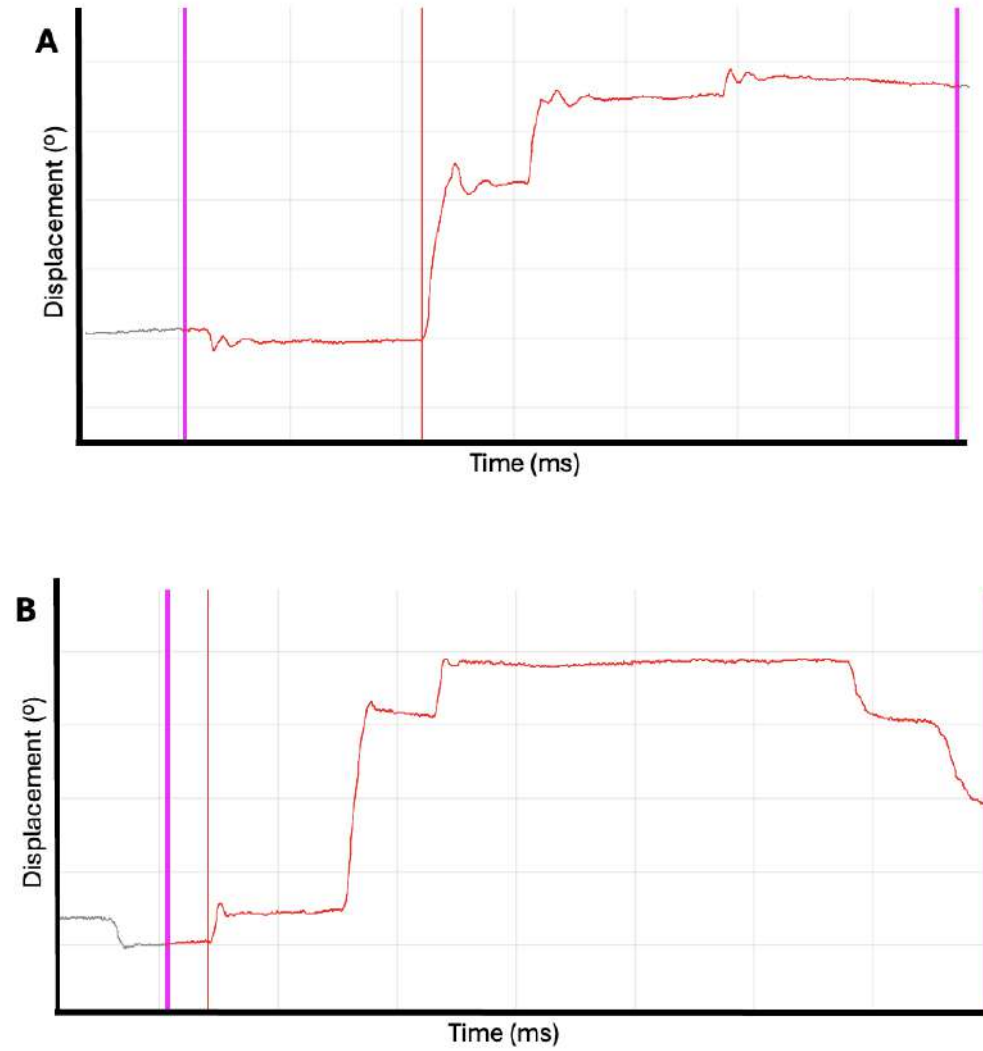


Figure 64: Hypometric Saccades in Parkinson's Disease. A) Hypometric Saccades in idiopathic Parkinson's disease B) Hypometric Saccades in GBA mutation Parkinson's disease;

Table 8: Qualitative Description of Reflexive Saccades Metrics in the LRRK2 Mutation PD Group.

Metric	LRRK2 Mutation PD Group Characteristics
Reflexive Saccade Average Velocity	High median velocity (225-250 deg/s) in Horizontal direction with narrow IQR; lower median (175-200 deg/s) in Vertical direction comparable to other PD groups and controls.
Reflexive Saccade Peak Velocity	High median peak velocity (600-700 deg/s) in Horizontal direction with compact IQR, comparable to controls; lower median (400-450 deg/s) in Vertical direction, consistent with other PD groups.
Reflexive Saccade Amplitude	Consistent amplitudes: 10-11 degrees Horizontal, 8-9 degrees Vertical with narrow IQRs, generally comparable to controls.
Reflexive Saccade Start Time	Consistent start times in both directions, median 180-200 ms with tight IQRs.
Reflexive Saccade End Time	Consistent end times in both directions, median 225-250 ms with narrow IQRs.
Reflexive Saccade Accuracy	Good and consistent accuracy (100 units median) in both Horizontal and Vertical directions.
Reflexive Saccade Correct Count	High and consistent correct counts: 20-22 Horizontal, 18-20 Vertical, indicating reliable saccadic generation.
Reflexive Saccade Hypermetric Count	Very low median count (0-1) in both directions, with some outliers; suggests minimal overshooting.
Reflexive Saccade Hypometric Count	Very low median count (0-1) in both directions, with some outliers; suggests minimal undershooting.

Timescale Analysis of Reflexive Saccades in Parkinson's Disease

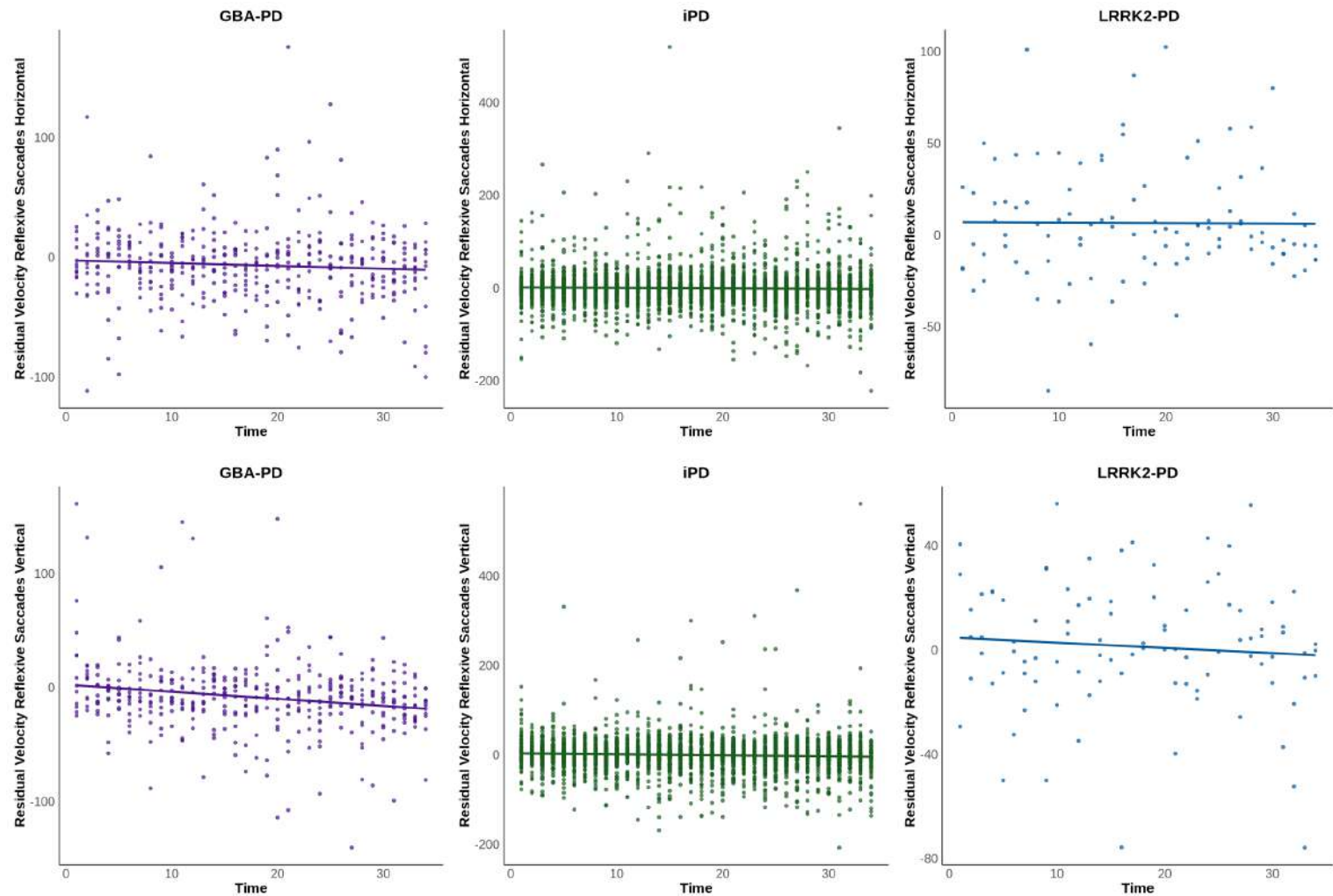


Figure 65: Timescale Analysis of Reflexive Saccades in Parkinson's Disease. Residual velocity calculated through the main sequence effect.

Volitional Saccades Horizontal Metrics in Parkinson's Disease

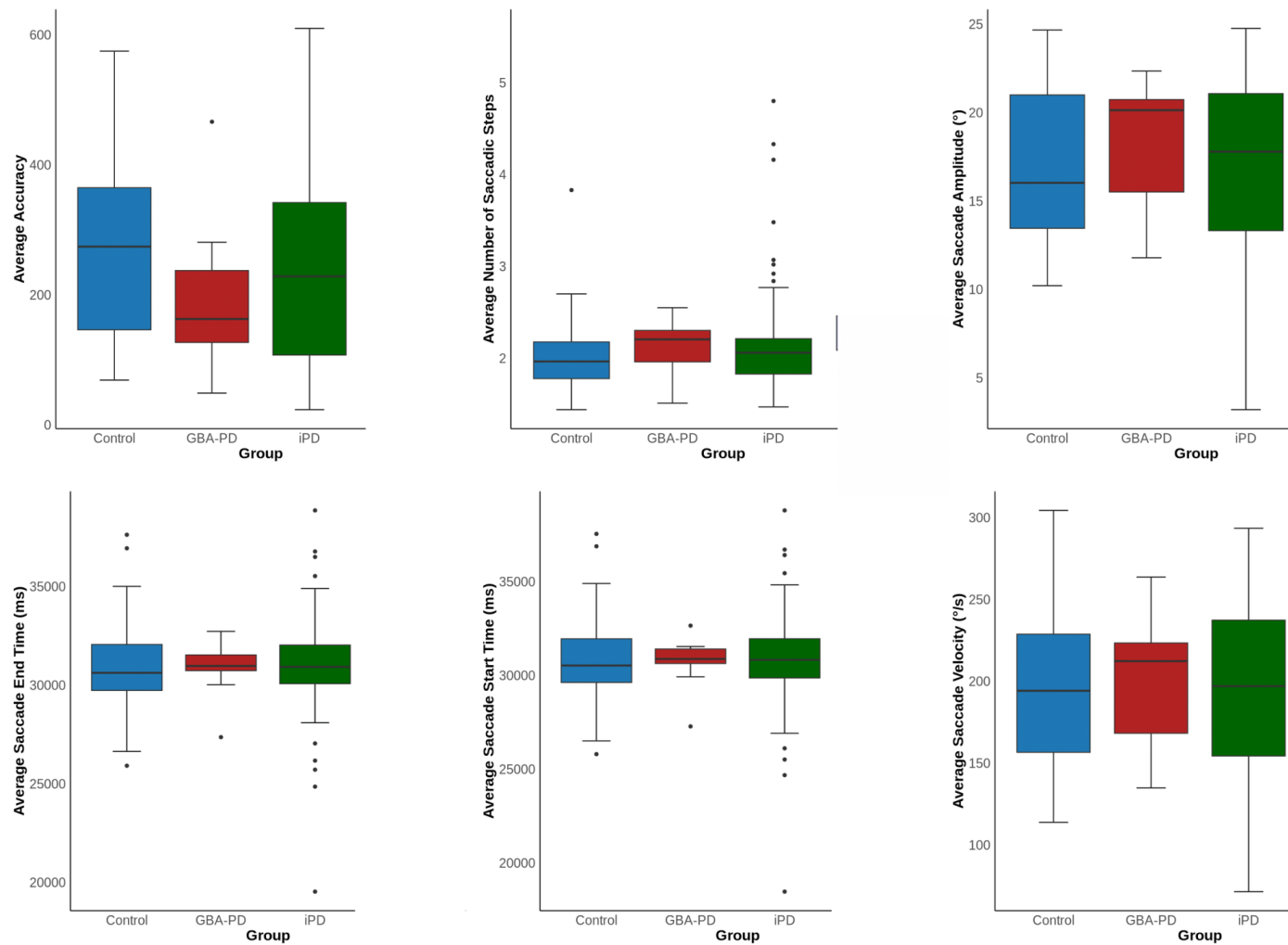


Figure 66: Volitional Saccades Horizontal Metrics in Parkinson's Disease. Box plots show the median, interquartile range, and full range. Generalized linear models were used to assess the effects of group, age, sex, LEDD, and disease duration. Statistical significance was set at $p < 0.05$.

Volitional Saccades Horizontal Metrics in Parkinson's Disease

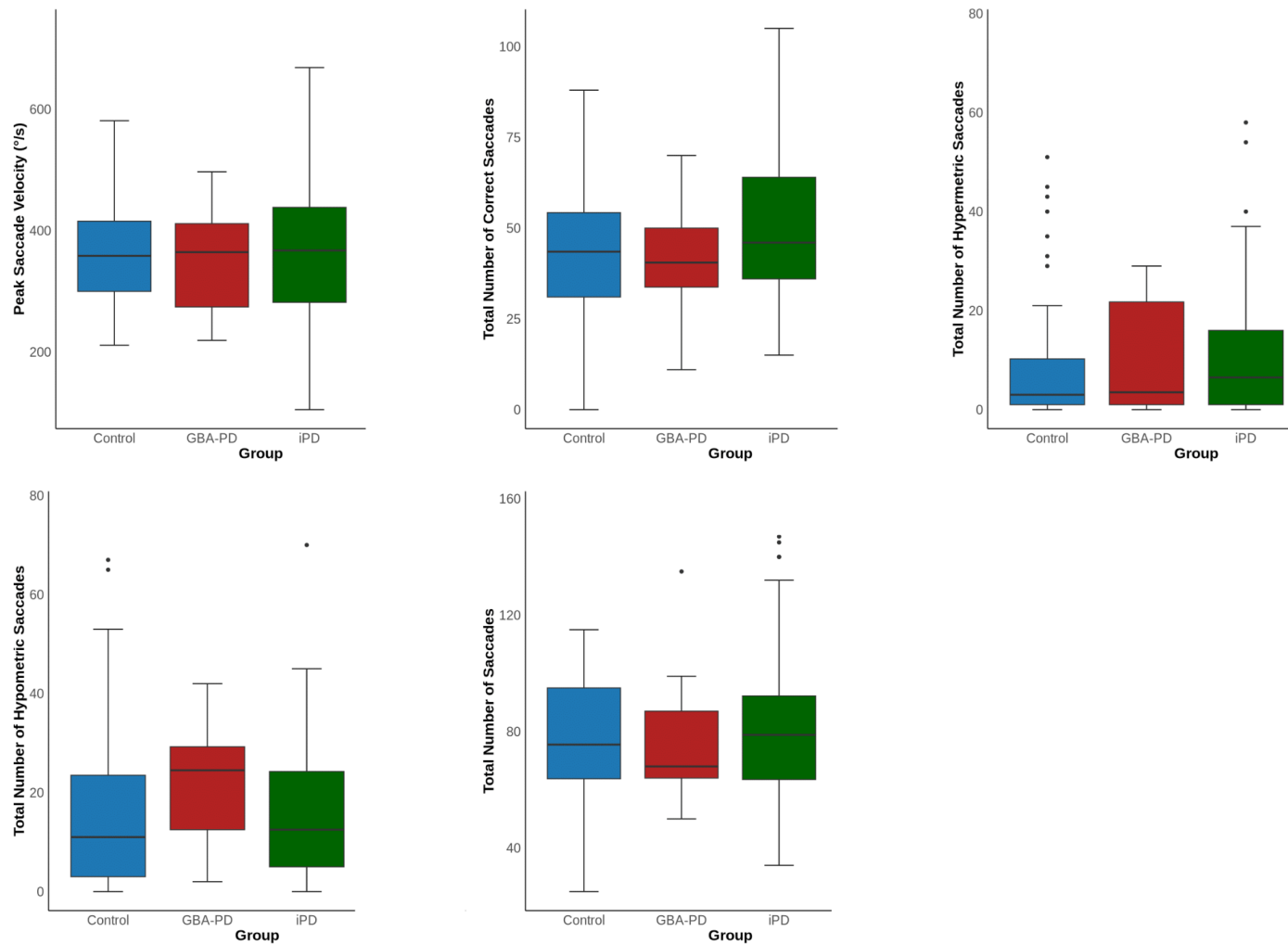


Figure 67: Volitional Saccades Horizontal Metrics in Parkinson's Disease. Box plots show the median, interquartile range, and full range. Generalized linear models were used to assess the effects of group, age, sex, LEDD, and disease duration. Statistical significance was set at $p < 0.05$.

Volitional Saccades Vertical Metrics in Parkinson's Disease

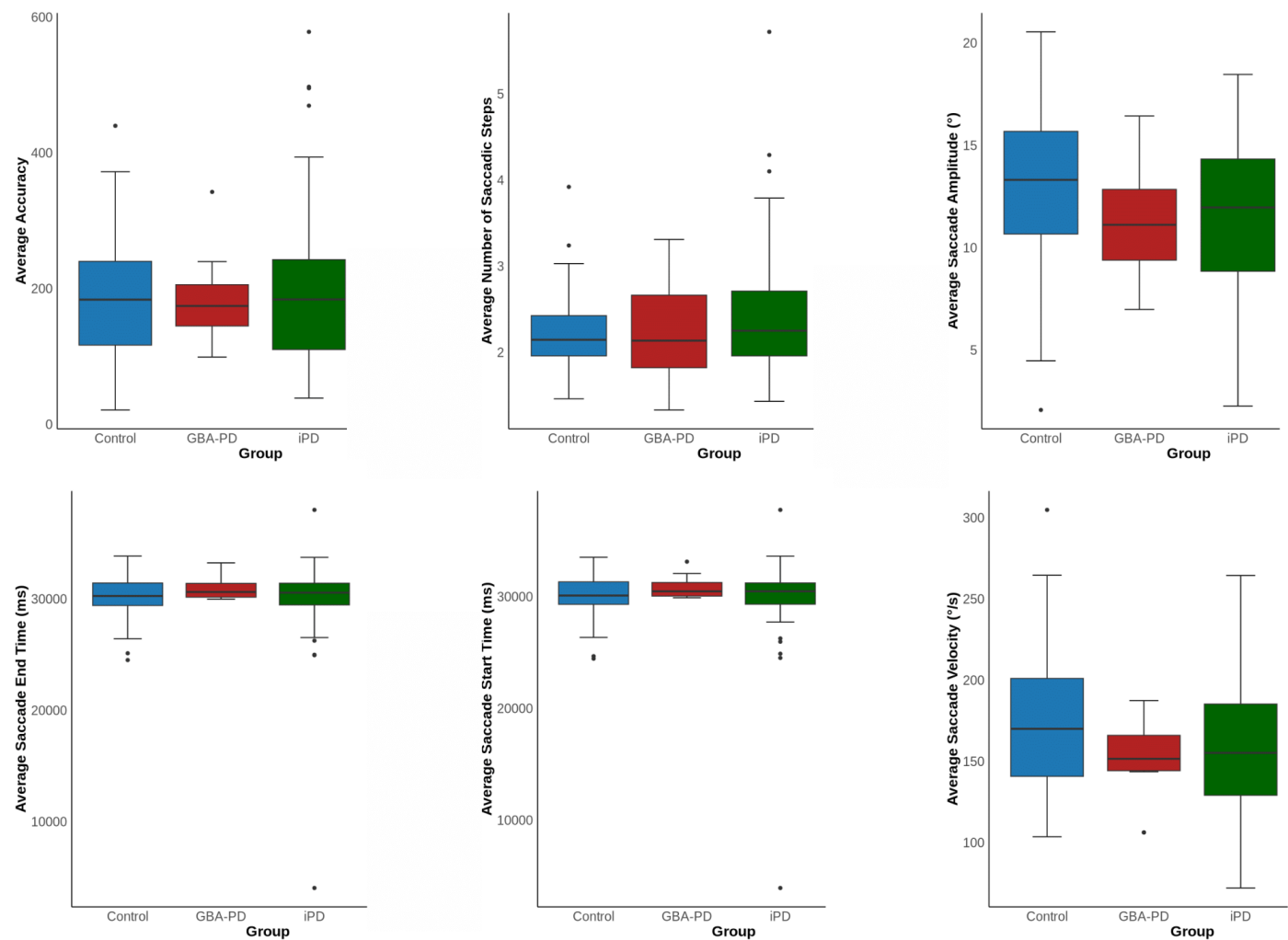


Figure 68: Volitional Saccades Vertical Metrics in Parkinson's Disease. Box plots show the median, interquartile range, and full range. Generalized linear models were used to assess the effects of group, age, sex, LEDD, and disease duration. Statistical significance was set at $p < 0.05$.

Volitional Saccades Vertical Metrics in Parkinson's Disease

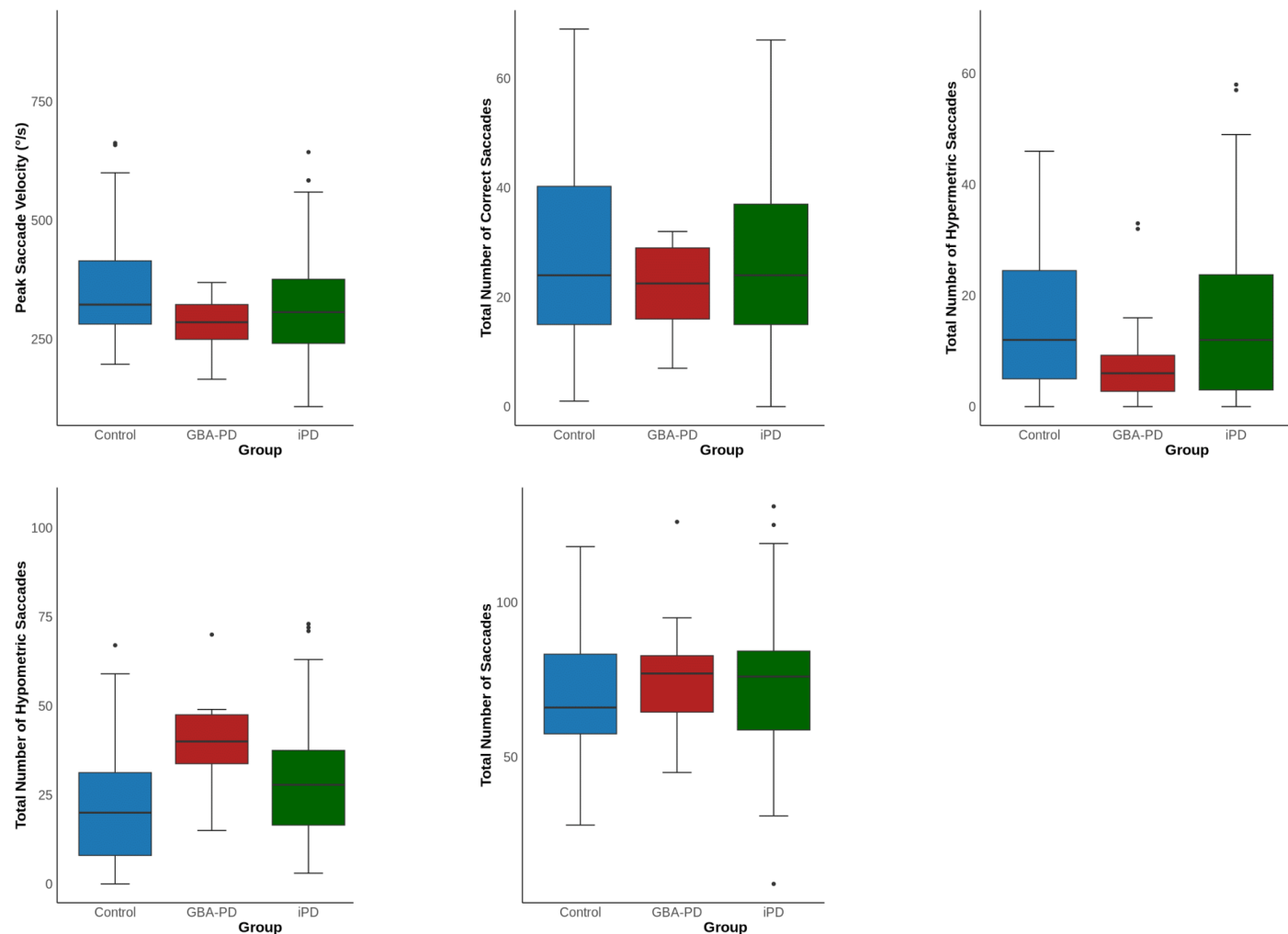


Figure 69: Volitional Saccades Vertical Metrics in Parkinson's Disease. Box plots show the median, interquartile range, and full range. Generalized linear models were used to assess the effects of group, age, sex, LEDD, and disease duration. Statistical significance was set at $p < 0.05$.

Table 9: Qualitative Description of Volitional Saccades Metrics in the LRRK2 Mutation PD Group.

Metric	LRRK2 Mutation PD Group Characteristics
Volitional Saccade Average Velocity	High median velocity (225-250 deg/s) in Horizontal direction with narrow IQR; lower median (175-200 deg/s) in Vertical direction comparable to other PD groups and controls.
Volitional Saccade Peak Velocity	High median peak velocity (600-700 deg/s) in Horizontal direction with compact IQR, similar to controls; lower median (400-450 deg/s) in Vertical direction, consistent with other PD groups.
Volitional Saccade Amplitude	Consistent amplitudes: 10-11 degrees Horizontal, 8-9 degrees Vertical with narrow IQRs, generally comparable to controls.
Volitional Saccade Start Time	Consistent start times in both directions, median 300-325 ms with tight IQRs.
Volitional Saccade End Time	Consistent end times in both directions, median 350-375 ms with narrow IQRs.
Volitional Saccade Accuracy	Good and consistent accuracy (100 units median) in both Horizontal and Vertical directions.
Volitional Saccade Correct Count	High and consistent correct counts: 95-100 Horizontal, 90-95 Vertical, indicating reliable saccadic generation.
Volitional Saccade Hypermetric Count	Very low median count (0-1) in both directions, with some outliers; minimal overshooting.
Volitional Saccade Hypometric Count	Very low median count (0-1) in both directions, with some outliers; minimal undershooting.
Volitional Saccade Total Number of Saccades	High median total saccades (100-110 Horizontal, 100 Vertical) with narrow IQRs, indicating good task compliance.
Volitional Saccade Saccadic Steps	Very low median number (0-5) of saccadic steps in both directions, with most data near zero; saccades typically executed in a single accurate movement.

Timescale Analysis of Volitional Saccades in Parkinson's Disease

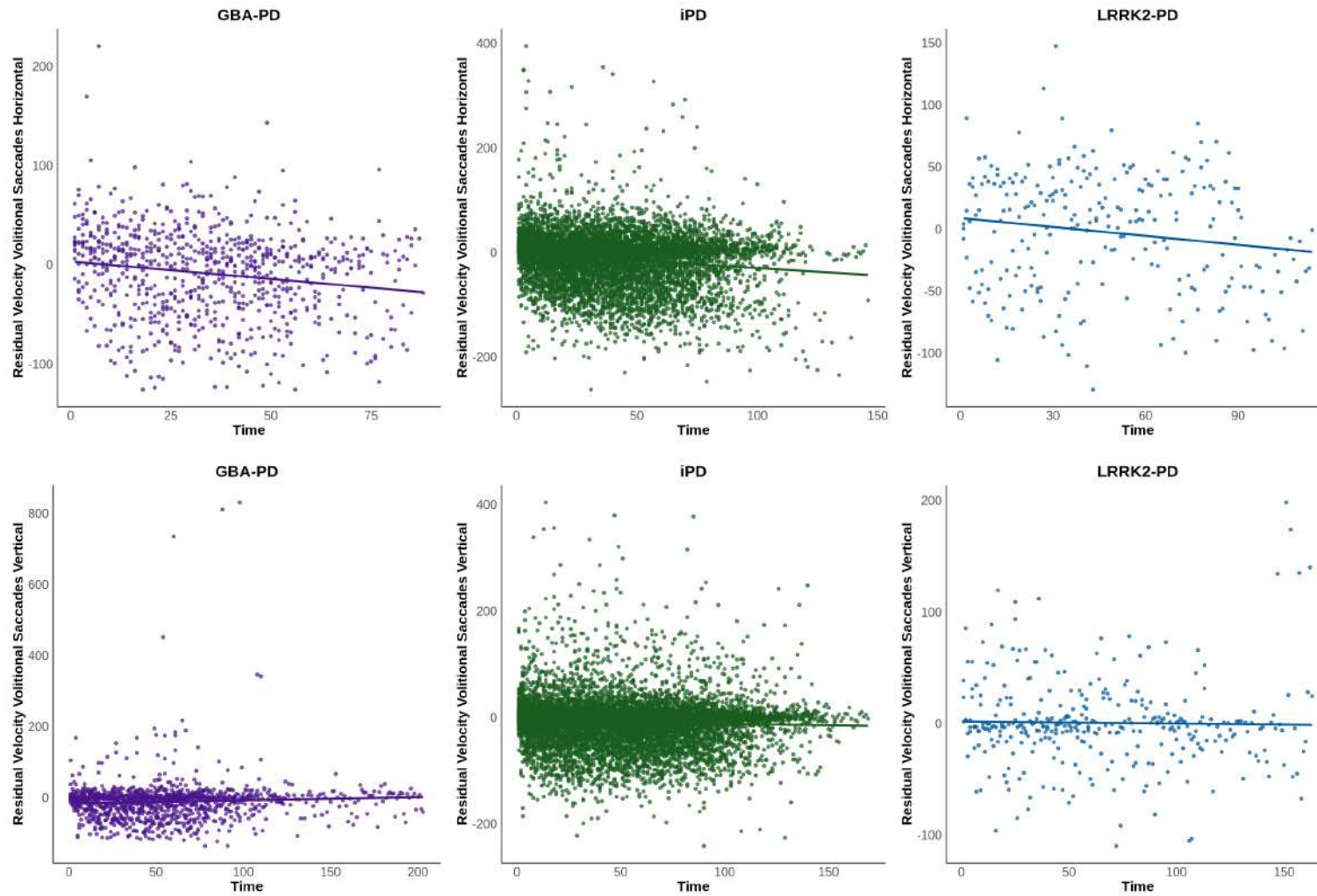


Figure 70: Timescale Analysis of Volitional Saccades in Parkinson's Disease. Residual velocity calculated through the main sequence effect.

Memory Guided Saccades Horizontal Metrics in Parkinson's Disease

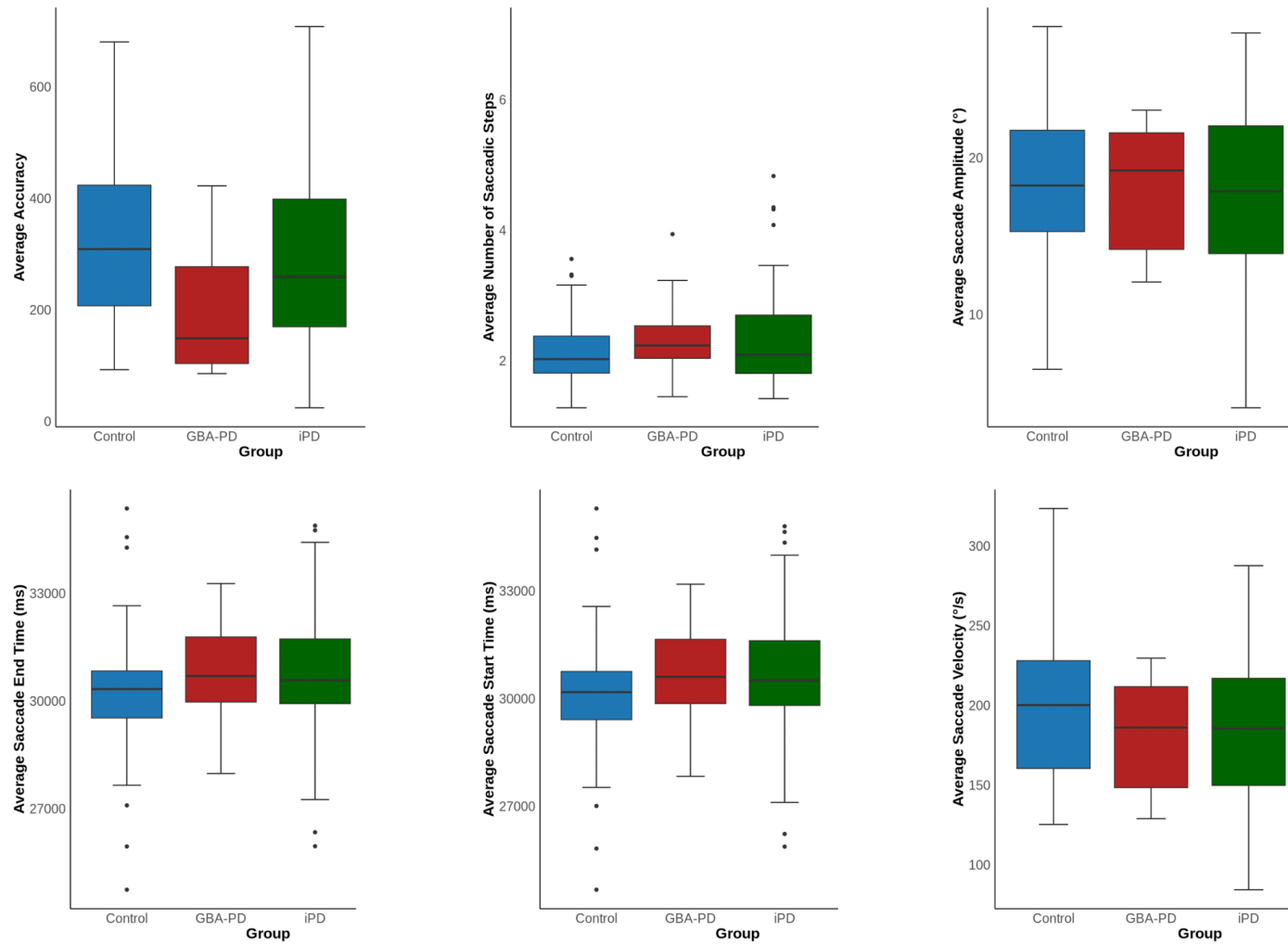


Figure 71: Memory Guided Saccades Horizontal Metrics in Parkinson's Disease. Box plots show the median, interquartile range, and full range. Generalized linear models were used to assess the effects of group, age, sex, LEDD, and disease duration. Statistical significance was set at $p < 0.05$.

Memory Guided Saccades Horizontal Metrics in Parkinson's Disease

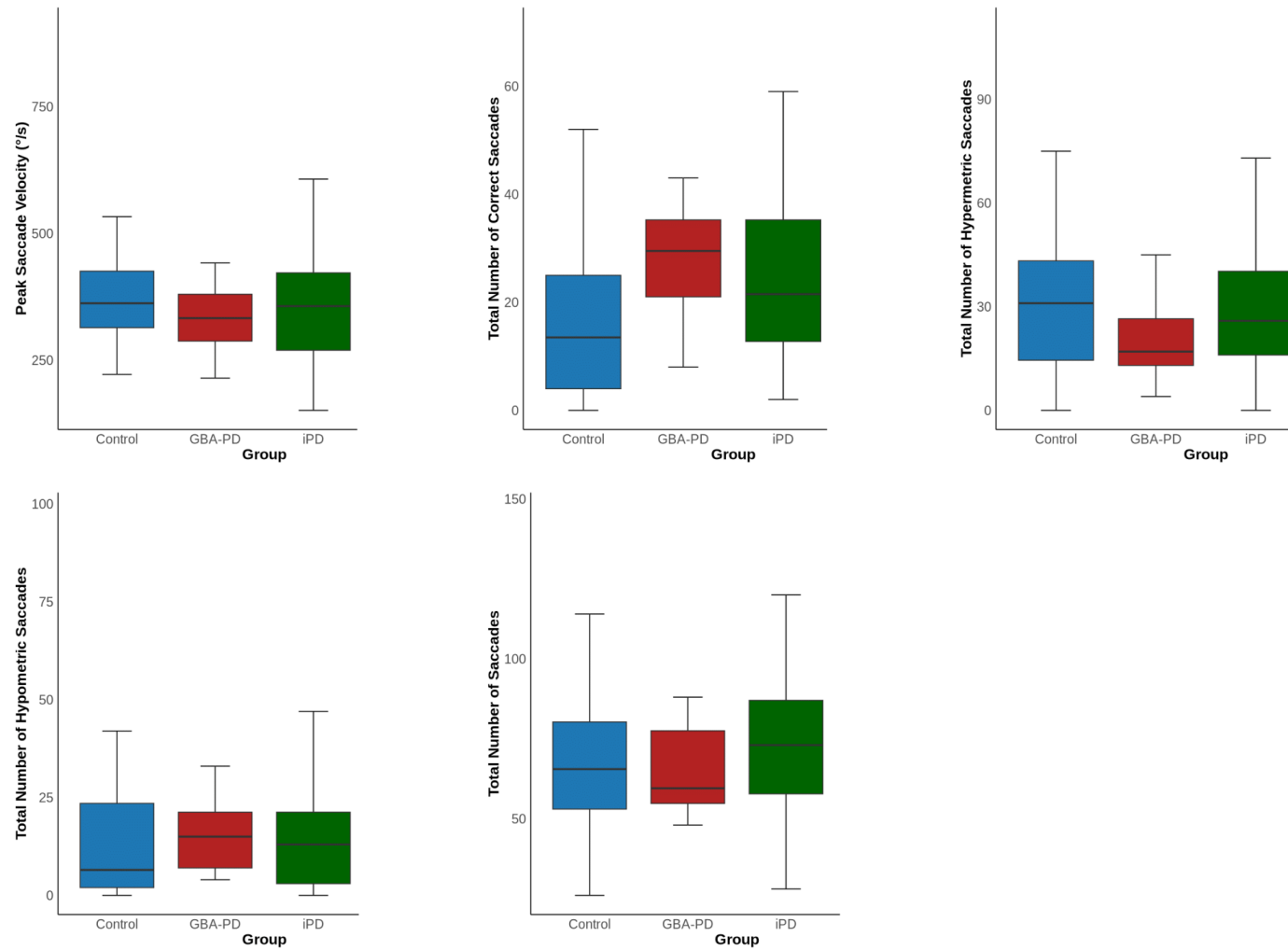


Figure 72: Memory Guided Saccades Horizontal Metrics in Parkinson's Disease. Box plots show the median, interquartile range, and full range. Generalized linear models were used to assess the effects of group, age, sex, LEDD, and disease duration. Statistical significance was set at $p < 0.05$.

Memory Guided Saccades Vertical Metrics in Parkinson's Disease

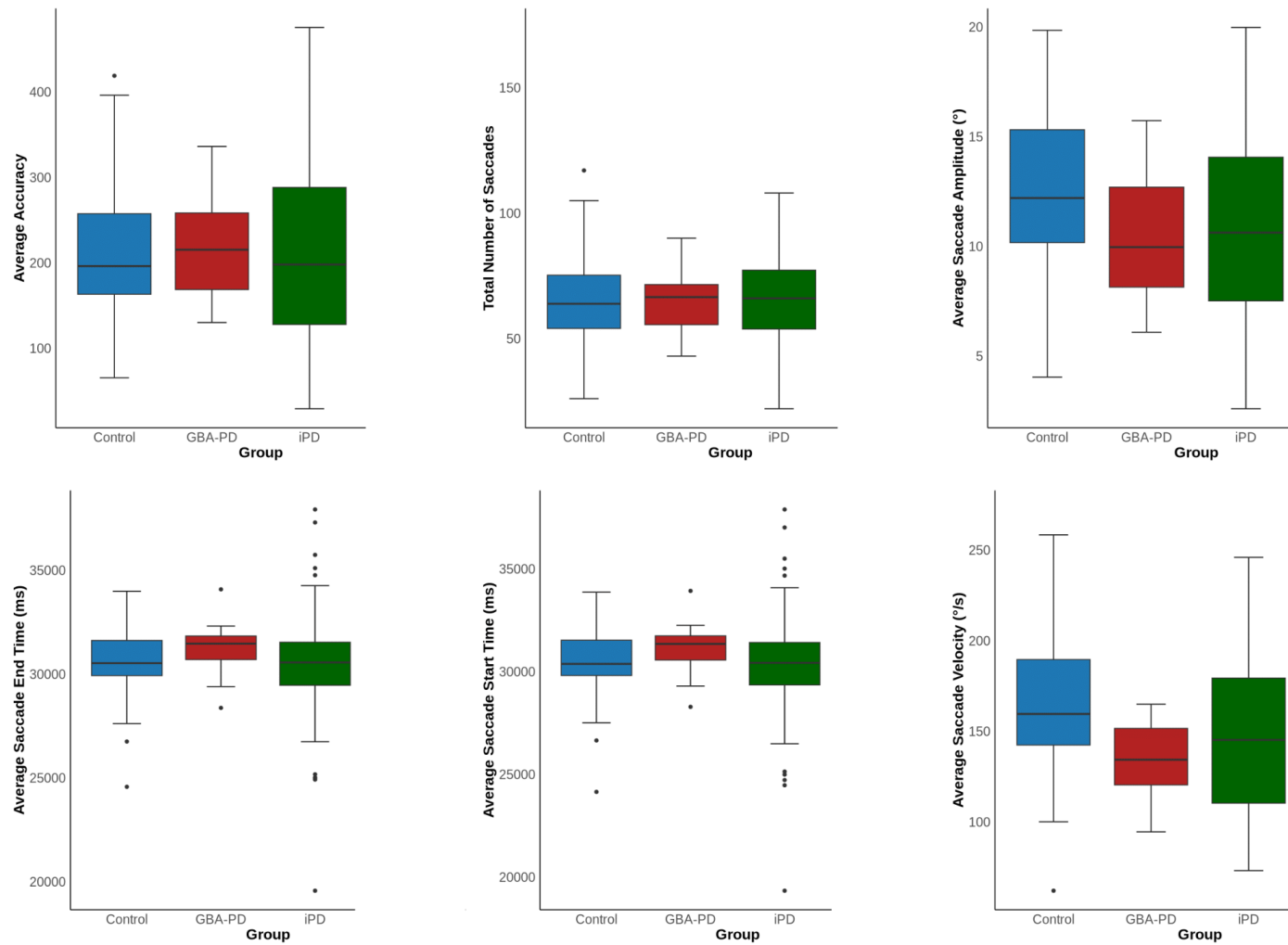


Figure 73: Memory Guided Saccades Vertical Metrics in Parkinson's Disease. Box plots show the median, interquartile range, and full range. Generalized linear models were used to assess the effects of group, age, sex, LEDD, and disease duration. Statistical significance was set at $p < 0.05$.

Memory Guided Saccades Vertical Metrics in Parkinson's Disease

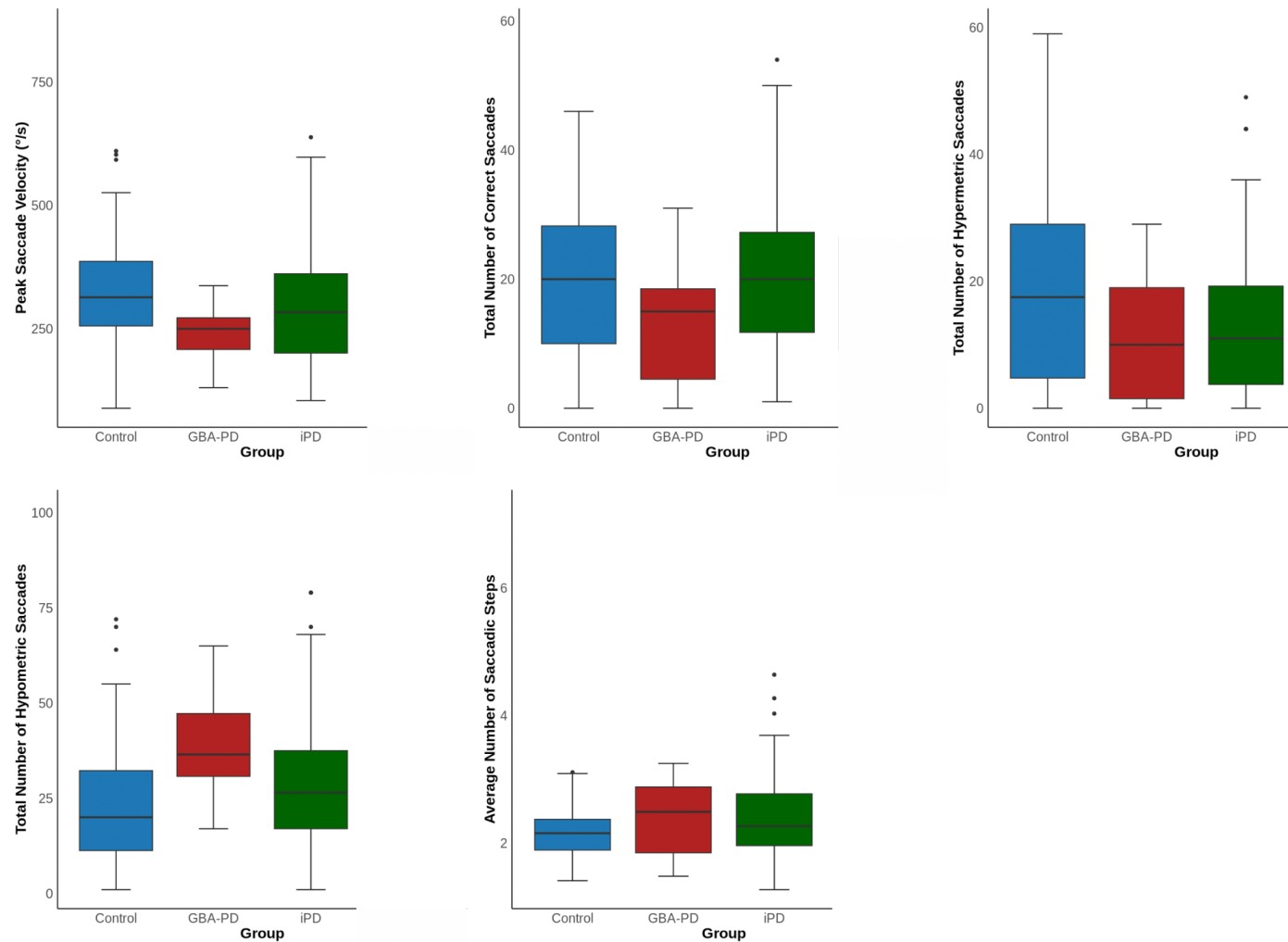


Figure 74: Memory Guided Saccades Vertical Metrics in Parkinson's Disease. Box plots show the median, interquartile range, and full range. Generalized linear models were used to assess the effects of group, age, sex, LEDD, and disease duration. Statistical significance was set at $p < 0.05$.

Table 10: Qualitative Description of Memory-Guided Saccades Metrics in the LRRK2 Mutation PD Group.

Metric		LRRK2 Mutation PD Group Characteristics
Memory-Guided Saccade Average Velocity	Sac-	Consistent median average velocities: 200-225 deg/s Horizontal, 150-175 deg/s Vertical; narrow IQRs; comparable to controls and other PD groups.
Memory-Guided Saccade Peak Velocity	Sac-	Consistent median peak velocities: 500-600 deg/s Horizontal, 350-400 deg/s Vertical; compact IQRs; in line with other groups.
Memory-Guided Saccade Amplitude	Sac-	Consistent amplitudes: 10-11 degrees Horizontal, 8-9 degrees Vertical; narrow IQRs; comparable to controls.
Memory-Guided Saccade Start Time	Sac-	Consistent start times in both directions, median 300-325 ms; narrow IQRs.
Memory-Guided Saccade End Time	Sac-	Consistent end times, median 350-375 ms Horizontal and Vertical; narrow IQRs.
Memory-Guided Saccade Accuracy	Sac-	Good and consistent accuracy (100 units median) in both Horizontal and Vertical directions.
Memory-Guided Saccade Correct Count	Sac-	High and consistent correct counts: 95-100 Horizontal, 90-95 Vertical; narrow IQRs indicating reliable spatial memory and execution.
Memory-Guided Saccade Hypermetric Count	Sac-	Very low median count (0-1) in both directions, with some outliers; minimal overshooting.
Memory-Guided Saccade Hypometric Count	Sac-	Very low median count (0-1) in both directions, with some outliers; minimal undershooting.
Memory-Guided Saccade Total Number of Saccades	Sac-	High median total saccades (100-110 Horizontal, 100 Vertical) with narrow IQRs; good task compliance.
Memory-Guided Saccade Saccadic Steps	Sac-	Very low median saccadic steps (0-5) in both directions; saccades usually executed in a single accurate movement.

Timescale Analysis of Memory Guided Saccades in Parkinson's Disease

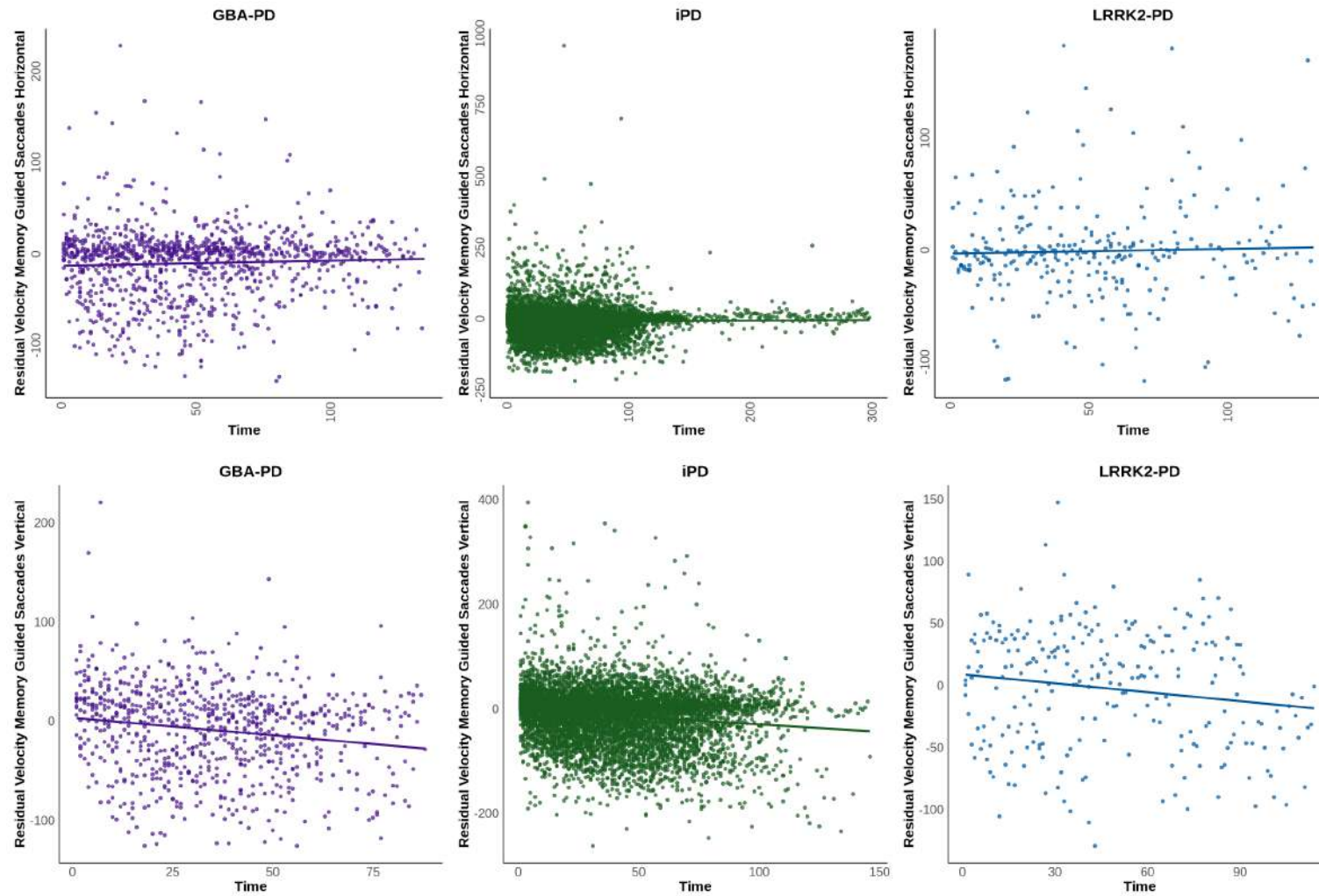


Figure 75: Timescale Analysis of Memory Guided Saccades in Parkinson's Disease. Residual velocity calculated through the main sequence effect.

Spider Diagram for Ocular Motor Metrics

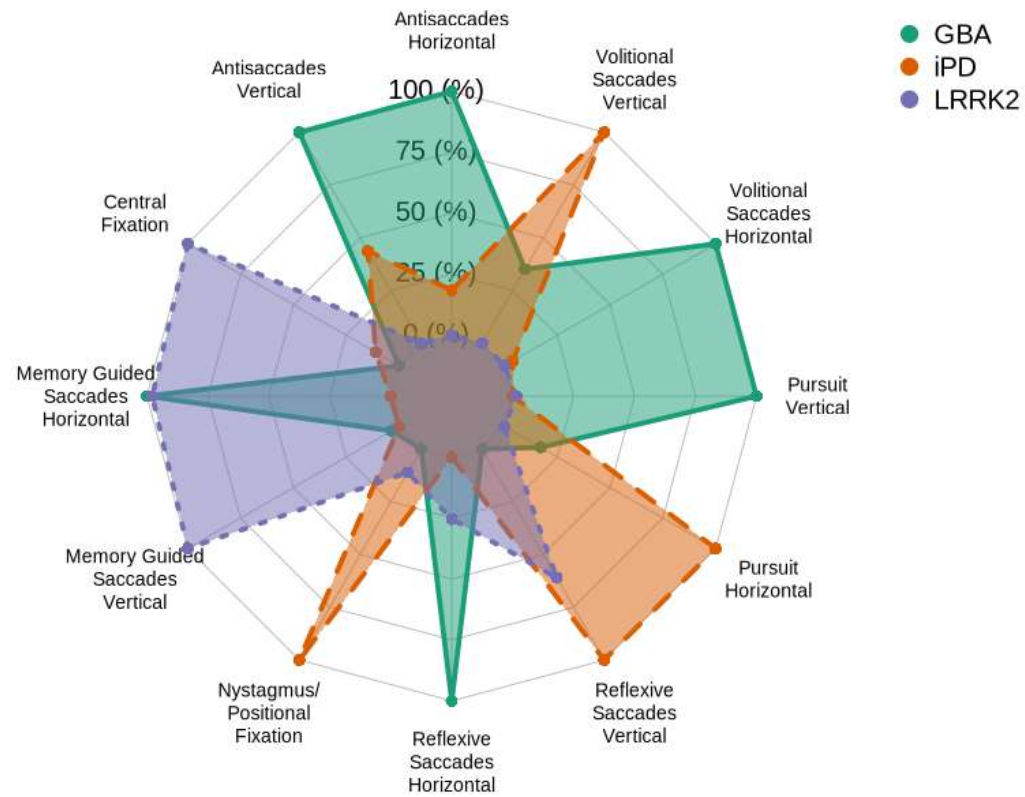


Figure 76: Spider Plot of Ocular Motor Paradigms in Parkinson's Disease. Composite score calculated using statistical outputs; higher composite scores indicate higher level of significance.

3.5 Discussion

This ocular motor study investigating a detailed battery of eye movements in iPD, GBA and LRRK2 mutation PD provided key information about the distinct patterns of ocular motor disturbance in these conditions. While iPD has been previously studied, there are very few studies looking at eye movements in genetic forms of PD. The findings from the iPD group are mostly consistent with previous literature, including fixation abnormalities and saccadic hypometria, along with some novel findings in oblique, volitional, and memory-guided saccades. The GBA and LRRK2 groups showed interesting patterns across paradigms, providing a new perspective on eye movements in these subgroups of PD. Each of these subgroups presents with a distinct ocular motor profile, suggesting that eye movements can potentially be used not only to identify PD at a higher level but also to differentiate between subtypes at a more granular level.

Previous literature has found that fixation instabilities in iPD manifest as increased numbers of SWJs (João Lemos and Eggenberger 2013; Otero-Millan, R. Schneider et al. 2013) and alterations in microsaccades (Otero-Millan, R. Schneider et al. 2013; R. G. Alexander, Macknik and Martinez-Conde 2018). This study found that while the number of small SWJs (less than 2° in amplitude) was significantly higher in iPD, there was no difference in the number of large SWJs (between 2–4° in amplitude). However, frequency of large SWJs was elevated in GBA-PD, and no differences were seen in LRRK2-PD. The lack of fixation control in iPD resulting in SWJs is caused by impairment of SNpr function, leading to decreased inhibitory control in the SC (Averbuch-Heller et al. 1999; O’Sullivan et al. 2003; Otero-Millan, R. Schneider et al. 2013). Additionally, increased compensatory activity in the FEF and disinhibition of the fastigial oculomotor region in the cerebellum could also contribute to the generation of SWJs (Shaikh, Xu-Wilson et al. 2011; White et al. 1983). The presence of larger SWJs in GBA-PD suggests a more severe disruption in the SNpr, leading to excessive inhibition and fixation instabilities (O’Regan et al. 2017; Vieira and Schapira 2022). Furthermore, greater cognitive impairment in GBA-PD, particularly in executive function, may impair top-down control from the FEF (Moran et al. 2021). The absence of significant SWJ changes in LRRK2-PD may reflect preserved cortical compensation and hyperactive striatal output, attributed to the less severe phenotype compared to iPD and GBA-PD (Healy et al. 2008).

A major limitation to consider in SWJ research is the lack of standardisation in quantification and classification methods. Some studies rely on manual identification, which is prone to subjective bias, while others

employ automated detection algorithms, which may have varying sensitivity thresholds. This variability could contribute to conflicting reports regarding the extent of SWJ abnormalities in PD and the lack of detail in quantification in the literature.

The microsaccade abnormalities of increased frequency and larger amplitude saccades seen in previous studies were not found in this study for any PD subgroup (Martinez-Conde, Otero-Millan and MacKnik 2013; Otero-Millan, Macknik, Langston et al. 2013; X. Ling et al. 2023). The microsaccade-triggering circuit, involving the SC, excitatory burst neuron (EBN), inhibitory burst neuron (IBN), and omnipause neuron (OPN) (Otero-Millan, Macknik, Serra et al. 2011), likely exhibits differential susceptibility in PD, leading to individual-specific microsaccade alterations. SC disinhibition due to BG dysfunction may drive early microsaccade dysregulation, particularly in GBA-PD, where faster neurodegeneration accelerates SC impairment. In contrast, brainstem OPN dysfunction, which affects fixation stability, may be more pronounced in advanced PD cases with gait instability (Seidel et al. 2015). EBN/IBN impairment may emerge later in PD or in atypical syndromes like PSP, where brainstem atrophy is more severe (Anagnostou et al. 2020). The lack of microsaccade abnormalities in this study may reflect high individual variability in which circuit component is most affected, with some individuals retaining cortical compensation, thereby masking group-level differences. Furthermore, microsaccade generation is influenced by task demands, attentional state, and individual variability, meaning that differences may only emerge under specific cognitive or visuomotor conditions rather than during passive fixation (A. Schneider et al. 2020).

There are conflicting results for pupil size in PD, with some studies finding an increase and others reporting a decrease compared to healthy controls (J. Huang et al. 2020; T. Sugiyama and Utsumi 1990; Micieli et al. 1991; Tsitsi, Nilsson et al. 2023; Tsitsi, Benfatto et al. 2021). In PD, increased pupil size is likely driven by a combination of locus coeruleus (LC) degeneration, cholinergic dysfunction, dopamine-norepinephrine (NE) dysregulation, and cortical impairments. The LC, a major NE-producing center, degenerates early in PD but may undergo a compensatory phase of hyperactivity before significant neuronal loss occurs, leading to excessive NE release and enhanced sympathetic pupil dilation (Delaville, Deurwaerdère and Benazzouz 2011; Espay, Lewitt and Kaufmann 2014; Larsen and Waters 2018). This could explain why pupil size is larger in PD despite autonomic dysfunction, with LRRK2-PD showing the greatest increase, potentially due to greater LC hyperactivity or delayed degeneration (Rocha et al. 2022). Simultaneously, early degeneration

of cholinergic neurons in the basal forebrain (nucleus basalis of Meynert) and brainstem (Edinger-Westphal nucleus) impairs pupillary constriction, resulting in a larger baseline pupil size. This effect may be more pronounced in GBA-PD, given its stronger cholinergic deficits and higher risk of dementia (Slingerland et al. 2024; Morawski et al. 2010; Biagioni et al. 2019). Additionally, dopamine and NE interact in autonomic regulation, and dopamine depletion in PD may disrupt sympathetic-parasympathetic balance, though baseline pupil dilation appears to be independent of medication status (Xing, Y. C. Li and W. J. Gao 2016). These combined mechanisms suggest that pupil size alterations in PD reflect a complex interplay between autonomic, neuromodulatory, and cortical dysfunctions, with subtype-specific variations based on LC integrity and cholinergic involvement.

The preservation of fixation precision and other fixation-related metrics in all PD subtypes suggests that not all components of the fixation control system are equally affected. While SWJs and pupil size abnormalities indicate disruptions in brainstem and BG circuits, fixation precision is primarily regulated by the cerebellum and visuo-oculomotor integration pathways, which may remain relatively intact in early- to mid-stage PD (Wu and Hallett 2013; Lewis et al. 2013). The vermis of the cerebellum, particularly the oculomotor vermis and fastigial nucleus, fine-tunes gaze stability by compensating for small fixation errors (Manto et al. 2012). If cerebellar compensation is effective, it could explain why fixation precision remains intact despite increased SWJs. Additionally, higher cortical areas, including the posterior parietal cortex (PPC), contribute to gaze stability through visuospatial processing, and their involvement in PD may be less pronounced in early stages (Yaoda Xu 2018).

The findings from the pursuit task indicate largely preserved smooth pursuit function across all PD subtypes, with no significant differences observed in pursuit gain or accuracy at either 0.2 Hz or 0.4 Hz in horizontal, vertical, or elliptical trajectories. Individuals with GBA-PD and LRRK2-PD demonstrated normal pursuit eye movements, suggesting that, unlike fixation abnormalities, pursuit deficits may not be a prominent feature of these genetic PD variants. However, in iPD, a distinct pattern emerged in elliptical pursuit, where gain was significantly increased in both the anticlockwise and clockwise directions at the higher speed (0.4 Hz). This localized difference suggests a potential disruption in predictive or anticipatory mechanisms specific to elliptical tracking, rather than a general impairment in smooth pursuit generation (Helmchen, Pohlmann et al. 2012). The involvement of the cerebellum—particularly the flocculus and paraflocculus, which con-

tribute to pursuit adaptation and predictive control—may be relevant here (Amir Kheradmand and David S. Zee 2011; Kakei et al. 2019). Increased gain could reflect a compensatory response to impaired cerebellar integration or reduced inhibition from the BG, resulting in an exaggerated response to the moving stimulus.

Further insights into pursuit abnormalities in iPD are revealed by saccadic pursuit metrics. Individuals with iPD exhibited the highest total saccade count across all amplitude bins, indicating increased reliance on corrective saccades—particularly those under 2° in amplitude. This suggests that, while overall pursuit gain remained relatively intact, there was a greater need for saccadic compensation, reflecting impaired smooth pursuit stability. The distribution of saccades followed a non-Gaussian pattern, consistent with previous reports that pursuit in PD is often fragmented and punctuated by small corrective saccades (Frei 2021).

GBA-PD exhibited a similar non-Gaussian saccadic distribution but with fewer large corrective saccades ($>2^\circ$), potentially reflecting greater impairment in voluntary pursuit control. This aligns with evidence suggesting that GBA-PD is associated with greater cognitive decline, particularly in executive function, which may hinder top-down modulation of pursuit (Moran et al. 2021; J. Ren et al. 2023). The reduced frequency of large corrective saccades may also reflect a diminished capacity to generate compensatory motor responses, suggesting that pursuit impairments in this subtype may be more strongly linked to cognitive dysfunction than motor instability alone.

In contrast, individuals with LRRK2-PD demonstrated the lowest total saccade count, with fewer small-amplitude saccades ($<1^\circ$), suggesting better gaze stability during pursuit compared to iPD and GBA-PD. This pattern implies a less fragmented pursuit strategy and may reflect relatively preserved ocular motor control in LRRK2-PD. The reduced reliance on small corrective saccades could indicate more effective visual motion integration, possibly due to differences in striatal-thalamic-cortical network compensation (C. Chen et al. 2020; Skelton, Tokars and Parisiadou 2022).

Despite these differences, the non-Gaussian distribution of saccadic behavior across all subtypes reinforces the idea that pursuit alterations in PD do not follow a simple linear decline, but instead reflect subtype-specific compensatory mechanisms and differential neural involvement. The absence of significant differences in pursuit gain and accuracy across most conditions highlights that smooth pursuit function—unlike fixation

control—remains relatively intact in PD, particularly in genetic subtypes. However, the presence of increased compensatory saccades in iPD and GBA-PD suggests subtle impairments that may not be captured by traditional gain measures alone. Future work should explore more dynamic measures of pursuit stability and predictive control to better characterise pursuit deficits in PD.

The results from the antisaccade task highlight distinct differences across PD subtypes, particularly in relation to saccadic velocity and amplitude. Notably, no significant differences were observed in the horizontal direction for iPD and LRRK2-PD, suggesting that, at least in these subtypes, horizontal antisaccade control remains largely intact. However, individuals with iPD exhibited significant impairments in the vertical antisaccade task, with reductions in saccadic amplitude, average velocity, and peak velocity compared to controls. These findings suggest that vertical antisaccades are more sensitive to ocular motor dysfunction in iPD, possibly due to differential BG-thalamocortical network involvement (G. E. Alexander, M. R. DeLong and Strick 1986; M. DeLong and Wichmann 2009). Vertical saccades are thought to be more dependent on brainstem structures, particularly the midbrain SC and the rostral interstitial nucleus of the medial longitudinal fasciculus, which may undergo early functional disruption in PD (Lal and Truong 2019; M. Takahashi, Sugiuchi and Shinoda 2024). The reduced saccadic velocity in iPD suggests impaired activation of the burst neuron pathways responsible for generating rapid eye movements, aligning with previous studies reporting hypometric and slowed saccades in PD (Quinet et al. 2020; Catz and Thier 2007). The accompanying amplitude reductions further support this interpretation, indicating that deficits in voluntary saccade generation extend beyond simple inhibitory control impairments to broader motor execution dysfunction.

In contrast, LRRK2-PD showed no significant differences from controls in either horizontal or vertical antisaccades, suggesting a more preserved saccadic control system in this genetic subtype. This finding aligns with previous reports that LRRK2-PD often presents with a milder phenotype and relatively intact ocular motor function in early disease stages (Giachino et al. 2022). The absence of antisaccade impairments indicates that cortical and brainstem circuitry responsible for voluntary saccade inhibition may remain functional in this group, possibly due to compensatory mechanisms or a less pronounced degree of neurodegeneration in the midbrain and SC compared to iPD and GBA-PD. However, given that LRRK2-PD has been associated with more pronounced striatal dopaminergic dysfunction in some studies, it remains possible that subtle deficits could emerge with disease progression or under increased cognitive load (Jeong and B. D. Lee 2020; X. Li

et al. 2010).

GBA-PD, on the other hand, demonstrated significant deficits in both horizontal and vertical antisaccades, with reduced saccadic amplitude and velocity across both planes. This global slowing of saccades suggests a broader impairment in voluntary saccade generation, potentially reflecting more widespread neurodegeneration, including early involvement of both cortical and subcortical structures (Everling and Fischer 1998). The reductions in amplitude and velocity are particularly noteworthy, as they imply that GBA-PD may involve greater dysfunction in pathways responsible for the execution of voluntary movements, beyond just deficits in inhibitory control. Given that GBA mutations have been linked to more severe cognitive decline in PD, the antisaccade impairments observed here may reflect a combination of motor and cognitive deficits, particularly involving the prefrontal cortex and supplementary eye fields (SEF), which are critical for the voluntary control of saccades (G. Liu et al. 2016; Stuphorn 2015; Pouget 2015). The greater impairment in vertical saccades further supports the hypothesis that brainstem circuits involved in vertical ocular motor control may be more affected in this subtype.

The findings from the oblique saccades task reveal a notable pattern of impairment in iPD and GBA-PD, but only at the highest level of eccentricity (10°), whereas performance remained intact at 4° and 8° across all subtypes. This suggests that saccadic control in PD is not uniformly impaired across all movement amplitudes but becomes more apparent as task difficulty increases. The greater demands placed on motor planning and execution at higher eccentricities likely expose subtle deficits that remain undetected in smaller-amplitude saccades. Interestingly, LRRK2-PD showed no significant differences in oblique saccades across all eccentricities, reinforcing previous findings that this genetic form of PD may be associated with more preserved ocular motor function, at least in early disease stages (Lage et al. 2024; Heidi C. Riek et al. 2024).

In iPD, significant deficits at 10° targets included reduced saccadic amplitude, decreased positional accuracy in both X and Y directions, fewer correct saccades, and a higher number of hypermetric saccades. The reduction in saccadic amplitude suggests impaired motor command generation, likely arising from BG dysfunction, which disrupts the balance of excitatory and inhibitory signals necessary for precise saccade execution (Matsumoto et al. 2012; J. Kim et al. 2017). The decreased positional accuracy further supports this interpretation, pointing to impaired cerebellar integration, which plays a critical role in refining saccadic

targeting (Koziol et al. 2014). The increased frequency of hypermetric saccades—where the eyes overshoot the target—suggests a failure in corrective feedback mechanisms, potentially involving dysfunction in the SC or the cerebellar oculomotor vermis, both of which contribute to saccadic calibration (Soetedjo and Albert F. Fuchs 2006; Enderle 2002). Notably, despite these deficits, saccadic velocity remained unaffected, indicating that the primary dysfunction in iPD may lie in saccadic precision and control, rather than in the generation of high-velocity eye movements.

The GBA-PD group exhibited a similar pattern of impairment, but with more widespread deficits at 10°. These included reductions in saccadic amplitude, average velocity, peak velocity, and positional accuracy, along with fewer correct saccades and an increased number of hypermetric saccades. The additional velocity impairments suggest a broader deficit in saccade generation compared to iPD, potentially reflecting more extensive neurodegeneration affecting both motor and cognitive control networks. The reduced number of correct saccades points to difficulties in suppressing erroneous movements and executing accurate goal-directed saccades, which may be linked to dysfunction in the FEF and BG circuits (Hikosaka, Takikawa and Kawagoe 2000). The higher number of hypermetric saccades, combined with reduced accuracy, suggests that motor calibration in GBA-PD is particularly impaired, possibly due to greater cerebellar involvement or disrupted striatal-thalamic feedback. Given the established link between GBA mutations and more severe cognitive decline, these broader oblique saccade impairments may also reflect deficits in executive function, which plays a critical role in voluntary saccadic suppression and trajectory correction (D. P. Munoz and Everling 2004; A. B. Sereno et al. 2009).

The presence of hypermetric saccades in the oblique saccade task—contrasting with the typically hypometric saccades seen in horizontal and vertical directions in PD—suggests that distinct underlying mechanisms govern oblique saccade control. One explanation is the differential involvement of the cerebellum, particularly the oculomotor vermis and fastigial nucleus, which regulate saccadic gain control and endpoint correction (Soetedjo and Albert F. Fuchs 2006; Desmurget et al. 2000). While hypometric saccades in PD are often attributed to excessive BG inhibition of the SC, oblique saccades may engage additional cerebellar feedback loops, which—when disrupted—result in overshooting the target instead. Oblique saccades also require simultaneous activation of both horizontal and vertical saccadic pathways, increasing computational demands and the risk of trajectory overestimation. The SC, which encodes saccadic vectors, may contribute to this

phenomenon; disruptions in its inhibitory-excitatory balance could exaggerate saccadic responses in non-cardinal planes.

Furthermore, cortical involvement—particularly from the (PEF)—is crucial for the spatial remapping needed for oblique movements. Dysfunction in these areas may impair trajectory estimation, resulting in hypermetric, rather than hypometric, errors (Culham, Cavina-Pratesi and Singhal 2006). The absence of hypermetric saccades in LRRK2-PD suggests that this subtype may retain better motor precision and feedback control, possibly due to preserved cerebellar function or more effective compensatory interactions within the cortical-striatal circuitry.

The findings from the reflexive saccades task reveal key differences in saccadic execution across PD subtypes, with impairments most evident in iPD and GBA-PD, while LRRK2-PD demonstrated preserved function. In iPD, reduced saccadic amplitude and an increased number of hypometric saccades were observed in both horizontal and vertical directions, while no differences were noted in saccadic velocity or timing measures. These results align with the well-established finding that PD is associated with hypometric saccades, likely due to BG dysfunction leading to excessive inhibition of the SC (Terao, Fukuda, Ugawa et al. 2013). The hypometric nature of reflexive saccades in iPD suggests impaired saccade initiation and motor scaling rather than a slowing of movement, reinforcing the notion that saccadic precision, rather than speed, is primarily affected in this subtype. Notably, the absence of significant differences in saccadic velocity indicates that the brainstem burst neuron circuits responsible for generating high-velocity movements remain relatively preserved in reflexive saccades (Mayà et al. 2024).

GBA-PD exhibited more pronounced reflexive saccade impairments than iPD, including reductions in amplitude, velocity, and accuracy across both horizontal and vertical directions. In addition to reduced amplitude and an increased number of hypometric saccades, individuals with GBA mutations showed significant decreases in average and peak saccadic velocity and a lower number of correct saccades. These additional velocity impairments suggest a broader deficit in motor command generation, potentially involving dysfunction in brainstem saccade-related structures such as the PPRF for horizontal saccades and the (riMLF) for vertical saccades (Termsarasab et al. 2015). Increased saccadic latency observed in GBA-PD further supports this interpretation, indicating a delay in saccade initiation likely reflecting disrupted interactions between

the SC and FEF (Do et al. 2019). Given that GBA mutations are associated with a more aggressive disease phenotype and earlier cognitive decline, these impairments may also reflect reduced top-down modulation of reflexive responses, particularly involving inhibitory control networks (Chan et al. 2005).

In contrast, LRRK2-PD exhibited no significant impairments in reflexive saccades, suggesting preserved function in both BG and brainstem ocular motor circuits. This finding aligns with prior literature indicating that LRRK2-PD typically presents with a milder ocular motor phenotype in early stages, possibly due to compensatory cortical-striatal mechanisms (Palermo et al. 2022). The absence of reflexive saccade abnormalities in this group further distinguishes LRRK2-PD from iPD and GBA-PD, underscoring the heterogeneity of ocular motor dysfunction in PD based on genetic background.

Timescale analysis of residual peak velocity provides further insights into the progression of reflexive saccade impairments across subtypes and links these to PD-related bradykinesia (Koohi et al. 2021). A significant decline in residual velocity was observed in both iPD and GBA-PD in horizontal and vertical directions, reinforcing the idea that saccadic hypometria in these groups is accompanied by a progressive reduction in movement vigor. This deterioration reflects an impaired capacity to sustain saccadic motor output over time and parallels the decremental pattern seen in limb movements in PD, a hallmark of bradykinesia (Berardelli et al. 2001). The observed decline in velocity may indicate progressive dysfunction of brainstem burst neurons and reduced dopaminergic input to the SC, resulting in weakened saccadic drive and impaired motor energetics (E. Benarroch 2023).

The results from the volitional saccades task indicate a largely preserved ability to generate voluntary saccades across all PD subtypes, with minimal differences observed compared to healthy controls. Neither iPD, GBA-PD, nor LRRK2-PD demonstrated significant impairments in volitional saccades in the horizontal direction, and only the GBA group exhibited an increased number of hypometric saccades in the vertical plane. The absence of widespread deficits suggests that, unlike reflexive or memory-guided saccades, volitional saccades may be less affected in early- or mid-stage PD, potentially due to preserved cortical control mechanisms (Pouget 2015). The FEF and supplementary eye fields (SEF) play a central role in the generation and planning of volitional saccades, and their relative sparing in PD may explain the lack of significant impairments in this task (Fernandes et al. 2014).

The increased number of hypometric saccades in the vertical plane observed in the GBA group, despite otherwise normal performance, suggests a subtle deficit in motor scaling rather than execution speed. Hypometric saccades in PD are typically attributed to BG dysfunction, specifically excessive inhibitory output from the substantia nigra pars reticulata (SNpr), resulting in under-scaling of movement amplitude (Terao, Fukuda, Yugeta et al. 2011). The selective involvement of vertical saccades may reflect early dysfunction of brainstem structures such as the rostral interstitial nucleus of the medial longitudinal fasciculus (riMLF), which is crucial for vertical saccade generation (C. Chen et al. 2020). Given the association of GBA mutations with accelerated disease progression and greater cognitive impairment, early deficits in vertical volitional saccades may serve as a subtle marker of broader cortical-striatal network dysfunction (Fernández-Vidal et al. 2024).

The timescale analysis of residual peak velocity in volitional saccades further supports the presence of latent motor deficits, even when standard saccadic metrics appear preserved. Both iPD and GBA-PD groups demonstrated significant declines in horizontal and vertical velocity over time, while the LRRK2-PD group showed a decline in horizontal but not vertical volitional saccades. This progressive reduction in velocity mirrors the decremental pattern characteristic of bradykinesia, where movement amplitude and speed diminish over repeated actions (Koohi et al. 2021; Wright et al. 2022). The observation that LRRK2-PD exhibited velocity decline only in the horizontal plane may indicate a more selective impairment in motor control, potentially due to differences in compensatory mechanisms or underlying pathophysiological features specific to the LRRK2 mutation. These findings suggest that while overt saccadic dysfunction may be absent, dynamic measures such as velocity over time can uncover subtle bradykinetic features in voluntary eye movements across PD subtypes.

Previous literature has found that voluntary saccades are often impaired earlier than reflexive saccades in Parkinson's disease, likely due to the involvement of fronto-striatal circuits responsible for executive control and planning (R. John Leigh and David S. Zee 2015b; Lal and Truong 2019). However, in this study, reflexive saccades appeared to be more affected than volitional ones. Several factors may account for this discrepancy. First, the volitional saccade task used in this study may have imposed relatively low cognitive demands, thereby allowing participants to perform adequately despite underlying cortical dysfunction. More complex paradigms involving working memory, inhibitory control, or task switching may be required to unmask subtle deficits in volitional saccade generation. Second, it is possible that cortical compensatory mechanisms,

particularly in the frontal eye fields (FEF) and supplementary eye fields (SEF), help preserve voluntary saccade function in early to mid-stage PD, whereas reflexive saccades—mediated primarily by subcortical and brainstem structures such as the superior colliculus (SC)—are more vulnerable to early dopaminergic depletion (Esposito et al. 2021; Terao, Fukuda, Ugawa et al. 2013). Third, the metrics used to assess reflexive saccades in this study, such as residual peak velocity, may have been more sensitive to early motor impairments than those employed for volitional saccades. Finally, differences in participant characteristics, including genetic subtype composition, disease duration, and medication status, could contribute to variability across studies. These findings suggest that the temporal pattern of ocular motor impairments in PD may be more nuanced than previously thought, and highlight the importance of task design and measurement sensitivity in interpreting results.

The results from the memory-guided saccades task reveal subtle yet detectable impairments, particularly in the GBA-PD and LRRK2-PD groups. While no significant group-level differences were observed in standard saccadic metrics in either direction, both subtypes exhibited a significantly increased number of hypometric saccades compared to healthy controls. In the vertical direction, individuals with GBA-PD also demonstrated reduced peak saccade velocity, suggesting a more pronounced deficit in motor execution for memory-guided saccades. Interestingly, while iPD participants did not show significant group-level differences in any direction, they did exhibit a progressive decline in vertical residual velocity over time, indicating emerging bradykinetic features not captured by baseline comparisons.

Memory-guided saccades place greater demands on cognitive control, particularly working memory, inhibition, and motor planning—functions mediated by interactions between the (FEF), (DLPFC), and (BG) (Sweeney et al. 2007; Cameron, Riddle and D’Esposito 2015; Pierrot-Deseilligny, Rivaud et al. 1991). Although conventional group comparisons did not reveal widespread impairments across all metrics, the increased number of hypometric saccades in both GBA-PD and LRRK2-PD suggests subtle impairments in the ability to retain and execute stored saccadic motor plans. These findings likely reflect early disruptions in prefrontal-striatal connectivity (Kraus et al. 2010). The presence of hypometria in the LRRK2 group, despite otherwise preserved saccadic measures, may indicate selective vulnerability of cognitive control mechanisms not evident in broader performance metrics.

Interestingly, the LRRK2-PD group demonstrated a significantly higher number of hypometric memory-guided saccades compared to healthy controls, despite the absence of broader impairments in other saccadic metrics. This finding contrasts with the commonly reported milder cognitive and motor phenotype associated with LRRK2-related PD, particularly in early disease stages (Taymans et al. 2023). One possible explanation is that memory-guided saccades, which rely on working memory, spatial encoding, and internally generated motor planning, may reveal subtle prefrontal-striatal dysfunction that is not yet detectable through standard clinical or reflexive tasks (H. H. Li and Curtis 2023). It is also plausible that individuals with LRRK2 mutations exhibit reduced compensatory cortical activation during tasks with high executive demand. Alternatively, this observation may reflect heterogeneity within the LRRK2-PD phenotype or early selective vulnerability of cognitive control mechanisms in a subset of mutation carriers. However, the relatively small sample size for the LRRK2 group raises the possibility that this finding may be an anomaly or driven by individual variability rather than a consistent subtype-specific effect. Further research with larger cohorts is needed to clarify whether increased hypometria in memory-guided saccades is a reproducible feature of LRRK2-associated PD.

The selective vertical plane impairment in memory-guided saccades mirrors the pattern seen in volitional saccades, suggesting that vertical saccades may be particularly vulnerable to PD-related neurodegeneration. This vulnerability could stem from early dysfunction in the riMLF and the interstitial nucleus of Cajal—key structures in vertical saccade control (Termsarasab et al. 2015). These findings align with previous research showing vertical saccades are more sensitive to PD-associated degeneration, potentially due to their greater reliance on brainstem and cerebellar pathways (C. A. Antoniades and Sperling 2024; Weil et al. 2016; T. J. Anderson and MacAskill 2013).

The timescale analysis of residual peak velocity adds further insight into the progression of memory-guided saccade deficits. A significant reduction in vertical residual velocity was observed across all three PD subtypes, whereas horizontal residual velocity was impaired only in iPD and GBA-PD, but preserved in LRRK2-PD. This progressive decline in velocity is consistent with bradykinetic features in PD, where motor vigor diminishes over time. The uniform impairment in vertical residual velocity across all groups supports the idea that vertical memory-guided saccades may serve as a sensitive early biomarker of neurodegeneration.

The more pronounced impairments in iPD and GBA-PD, compared to LRRK2-PD, point to greater disruption of prefrontal-BG connectivity, which is crucial for executing memory-based saccades. Given the well-established link between GBA mutations and heightened cognitive decline, the additional slowing in GBA-PD may indicate early deficits in cognitive-motor integration. Conversely, the relative preservation in LRRK2-PD suggests intact top-down control mechanisms in early disease stages, supporting the hypothesis of subtype-specific ocular motor pathophysiology.

3.5.1 Clinical Implications

The findings of this study have significant clinical implications, particularly in enhancing the differentiation of PD subtypes and distinguishing PD from atypical parkinsonian syndromes. The distinct patterns of ocular motor deficits observed in idiopathic PD (iPD), GBA-associated PD (GBA-PD), and LRRK2-associated PD (LRRK2-PD) suggest that eye movement testing could serve as a valuable biomarker for disease characterization and progression tracking. The presence of hypometric reflexive and memory-guided saccades in iPD and GBA-PD, combined with a decline in residual velocity over time, indicates that these subtypes exhibit bradykinetic ocularmotor features that mirror the classic limb bradykinesia seen in PD. In contrast, the relative preservation of saccadic function in LRRK2-PD underscores the heterogeneity of ocularmotor impairment across genetic variants of PD.

Beyond subclassification of PD, these findings are particularly relevant for distinguishing PD from atypical parkinsonian syndromes such as PSP, MSA, and corticobasal degeneration (CBS). In PSP, vertical gaze palsy and markedly slowed saccades are hallmark features, whereas in PD, vertical saccades are preserved but hypometric. The increased frequency of small SWJs observed in iPD and GBA-PD may resemble findings seen in MSA and CBS; however, the absence of cerebellar-driven gaze instability in PD helps distinguish it from these disorders. Moreover, the progressive decline in residual saccadic velocity in iPD and GBA-PD highlights the bradykinetic nature of ocularmotor control in these subtypes, in contrast to the uniformly slow saccades characteristic of PSP.

The ability to objectively measure saccadic function through eye-tracking technology provides a non-invasive tool for early detection and longitudinal monitoring of disease. Integrating ocular motor assessments into routine clinical evaluations could enhance diagnostic accuracy and allow neurologists to track subtle motor

and cognitive changes over time. Additionally, saccadic metrics may prove useful in evaluating treatment efficacy, as improvements in saccadic performance could reflect responses to dopaminergic therapy, deep brain stimulation (DBS), or cognitive rehabilitation. Given this potential, future studies should examine how saccadic testing can be systematically integrated into clinical workflows and whether eye movement abnormalities can serve as predictors of disease progression and cognitive decline in PD.

3.5.2 Limitations

Despite the comprehensive approach undertaken in this study to investigate ocular motor deficits in Parkinson's disease (PD) subtypes, several limitations must be acknowledged. These primarily relate to sample size constraints, subgroup imbalances, methodological considerations, technical limitations in eye-tracking assessments, and potential confounding factors.

A major limitation was the small sample size of the genetic PD subgroups, particularly the LRRK2-PD and GBA-PD cohorts. With only three participants in the LRRK2-PD group and twelve in the GBA-PD group, statistical comparisons were underpowered, limiting the ability to detect significant group differences. This increases the risk of Type II errors (false negatives) and reduces the generalizability of the findings. In contrast, the idiopathic PD (iPD) group had a much larger sample ($n = 104$), which may have skewed comparative analyses due to greater statistical sensitivity. Bootstrapping was employed to mitigate the effects of small sample sizes; however, this technique cannot fully address the potential biases introduced by such disparities. Furthermore, the small sample size limits the generalizability of results and makes the dataset more susceptible to significant effects from outliers. Future research should prioritise larger and more balanced group sizes, especially for genetic subtypes, to enhance statistical reliability and reduce sampling variability.

Recruitment was conducted through specialist PD clinics and research centres, introducing possible selection bias. Participants may have been higher functioning and more motivated, thus not representative of the broader PD population, particularly those with severe motor or cognitive impairments. Furthermore, the study excluded individuals with advanced PD, severe psychiatric illness, or cognitive decline, limiting the generalisability of the findings to milder or moderate disease phenotypes. The age range of 40–80 years excluded younger-onset PD, which may exhibit distinct ocular motor characteristics—particularly relevant

given that GBA and LRRK2 mutations are associated with earlier onset.

Although high-resolution infrared eye-tracking was used, several technical limitations remain:

- **Calibration errors:** The precision of ocular motor measurements depends on effective calibration, which may be affected by fatigue, anatomical differences, and head drift.
- **Head movements:** Despite instructions to remain still, subtle head shifts may have impacted gaze position measurements, particularly in fixation tasks.
- **Blink artifacts:** Blinks can introduce noise into eye-tracking data, affecting metrics such as saccade endpoint, fixation stability, and pupil size, even after cleaning.

In addition, the absence of a standardised method to quantify fixation stability across studies complicates comparisons with existing literature, despite the meaningful differences observed in the positional fixation task.

Another important limitation is that participants were tested in their medicated “ON” and “OFF” state. Dopaminergic therapy, particularly levodopa, may influence ocular motor performance—improving some metrics while leaving others unchanged. This study did not take into account the medication state during the ocular motor assessment, preventing assessment of which ocular motor impairments are dopamine-responsive. While LEDD was included as a covariate in the GLMs, it may not fully account for individual differences in medication response, leaving residual confounding effects.

Cognitive impairment—known to influence saccadic control—was not formally assessed. Since tasks like antisaccades and memory-guided saccades rely on executive function, working memory, and attention, the absence of neuropsychological measures (e.g., Montreal Cognitive Assessment, Stroop Task, or Digit Span) limits the ability to disentangle motor from cognitive contributions to task performance. Including such assessments in future studies would provide a more complete picture of the cognitive-ocular motor relationship.

Finally, the large number of statistical comparisons across multiple eye movement tasks (fixation, pursuit, reflexive, antisaccade, memory-guided, and volitional saccades) increases the risk of Type I errors (false positives). Although Bonferroni correction was applied, small genetic subgroup sizes reduce the reliability

of these adjustments. While GLMs were employed to adjust for covariates including age, sex, LEDD, and disease duration, limited power in the genetic groups restricts the strength of the conclusions. Some effect sizes may have been inflated or underestimated due to sample variability. Larger, multicentre studies are needed to confirm these findings and strengthen their clinical relevance.

3.5.3 Future Directions

The results of this study highlight several promising avenues for future research in PD diagnostics and management. One key area is longitudinal assessment, where tracking saccadic impairments over time could offer insights into disease progression. Future studies should evaluate whether worsening saccadic performance correlates with motor or cognitive decline, and whether specific eye movement metrics can predict the transition to more advanced disease stages.

Another important direction involves examining treatment effects on saccadic performance. While dopaminergic medications have shown variable efficacy, some studies report partial improvements in certain saccade types, while others show no significant change. Investigating the effects of dopaminergic therapy, deep brain stimulation (DBS), and non-dopaminergic interventions such as cholinergic modulation could yield valuable information on the neural circuits underlying ocular motor dysfunction. Additionally, rehabilitative approaches targeting eye movement control should be explored as potential therapeutic strategies.

The development of portable, high-resolution eye-tracking technology presents a significant opportunity to integrate saccadic assessments into routine clinical workflows. Establishing standardised ocular motor testing protocols could enable clinicians to utilise eye-tracking as a rapid, objective tool for early diagnosis, disease monitoring, and treatment evaluation. This technology may be especially valuable for screening at-risk individuals, such as asymptomatic GBA and LRRK2 mutation carriers, potentially allowing for the detection of early-stage neurodegeneration prior to the onset of overt motor symptoms.

The application of machine learning and artificial intelligence to saccadic data analysis is another exciting future direction. artificial intelligence (AI) models could be trained to recognise distinct ocular motor profiles characteristic of different PD subtypes and atypical parkinsonian syndromes, thereby improving diagnostic

precision. Integrating ocular motor data with other biomarkers, such as neuroimaging and genetic information, may enhance early disease detection and classification.

Lastly, multimodal neuroimaging studies correlating saccadic abnormalities with structural and functional changes in key brain regions—including the superior colliculus, cerebellum, and frontal eye fields—could improve our understanding of the pathophysiological basis of ocular motor dysfunction in PD. Such studies may also clarify the compensatory mechanisms employed by different PD subtypes and inform the development of targeted therapeutic interventions.

Advancing these research directions could establish saccadic testing as a powerful clinical tool for early diagnosis, subtype differentiation, and treatment monitoring in PD, ultimately contributing to better patient outcomes.

3.6 Chapter Summary

This study provides critical insights into the distinct ocular motor impairments in iPD, GBA-PD, and LRRK2-PD, revealing subtype-specific deficits across fixation, pursuit, reflexive saccades, antisaccades, volitional saccades, and oblique saccades. These findings underscore the utility of ocular motor assessments as potential biomarkers for differentiating PD subtypes and tracking disease progression. The preservation of specific ocular motor functions in LRRK2-PD, contrasted with the more severe impairments observed in GBA-PD, suggests differential patterns of neurodegeneration between genetic and idiopathic forms of PD.

Despite the study's limitations, the results highlight the need for longitudinal, multimodal investigations that integrate eye-tracking, neuroimaging, and computational modelling to further elucidate the neural mechanisms underlying ocular motor dysfunction in PD. The findings also support the exploration of non-dopaminergic therapies aimed at improving eye movement control. Future research should prioritise the clinical translation of eye movement biomarkers, ensuring their integration into diagnostic workflows and therapeutic strategies for PD and its genetic variants.

4 Ocular Motor Function in Atypical Parkinsonian Syndromes

4.1 Introduction

Atypical parkinsonian syndromes, also referred to as atypical parkinsonism, encompass a group of neurodegenerative disorders that share clinical features with PD but differ significantly in their pathophysiology, progression, and treatment response (Dickson 2018). Atypical parkinsonian syndromes are characterised by a broader spectrum of symptoms, faster disease progression, poor or transient response to dopaminergic therapy, and prominent non-motor manifestations such as cognitive decline, autonomic dysfunction, psychiatric symptoms, and visual disturbances (Catalan et al. 2021). The most commonly recognised atypical parkinsonian syndromes include PSP, MSA, CBS, and, in some classifications, DLB (Mcfarland 2016; Coakeley and Strafella 2015).

A defining clinical feature of atypical parkinsonian syndromes is the poor or absent response to levodopa, the mainstay of treatment in idiopathic PD. While some individuals may exhibit temporary improvement, this is rarely sustained, and symptoms continue to progress (Przewodowska, Marzec and Madetko 2021; Likitgorn, Yan and Y. J. Liao 2021). In addition to severe motor symptoms, such as early postural instability and gait impairment, atypical parkinsonian syndromes also involve distinctive ocular motor abnormalities, deficits in language and executive function, ideomotor apraxia, and visuospatial processing difficulties (Stamelou and Bhatia 2015; Banta et al. 2023; Madetko-Alster et al. 2024). Neuroimaging can aid in the differentiation of atypical parkinsonian syndromes from PD, often revealing characteristic patterns of grey matter atrophy in regions such as the cortex, thalamus, midbrain, striatum, and cerebellum (Eimeren et al. 2019; F. Yu et al. 2015).

Despite these distinguishing features, there remains a lack of definitive, validated biomarkers that can reliably differentiate PD from atypical parkinsonian syndromes, or distinguish between the different subtypes. The clinical overlap, particularly in early stages, contributes to high rates of misdiagnosis. In many cases, definitive diagnosis is only confirmed post-mortem (Stamelou and Bhatia 2015). Furthermore, individuals who present with atypical clinical features may not meet the strict pathological criteria for any one atypical parkinsonian syndrome subtype, resulting in diagnostic ambiguity and the classification of such cases as “atypical” (Koga et al. 2015; Batla et al. 2013; Wenning et al. 1997). The emergence of genetic mutations associated with atypical parkinsonian phenotypes, such as *dctn1* and *mapt*, further complicates the diagnostic landscape

(Stamelou, N. P. Quinn and Bhatia 2013). These “atypical look-alikes” present additional challenges for differential diagnosis and underscore the need for improved clinical, neurophysiological, and biomarker-based tools.

4.1.1 Progressive Supranuclear Palsy

PSP has several recognised syndromic presentations, including Richardson syndrome, PSP with parkinsonism (PSP-P) (D. R. Williams, De Silva et al. 2005), the rare PSP with pure akinesia and gait freezing (PSP-PAGF) (D. R. Williams, Holton et al. 2007), PSP with corticobasal syndrome, and PSP with progressive nonfluent aphasia (PSP-PNFA) (D. R. Williams and Lees 2009). PSP is a tauopathy characterised by the accumulation of four-repeat tau aggregates in the brain. These aggregates form neurofibrillary tangles, tufted astrocytes, and coiled bodies, particularly in regions such as the basal ganglia. Affected structures include the SN, globus pallidus, and subthalamic nucleus, resulting in hallmark motor symptoms such as bradykinesia, rigidity, and postural instability (Dickson, Rademakers and M. L. Hutton 2007; Jennifer L. Whitwell, Lowe et al. 2017). The midbrain is also implicated, especially the oculomotor nuclei responsible for vertical gaze control, contributing to vertical gaze palsy—a core clinical feature of PSP (Ali, Botha et al. 2019). MRI often reveals midbrain atrophy, which can manifest as the “hummingbird sign,” a characteristic radiological marker of PSP (J. L. Whitwell et al. 2013). Involvement of the frontal cortex by tau pathology leads to additional cognitive and behavioural impairments (Mendez et al. 2024).

The accumulation of misfolded tau proteins in neurons and glial cells disrupts cellular functioning, leading to neuroinflammation and mitochondrial dysfunction. Activated microglia and astrocytes contribute to a pro-inflammatory environment that exacerbates neuronal injury. Although this neuroinflammatory response may initially serve a compensatory role, it ultimately promotes further neurodegeneration (Fernández-Botrán et al. 2011). Concurrent mitochondrial impairments—such as reduced bioenergetics and elevated oxidative stress—can result in neuronal energy failure and apoptosis (Prasuhn et al. 2022).

4.1.2 Eye Movements in Progressive Supranuclear Palsy

Ocular motor disturbances are among the most defining features of PSP. These include vertical supranuclear gaze palsy, slowed vertical saccades, and frequent square wave jerks (Höglinger et al. 2017). Disproportionate

slowing of vertical saccadic velocity relative to horizontal saccades is one of the earliest and most specific features of PSP. The reduced vertical saccade velocity often results in an oblique, curved trajectory—a phenomenon referred to as “round-the-houses” saccades (N. Quinn and R. J. Leigh 1996). This supports brainstem involvement and is accompanied by increased square wave jerks and gaze instability (Fearon et al. 2020). Square wave jerks in PSP are of higher frequency and amplitude than in other parkinsonian syndromes and are thought to arise from dysfunction in supratentorial cortical structures, including the temporal lobe. Although one study suggested that square wave jerk amplitude is more important than group classification for predicting occurrence (Anagnostou et al. 2020), this study excluded disorders like MSA and CBS, where square wave jerks are also common. In advanced stages of PSP, vertical gaze limitation often progresses to involve horizontal movements as well (Becker et al. 2023).

Saccades in PSP are characteristically hypometric, which may result from reduced firing of EBN in the brainstem (Terao, Tokushige et al. 2022 J. Lemos et al. 2017). Some individuals display a “zig-zag” or “saw-tooth” saccadic pattern, where hypometric vertical saccades are accompanied by horizontal corrections. This may reflect the combination of square wave jerks and hypometric saccades, possibly representing a compensatory mechanism due to impaired vertical control (Troost and Daroff 1977; Shaikh, Factor and Juncos 2017).

Volitional and memory-guided saccade function in PSP is less well studied. However, evidence suggests that volitional saccades are less accurate and slower than reflexive saccades, possibly due to frontal eye field dysfunction (Wright et al. 2022; Bruce and Goldberg 1985). Interestingly, saccade velocity and accuracy remain stable over short time scales (e.g., one minute), which contrasts with observations in PD, where performance can deteriorate over time (Koohi et al. 2021; Wright et al. 2022).

Smooth pursuit in PSP is impaired, often appearing as “cogwheel” or saccadic pursuit, with small corrective saccades superimposed on slow phases (Bruce and Goldberg 1985). OKN is also abnormal—particularly due to intrusions of eye drift in the direction of the slow phase during the fast phase—and may serve as a useful clinical sign (Lal and Truong 2019). Loss of quick phases in torsional vestibulo-ocular reflexes has also been reported in PSP (X. Ling et al. 2023). Lastly, PSP is associated with severe disinhibition during antisaccade tasks, reflected in significantly increased error rates (S. Rivaud-Péchoix et al. 2007). In summary,

the ocular motor profile of PSP is defined by vertical gaze palsy, slowed vertical saccades, high-frequency square wave jerks, broken smooth pursuit, and impaired antisaccade performance—all of which provide valuable diagnostic information.

4.1.3 Multiple System Atrophy

MSA is an α -synucleinopathy characterised by the pathological accumulation of misfolded α -synuclein protein, leading to neurodegeneration through various mechanisms. MSA is clinically divided into two main subtypes: MSA-P (predominantly parkinsonian) and MSA-C (predominantly cerebellar) (Massey et al. 2013; Fanciulli et al. 2022). MSA-P is marked by classic parkinsonian features, including bradykinesia, rigidity, and postural instability. However, in contrast to PD, individuals with MSA-P typically show a poor or transient response to dopaminergic therapies. Additionally, autonomic dysfunction, cognitive impairments affecting executive function, memory and attention, and rapid eye movement (REM) sleep behaviour disorder are commonly observed (Santaella et al. 2020; Schrag et al. 2010; Kadodwala et al. 2019). MSA-C, on the other hand, presents with cerebellar ataxia, including unsteady gait, balance impairment, and coordination difficulties (P. A. Low et al. 2015). Like MSA-P, MSA-C also exhibits autonomic dysfunction and cognitive decline, often coupled with mood disorders and sleep disturbances (S. Ren et al. 2019; A. Sugiyama et al. 2020).

The pathological hallmark of MSA is the presence of glial cytoplasmic inclusions composed of aggregated α -synuclein, which lead to ROS production, mitochondrial dysfunction, and neuroinflammatory processes (Liang et al. 2008; Lingyu Zhang et al. 2022; Mandler et al. 2015). The most affected brain regions include the striatonigral system, olivopontocerebellar system, and the autonomic nervous system (Sturm et al. 2016; Kasai et al. 2016). Within the striatonigral system, significant neuronal loss occurs in the putamen and SN, resulting in parkinsonian features (Y. Watanabe et al. 2023; Sekiya et al. 2019). In the olivopontocerebellar system, degeneration of Purkinje cells and neuronal loss in the inferior olivary nucleus and pontine nuclei lead to cerebellar signs (Meng et al. 2023; Miki et al. 2022).

4.1.4 Eye Movements in Multiple System Atrophy

Ocular motor abnormalities are common in MSA and reflect the underlying neuropathology. Prominent features include excessive SWJs, mild supranuclear gaze palsy, gaze-evoked nystagmus, positional downbeat nystagmus, saccadic hypometria, impaired smooth pursuit, and abnormal suppression of the VOR—consistent with striatonigral and olivopontocerebellar degeneration (T. J. Anderson and MacAskill 2013).

Smooth pursuit gain is significantly reduced in MSA compared to healthy controls (T. J. Anderson and MacAskill 2013). Notably, individuals with MSA-C demonstrate lower smooth pursuit gain than those with MSA-P (H. Zhou et al. 2022). Although pursuit deficits are observed in both MSA and PSP, PSP is not typically associated with volume loss in pontocerebellar regions, a key neural substrate for smooth pursuit (Vintonyak et al. 2017; Lanfranchi, Jerman and Vianello 2009). Saccadic intrusions during pursuit, such as catch-up saccades, are also observed in MSA (Lal and Truong 2019). While MSA-C is characterised by fragmented or “broken-up” pursuit due to decreased gain, MSA-P can exhibit anticipatory saccades that precede the target’s movement (Pinkhardt, Kassubek et al. 2009).

Saccadic velocity is generally preserved in MSA, though mild-to-moderate saccadic hypometria is often reported (Linder et al. 2012). Some individuals may also exhibit vertical supranuclear gaze palsy, albeit less severe than in PSP (T. Anderson et al. 2008). In antisaccade tasks, MSA individuals (subtype not always specified) demonstrate higher error rates than controls and individuals with PD. Moreover, antisaccade latency in MSA does not improve over time, in contrast to controls and PD, suggesting its utility as a progression marker (Brooks et al. 2017).

Compared to PD and CBS, individuals with MSA exhibit more frequent SWJs, although the frequency remains lower than in PSP (Otero-Millan, Serra et al. 2011). In MSA, SWJs can occasionally be larger in amplitude, termed “macro-square wave jerks” (Yamamoto et al. 1992). Gaze-evoked, downbeat, and rebound nystagmus are often observed in MSA-C and are linked to cerebellar dysfunction (Gilman et al. 2008). Abnormal VOR suppression is a particularly useful clinical sign distinguishing MSA from other parkinsonian syndromes (Rascol et al. 1995). Interestingly, MSA-P individuals without overt cerebellar signs may still exhibit cerebellar ocular motor abnormalities, complicating differential diagnosis (J. Y. Lee et al. 2009).

Overall, the combination of frequent SWJs, saccadic hypometria, disrupted pursuit, and impaired VOR suppression is strongly indicative of MSA-P over PD, where cerebellar involvement is not expected. Notably, convergence eye movements are typically preserved in MSA, whereas abnormalities are more frequently reported in DLB and PD.

4.1.5 Corticobasal Syndrome

CBS, also referred to as corticobasal degeneration, is a 4-repeat tauopathy characterised by neuronal loss and gliosis (Isella et al. 2018). The clinical presentation is heterogeneous and frequently includes parkinsonian features. Affected individuals often exhibit asymmetric rigidity and bradykinesia, accompanied by dystonia and myoclonus (Boeve 2011; Dopper et al. 2011). A hallmark symptom is limb apraxia—the inability to perform purposeful movements despite intact motor function—commonly manifesting as the “alien limb phenomenon,” in which the limb appears to act independently (Constantinides et al. 2019). Additional features include cognitive deficits in executive function, language, and memory, as well as impairments in sensory recognition (Fekete et al. 2012; Constantinides et al. 2019).

Neurodegeneration in CBS results from the accumulation of hyperphosphorylated tau protein, forming neurofibrillary tangles and other tau aggregates. Affected regions typically include the frontal and parietal cortices—particularly the parasagittal superior frontoparietal regions—as well as structures within the BG, including the SN and putamen (Isella et al. 2018; Constantinides et al. 2019). This is accompanied by reactive gliosis, a pathological increase in glial cell proliferation (Isella et al. 2018; Constantinides et al. 2019). Astrocytic plaques and thread-like tau pathology are also observed in both grey and white matter (Dickson, Braak et al. 2009).

4.1.6 Eye Movements in Corticobasal Syndrome

Ocular motor abnormalities in CBS primarily include saccadic apraxia, or increased saccadic latency—the delay between target appearance and saccade initiation (S. Rivaud-Péchoux et al. 2007). Given the lateralised nature of degeneration in CBS, these latency increases are often ipsilateral to the most affected side

(Anderson 2008; Oculomotor individuals; Sophie Rivaud-Péchoix et al. 2000). Importantly, while latency is impaired, saccadic metrics such as velocity and amplitude remain relatively preserved compared to PD and PSP, providing a useful clinical distinction (Mosimann et al. 2005).

CBS individuals also show elevated error rates and longer latencies in antisaccade tasks compared to both controls and PD individuals. Notably, they often fail to spontaneously self-correct their errors (S. Rivaud-Péchoix et al. 2007; Siobhan Garbutt et al. 2008). Atrophy in the PC has been linked to increased latency in prosaccades, while dysfunction in the FEF may underlie impairments in both pro- and antisaccade generation. Interestingly, in single-task paradigms (prosaccades or antisaccades alone), antisaccade error rates were comparable between CBS and PD, whereas PSP individuals exhibited significantly higher error rates. However, in mixed-task paradigms, CBS individuals showed a marked increase in both prosaccade and antisaccade errors, suggesting that task-switching exacerbates executive deficits (S. Rivaud-Péchoix et al. 2007).

Additional ocular motor abnormalities have been documented in CBS, although they are generally milder than in other atypical parkinsonian syndromes. Impaired OKN and increased SWJs are observed in some cases. Reduced pursuit gain, restricted ocular range, and “jolting” or abrupt eye movements during smooth pursuit have also been reported (Rinne et al. 1994). Vertical supranuclear gaze palsy occurs less frequently than in PSP but may be present in up to 20% of CBS individuals early in the disease, increasing to 50% in those with overlapping PSP pathology (H. Ling et al. 2014). Atypical cases may also exhibit impaired vertical saccades and early reductions in horizontal saccadic velocity (Rinne et al. 1994), though early SWJs and pronounced saccadic delays remain more indicative of PSP.

In summary, CBS is defined by ocular motor apraxia, particularly manifesting as increased latency of voluntary saccades. These impairments are often lateralised to the more affected apraxic limb, and while milder than in PSP or MSA, they may still hold diagnostic value when integrated with broader clinical and cognitive assessments.

4.1.7 Dementia with Lewy Bodies

DLB is defined by the presence of Lewy bodies and Lewy neurites, which are primarily composed of aggregated alpha-synuclein protein (Hansen et al. 2019). The accumulation of these misfolded proteins leads to neuronal dysfunction and cell death in the cerebral cortex, SN, and limbic system (Surendranathan, Rowe and O'Brien 2015). DLB frequently coexists with other neurodegenerative pathologies, most notably Alzheimer's disease (AD), with a significant number of cases also displaying amyloid plaques and neurofibrillary tangles characteristic of AD (Compta et al. 2011). As in other forms of dementia, neuroinflammation is a key feature, driven by activated microglia and astrocytes, which exacerbate neuronal degeneration (Gate et al. 2021; Zirra and Huxford 2022).

Lewy body dementia includes two clinical presentations: dementia with Lewy bodies and Parkinson's disease dementia (PDD). The clinical implications of DLB differ from those of PD and other atypical parkinsonian syndromes, primarily due to the predominant cortical involvement in DLB. The distribution of Lewy bodies differs between these two presentations: in DLB, they are more widespread, affecting the neocortex, limbic areas, and brainstem, while in PDD, they are largely concentrated in the SN and other regions of the BG (Hansen et al. 2019; Surendranathan, Rowe and O'Brien 2015). Consequently, DLB is associated with cognitive fluctuations, visual hallucinations, and other neuropsychiatric symptoms, whereas PDD more commonly presents with predominant motor features (Compta et al. 2011).

4.1.8 Eye Movements in Dementia with Lewy Bodies

Systematic reporting of ocular motor abnormalities in DLB is limited, both in clinical and experimental settings. In one study involving 20 individuals with DLB, saccadic eye movements were compared to those of individuals with PDD. The DLB group exhibited impairments in both reflexive and voluntary saccade generation, as well as difficulties with more complex tasks such as saccadic prediction, decision-making, and antisaccades (Mosimann et al. 2005). Compared to individuals with AD and PD, those with DLB demonstrated more severe saccadic dysfunction, potentially due to the widespread cortical and subcortical degeneration characteristic of DLB.

Other studies have identified prolonged latencies across various horizontal saccade types, impairments in

predictive saccades, and deficits in saccadic suppression (Mosimann et al. 2005; Kapoula et al. 2010). A detailed examination of horizontal and vertical saccades in DLB individuals showed a reduced tendency to generate short-latency “express saccades” in gap tasks, where a temporal gap separates fixation offset from target onset (Mosimann et al. 2005). These individuals also showed reduced saccadic velocity and gain, as well as increased latency in both reflexive and voluntary saccades, with deficits worsening alongside disease progression (Sophie Rivaud-Péchoux et al. 2000).

Case reports have described a subset of DLB individuals who develop vertical gaze palsy, often accompanied by horizontal gaze disturbances (Nakashima et al. 2003; Brett, Henson and Staunton 2002; Kapoula et al. 2010). These cases can closely resemble clinical presentations of PSP, highlighting the importance of careful differential diagnosis when vertical gaze deficits are observed. Additionally, convergence insufficiency has been reported in DLB, although it is not specific to the condition and may also be seen in PD.

In summary, DLB is typically associated with increased saccadic latency, reduced saccade gain, and a higher number of errors during complex saccadic tasks. These deficits reflect cortical and subcortical involvement and, when present alongside characteristic cognitive and neuropsychiatric symptoms, may aid in the differential diagnosis of dementia-related parkinsonism.

4.2 Project Aims

1. To assess the distinct ocular motor profiles of PSP, MSA, CBS, and DLB.
2. To identify ocular motor biomarkers that can differentiate atypical parkinsonian syndromes from idiopathic PD.

4.3 Methods

4.3.1 Participants

Participants were recruited for the ocular motor study in atypical parkinsonian syndromes through the methods described in Chapter 2: General Methods. Inclusion criteria were: (1) a confirmed diagnosis of an atypical

parkinsonian syndrome or a working diagnosis of atypical parkinsonism; (2) exclusion of idiopathic PD or genetically confirmed PD through genetic testing; (3) age between 40–80 years; (4) normal or corrected-to-normal vision; (5) ability to provide informed consent; (6) ability to follow verbal instructions; and (7) ability to sit comfortably for the duration of the testing. Exclusion criteria included: (1) presence of other neurological conditions or a history of head trauma or stroke; (2) bilateral visual impairments (recordings were permitted if vision was intact in one eye); (3) movement-related visual disturbances such as diplopia; (4) severe psychiatric conditions (e.g., psychosis); (5) systemic health conditions affecting vision, such as diabetic retinopathy; (6) pregnancy (self-declared); (7) history of epilepsy; (8) eyelid-opening apraxia; (9) inability to remain seated; and (10) severely impaired ocular motor function that prevented successful calibration/validation.

Healthy controls were also recruited through the methods outlined in Chapter 2. Inclusion criteria were: (1) no history of neurodegenerative, neurological, or movement disorders; (2) normal or corrected vision; (3) normal cognitive function; and (4) ability to provide informed consent and comply with procedures. Exclusion criteria mirrored those of the patient cohort, including: (1) bilateral visual impairments or diplopia; (2) severe psychiatric conditions; (3) systemic vision-affecting conditions such as diabetes with retinopathy; (4) pregnancy (self-declared); and (5) history of epilepsy.

Participants were categorised into six groups based on established diagnostic criteria: PSP, MSA, CBS, DLB, atypical parkinsonism (ATP), and healthy controls. A total of 92 participants were included: 16 with PSP, 11 with MSA, 6 with CBS, 2 with DLB, 10 with ATP, and 51 healthy controls. The study received ethical approval from the UCL Research Ethics Committee. Written informed consent was obtained from all participants.

4.3.2 Ocular Motor Assessment

All participants underwent the standard ocular motor battery detailed in Chapter 2: General Methods. The experimental setup, including calibration and validation procedures, was identical to those previously described.

4.3.3 Data Processing and Analysis

Data processing and metric extraction followed the procedures in Chapter 2. Additional analyses were conducted to explore patterns in eye movements in greater detail.

Saccadic analysis during pursuit tasks involved generating a saccade report for each participant, which included the total number of saccades and individual saccade characteristics such as amplitude, peak velocity, average velocity, start and end times, and end position. Saccades were binned into six amplitude-based buckets: $<1^\circ$, $1\text{--}2^\circ$, $2\text{--}3^\circ$, $3\text{--}4^\circ$, $4\text{--}5^\circ$, and $>5^\circ$. For each bucket, the number of saccades and average metrics were calculated. This analysis was conducted separately for horizontal, vertical, and elliptical pursuit directions. Histograms were generated to visualise saccade distribution across amplitude bins.

To account for the main sequence effect—the nonlinear relationship between saccade amplitude and peak velocity—saccadic velocities were corrected using equations detailed in Chapter 2. These adjusted values were used for further analysis. For oblique, reflexive, volitional, and memory-guided saccades, a temporal analysis was performed by plotting accuracy and peak velocity of successive saccades over time. Each saccade was represented as a point, and linear regression was applied to derive the slope and coefficient of determination (R^2).

In horizontal and vertical paradigms, true displacements were calculated using eye position coordinates: Y-axis displacement for horizontal tasks and X-axis displacement for vertical tasks. This was especially relevant for reflexive, volitional, and memory-guided saccades.

To identify qualitative features not captured by quantitative metrics, eye movement traces were mapped and overlaid with target locations for oblique, reflexive, volitional, and memory-guided tasks. This allowed visual detection of abnormal saccadic patterns such as “round-the-houses” and “zig-zag” trajectories.

To identify which ocular motor measures were most sensitive in detecting PD-related changes, a composite score was computed for each type of eye movement. Hybrid-weighted composite z -scores were calculated by incorporating both statistical significance (p -values) and precision (confidence interval widths) into the weighting process. First, the z -scores for each group’s effect size were computed using the formula:

$$z = \frac{x - \mu}{\sigma}$$

where x is the group's effect size, μ is the mean effect size across groups, and σ is the standard deviation.

The CI width for each metric was calculated as:

$$\text{CI Width} = \text{Upper CI} - \text{Lower CI}$$

The hybrid weight for each metric was then computed as:

$$\text{Weight} = \frac{1}{(\text{p-value} \times \text{CI Width}) + \varepsilon'}$$

where ε' is a small constant to prevent division by zero. Each z -score was multiplied by its corresponding hybrid weight, and the weighted z -scores were summed across all metrics for each group. The final composite z -score was obtained by normalising the weighted sum by the total hybrid weight for each group. This approach ensures that the composite scores reflect both the statistical significance and the precision of the effect sizes, providing a robust measure of relative group performance across paradigms.

4.3.4 Statistical Analyses

Demographic data were summarised using descriptive statistics. The dataset was inspected for missing values, and participants with incomplete data were excluded from further analysis. To address the limited sample sizes of the CBS and DLB groups, bootstrapping (1,000 resamples) was used to compute CIs and p-values.

The bootstrapped values were subsequently used for further analysis. A series of GLMs were fitted to evaluate the effects of group, age, sex, LEDD, and disease duration on each ocular motor metric using the `glm2` function in R. Model estimates included regression coefficients (β estimates), 95% CIs, p-values, AIC, and BIC for model comparison. Multiple comparisons were accounted for using the Bonferroni correction. Following the GLM analysis, post hoc pairwise comparisons were conducted among all the groups using the estimated marginal means package in R. Multiple comparisons were adjusted using the Bonferroni correction. The significance level for all analyses was set at $\alpha = 0.05$. All analyses were conducted using R (Version 2023.09.1+494, R Core Team, Vienna, Austria). The data tables for all the analyses are provided in the

appendix.

4.4 Results

4.4.1 Participants

After account for data loss and exclusions the control group comprised 48 individuals (26 females and 22 males) with a mean age of 62.66 years ($SD = 13.68$, range = 22.25–79.59). The ATP group included 10 participants (5 males and 5 females) with a mean age of 68.90 years ($SD = 2.96$, range = 65.08–73.45). The CBS group consisted of 6 individuals (3 males and 3 females), with a mean age of 70.33 years ($SD = 8.10$, range = 57.91–79.34). The DLB group included 2 males with a mean age of 64.50 years ($SD = 7.78$, range = 59.00–70.00). The MSA group comprised 11 individuals (7 males and 4 females), with a mean age of 67.00 years ($SD = 5.51$, range = 60.06–75.84). The PSP group consisted of 16 participants (9 males and 7 females) with a mean age of 68.71 years ($SD = 3.31$, range = 64.10–75.31). The mean disease duration was 4.15 years ($SD = 1.50$) for the ATP group, 2.33 years ($SD = 1.03$) for the CBS group, 5.00 years ($SD = 0.00$) for the DLB group, 3.67 years ($SD = 1.10$) for the MSA group, and 4.00 years ($SD = 1.34$) for the PSP group.

Table 11: Demographic and clinical characteristics of the study cohort. Values are presented as mean \pm standard deviation (SD). Age is reported for all participants, while disease duration is reported for disease groups only. Data are stratified by group and sex. “-” indicates not applicable or unavailable.

Group	Age (Mean \pm SD)	Disease Duration (Mean \pm SD)
ATP (N = 10)	68.89 \pm 2.85	4.11 \pm 1.36
Males (N = 5)	68.80 \pm 2.59	3.80 \pm 1.10
Females (N = 5)	69.00 \pm 3.56	4.50 \pm 1.73
CBS (N = 6)	69.50 \pm 8.10	2.50 \pm 1.00
Males (N = 3)	72.00 \pm 9.56	2.00 \pm 0.90
Females (N = 3)	68.67 \pm 9.71	2.67 \pm 1.15
Healthy Controls (N = 48)	62.89 \pm 14.10	-
Males (N = 22)	63.16 \pm 15.44	-
Females (N = 26)	62.65 \pm 13.14	-
DLB (N = 2)	64.50 \pm 7.78	5.00 \pm 0.00
Males (N = 2)	64.50 \pm 7.78	5.00 \pm 0.00
Females (N = 0)	-	-
MSA (N = 11)	67.00 \pm 5.96	3.60 \pm 0.97
Males (N = 7)	67.00 \pm 3.46	4.33 \pm 1.15
Females (N = 4)	67.00 \pm 7.02	3.29 \pm 0.76
PSP (N = 16)	68.73 \pm 3.22	4.00 \pm 1.36
Males (N = 9)	68.12 \pm 3.36	3.50 \pm 1.69
Females (N = 7)	69.43 \pm 3.15	4.57 \pm 0.53

4.4.2 Eye Movements in Progressive Supranuclear Palsy

In the fixation task, the PSP group exhibited an increased number of large SWJs ($\beta = 9.677$, 95% CI [5.713, 13.641], $p < 0.001$), intrusive saccades ($\beta = 22.093$, 95% CI [12.456, 31.729], $p < 0.001$), and overall saccade count ($\beta = 24.157$, 95% CI [10.656, 37.658], $p < 0.001$) compared to healthy controls. However, no significant differences were noted in the number of small SWJs or microsaccades. Additionally, other measures of fixation, including average pupil size, average fixation duration, and fixation precision metrics, were similar to controls in PSP.

In the positional fixation/nystagmus task, the PSP group exhibited an increased number of large SWJs across trials, with significant differences in the up ($\beta = 4.717$, 95% CI [2.085, 7.349], $p = 0.0007$), down ($\beta = 4.875$, 95% CI [2.419, 7.331], $p = 0.0002$), right ($\beta = 4.333$, 95% CI [2.387, 6.279], $p < 0.0001$), and left positions ($\beta = 4.771$, 95% CI [2.572, 6.970], $p < 0.0001$) compared to healthy controls. Additionally, PSP individuals showed significantly increased numbers of intrusive saccades in the up ($\beta = 22.880$, 95% CI [12.776, 32.984], $p < 0.0001$), down ($\beta = 19.159$, 95% CI [10.395, 27.923], $p < 0.0001$), right ($\beta = 17.037$, 95% CI [8.248, 25.825], $p = 0.0003$), and left positions ($\beta = 22.814$, 95% CI [12.120, 33.508], $p < 0.0001$) compared to controls.

In the pursuit task, the PSP group exhibited significantly increased average RMSE gaze error across multiple trial conditions compared to healthy controls. Specifically, RMSE gaze error was higher during horizontal pursuit at 0.2 Hz ($\beta = 1.446$, 95% CI [0.208, 2.684], $p = 0.025$) and 0.4 Hz ($\beta = 1.497$, 95% CI [0.122, 2.871], $p = 0.036$) compared to controls. Similarly, RMSE gaze error was significantly elevated during vertical pursuit at 0.2 Hz ($\beta = 0.980$, 95% CI [0.194, 2.154], $p = 0.011$) and 0.4 Hz ($\beta = 1.285$, 95% CI [0.452, 2.118], $p = 0.003$) compared to controls. Impairments were also observed in circular pursuit, with increased RMSE gaze error during anticlockwise pursuit at 0.2 Hz ($\beta = 1.810$, 95% CI [0.565, 3.054], $p = 0.006$) and 0.4 Hz ($\beta = 2.743$, 95% CI [0.651, 4.214], $p < 0.001$), as well as during clockwise pursuit at 0.2 Hz ($\beta = 2.119$, 95% CI [0.650, 3.262], $p = 0.002$) and 0.4 Hz ($\beta = 2.777$, 95% CI [0.701, 3.961], $p < 0.001$) compared to controls. Additionally, velocity gain was significantly reduced in PSP during vertical pursuit at 0.2 Hz ($\beta = -0.626$, 95% CI [-1.182, -0.069], $p = 0.030$) and 0.4 Hz ($\beta = -0.147$, 95% CI [-0.455, -0.023], $p = 0.045$) compared to controls.

In the horizontal antisaccade task, the PSP group exhibited significantly reduced antisaccade amplitude ($\beta = -6.321$, 95% CI [-7.530, -5.112], $p < 0.001$), peak velocity ($\beta = -172.802$, 95% CI [-221.958, -123.646], $p < 0.001$), and saccade average velocity ($\beta = -71.977$, 95% CI [-89.645, -54.309], $p < 0.001$) compared to healthy controls. Additionally, the PSP group made significantly more antisaccade errors ($\beta = 4.767$, 95% CI [2.027, 7.506], $p = 0.001$) and fewer correct antisaccades ($\beta = -5.034$, 95% CI [-7.742, -2.326], $p < 0.001$) compared to controls. In the vertical antisaccade task, the PSP group demonstrated a significant reduction in antisaccade amplitude ($\beta = -4.348$, 95% CI [-5.387, -3.308], $p < 0.001$), peak velocity ($\beta = -191.857$, 95% CI [-254.151, -129.562], $p < 0.001$), and saccade average velocity ($\beta = -72.654$, 95% CI [-88.268, -57.039], $p < 0.001$) compared to healthy controls. Additionally, PSP individuals exhibited a higher saccadic latency

($\beta = 98.126$, 95% CI [23.089, 173.162], $p = 0.012$) and a greater number of self-corrected antisaccades ($\beta = 2.438$, 95% CI [0.453, 4.424], $p = 0.018$) compared to controls.

Significant differences were observed in oblique saccades at 4°, 8°, and 10° in the PSP group compared to controls. The PSP group exhibited a significant decrease in saccade amplitude at 4° ($\beta = -0.670$, 95% CI [-1.118, -0.223], $p = 0.004$), 8° ($\beta = -2.101$, 95% CI [-2.863, -1.339], $p < 0.001$), and 10° ($\beta = -2.928$, 95% CI [-3.865, -1.990], $p < 0.001$) compared to controls. Average saccade velocity was decreased in PSP at 4° ($\beta = -23.862$, 95% CI [-34.745, -12.978], $p < 0.001$), 8° ($\beta = -39.096$, 95% CI [-53.952, -24.240], $p < 0.001$), and 10° ($\beta = -49.226$, 95% CI [-65.751, -32.701], $p < 0.001$) compared to controls. Additionally, PSP participants demonstrated lower accuracy in both the X (4°: $\beta = 44.399$, 95% CI [14.506, 74.293], $p = 0.005$; 8°: $\beta = 67.479$, 95% CI [23.889, 111.070], $p = 0.003$; 10°: $\beta = 108.708$, 95% CI [58.054, 159.363], $p < 0.001$) and Y (4°: $\beta = 54.172$, 95% CI [22.040, 86.305], $p = 0.001$; 8°: $\beta = 108.568$, 95% CI [62.014, 155.122], $p < 0.001$; 10°: $\beta = 172.728$, 95% CI [118.458, 226.997], $p < 0.001$) dimensions compared to controls. The proportion of correct responses was significantly lower in PSP at 8° ($\beta = -3.676$, 95% CI [-6.045, -1.306], $p = 0.003$) and 10° ($\beta = -4.831$, 95% CI [-7.643, -2.020], $p = 0.001$) compared to controls. A significant increases in hypometric saccades was noted in PSP at 4° ($\beta = 10.169$, 95% CI [5.917, 14.422], $p < 0.001$), 8° ($\beta = 11.340$, 95% CI [6.772, 15.908], $p < 0.001$), and 10° ($\beta = 12.999$, 95% CI [8.813, 17.185], $p < 0.001$) compared to controls. Additionally, hypermetric saccades were significantly increased at 4° ($\beta = 11.216$, 95% CI [6.938, 15.494], $p < 0.001$), 8° ($\beta = 14.221$, 95% CI [9.544, 18.898], $p < 0.001$), and 10° ($\beta = 16.896$, 95% CI [12.531, 21.260], $p < 0.001$) compared to controls.

In the horizontal reflexive saccade task, the PSP group exhibited significantly reduced saccade accuracy ($\beta = 127.392$, 95% CI [31.157, 223.628], $p = 0.011$) and reduced saccade average velocity ($\beta = -47.036$, 95% CI [-64.860, -29.212], $p < 0.001$) compared to healthy controls. Additionally, PSP individuals showed a significant decrease in current saccade peak velocity ($\beta = -140.426$, 95% CI [-205.149, -75.703], $p < 0.001$) and reduced saccade amplitude ($\beta = -2.711$, 95% CI [-3.736, -1.685], $p < 0.001$) compared to controls. PSP individuals also made significantly fewer correct reflexive saccades ($\beta = -8.748$, 95% CI [-13.058, -4.439], $p < 0.001$) and more hypometric saccades ($\beta = 9.383$, 95% CI [5.215, 13.551], $p < 0.001$) compared to controls. In the vertical reflexive saccade task, PSP individuals demonstrated a significantly reduced saccade accuracy ($\beta = 153.349$, 95% CI [85.332, 221.365], $p < 0.001$) and a reduction in saccade average velocity (β

= -59.422, 95% CI [-78.164, -40.679], $p < 0.001$) compared to controls. PSP individuals also exhibited a significant decrease in current saccade peak velocity ($\beta = -164.748$, 95% CI [-233.152, -96.344], $p < 0.001$) and increased saccadic latency ($\beta = 104.557$, 95% CI [27.076, 182.038], $p = 0.010$) compared to controls. Additionally, saccade amplitude was significantly reduced ($\beta = -3.418$, 95% CI [-4.576, -2.259], $p < 0.001$) compared to controls. Similar to the horizontal direction, PSP individuals made fewer correct reflexive saccades ($\beta = -7.185$, 95% CI [-10.889, -3.480], $p < 0.001$) while exhibiting more hypometric saccades ($\beta = 9.161$, 95% CI [5.275, 13.047], $p < 0.001$) compared to controls.

In the volitional saccade task, the PSP group showed significantly altered eye movement characteristics compared to controls. The PSP group demonstrated an increased number of saccadic steps ($\beta = 0.753$, 95% CI [0.351, 1.155], $p = 0.0004$) and a reduced number of correct saccades ($\beta = -14.607$, 95% CI [-26.002, -3.213], $p = 0.0140$) compared to controls. Additionally, saccadic amplitude was significantly lower in PSP ($\beta = -6.605$, 95% CI [-9.505, -3.705], $p < 0.001$), along with decreased average saccade velocity ($\beta = -65.223$, 95% CI [-94.400, -36.047], $p < 0.001$) and saccade peak velocity ($\beta = -157.951$, 95% CI [-221.439, -94.463], $p < 0.001$) compared to controls. In the vertical volitional saccade task, the PSP group had a significantly higher number of saccadic steps ($\beta = 0.228$, 95% CI [0.060, 0.516], $p = 0.0124$) and reduced saccade accuracy ($\beta = 168.040$, 95% CI [109.034, 227.045], $p < 0.001$) compared to controls. Furthermore, PSP participants exhibited a lower number of correct saccades ($\beta = -17.057$, 95% CI [-27.066, -7.047], $p = 0.0013$), an increased number of hypometric saccades ($\beta = 12.270$, 95% CI [1.643, 22.898], $p = 0.0264$), and reduced saccade amplitude ($\beta = -6.086$, 95% CI [-8.406, -3.767], $p < 0.001$) compared to controls. Additionally, the PSP group had lower average saccade velocity ($\beta = -65.004$, 95% CI [-90.069, -39.939], $p < 0.001$) and peak saccadic velocity ($\beta = -165.445$, 95% CI [-241.558, -89.332], $p < 0.001$) compared to controls.

In the memory-guided saccade task, the PSP group exhibited significant differences compared to healthy controls. In the horizontal direction, PSP participants showed an increased number of saccadic steps ($\beta = 0.698$, 95% CI [0.263, 1.133], $p = 0.002$) and decreased saccadic accuracy ($\beta = 153.458$, 95% CI [48.996, 257.920], $p = 0.005$), while the number of correct saccades was significantly lower ($\beta = -8.961$, 95% CI [-17.412, -0.510], $p = 0.041$) compared to controls. Additionally, PSP participants demonstrated reduced saccadic performance, with decreased saccadic amplitude ($\beta = -8.893$, 95% CI [-12.125, -5.662], $p < 0.001$), average saccade velocity ($\beta = -74.795$, 95% CI [-102.156, -47.435], $p < 0.001$), and saccade peak velocity

($\beta = -171.861$, 95% CI [-230.600, -113.123], $p < 0.001$) compared to controls. Similarly, in the vertical direction, the number of saccadic steps ($\beta = 0.308$, 95% CI [0.026, 0.590], $p = 0.035$) was higher and accuracy ($\beta = 163.045$, 95% CI [108.244, 217.846], $p < 0.001$) were lower, resulting in a lower number of correct saccades ($\beta = -14.203$, 95% CI [-21.291, -7.116], $p < 0.001$) compared to controls. Furthermore, PSP participants showed an increased number of hypometric saccades ($\beta = 17.378$, 95% CI [6.706, 28.049], $p = 0.002$) compared to controls. As observed in the horizontal direction, PSP participants exhibited significantly reduced saccadic amplitude ($\beta = -7.092$, 95% CI [-9.154, -5.031], $p < 0.001$), average saccade velocity ($\beta = -64.906$, 95% CI [-88.675, -41.136], $p < 0.001$), and saccade peak velocity ($\beta = -169.904$, 95% CI [-242.698, -97.110], $p < 0.001$) compared to controls.

4.4.3 Eye Movements in Corticobasal Syndrome

In the fixation task, the CBS group exhibited a significant increase in fixation precision score as measured by RMS and SD ($\beta = 0.0259$, 95% CI [0.0092, 0.0427], $p = 0.0033$ and $\beta = 0.0361$, 95% CI [0.0090, 0.0632], $p = 0.0108$, respectively) compared to controls. The microsaccade count ($\beta = 34.388$, 95% CI [14.758, 54.018], $p = 0.00095$) and small SWJ count ($\beta = 29.542$, 95% CI [15.953, 43.130], $p < 0.0001$) was also higher compared to healthy controls. In the positional fixation/nystagmus task where the target was positioned in four different positions, up, down, right and left, the CBS group had an increased number of large intrusive saccades only in the right direction ($\beta = 16.643$, 95% CI [1.799, 31.487], $p = 0.031$).

In the pursuit task, the CBS group exhibited significantly higher RMSE in gaze across multiple conditions. Specifically, RMSE was elevated in horizontal pursuit at 0.2 Hz ($\beta = 4.336$, 95% CI [2.245, 6.427], $p = 0.0001$) and 0.4 Hz ($\beta = 4.241$, 95% CI [1.920, 6.563], $p = 0.0006$) compared to controls. Similarly, deficits were observed in vertical pursuit at 0.2 Hz ($\beta = 2.305$, 95% CI [0.322, 4.289], $p = 0.0254$) and 0.4 Hz ($\beta = 2.619$, 95% CI [1.211, 4.026], $p = 0.0005$) compared to controls. Impairments were also evident in anticlockwise pursuit at 0.2 Hz ($\beta = 4.994$, 95% CI [2.892, 7.096], $p < 0.0001$) and 0.4 Hz ($\beta = 4.349$, 95% CI [2.194, 6.504], $p = 0.0002$), as well as in clockwise pursuit at 0.2 Hz ($\beta = 4.386$, 95% CI [2.236, 6.536], $p = 0.0001$) and 0.4 Hz ($\beta = 4.510$, 95% CI [2.189, 6.831], $p = 0.0003$) compared to healthy controls. Gain was lower in the CBS group in the clockwise direction at 0.4Hz ($\beta = -0.267$, 95% CI [-0.514, -0.019], $p = 0.037$) compared to controls.

In the antisaccade task, individuals with CBS exhibited significant differences compared to healthy controls. In the horizontal direction, the CBS group had prolonged antisaccade end time ($\beta = -86.266$, 95% CI [-170.319, -2.212], $p = 0.0477$) and start time ($\beta = -121.384$, 95% CI [-201.370, -41.398], $p = 0.0039$), along with a higher number of errors ($\beta = 7.440$, 95% CI [2.813, 12.066], $p = 0.0023$) and fewer correct responses ($\beta = -7.524$, 95% CI [-12.099, -2.950], $p = 0.0018$) compared to controls. In the vertical direction, the CBS group exhibited reduced antisaccade amplitude ($\beta = -3.160$, 95% CI [-4.917, -1.404], $p = 0.0007$) and lower average velocity ($\beta = -47.531$, 95% CI [-73.904, -21.159], $p = 0.0007$) compared to controls.

No significant differences were observed in the oblique saccades task at 4°, 8°, and 10° between the CBS group and healthy controls. In all conditions, the CBS group exhibited performance levels comparable to those of controls, with no statistically significant differences found in metrics such as saccade amplitude, latency, accuracy, or error types.

In the reflexive saccade task, individuals with CBS demonstrated significant impairments in the vertical direction. The CBS group exhibited a significantly reduced correct saccades ($\beta = -6.965$, 95% CI [-13.222, -0.709], $p = 0.032$) compared to healthy controls. Additionally, the number of hypometric saccades was significantly increased in CBS ($\beta = 7.948$, 95% CI [1.385, 14.512], $p = 0.020$) compared to controls. No significant differences were observed in the horizontal reflexive saccades.

In the volitional saccade task, no significant differences were observed between individuals with CBS and healthy controls. Analyses of key parameters, including saccade amplitude, peak velocity, latency, and accuracy, yielded p-values greater than 0.05, indicating no statistically significant impairments in volitional eye movements in CBS.

In the memory-guided saccade task, individuals with CBS exhibited significant impairments compared to healthy controls. In the horizontal direction, CBS participants demonstrated a significantly increased number of hypometric saccades ($\beta = 26.555$, 95% CI [4.185, 48.925], $p = 0.023$) compared to controls. Additionally, they exhibited a significantly reduced saccadic amplitude ($\beta = -7.152$, 95% CI [-12.610, -1.694], $p = 0.012$), along with a delayed saccade end time ($\beta = 3296.902$, 95% CI [1094.753, 5499.051], $p = 0.004$) and saccade start time ($\beta = 3514.543$, 95% CI [1271.439, 5757.648], $p = 0.003$), compared to controls. In the vertical

direction, CBS participants also showed an increased number of hypometric saccades ($\beta = 9.574$, 95% CI [8.450, 27.599], $p = 0.030$) and a delayed saccade start time ($\beta = 177.378$, 95% CI [4.598, 350.159], $p = 0.048$), compared to controls.

4.4.4 Eye Movements in Multiple System Atrophy

In the central fixation task, no significant differences were observed between individuals with MSA and healthy controls. Analyses of key fixation stability metrics, including fixation duration, precision, and microsaccade frequency, yielded p-values greater than 0.05, indicating no statistically significant impairments in central fixation in MSA. In the positional fixation task, individuals with MSA exhibited a significant increase in the number of saccades across multiple trials. Specifically, the number of large intrusive saccades was significantly higher in the up ($\beta = 10.782$, 95% CI [0.451, 22.014], $p = 0.044$), down ($\beta = 9.986$, 95% CI [0.242, 19.729], $p = 0.048$), right ($\beta = 15.328$, 95% CI [5.558, 25.098], $p = 0.003$), and left positions ($\beta = 13.178$, 95% CI [1.290, 25.067], $p = 0.033$) compared to healthy controls. The MSA group also had an increased pupil size in the the left position ($\beta = 558.101$, 95% CI [11.329, 1104.874], $p = 0.048$) and a increased number of total saccades in the up position ($\beta = 16.830$, 95% CI [0.654, 33.006], $p = 0.044$) compared to controls.

In the pursuit task, individuals with MSA exhibited significant impairments in pursuit accuracy and pursuit gain. Pursuit accuracy was significantly reduced in anticlockwise pursuit at 0.4 Hz ($\beta = 2.046$, 95% CI [0.628, 3.464], $p = 0.006$) and in clockwise pursuit at 0.4 Hz ($\beta = 2.416$, 95% CI [0.889, 3.944], $p = 0.003$), compared to controls. Additionally, pursuit gain was significantly reduced in anticlockwise pursuit at 0.4 Hz ($\beta = -0.175$, 95% CI [-0.348, -0.001], $p = 0.042$) and in clockwise pursuit at 0.4 Hz ($\beta = -0.202$, 95% CI [-0.365, -0.039], $p = 0.017$), compared to controls. No significant differences were observed in the other directions and speeds.

In the antisaccade task, individuals with MSA exhibited significant impairments in both the horizontal and vertical directions. In the horizontal direction, the MSA group demonstrated a significantly reduced saccade amplitude ($\beta = -1.428$, 95% CI [-2.773, -0.084], $p = 0.041$) and a higher number of antisaccade errors ($\beta = 6.552$, 95% CI [3.507, 9.597], $p < 0.001$) compared to controls. The number of correct antisaccades was

significantly lower ($\beta = 5.034$, 95% CI [2.326, 7.742], $p < 0.001$), and the number of self corrected errors was higher ($\beta = 2.985$, 95% CI [0.445, 5.524], $p = 0.024$) compared to controls. In the vertical direction, the MSA group also exhibited a significantly reduced saccade amplitude ($\beta = -2.582$, 95% CI [-3.738, -1.427], $p < 0.001$), saccade peak velocity ($\beta = -32.595$, 95% CI [-49.954, -15.237], $p < 0.001$), and saccade average velocity ($\beta = -89.928$, 95% CI [-159.181, -20.676], $p = 0.013$) compared to controls. Additionally, the MSA group made significantly more antisaccade errors ($\beta = 6.686$, 95% CI [4.244, 9.127], $p < 0.001$), while the number of correct antisaccades was significantly lower ($\beta = -6.650$, 95% CI [-9.189, -4.111], $p < 0.001$) compared to controls. The MSA group also had an increased number of self-correct errors ($\beta = 2.873$, 95% CI [0.665, 5.081], $p = 0.012$) compared to controls.

In the oblique saccade task, individuals with MSA exhibited significant impairments in saccade amplitude at higher eccentricities. Specifically, saccade amplitude was significantly reduced at 8° ($\beta = -1.082$, 95% CI [-1.929, -0.235], $p = 0.014$) and at 10° ($\beta = -1.245$, 95% CI [-2.288, -0.203], $p = 0.022$) compared to healthy controls. No significant differences were observed at 4° and in other saccadic metrics at 8° and 10° .

In the reflexive saccade task, individuals with MSA exhibited significant impairments in both the horizontal and vertical directions. In the horizontal direction, saccade accuracy was significantly decreased ($\beta = 155.052$, 95% CI [48.068, 262.037], $p = 0.006$), while saccade end time ($\beta = 251.288$, 95% CI [110.717, 391.859], $p = 0.001$) and saccade start time ($\beta = 245.169$, 95% CI [106.690, 383.647], $p = 0.001$) were significantly higher, compared to controls. Additionally, saccadic amplitude was significantly lower ($\beta = -1.818$, 95% CI $p = 0.002$), compared to controls. The MSA group also made significantly fewer correct reflexive saccades ($\beta = -7.636$, 95% CI [-12.427, -2.845], $p = 0.002$) and exhibited a higher number of hypometric saccades ($\beta = 7.766$, 95% CI [3.132, 12.400], $p = 0.002$) in the horizontal direction compared to controls. In the vertical direction, MSA participants also showed significantly reduced saccade peak velocity ($\beta = -21.672$, 95% CI [-42.508, -0.836], $p = 0.045$) and saccade amplitude ($\beta = -1.653$, 95% CI [-2.941, -0.365], $p = 0.014$) compared to controls. Additionally, the number of correct reflexive saccades was significantly lower ($\beta = -4.336$, 95% CI [-8.454, -0.218], $p = 0.042$), while the number of hypometric saccades was significantly higher ($\beta = 7.596$, 95% CI [3.275, 11.916], $p = 0.001$) compared to controls.

In the volitional saccade task, individuals with MSA exhibited a significant increase in the number of hyper-

metric saccades ($\beta = 11.622$, 95% CI [1.048, 22.195], $p = 0.034$), compared to controls. No other significant differences were observed in saccade amplitude, velocity, or latency.

In the memory-guided saccade task, individuals with MSA exhibited significant differences in saccadic accuracy and amplitude. In the horizontal direction, accuracy was significantly decreased ($\beta = 163.192$, 95% CI [47.062, 279.322], $p = 0.007$), compared to controls. In the vertical direction, saccade amplitude was significantly reduced ($\beta = -2.771$, 95% CI [-5.062, -0.479], $p = 0.020$), compared to controls. No other significant differences were observed.

4.4.5 Eye Movements in Dementia with Lewy Bodies

In the central fixation task, individuals with DLB exhibited significant differences in fixation precision compared to healthy controls. Precision measured by RMS was significantly decreased ($\beta = 0.039$, 95% CI [0.016, 0.063], $p = 0.002$), as was precision measured by SD ($\beta = 0.058$, 95% CI [0.020, 0.096], $p = 0.004$), compared to controls. In the positional fixation task, individuals with DLB exhibited significant impairments in fixation precision across multiple positions. Fixation precision was significantly decreased when looking upward ($\beta = 0.023$, 95% CI [0.002, 0.044], $p = 0.038$), downward ($\beta = 0.035$, 95% CI [0.007, 0.063], $p = 0.016$), rightward ($\beta = 0.031$, 95% CI [0.004, 0.058], $p = 0.027$), and leftward ($\beta = 0.023$, 95% CI [0.006, 0.051], $p = 0.012$), measured by RMS compared to controls. Additionally, fixation precision measured by SD was also significantly lower across upward ($\beta = 0.035$, 95% CI [0.001, 0.072], $p = 0.043$), downward ($\beta = 0.052$, 95% CI [0.009, 0.095], $p = 0.020$), rightward ($\beta = 0.053$, 95% CI [0.012, 0.094], $p = 0.013$), and leftward ($\beta = 0.039$, 95% CI [0.008, 0.085], $p = 0.011$) directions compared to controls.

In the pursuit task, individuals with DLB exhibited significant impairments in pursuit accuracy. Pursuit accuracy was significantly reduced in horizontal pursuit at 0.4 Hz ($\beta = 5.472$, 95% CI [2.210, 8.733], $p = 0.002$), vertical pursuit at 0.2 Hz ($\beta = 2.859$, 95% CI [0.072, 5.646], $p = 0.047$), vertical pursuit at 0.4 Hz ($\beta = 4.895$, 95% CI [2.917, 6.873], $p < 0.001$), anticlockwise pursuit at 0.4 Hz ($\beta = 4.989$, 95% CI [1.962, 8.017], $p = 0.002$), and clockwise pursuit at 0.2 Hz ($\beta = 3.695$, 95% CI [0.673, 6.717], $p = 0.019$) compared to controls. No significant differences were observed in pursuit accuracy at 0.2 Hz for any direction.

In the oblique saccade task, individuals with DLB exhibited significant impairments in saccade velocity, timing, and error patterns. Saccade average velocity was significantly reduced at 8° ($\beta = -57.324$, 95% CI [-92.586, -22.062], $p = 0.002$), compared to controls. Additionally, saccadic latency at 4° was significantly prolonged ($\beta = 61.730$, 95% CI [3.849, 127.310], $p = 0.048$) and at 8° ($\beta = 260.822$, 95% CI [155.504, 366.140], $p < 0.001$), compared to controls. As were saccade end time at 4° ($\beta = 214.857$, 95% CI [132.698, 297.016], $p < 0.001$), 8° ($\beta = 570.684$, 95% CI [477.155, 664.214], $p < 0.001$) and at 10° ($\beta = 207.366$, 95% CI [109.224, 305.508], $p < 0.001$), compared to controls. Accuracy measures were also significantly altered, with DLB individuals having a higher error margin ($\beta = 88.810$, 95% CI [17.856, 159.765], $p = 0.016$), compared to controls. The DLB group had an increased number of hypometric saccades at 4° ($\beta = 10.503$, 95% CI [0.410, 20.597], $p < 0.044$) and 8° ($\beta = 13.443$, 95% CI [2.600, 24.285], $p < 0.017$) compared to controls.

In the antisaccade task, individuals with DLB exhibited significant impairments in both the horizontal and vertical directions. In the horizontal direction, saccadic amplitude was significantly reduced ($\beta = -2.377$, 95% CI [-4.845, -0.090], $p = 0.042$), while saccadic latency was significantly increased ($\beta = 613.053$, 95% CI [494.934, 731.172], $p < 0.001$), compared to controls. Additionally, saccade peak velocity was significantly reduced ($\beta = -114.408$, 95% CI [-231.081, -2.265], $p = 0.048$), and saccade end time was significantly prolonged ($\beta = 325.198$, 95% CI [212.795, 437.600], $p < 0.001$), compared to controls. In the vertical direction, saccadic amplitude was significantly reduced ($\beta = -2.413$, 95% CI [-5.283, -0.457], $p = 0.010$), and saccadic latency was significantly increased ($\beta = 433.990$, 95% CI [234.159, 633.821], $p < 0.001$) compared to controls. Similarly, saccade peak velocity was significantly reduced ($\beta = -89.108$, 95% CI [-236.967, -58.751], $p = 0.024$), and saccade end time was significantly prolonged ($\beta = 315.034$, 95% CI [136.931, 493.138], $p < 0.001$) compared to controls.

In the reflexive saccade task, individuals with DLB exhibited significant impairments in both the horizontal and vertical directions. In the horizontal direction, accuracy was significantly reduced ($\beta = 306.446$, 95% CI [78.026, 534.867], $p = 0.010$), while saccade peak velocity was significantly reduced ($\beta = -202.804$, 95% CI [-356.427, -49.182], $p = 0.012$) compared to controls. Average saccade velocity was significantly lower ($\beta = -457.793$, 95% CI [-753.456, -162.131], $p = 0.003$) compared to controls. Saccade end time was higher in the DLB group ($\beta = 463.282$, 95% CI [163.152, 763.412], $p = 0.003$) compared to controls. In the vertical

direction, accuracy was significantly reduced ($\beta = 169.147$, 95% CI [7.706, 330.588], $p = 0.043$), while peak saccade velocity was significantly reduced ($\beta = -187.803$, 95% CI [-350.163, -25.444], $p = 0.026$) compared to controls. Additionally, saccadic end time was significantly increased ($\beta = 482.219$, 95% CI [283.922, 680.516], $p < 0.001$), and average saccade velocity was significantly lower ($\beta = -67.587$, 95% CI [-112.073, -23.100], $p = 0.004$) compared to controls.

In the volitional saccade task, individuals with DLB exhibited significant impairments in both the horizontal and vertical directions. In the horizontal direction, the total number of volitional saccades completed in the horizontal direction was significantly reduced ($\beta = -31.766$, 95% CI [-63.103, -0.428], $p = 0.040$), compared to controls. Additionally, accuracy was significantly decreased ($\beta = 277.744$, 95% CI [45.986, 509.502], $p = 0.021$), compared to controls. The number of correct volitional saccades was significantly lower ($\beta = -37.837$, 95% CI [-64.882, -10.791], $p = 0.008$), while saccadic amplitude was significantly reduced ($\beta = -8.097$, 95% CI [-14.979, -1.214], $p = 0.024$), compared to controls. In the vertical direction accuracy was decreased showing a significant difference ($\beta = 116.585$, 95% CI [23.469, 256.638], $p = 0.011$) compared to controls. Additionally, the number of correct volitional saccades was significantly reduced ($\beta = -19.932$, 95% CI [-43.690, -3.827], $p = 0.010$), and saccadic amplitude was significantly decreased ($\beta = -4.864$, 95% CI [-10.370, -0.642], $p = 0.047$) compared to controls. Lastly the total number of volitional saccades completed in the vertical direction was significantly reduced ($\beta = -41.082$, 95% CI [-69.137, -13.027], $p = 0.005$) compared to controls.

In the memory-guided saccade task, individuals with DLB exhibited significant impairments in both the horizontal and vertical directions. In the horizontal direction, the total number of memory guided saccades completed was significantly reduced ($\beta = -27.347$, 95% CI [-56.916, -2.221], $p = 0.044$), compared to controls. Additionally, accuracy was lower ($\beta = 306.018$, 95% CI [58.072, 553.965], $p = 0.018$), compared to controls. Saccade amplitude was significantly lower ($\beta = -12.091$, 95% CI [-19.761, -4.420], $p = 0.003$) compared to controls. Furthermore, both average saccade velocity ($\beta = -95.288$, 95% CI [-160.230, -30.345], $p = 0.005$) and saccade peak velocity ($\beta = -169.608$, 95% CI [-309.026, -30.189], $p = 0.020$) were significantly reduced, compared to controls. In the vertical direction, the total number of memory guided saccades completed was significantly lower in DLB ($\beta = -37.110$, 95% CI [-65.047, -9.174], $p = 0.011$) compared to controls. Accuracy was significantly reduced ($\beta = 190.323$, 95% CI [60.251, 320.396], $p = 0.005$) compared to controls.

Additionally, both average saccade velocity ($\beta = -74.301$, 95% CI [-130.719, -17.884], $p = 0.012$) and peak saccade velocity ($\beta = -177.378$, 95% CI [-350.159, -4.598], $p = 0.048$) were significantly reduced, compared to controls.

4.4.6 Eye Movements in Atypical Cases

No significant differences were observed in the ATP group for the fixation task. Analyses of fixation precision, stability, microsaccade and saccade frequency yielded p-values greater than 0.05, indicating that fixation control in ATP remains comparable to that of healthy controls. In the positional fixation task, individuals with ATP exhibited significant impairments in fixation precision across multiple trials. RMS precision measure was significantly decreased in the up ($\beta = 0.009$, 95% CI [0.001, 0.019], $p = 0.049$), down ($\beta = 0.016$, 95% CI [0.003, 0.030], $p = 0.022$), right ($\beta = 0.012$, 95% CI [0.001, 0.026], $p = 0.043$), and left ($\beta = 0.017$, 95% CI [0.003, 0.031], $p = 0.020$) positions, compared to controls. Additionally, SD precision measure was significantly decreased in the up ($\beta = 0.014$, 95% CI [0.004, 0.032], $p = 0.014$), down ($\beta = 0.025$, 95% CI [0.004, 0.046], $p = 0.024$), right ($\beta = 0.020$, 95% CI [0.000, 0.041], $p = 0.041$), and left ($\beta = 0.034$, 95% CI [0.011, 0.057], $p = 0.004$) positions compared to controls.

No significant differences were observed in the ATP group for the pursuit task. Analyses of pursuit accuracy and pursuit gain across all tested conditions, including horizontal, vertical, anticlockwise, and clockwise directions at 0.2 Hz and 0.4 Hz, yielded p-values greater than 0.05.

In the oblique saccade task, individuals with ATP exhibited significant impairments in saccade amplitude, velocity, accuracy, and error patterns. Saccadic amplitude at 4° was significantly reduced ($\beta = -1.002$, 95% CI [-1.525, -0.480], $p = 0.0003$), as was saccade amplitude at 8° ($\beta = -2.342$, 95% CI [-3.231, -1.452], $p < 0.001$) and at 10° ($\beta = -2.909$, 95% CI [-4.004, -1.815], $p < 0.001$), compared to controls. Saccade velocity was also significantly lower in ATP, with peak saccade velocity reduced at 4° ($\beta = -25.416$, 95% CI [-38.120, -12.713], $p < 0.001$), as well at 8° ($\beta = -36.396$, 95% CI [-53.737, -19.056], $p < 0.001$) and at 10° ($\beta = -45.662$, 95% CI [-64.950, -26.374], $p < 0.001$) compared to controls. Average saccade velocity was also reduced at 4° ($\beta = -63.508$, 95% CI [-108.595, -18.422], $p = 0.007$), 8° ($\beta = -99.046$, 95% CI [-153.089, -45.002], $p < 0.001$), and 10° ($\beta = -105.680$, 95% CI [-162.237, -49.123], $p < 0.001$) compared to

controls. Accuracy deficits were evident, with reduced accuracy in the Y plane at 8° ($\beta = 102.422$, 95% CI [48.083, 156.760], $p < 0.001$) and at 10° ($\beta = 137.741$, 95% CI [74.397, 201.086], $p < 0.001$) compared to controls. Error analysis revealed significantly fewer correct oblique responses ($\beta = -4.268$, 95% CI [-7.550, -0.987], $p = 0.013$), along with a reduction in hypometric saccades at 4° ($\beta = -7.115$, 95% CI [-12.079, -2.151], $p = 0.006$), 8° ($\beta = -11.400$, 95% CI [-16.732, -6.068], $p < 0.001$), and 10° ($\beta = -10.137$, 95% CI [-15.023, -5.251], $p < 0.001$), compared to controls. However, the number of hypermetric saccades at 4° ($\beta = 7.358$, 95% CI [2.365, 12.351], $p = 0.005$), 8° ($\beta = 13.656$, 95% CI [8.197, 19.115], $p < 0.001$), and 10° ($\beta = 12.859$, 95% CI [7.765, 17.954], $p < 0.001$) errors was significantly increased, compared to controls.

In the antisaccade task, individuals with ATP exhibited significant impairments in both the horizontal and vertical directions. In the horizontal direction, saccadic amplitude was significantly reduced ($\beta = -4.473$, 95% CI [-5.885, -3.062], $p < 0.001$), along with a significant decrease in peak saccade velocity ($\beta = -50.866$, 95% CI [-71.488, -30.243], $p < 0.001$) and average saccade velocity ($\beta = -101.880$, 95% CI [-159.255, -44.505], $p = 0.001$) compared to controls. Additionally, ATP participants made significantly more antisaccade errors ($\beta = 3.972$, 95% CI [0.775, 7.169], $p = 0.017$) and fewer correct responses ($\beta = -4.002$, 95% CI [-7.163, -0.841], $p = 0.015$), compared to controls. In the vertical direction, ATP participants exhibited significantly reduced saccadic amplitude ($\beta = -3.797$, 95% CI [-5.011, -2.584], $p < 0.001$) and saccade peak velocity ($\beta = -59.019$, 95% CI [-77.244, -40.794], $p < 0.001$) compared to controls. Saccadic latency was significantly increased ($\beta = 117.492$, 95% CI [19.224, 215.761], $p = 0.022$), compared to controls. Additionally, average saccade velocity ($\beta = -142.088$, 95% CI [-214.799, -69.377], $p < 0.001$) was significantly lower, while saccade end time was significantly prolonged ($\beta = 146.741$, 95% CI [59.158, 234.325], $p = 0.002$) compared to controls.

In the reflexive saccade task, individuals with ATP exhibited significant impairments in both the horizontal and vertical directions. In the horizontal direction, peak saccade velocity was significantly reduced ($\beta = -24.509$, 95% CI [-45.314, -3.705], $p = 0.024$), along with a significant decrease in saccadic amplitude ($\beta = -1.267$, 95% CI [-2.464, -0.069], $p = 0.041$) compared to controls. The number of correct reflexive responses was significantly lower ($\beta = -7.745$, 95% CI [-12.776, -2.715], $p = 0.003$), while the number of hypometric saccades was significantly higher ($\beta = 9.226$, 95% CI [4.361, 14.091], $p < 0.001$), compared to controls. In the vertical direction, ATP participants exhibited significantly decreased saccade accuracy ($\beta = 102.831$, 95% CI [23.441, 182.220], $p = 0.013$), compared to controls. Additionally, peak saccade velocity was significantly

reduced ($\beta = -51.244$, 95% CI $[-73.120, -29.367]$, $p < 0.001$), while saccadic latency was significantly increased ($\beta = 112.613$, 95% CI $[15.099, 210.127]$, $p = 0.026$) compared to controls. Furthermore, average saccade velocity was significantly lower ($\beta = -127.143$, 95% CI $[-206.984, -47.301]$, $p = 0.003$), and saccade end time was significantly prolonged ($\beta = 151.074$, 95% CI $[60.637, 241.511]$, $p = 0.002$) compared to controls. Additionally, ATP participants made significantly fewer correct responses ($\beta = -6.505$, 95% CI $[-10.828, -2.181]$, $p = 0.004$), while the number of hypometric saccades was significantly higher ($\beta = 9.430$, 95% CI $[4.894, 13.965]$, $p < 0.001$) compared to controls.

In the volitional saccade task, individuals with ATP exhibited significant impairments in both the horizontal and vertical directions. In the horizontal direction, the total number of volitional saccades was significantly reduced ($\beta = -20.581$, 95% CI $[-35.992, -5.171]$, $p = 0.011$), compared to controls. Additionally, accuracy was significantly decreased ($\beta = 1.228$, 95% CI $[0.758, 1.697]$, $p < 0.001$), compared to controls. Saccade amplitude was significantly lower ($\beta = -75.952$, 95% CI $[-150.056, -1.848]$, $p = 0.048$), compared to controls. In the vertical direction, the total number of volitional saccades was significantly lower in ATP ($\beta = -18.485$, 95% CI $[-32.281, -4.689]$, $p = 0.010$), compared to controls. Accuracy was significantly decreased ($\beta = 79.051$, 95% CI $[10.179, 147.923]$, $p = 0.027$) compared to controls. Additionally, both the number of correct saccades ($\beta = -16.785$, 95% CI $[-28.468, -5.102]$, $p = 0.006$) and saccadic amplitude ($\beta = -6.870$, 95% CI $[-9.577, -4.162]$, $p < 0.001$) were significantly reduced, compared to controls. Furthermore, average saccade velocity ($\beta = -71.841$, 95% CI $[-101.097, -42.585]$, $p < 0.001$) and peak saccade velocity ($\beta = -154.811$, 95% CI $[-243.651, -65.971]$, $p = 0.001$) were significantly reduced, compared to controls.

In the memory-guided saccade task, individuals with ATP exhibited significant impairments in both the horizontal and vertical directions. In the horizontal direction, the total number of memory guided saccades was significantly reduced ($\beta = -20.385$, 95% CI $[-34.925, -5.844]$, $p = 0.007$), compared to controls. Additionally, saccadic steps was significantly increased ($\beta = 1.596$, 95% CI $[1.089, 2.104]$, $p < 0.001$), compared to controls. Saccade amplitude was significantly lower ($\beta = -6.230$, 95% CI $[-10.002, -2.458]$, $p = 0.002$), compared to controls. Furthermore, both average saccade velocity ($\beta = -49.981$, 95% CI $[-81.917, -18.045]$, $p = 0.003$) and peak saccade velocity ($\beta = -96.266$, 95% CI $[-164.826, -27.706]$, $p = 0.007$) were significantly reduced, compared to controls. In the vertical direction, total number of memory guided saccades was significantly lower in ATP ($\beta = -7.707$, 95% CI $[-21.445, -6.031]$, $p = 0.027$), compared to controls. Saccadic steps were increased,

compared to controls ($\beta = 0.587$, 95% CI [0.257, 0.916], $p < 0.001$). Additionally, the number of correct saccades was significantly reduced ($\beta = -13.521$, 95% CI [-21.794, -5.249], $p = 0.002$), while hypometric saccades was significantly increased ($\beta = 20.098$, 95% CI [7.642, 32.554], $p = 0.002$), compared to controls. Saccade amplitude was significantly lower ($\beta = -7.776$, 95% CI [-10.182, -5.370], $p < 0.001$) compared to controls. Additionally, saccade end time was significantly prolonged ($\beta = 1780.152$, 95% CI [287.120, 3273.185], $p = 0.022$), peak saccade velocity ($\beta = -161.405$, 95% CI [-246.371, -76.439], $p < 0.001$) and average saccade velocity ($\beta = -72.949359$, 95% CI [-100.69, -45.205], $p < 0.001$) were lower compared to controls.

4.4.7 Composite Score

Hybrid-weighted composite z-scores were calculated for each ocular motor paradigm across five atypical parkinsonian syndromes: ATP, CBS, DLB, MSA, and PSP. These scores were computed by combining z-transformed effect sizes with weights derived from the product of p-values and confidence interval widths, such that higher composite scores reflect a greater combination of statistical significance and precision. For the ATP group, the highest composite scores were observed in memory-guided saccades horizontal (1.51), memory-guided saccades vertical (1.18), antisaccades vertical (0.61), and antisaccades horizontal (0.58). In the CBS group, central fixation yielded the highest score (0.69), followed by antisaccades horizontal (0.27), memory-guided saccades vertical (0.18), and antisaccades vertical (0.12). In the DLB group, the highest composite scores were found in antisaccades horizontal (1.78), antisaccades vertical (1.56), central fixation (1.44), and memory-guided saccades horizontal (1.30). For the MSA group, the top scores were central fixation (0.96), antisaccades vertical (0.70), and memory-guided saccades vertical (0.45). The PSP group showed the highest composite scores in central fixation (1.63), antisaccades vertical (1.38), antisaccades horizontal (1.16), memory-guided saccades vertical (0.78), and memory-guided saccades horizontal (0.55).

4.4.8 Timescale Analysis

PSP, MSA, CBS, ATP, and DLB groups did not show significant differences from controls in most conditions. For reflexive saccades, none of these groups exhibited significant changes in either horizontal or vertical residual velocity, with p-values well above 0.05. Similarly, for volitional saccades, these groups did not display significant velocity changes. In memory-guided saccades, the MSA group showed a significant

reduction in vertical residual velocity ($p = 0.003$), but all other groups did not show any significant differences in either horizontal or vertical residual velocity. These findings suggest that while iPD, GBA, and LRRK2 mutations are associated with significant changes in saccadic velocity over time, other Parkinsonian syndromes and related disorders show little to no significant variation in residual velocity compared to controls.

4.4.9 Saccadic Pursuit

For atypical Parkinsonian syndromes, the Shapiro-Wilk test results reveal a significant deviation from normality in saccade-related metrics, with W values consistently below 0.80 and p-values under 0.01 for all conditions. These results suggest that saccadic impairments in atypical syndromes are highly variable, potentially due to the differential impact of these disorders on ocular motor networks. CBS and PSP, which frequently involve frontal and brainstem circuits critical for voluntary saccades, showed particularly skewed distributions, indicating greater inter-individual variability. Given the severity of saccadic dysfunction in atypical syndromes, the non-normal distribution may reflect a more abrupt or heterogeneous decline in ocular motor control compared to idiopathic PD.

Central Fixation Metrics in Atypical Parkinsonian Syndromes

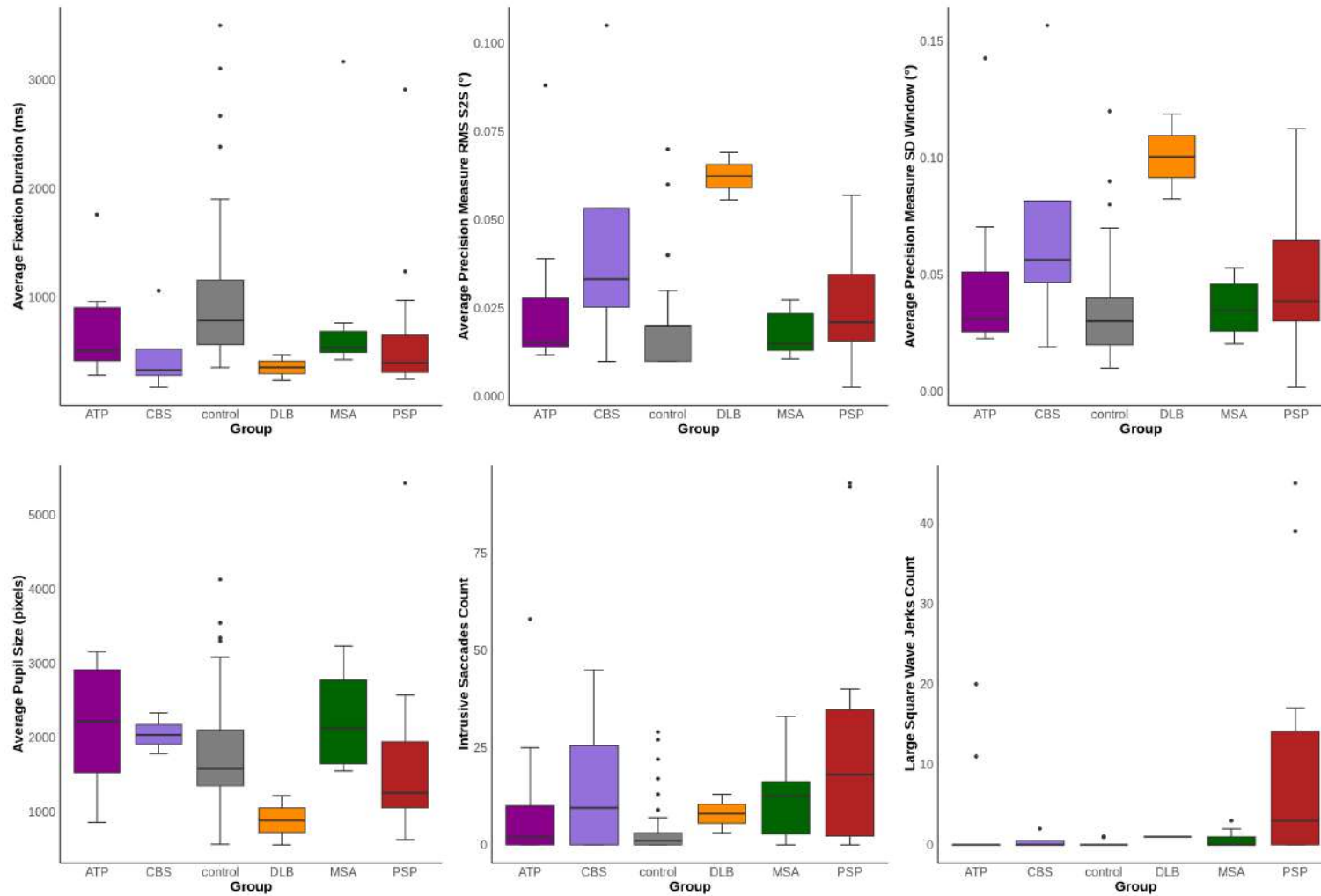


Figure 77: Central Fixation Metrics in Atypical Parkinsonian Syndromes. Box plots show the median, interquartile range, and full range. Generalized linear models were used to assess the effects of group, age, sex, and disease duration. Statistical significance was set at $p < 0.05$.

Central Fixation Metrics in Atypical Parkinsonian Syndromes

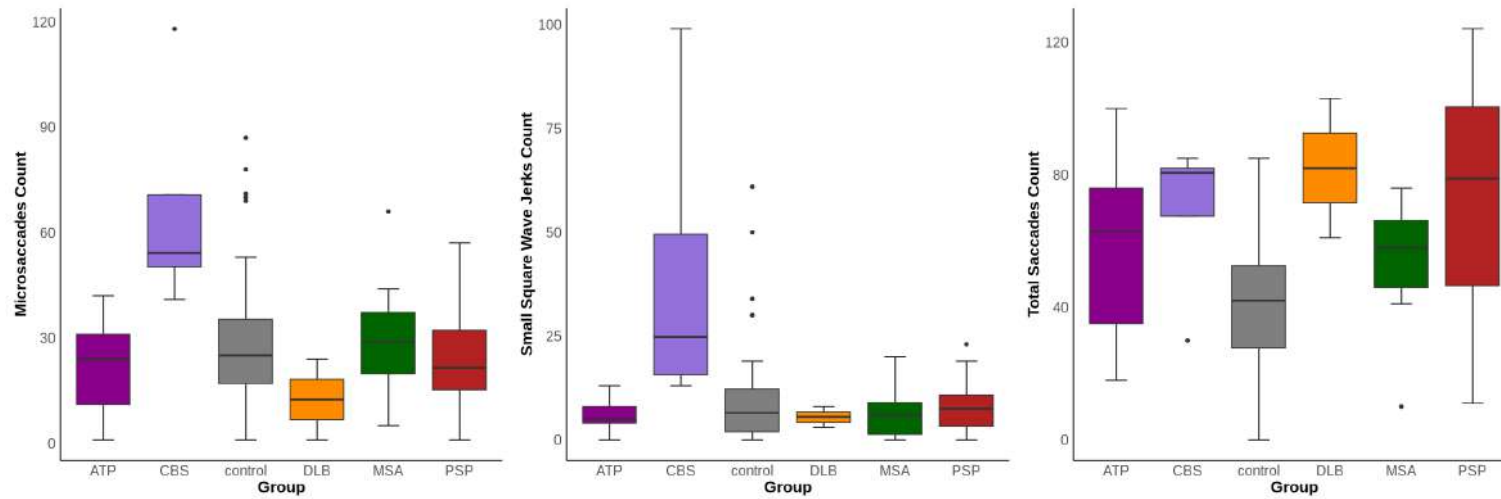


Figure 78: Central Fixation Metrics in Atypical Parkinsonian Syndromes. Box plots show the median, interquartile range, and full range. Generalized linear models were used to assess the effects of group, age, sex, and disease duration. Statistical significance was set at $p < 0.05$.

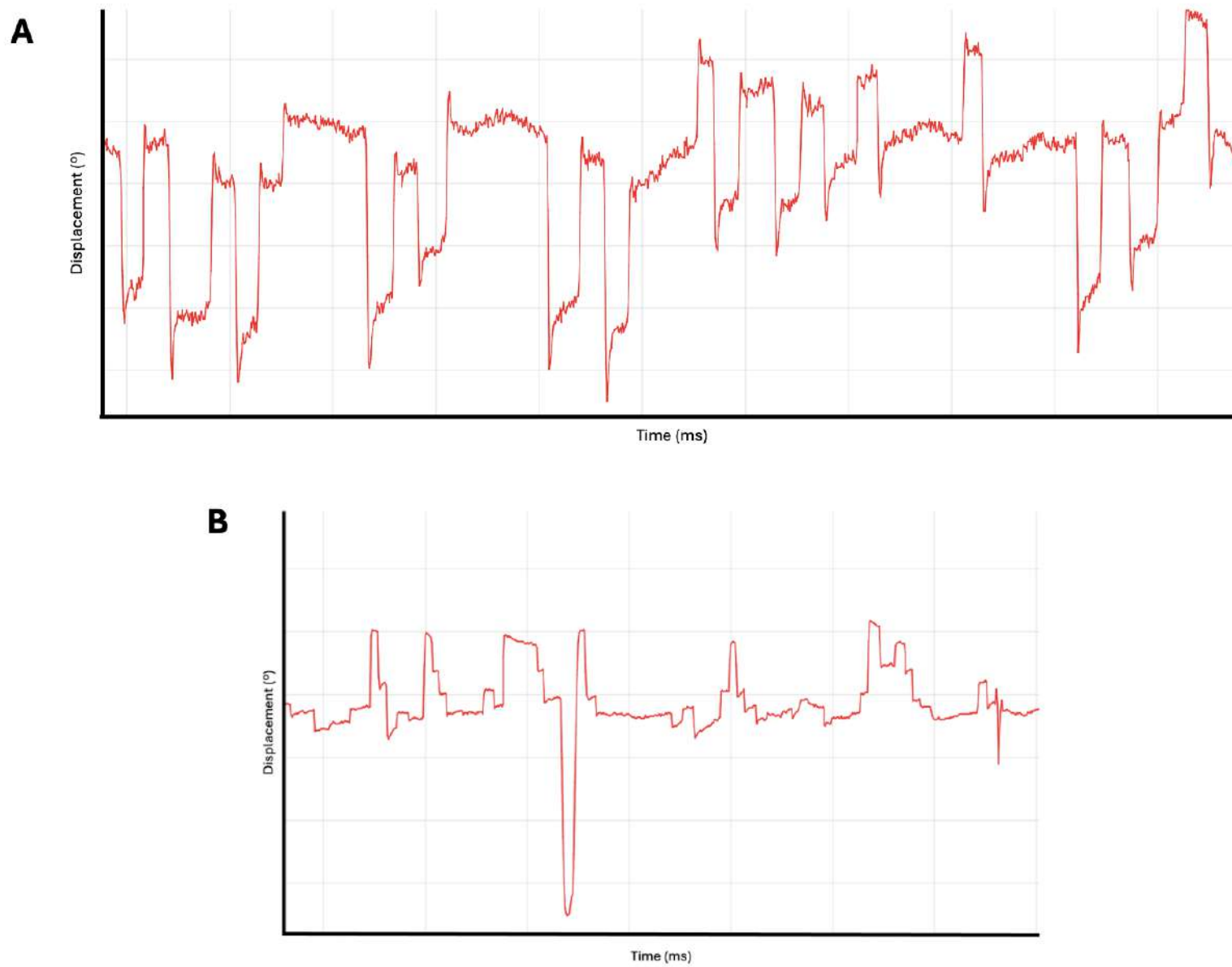


Figure 79: Fixation Traces in Progressive Supranuclear Palsy. A) Large square wave jerks; B) Multi-step square wave jerks.

Positional Fixation/ Nystagmus Metrics in Atypical Parkinsonian Syndromes

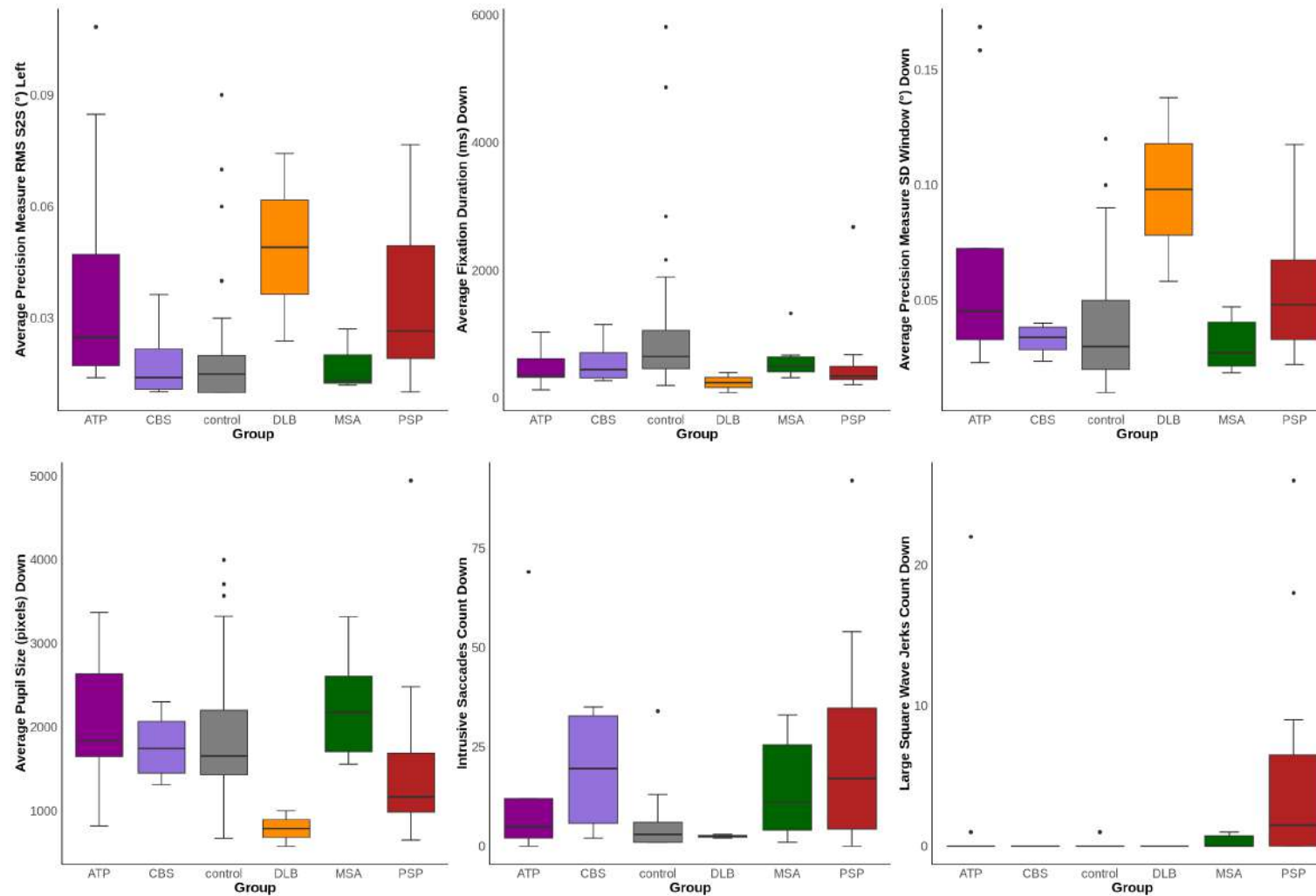


Figure 80: Positional Fixation/ Nystagmus Metrics in Atypical Parkinsonian Syndromes. Box plots show the median, interquartile range, and full range. Generalized linear models were used to assess the effects of group, age, sex, and disease duration. Statistical significance was set at $p < 0.05$.

Positional Fixation/ Nystagmus Metrics in Atypical Parkinsonian Syndromes

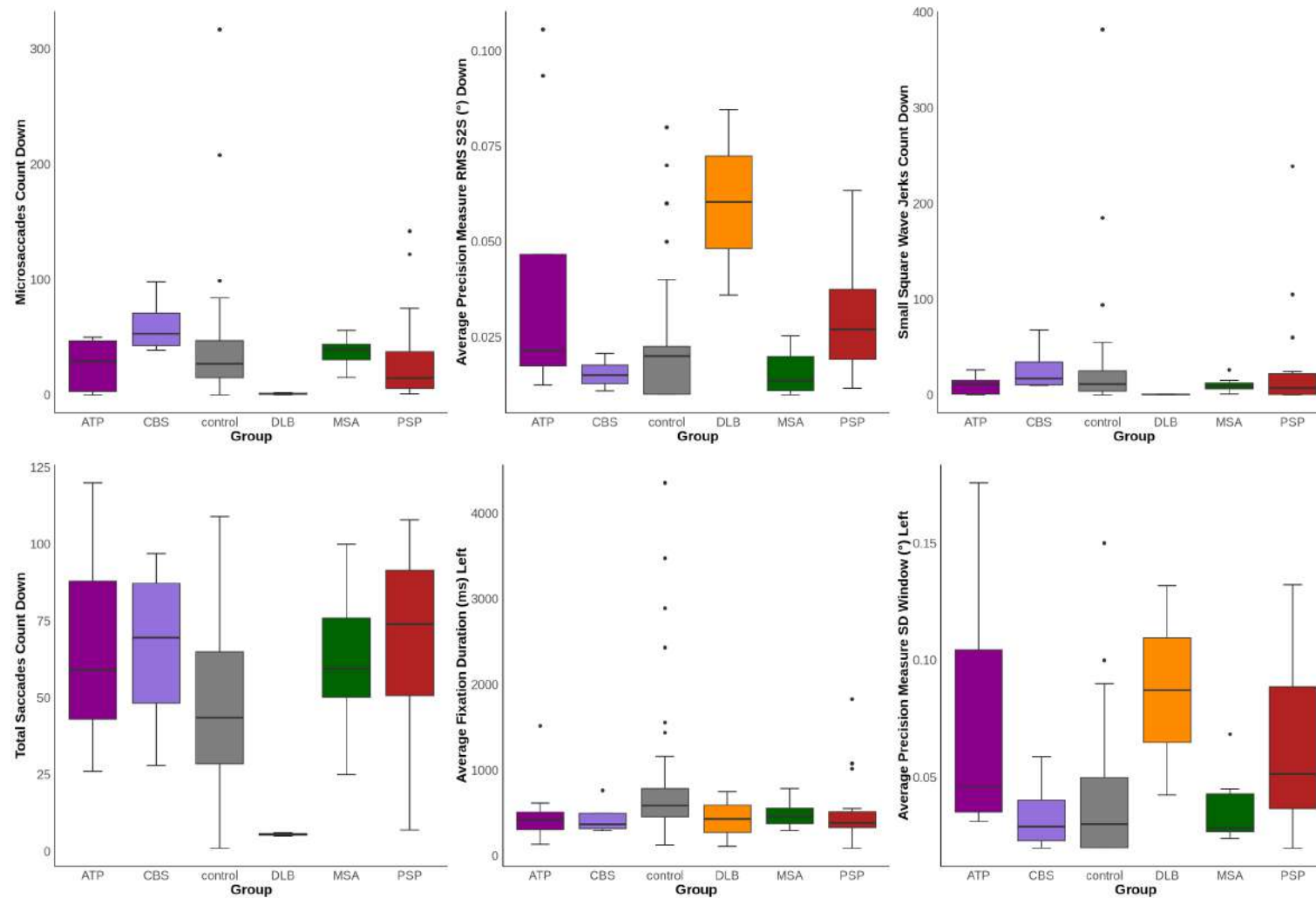


Figure 81: Positional Fixation/ Nystagmus Metrics in Atypical Parkinsonian Syndromes. Box plots show the median, interquartile range, and full range. Generalized linear models were used to assess the effects of group, age, sex, and disease duration. Statistical significance was set at $p < 0.05$.

Positional Fixation/ Nystagmus Metrics in Atypical Parkinsonian Syndromes

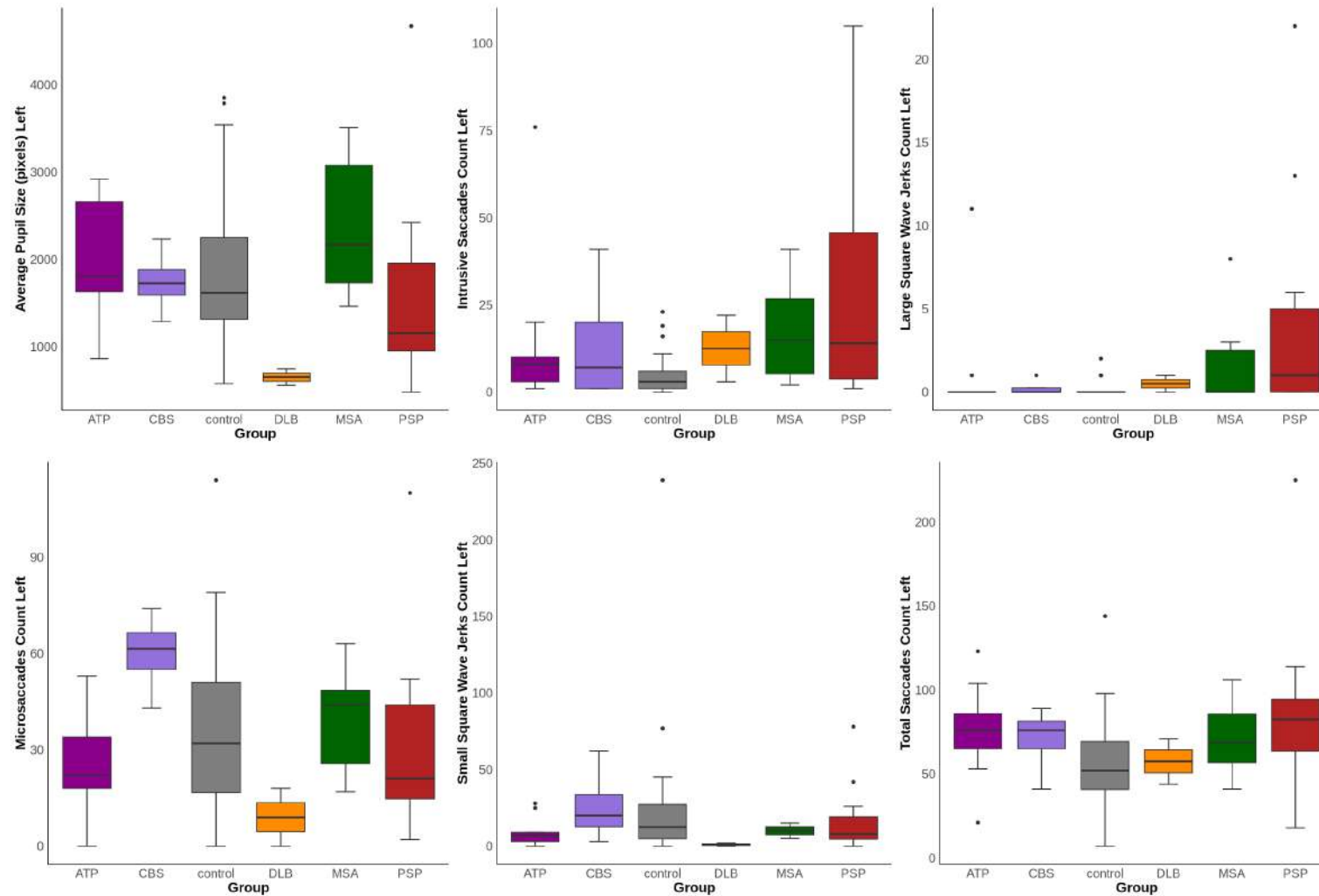


Figure 82: Positional Fixation/ Nystagmus Metrics in Atypical Parkinsonian Syndromes. Box plots show the median, interquartile range, and full range. Generalized linear models were used to assess the effects of group, age, sex, and disease duration. Statistical significance was set at $p < 0.05$.

Positional Fixation/ Nystagmus Metrics in Atypical Parkinsonian Syndromes

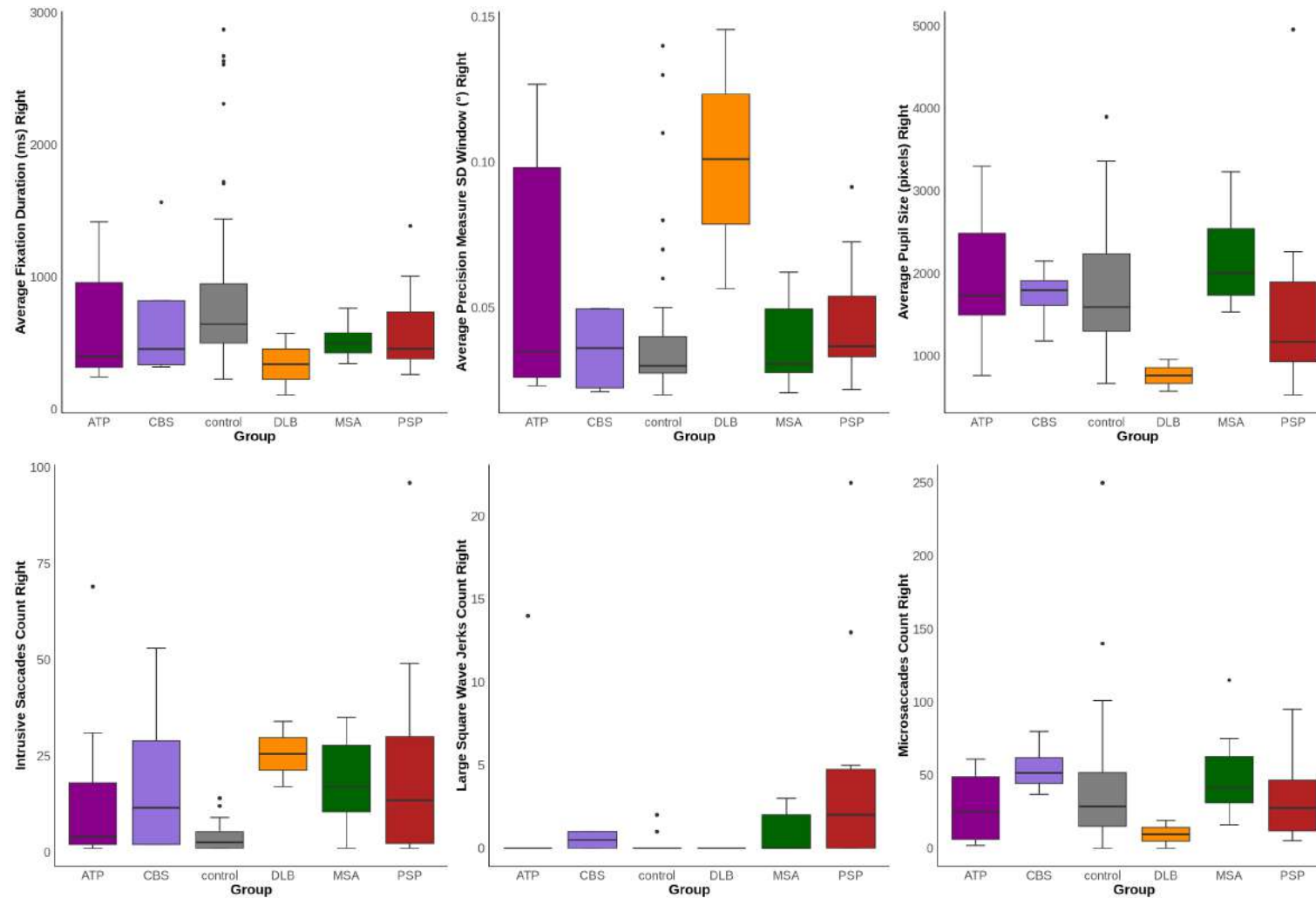


Figure 83: Positional Fixation/ Nystagmus Metrics in Atypical Parkinsonian Syndromes. Box plots show the median, interquartile range, and full range. Generalized linear models were used to assess the effects of group, age, sex, and disease duration. Statistical significance was set at $p < 0.05$.

Positional Fixation/ Nystagmus Metrics in Atypical Parkinsonian Syndromes

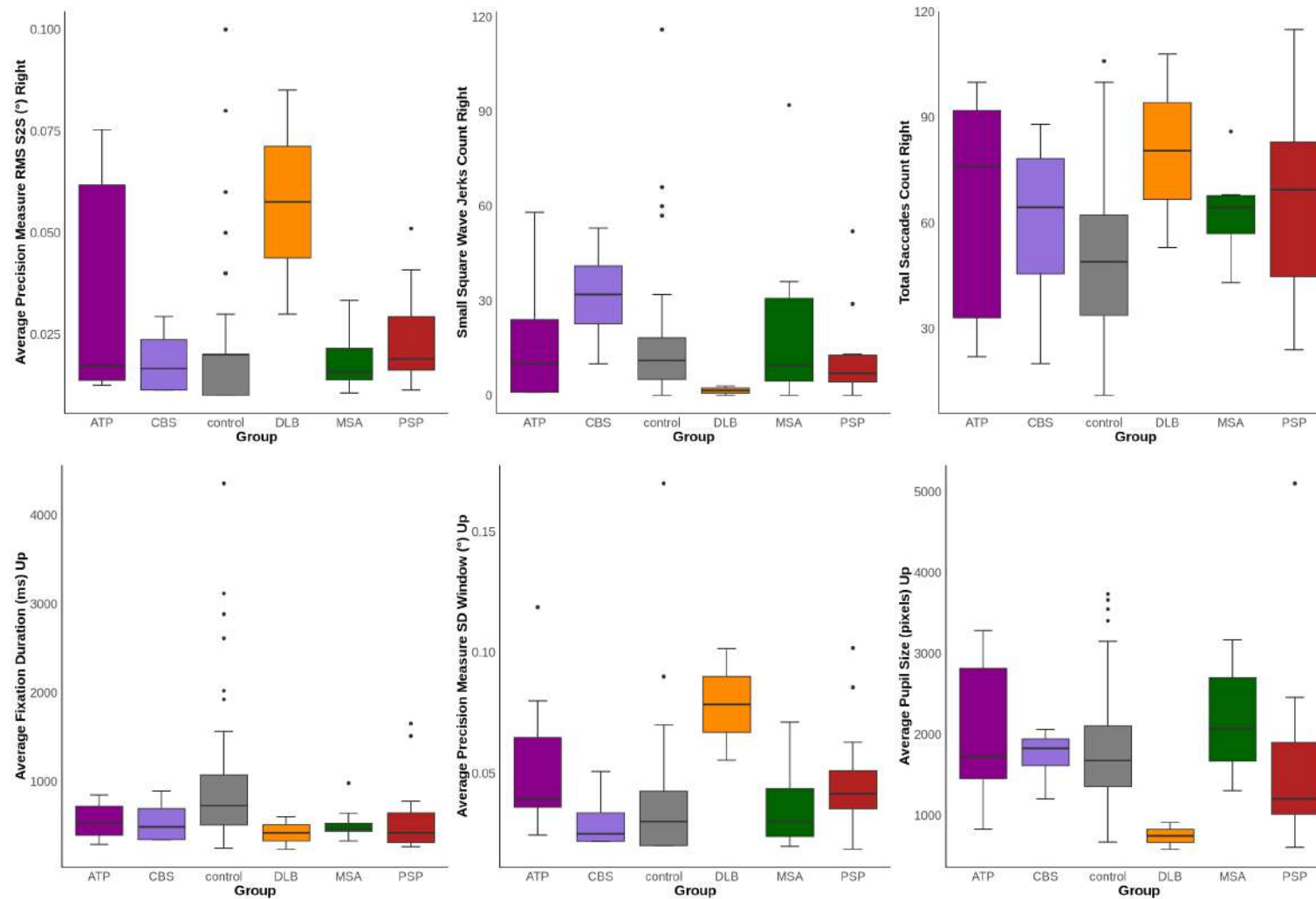


Figure 84: Positional Fixation/ Nystagmus Metrics in Atypical Parkinsonian Syndromes. Box plots show the median, interquartile range, and full range. Generalized linear models were used to assess the effects of group, age, sex, and disease duration. Statistical significance was set at $p < 0.05$.

Positional Fixation/ Nystagmus Metrics in Atypical Parkinsonian Syndromes

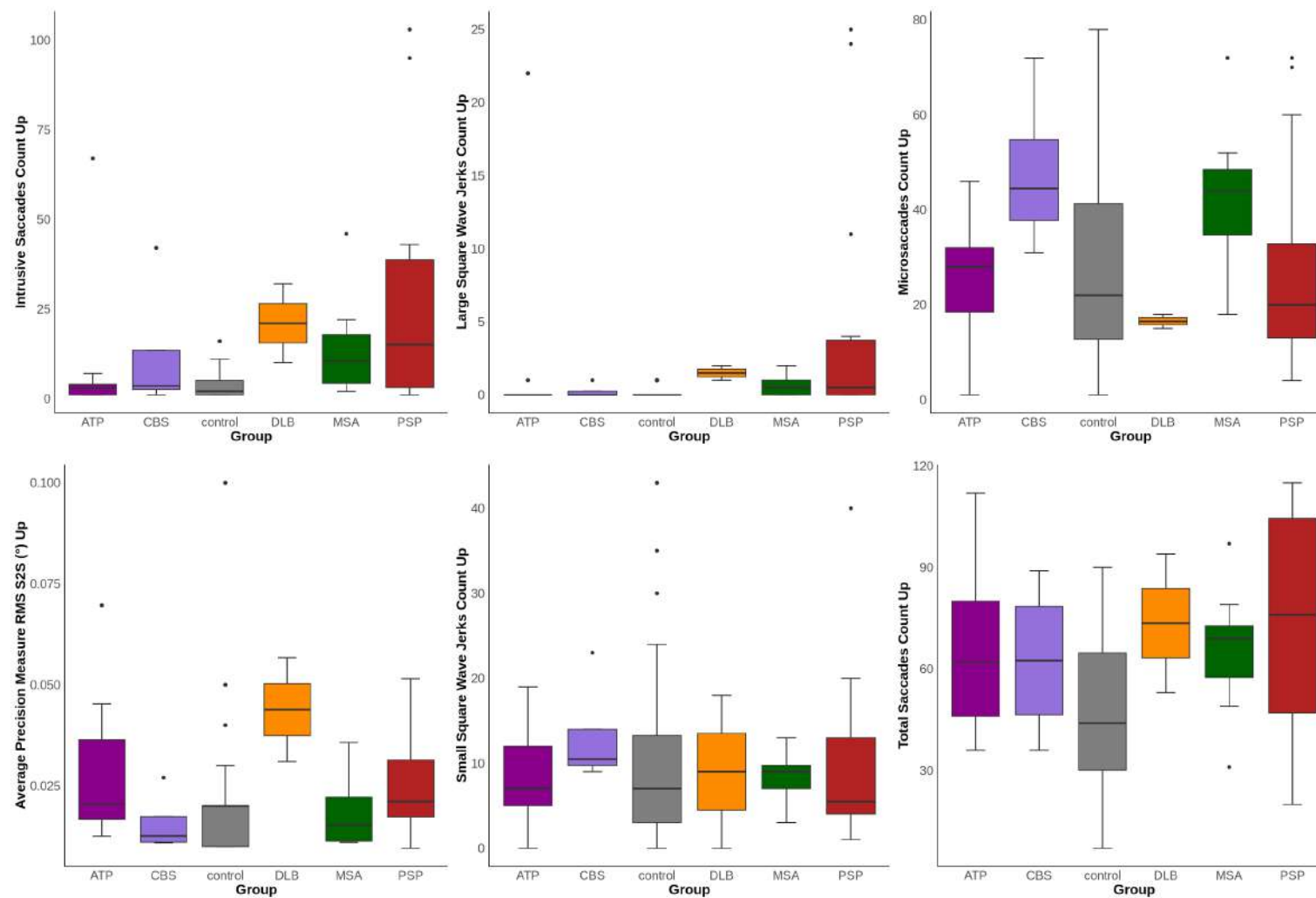


Figure 85: Positional Fixation/ Nystagmus Metrics in Atypical Parkinsonian Syndromes. Box plots show the median, interquartile range, and full range. Generalized linear models were used to assess the effects of group, age, sex, and disease duration. Statistical significance was set at $p < 0.05$.

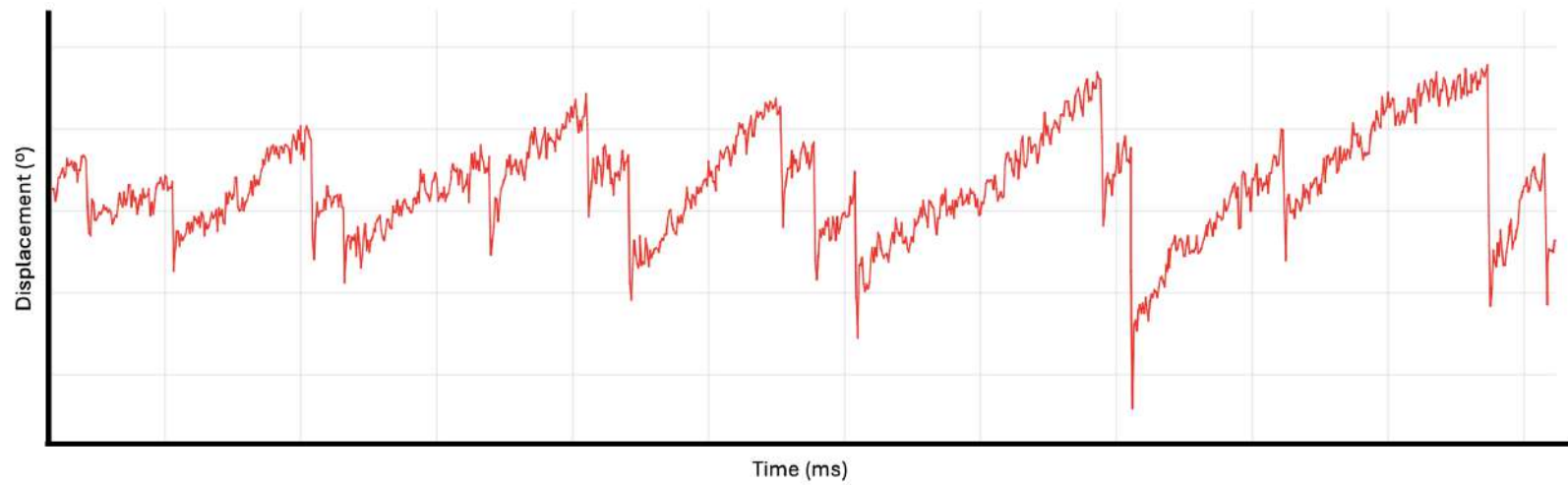


Figure 86: Positional Fixation/ Nystagmus Traces in Multiple System Atrophy.

Smooth Pursuit Metrics in Atypical Parkinsonian Syndromes

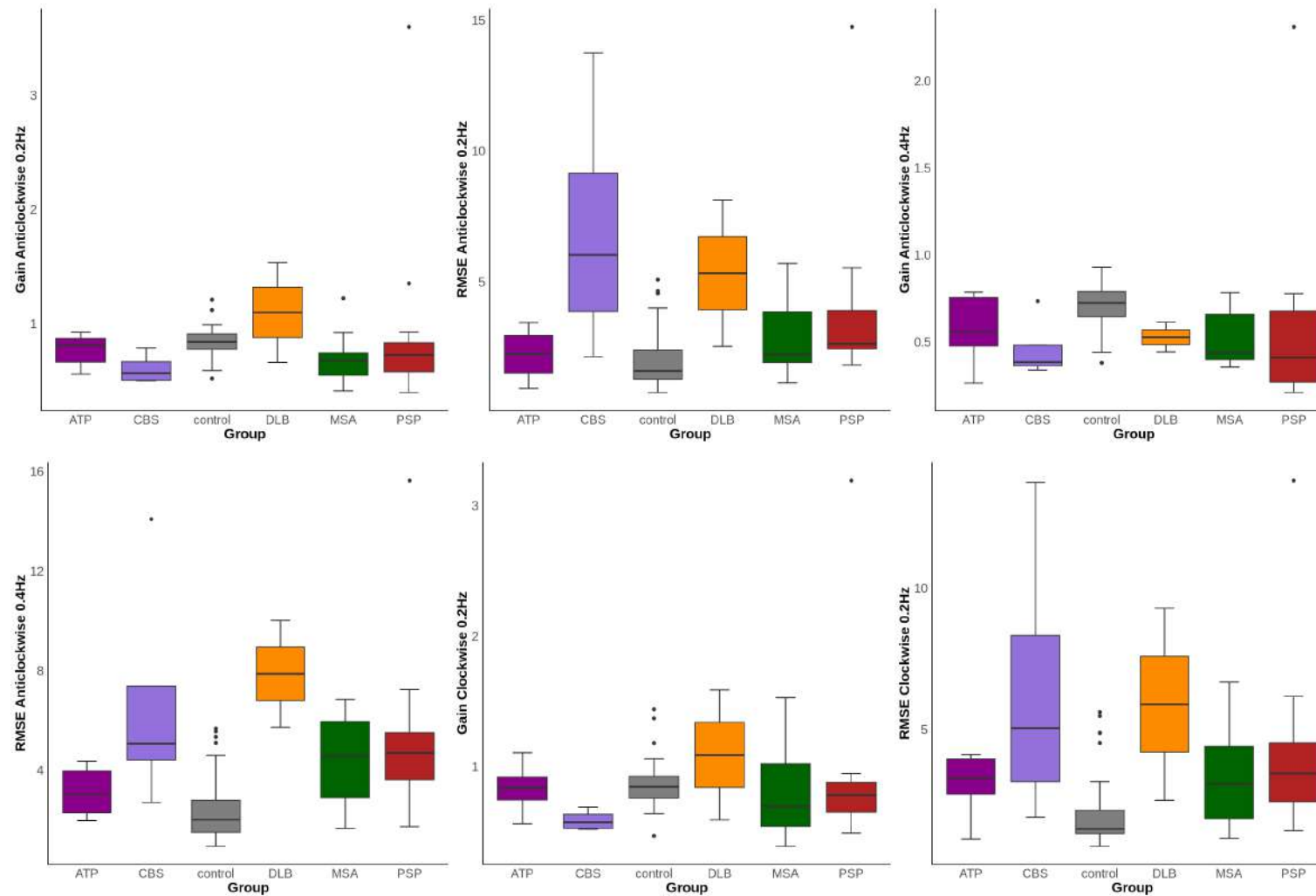


Figure 87: Smooth Pursuit Metrics in Atypical Parkinsonian Syndromes. Box plots show the median, interquartile range, and full range. Generalized linear models were used to assess the effects of group, age, sex, and disease duration. Statistical significance was set at $p < 0.05$.

Smooth Pursuit Metrics in Atypical Parkinsonian Syndromes

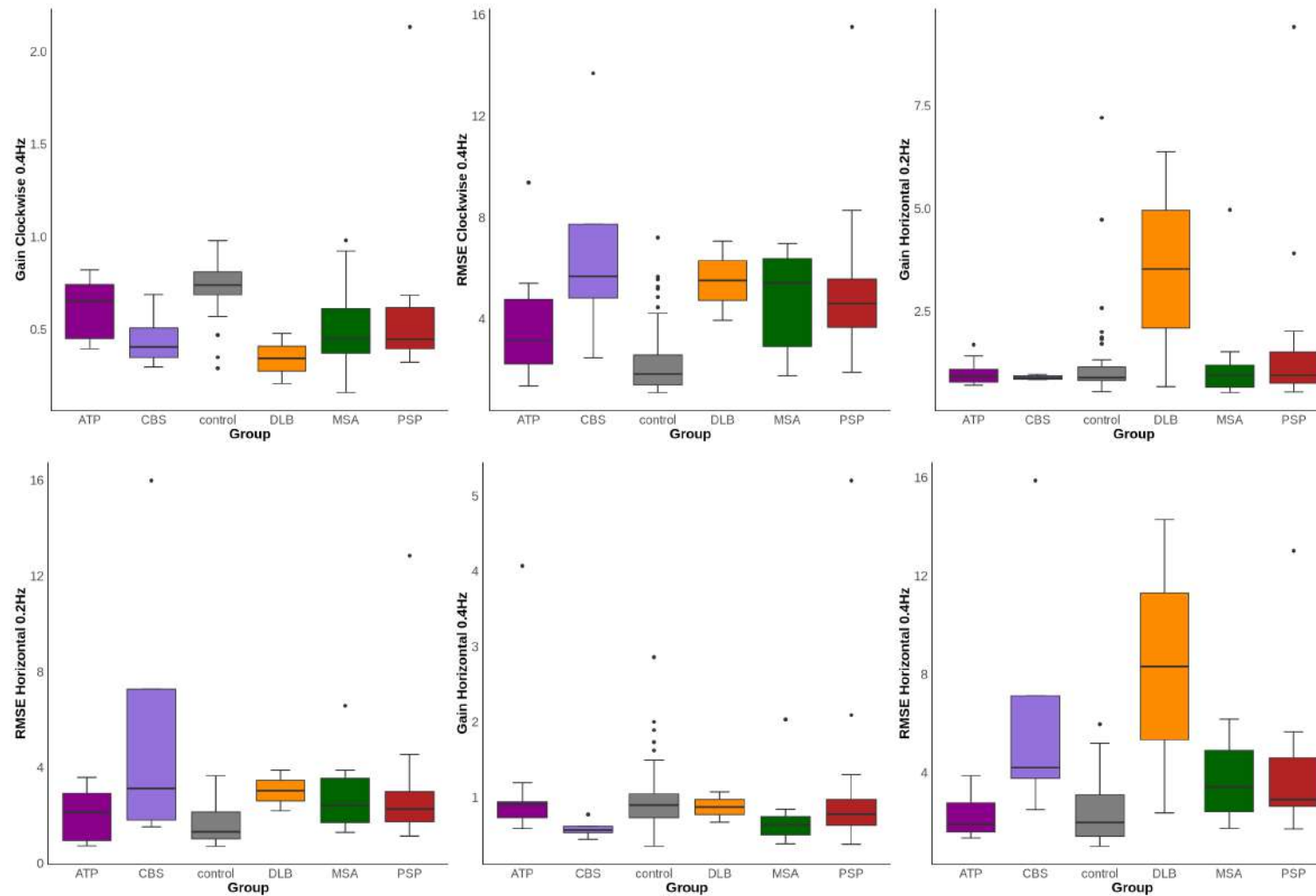


Figure 88: Smooth Pursuit Metrics in Atypical Parkinsonian Syndromes. Box plots show the median, interquartile range, and full range. Generalized linear models were used to assess the effects of group, age, sex, and disease duration. Statistical significance was set at $p < 0.05$.

Smooth Pursuit Metrics in Atypical Parkinsonian Syndromes

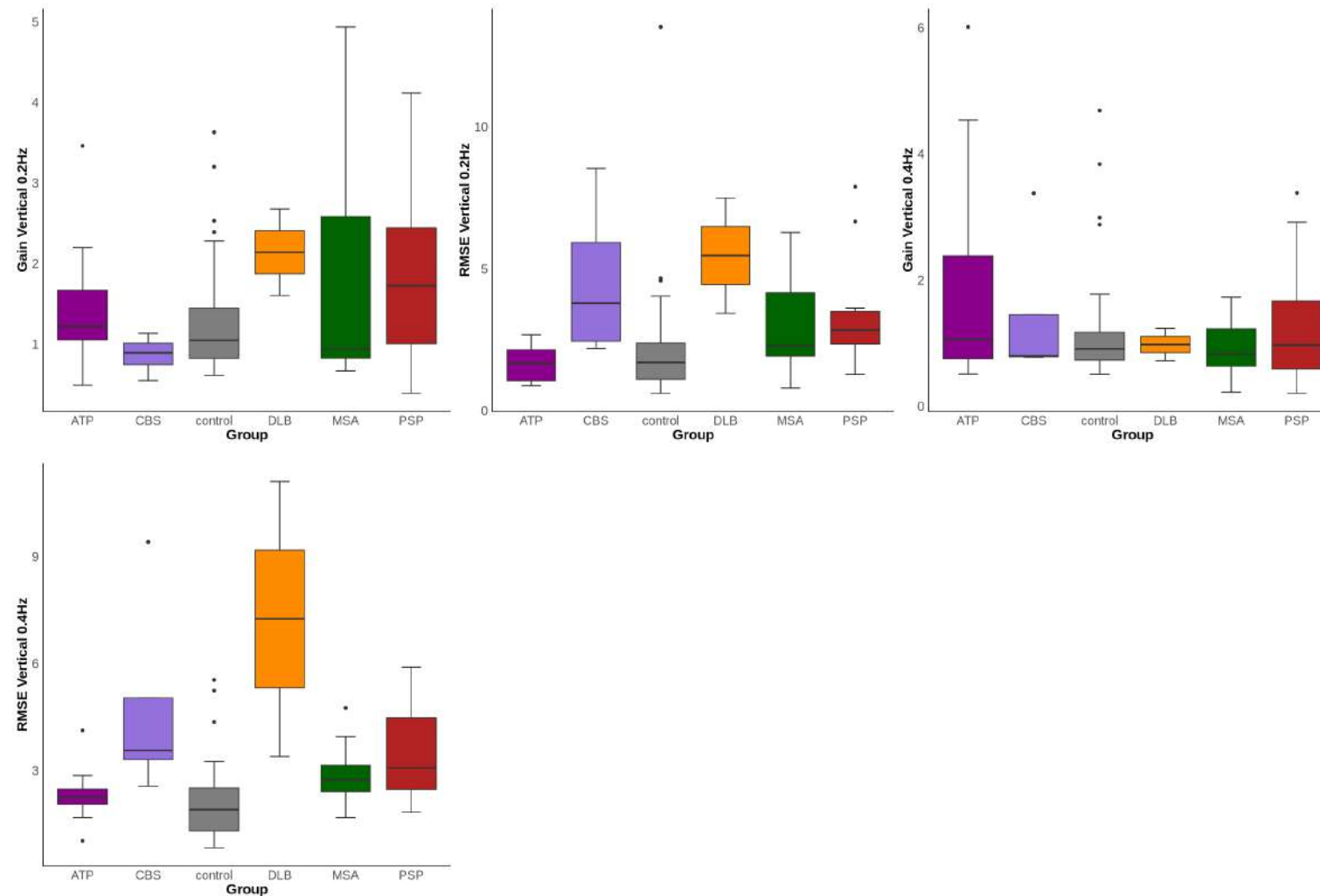


Figure 89: Smooth Pursuit Metrics in Atypical Parkinsonian Syndromes. Box plots show the median, interquartile range, and full range. Generalized linear models were used to assess the effects of group, age, sex, and disease duration. Statistical significance was set at $p < 0.05$.

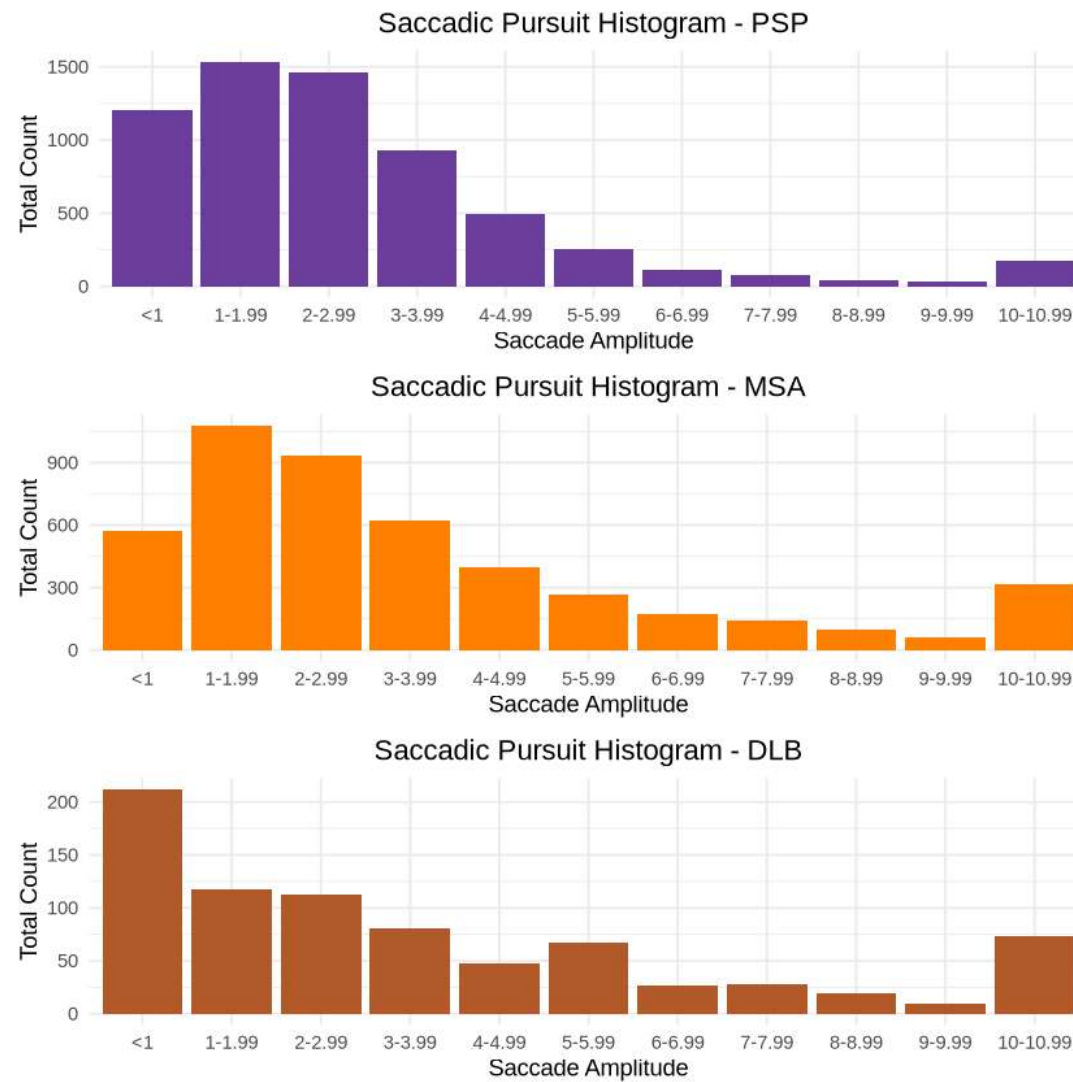
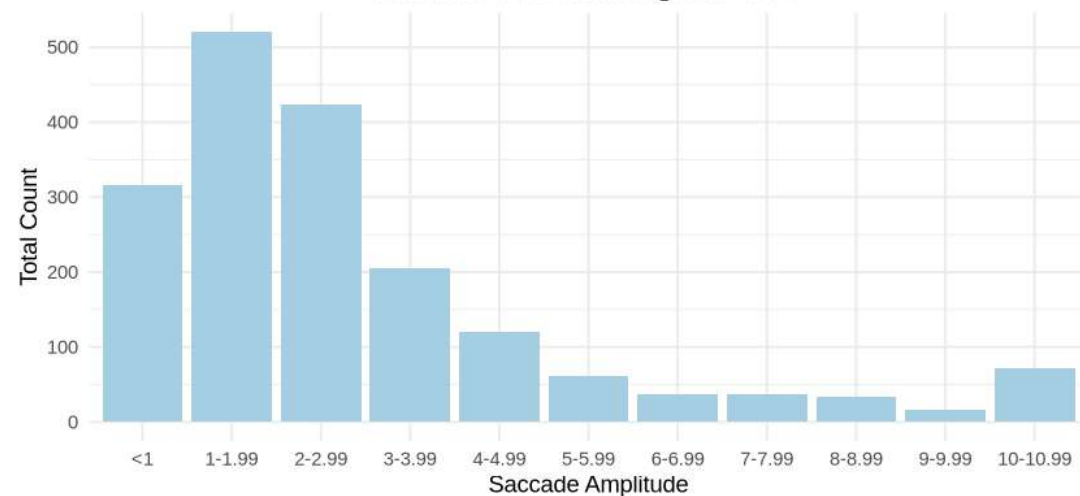


Figure 90: Saccadic Pursuit Histogram in Atypical Parkinsonian Syndromes. Saccades grouped by amplitude.

Saccadic Pursuit Histogram - CBS



Saccadic Pursuit Histogram - ATP

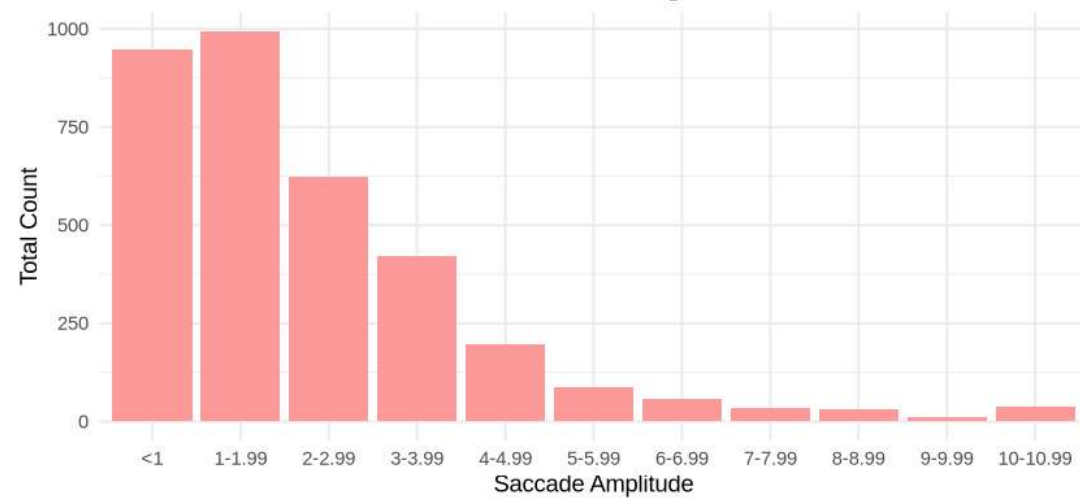


Figure 91: Saccadic Pursuit Histogram in Atypical Parkinsonian Syndromes. Saccades grouped by amplitude.

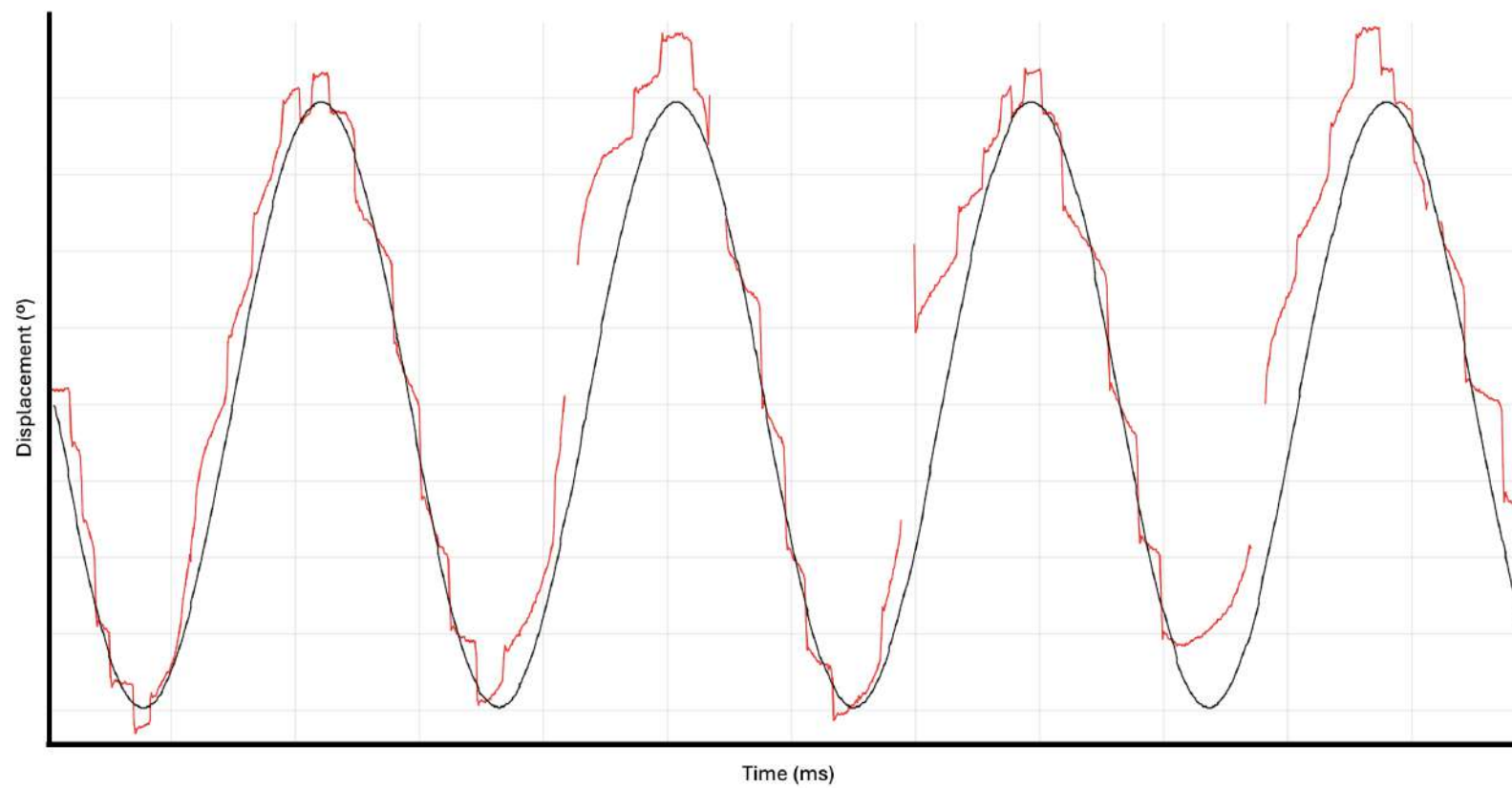


Figure 92: Smooth Pursuit Trace in Corticobasal Syndrome. A) Horizontal pursuit at 0.4Hz

Oblique Saccades Metrics in Atypical Parkinsonian Syndromes

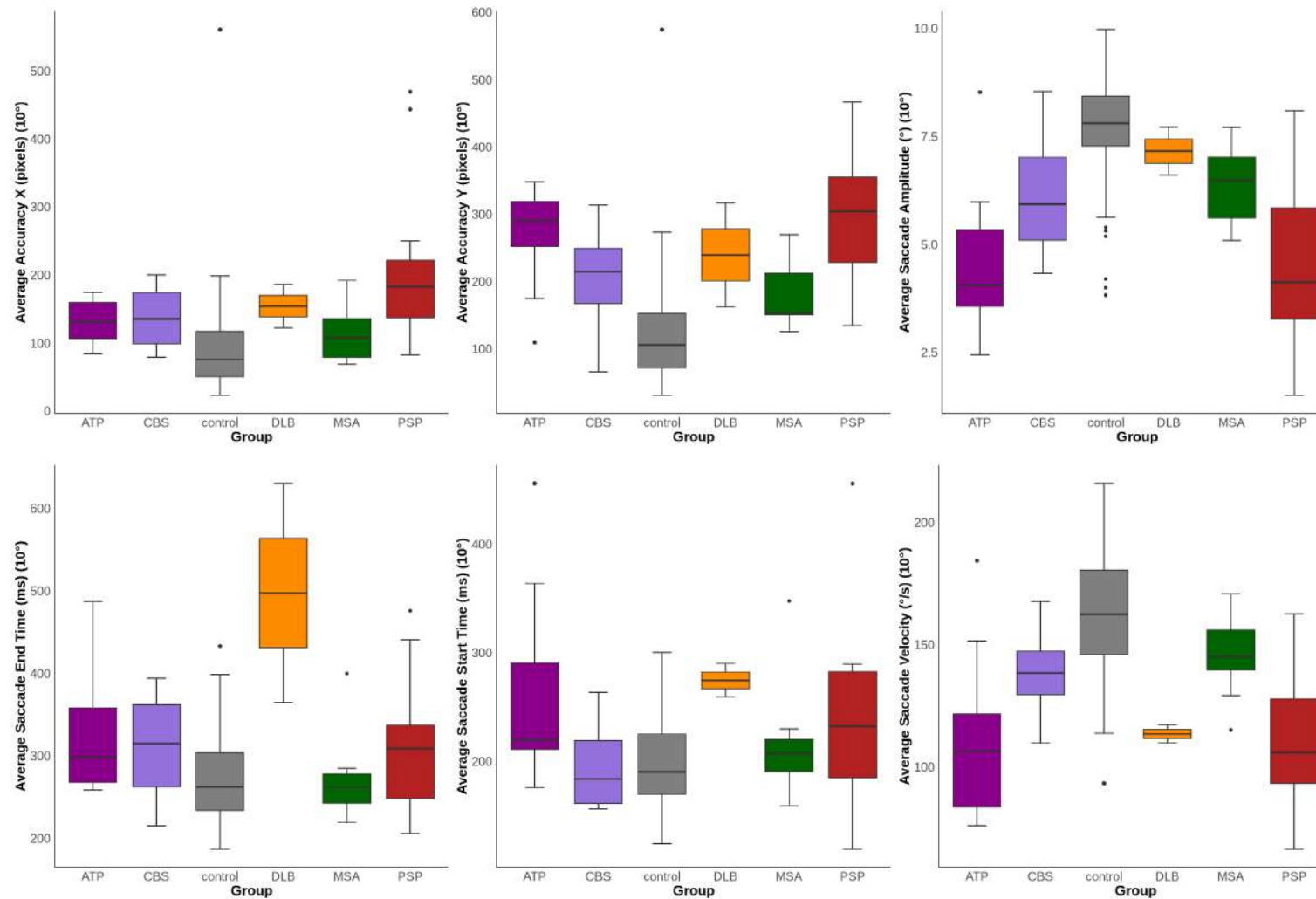


Figure 93: Oblique Saccades Metrics in Atypical Parkinsonian Syndromes. Box plots show the median, interquartile range, and full range. Generalized linear models were used to assess the effects of group, age, sex, and disease duration. Statistical significance was set at $p < 0.05$.

Oblique Saccades Metrics in Atypical Parkinsonian Syndromes

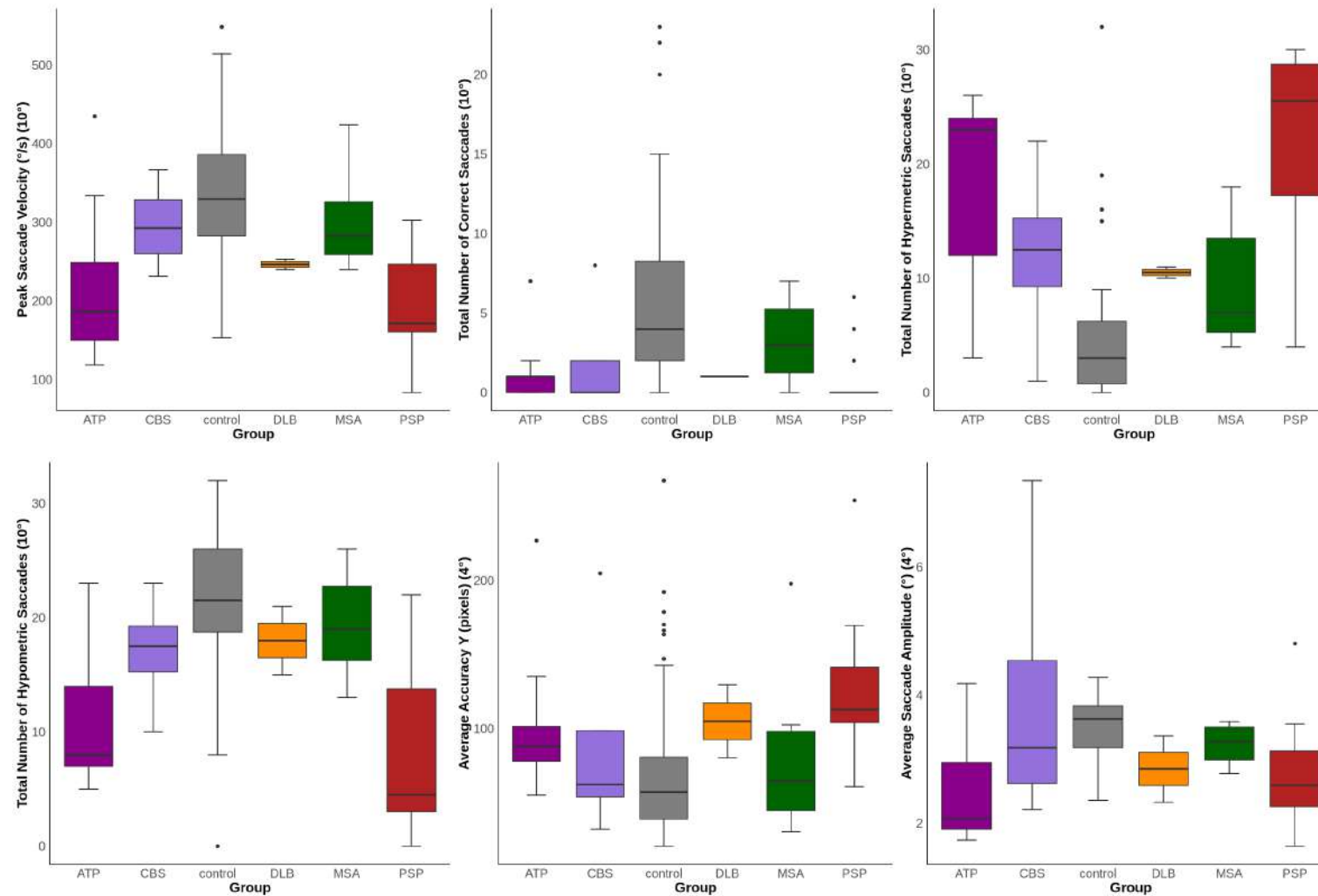


Figure 94: Oblique Saccades Metrics in Atypical Parkinsonian Syndromes. Box plots show the median, interquartile range, and full range. Generalized linear models were used to assess the effects of group, age, sex, and disease duration. Statistical significance was set at $p < 0.05$.

Oblique Saccades Metrics in Atypical Parkinsonian Syndromes

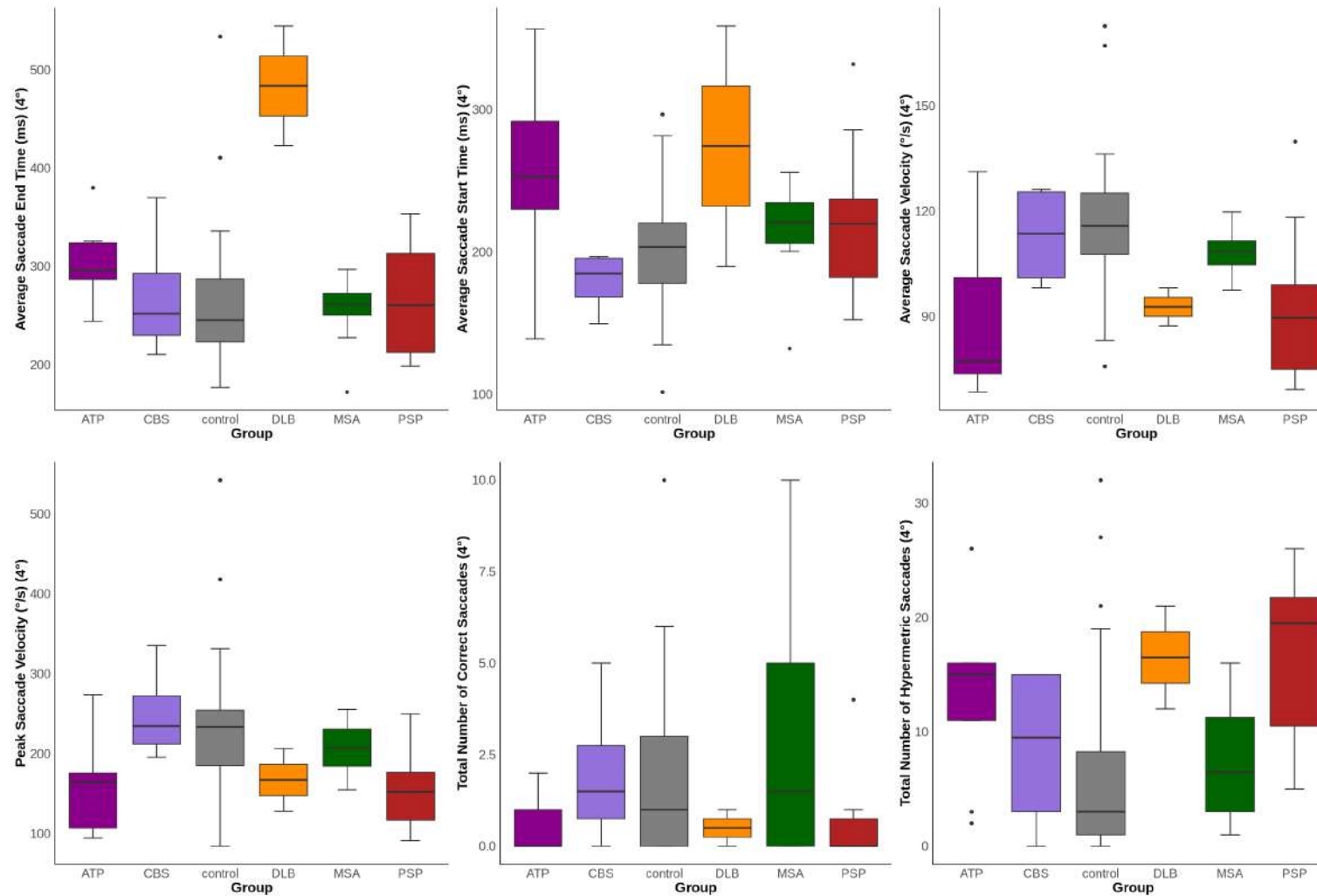


Figure 95: Oblique Saccades Metrics in Atypical Parkinsonian Syndromes. Box plots show the median, interquartile range, and full range. Generalized linear models were used to assess the effects of group, age, sex, and disease duration. Statistical significance was set at $p < 0.05$.

Oblique Saccades Metrics in Atypical Parkinsonian Syndromes

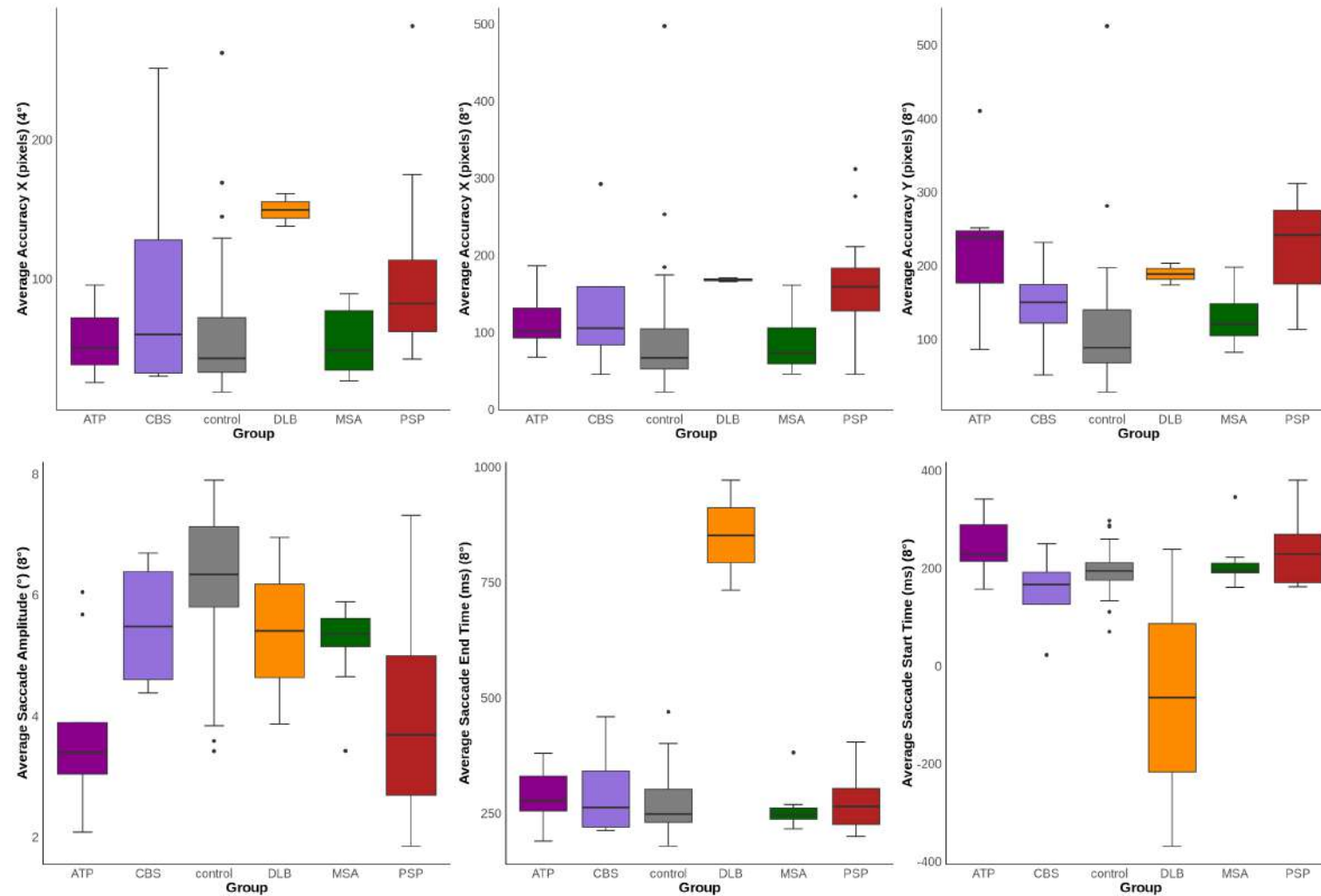


Figure 96: Oblique Saccades Metrics in Atypical Parkinsonian Syndromes. Box plots show the median, interquartile range, and full range. Generalized linear models were used to assess the effects of group, age, sex, and disease duration. Statistical significance was set at $p < 0.05$.

Oblique Saccades Metrics in Atypical Parkinsonian Syndromes

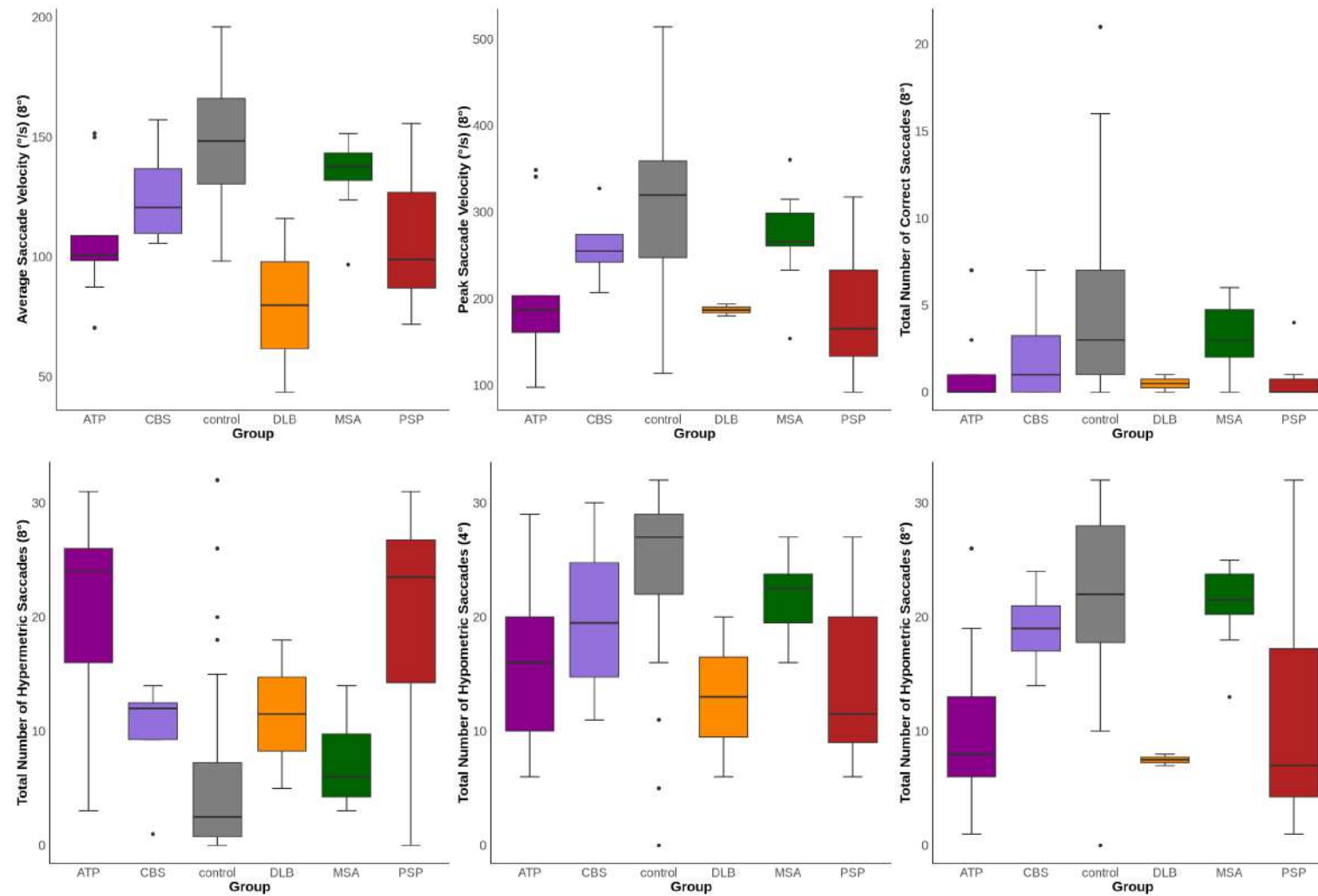


Figure 97: Oblique Saccades Metrics in Atypical Parkinsonian Syndromes. Box plots show the median, interquartile range, and full range. Generalized linear models were used to assess the effects of group, age, sex, and disease duration. Statistical significance was set at $p < 0.05$.

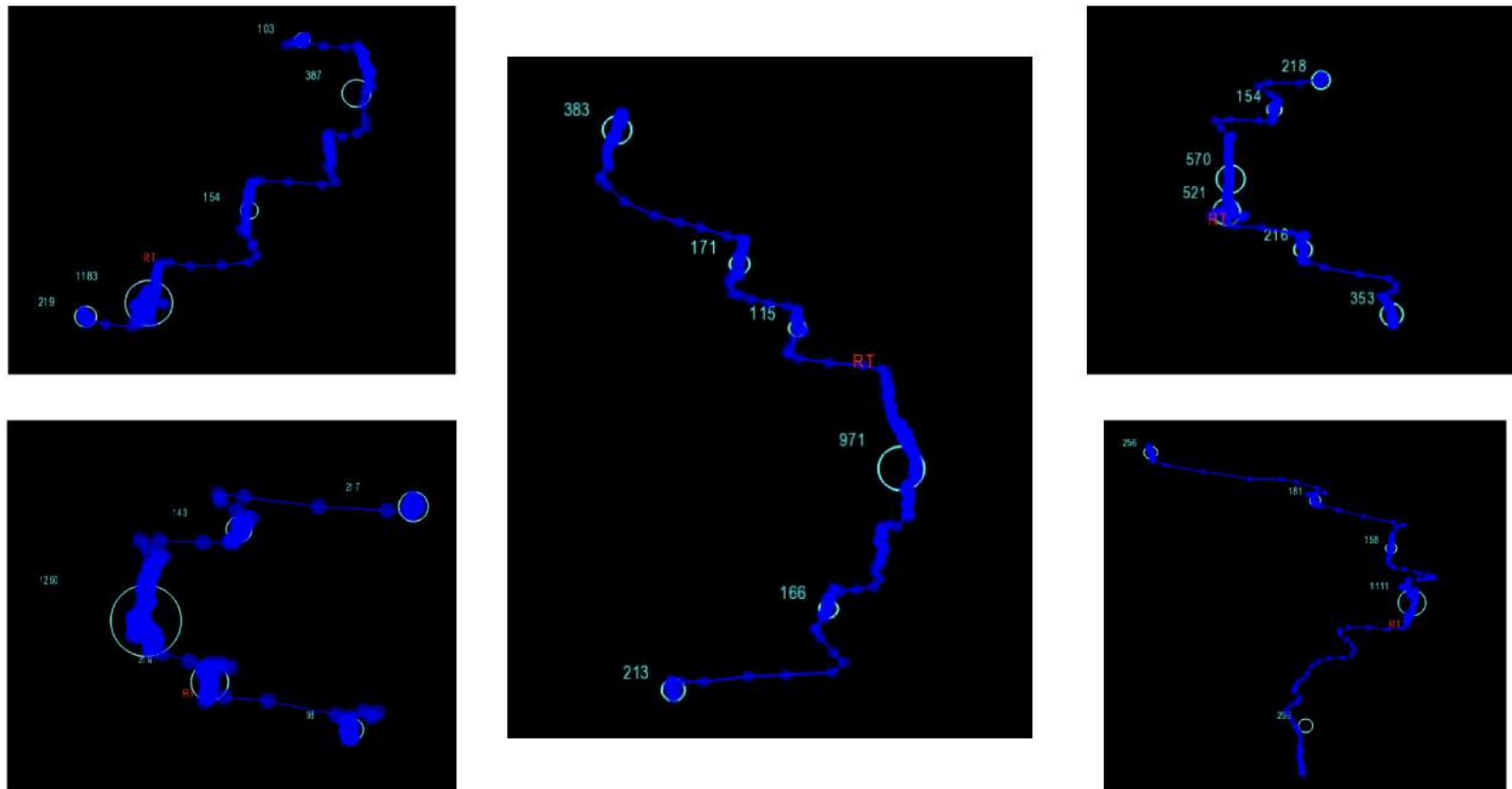


Figure 98: Oblique Saccades Trace in Progressive Supranuclear Palsy. Images from 10° targets at different positions on the screen; trajectories were mapped using the position of the pupils. Curved trajectories suggest "round the houses" mechanism for oblique saccades in progressive supranuclear palsy.

Antisaccades Horizontal Metrics in Atypical Parkinsonian Syndromes

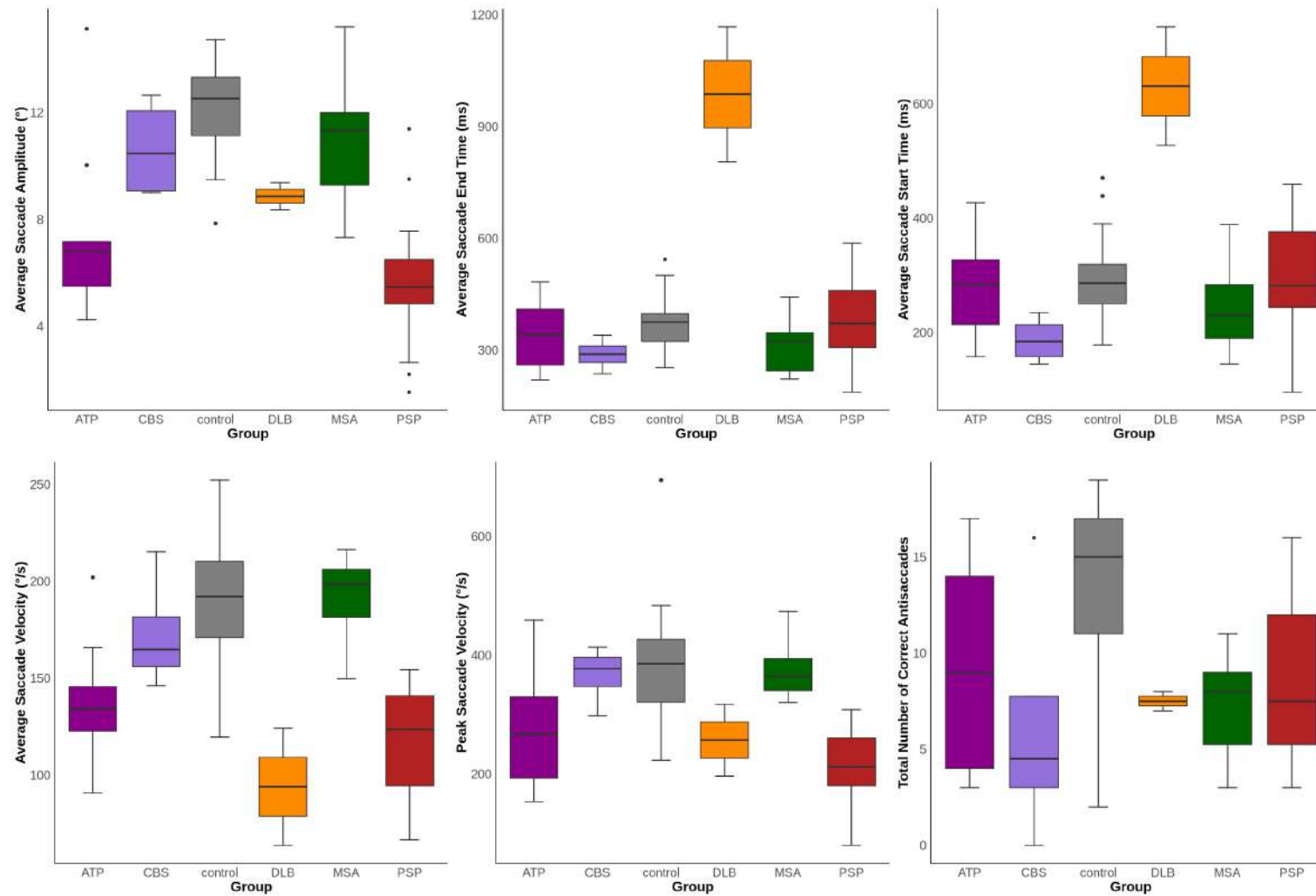


Figure 99: Antisaccades Horizontal Metrics in Atypical Parkinsonian Syndromes. Box plots show the median, interquartile range, and full range. Generalized linear models were used to assess the effects of group, age, sex, and disease duration. Statistical significance was set at $p < 0.05$.

Antisaccades Horizontal Metrics in Atypical Parkinsonian Syndromes

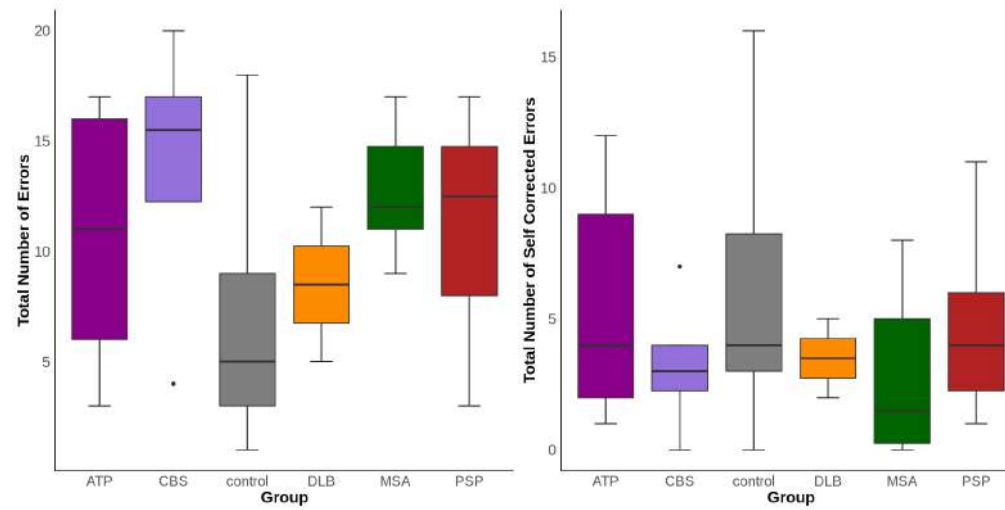


Figure 100: Antisaccades Horizontal Metrics in Atypical Parkinsonian Syndromes. Box plots show the median, interquartile range, and full range. Generalized linear models were used to assess the effects of group, age, sex, and disease duration. Statistical significance was set at $p < 0.05$.

Antisaccades Vertical Metrics in Atypical Parkinsonian Syndromes

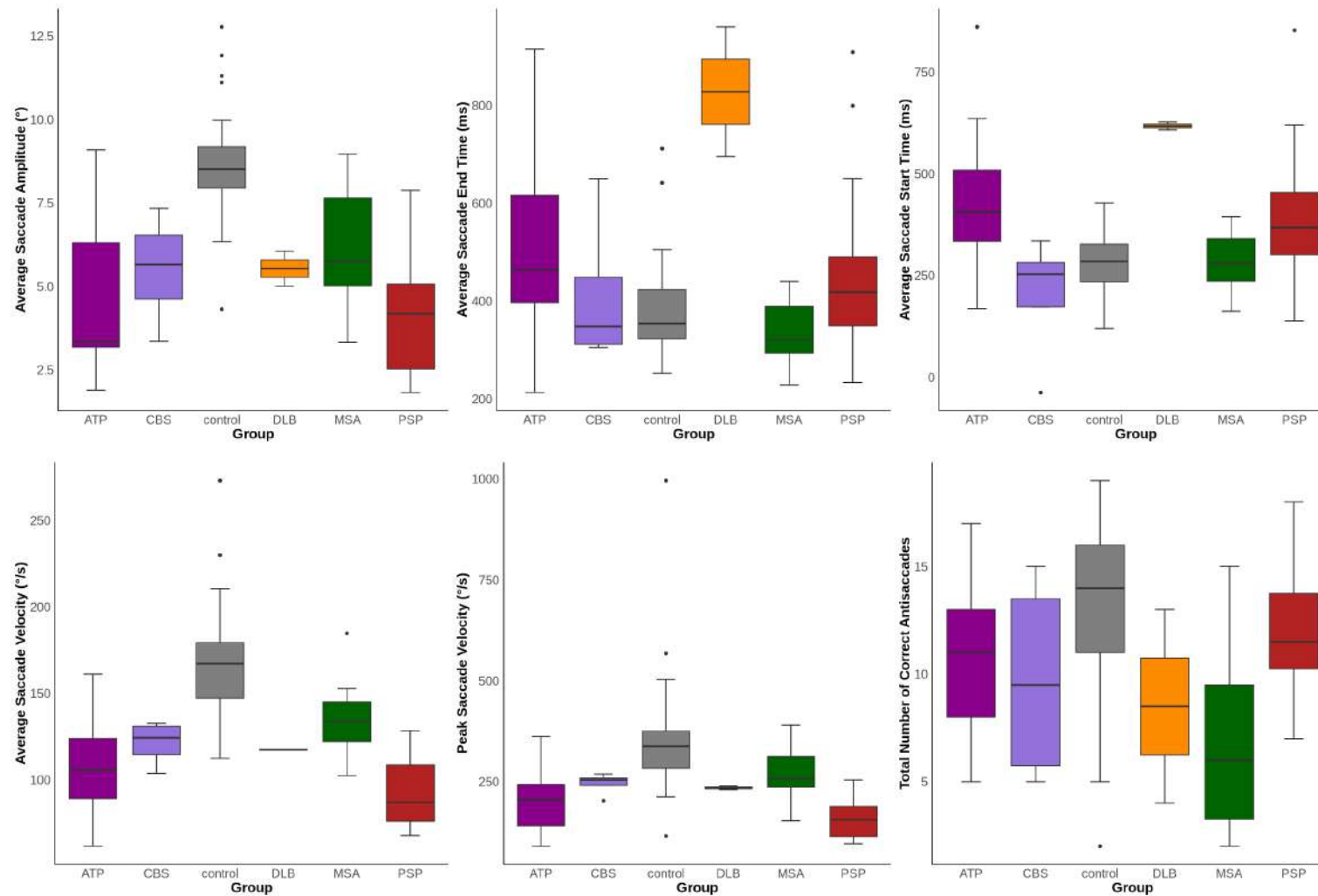


Figure 101: Antisaccades Vertical Metrics in Atypical Parkinsonian Syndromes. Box plots show the median, interquartile range, and full range. Generalized linear models were used to assess the effects of group, age, sex, and disease duration. Statistical significance was set at $p < 0.05$.

Antisaccades Vertical Metrics in Atypical Parkinsonian Syndromes

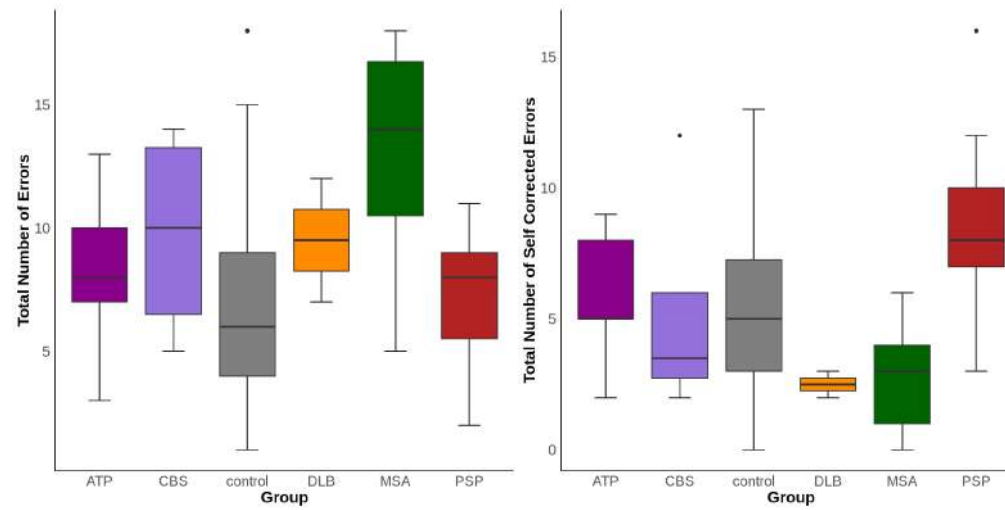


Figure 102: Antisaccades Vertical Metrics in Atypical Parkinsonian Syndromes. Box plots show the median, interquartile range, and full range. Generalized linear models were used to assess the effects of group, age, sex, and disease duration. Statistical significance was set at $p < 0.05$.

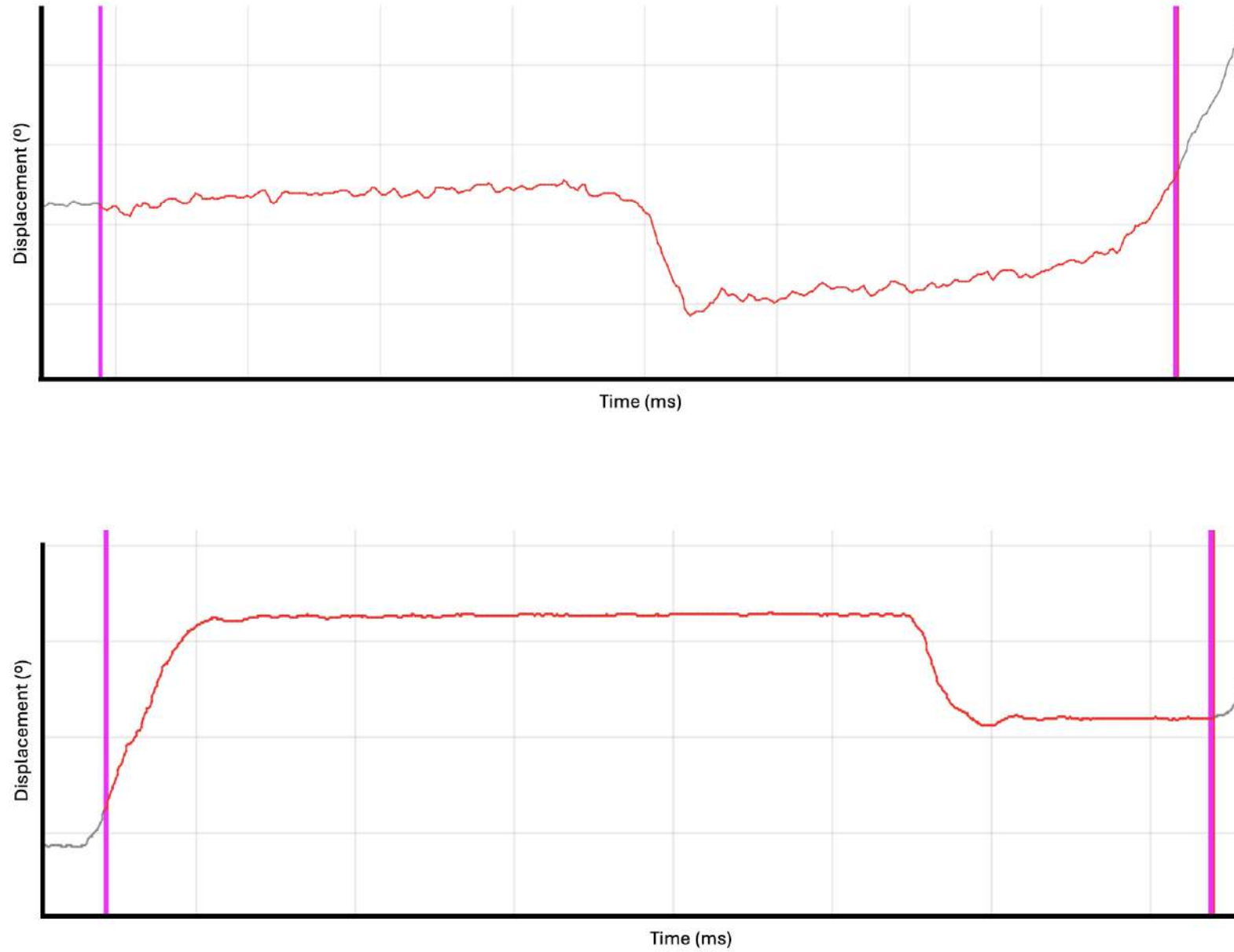


Figure 103: Antisaccades Trace in Multiple System Atrophy.A) Correct antisaccade; B) Self corrected error in antisaccade.

Reflexive Saccades Horizontal Metrics in Atypical Parkinsonian Syndromes

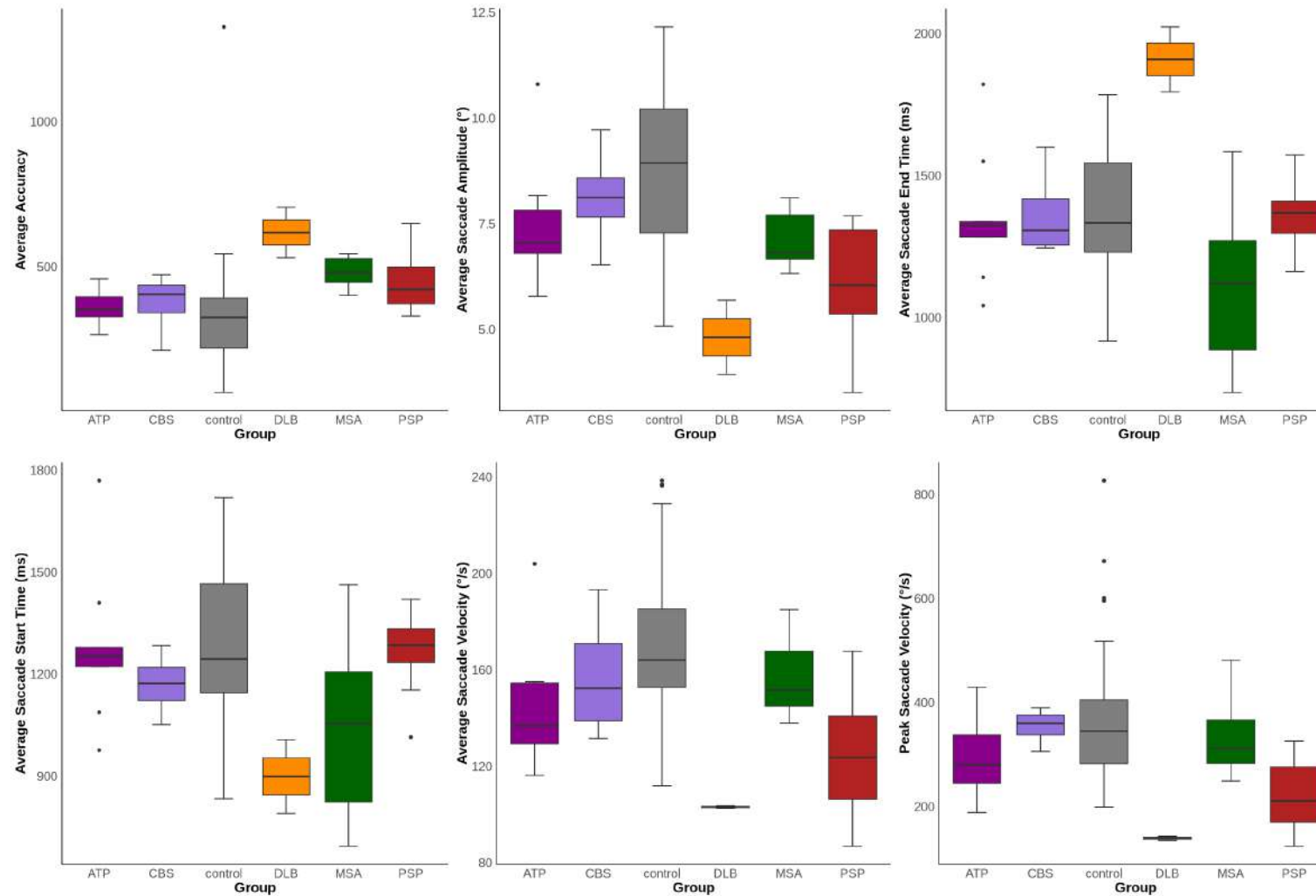


Figure 104: Reflexive Saccades Horizontal Metrics in Atypical Parkinsonian Syndromes. Box plots show the median, interquartile range, and full range. Generalized linear models were used to assess the effects of group, age, sex, and disease duration. Statistical significance was set at $p < 0.05$.

Reflexive Saccades Horizontal Metrics in Atypical Parkinsonian Syndromes

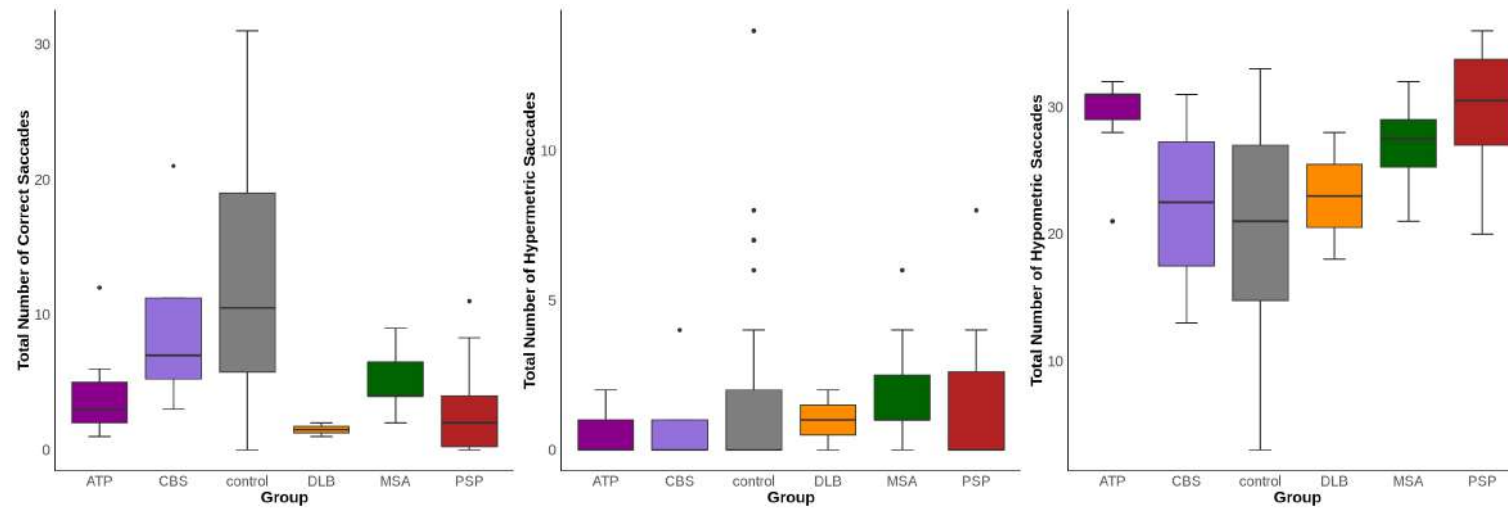


Figure 105: Reflexive Saccades Horizontal Metrics in Atypical Parkinsonian Syndromes. Box plots show the median, interquartile range, and full range. Generalized linear models were used to assess the effects of group, age, sex, and disease duration. Statistical significance was set at $p < 0.05$.

Reflexive Saccades Vertical Metrics in Atypical Parkinsonian Syndromes

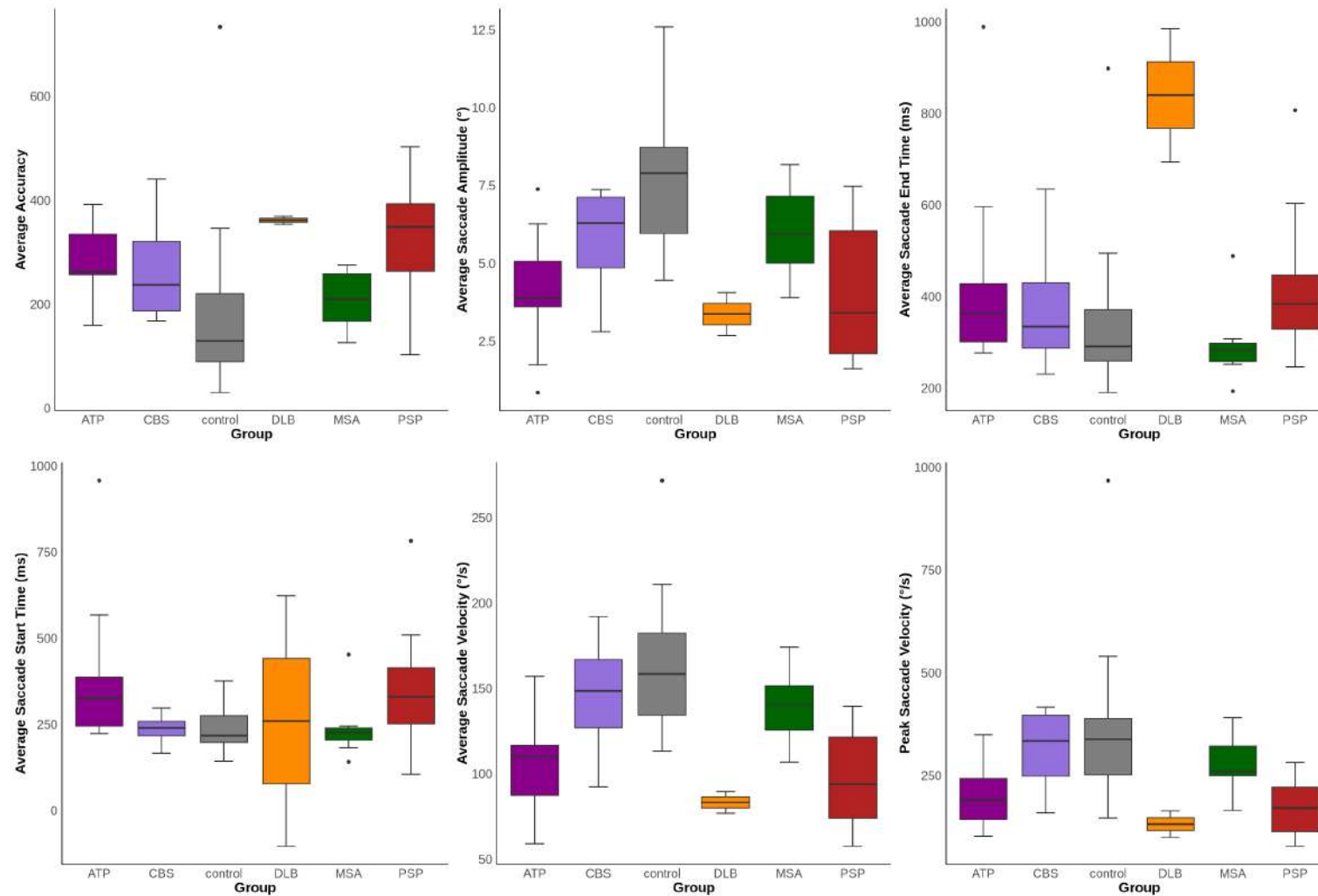


Figure 106: Reflexive Saccades Vertical Metrics in Atypical Parkinsonian Syndromes. Box plots show the median, interquartile range, and full range. Generalized linear models were used to assess the effects of group, age, sex, and disease duration. Statistical significance was set at $p < 0.05$.

Reflexive Saccades Vertical Metrics in Atypical Parkinsonian Syndromes

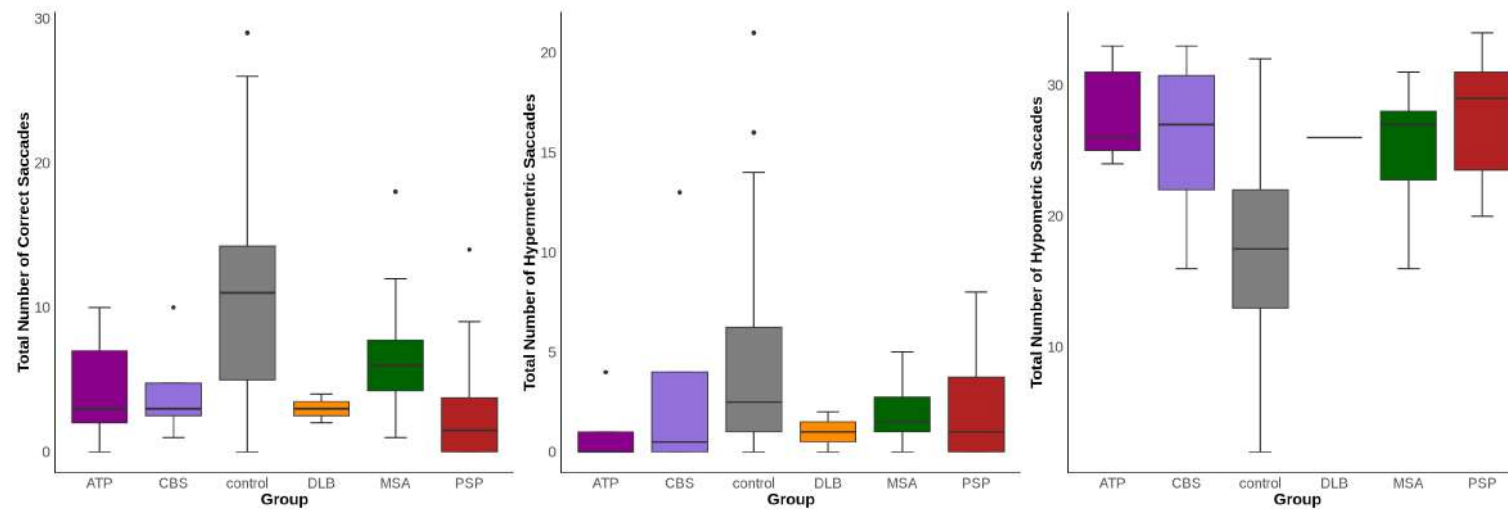


Figure 107: Reflexive Saccades Vertical Metrics in Atypical Parkinsonian Syndromes. Box plots show the median, interquartile range, and full range. Generalized linear models were used to assess the effects of group, age, sex, and disease duration. Statistical significance was set at $p < 0.05$.

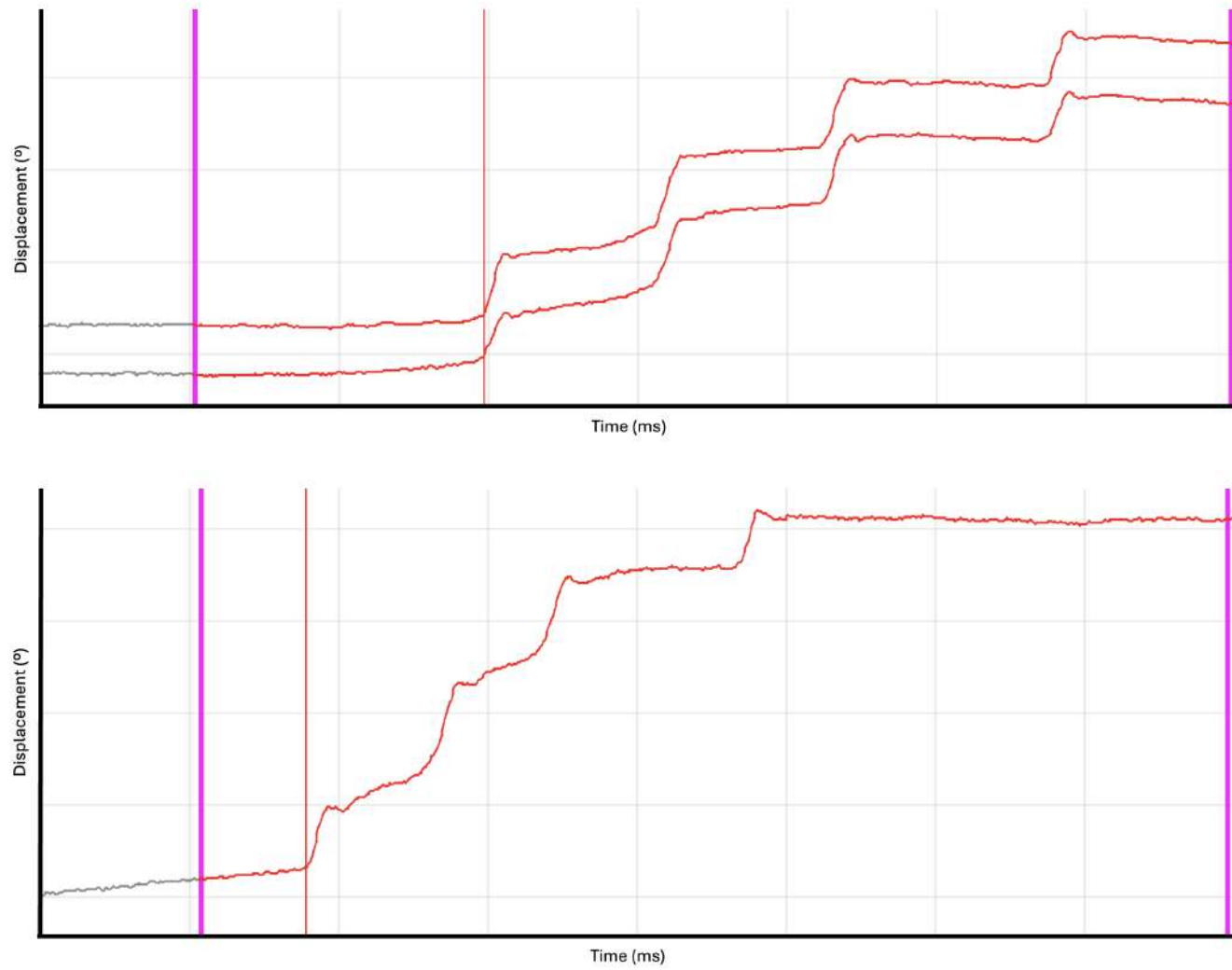


Figure 108: Hypometric Saccades in Atypical Parkinsonian Syndromes. A) Hypometric Saccades in Progressive Supranuclear Palsy; B) Hypometric Saccades in Corticobasal Syndrome.;

Timescale Analysis of Reflexive Saccades in Atypical Parkinsonian Syndromes

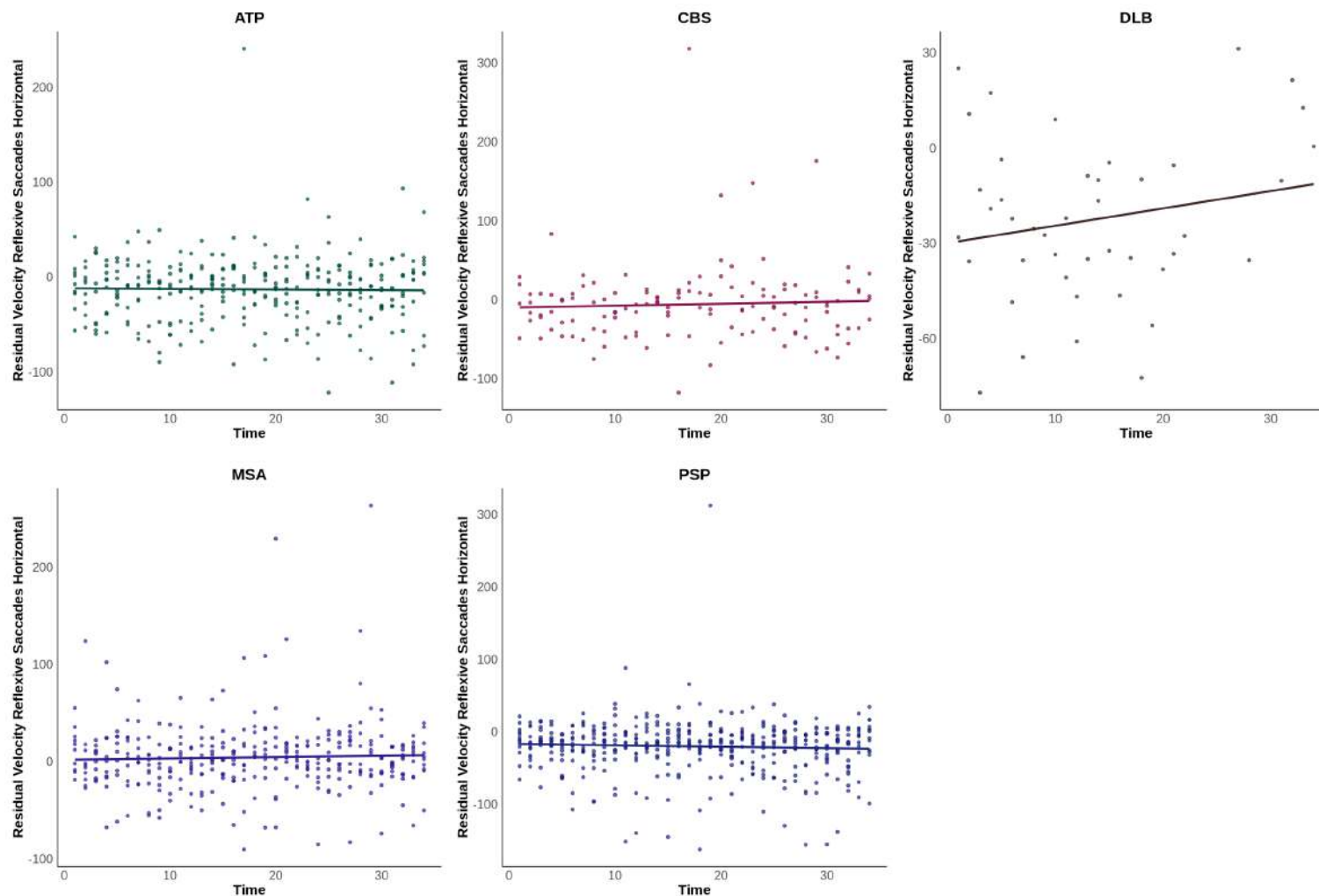


Figure 109: Timescale Analysis of Reflexive Saccades in Atypical Parkinsonian Syndromes. Residual velocity calculated through the main sequence effect.

Timescale Analysis of Reflexive Saccades in Atypical Parkinsonian Syndromes

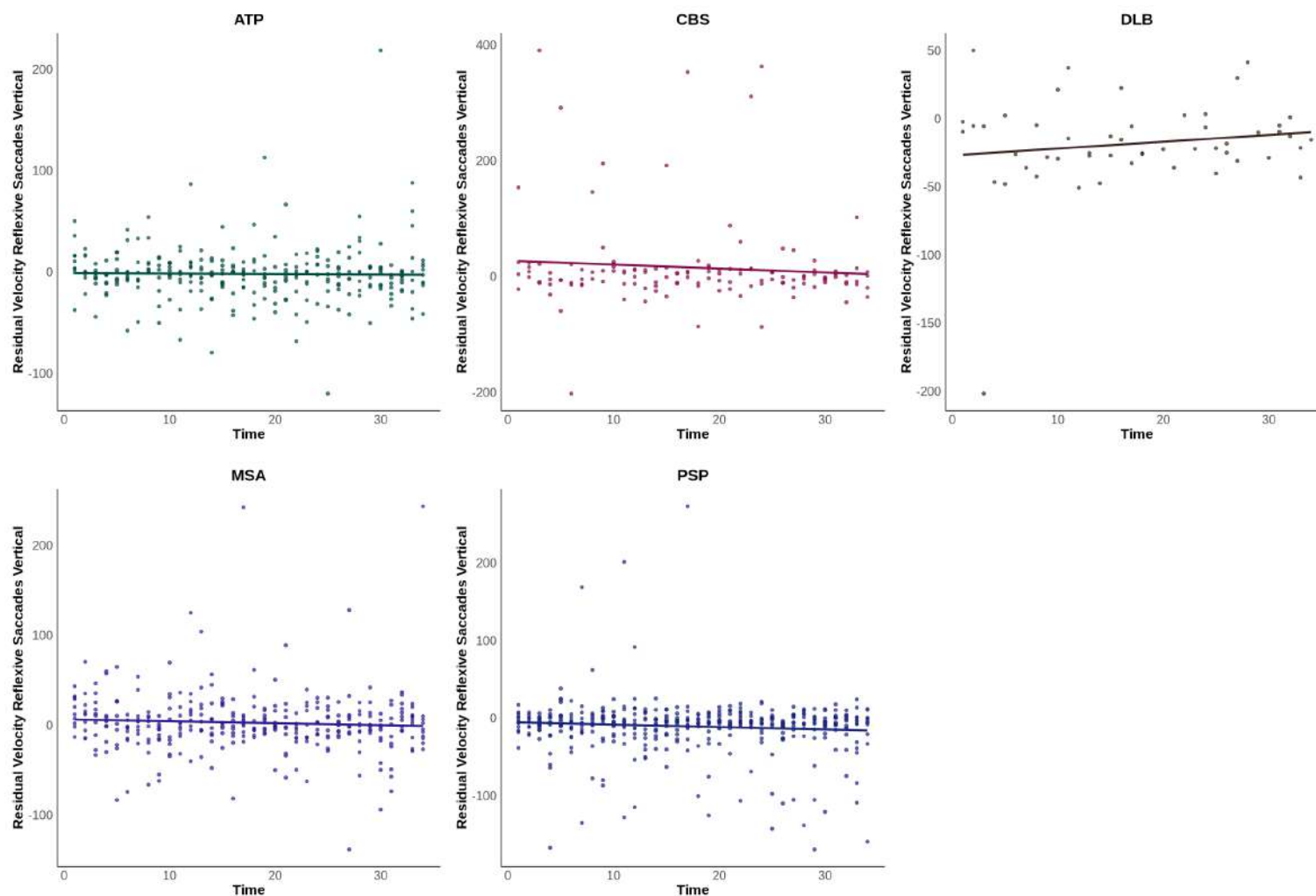


Figure 110: Timescale Analysis of Reflexive Saccades in Atypical Parkinsonian Syndromes. Residual velocity calculated through the main sequence effect.

Volitional Saccades Horizontal Metrics in Atypical Parkinsonian Syndromes

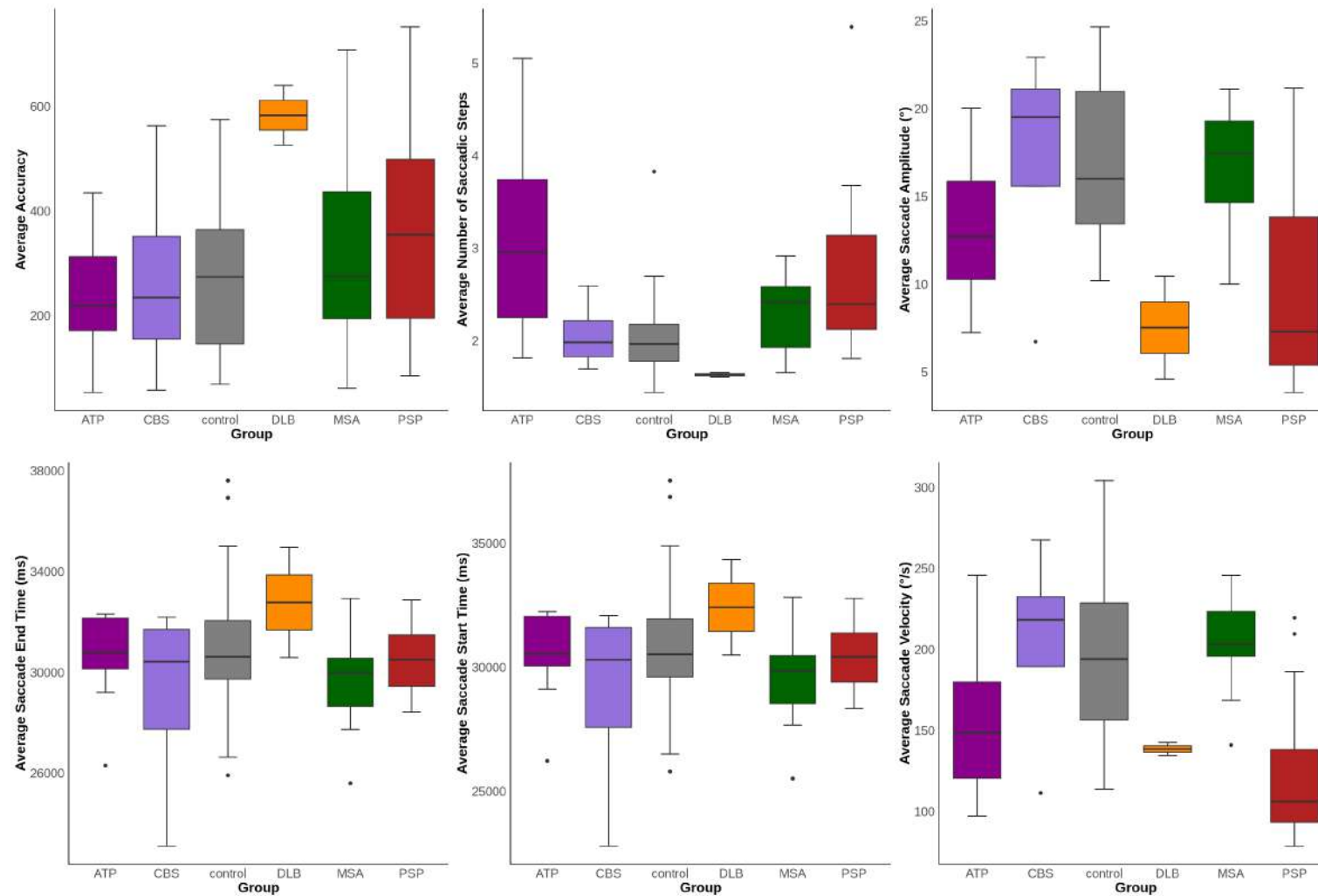


Figure 111: Volitional Saccades Horizontal Metrics in Atypical Parkinsonian Syndromes. Box plots show the median, interquartile range, and full range. Generalized linear models were used to assess the effects of group, age, sex, and disease duration. Statistical significance was set at $p < 0.05$.

Volitional Saccades Horizontal Metrics in Atypical Parkinsonian Syndromes

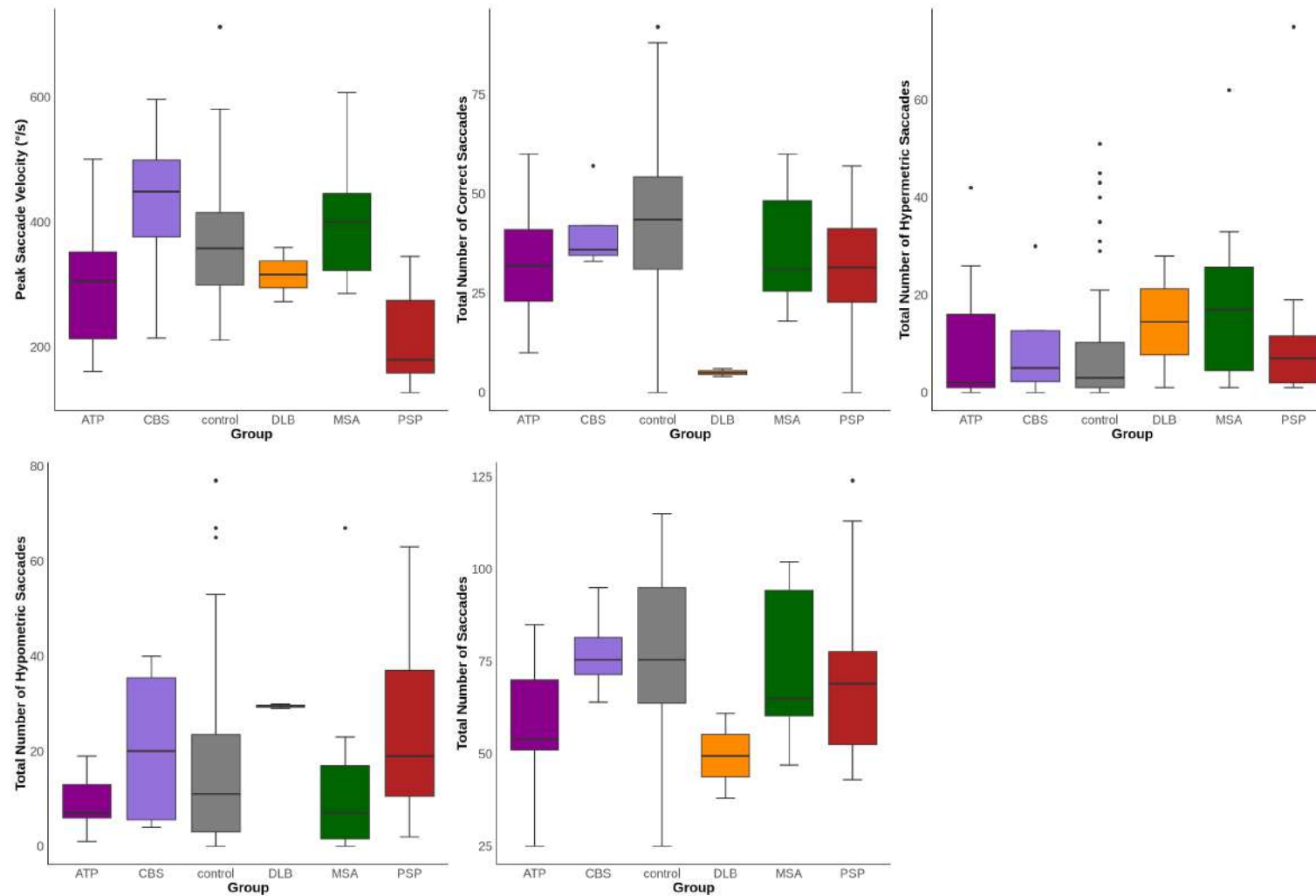


Figure 112: Volitional Saccades Horizontal Metrics in Atypical Parkinsonian Syndromes. Box plots show the median, interquartile range, and full range. Generalized linear models were used to assess the effects of group, age, sex, and disease duration. Statistical significance was set at $p < 0.05$.

Volitional Saccades Vertical Metrics in Atypical Parkinsonian Syndromes

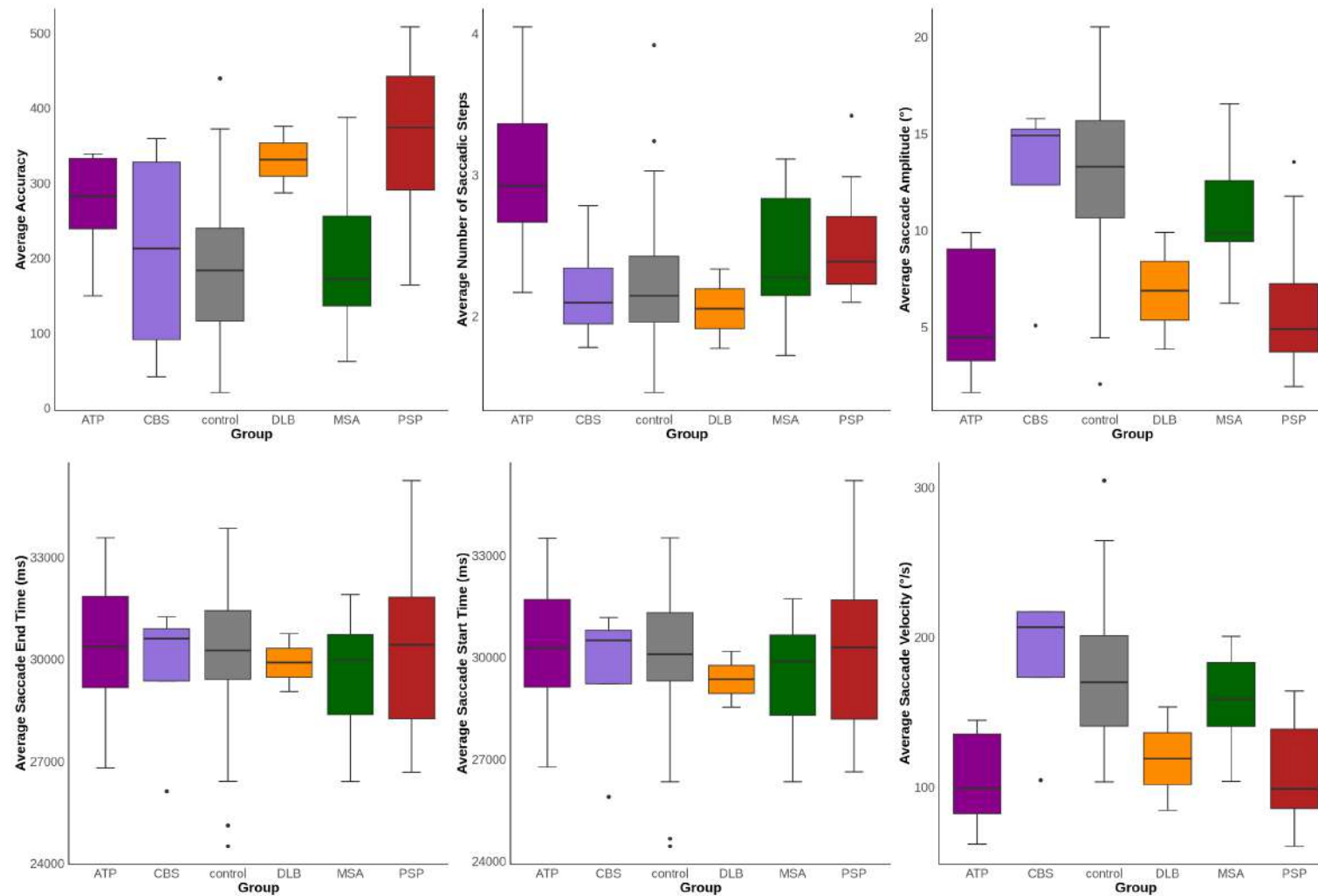


Figure 113: Volitional Saccades Vertical Metrics in Atypical Parkinsonian Syndromes. Box plots show the median, interquartile range, and full range. Generalized linear models were used to assess the effects of group, age, sex, and disease duration. Statistical significance was set at $p < 0.05$.

Volitional Saccades Vertical Metrics in Atypical Parkinsonian Syndromes

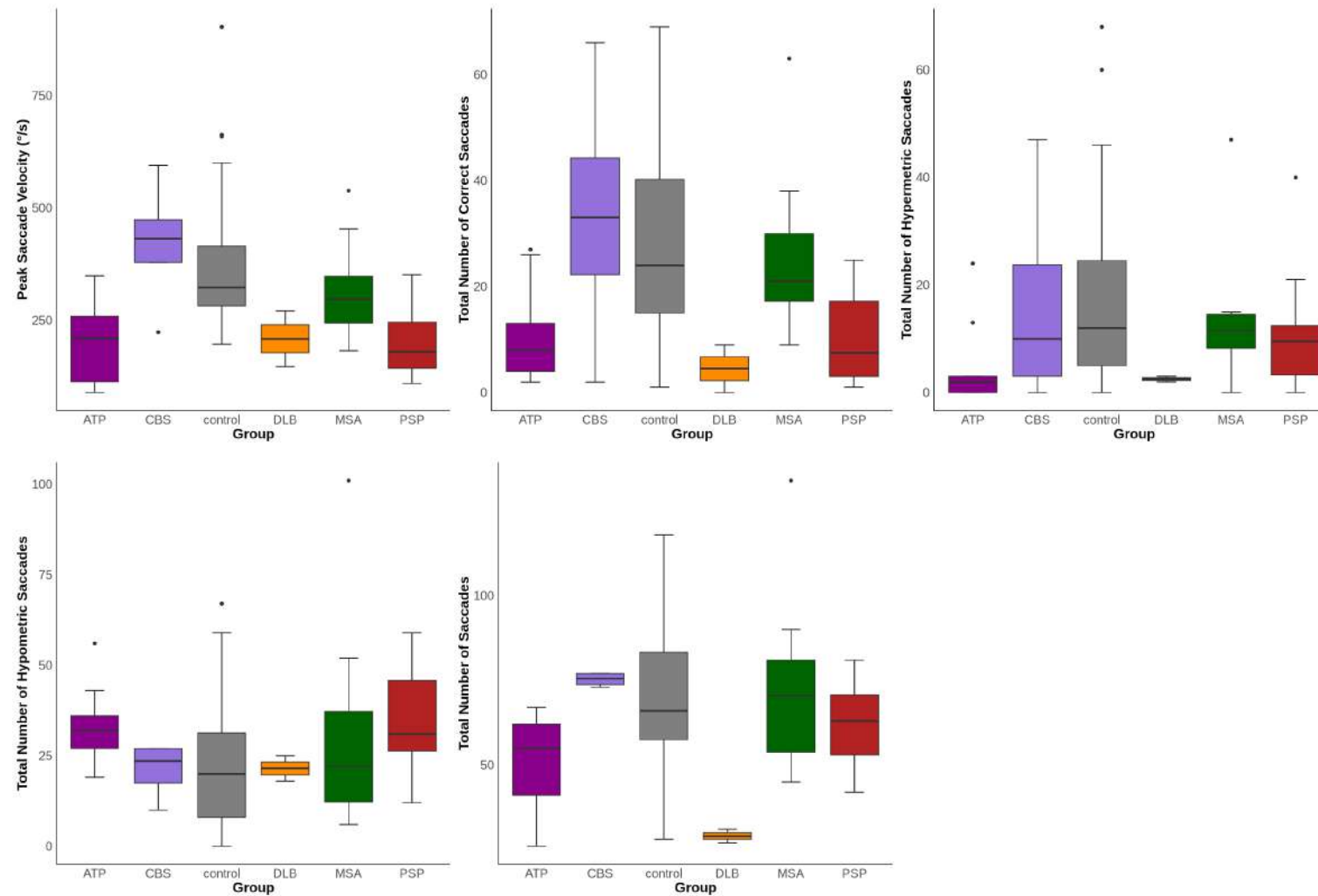


Figure 114: Volitional Saccades Vertical Metrics in Atypical Parkinsonian Syndromes. Box plots show the median, interquartile range, and full range. Generalized linear models were used to assess the effects of group, age, sex, and disease duration. Statistical significance was set at $p < 0.05$.

Timescale Analysis of Volitional Saccades in Atypical Parkinsonian Syndromes

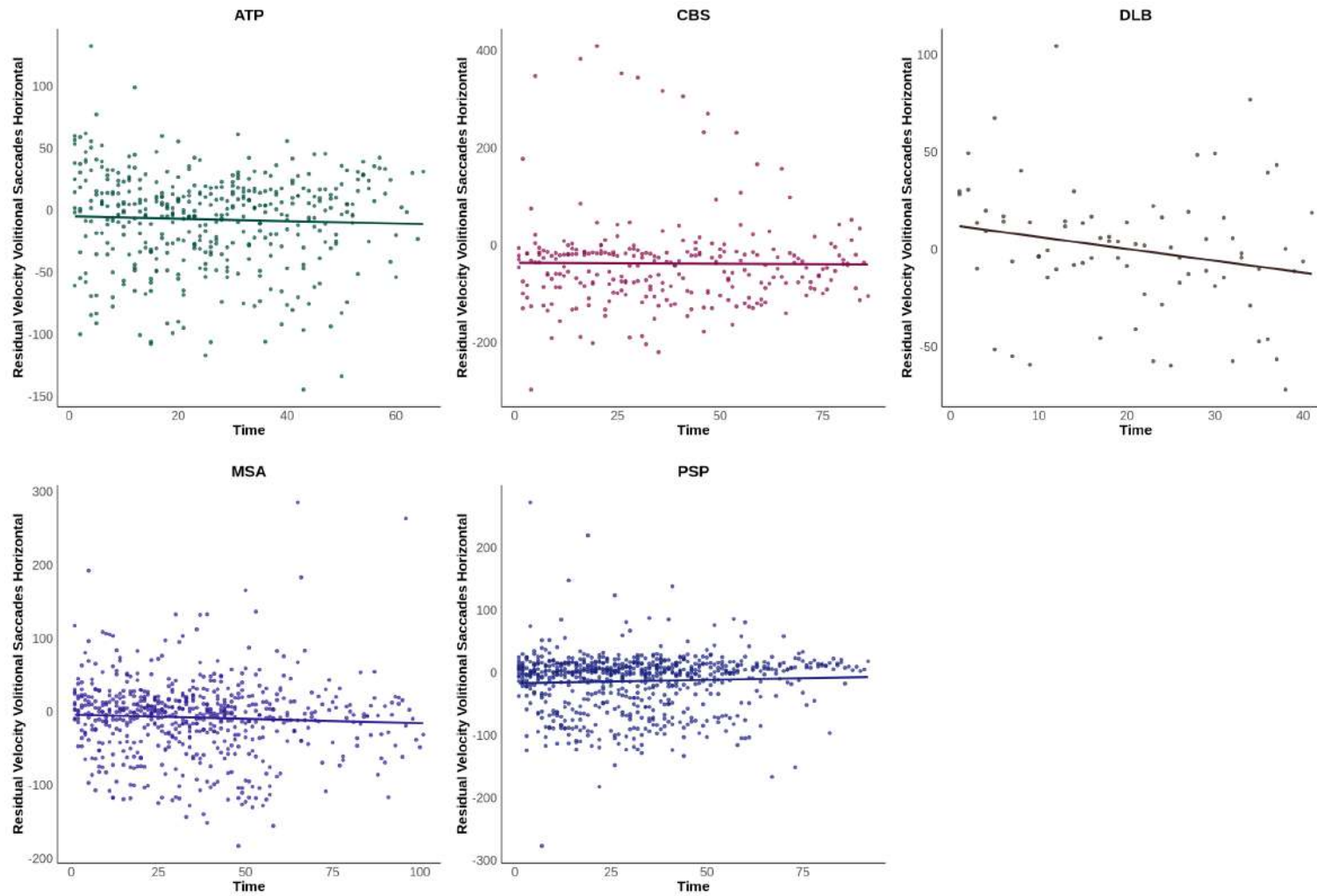


Figure 115: Timescale Analysis of Volitional Saccades in Atypical Parkinsonian Syndromes. Residual velocity calculated through the main sequence effect.

Timescale Analysis of Volitional Saccades in Atypical Parkinsonian Syndromes

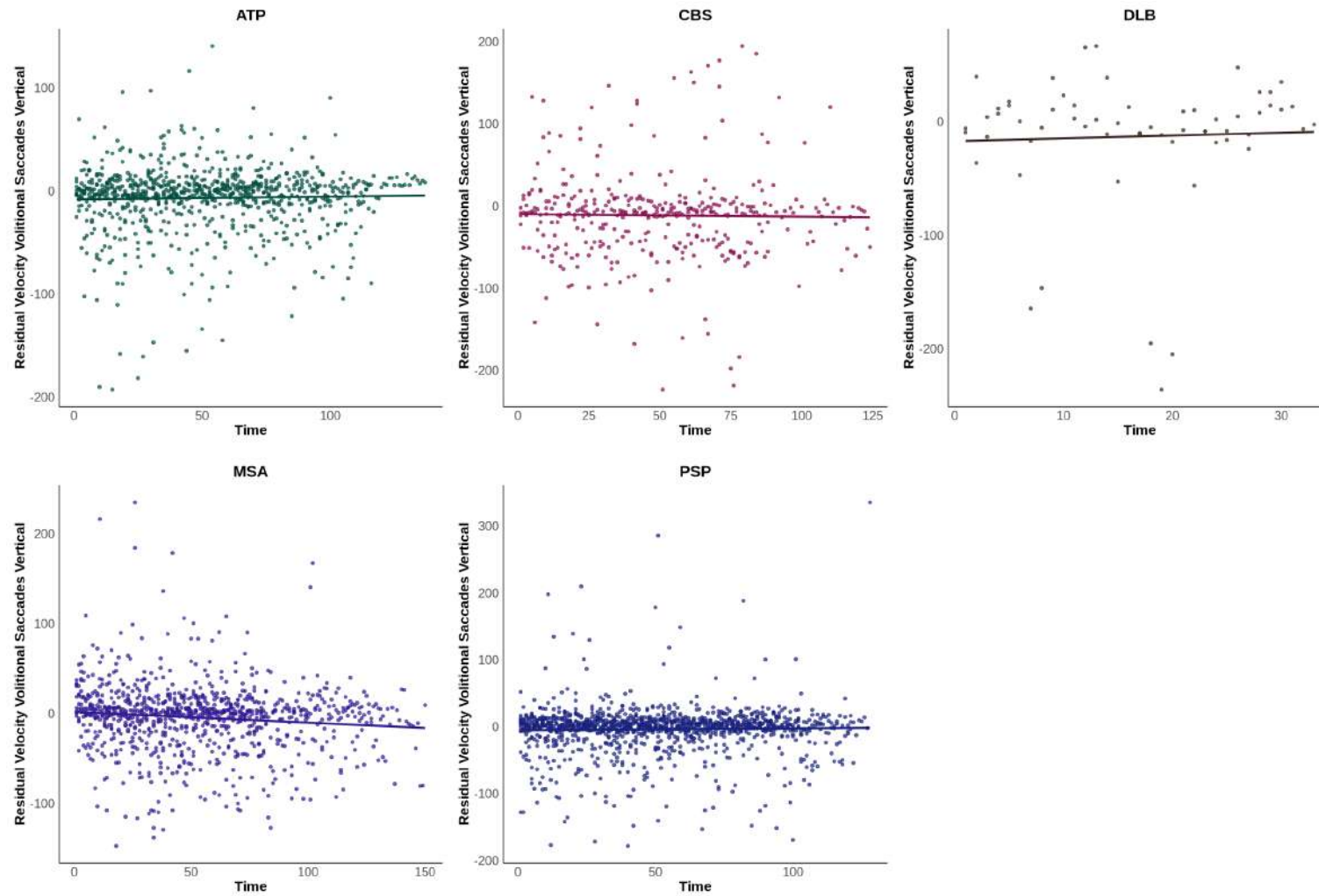


Figure 116: Timescale Analysis of Volitional Saccades in Atypical Parkinsonian Syndromes. Residual velocity calculated through the main sequence effect.

Memory Guided Saccades Horizontal Metrics in Atypical Parkinsonian Syndromes

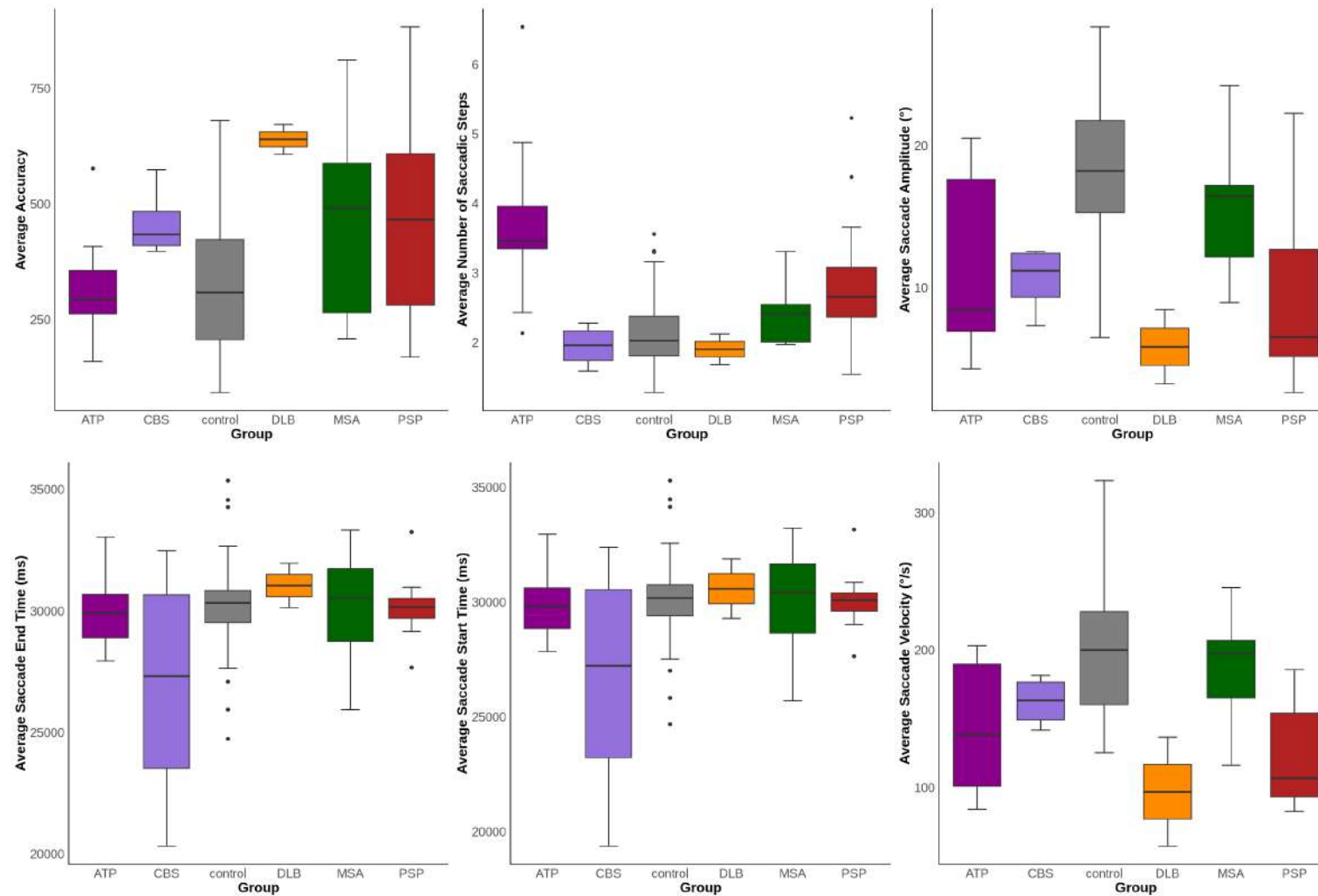


Figure 117: Memory Guided Saccades Horizontal Metrics in Atypical Parkinsonian Syndromes.

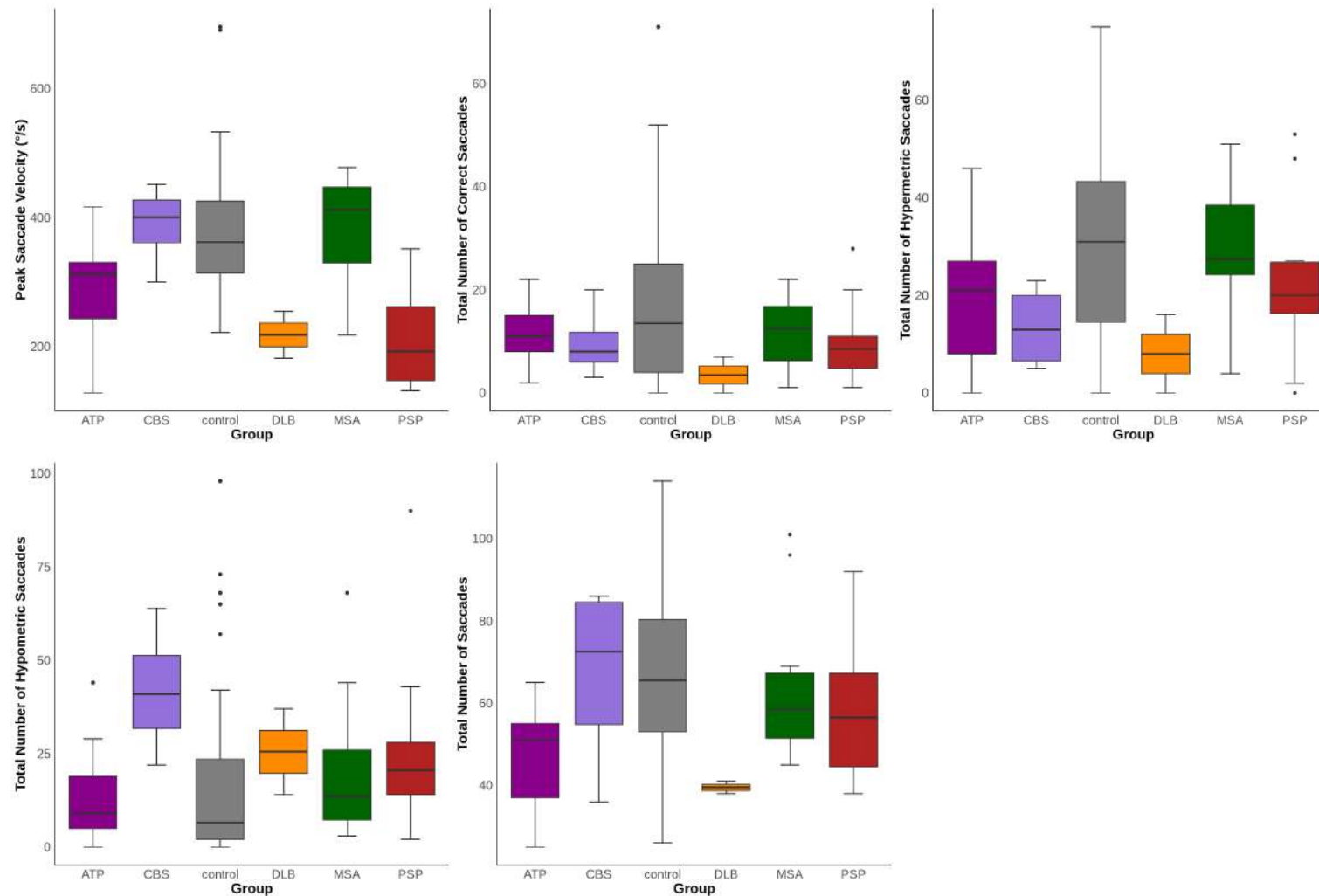


Figure 118: Memory Guided Saccades Horizontal Metrics in Atypical Parkinsonian Syndromes. Box plots show the median, interquartile range, and full range. Generalized linear models were used to assess the effects of group, age, sex, and disease duration. Statistical significance was set at $p < 0.05$.

Memory Guided Saccades Vertical Metrics in Atypical Parkinsonian Syndromes

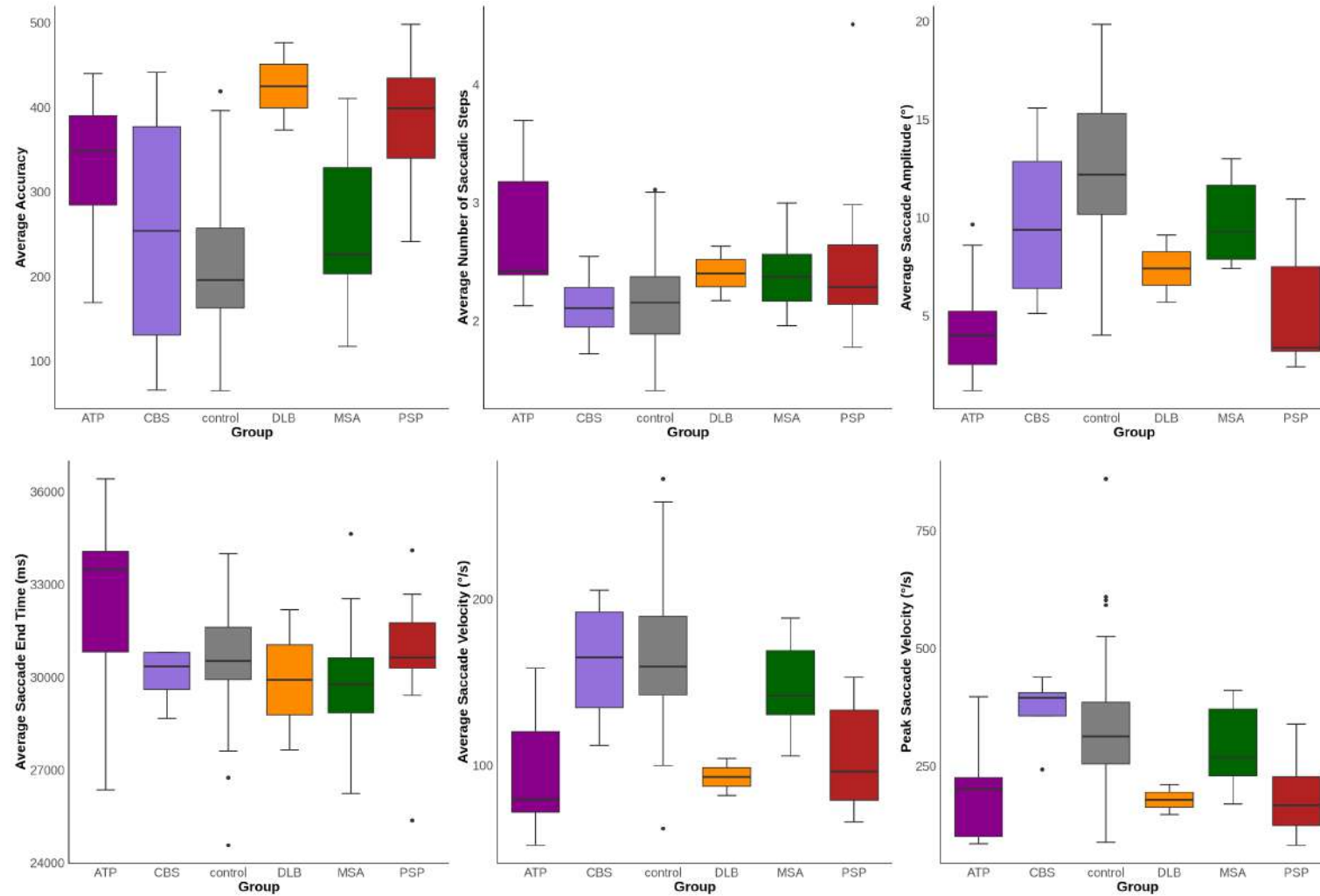


Figure 119: Memory Guided Saccades Vertical Metrics in Atypical Parkinsonian Syndromes. Box plots show the median, interquartile range, and full range. Generalized linear models were used to assess the effects of group, age, sex, and disease duration. Statistical significance was set at $p < 0.05$.

Memory Guided Saccades Vertical Metrics in Atypical Parkinsonian Syndromes

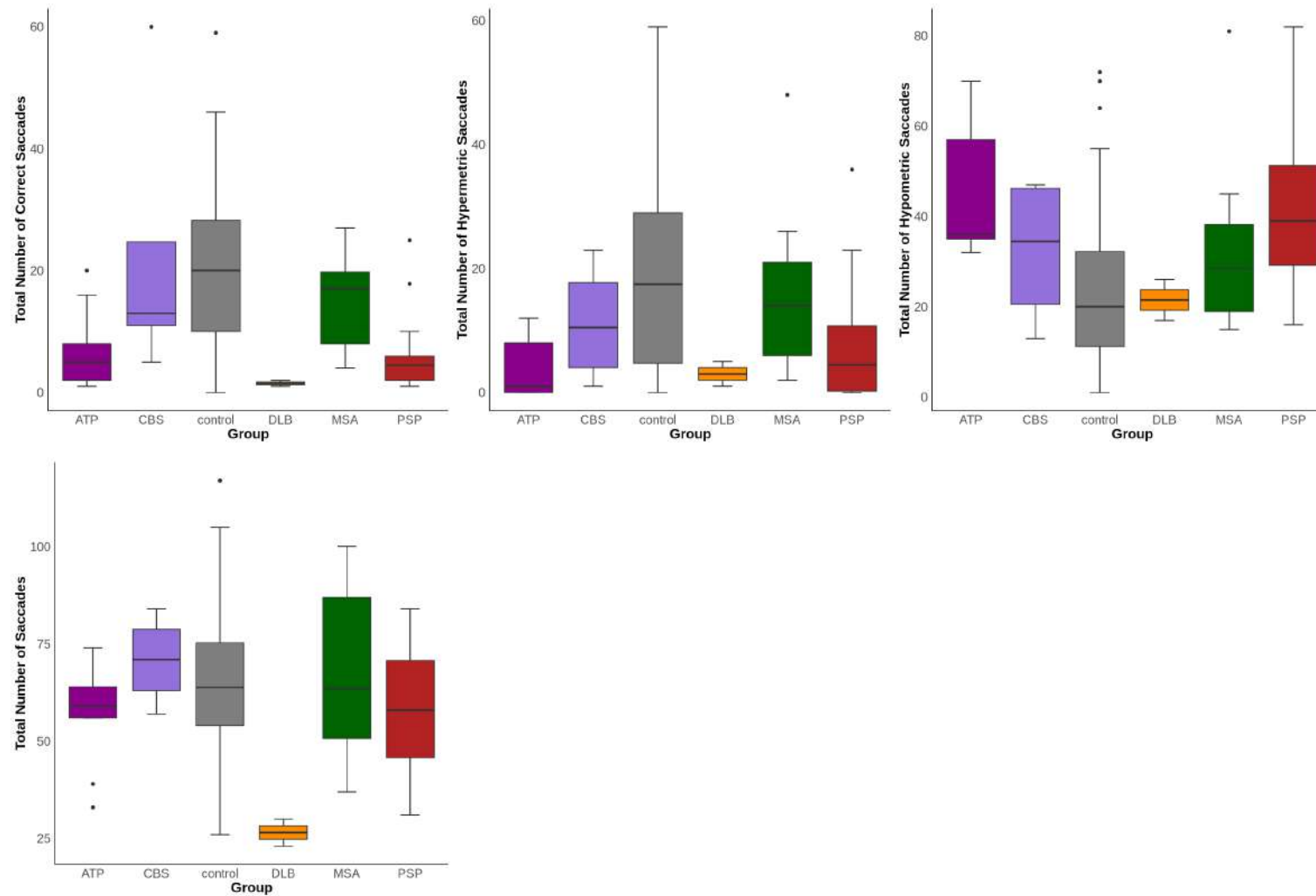


Figure 120: Memory Guided Saccades Vertical Metrics in Atypical Parkinsonian Syndromes. Box plots show the median, interquartile range, and full range. Generalized linear models were used to assess the effects of group, age, sex, and disease duration. Statistical significance was set at $p < 0.05$.

Timescale Analysis of Memory Guided Saccades in Atypical Parkinsonian Syndromes

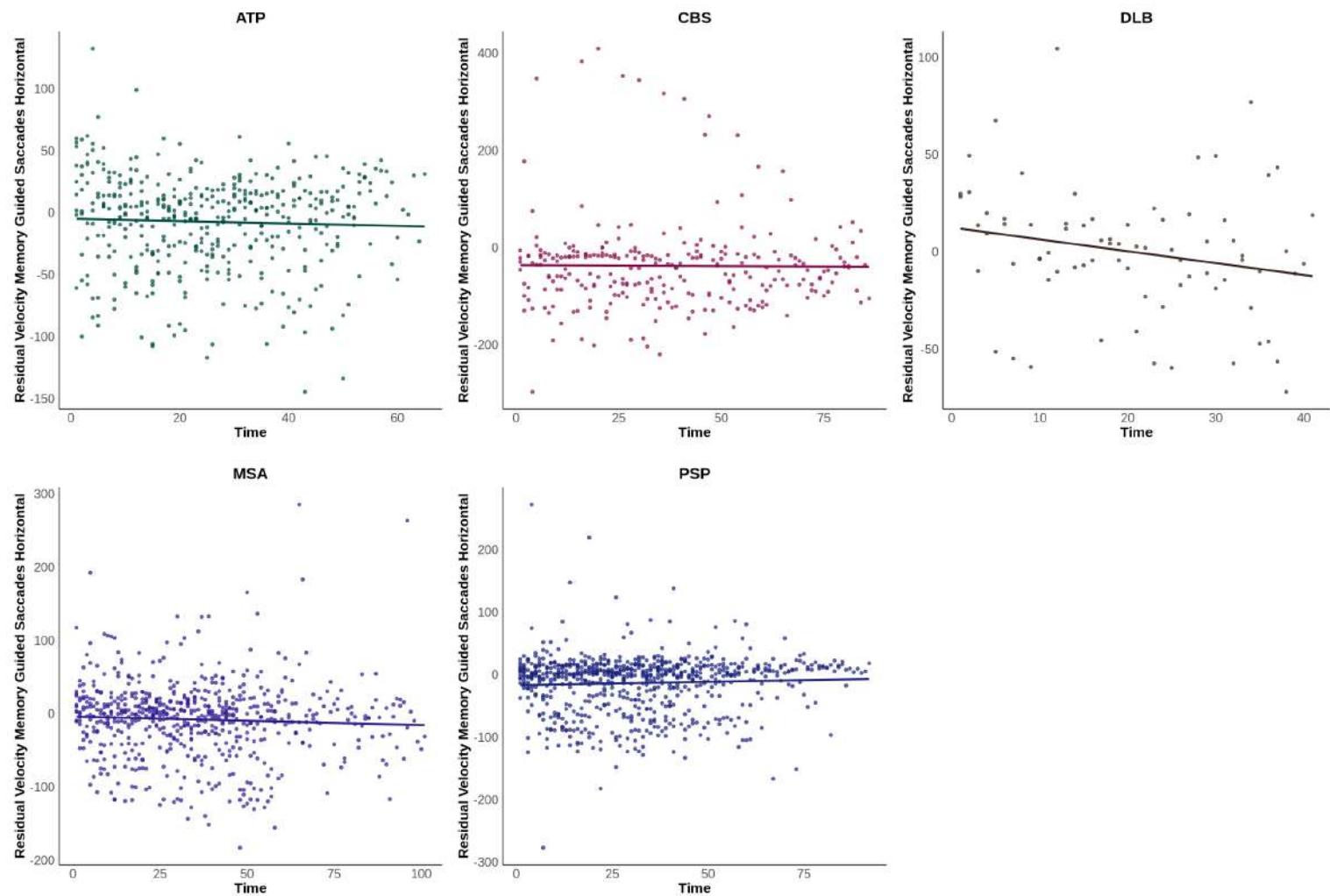


Figure 121: Timescale Analysis of Memory Guided Saccades in Atypical Parkinsonian Syndromes. Residual velocity calculated through the main sequence effect.

Timescale Analysis of Memory Guided Saccades in Atypical Parkinsonian Syndromes

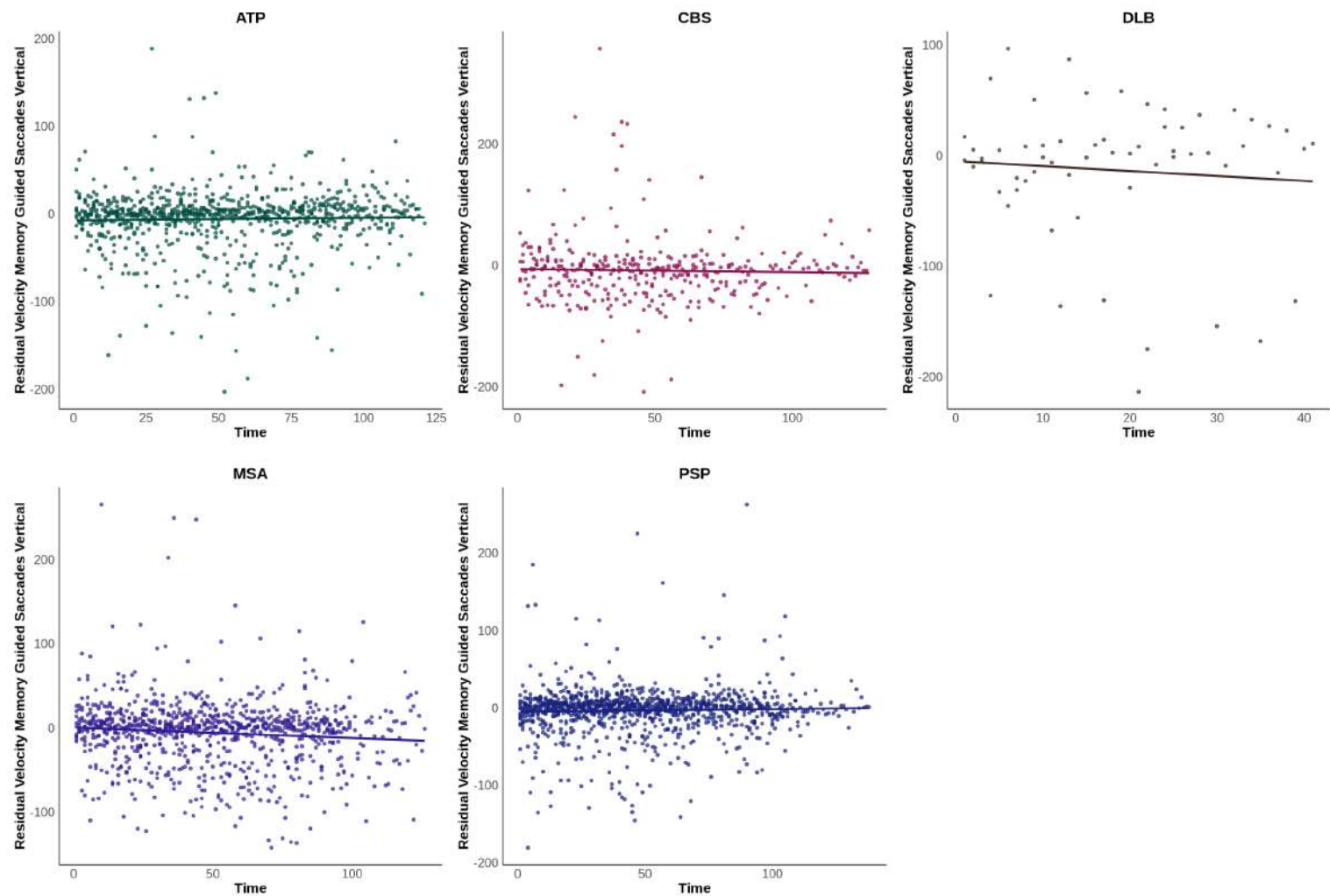


Figure 122: Timescale Analysis of Memory Guided Saccades in Atypical Parkinsonian Syndromes. Residual velocity calculated through the main sequence effect.

Spider Diagram for Ocular Motor Metrics

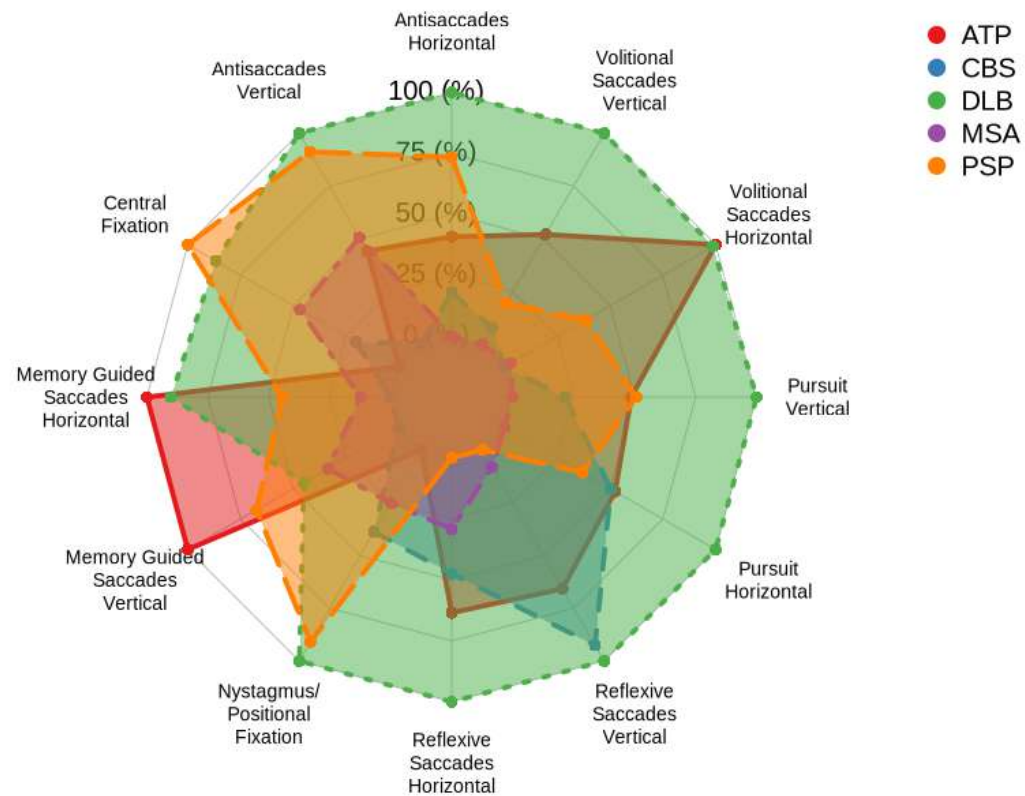


Figure 123: Spider Plot of Ocular Motor Paradigms in Atypical Parkinsonian Syndromes. Composite score calculated using statistical outputs; higher composite scores indicate higher level of significance.

4.5 Discussion

Understanding ocular motor dysfunction in atypical parkinsonian syndromes provides a unique window into the neural mechanisms underlying these complex disorders, offering both potential diagnostic biomarkers and insights into disease progression. Unlike PD, which primarily affects the dopaminergic pathways of the BG, atypical parkinsonian syndromes involve widespread neurodegeneration across cortical, subcortical, and brainstem structures. This results in distinct patterns of eye movement impairment. In this study, fixation stability, smooth pursuit, and multiple saccadic paradigms—including antisaccades, reflexive, oblique, volitional, and memory-guided saccades—were systematically evaluated in individuals with PSP, CBS, MSA, DLB, and atypical parkinsonian cases. The results revealed divergent ocular motor profiles across these syndromes, reflecting disease-specific impairments in key neural circuits such as the SC, FEF, SEF, cerebellum, and output pathways of the BG. These findings contribute to the growing body of literature on eye movement dysfunction in atypical parkinsonian syndromes and emphasize the clinical utility of ocular motor testing. Given its non-invasive nature and sensitivity to functional changes in neurodegenerative disease, eye-tracking may serve as an objective tool for differential diagnosis, disease monitoring, and future biomarker development.

Fixation stability is a fundamental ocular motor function that relies on coordinated activity across cortical, subcortical, and brainstem structures, including the SC, cerebellum, BG, and frontal-parietal eye fields (Robert H. Wurtz 2008). The impairments observed across PSP, CBS, MSA, DLB, and ATP suggest distinct underlying pathophysiologies affecting different neural circuits involved in fixation control.

While PSP, CBS, and MSA exhibited specific impairments in fixation stability and intrusive saccades, DLB and ATP were marked by increased fixation variability, reflecting broader cortical-subcortical dysfunction. PSP demonstrated severe fixation instability, characterized by a significant increase in large SWJs, intrusive saccades, and total saccade count. Notably, small SWJs and microsaccades remained unaffected, suggesting dysfunction in large gaze-holding mechanisms rather than micro-fixational control. This aligns with PSP's known pathology involving degeneration of the midbrain and SC, regions critical for saccade suppression and fixation control (Righini et al. 2004; Hanes and Robert H. Wurtz 2001).

The increased frequency of large intrusive saccades in PSP likely reflects impaired inhibitory control from the BG and SC hyperactivity (N. M. Warren et al. 2007; Shaikh, Factor and Juncos 2017). Normally, the

SNpr exerts tonic inhibition on the SC to regulate reflexive saccade generation (Kojima, Koketsu and May 2023). In PSP, tau-related neurodegeneration in the SNpr leads to SC disinhibition, resulting in increased spontaneous saccades. This may also account for the premature saccade initiation and gaze-holding deficits observed in PSP (Shaikh and David S. Zee 2018). Interestingly, pupil size and fixation precision remained preserved in PSP, contrasting with DLB and CBS, where increased fixation variability was observed. This suggests that PSP-related ocular motor dysfunctions are primarily driven by SC and brainstem circuitry, rather than the broader cortical degeneration seen in DLB and CBS.

In the positional fixation task, PSP exhibited an increased frequency of large SWJs and intrusive saccades across all gaze positions (up, down, left, right), confirming that fixation instability in PSP is not directionally selective. This supports previous findings indicating that midbrain atrophy disrupts both vertical and horizontal saccadic control (J. Lemos et al. 2017; Gorges, Pinkhardt and Kassubek 2014). The presence of intrusive saccades also suggests impaired regulation from the cerebellar fastigial nucleus, contributing further to fixation instability (M. Yu and S.-M. Wang 2020).

CBS showed a distinct fixation profile, with increased microsaccades and small SWJs, along with elevated fixation variability measured by RMS and SD. This pattern is consistent with impaired cortical modulation of fixation stability due to frontal and parietal degeneration (J. Y. Lee et al. 2009). The FEF and DLPFC are crucial for suppressing inappropriate saccades and maintaining steady gaze (Cameron, Riddle and D'Esposito 2015). In CBS, degeneration in these areas likely weakens top-down control, resulting in excessive microsaccade generation. Interestingly, CBS did not exhibit significant deficits in positional fixation, suggesting that fixation instability is more evident during central fixation. This may reflect a breakdown in sustained gaze maintenance, rather than SC-mediated reflexive control as seen in PSP and MSA. The absence of positional fixation impairments thus helps distinguish CBS from PSP.

MSA presented a markedly different fixation profile. Central fixation was preserved, indicating intact baseline gaze stability. However, significant increases in large intrusive saccades were observed in positional fixation tasks across all gaze directions. This pattern suggests that cerebellar degeneration in MSA—particularly affecting the ocular motor vermis and FN—impairs the ability to maintain eccentric gaze positions (Lal and Truong 2019; Manto et al. 2012). The cerebellum plays a critical role in stabilizing gaze during po-

sitional fixation, and its dysfunction in MSA aligns with clinical cerebellar ataxia and associated ocular motor instability (S. Ren et al. 2019). In contrast to PSP and CBS, which affect central fixation, MSA's fixation impairments appear to arise from cerebellar dysfunction during more challenging gaze-holding conditions.

DLB demonstrated marked fixation instability across both central and positional tasks, primarily reflected by increased variability (RMS and SD), rather than increased saccadic intrusions. This suggests that DLB individuals struggle to maintain steady gaze, potentially due to widespread cortical involvement rather than discrete motor dysfunction. The PPC and visual association areas—commonly affected in DLB by α -synuclein pathology—play essential roles in visuospatial integration and gaze stability (Taylor et al. 2012; J. F. Stein 2023). Degeneration in these areas, along with widespread cholinergic dysfunction, likely contributes to impaired cortical modulation of the SC and brainstem circuits (Okkels et al. 2024; Segovia, Górriz et al. 2019). Notably, fixation precision was impaired across all gaze directions, highlighting diffuse cortical-subcortical dysfunction.

ATP participants did not show central fixation impairments. However, in positional fixation, ATP individuals exhibited significantly increased variability (RMS and SD) across multiple trials. This suggests that fixation instability in ATP may be more subtle and emerge primarily under higher task demands. The pattern of variability suggests that cognitive factors, such as attentional control or executive function, may contribute more strongly to fixation instability in ATP than motor dysfunction alone.

Smooth pursuit eye movements require precise coordination of cortical, subcortical, and cerebellar networks to enable continuous tracking of a moving target. The FEF, MT and MST cortices, BG, SC, brainstem burst neurons, and cerebellum all contribute to pursuit generation and stabilization (Ono). Disruptions within these circuits can lead to impaired gaze tracking, as seen in atypical parkinsonian syndromes such as PSP, CBS, MSA, DLB, and atypical parkinsonism.

Unlike idiopathic PD, where pursuit deficits are typically mild and uniform, atypical parkinsonian syndromes exhibit distinct impairments in pursuit accuracy, velocity gain, and compensatory saccades—each reflecting syndrome-specific neural dysfunction. PSP demonstrated the most severe pursuit impairments across all directions, including elevated RMSE gaze error and reduced velocity gain, particularly during vertical pursuit.

This is consistent with PSP's hallmark midbrain degeneration (Buch et al. 2022). The SC and riMLF play essential roles in stabilizing gaze and generating vertical movements (Kato, Arai and T. Hattori 2003). Neurodegeneration in these regions leads to disinhibition of the SC, resulting in excessive intrusive saccades and poor fixation stability, as confirmed by the abundance of large corrective saccades, greater than 5° , observed in amplitude distribution analyses. The riMLF's role in vertical pursuit explains the disproportionately greater deficits observed in PSP for vertical tracking, distinguishing it from PD, where vertical pursuit is generally preserved (J. Lemos et al. 2017).

CBS also exhibited severe pursuit impairments, albeit with greater variability across individuals compared to PSP. While PSP-related deficits stem from midbrain pathology, CBS-related pursuit dysfunction likely arises from cortical degeneration in the frontal and parietal lobes, affecting top-down control of smooth tracking (Constantinides et al. 2019). The PPC and FEF are responsible for integrating visual motion cues and suppressing erroneous corrective saccades (Baltaretu et al. 2020). In CBS, damage to these areas results in erratic gaze shifts, frequent microsaccades, and variability in saccadic amplitude. Some CBS individuals generated excessive small corrective saccades ($<2^\circ$), while others exhibited large gaze shifts ($>5^\circ$), highlighting the asymmetric and heterogeneous nature of CBS-related cortical dysfunction (Jennifer L. Whitwell, Graff-Radford et al. 2017).

In contrast, MSA showed more selective impairments, with deficits predominantly in circular pursuit at 0.4 Hz and relatively preserved horizontal and vertical tracking. This pattern corresponds with known cerebellar involvement in MSA, where degeneration disrupts the cerebellum's role in pursuit gain modulation and trajectory smoothing (Ortiz et al. 2020). The oculomotor vermis and fastigial nucleus fine-tune pursuit velocity to accommodate target motion changes (Helmchen, Machner et al. 2022). In MSA, cerebellar atrophy weakens these mechanisms, resulting in increased pursuit error and a reliance on small-amplitude corrective saccades. Unlike PSP and CBS, where large saccades are common, MSA pursuit errors are subtler and more uniformly distributed, supporting the view of a cerebellar-mediated ocular motor instability. Notably, the greater deficits in circular pursuit over linear directions suggest that cerebellar dysfunction in MSA primarily affects complex, velocity-dependent adjustments.

DLB individuals showed pursuit impairments primarily at 0.4 Hz in horizontal and vertical directions, while

circular pursuit remained relatively intact. Unlike the other subtypes, DLB did not exhibit frequent large corrective saccades. Instead, deficits were characterized by poor gaze stability and high RMSE error, pointing toward impaired visuospatial processing rather than primary motor dysfunction. The PPC and lateral occipital cortex, often affected in DLB due to α -synuclein pathology, play a central role in visuospatial attention and pursuit tracking (T. Yousaf et al. 2019; Hinkley et al. 2009). Furthermore, cholinergic deficits in DLB impair sustained visual attention, further contributing to unstable pursuit (Sarter, Givens and Bruno 2001). The absence of large compensatory saccades, despite significant tracking error, suggests that pursuit impairments in DLB stem more from cognitive-perceptual dysfunction than from failures in ocular motor execution.

ATP exhibited high inter-individual variability in pursuit performance. Some participants demonstrated significant tracking deficits with frequent large corrective saccades, while others displayed relatively preserved pursuit. This variability indicates that ATP encompasses a spectrum of underlying pathologies resembling PSP-, CBS-, or MSA-like presentations. The broad distribution of saccade amplitudes and RMSE errors in ATP underscores its heterogeneous nature and the need for refined subtyping within this clinical category. Overall, smooth pursuit abnormalities in atypical parkinsonian syndromes reflect the distributed, syndrome-specific nature of neural degeneration—ranging from midbrain dysfunction in PSP to cortical breakdown in CBS and cerebellar degradation in MSA. These distinct pursuit signatures provide a valuable foundation for future diagnostic stratification using ocular motor biomarkers.

The findings from the antisaccades paradigms found deficits across all conditions, each reflecting syndrome-specific ocular motor profiles. PSP exhibited the most pronounced vertical antisaccade impairment, consistent with its characteristic vertical supranuclear gaze palsy due to early degeneration of midbrain structures, including the riMLF and interstitial nucleus of Cajal (S. Rivaud-Péchoix et al. 2007; A. L. Chen et al. 2010). PSP individuals showed hypometric or slowed vertical antisaccades and frequent reflexive errors, with horizontal antisaccades being comparatively less impaired, suggesting a directional asymmetry. In contrast, MSA displayed relatively symmetric antisaccade performance, with preserved vertical eye movements and only mildly prolonged latencies. This aligns with the absence of supranuclear gaze palsy in MSA, where ocular motor control is typically spared due to limited involvement of vertical gaze centers and largely intact FEF (Brooks et al. 2017). CBS showed impaired initiation and accuracy in both directions, with prolonged antisaccade latencies linked to dysfunction within the fronto-parietal network, including the DLPFC and

posterior parietal cortex, which support voluntary saccade generation (Parmera et al. 2016; Heidi C Riek et al. 2023). However, vertical range was preserved, distinguishing CBS from PSP. DLB was characterized by bilateral antisaccade impairment without a vertical–horizontal discrepancy. Latencies were prolonged and error rates high, likely due to executive dysfunction from cortical Lewy body pathology affecting the prefrontal cortex, alongside generalized saccadic slowing from parkinsonian bradykinesia (Mosimann et al. 2005; Garcia-Esparcia et al. 2017). Importantly, DLB individuals retained full vertical range, contrasting with PSP. These syndrome-specific patterns can enhance early differentiation of atypical parkinsonian syndromes. Markedly impaired vertical antisaccades with preserved horizontals are a key indicator for PSP. In contrast, symmetric slowing with preserved vertical saccades points to MSA or DLB. High antisaccade error rates in both PSP and DLB reflect frontal executive dysfunction, but only PSP shows associated vertical gaze palsy (D. R. Williams, De Silva et al. 2005; Mosimann et al. 2005). If CBS present with severe vertical antisaccade deficits, underlying PSP pathology could be considered.

Oblique saccades involve the coordinated activation of both horizontal and vertical eye movement systems, requiring precise integration of signals from the SC, cerebellum, brainstem burst neurons, and cortical ocular motor control regions (Mayu Takahashi et al. 2022). Disruption of these pathways can lead to misdirected, delayed, or inaccurate oblique saccades, as observed across atypical parkinsonian syndromes. The findings from this study highlight distinct syndrome-specific impairments in oblique saccade generation, further differentiating PSP, CBS, MSA, DLB, and ATP.

PSP exhibited pronounced deficits in oblique saccade accuracy, amplitude, and latency, with impairments worsening at higher eccentricities (4°, 8°, and 10°). These deficits reflect PSP’s characteristic midbrain pathology, which disrupts the integration of vertical and horizontal saccadic components (J. Lemos et al. 2017). Interestingly, PSP individuals often demonstrated hypermetric oblique saccades, in contrast to the hypometric horizontal and vertical saccades typically observed in PD. This directional shift in error patterns aligns with the characteristic “round-the-houses” and “zig-zag” trajectories in PSP, where saccades deviate from the direct path and exhibit looping or stair-step patterns (Termsarasab et al. 2015; Fearon et al. 2020). These hypermetric errors suggest instability in the SC-mediated vector summation process, which normally balances horizontal and vertical saccade components to produce accurate oblique movements (D. Li et al. 2024). In addition, dysfunction in the fastigial oculomotor region of the cerebellum impairs mid-course

trajectory corrections, resulting in increased positional variability in both X and Y axes (Guerrasio et al. 2010).

In contrast, CBS did not show significant impairments in oblique saccades at any eccentricity, suggesting relatively intact brainstem and SC-mediated circuits. This contrasts with the cortical-driven deficits in voluntary saccades and smooth pursuit observed in CBS. The preserved oblique saccade performance further supports the notion that CBS is primarily a cortical syndrome affecting motor planning rather than subcortical or brainstem execution pathways, offering an important diagnostic distinction from PSP.

MSA displayed moderate impairments in oblique saccades, specifically reduced saccade amplitude at 8° and 10°, with relatively normal performance at 4°. This amplitude-dependent decline suggests that cerebellar degeneration in MSA disrupts gain modulation during larger saccades, consistent with cerebellar ocular motor ataxia. Unlike PSP, where saccades are typically hypermetric, MSA showed progressive hypometria, in line with dysfunction of the oculomotor vermis and fastigial nucleus, which fine-tune saccadic amplitude and precision (Helmchen, Pohlmann et al. 2012). The relative preservation of smaller oblique saccades in MSA implies that early cerebellar dysfunction selectively affects higher amplitude saccades that demand more precise calibration.

DLB exhibited substantial impairments in oblique saccade timing, accuracy, and velocity, particularly at higher eccentricities. Individuals showed prolonged latencies and extended saccade durations, with increased horizontal error margins and positional variability. Unlike PSP, where errors were hypermetric and stereotyped, DLB's impairments appeared more variable and spatially diffuse. These findings suggest disruptions in visuospatial processing, rather than motor execution per se. The PPC and lateral occipital cortex—regions heavily impacted by α -synuclein pathology in DLB—are critical for spatial localization and saccade planning (Taylor et al. 2012; Cheviet, Pisella and Pélisson 2021). Delayed saccade initiation and prolonged execution in DLB align with clinical features such as bradyphrenia and attentional disengagement, indicating a cognitive rather than purely motor origin for oblique saccade deficits (Rafal et al. 1984).

ATP individuals demonstrated widespread and heterogeneous impairments across all eccentricities. These included reduced saccade amplitude, decreased peak velocity, and impaired accuracy, with error patterns shifting between hypometria and hypermetria. This variability suggests that ATP encompasses mixed patho-

logies, including PSP-like midbrain dysfunction, MSA-like cerebellar deficits, and DLB-like visuospatial impairments. Increased positional variability, particularly in the Y-direction, further indicates vertical saccade instability, potentially reflecting early midbrain or brainstem involvement. However, unlike classic PSP, vertical saccadic slowing was less severe or consistent.

Compared to idiopathic PD, where oblique saccades are typically preserved and hypometria is mild and uniform due to basal ganglia dysfunction, atypical parkinsonian syndromes demonstrate pronounced, direction-specific impairments. These findings reflect broader and more complex neurodegenerative processes. PSP is characterized by hypermetric, unstable oblique saccades driven by midbrain atrophy and SC disinhibition. MSA demonstrates progressive hypometria at larger amplitudes due to cerebellar gain adaptation failure. DLB presents with prolonged latency and high spatial variability linked to visuospatial network degeneration. ATP, with its diverse impairments, further underscores the need for refined diagnostic stratification using detailed ocular motor profiling.

PSP exhibited severe reflexive saccade impairments in both horizontal and vertical directions, marked by significantly reduced saccade amplitude, velocity, and accuracy, alongside prolonged latencies. Notably, vertical reflexive saccades were more severely affected than horizontal ones—a hallmark of PSP—reflecting midbrain degeneration involving the riMLF and SC (Sequeira, Rizzo and Rucker 2017; Vinny and Lal 2016). The high proportion of hypometric saccades suggests insufficient saccadic drive, likely due to disrupted burst neuron activity within the PPRF and mesencephalic reticular formation (Walton and Freedman 2014). This is consistent with the characteristic “staircase” saccade pattern and vertical gaze palsy observed in PSP, wherein individuals require multiple small corrective saccades to reach the intended target (R. Schneider et al. 2011). Additionally, impaired SC suppression mechanisms may underlie erratic saccadic behavior and reduced spatial precision (Pin et al. 2023). These features clearly differentiate PSP from other atypical parkinsonian syndromes such as CBS and MSA, where reflexive saccade deficits are either milder or follow different trajectories of dysfunction.

CBS demonstrated selective impairments in vertical reflexive saccades, with reduced correct response rates and increased hypometria. Unlike PSP, which showed profound impairments across both axes, CBS impairments were more localized to vertical saccades, reflecting asymmetric cortical degeneration rather than

brainstem dysfunction (Aiba et al. 2023). Degeneration in the PPC and SEF likely impairs visuomotor coordination and spatial mapping, contributing to increased undershooting and reduced spatial accuracy (W. Ma et al. 2022). Importantly, the absence of significant horizontal impairments further distinguishes CBS from PSP and MSA, where reflexive saccades are broadly impaired.

MSA exhibited moderate but widespread reflexive saccade abnormalities, with decreased amplitude, velocity, and accuracy across both horizontal and vertical directions. Unlike PSP, where vertical impairments dominate, MSA showed a more balanced impairment profile, consistent with diffuse cerebellar and brainstem pathology. Dysfunction in the fastigial nucleus and oculomotor vermis of the cerebellum likely contributes to hypometric saccades, increased latency, and prolonged end times (Kojima, Soetedjo and Albert F. Fuchs 2010). These prolonged saccadic responses mirror the bradykinetic features of MSA, particularly in the MSA-C subtype (David S. Zee et al. 1976). The increased rate of hypometric saccades supports impaired gain adaptation, a common marker of cerebellar ataxia and brainstem dysfunction (Jensen, Sinem Balta Beylergil and Shaikh 2019). The profile of reflexive saccade impairments in MSA is thus distinct from PSP, with more modest velocity reductions and less directional asymmetry.

DLB showed global reflexive saccade dysfunction, including prolonged latencies, reduced velocities, and poor spatial accuracy in both directions. This uniform impairment pattern differs from PSP's vertical predominance or CBS's parietal asymmetry, indicating a more cortical-subcortical origin. The PPC and BG, which are affected by α -synuclein pathology in DLB, are essential for reflexive saccade planning and execution (Nimmo et al. 2020; Hikosaka, Takikawa and Kawagoe 2000). The extended saccadic latencies likely reflect cognitive slowing and attentional disengagement, rather than pure motor impairment (Bradshaw et al. 2006). DLB individuals also exhibited significant reductions in saccade accuracy, which aligns with previous findings linking saccadic instability to visuospatial processing deficits and posterior cortical atrophy (Shakespeare et al. 2015). The absence of a high hypometric error rate (as seen in PSP and MSA) further suggests that DLB's reflexive saccade impairments stem primarily from cortical visuospatial dysfunction.

ATP individuals exhibited a heterogeneous profile, encompassing impairments in amplitude, velocity, latency, and accuracy. The presence of increased hypometric errors and prolonged latencies suggests combined dysfunction across multiple neural systems, including brainstem burst neurons, cerebellar gain circuits, and

cortical visuomotor networks. Unlike PSP, where vertical deficits predominate, or MSA, where hypometria is cerebellar-driven, ATP individuals showed balanced impairments across directions. This likely reflects the syndromic heterogeneity of ATP, which may include undiagnosed or evolving forms of PSP, MSA, or DLB. Future stratification of ATP subtypes based on ocular motor characteristics may aid in better classification and early diagnosis of these individuals.

PSP exhibited severe impairments in volitional saccade execution, characterized by reduced saccade amplitude, slower velocities, and an increased number of saccadic steps (i.e., multiple corrective saccades required to reach the target). Notably, PSP individuals made significantly fewer correct volitional saccades, particularly in the vertical direction, highlighting midbrain-driven deficits in voluntary gaze control. The SC, FEF, and SEF are all significantly affected in PSP, resulting in poor inhibitory control, excessive saccadic fragmentation, and increased hypometric errors (Lal and Truong 2019; Jensen, Sinem Balta Beylergil and Shaikh 2019; Shaikh and David S. Zee 2018). The increased number of saccadic steps aligns with the “staircase” saccade patterns commonly observed in PSP, where individuals struggle to produce single large gaze shifts and instead rely on a series of small-amplitude corrections (B. Chen et al. 2023; R. M. Schneider et al. 2013). These features clearly distinguish PSP from CBS and MSA, where volitional saccades are either relatively preserved or exhibit distinct error profiles.

In contrast to PSP, CBS showed no significant differences from healthy controls in volitional saccade metrics, suggesting that voluntary saccade control remains relatively preserved. This is somewhat unexpected given CBS-associated degeneration in cortical ocular motor regions such as the FEF, PPC, and DLPFC, all of which contribute to top-down control of volitional saccades (Burrell et al. 2014; McDowell, Dyckman et al. 2008). One possible explanation is that CBS-related deficits manifest more prominently in antisaccade and reflexive saccade tasks, where sensory-motor integration and inhibitory control play larger roles. The relative preservation of volitional saccades helps differentiate CBS from PSP and DLB, where impairments are more global.

MSA demonstrated moderate volitional saccade deficits, particularly an increased proportion of hypermetric (overshooting) saccades. Unlike the hypometric saccades seen in PSP due to midbrain dysfunction, MSA’s hypermetric errors likely result from cerebellar degeneration—specifically impaired saccadic gain regulation

in the fastigial nucleus and oculomotor vermis (Inomata-Terada et al. 2023; Kojima, Soetedjo and Albert F. Fuchs 2010). The cerebellum is crucial for fine-tuning saccade amplitude, and its dysfunction in MSA may lead to excessive gaze shifts and overshooting of targets (Manto et al. 2012). Despite this, other volitional saccade parameters such as latency and velocity were relatively preserved, suggesting milder ocular motor dysfunction compared to PSP and DLB.

DLB exhibited widespread volitional saccade impairments, including reduced amplitude, slower velocities, increased endpoint variability, and fewer executed saccades across both horizontal and vertical axes. Unlike PSP, where the impairments are motoric in origin, DLB-related deficits are likely due to higher-order dysfunction in visuospatial processing and executive control, consistent with posterior cortical atrophy and α -synuclein pathology affecting the PPC and precuneus (Jennifer L. Whitwell, Graff-Radford et al. 2017). The increased endpoint variability suggests that DLB individuals struggle with spatial localization and target acquisition. Furthermore, the reduction in saccade frequency reflects cognitive slowing and attentional disengagement, differentiating DLB from PSP and MSA, where impairments are driven more by motor execution pathways.

ATP individuals exhibited a combination of volitional saccade impairments observed in PSP, MSA, and DLB, including reduced saccade amplitude, slower velocities, increased endpoint variability, and fewer correct responses. The mixed presentation—ranging from PSP-like hypometria to MSA-like hypermetria—suggests that ATP encompasses a heterogeneous set of ocular motor pathologies. This supports the hypothesis that ATP includes underlying cases of unclassified PSP, MSA, or DLB phenotypes. The diffuse deficits across amplitude, velocity, and accuracy highlight dysfunction across multiple neural systems, including midbrain ocular motor circuits, cerebellar gain control pathways, and frontoparietal networks involved in motor planning.

In contrast to idiopathic PD, where volitional saccade deficits are typically mild and limited to increased latency and slight hypometria due to basal ganglia dysfunction, APS subtypes display more severe and varied impairments. PSP is marked by fragmented, hypometric, staircase-like saccades; MSA by cerebellar-driven hypermetria; DLB by cognitive-executive dysfunction and endpoint inaccuracy; and ATP by a heterogeneous combination of features. These findings underscore the diagnostic utility of volitional saccade testing for differentiating between APS subtypes and PD, and for identifying syndrome-specific neural circuit impairments.

PSP exhibited severe deficits in memory-guided saccade performance, characterised by increased saccadic steps, reduced accuracy, hypometric errors, and a lower number of correct responses in both horizontal and vertical directions. The substantially reduced saccade amplitude and velocity suggest impaired voluntary saccade initiation and execution, driven by dysfunction in the SC, FEF, and BG. The SC plays a key role in maintaining the spatial representation of saccadic targets, while the FEF and SEF are responsible for motor planning and inhibition—all of which are significantly affected by tau pathology in PSP (A. B. Wolf et al. 2015; Kovacs 2015). The increased hypometric saccades and stepwise corrections align with the characteristic “staircase” saccade behaviour seen in PSP, reflecting a failure to generate large, single-step saccades to remembered locations (Rucker 2014). These deficits are more pronounced in vertical saccades, further differentiating PSP from CBS and MSA, where MGS impairments follow different patterns.

CBS exhibited selective impairments in memory-guided saccades, with increased hypometric errors, reduced saccadic amplitude, and delayed execution times. Unlike PSP, where both horizontal and vertical saccades were severely impaired, CBS individuals demonstrated delayed saccade execution and reduced amplitude, particularly in the horizontal direction. These findings suggest a breakdown in motor planning and working memory storage, likely driven by parietal and premotor cortical degeneration, including the PPC and supplementary motor area (Boxer et al. 2006). The PPC is critical for maintaining spatial representations and guiding eye movements, and its degeneration in CBS may lead to deficits in retaining target location over the memory delay period (Merriam, Genovese and Colby 2003). Additionally, the delayed saccade start and end times point to dysfunction in motor preparation and execution, further linking CBS-related impairments to disrupted frontoparietal networks (Alkan et al. 2011).

MSA exhibited moderate deficits in memory-guided saccade performance, primarily affecting saccadic accuracy and amplitude. Unlike PSP, where vertical impairments dominate, or CBS, where execution delays are prominent, MSA individuals demonstrated more subtle reductions in saccade amplitude and accuracy, suggesting a cerebellar contribution. The fastigial nucleus and oculomotor vermis in the cerebellum are involved in saccadic gain adaptation, and their dysfunction in MSA likely contributes to impaired saccade precision (Cassanello, Ohl and Rolfs 2016). The absence of substantial latency increases or excessive hypometria in MSA differentiates it from PSP, where midbrain and frontal dysfunction lead to severe gaze instability, and CBS, where motor planning delays are more evident.

DLB exhibited widespread impairments in memory-guided saccades, including reduced saccade generation, lower amplitude, increased endpoint variability, and slower velocities. Unlike PSP and CBS, where impairments are primarily motor-driven, DLB individuals displayed a global reduction in MGS execution, likely reflecting cognitive dysfunction. The PPC, precuneus, and BG, which are affected by α -synuclein pathology in DLB, play essential roles in spatial attention, working memory, and saccadic control (Schulz-Schaeffer 2010; Y. Zhang et al. 2018; Hikosaka, Takikawa and Kawagoe 2000). The reduction in total saccades executed aligns with bradyphrenia (cognitive slowing) and attentional disengagement, key features of DLB (Schumacher et al. 2019). Additionally, the greater endpoint variability in DLB compared to PSP and MSA suggests a breakdown in target localisation and visuospatial processing, rather than purely motor deficits. The significant slowing of saccade velocity further supports cognitive impairment as a driving factor, distinguishing DLB from CBS, where MGS execution delays are more related to parietal degeneration.

ATP exhibited a combination of impairments found across PSP, MSA, and DLB, including increased saccadic steps, reduced amplitude, slower velocities, and greater endpoint variability. Like DLB, ATP individuals executed fewer memory-guided saccades overall, suggesting an underlying cognitive deficit affecting motor planning and working memory storage. However, ATP also exhibited increased hypometric errors and stepwise corrections, similar to PSP, indicating potential overlap in midbrain pathology affecting the SC and FEF. The significant prolongation of saccade execution times in ATP further suggests disruptions in both cortical motor planning circuits (PPC, SMA) and brainstem execution centres (SC, cerebellum). These findings indicate that ATP represents a heterogeneous group with variable impairments in saccade control, dependent on the underlying neurodegenerative pathology.

The presence of hypometric saccades, although commonly observed across parkinsonian disorders, is not a sensitive diagnostic marker due to their prevalence in both typical and atypical forms of parkinsonism. In contrast, hypermetric saccades, characterized by consistent overshooting, appear to be more diagnostically informative. Hypermetric errors observed in conditions such as MSA and PSP—particularly prominent in oblique saccade tasks in PSP and volitional saccades in MSA—likely reflect distinct cerebellar or midbrain pathologies. Consequently, hypermetric saccades may represent a more useful clinical marker for differentiating atypical parkinsonian syndromes from idiopathic PD, which typically shows uniform hypometric

saccadic errors.[±]

Consistent with known clinical features, PSP individuals demonstrated markedly greater impairment in vertical antisaccades compared to horizontal antisaccades. This vertical predominance aligns closely with PSP's hallmark midbrain pathology, specifically affecting vertical gaze centers such as the riMLF and interstitial nucleus of Cajal. Thus, pronounced vertical antisaccade impairment—particularly increased latency, hypometria, and higher error rates—strongly supports a PSP diagnosis, differentiating it from other atypical syndromes such as CBS or MSA, which exhibit more symmetric or horizontally dominated profiles. Interestingly, CBS presented distinct antisaccade profiles across horizontal and vertical directions. CBS individuals exhibited significant impairments predominantly in vertical antisaccade tasks, characterized by prolonged latencies and increased errors, while horizontal antisaccades remained relatively intact. This directional asymmetry likely results from asymmetric cortical degeneration involving frontoparietal networks, such as the PPC and DLPFC, which differentially affect vertical versus horizontal saccadic generation. Thus, evaluating antisaccades separately in horizontal and vertical directions provides a valuable diagnostic distinction between CBS and other atypical parkinsonian syndromes. A striking distinction in MSA's ocular motor profile emerged in fixation tasks, where central fixation stability was largely preserved, but significant impairment appeared specifically during positional (eccentric) fixation. This pattern aligns closely with MSA's known cerebellar degeneration, particularly within the oculomotor vermis and fastigial nucleus, critical for maintaining eccentric gaze positions. Thus, examining positional fixation stability may serve as a sensitive measure for identifying early cerebellar ocular motor dysfunction in MSA, distinguishing it from syndromes like PSP and CBS, where central fixation stability itself is notably impaired. In smooth pursuit assessments, MSA demonstrated notably greater impairments in elliptical (circular) pursuit at higher frequencies (0.4 Hz) compared to linear (horizontal or vertical) directions. This selective deficit likely arises from the cerebellum's critical role in dynamically adjusting pursuit gain during complex trajectories and higher velocity demands. Cerebellar degeneration in MSA disrupts these velocity-dependent adjustments, resulting in pronounced elliptical pursuit impairments. Thus, pursuit paradigms involving complex trajectories and higher speeds might serve as particularly sensitive markers for cerebellar ocular motor dysfunction in MSA. Interestingly, DLB individuals exhibited disproportionately greater ocular motor deficits at lower eccentricities across multiple tasks, including oblique and reflexive saccades. This pattern likely results from impaired visuospatial attention and cortical integration involving the PPC and lateral occipital regions, which are more severely disrupted at central or near-central visual fields where precise attentional allocation

and spatial discrimination are required. Consequently, DLB's pronounced deficits at smaller eccentricities suggest a fundamental dysfunction in visuospatial processing rather than primary motor deficits, further differentiating DLB from other atypical parkinsonian syndromes with more peripheral ocular motor impairments.

Compared to idiopathic PD, atypical parkinsonian syndromes exhibited markedly more severe and heterogeneous ocular motor impairments across all paradigms assessed. Idiopathic PD typically presents mild, uniform ocular motor deficits such as slight saccadic hypometria, mildly increased latencies, and subtle pursuit impairment. In contrast, atypical syndromes such as PSP, CBS, MSA, and DLB showed pronounced, directionally-specific, or amplitude-dependent impairments linked clearly to discrete neural degeneration involving midbrain, cerebellar, or cortical-subcortical networks. This stark contrast underscores the diagnostic utility of comprehensive ocular motor testing in distinguishing idiopathic PD from atypical parkinsonian syndromes.

4.5.1 Clinical Implications

The findings from this study highlight the potential of ocular motor testing as a valuable clinical tool for distinguishing atypical parkinsonian syndromes from idiopathic PD and from each other. Each atypical parkinsonian subtype exhibited distinct patterns of saccadic and pursuit impairments, which may serve as diagnostic biomarkers. For instance, PSP was characterised by vertical saccadic deficits, increased stepwise corrections, and round-the-houses eye movements, aligning with midbrain degeneration affecting the SC and FEF. In contrast, CBS displayed pronounced execution delays and spatial inaccuracies in voluntary saccades, suggesting parietal and premotor cortical involvement. MSA presented with subtle impairments in pursuit and reflexive saccades, likely reflecting cerebellar dysfunction, while DLB exhibited widespread reductions in saccade execution, increased endpoint variability, and slower velocities, consistent with cognitive and visuospatial deficits due to Lewy body pathology.

From a clinical differentiation standpoint, these results reinforce the importance of integrating eye movement assessments into diagnostic protocols for atypical parkinsonian syndromes. Current diagnostic criteria for atypical parkinsonian syndromes are largely based on clinical motor symptoms, imaging, and cognitive assessments, yet many of these syndromes have overlapping features, particularly in early disease stages.

The distinct ocular motor profiles seen here suggest that a structured ocular motor battery could provide additional objective markers to aid in differential diagnosis, reducing misclassification rates. Additionally, eye movement biomarkers may be useful in tracking disease progression and evaluating treatment response, particularly in clinical trials for atypical parkinsonian syndromes, where early and reliable outcome measures are needed.

4.5.2 Limitations

Despite the robust statistical and methodological approach used in this study, several limitations should be acknowledged. Sample size variability across atypical parkinsonian subtypes posed a challenge, particularly for CBS and DLB cohorts, which had the smallest participant numbers. While bootstrapping and adjusted statistical methods were employed to mitigate the impact of small sample sizes, larger cohorts are necessary to confirm these findings and ensure broader generalisability.

Another limitation lies in the potential influence of cognitive impairment on ocular motor performance. Atypical Parkinsonian syndromes, particularly DLB and CBS, are associated with executive dysfunction and visuospatial deficits, which could have contributed to the observed impairments in voluntary saccades and memory-guided tasks. However, differentiating primary motor-related deficits from cognitive influences remains challenging, and future studies should incorporate neuropsychological assessments alongside ocular motor testing to clarify these relationships.

Technical challenges were also present. Individuals with severe gaze dysfunction, particularly in PSP and ATP, often had difficulty maintaining stable fixation, which could impact calibration and data accuracy. Additionally, variability in disease duration and medication status across groups could have influenced results, particularly since dopaminergic treatments and disease severity may differentially affect saccadic performance. Further research is required to determine the extent to which ocular motor deficits change over time and whether they can serve as longitudinal biomarkers of disease progression.

4.5.3 Future Directions

This study provides a strong foundation for further research into ocular motor biomarkers in atypical Parkinsonian syndromes, yet several key areas warrant additional investigation. Longitudinal studies are needed to track the progression of ocular motor deficits over time, helping determine their clinical utility in monitoring disease trajectory and treatment effects. Given the variability in findings between atypical Parkinsonian subtypes, future research should also explore whether ocular motor impairments emerge before overt motor symptoms, potentially serving as an early diagnostic marker for prodromal atypical Parkinsonian syndromes.

Another avenue for exploration is multimodal integration with imaging and neurophysiological data. Functional MRI and diffusion tensor imaging studies could help map the neural correlates of specific ocular motor impairments, providing deeper insight into how different neurodegenerative pathologies impact eye movement control networks. Similarly, combining eye tracking with EEG or magnetoencephalography could shed light on the cortical and subcortical mechanisms driving atypical Parkinsonian syndromes-related ocular motor dysfunctions. Additionally, machine learning and AI approaches could enhance automated classification of atypical Parkinsonian subtypes based on ocular motor metrics. By developing predictive models that integrate eye movement data with clinical and imaging variables, future studies could pave the way for more accurate, non-invasive diagnostic tools for atypical Parkinsonian syndromes.

4.6 Chapter Summary

This study investigated ocular motor dysfunction in atypical parkinsonian syndromes atypical Parkinsonian syndromes, including PSP, CBS, MSA, DLB, and ATP, using a comprehensive battery of eye movement paradigms. Each atypical Parkinsonian subtype demonstrated distinctive impairments in saccadic control, pursuit accuracy, and memory-guided eye movements, highlighting potential ocular motor biomarkers for disease differentiation. Key findings revealed that PSP exhibited profound vertical saccadic impairments, CBS displayed execution delays and hypometric errors, MSA demonstrated cerebellar-linked impairments in pursuit and reflexive saccades, DLB was characterised by widespread slowing and increased endpoint variability, and ATP exhibited mixed deficits across multiple domains. These results underscore the potential clinical value of ocular motor testing in atypical Parkinsonian syndromes, both for diagnostic refinement and

disease tracking. Despite methodological strengths, including detailed statistical modelling and composite score analysis, limitations such as small sample sizes, cognitive influences, and calibration challenges necessitate further investigation. Future research should focus on longitudinal studies, multimodal integration with imaging, and AI-based classification models to enhance diagnostic precision and disease monitoring in atypical Parkinsonian syndromes. This study lays the groundwork for incorporating ocular motor assessments into clinical practice, potentially improving early detection and personalised treatment strategies for atypical Parkinsonian syndromes individuals.

5 Longitudinal Study of Eye Movements in Parkinson's Disease

5.1 Introduction

PD is a progressive neurodegenerative condition characterised by a decline in both motor and non-motor functions. Motor symptoms include bradykinesia, rigidity, tremor, and postural instability, while non-motor symptoms encompass cognitive decline, sleep disturbances, and psychiatric issues. This deterioration is primarily driven by the gradual loss of dopaminergic neurons in the SN, leading to increased disease severity and reduced quality of life (Antonini, Reichmann et al. 2023).

The progression of PD is heterogeneous, influenced by factors such as genetics, lifestyle, environmental exposures, and disease subtypes. Clinical staging tools including the hoehn and yahr (H&Y) scale and the unified parkinson's disease rating scale (UPDRS) are commonly used to monitor the progression of motor symptoms over time (Goetz et al. 2008; Martinez-Martin et al. 2018). Longitudinal studies have shown that as PD advances, there is a progressive worsening of gait, balance, axial motor symptoms, and freezing of gait, particularly in the later stages (Deng et al. 2020; Shalash et al. 2022). Non-motor symptoms such as REM sleep behavior disorder (RBD) have also been identified as early indicators of disease progression, often appearing before the onset of motor symptoms (Z. Xu, K. N. Anderson and Pavese 2022). The Oxford Discovery Cohort and other studies have demonstrated that individuals with comorbid RBD exhibit faster cognitive and motor decline (Y. Liu et al. 2021).

Cross-sectional studies correlating eye movements with disease severity and cognitive decline provide a starting point for assessing longitudinal changes in eye movements. Decreased fixation instability, reflected by more frequent SWJs, has been associated with greater disease severity, particularly the worsening of axial motor symptoms such as postural instability (Przybyszewski et al. 2023). Furthermore, fixation instability has been linked to prodromal features like RBD, with PD individuals with RBD showing greater fixation instability compared to non-RBD PD patients and healthy controls. Smooth pursuit deficits, particularly an increase in saccadic intrusions, are also more pronounced in the advanced stages of the disease (Frei 2021). Progressive saccadic hypometria and increased latency mirror the global motor slowing observed in bradykinesia (White et al. 1983). Additionally, reductions in saccadic amplitude correlate with cognitive impairment (MacAskill, Graham et al. 2012). While average saccadic velocity tends to remain stable, peak

velocity declines with increased disease severity, likely due to impaired co-activation of opposing ocular muscles (Waldthaler, Tsitsi and Svenningsson 2019). Antisaccade tasks have demonstrated increased latency and error rates in individuals with cognitive impairment, reinforcing the link between executive dysfunction, global cognitive decline, and eye movement control (J. Y. Zhang et al. 2021). It is also possible that ocular motor dysfunction precedes cognitive decline in PD, highlighting the potential of eye movement metrics as early indicators of both motor and non-motor disease progression.

Although wearable devices are increasingly used for continuous monitoring of motor symptoms, and cognitive changes have been studied longitudinally, eye movement changes over time in PD remain understudied. In particular, the long-term effects of dopaminergic therapy on ocular motor function are not well understood. Given the utility of eye movements as a non-invasive, quantitative measure, examining longitudinal changes using a comprehensive ocular motor battery may help validate eye tracking as a disease progression biomarker and assess the impact of medication and therapeutic interventions on PD symptoms.

5.2 Project Aims

1. To investigate changes in ocular motor function over a one-year period in individuals with PD.
2. To explore the potential of eye movement metrics as biomarkers for disease progression in PD.

5.3 Methods

5.3.1 Participants

Participants with idiopathic PD whose eye movements were recorded at baseline in the ocular motor study discussed in Chapter 3 were invited for a follow-up one year later. Follow-up recordings were conducted within a one-month window, 12 months after the baseline recording. Participants were excluded if any of the following criteria were met: (1) development of other neurological conditions or movement disorders, (2) emergence of eye movement abnormalities such as diplopia, (3) receipt of deep brain stimulation (DBS) within the past year, or (4) receipt of a positive genetic test result for GBA or LRRK2.

A total of 23 participants met the timeline and inclusion criteria for the follow-up study. Of these, 21 participated, while two were unable to take part due to scheduling conflicts, pre-existing health conditions, or newly acquired genetic status. Informed consent was obtained, and ethical approval was granted by the UCL Research Ethics Committee.

5.3.2 Ocular Motor Battery

The standard ocular motor battery described in Chapter 2: General Methods was used at both baseline and follow-up. The experimental setup, including calibration and validation procedures, remained consistent across time points.

5.3.3 Data Processing and Analysis

Data processing methods and metric extraction followed the procedures detailed in Chapter 2: General Methods.

5.3.4 Statistical Analyses

Descriptive statistics were calculated for demographics at baseline and after one year. Paired t-tests were used to assess within-subject changes. Because the data was not normally distributed as determined by the Shapiro–Wilk test, (linear mixed models (LMM)s) were fitted separately for each eye movement metric. Fixed effects included age, sex, disease duration, and LEDD, while participant ID was entered as a random effect. Bonferroni correction was applied to adjust for multiple comparisons, and 95% CIs were reported for all fixed effects. Model fit was evaluated using the AIC and the BIC. To test whether changes in metrics over time differed across subgroups, interaction terms were added to the (LMMs): time disease severity (mild vs. severe), time LEDD class (low vs. high), time age, and time sex. Post hoc analyses used estimated marginal means and pairwise comparisons. Participants were grouped as “low” or “high” based on whether their age, disease duration, or LEDD values fell below or above the respective group means at baseline and follow-up. Significant interaction terms were interpreted as indicating subgroup-specific effects of time. Multicollinearity was assessed via variance inflation factor (VIF)s, with values greater than 5 indicating

potential concern. All analyses were performed using R (Version 2023.09.1+494, R Core Team, Vienna, Austria). The data tables with all the results are presented in the appendix.

5.3.5 Participants

A total of 20 participants were included in the final analysis; one individual was excluded due to incomplete data. The cohort consisted of 12 males and 8 females. At baseline, the mean age was 62.25 ± 7.95 years, with an average disease duration of 6.35 ± 5.92 years and a mean LEDD of 391.15 ± 305.73 mg. After one year, the mean age increased to 63.30 ± 7.98 years, the average disease duration rose to 7.30 ± 5.86 years, and the mean LEDD increased to 461.40 ± 282.19 mg. Paired t-tests revealed significant changes in disease duration ($p < 0.001$) and LEDD ($p = 0.009$) between baseline and follow-up, while no significant change was observed in age ($p = 0.102$). Multicollinearity analysis of the fixed-effect predictors—age, sex, disease duration, and LEDD—showed no evidence of collinearity, with all VIFs values falling below the threshold of 5.

Table 12: Demographic and clinical characteristics of the study cohort at baseline and one year. Values are presented as mean \pm standard deviation (SD). Age is reported for all participants, while disease duration and LEDD are reported for disease groups only. Data are stratified by group and sex. “-” indicates not applicable or unavailable.

Group	Age (Mean \pm SD)	Disease Duration (Mean \pm SD)	LEDD (Mean \pm SD)
Baseline (N = 20)	62.25 ± 7.95	6.35 ± 5.92	391.15 ± 305.73
Males (N = 12)	64.17 ± 6.82	5.83 ± 6.18	401.08 ± 312.70
Females (N = 8)	59.38 ± 9.09	7.13 ± 5.84	376.25 ± 315.65
Follow Up (N = 20)	63.30 ± 7.98	7.30 ± 5.86	461.40 ± 282.19
Males (N = 12)	65.17 ± 6.82	6.83 ± 6.18	452.75 ± 273.53
Females (N = 8)	60.50 ± 9.21	8.00 ± 5.68	474.38 ± 313.44

5.3.6 Ocular Motor Function

For the central fixation task, there were no significant differences in average fixation duration, RMS precision measure, SD precision measure, average pupil size, number of large intrusive saccades, number of large SWJs, or number of microsaccades between baseline and one-year follow-up. However, the overall saccade

count significantly decreased ($\beta = -14.82$, 95% CI [-29.02, -0.75], $p = 0.05$), as did the number of small SWJs ($\beta = -19.47$, 95% CI [-30.46, -8.48], $p = 0.002$). Pairwise comparisons revealed that the number of small SWJs significantly decreased in individuals with low disease duration ($p = 0.003$) and in those with high LEDD ($p = 0.05$). Similarly, the total number of saccades decreased significantly in individuals with low disease duration ($p = 0.02$) and those with high LEDD ($p = 0.05$).

Fixation across all eccentric positions (up, down, right, and left) showed no significant differences in average fixation duration, RMS precision measure, SD precision measure, average pupil size, number of large intrusive saccades, total number of saccades, or number of microsaccades between baseline and follow-up. However, in the up position, both small SWJs ($\beta = -16.68$, 95% CI [-27.20, -6.10], $p = 0.005$) and large SWJs ($\beta = -0.41$, 95% CI [-0.75, -0.07], $p = 0.02$) significantly decreased. Pairwise comparisons showed that individuals with low disease duration ($p = 0.002$) and high LEDD ($p = 0.01$) exhibited a significant reduction in small SWJs in the up position.

No significant differences were observed in pursuit gain or pursuit accuracy across all directions (horizontal, vertical, elliptical) and speeds (0.2 Hz and 0.4 Hz) between baseline and follow-up.

Antisaccades in the horizontal direction showed no significant changes in saccade amplitude, average velocity, peak velocity, latency, end time, number of errors, or number of self-corrected errors. In the vertical direction, no significant differences were found for amplitude, average velocity, peak velocity, or number of errors. However, saccade end time ($\beta = 42.30$, 95% CI [4.12, 80.10], $p = 0.04$), latency ($\beta = 38.47$, 95% CI [8.75, 67.68], $p = 0.02$), and number of self-corrected errors ($\beta = 1.90$, 95% CI [0.21, 3.59], $p = 0.04$) increased significantly. Pairwise comparisons indicated that end time and latency significantly increased in individuals with low LEDD ($p = 0.03$ and $p = 0.02$, respectively), while the number of self-corrected errors significantly increased in individuals with low disease duration ($p = 0.05$).

Oblique saccades at 4°, 8°, and 10° eccentricities showed no significant changes in amplitude, average velocity, peak velocity, latency, end time, X and Y positional accuracy, number of correct saccades, or hypermetric saccades. However, the number of hypometric saccades at 10° increased significantly ($\beta = 3.38$, 95% CI [1.25, 5.54], $p = 0.005$). Pairwise comparisons showed increased hypometric saccades in individuals with

high and low disease duration and low LEDD ($p = 0.02$, $p = 0.05$, and $p = 0.01$, respectively).

No significant differences were found in reflexive saccade metrics—amplitude, average velocity, peak velocity, latency, end time, accuracy, number of correct, hypometric, or hypermetric saccades—in either the horizontal or vertical direction.

Volitional saccades in both horizontal and vertical directions also revealed no significant changes in amplitude, average velocity, peak velocity, latency, end time, accuracy, number of correct, hypometric, or hypermetric saccades, total number of saccades completed, or number of saccadic steps.

Similarly, memory-guided saccades in both planes showed no significant changes across amplitude, average velocity, peak velocity, accuracy, number of correct, hypometric, or hypermetric saccades, total number of saccades completed, or number of saccadic steps. Significant increases were observed in the horizontal direction for saccade end time ($\beta = 1367.15$, 95% CI [57.01, 2679.21], $p = 0.05$) and latency ($\beta = 1352.95$, 95% CI [31.19, 2676.95], $p = 0.05$), though these changes were not observed in the vertical direction. Pairwise comparisons showed no significant effects of disease duration or LEDD.

Longitudinal Change Central Fixation

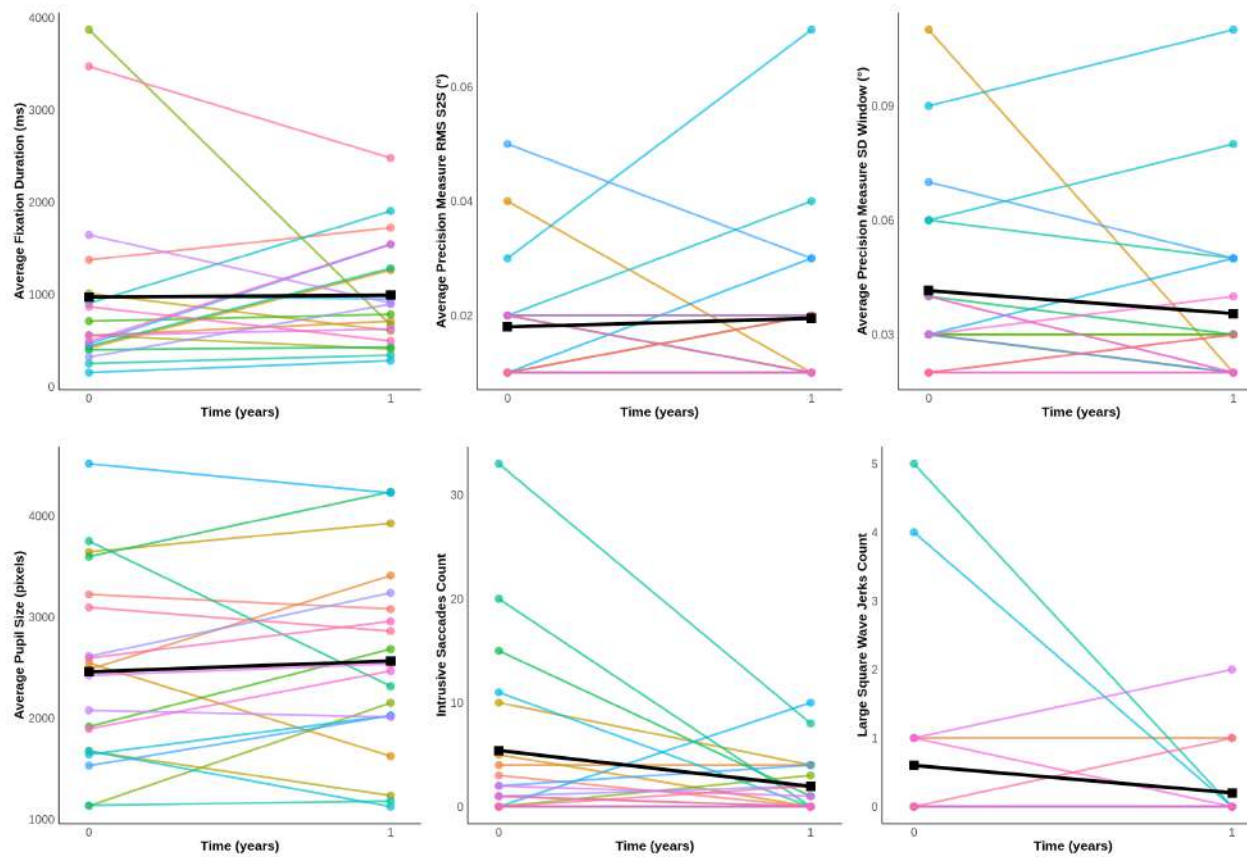


Figure 124: Central Fixation Metrics. Each line represents an individual; black line represents the mean change over time. Linear mixed-effects models were fitted separately for each metric, with age, sex, disease duration, and levodopa equivalent daily dose (LEDD) as fixed effects, and participant ID as a random effect. Statistical significance was set at $p < 0.05$.

Longitudinal Change Central Fixation

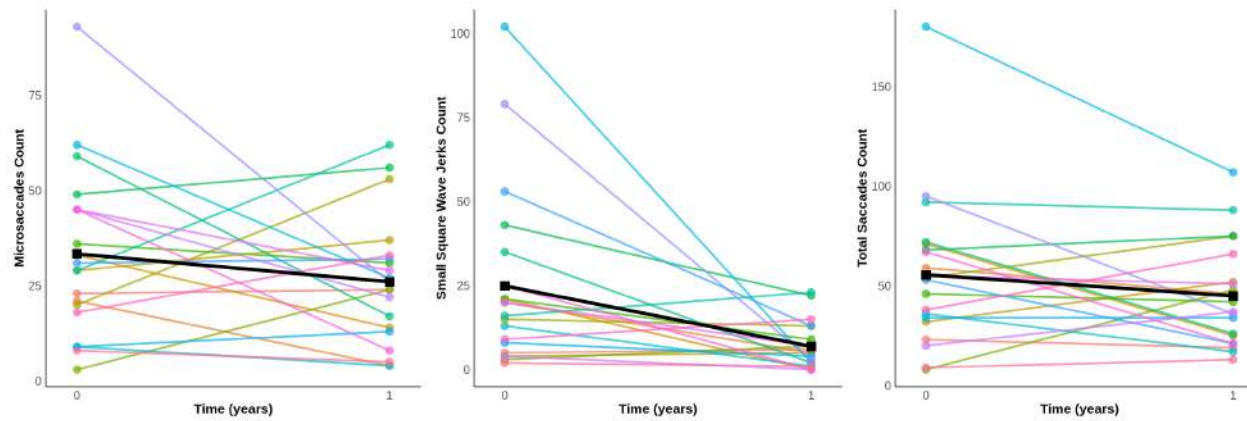


Figure 125: Central Fixation Metrics. Each line represents an individual; black line represents the mean change over time. Linear mixed-effects models were fitted separately for each metric, with age, sex, disease duration, and levodopa equivalent daily dose (LEDD) as fixed effects, and participant ID as a random effect. Statistical significance was set at $p < 0.05$.

Longitudinal Change Positional Fixation/ Nystagmus

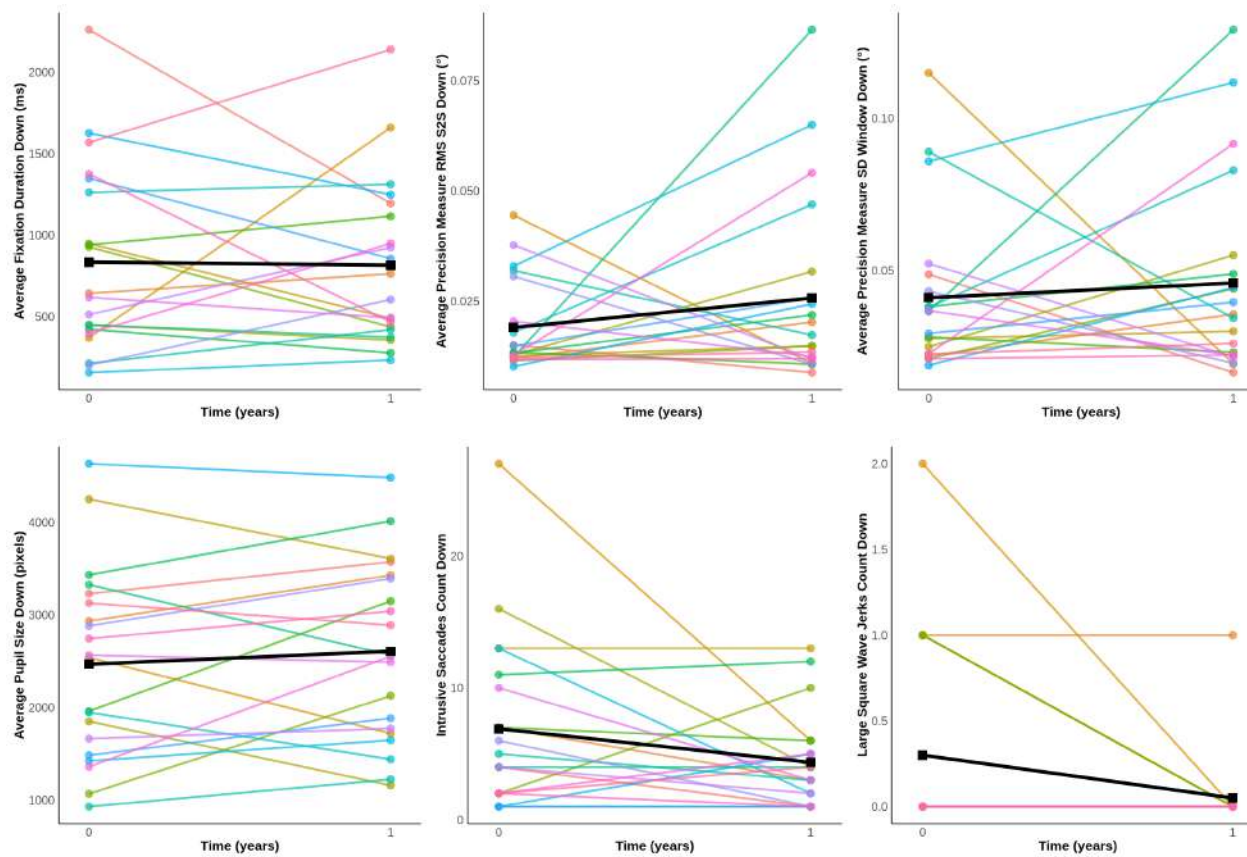


Figure 126: Positional Fixation/ Nystagmus Metrics. Each line represents an individual; black line represents the mean change over time. Linear mixed-effects models were fitted separately for each metric, with age, sex, disease duration, and levodopa equivalent daily dose (LEDD) as fixed effects, and participant ID as a random effect. Statistical significance was set at $p < 0.05$.

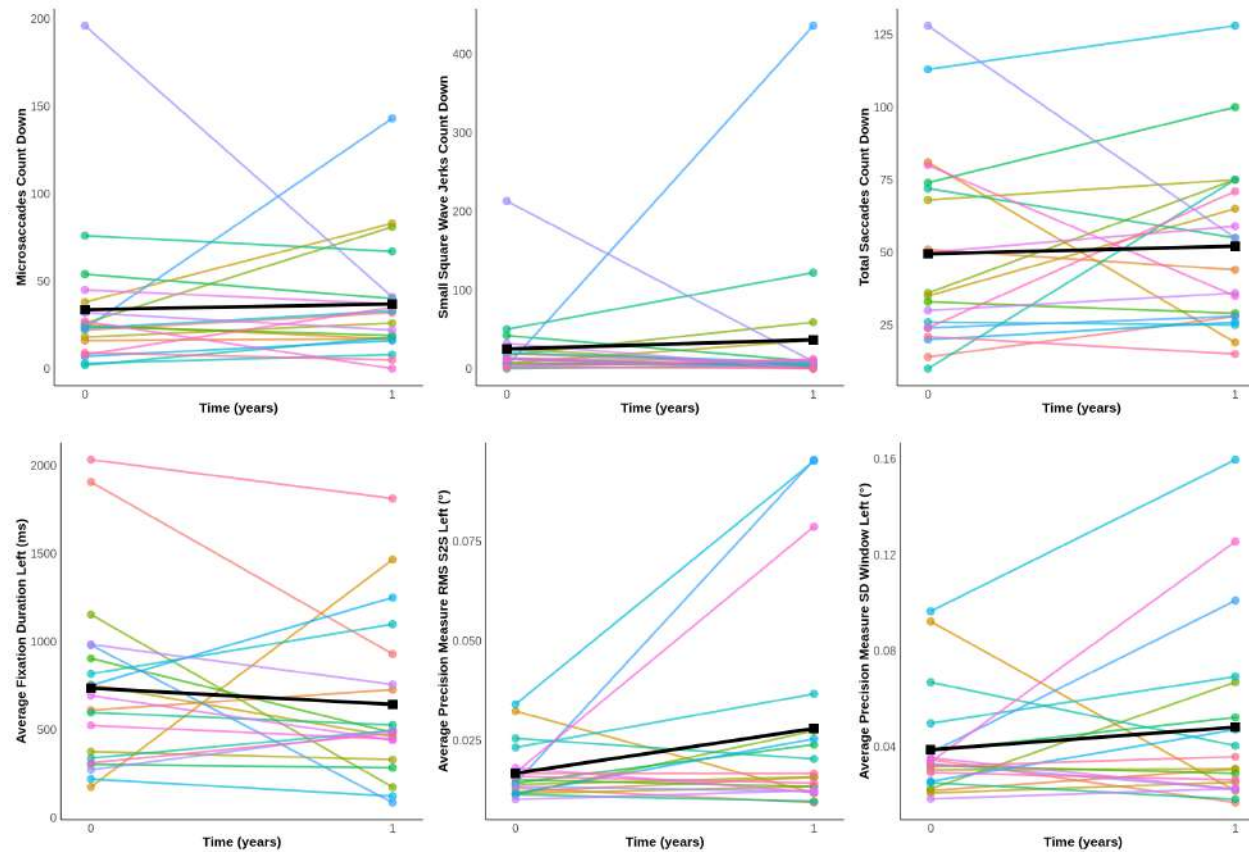


Figure 127: Positional Fixation/ Nystagmus Metrics. Each line represents an individual; black line represents the mean change over time. Linear mixed-effects models were fitted separately for each metric, with age, sex, disease duration, and levodopa equivalent daily dose (LEDD) as fixed effects, and participant ID as a random effect. Statistical significance was set at $p < 0.05$.

Longitudinal Change Positional Fixation/ Nystagmus

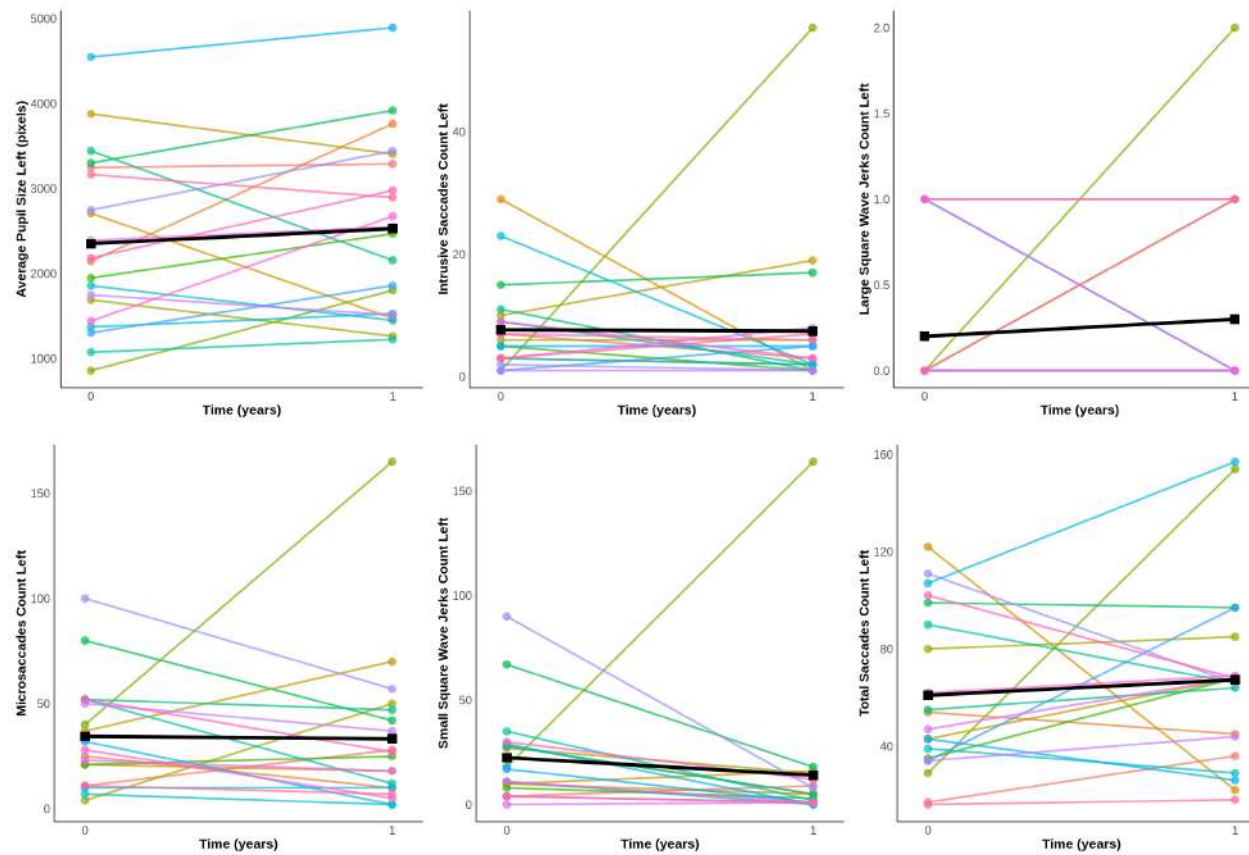


Figure 128: Positional Fixation/ Nystagmus Metrics. Each line represents an individual; black line represents the mean change over time. Linear mixed-effects models were fitted separately for each metric, with age, sex, disease duration, and levodopa equivalent daily dose (LEDD) as fixed effects, and participant ID as a random effect. Statistical significance was set at $p < 0.05$.

Longitudinal Change Positional Fixation/ Nystagmus

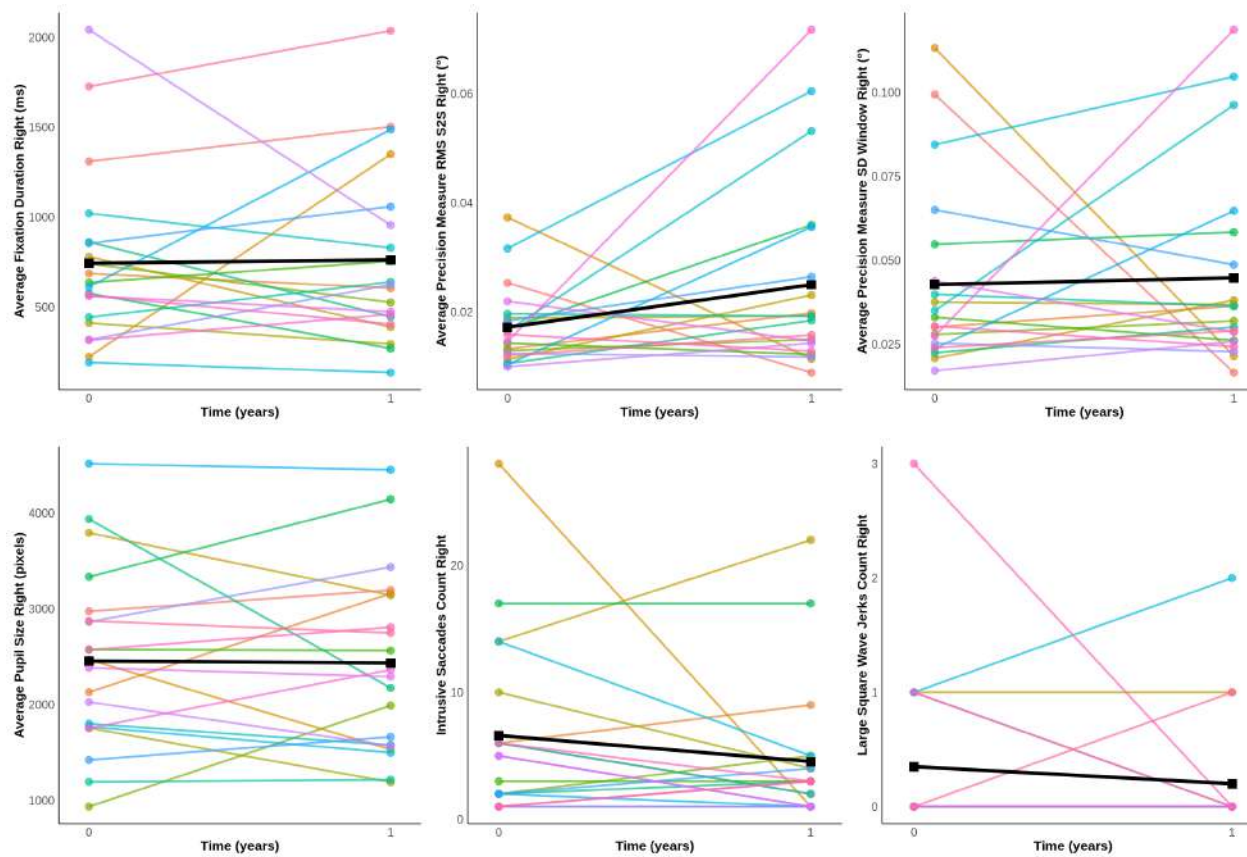


Figure 129: Positional Fixation/ Nystagmus Metrics. Each line represents an individual; black line represents the mean change over time. Linear mixed-effects models were fitted separately for each metric, with age, sex, disease duration, and levodopa equivalent daily dose (LEDD) as fixed effects, and participant ID as a random effect. Statistical significance was set at $p < 0.05$.

Longitudinal Change Positional Fixation/ Nystagmus

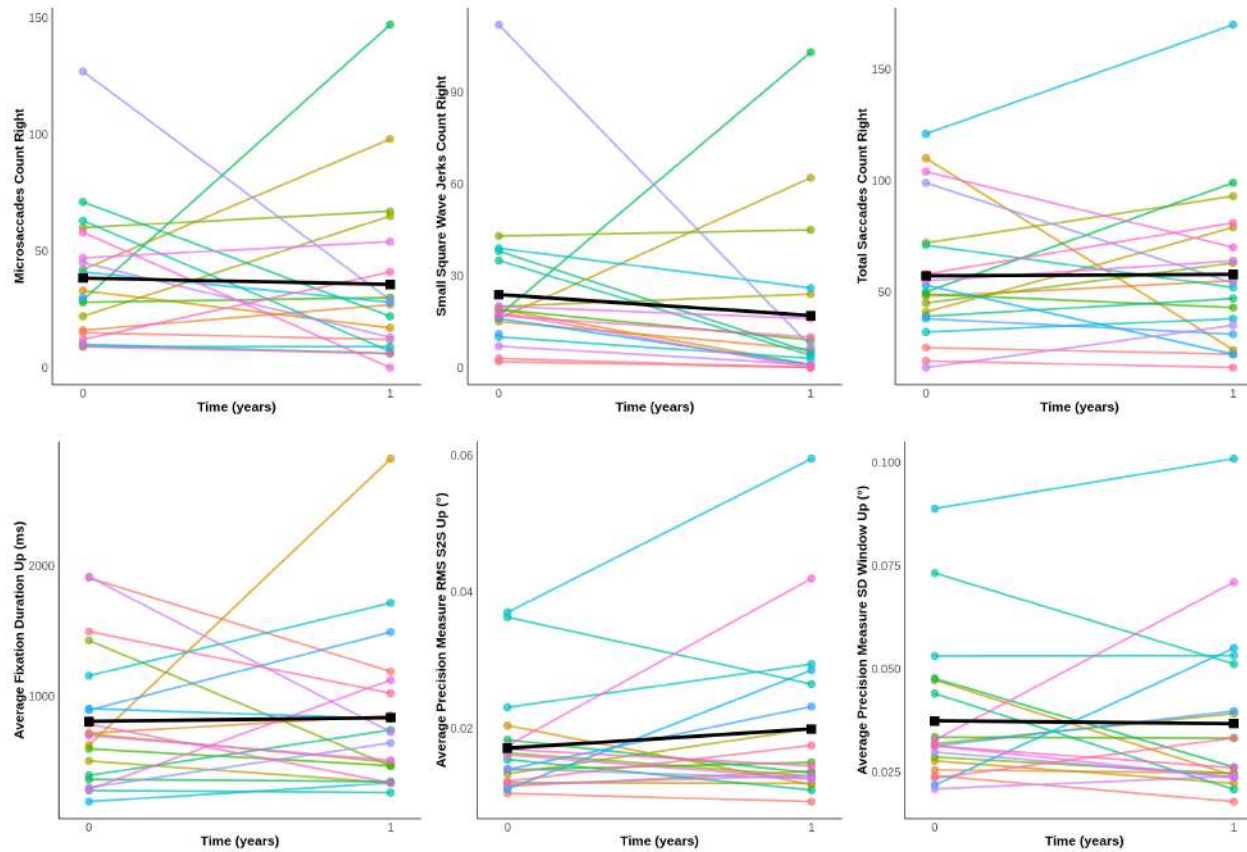


Figure 130: Positional Fixation/ Nystagmus Metrics. Each line represents an individual; black line represents the mean change over time. Linear mixed-effects models were fitted separately for each metric, with age, sex, disease duration, and levodopa equivalent daily dose (LEDD) as fixed effects, and participant ID as a random effect. Statistical significance was set at $p < 0.05$.

Longitudinal Change Pursuit

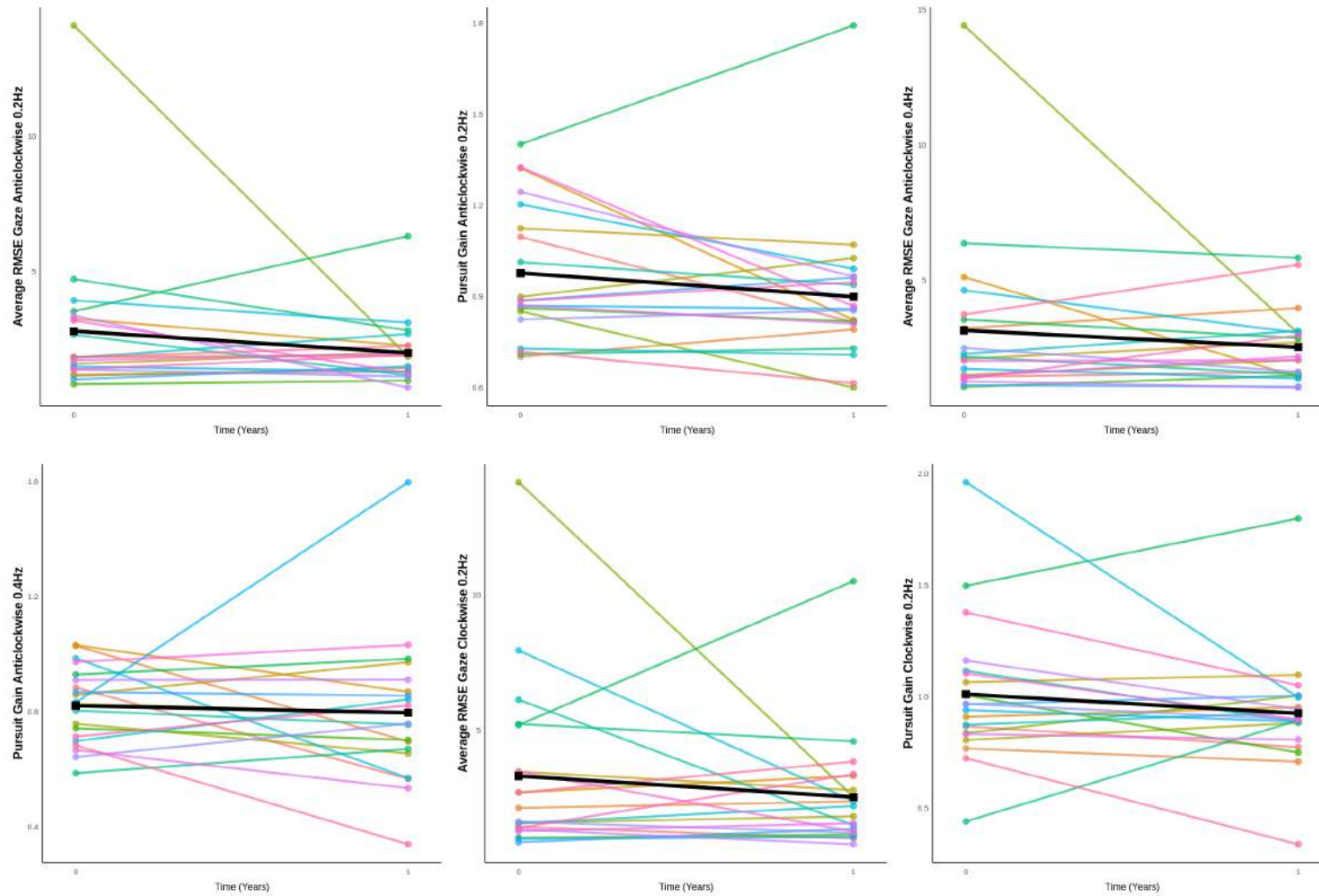


Figure 131: Longitudinal Change Pursuit Metrics. Each line represents an individual; black line represents the mean change over time. Linear mixed-effects models were fitted separately for each metric, with age, sex, disease duration, and levodopa equivalent daily dose (LEDD) as fixed effects, and participant ID as a random effect. Statistical significance was set at $p < 0.05$.

Longitudinal Change Pursuit

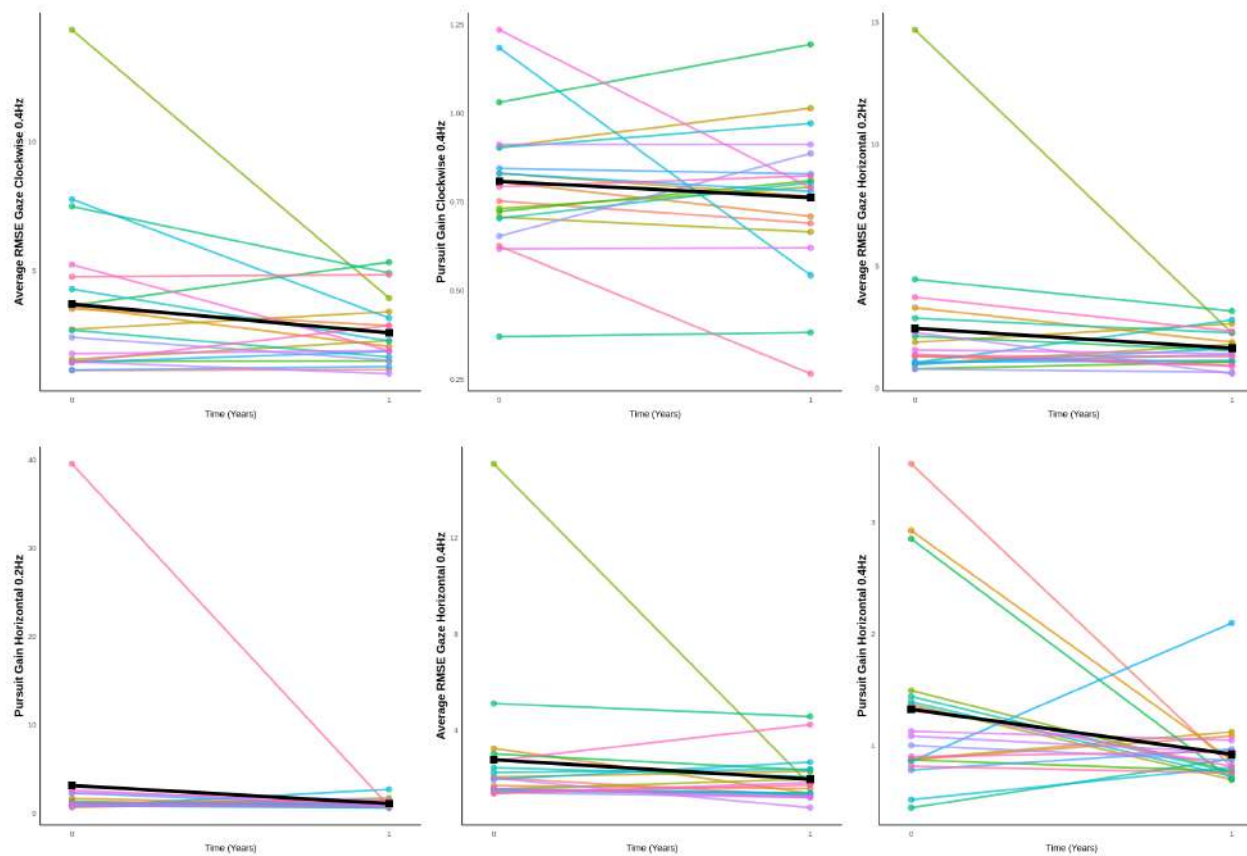


Figure 132: Longitudinal Change Pursuit Metrics. Each line represents an individual; black line represents the mean change over time.

Linear mixed-effects models were fitted separately for each metric, with age, sex, disease duration, and levodopa equivalent daily dose (LEDD) as fixed effects, and participant ID as a random effect. Statistical significance was set at $p < 0.05$.

Longitudinal Change Pursuit

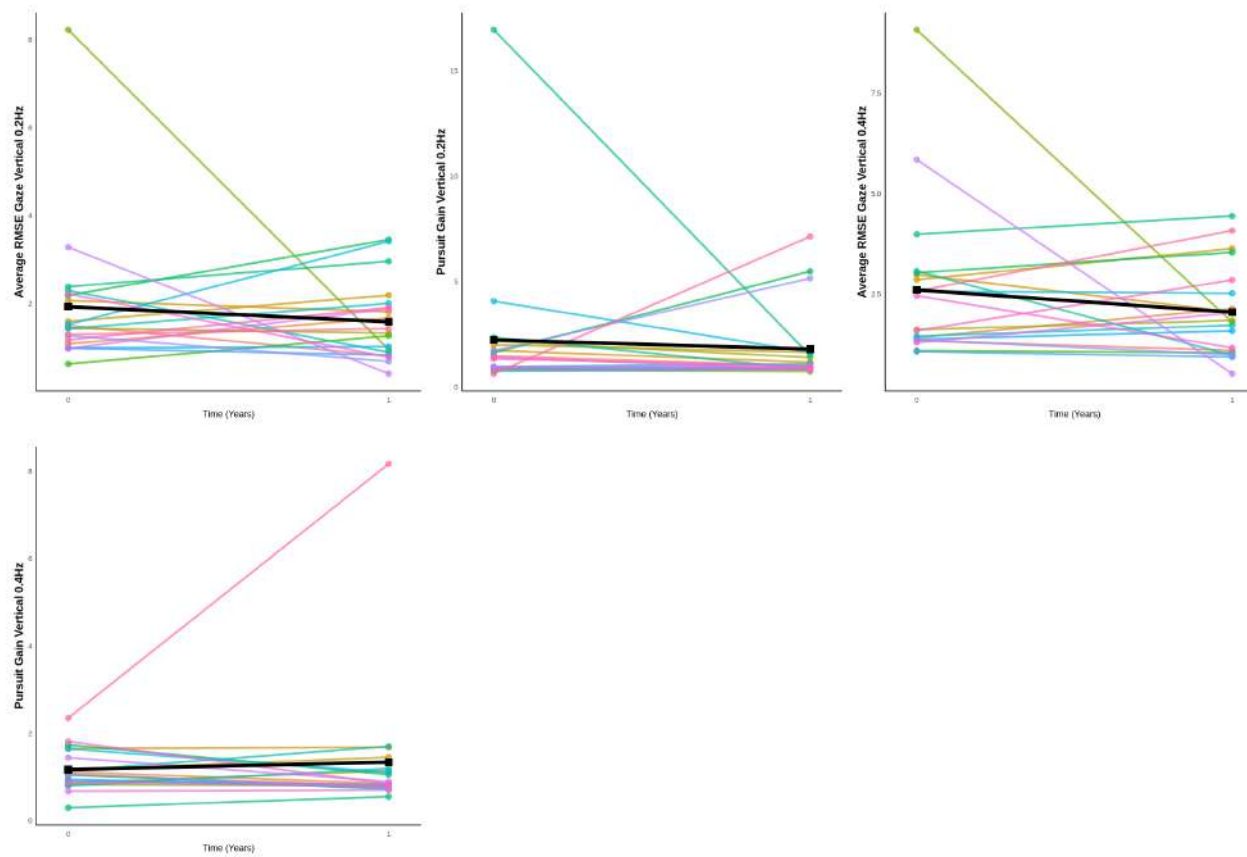


Figure 133: Pursuit Metrics. Each line represents an individual; black line represents the mean change over time. Linear mixed-effects models were fitted separately for each metric, with age, sex, disease duration, and levodopa equivalent daily dose (LEDD) as fixed effects, and participant ID as a random effect. Statistical significance was set at $p < 0.05$.

Longitudinal Change Oblique Saccades

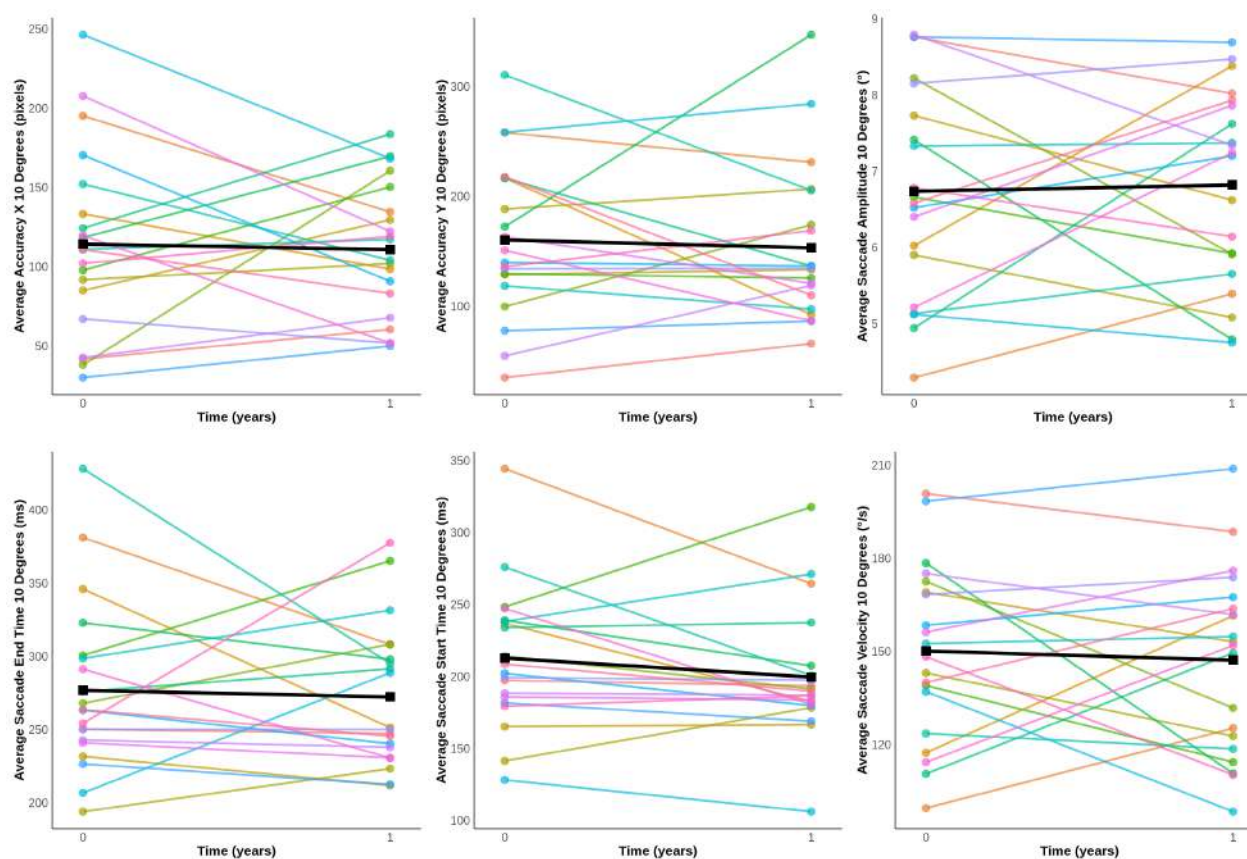


Figure 134: Oblique Saccades Metrics. Each line represents an individual; black line represents the mean change over time. Linear mixed-effects models were fitted separately for each metric, with age, sex, disease duration, and levodopa equivalent daily dose (LEDD) as fixed effects, and participant ID as a random effect. Statistical significance was set at $p < 0.05$.

Longitudinal Change Oblique Saccades

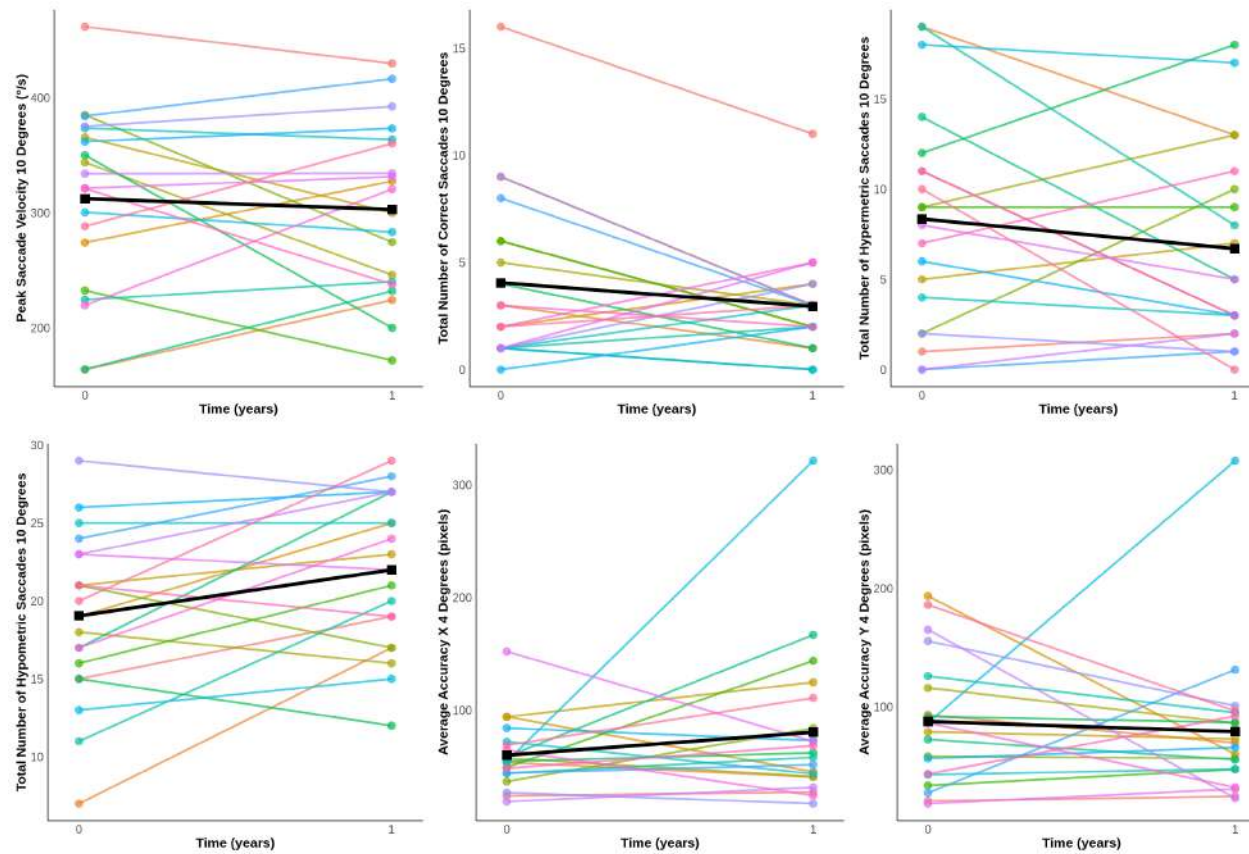


Figure 135: Oblique Saccades Metrics. Each line represents an individual; black line represents the mean change over time. Linear mixed-effects models were fitted separately for each metric, with age, sex, disease duration, and levodopa equivalent daily dose (LEDD) as fixed effects, and participant ID as a random effect. Statistical significance was set at $p < 0.05$.

Longitudinal Change Oblique Saccades

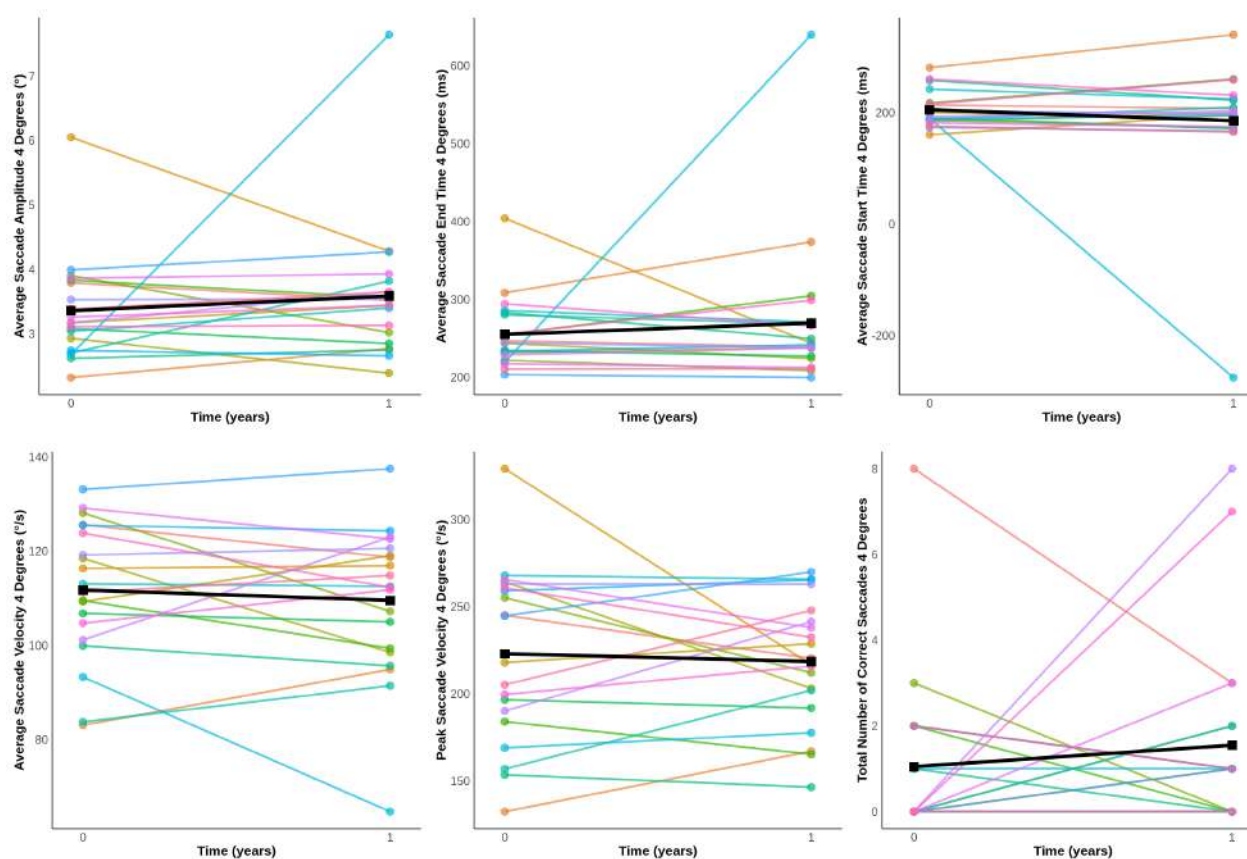


Figure 136: Oblique Saccades Metrics. Each line represents an individual; black line represents the mean change over time. Linear mixed-effects models were fitted separately for each metric, with age, sex, disease duration, and levodopa equivalent daily dose (LEDD) as fixed effects, and participant ID as a random effect. Statistical significance was set at $p < 0.05$.

Longitudinal Change Oblique Saccades

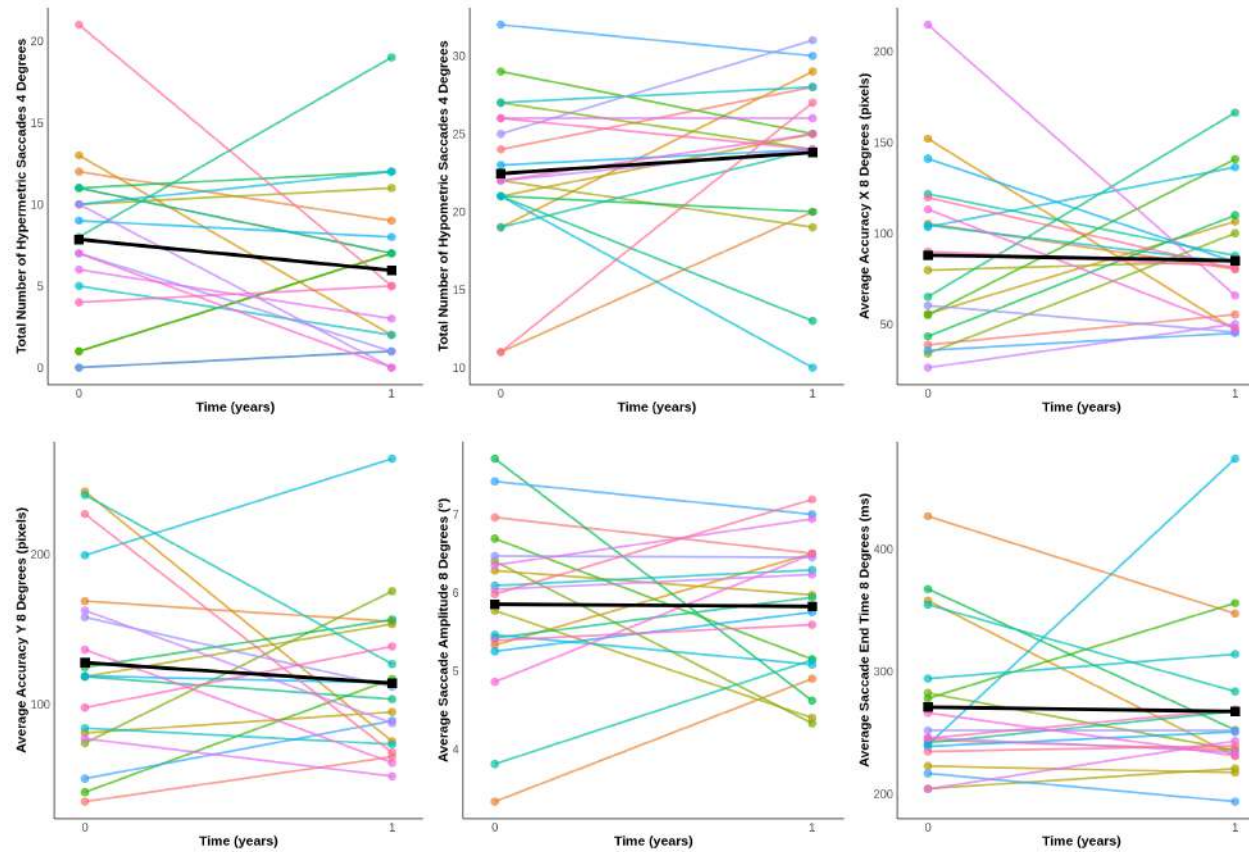


Figure 137: Oblique Saccades Metrics. Each line represents an individual; black line represents the mean change over time. Linear mixed-effects models were fitted separately for each metric, with age, sex, disease duration, and levodopa equivalent daily dose (LEDD) as fixed effects, and participant ID as a random effect. Statistical significance was set at $p < 0.05$.

Longitudinal Change Oblique Saccades

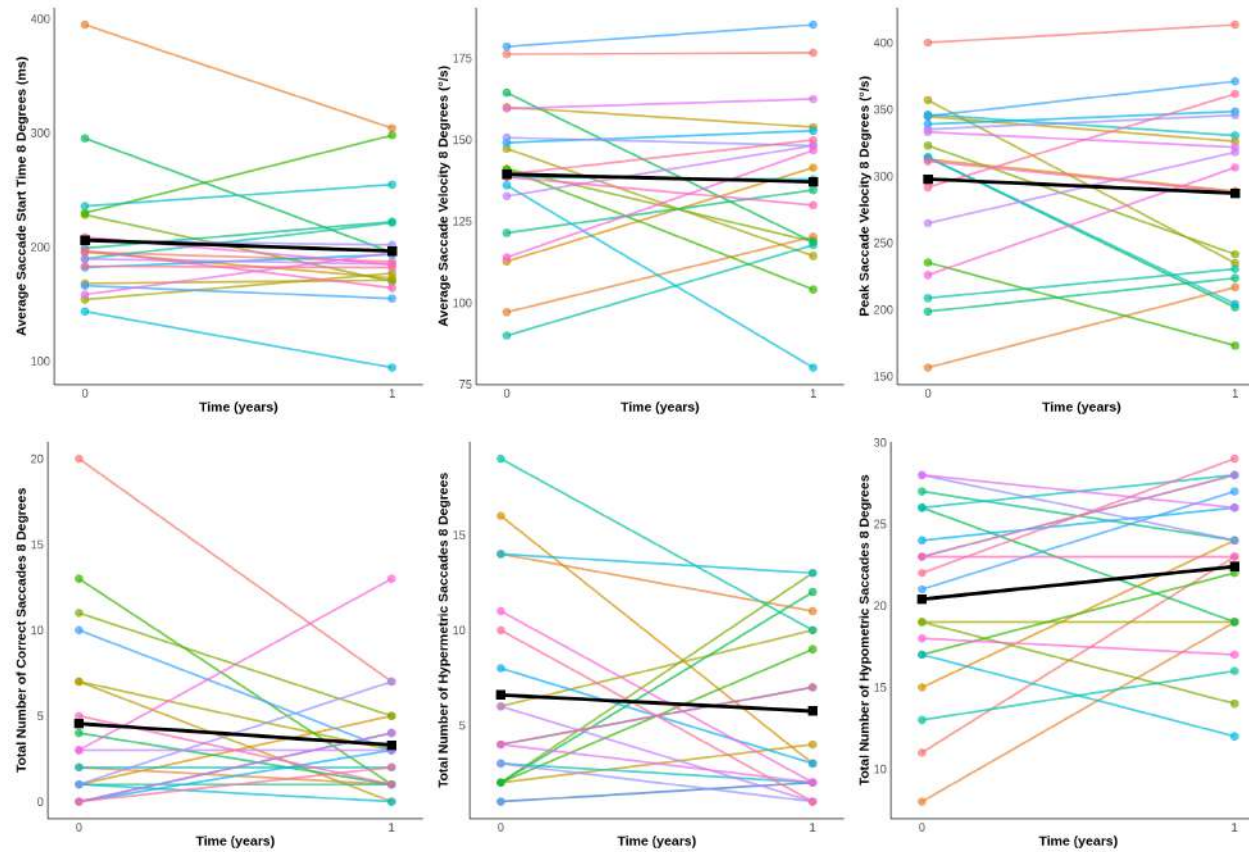


Figure 138: Oblique Saccades Metrics. Each line represents an individual; black line represents the mean change over time. Linear mixed-effects models were fitted separately for each metric, with age, sex, disease duration, and levodopa equivalent daily dose (LEDD) as fixed effects, and participant ID as a random effect. Statistical significance was set at $p < 0.05$.

Longitudinal Change Antisaccades Horizontal

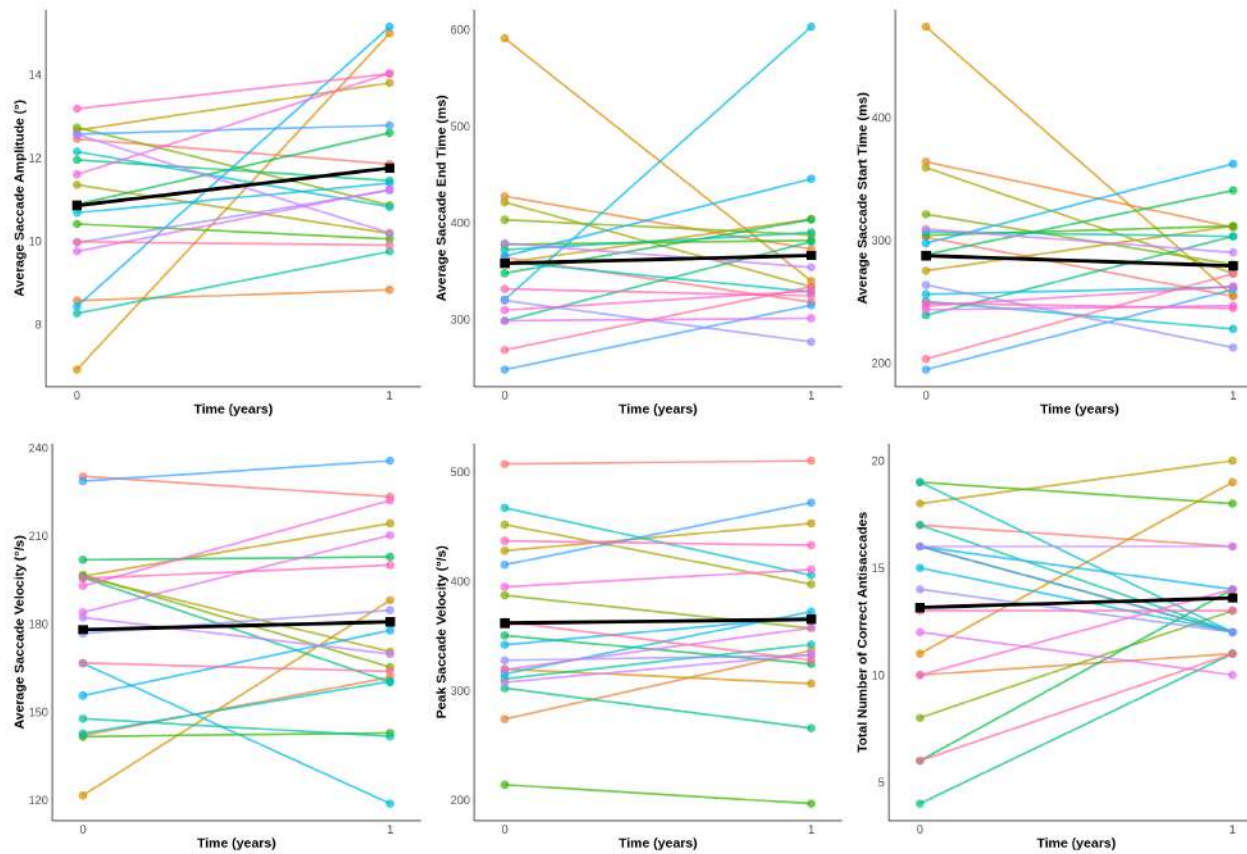


Figure 139: Antisaccades Horizontal Metrics. Each line represents an individual; black line represents the mean change over time. Linear mixed-effects models were fitted separately for each metric, with age, sex, disease duration, and levodopa equivalent daily dose (LEDD) as fixed effects, and participant ID as a random effect. Statistical significance was set at $p < 0.05$.

Longitudinal Change Antisaccades Horizontal

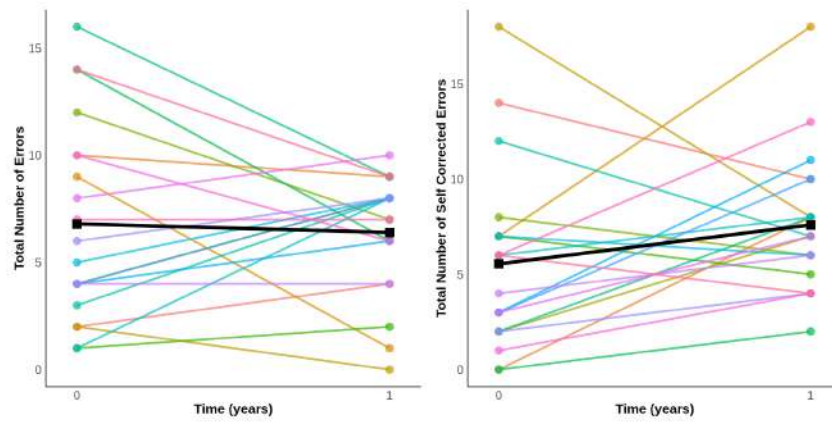


Figure 140: Antisaccades Horizontal Metrics. Each line represents an individual; black line represents the mean change over time. Linear mixed-effects models were fitted separately for each metric, with age, sex, disease duration, and levodopa equivalent daily dose (LEDD) as fixed effects, and participant ID as a random effect. Statistical significance was set at $p < 0.05$.

Longitudinal Change Antisaccades Vertical

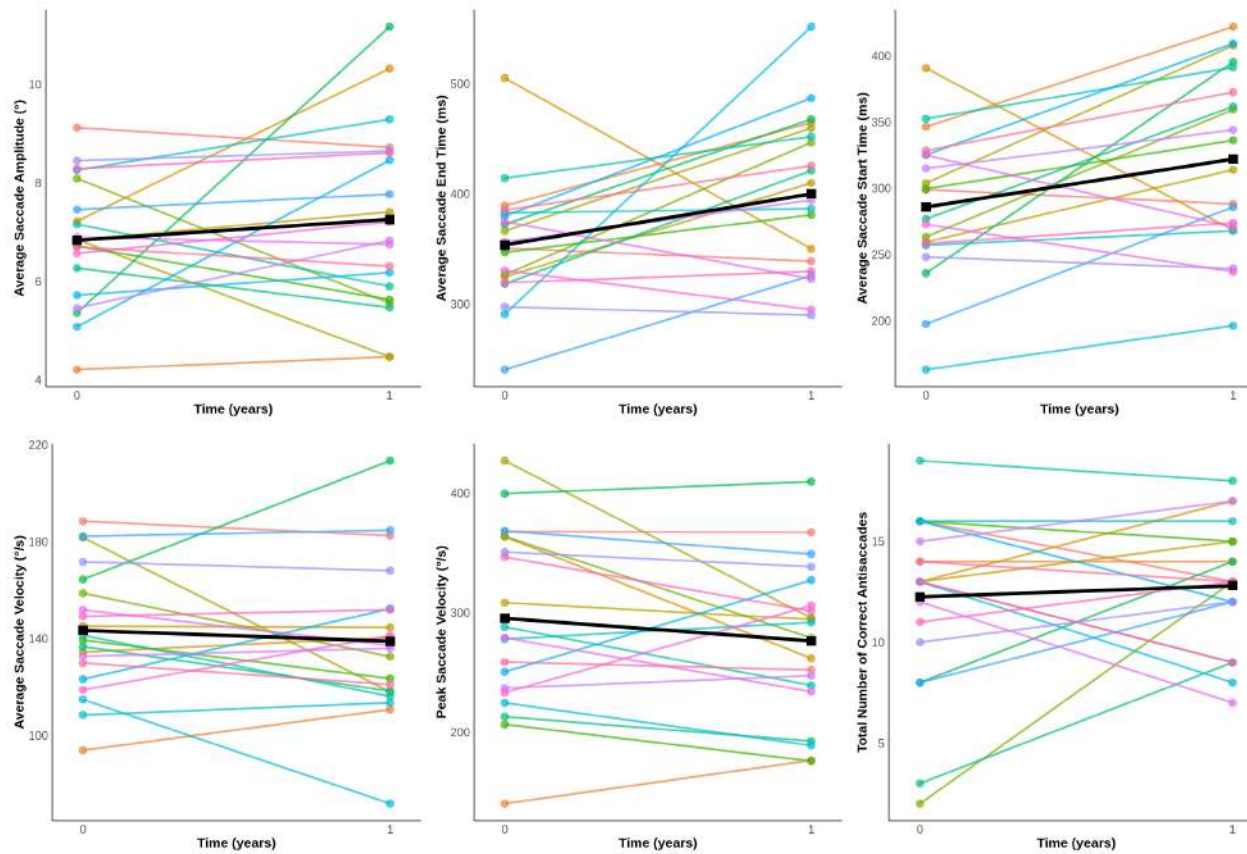


Figure 141: Antisaccades Vertical Metrics. Each line represents an individual; black line represents the mean change over time. Linear mixed-effects models were fitted separately for each metric, with age, sex, disease duration, and levodopa equivalent daily dose (LEDD) as fixed effects, and participant ID as a random effect. Statistical significance was set at $p < 0.05$.

Longitudinal Change Antisaccades Vertical

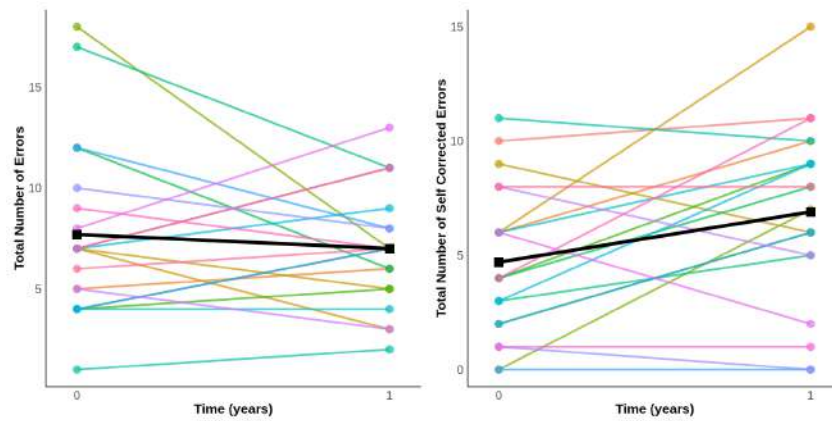


Figure 142: Antisaccades Vertical Metrics. Each line represents an individual; black line represents the mean change over time. Linear mixed-effects models were fitted separately for each metric, with age, sex, disease duration, and levodopa equivalent daily dose (LEDD) as fixed effects, and participant ID as a random effect. Statistical significance was set at $p < 0.05$.

Longitudinal Change Reflexive Saccades Horizontal

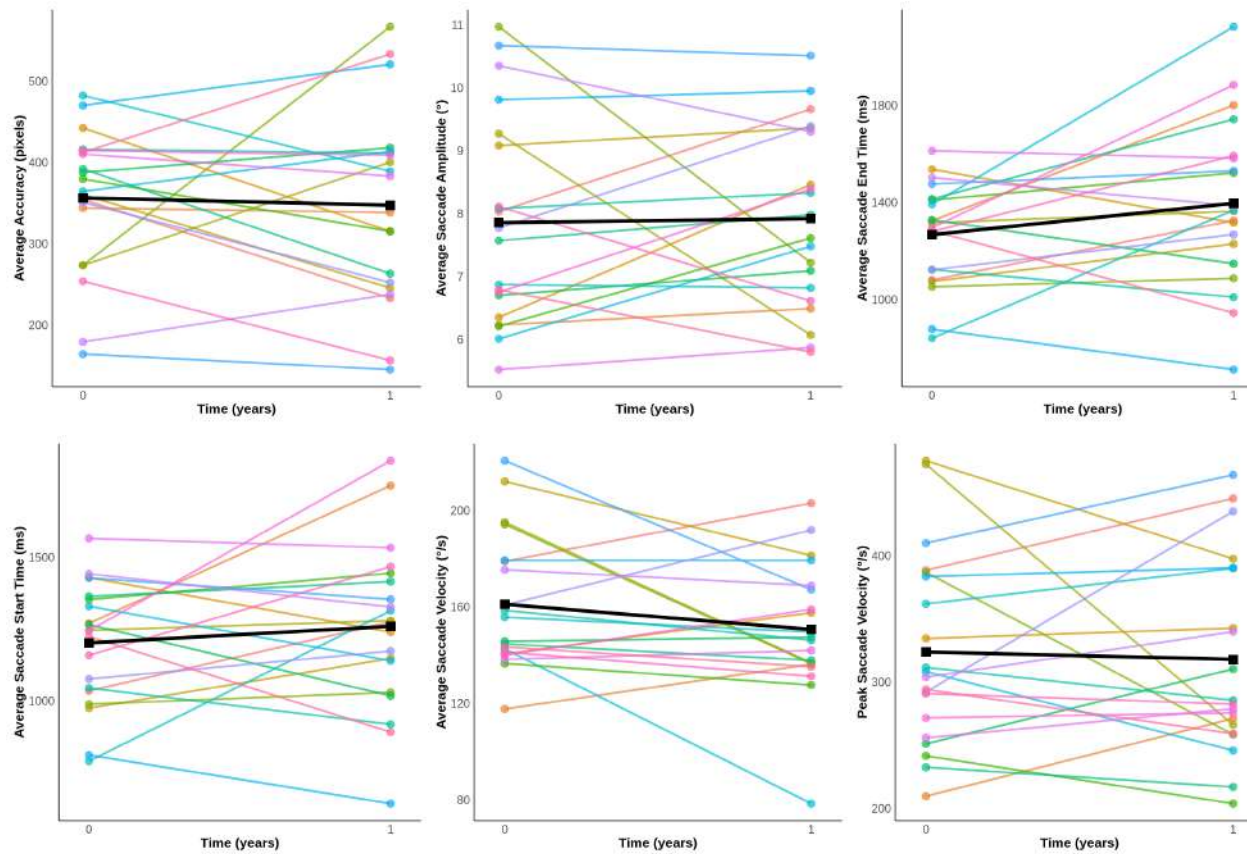


Figure 143: Reflexive Saccades Horizontal Metrics. Each line represents an individual; black line represents the mean change over time. Linear mixed-effects models were fitted separately for each metric, with age, sex, disease duration, and levodopa equivalent daily dose (LEDD) as fixed effects, and participant ID as a random effect. Statistical significance was set at $p < 0.05$.

Longitudinal Change Reflexive Saccades Horizontal

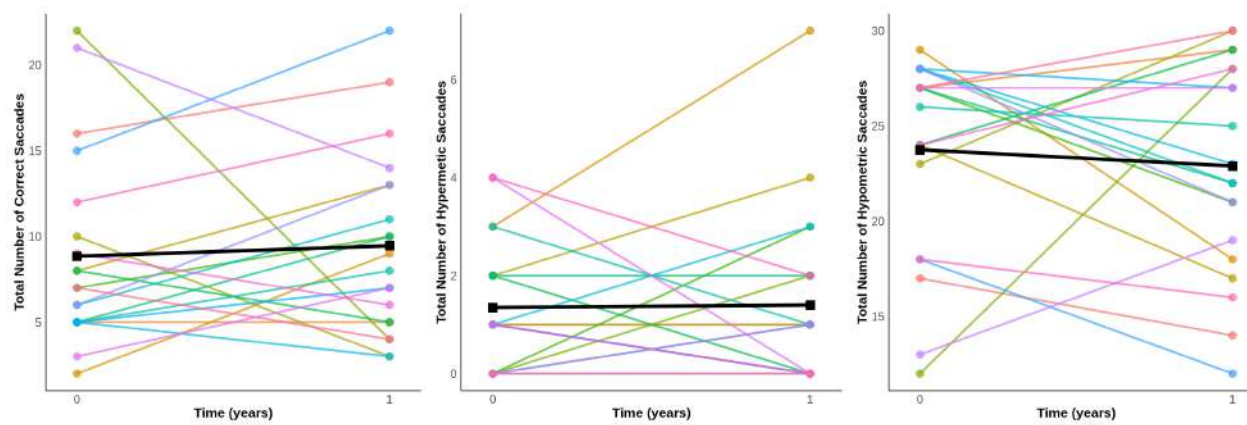


Figure 144: Reflexive Saccades Horizontal Metrics. Each line represents an individual; black line represents the mean change over time. Linear mixed-effects models were fitted separately for each metric, with age, sex, disease duration, and levodopa equivalent daily dose (LEDD) as fixed effects, and participant ID as a random effect. Statistical significance was set at $p < 0.05$.

Longitudinal Change Reflexive Saccades Vertical

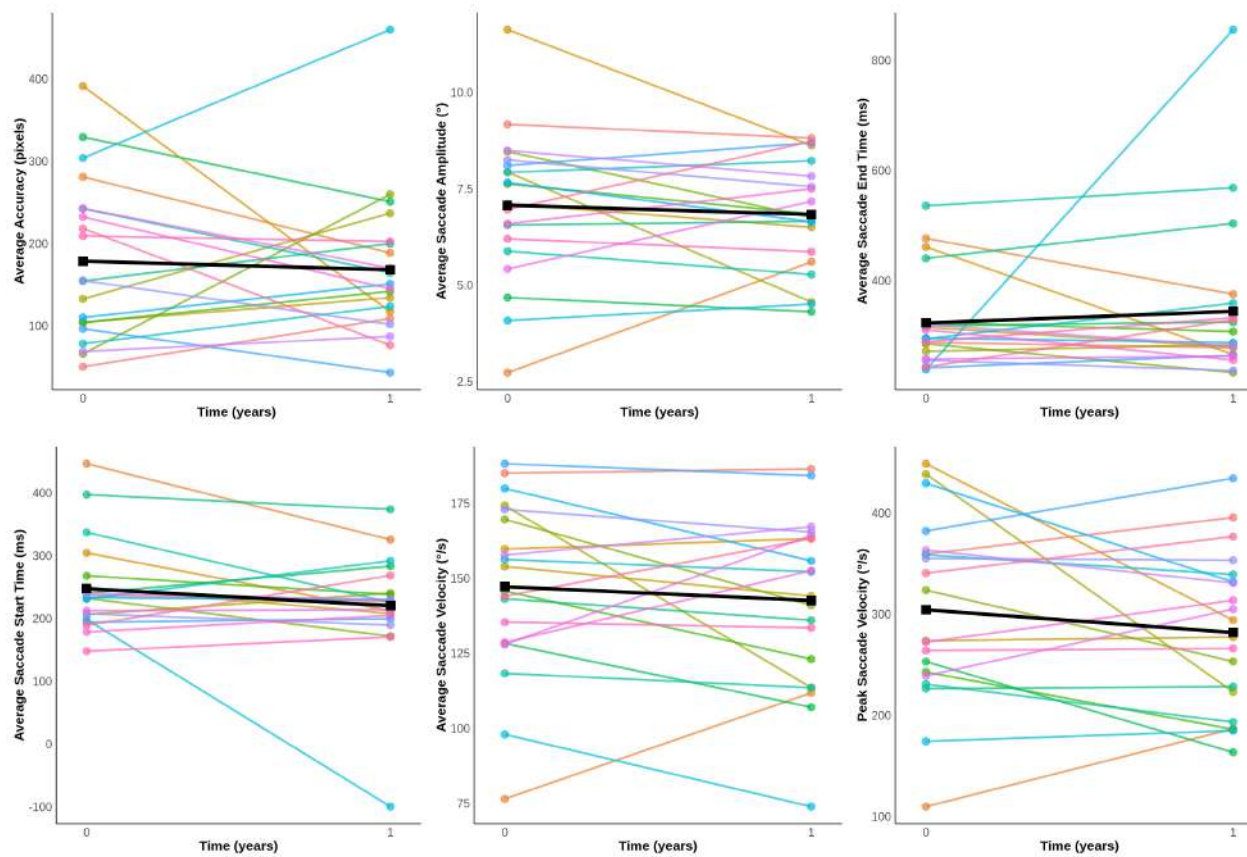


Figure 145: Reflexive Saccades Vertical Metrics. Each line represents an individual; black line represents the mean change over time. Linear mixed-effects models were fitted separately for each metric, with age, sex, disease duration, and levodopa equivalent daily dose (LEDD) as fixed effects, and participant ID as a random effect. Statistical significance was set at $p < 0.05$.

Longitudinal Change Reflexive Saccades Vertical

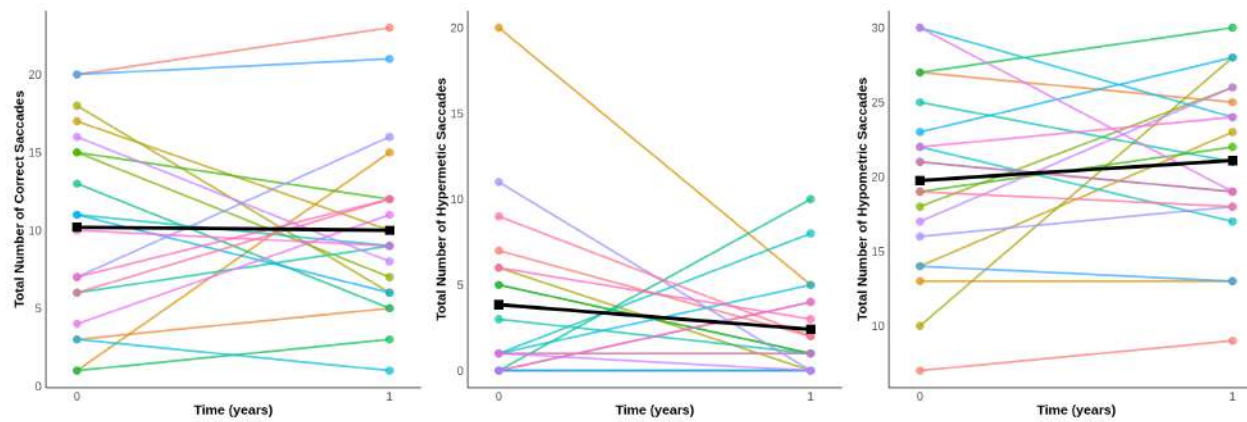


Figure 146: Reflexive Saccades Vertical Metrics. Each line represents an individual; black line represents the mean change over time. Linear mixed-effects models were fitted separately for each metric, with age, sex, disease duration, and levodopa equivalent daily dose (LEDD) as fixed effects, and participant ID as a random effect. Statistical significance was set at $p < 0.05$.

Longitudinal Change Volitional Saccades Horizontal

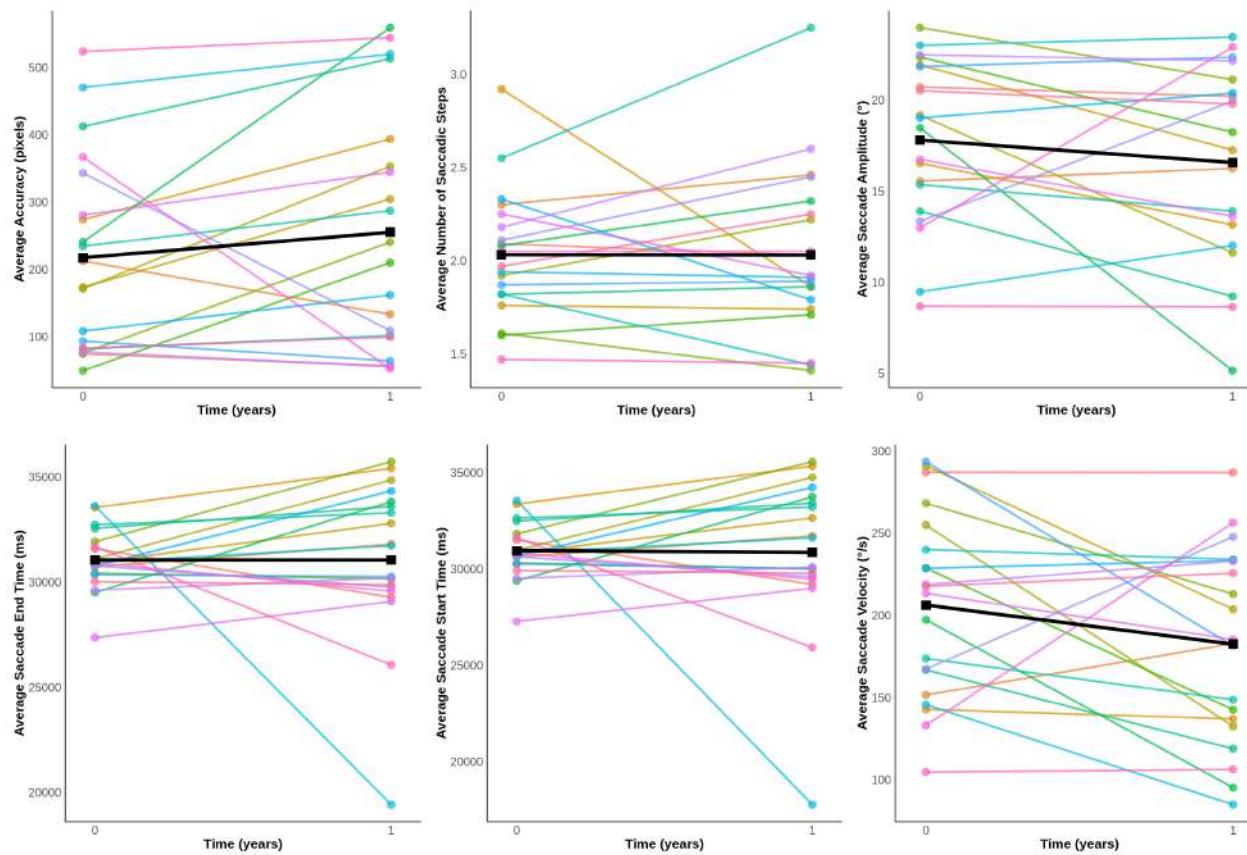


Figure 147: Volitional Saccades Horizontal Metrics. Each line represents an individual; black line represents the mean change over time. Linear mixed-effects models were fitted separately for each metric, with age, sex, disease duration, and levodopa equivalent daily dose (LEDD) as fixed effects, and participant ID as a random effect. Statistical significance was set at $p < 0.05$.

Longitudinal Change Volitional Saccades Horizontal

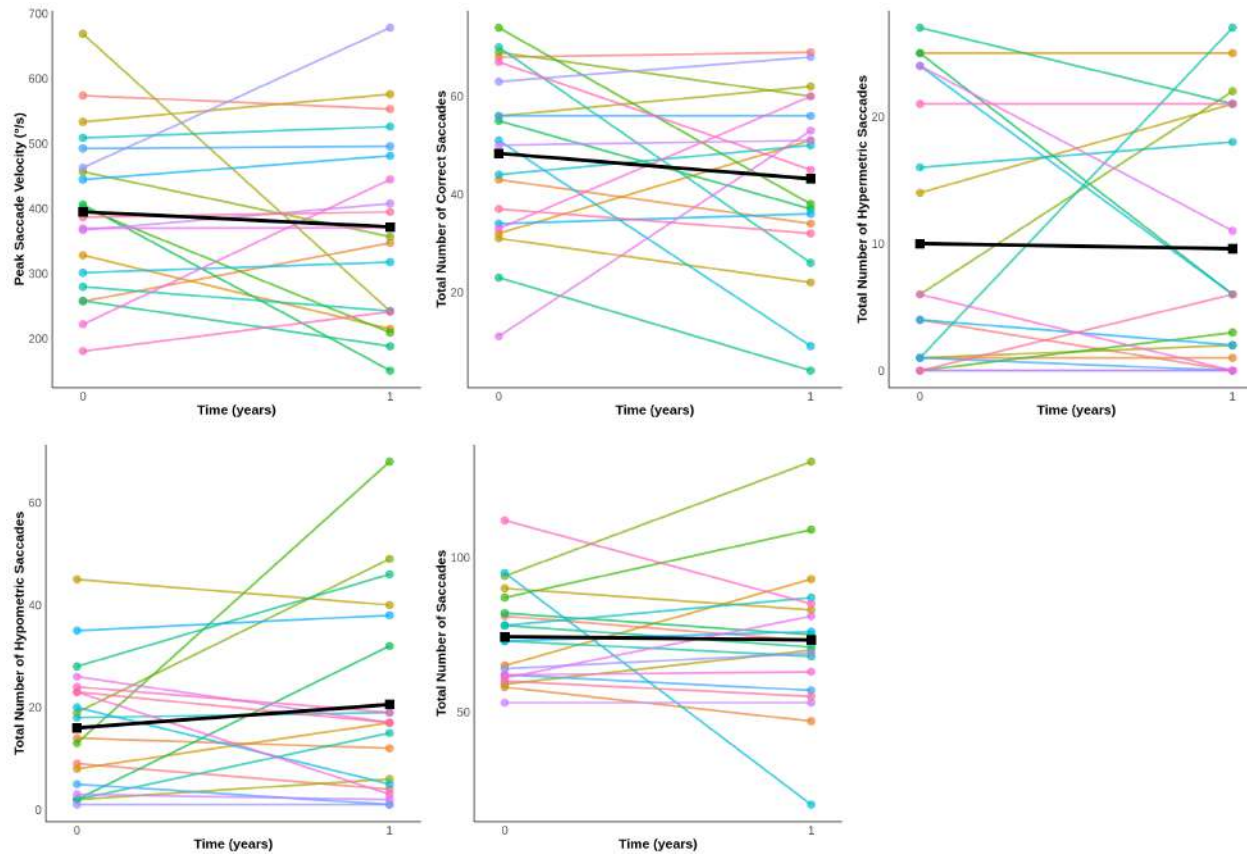


Figure 148: Volitional Saccades Horizontal Metrics. Each line represents an individual; black line represents the mean change over time. Linear mixed-effects models were fitted separately for each metric, with age, sex, disease duration, and levodopa equivalent daily dose (LEDD) as fixed effects, and participant ID as a random effect. Statistical significance was set at $p < 0.05$.

Longitudinal Change Volitional Saccades Vertical

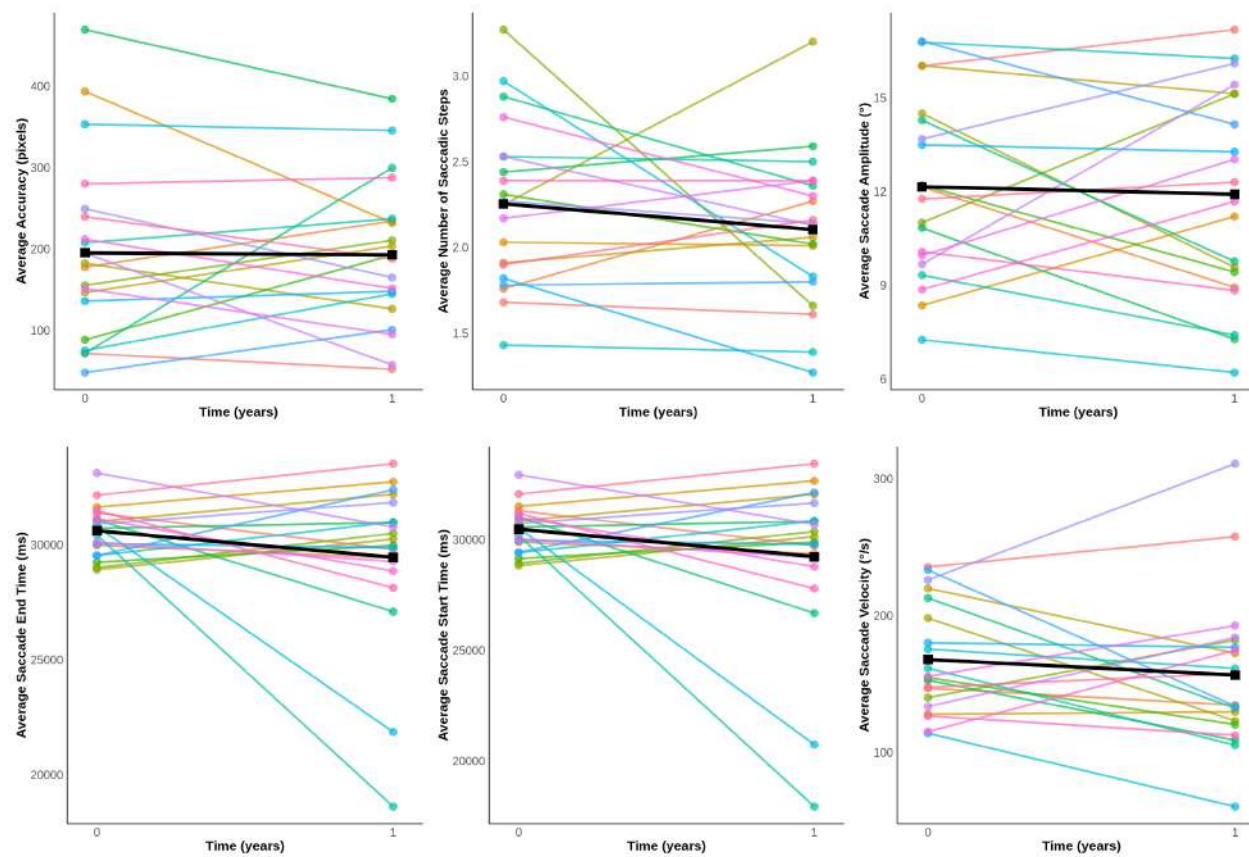


Figure 149: Volitional Saccades Vertical Metrics. Each line represents an individual; black line represents the mean change over time. Linear mixed-effects models were fitted separately for each metric, with age, sex, disease duration, and levodopa equivalent daily dose (LEDD) as fixed effects, and participant ID as a random effect. Statistical significance was set at $p < 0.05$.

Longitudinal Change Volitional Saccades Vertical

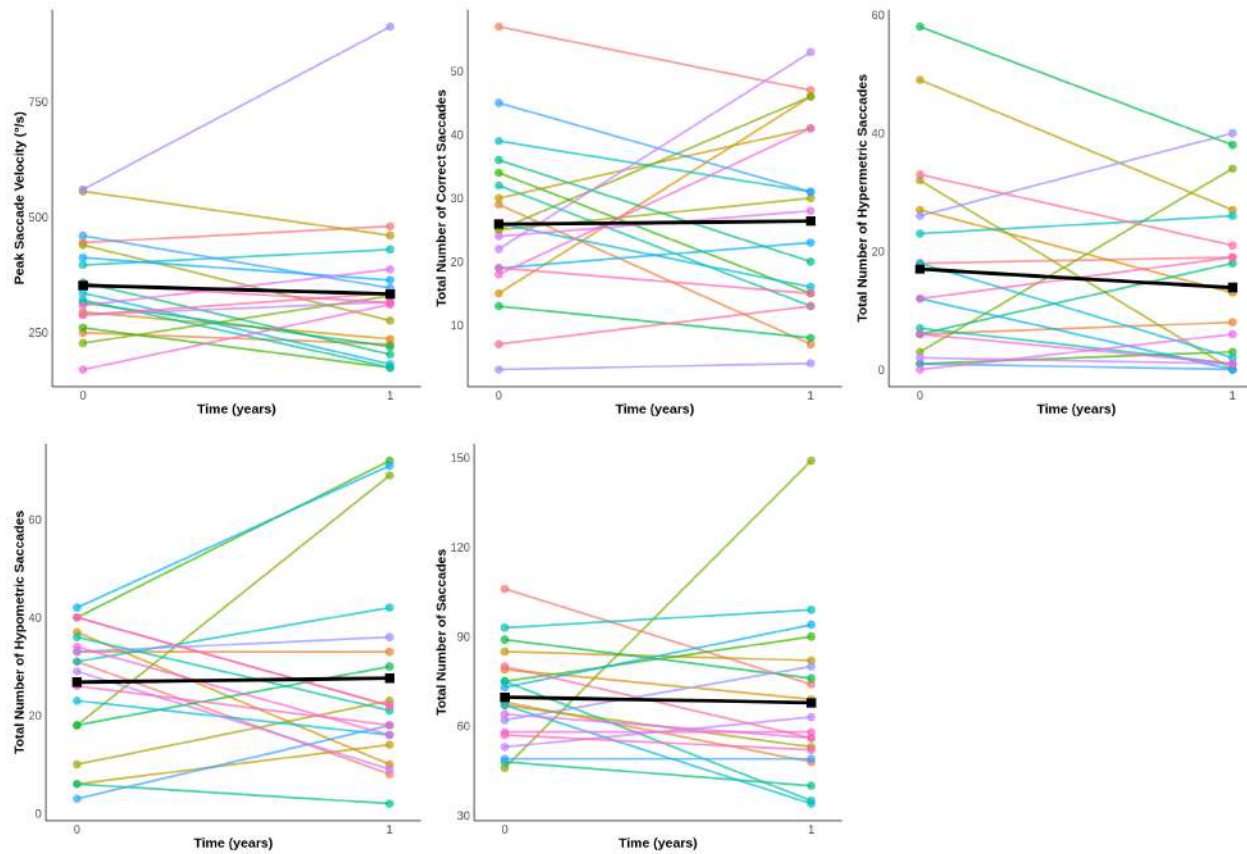


Figure 150: Volitional Saccades Vertical Metrics. Each line represents an individual; black line represents the mean change over time. Linear mixed-effects models were fitted separately for each metric, with age, sex, disease duration, and levodopa equivalent daily dose (LEDD) as fixed effects, and participant ID as a random effect. Statistical significance was set at $p < 0.05$.

Longitudinal Change Memory Guided Saccades Horizontal

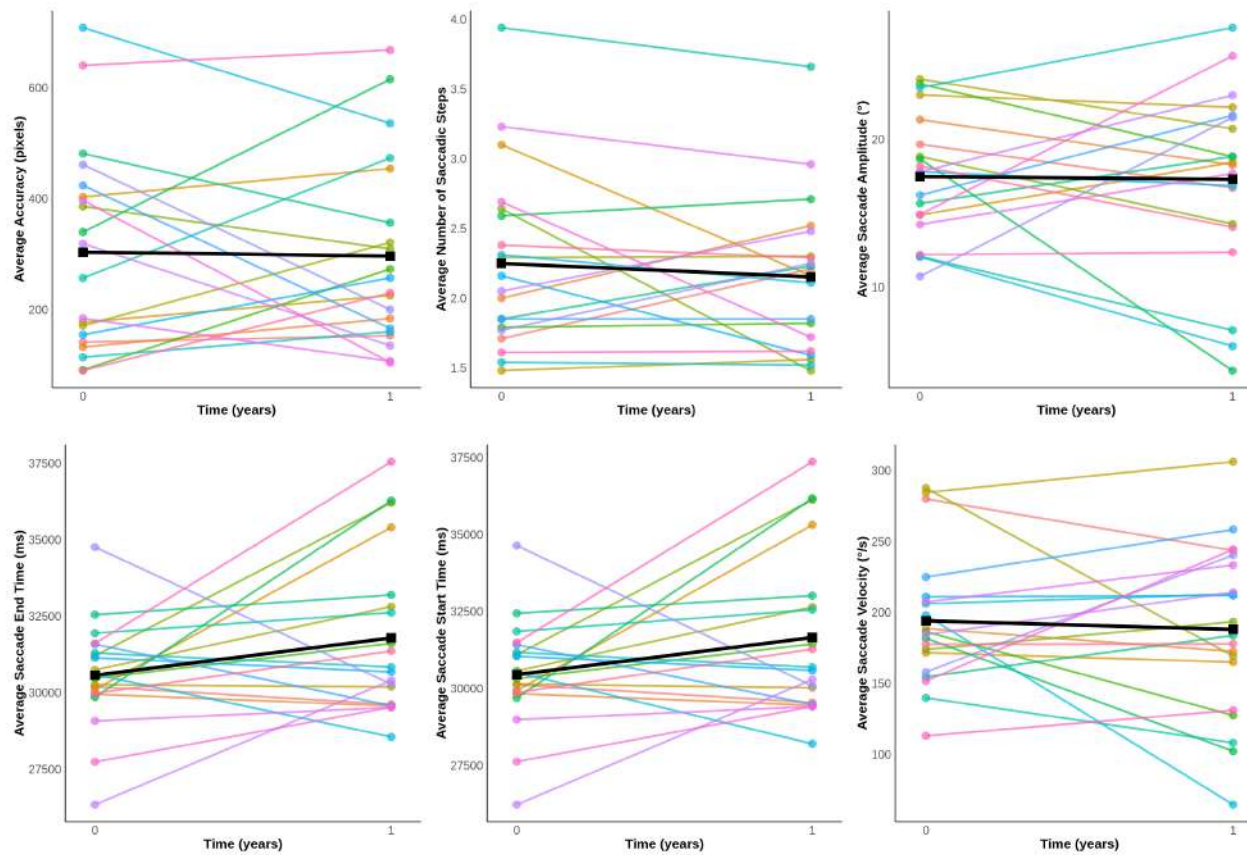


Figure 151: Memory Guided Saccades Horizontal Metrics. Each line represents an individual; black line represents the mean change over time. Linear mixed-effects models were fitted separately for each metric, with age, sex, disease duration, and levodopa equivalent daily dose (LEDD) as fixed effects, and participant ID as a random effect. Statistical significance was set at $p < 0.05$.

Longitudinal Change Memory Guided Saccades Horizontal

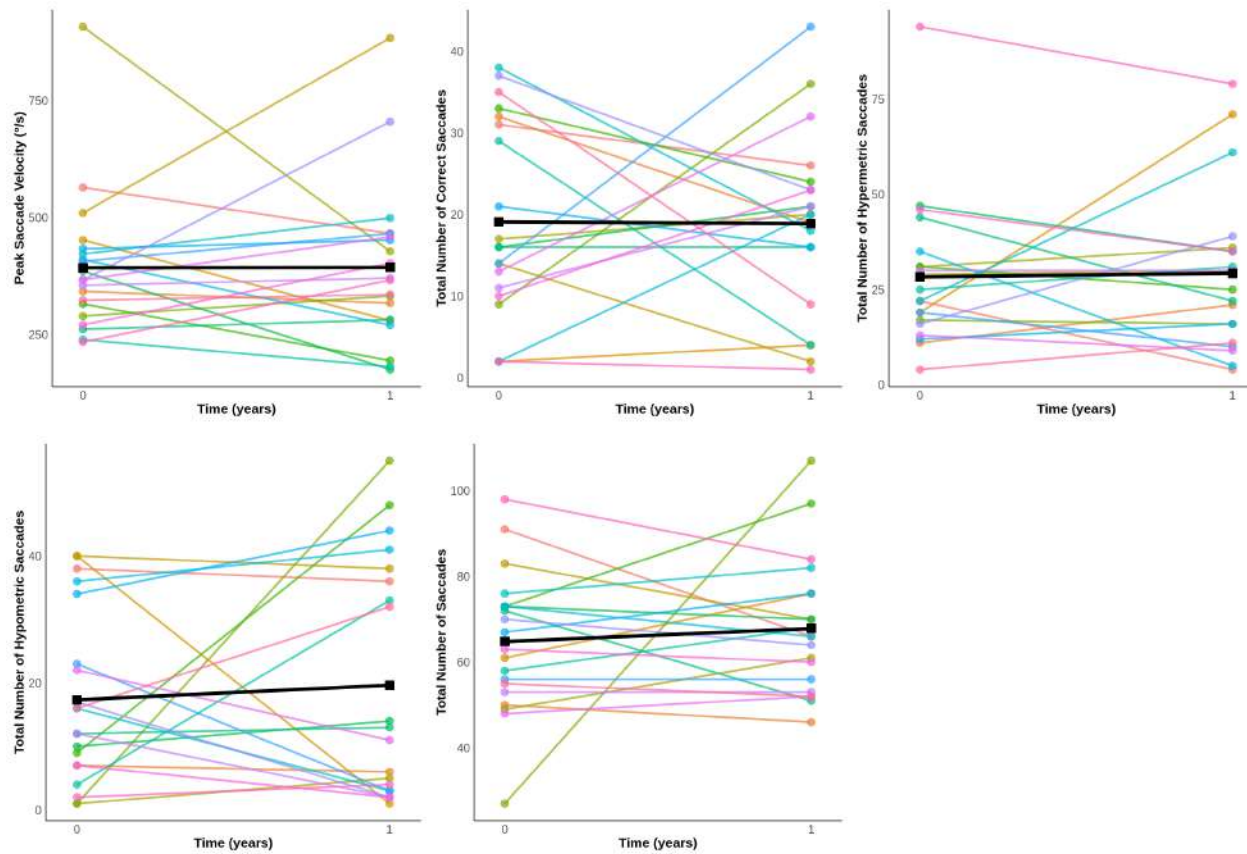


Figure 152: Memory Guided Saccades Horizontal Metrics. Each line represents an individual; black line represents the mean change over time. Linear mixed-effects models were fitted separately for each metric, with age, sex, disease duration, and levodopa equivalent daily dose (LEDD) as fixed effects, and participant ID as a random effect. Statistical significance was set at $p < 0.05$.

Longitudinal Change Memory Guided Saccades Vertical

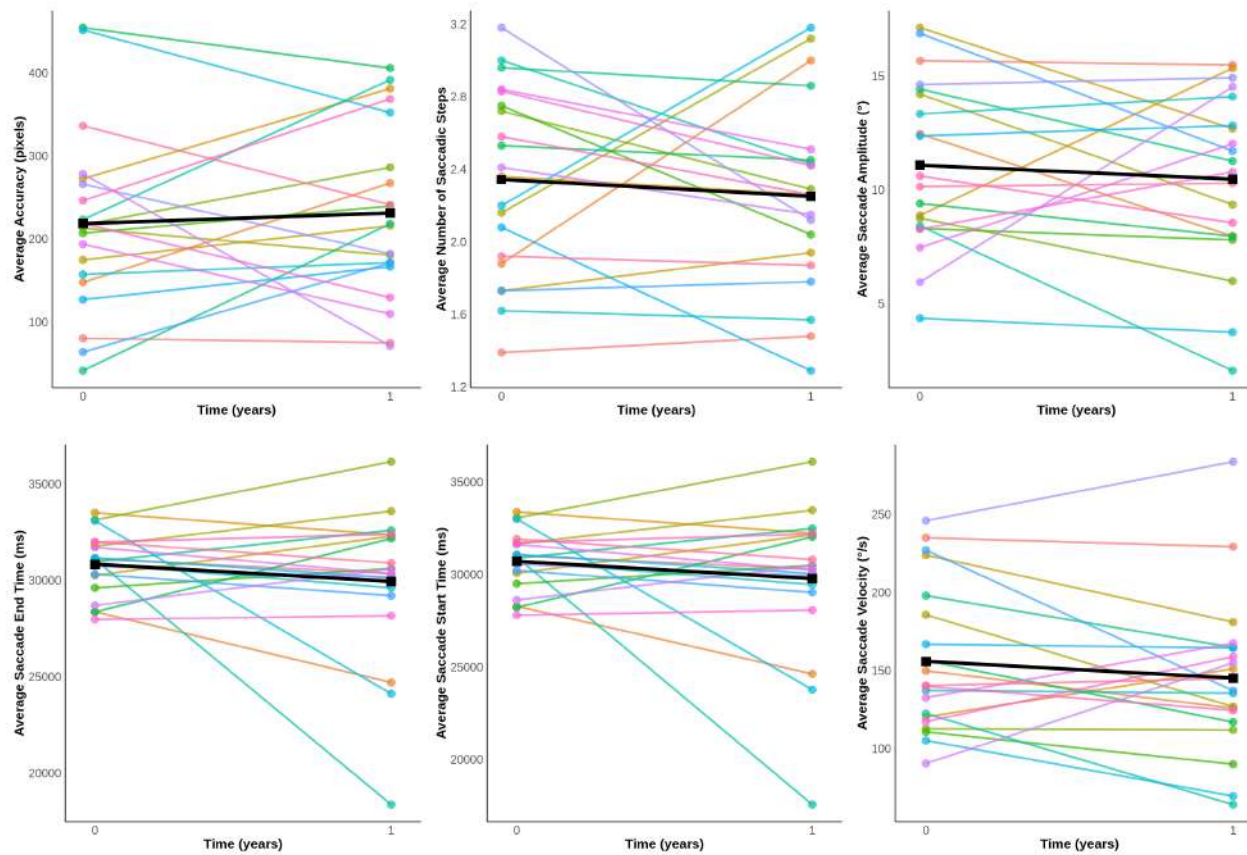


Figure 153: Memory Guided Saccades Vertical Metrics. Each line represents an individual; black line represents the mean change over time. Linear mixed-effects models were fitted separately for each metric, with age, sex, disease duration, and levodopa equivalent daily dose (LEDD) as fixed effects, and participant ID as a random effect. Statistical significance was set at $p < 0.05$.

Longitudinal Change Memory Guided Saccades Vertical

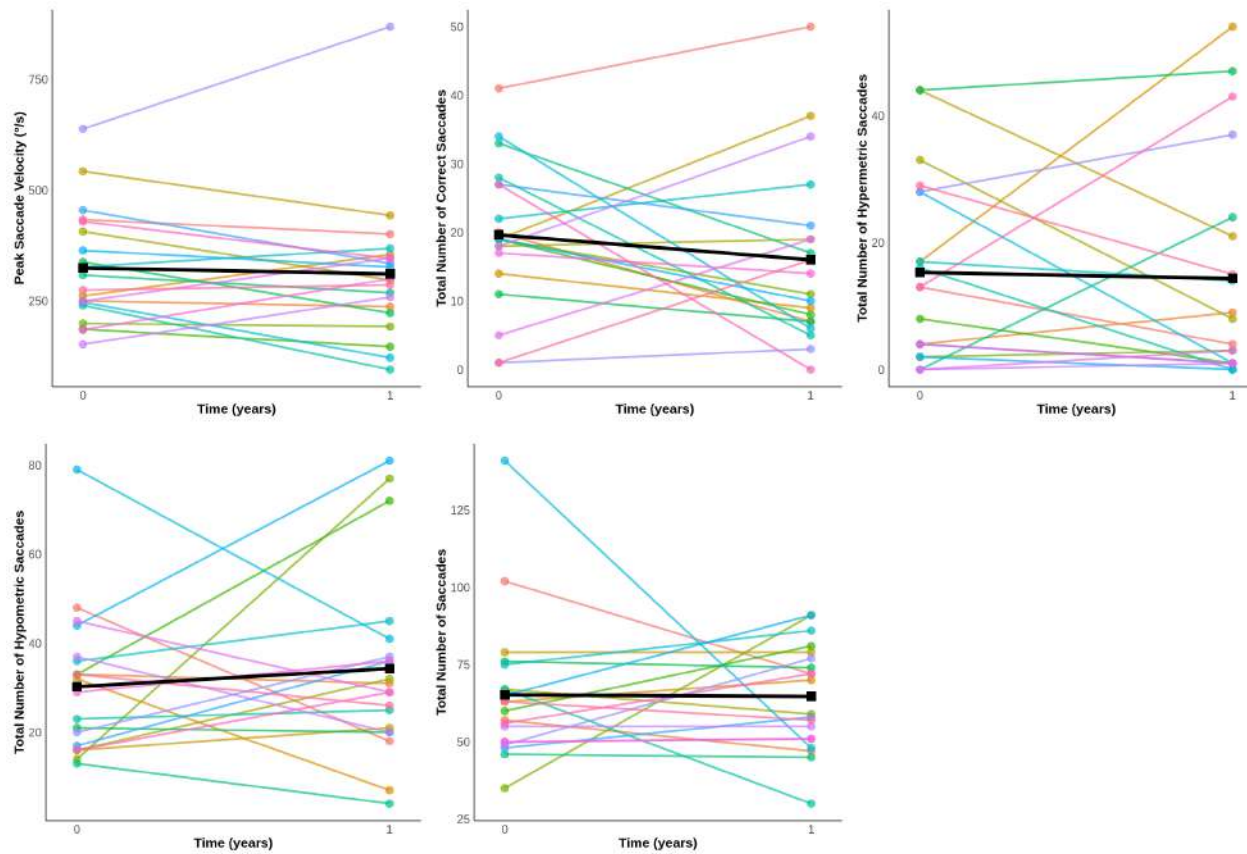


Figure 154: Memory Guided Saccades Vertical Metrics. Each line represents an individual; black line represents the mean change over time. Linear mixed-effects models were fitted separately for each metric, with age, sex, disease duration, and levodopa equivalent daily dose (LEDD) as fixed effects, and participant ID as a random effect. Statistical significance was set at $p < 0.05$.

5.4 Discussion

This project investigates the longitudinal changes in ocular motor function over a one-year period in PD. While previous studies have established cross-sectional correlations between eye movement metrics and disease severity, they have not explored how these metrics evolve over time. Moreover, the effects of dopaminergic medication, as measured by LEDD, on longitudinal changes in eye movements remain understudied. By addressing these gaps, this research evaluates eye movement metrics as potential biomarkers for disease progression and treatment efficacy. The findings of this study indicate that most eye movement metrics in fixation, pursuit, and saccades remain stable over one year. However, notable differences were observed in the number of SWJs, the antisaccade task, and the number of hypometric saccades. These findings provide quantitative evidence that specific eye movement metrics are sensitive to subtle changes in motor and cognitive function over time, potentially influenced by disease progression and dopaminergic treatment.

The observed decrease in the number of small SWJs after one year may reflect improved voluntary control due to medication effects, or potentially increased fatigue or declines in attentional and inhibitory control (Iakovakis et al. 2018). The modulatory effect of dopaminergic medication on fixation appears more prominent in the early stages of PD, as shown by the pairwise comparisons. Dopaminergic treatment in early PD may restore regularity in fixation, but as the disease progresses, alternative pathophysiological mechanisms may dominate, leading to greater variability (Adams et al. 2023). The decrease in SWJs with treatment aligns with broader motor improvements following dopamine agonists. Prior studies have found that early intervention can slow symptom progression (Y. Lee et al. 2019) (Poewe 2009 Adams et al. 2023 Iakovakis et al. 2018), though the efficacy of dopaminergic therapy declines in later disease stages (Poewe 2009). This reflects dopamine's known role in BG circuits, which suppress involuntary movements. However, the absence of changes in pursuit gain and reflexive saccades suggests dopaminergic therapy has limited impact on ocular motor functions reliant on non-dopaminergic pathways (Pinkhardt, Jürgens et al. 2012).

Antisaccade performance, reflecting executive dysfunction, declined over the year, likely due to progression of extra-nigral pathology affecting frontal-subcortical circuits (Poewe 2009). Dopaminergic replacement may not fully restore these deficits, highlighting the contribution of non-dopaminergic circuits (Antonini, D'Onofrio and Guerra 2023 Jankovic 2008). The increase in saccadic latency and self-corrected errors aligns with findings that these impairments reflect early cognitive decline even in non-demented PD (O. W. Wong

et al. 2018). Vertical antisaccade impairments suggest differential vulnerability of circuits controlling vertical versus horizontal saccades (Pinkhardt, Jürgens et al. 2012). Medial frontal cortex, linked to vertical control, may be more affected early in PD (Barbosa et al. 2019). The absence of changes in reflexive vertical saccades suggests impairments are specific to tasks requiring higher voluntary control (MacAskill, Graham et al. 2012).

The increase in hypometric saccades in oblique saccades at high eccentricities may reflect PD's nuanced impact on motor planning for large movements. Saccadic hypometria, linked to bradykinesia, is more evident with disease progression (Terao, Fukuda, Yugeta et al. 2011 MacAskill, Graham et al. 2012). Larger saccades require greater coordination, potentially explaining their vulnerability (Barbosa et al. 2019). In contrast, smaller saccades may be preserved longer (MacAskill, Graham et al. 2012). Individuals with shorter disease duration showed more changes in SWJs and antisaccades, while those with longer duration exhibited stability. This may reflect a ceiling effect, where advanced PD leaves little room for further decline over one year. Alternatively, early PD may show more variability and responsiveness to treatment. It is important to interpret these findings cautiously, as only specific metrics changed, not entire domains of ocular motor function. The significant changes in metrics such as hypometric saccades and antisaccadic latency raise the question of ageing versus disease progression. Including healthy controls in future studies could clarify age-related changes, enhancing the interpretability of eye movement metrics as a biomarker.

A key finding is the stability of most ocular motor metrics compared to the typical decline in other PD motor symptoms. This may reflect unique neuroanatomical substrates of eye movements. Unlike limb motor functions dependent on BG circuits, ocular motor control involves non-dopaminergic pathways, such as the SC, brainstem nuclei, and cerebellum (Pinkhardt, Jürgens et al. 2012). These circuits may be less susceptible to early degeneration or better compensated. Additionally, a one-year period may be too short to detect changes in ocular motor metrics. Unlike limb movements, eye movements are less affected by musculoskeletal constraints (Y. Lee et al. 2019).

Despite PD's neurodegeneration, the relative ocular motor stability may suggest adaptive neuroplasticity (O. W. Wong et al. 2018). Compensatory mechanisms, such as cerebellar support or recruitment of alternative circuits, may help preserve ocular motor function (Manto et al. 2012; Mitoma et al. 2020). These mechanisms may support less cognitively demanding tasks like reflexive saccades or pursuit in the short term. The

trajectory of ocular motor impairments may be non-linear, with early PD marked by dynamic change and advanced PD showing stable deficits. This implies a "window of sensitivity" in which eye movements are more responsive to disease progression and treatment. This window may be shaped by cognitive reserve—the brain's ability to compensate for neurodegeneration (Stern et al. 2019). An "ocular motor reserve" may preserve eye movement control through efficient or redundant pathways supported by visual engagement, plasticity, and genetics (Mitoma et al. 2020).

Other theories may explain ocular motor stability. Adaptive internal models, generated by the cerebellum and ocular motor system, predict and compensate for changes to preserve function (Wolpert, Ghahramani and Jordan 1995). Alternatively, the differential vulnerability hypothesis posits that not all neural circuits degenerate at the same rate in PD. Ocular motor pathways may be structurally or functionally more resilient. Microarray studies and laser capture of ocular motor neurons suggest lower susceptibility to excitotoxicity (Brockington et al. 2013). Understanding these mechanisms could inform therapies aimed at enhancing plasticity and compensatory pathways, ultimately supporting motor preservation in PD.

5.4.1 Clinical Implications

The findings of this study have significant clinical implications for the assessment and management of Parkinson's Disease (PD). First, the observation that specific ocular motor metrics—such as the number of SWJs, antisaccade task performance, and hypometric saccades—change over time suggests that these metrics may serve as valuable biomarkers for monitoring disease progression. Unlike traditional motor assessments, which can be subject to variability due to medication effects and patient fatigue, eye movement metrics provide objective, quantifiable data that could complement existing clinical evaluations.

The stability of most ocular motor metrics over a one-year period, despite the progressive nature of PD, suggests the presence of compensatory mechanisms that may maintain function in the early stages of the disease. This raises the possibility that early intervention strategies, such as neuroprotective treatments or rehabilitative therapies, could be designed to enhance these compensatory pathways and delay disease progression. Furthermore, the differential effects of dopaminergic therapy on specific eye movement metrics highlight the selective influence of dopamine replacement on certain motor circuits. For instance, the improvement in fixation regu-

larity and reduction in SWJs with dopaminergic therapy suggest that fixation abnormalities in early-stage PD may be responsive to treatment. However, the limited impact of medication on antisaccadic performance and hypometric saccades underscores the involvement of non-dopaminergic pathways in ocular motor dysfunction.

From a diagnostic perspective, incorporating eye movement testing into routine clinical evaluations could aid in the early detection of PD. Given that impairments in antisaccades and hypometric saccades reflect executive dysfunction and bradykinesia, respectively, these metrics could be particularly useful in identifying patients at risk of cognitive decline or more severe motor impairment. Additionally, the observed directional bias in vertical antisaccadic impairments suggests that eye movement testing could help differentiate PD from other parkinsonian syndromes with distinct neuroanatomical involvement.

5.4.2 Limitations

The follow-up study examining eye movements in PD after one year also has several limitations that should be considered. Firstly, the sample size remains relatively small, with only 20 participants completing the study. This limited sample may reduce the statistical power to detect subtle changes in eye movement metrics over time, particularly when examining subgroup interactions such as disease severity, age, and medication effects.

Another limitation is the reliance on a one-year follow-up period. While this provides valuable insights into short-term progression, it does not capture the long-term trajectory of ocular motor decline in PD. A longer follow-up period, with multiple assessment points, would allow for a more detailed characterization of disease-related changes in eye movements.

Additionally, while statistical models were used to account for individual variability and multiple comparisons, the presence of unmeasured confounding factors cannot be ruled out. Factors such as cognitive decline, fluctuations in attention, and subtle changes in visual function could influence eye movement metrics over time.

Lastly, participants were assessed while on their usual dopaminergic medication regimen. Since levodopa and other dopaminergic treatments can modulate eye movements, future studies should consider evaluating participants in both medicated and unmedicated states to determine the direct effects of disease progression

independent of pharmacological influence.

5.4.3 Future Directions

To build on these findings, future research should extend the follow-up period to capture longer-term changes in ocular motor function, allowing for better correlation with the progression of motor symptoms. Additionally, investigating the neuroanatomical basis of the directional bias observed in vertical antisaccadic impairments could provide insights into the differential involvement of cortical and subcortical structures in PD. It would also be valuable to explore the impact of specific dopaminergic therapies on ocular motor metrics, including the effects of combinations of medication and non-pharmacological interventions. Including larger and more diverse cohorts, particularly individuals with genetic PD and atypical parkinsonian syndromes, would help generalize findings across different subtypes. Finally, investigating potential interactions between ocular motor metrics and other non-motor symptoms, such as sleep disturbances and cognitive decline, could uncover shared pathways of neurodegeneration.

Overall, the current study offers many insights into the longitudinal changes occurring in ocular motor function in PD over a one-year period. Indeed, most of the eye movement metrics remained relatively stable, though important changes were recorded in specific tasks, such as antisaccade performance and hypometric saccades, as subtle shifts reflective of motor and cognitive function may also be influenced by disease progression and treatment with dopaminergic drugs. The relative preservation of ocular motor metrics, despite the inherently progressive nature of PD, likely underscores the presence of compensatory mechanisms, including neuroplasticity, which may underpin the preservation of certain eye movement functions in the earliest stages of disease progression. However, the trajectory of ocular motor impairment appears to evolve in a non-linear fashion with dynamic changes observed in early-stage PD and relatively, yet persistently abnormal, profiles in the advanced stages of disease. These observations emphasize the requirement for longer assessments to fully define the evolution of eye movement deficits and their usefulness as biomarkers for disease progression. Future research should determine the neuroanatomical underpinnings of observed directional biases, investigate the role of dopaminergic therapies, and include larger, more diverse cohorts to explore the broader applicability of these findings. We can extend our knowledge of the complex relationship between ocular motor function and PD, and perhaps from that, new targets for therapeutic interventions will

emerge that will improve the quality of life for people with Parkinson's disease.

5.5 Chapter Summary

This chapter explored the longitudinal changes in ocular motor function over a one-year period in PD, addressing gaps in previous research that primarily focused on cross-sectional analyses. The study found that while most eye movement metrics remained stable, significant changes were observed in SWJs, antisaccade task performance, and hypometric saccades. These findings suggest that specific ocular motor impairments may be sensitive to disease progression and dopaminergic treatment effects, offering potential biomarkers for monitoring PD.

6 Saccadic Adaptation in Parkinson's Disease and Multiple System Atrophy

6.1 Introduction

Saccadic adaptation is one of the neurophysiological processes that allows the ocular motor system to adjust the amplitude of saccades in response to visual errors (Havermann, Volcic and Lappe 2012). The implications of saccadic adaptation extend beyond eye movements, encompassing overall cognitive and motor function. This suggests that the ocular motor system is not only reactive but also anticipatory, as it can adjust saccadic behaviour based on contextual factors and prior experiences (A. L. Wong and Shelhamer 2011).

During saccadic motion, when there is a rapid movement to change the field of view, discrepancies between the intended and actual end position of the eye can lead to misperceptions of objects within the visual field. Saccadic adaptation allows the recalibration of motor commands to reduce discrepancies and stabilise visual perception. This adaptation is aided by sensory feedback and corollary discharge signals, allowing the brain to predict the expected end position of visual targets (Havermann, Volcic and Lappe 2012; Panouillères, Urquizar et al. 2011). Furthermore, saccadic adaptation also modifies the perceptual accuracy of visual stimuli, ensuring that the perceived location of objects is in line with their actual position in the environment, as deviations in saccade end points can lead to the mislocalisation of visual stimuli (Tyralla, Pomè and Zimmermann 2023; Stefan Van der Stigchel et al. 2020; Awater et al. 2005). Lastly, as the ocular motor system operates through a preprogrammed mechanism, it is susceptible to systematic errors such as consistently overshooting or undershooting a target. Saccadic adaptation allows the recalibration of saccadic gain, which is the ratio between the amplitude of the saccade and the target distance, and highlights the system's ability to learn and maintain optimum ocular motor performance (Waespe and Baumgartner 1992; A. Z. Khan, Heinen and McPeck 2010). Interestingly, the process of saccadic adaptation does not only rely on corrective saccades. Research has shown that there is a dissociation between the neural mechanisms that are responsible for adaptation and those generating corrective saccades, suggesting that the brain can possibly adapt saccadic commands without necessarily producing a corrective saccade (Panouillères, Urquizar et al. 2011).

6.1.1 Neural Circuitry of Saccadic Adaptation

Saccadic adaptation primarily involves neural circuits including the superior colliculus (SC), the cerebellum, and cortical areas. In the adaptation process, the SC acts as the major hub for integrating sensory information and generating motor commands for saccades. The SC receives input from various cortical areas including the frontal eye fields (FEF) and lateral intraparietal area, which are pivotal for the planning and execution of eye movements (Ipata et al. 2006; Schütz, Kerzel and Souto 2014). The output of the SC is directed towards brainstem nuclei involved in the execution of saccades, and adaptive saccades modify the efficacy of these commands (Takeichi, Kaneko and Albert F. Fuchs 2007). The SC is also involved in the adaptation of saccadic commands based on visual feedback (Kojima, Soetedjo and Albert F. Fuchs 2011).

Regions of the cerebellum, including the ocular motor vermis and lobules VI and VII, are involved in saccadic adaptation through the fine-tuning of motor commands by adjusting saccadic amplitude in response to visual errors (Salman et al. 2006; Golla et al. 2008). The adaptive role of the cerebellum not only involves a reflexive response but also learning mechanisms that alter the motor output based on previous error learning (Salman et al. 2006; Panouillères, Urquizar et al. 2011). Some studies have also highlighted that different parts of the cerebellum might have a specialised role for adaptation of different types of saccades. It was found that medial focal lesions impaired the adaptation of reflexive saccades but not scanning voluntary saccades, whereas a lateral lesion impaired adaptation of scanning voluntary saccades but not reflexive saccades (Alahyane et al. 2008).

In addition to the SC and the cerebellum, the nucleus reticularis tegmenti pontis, which is a bridge between the basal ganglia and the cerebellum, is also involved in the neural circuitry for saccadic adaptation. This region receives input from the SC and has projections to the brainstem areas involved in saccadic control. Changes have been observed in the neural pathways involving the nucleus reticularis tegmenti pontis during saccadic adaptation, suggesting that it plays a role in modulating the signals driving the adaptation process (Quessy, Quinet and Freedman 2010).

The cortical areas also play a significant role in saccadic adaptation, particularly the FEFs and the supplementary eye fields. Both regions have been found to be activated in functional imaging studies during saccadic adaptation tasks, highlighting their role in the planning and execution of adapted saccades (Blurton, Raabe

and Greenlee 2012). The interaction between the cortical and subcortical regions, along with the SC and the cerebellum, forms a neural network involved in processing visual errors and adjusting motor commands accordingly (Zimmermann, D. Burr and Morrone 2011).

6.1.2 Saccadic Adaptation in Parkinson's Disease

In PD, saccadic adaptation exhibits selective impairments, particularly in memory-guided saccades, while visually guided saccades remain largely intact (MacAskill, T. J. Anderson and R. D. Jones 2002). PD is characterised by degeneration of the basal ganglia, which play a crucial role in modulating motor output, including eye movements (Lang and Lozano 1998). Research suggests that the basal ganglia do not directly govern saccadic adaptation but may influence its execution by disrupting communication between the frontal cortical regions—responsible for volitional eye movement control—and subcortical ocular motor centres (Brainard and Doupe 2000; Lawrence 2000). This impairment is evident in the adaptive mechanisms required to modify memory-guided saccades, which rely more on frontal circuits than cerebellar pathways (Optican and David S. Zee 1984; Takagi, David S. Zee and Tamargo 1998). Parkinsonian patients typically exhibit saccadic hypometria, a tendency to undershoot visual targets, and while they retain the ability to adaptively increase or decrease saccade amplitude in reflexive saccades, their capacity to adjust memory-guided saccades is markedly diminished (Deubel 1999; C. J. Erkelens and Hulleman 1993). These findings align with a broader understanding of PD-related deficits, where automatic or externally cued movements are better preserved than internally generated, volitional movements (C. A. Antoniadis and Spering 2024). The differential effects of PD on saccadic adaptation underscore the importance of the basal ganglia-frontal cortex pathways in motor learning and highlight potential avenues for rehabilitative strategies aimed at enhancing adaptive eye movement control in these patients.

6.1.3 Saccadic Adaptation in Multiple System Atrophy

Unlike PD, MSA remains largely unstudied in the context of saccadic adaptation, creating a significant gap in our understanding of how this disorder affects eye movement recalibration. MSA is a progressive neurodegenerative condition characterised by varying degrees of basal ganglia and cerebellar involvement, depending on whether it manifests primarily as multiple system atrophy - parkinsonian (MSA-P) (parkinsonian subtype) or

multiple system atrophy - cerebellar (MSA-C) (cerebellar subtype) (Ubhi, P. Low and Masliah 2011). Given the established role of the cerebellum in saccadic adaptation, it is plausible that MSA patients—particularly those with predominant cerebellar degeneration—would exhibit pronounced deficits in their ability to adapt saccade amplitudes (Optican and David S. Zee 1984; Takagi, David S. Zee and Tamargo 1998). Studies in cerebellar disorders show that lesions can impair or completely abolish saccadic adaptation, leading to persistent dysmetria, either as hypometria or hypermetria (Waespe and Baumgartner 1992; Straube and Deubel 1995; Straube, Deubel et al. 1995). If a similar mechanism operates in MSA, affected individuals may struggle to adjust their saccades to compensate for inaccuracies, resulting in a progressive decline in eye movement control. However, without empirical research explicitly investigating saccadic adaptation in MSA, these assumptions remain speculative. Future studies are necessary to determine the extent to which saccadic adaptation is impaired in MSA and whether deficits in this process contribute to the broader ocular motor dysfunction observed in these patients.

6.2 Project Aims

1. To investigate deficits in saccadic adaptation in PD and MSA.
2. To explore the implications of saccadic adaptation impairments for motor learning and neural plasticity in these conditions.

6.3 Methods

6.3.1 Participants

Participants were recruited for the saccadic adaptation study in PD and MSA through the methods described in Chapter 2: General Methods. Inclusion criteria were: (1) a confirmed diagnosis of MSA as per Chapter 2, (2) a confirmed diagnosis of idiopathic PD, (3) age between 40–80 years, (4) normal or corrected-to-normal vision, (5) ability to provide informed consent, (6) ability to follow verbal instructions, and (7) ability to sit for the duration of testing. Participants were excluded if they: (1) had other neurological conditions or a history of head trauma or stroke, (2) had bilateral visual impairments (if one eye was impaired, the other was recorded) or movement-related impairments such as diplopia, (3) had severe psychiatric conditions (e.g., psychosis), (4)

had systemic conditions affecting vision (e.g., diabetic retinopathy), (5) were pregnant or potentially pregnant (self-reported), (6) had a history of epilepsy, (7) had eyelid opening apraxia, (8) were physically unable to sit for testing, or (9) had severe ocular motor impairment preventing successful calibration and validation during the eye-tracking setup.

Healthy controls were recruited using the same procedures described in Chapter 2. Inclusion criteria were: (1) no history of neurodegenerative, neurological, or movement disorders, (2) normal or corrected vision, (3) normal cognitive function, and (4) ability to provide consent and comply with procedures. Exclusion criteria matched the clinical group, including bilateral visual impairments, psychosis, systemic visual-affecting conditions, pregnancy, or a history of epilepsy.

Participants were grouped into three cohorts: idiopathic PD, MSA, and healthy controls. A total of 31 participants were included: 18 with idiopathic PD, 4 with MSA, and 9 healthy controls. The study was approved by the UCL research ethics committee, and informed consent was obtained from all participants prior to testing.

6.3.2 Experimental Protocol

The experimental setup followed procedures described in Chapter 2: General Methods, including standard calibration and validation.

The experimental paradigm had two phases: (1) the adaptation phase with a stepped target, and (2) the test phase with a standard target. The adaptation phase comprised 100 trials where the target first moved 10° horizontally and then stepped inward by 2°. The test phase also comprised 100 trials with the target moving 10° horizontally without stepping. A gaze-contingent drift check was employed, triggering recalibration if eye drift exceeded 2°. Breaks were allowed between blocks, with recalibration as needed.

6.3.3 Data Processing and Analysis

Eye-tracking data were processed using Data Viewer (SR Research). Saccade reports included amplitude, average and peak velocity, and saccade start time. Trials were divided into adaptation and test phases, and

saccadic gain was calculated as the ratio of saccade amplitude to the original target amplitude (10°). Mean saccadic metrics and gain were computed for each participant per phase. Additionally, trials were grouped into blocks of 10 (e.g., trials 1–10, 11–20), and block-wise average gain was calculated.

6.3.4 Statistical Analyses

Descriptive statistics were used to summarise participant demographics and saccadic metrics per task phase. Normality was assessed using the Shapiro–Wilk test, and since most data were not normally distributed, non-parametric analyses were performed. Between-group comparisons (e.g., PD vs. controls, MSA vs. controls) were conducted using Mann–Whitney U tests. Within-group comparisons (e.g., early vs. late adaptation) were assessed using Wilcoxon signed-rank tests. Saccadic gain from the first 10 trials was compared to that from the last 10 trials of each phase to assess adaptation. Between-group differences in gain change were also tested. Bonferroni correction was applied to all multiple comparisons. Additionally, percentage change in gain was calculated between the first and last trial blocks per group and phase. Significance was defined as $\alpha = 0.05$. All analyses were performed in R (Version 2023.09.1+494, R Core Team, Vienna, Austria).

6.4 Results

6.4.1 Participants

The final cohort included 31 participants: 9 controls, 4 with MSA, and 18 with PD. The control group had a mean age of 56.49 years (SD = 16.39) and comprised 5 males and 4 females. The MSA group had a mean age of 66.75 years (SD = 7.93), with 1 male and 3 females, and a mean disease duration of 6.67 years. The PD group had a mean age of 66.35 years (SD = 6.82), with 12 males and 6 females, and a mean disease duration of 5.34 years.

Table 13: Demographic and clinical characteristics of the study cohort. Values are presented as mean \pm standard deviation (SD). Age is reported for all participants. Data are stratified by group and sex. “-” indicates not applicable or unavailable.

Group	Age (Mean \pm SD)
MSA (N = 4)	66.75 \pm 7.93
Males (N = 1)	55.00 \pm -
Females (N = 3)	70.67 \pm 1.53
PD (N = 18)	66.35 \pm 6.82
Males (N = 12)	67.01 \pm 6.21
Females (N = 6)	65.05 \pm 8.39
Control (N = 9)	56.49 \pm 16.39
Males (N = 5)	51.23 \pm 20.03
Females (N = 4)	63.06 \pm 8.81

6.5 Results

6.5.1 Participants

The study included 31 participants: 9 controls, 4 MSA, and 18 PD. The control group had a mean age of 56.49 years (SD = 16.39), with 5 males and 4 females. The MSA group had a mean age of 66.75 years (SD = 7.93), with 1 male and 3 females, and a mean disease duration of 6.67 years. The PD group had a mean age of 66.35 years (SD = 6.82), with 12 males and 6 females, and a mean disease duration of 5.34 years.

6.5.2 Saccadic Adaptation in Controls

In the adaptation phase, controls exhibited a significant decrease in gain of 17.44% between the first 10 trials and the last 10 trials ($p = 0.001$). Peak saccade velocity and average saccade velocity decreased by 13.87% and 13.03%, respectively. Saccade duration increased by 192.31%, and saccade start time increased by 19.78%. However, these changes in saccadic metrics were not statistically significant. In the test phase, gain significantly increased by 13.60% ($p = 0.04$), while other saccadic metrics showed no significant differences. Average saccade velocity marginally increased, whereas saccade duration, peak saccade velocity, and saccade

start time decreased across the test phase.

6.5.3 Saccadic Adaptation in Parkinson's Disease

Mann–Whitney U tests comparing gain and saccadic metrics between PD and controls revealed no significant differences in either the adaptation or test phase. Similarly, Wilcoxon signed-rank tests within the PD group indicated no significant intra-group differences. Nonetheless, during the adaptation phase, individuals with PD showed a significant gain reduction of 12.14% ($p = 0.002$) between the first 10 and the last 10 trials. Saccade duration and start time increased by 27.73% and 16.25%, respectively, while average and peak saccade velocities slightly decreased. In the test phase, gain increased by 3.87%, and saccade start time increased by 17.40%, with small reductions in average velocity, peak velocity, and saccade duration. These changes were not statistically significant. Overall, the PD group exhibited a clear reduction in gain during the adaptation phase.

6.5.4 Saccadic Adaptation in Multiple System Atrophy

Mann–Whitney U tests comparing gain and saccadic metrics between MSA and controls showed no significant differences in either the adaptation or test phase. Wilcoxon signed-rank tests within the MSA group also indicated no significant intra-group differences. Nonetheless, descriptive analysis revealed that, compared to PD and controls, MSA participants showed only a 4.28% decrease in gain during the adaptation phase, which was not significant. Saccade duration increased by 21.40%, and unlike the other groups, start time decreased by 9.36%. Peak and average saccade velocities remained relatively stable (less than 1% change). In the test phase, gain increased by 5.76%, which was greater than in PD but less than in controls. Average saccade velocity decreased by 5.81%, while peak velocity increased by 3.49%. Saccade duration and start time increased by 65.01% and 13.16%, respectively. No significant differences in gain or saccadic metrics were observed between the first and last 10 trials of the test phase.

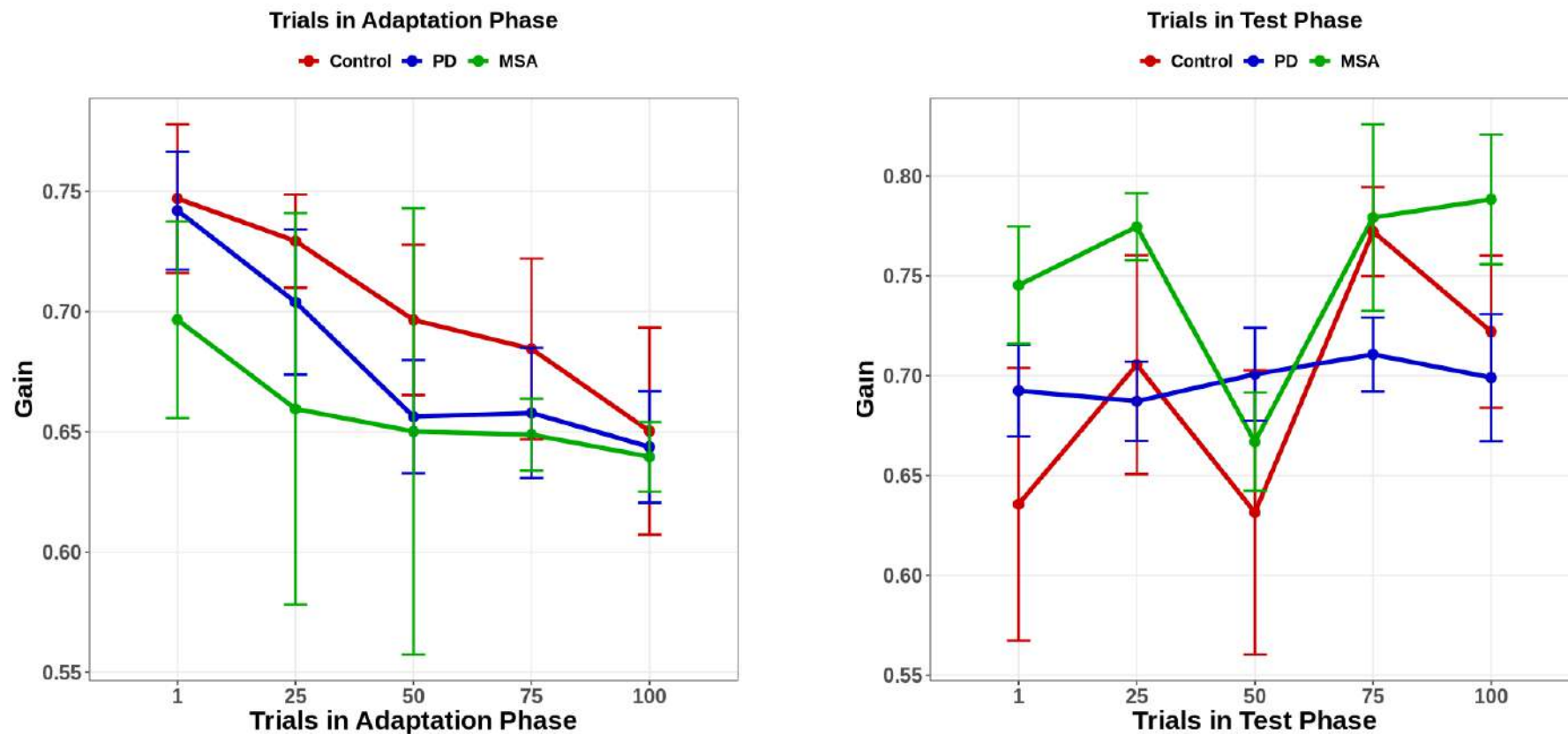


Figure 155: Gain in Adaptation and Test Phases. Mean gain for increments of 25 trials were plotted with SD. Line graphs show the mean saccadic gain (\pm standard error) across trial blocks for each group and phase. Percentage change in gain was calculated to assess adaptation within groups, and between-group differences in gain change were evaluated using non-parametric tests. Bonferroni correction was applied for multiple comparisons. Statistical significance was defined as $p < 0.05$.

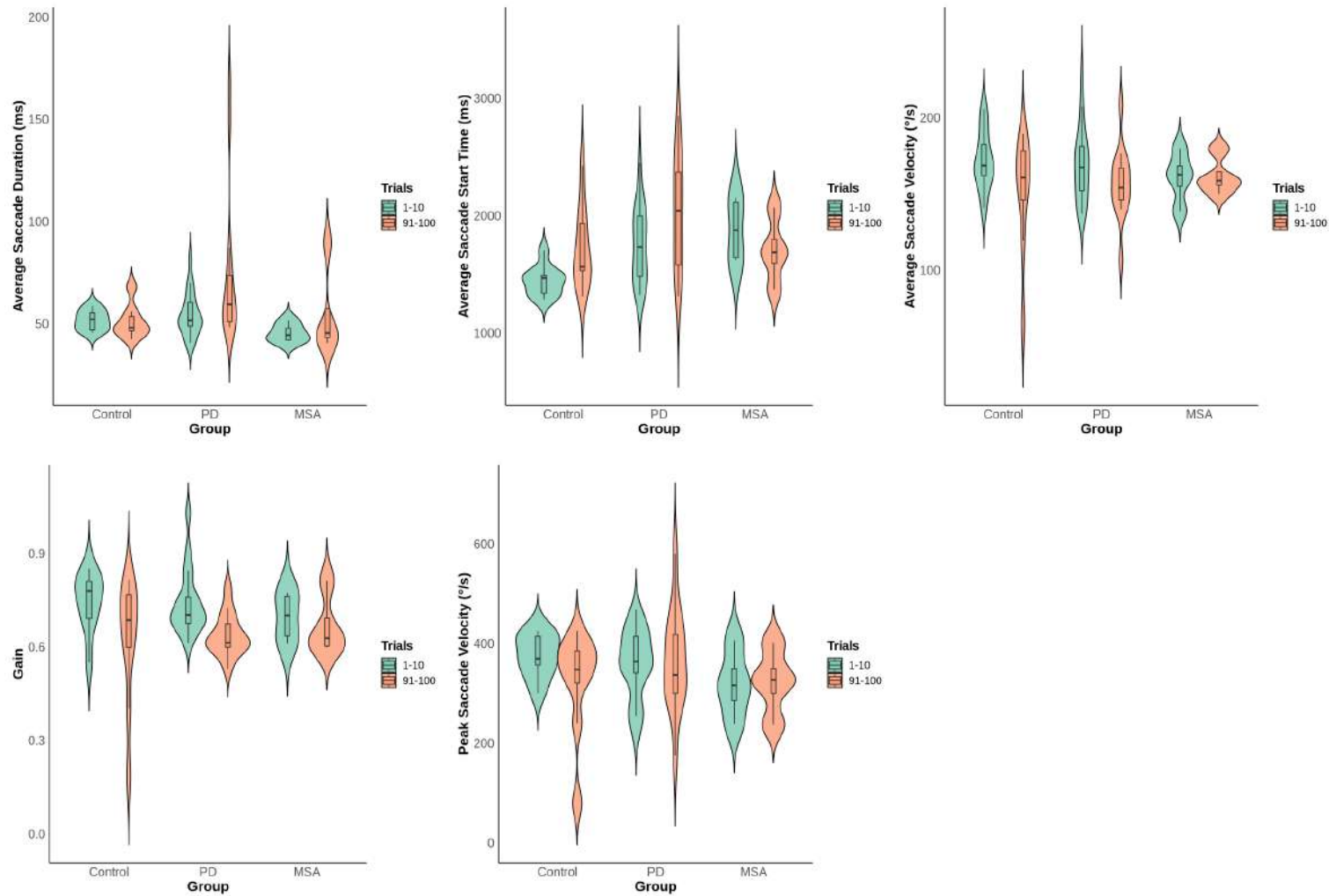


Figure 156: Metrics in Adaptation Phase. Average metrics for trial 1-10 and trials 91-100 are plotted. Between-group comparisons (e.g., PD vs. controls, MSA vs. controls) were conducted using Mann–Whitney U tests, while within-group comparisons (e.g., early vs. late adaptation) were assessed using Wilcoxon signed-rank tests. Bonferroni correction was applied to adjust for multiple comparisons. Statistical significance was set at $p < 0.05$.

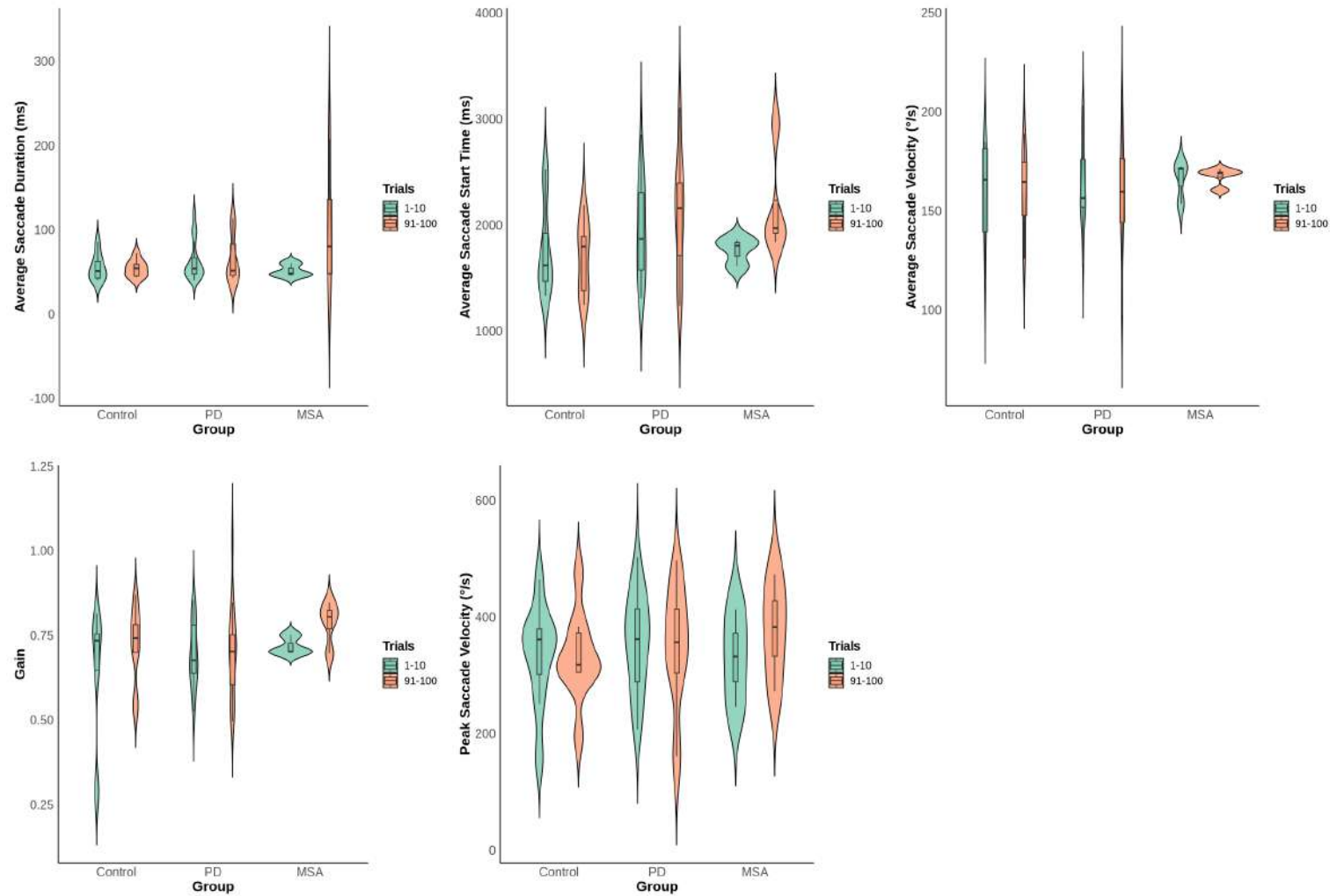


Figure 157: Metrics in Test Phase. Average metrics for trial 1-10 and trials 91-100 are plotted. Between-group comparisons (e.g., PD vs. controls, MSA vs. controls) were conducted using Mann–Whitney U tests, while within-group comparisons (e.g., early vs. late adaptation) were assessed using Wilcoxon signed-rank tests. Bonferroni correction was applied to adjust for multiple comparisons. Statistical significance was set at $p < 0.05$.

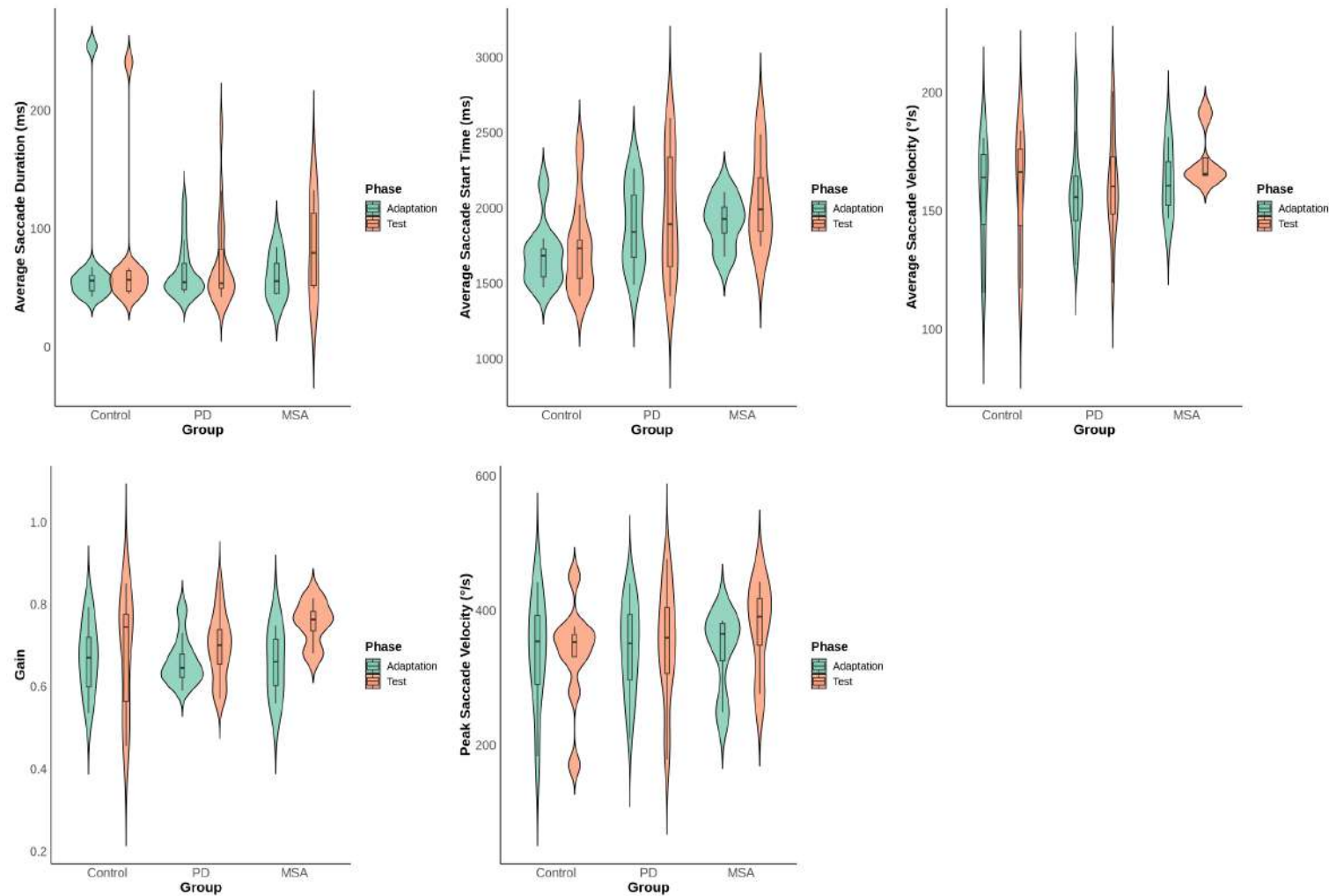


Figure 158: Metrics in Adaptation and Test Phases. Average metrics for each phase. Between-group comparisons (e.g., PD vs. controls, MSA vs. controls) were conducted using Mann–Whitney U tests, while within-group comparisons (e.g., early vs. late adaptation) were assessed using Wilcoxon signed-rank tests. Bonferroni correction was applied to adjust for multiple comparisons. Statistical significance was set at $p < 0.05$.

6.6 Discussion

This study aimed to investigate saccadic adaptation in individuals with idiopathic PD, MSA, and healthy controls to better understand motor learning and neural plasticity differences across these groups. The findings provide insights into the integrity of sensorimotor recalibration mechanisms and the neural substrates supporting such adaptation. Saccadic adaptation is primarily regulated by the cerebellum, which plays a role in adjusting movements to maintain accuracy. The ocular motor vermis and the caudal fastigial nucleus are key structures that help fine-tune saccadic gain, ensuring that eye movements remain precise over time (Helmchen, Machner et al. 2022). Other regions, such as the SC and FEF, also contribute to this adaptation (Métais et al. 2022).

Healthy controls demonstrated a robust saccadic adaptation response, evidenced by a significant reduction in gain across the adaptation phase, followed by clear deadaptation in the test phase. These results are consistent with established literature, indicating intact error-based learning mechanisms in healthy adults (Métais et al. 2022). Neuroimaging work has advanced our understanding of the neural architecture underlying saccadic adaptation in healthy individuals. Beyond the cerebellum, saccadic adaptation involves a broad network of cortical and subcortical regions, including the medial temporal areas, FEF, parietal eye fields (PEF), precuneus, and right pallidum, each contributing uniquely to motor recalibration, visual error processing, and directional adaptation (Blurton, Raabe and Greenlee 2012; Gerardin et al. 2012; Guillaume et al. 2018). Furthermore, the visual and parietal cortices have also been implicated in error detection and trans-saccadic spatial updating, suggesting that adaptation encompasses both motor execution and perceptual recalibration components (Cheviet, Pisella and Pélisson 2021; Baltaretu et al. 2020). Altogether, saccadic adaptation in healthy individuals is a multistage process, engaging a hierarchical network where the cerebellum executes fast motor recalibration, subcortical structures relay signals, and cortical areas support perceptual remapping, attention shifts, and integration of error feedback.

In contrast, individuals with PD also exhibited a significant but more modest gain reduction during adaptation and a blunted deadaptation. Although these changes were not statistically different from controls, they suggest some degree of preserved but attenuated adaptive plasticity in PD. This is noteworthy given the dopaminergic system's central role in reward prediction and error correction—functions critical for adaptation (Keiflin and Janak 2015). Dopaminergic deficits reduce sensitivity to performance feedback, resulting in attenuated

trial-by-trial updates in adaptation. In PD, while the cerebellum is relatively spared, dopaminergic depletion in the basal ganglia, particularly in the striatum, may indirectly affect saccadic adaptation by impairing motivation and internal performance monitoring (Zhong et al. 2022; Zhai et al. 2023). This could explain the reduced but preserved adaptation observed. Additionally, PD-related impairments in internal prediction of movement outcomes may hinder error detection and correction.

MSA participants showed the least change in gain during the adaptation phase and only moderate deadadaptation. This flattened adaptation curve points to cerebellar circuitry dysfunction, often compromised in MSA, particularly in the cerebellar subtype (S. Ren et al. 2019). Unlike PD, where the basal ganglia are predominantly affected, MSA encompasses widespread neurodegeneration, including brainstem and cerebellar structures crucial for visuomotor recalibration (Block and Celnik 2013; Abrahão et al. 2011). Brainstem atrophy likely contributes to deficits in coordinating saccade generation via the paramedian pontine reticular formation and feedback modulation from the cerebellum (E. E. Benarroch 2003; Ramat et al. 2007). Furthermore, disruption in the cerebello-thalamo-cortical loop may impair predictive coding, interfering with both detection and correction of saccadic errors (Cao et al. 2018).

In healthy controls, the adaptation phase was associated with a substantial increase in saccade duration, reflecting more controlled and effortful motor recalibration. This supports the idea that the ocular motor system becomes temporarily less efficient while compensating for visual error (Masselink and Lappe 2021; Wagner, C. Wolf and Schütz 2021). Saccadic latency also increased moderately, indicating cautious initiation during adaptation. Both average and peak saccade velocities decreased, though not significantly, suggesting reduced motor drive or deliberate slowing for precision. During the test phase, most metrics returned toward baseline—saccade duration and latency decreased, while velocity increased—demonstrating the system's dynamic flexibility.

In the PD group, saccade duration and latency increased during adaptation, mirroring but less pronounced than in controls. Slight decreases in velocity were also noted. These changes may reflect bradykinesia, a hallmark of PD, even in ocular motor function (Berardelli et al. 2001; Koohi et al. 2021). In the test phase, gain increased modestly, but other metrics suggested persistent inefficiency: saccade duration decreased, velocities declined, and latency increased. Unlike controls, PD participants failed to re-engage automatic

saccade programs effectively, likely due to impaired internal feedback and basal ganglia dysfunction (J. S. Li et al. 2023; McGregor and Nelson 2019; Blandini et al. 2000).

The MSA group showed the most atypical saccadic profiles. During adaptation, saccade duration increased modestly, while latency decreased (9.4%), diverging from the PD and control trends. This suggests premature or erratic saccade initiation, possibly due to disrupted cerebellar timing (Johansson, Hesslow and Medina 2016). Velocity metrics changed minimally, indicating unresponsive or impaired scaling. In the test phase, duration and start time increased without corresponding amplitude adjustment. This highlights an inability to coordinate timing and amplitude, consistent with cerebellar or brainstem dysfunction (S. Ren et al. 2019). The dissociation between gain and other metrics underscores a broader breakdown in the ocular motor system's integration of planning, execution, and error correction.

The gain trajectories across both adaptation and test phases displayed irregularities, deviating from smooth, exponential-like learning curves typically observed (Panouillères, Sebastiaan F.W. Neggers et al. 2012). Long task duration may have introduced cognitive fatigue and attentional lapses, especially in neurodegenerative groups. Despite drift checks, inconsistent attention could impact trial-to-trial consistency. Both MSA and PD are linked to elevated motor variability due to neural noise and unreliable internal models (Wiegel et al. 2022; Torres, Cole and Poizner 2014). In controls, plateauing or non-linear learning may have led to jagged gain curves. Most importantly, the small sample size—particularly for the MSA group—could amplify inter-individual effects, exaggerating variability in group-level plots.

6.6.1 Clinical Implications

The findings from this study offer valuable clinical insights into the neurophysiological underpinnings of motor learning deficits in PD and MSA. The observation that individuals with PD demonstrate partially preserved saccadic adaptation suggests that despite basal ganglia dysfunction, some elements of visuomotor plasticity remain intact—likely mediated through compensatory cerebellar and cortical mechanisms. This could inform therapeutic strategies aimed at enhancing residual learning capacity, such as adaptive training paradigms that leverage intact cerebellar circuitry to reinforce motor recalibration. In contrast, the severely blunted adaptation response in MSA, coupled with erratic saccadic metrics, points to more profound disrup-

tion in sensorimotor learning and timing. This supports the clinical differentiation between PD and MSA, particularly in early or ambiguous cases. Quantitative assessment of saccadic adaptation may therefore serve as a sensitive biomarker to distinguish between these conditions and track disease progression. Furthermore, the increased saccade duration and latency in both groups highlight ocular motor slowing as a general feature of neurodegeneration, which could impact daily activities such as reading, driving, and navigation. Clinically, these deficits emphasize the need for early detection and patient-specific interventions to preserve functional independence.

6.6.2 Limitations

Despite the important insights gained, several limitations should be acknowledged. First, the sample size for the MSA group was small ($n = 4$), which limits statistical power and generalizability. The heterogeneity within MSA, particularly between MSA-C and MSA-P subtypes, may have further confounded the results, as these phenotypes likely show distinct ocular motor profiles. Second, although the gain changes were statistically significant in PD and controls, many of the changes in other saccadic metrics (e.g., velocity, latency) did not reach significance, potentially due to inter-individual variability or insufficient trial density for fine-grained temporal analysis. Additionally, the long experimental duration may have introduced fatigue effects, especially in neurodegenerative cohorts, possibly impacting attentional consistency and motor execution over time. Eye tracking was performed under laboratory-controlled conditions, which may not fully reflect ecological visual behavior. Finally, while this study inferred neural mechanisms based on behavioral outcomes and prior literature, direct neuroimaging or electrophysiological correlates were not obtained to confirm the involvement of specific circuits in the observed effects.

6.6.3 Future Directions

Future research should prioritize expanding the sample size, particularly for the MSA group, and consider stratifying participants by clinical phenotype to better understand subtype-specific impairments. Incorporating neuroimaging modalities such as high-resolution functional MRI or diffusion tensor imaging would enable direct mapping of the cerebello-cortical and basal ganglia circuits involved in saccadic adaptation, thereby validating and refining the circuit-level interpretations proposed in this study. Additionally, longitudinal

studies could assess how saccadic adaptation evolves with disease progression and how it correlates with other motor and cognitive symptoms. There is also scope to investigate the impact of dopaminergic medication or targeted cerebellar stimulation on saccadic adaptation performance in PD. Finally, developing shorter, adaptive versions of the saccadic adaptation paradigm suitable for bedside or clinical deployment could help translate this task into a viable biomarker for early diagnosis and treatment monitoring in parkinsonian syndromes.

6.7 Chapter Summary

This chapter explored saccadic adaptation and deadaptation in healthy controls, idiopathic PD, and MSA. Using a visual error paradigm, it was found that healthy individuals exhibited robust, bidirectional gain modulation and coordinated changes in other saccadic metrics, reflecting intact sensorimotor learning. PD participants showed significant but attenuated adaptation, with prolonged saccade duration and latency, indicative of slowed but preserved motor learning, potentially mediated by cerebellar compensation. MSA participants, by contrast, showed minimal adaptation and highly irregular timing patterns, likely due to widespread cerebellar and brainstem degeneration. The differential adaptation profiles offer mechanistic insight into the neural circuitry underlying ocular motor plasticity and underscore the distinct pathophysiological bases of PD and MSA. Although limited by sample size and lack of direct neural recordings, the findings highlight the potential for saccadic adaptation as a clinical tool to assess motor learning and disease-specific dysfunction. Future work should focus on expanding cohort sizes, incorporating neuroimaging, and developing translational applications to harness saccadic metrics as sensitive, non-invasive biomarkers of neurodegeneration.

7 Effect of Levodopa on Eye Movements in Parkinson's Disease

7.1 Introduction

Levodopa, also known as L-dopa, is the primary pharmacological agent used in the management of PD. It acts as the metabolic precursor for the synthesis of dopamine, the neurotransmitter deficient in the nigrostriatal pathway in PD. Dopa decarboxylase is the enzyme responsible for converting levodopa into dopamine via decarboxylation (Lahlou et al. 2019; Beigi et al. 2016). In a healthy brain, dopamine modulates the activity of striatal neurons in the basal ganglia, including both the direct and indirect pathways that initiate and inhibit movement. Levodopa restores some of this modulation by enhancing the activity of the direct pathway and suppressing the indirect pathway, alleviating hallmark symptoms of PD such as bradykinesia, rigidity, and tremor (Ryan, Bair-Marshall and Nelson 2018; Heiman et al. 2014).

Motor fluctuations in PD are commonly referred to as *ON* and *OFF* states. During the *ON* state, levodopa leads to significant improvement in motor symptoms, as individuals often experience enhanced mobility. This immediate benefit is primarily attributed to dopamine restoration in the striatum. Clinical studies have shown that levodopa improves UPDRS scores and reduces resting tremor (Zach, Dirkx, Roth et al. 2020; Miyasaki 2010; Heiman et al. 2014). However, Zach et al. noted that although tremor severity decreased during *ON* states, tremor variability and irregular tremor frequencies increased—possibly due to desynchronised oscillatory activity in the basal ganglia, highlighting the complexity of levodopa's short-term effects (Zach, Dirkx, Pasman et al. 2017).

Some studies have also found cognitive benefits of levodopa during *ON* states, particularly in tasks involving attention and executive function. However, these effects are not consistent across individuals, with some reporting worsened cognitive function (Landes et al. 2022). Conversely, during *OFF* states, cognitive and motor impairments can become more pronounced, not only due to dopamine depletion but also as a result of disturbances in cholinergic, glutamatergic, and serotonergic systems—also implicated in PD pathophysiology (Warren Olanow et al. 2013).

In the context of eye movements, relatively few studies have comprehensively examined *ON* vs. *OFF* states. Hood et al. investigated prosaccades and antisaccades before and after levodopa administration, finding that

levodopa significantly increased reflexive saccade latency but reduced antisaccade error rates (Hood et al. 2007). This aligns with another study (Vermersch et al. 1994) and may be explained by the tonic inhibition model, wherein levodopa enhances inhibition of reflexive responses (Anne B. Sereno 1992).

Other investigations by M. J. Munoz, Reilly et al. 2022 and M. J. Munoz, Arora et al. 2023 assessed the effects of antiparkinsonian medication on visually guided saccades and reaching tasks over several days. M. J. Munoz, Reilly et al. 2022 examined paradigms with step, gap, and overlap fixation conditions at 10° and 15° eccentricities, while M. J. Munoz, Arora et al. 2023 evaluated a reaching task where participants looked at and touched target LEDs. Both studies reported increased saccadic latency and decreased gain and peak velocity following medication. These discrepancies suggest that while antiparkinsonian medications do impact eye movements, results may vary depending on the specific paradigms employed. Moreover, other paradigms such as pursuit and fixation remain underexplored in this context.

This project aims to systematically compare eye movements during ON and OFF states to assess the short-term effects of levodopa. A comprehensive ocular motor battery is used to evaluate various eye movement classes, offering an opportunity to replicate previously reported findings and uncover novel insights. Understanding the short-term modulation of ocular motor behaviour may help determine whether eye movements, like limb motor functions, can be temporarily improved to support daily tasks that require accurate visual tracking and rapid eye responses. These findings may also inform best practices for ocular motor testing in PD, particularly regarding the timing of medication administration.

7.2 Project Aims

1. To evaluate the short-term impact of levodopa on ocular motor function in PD, focusing on changes in metrics such as latency, error rates, and gain.
2. To determine which ocular motor metrics are most sensitive to dopaminergic therapy.

7.3 Methodology

7.3.1 Participants

Individuals scheduled for a levodopa challenge test at the Functional Neurosurgery Unit at 33 Queen Square were approached and informed about the study. Inclusion criteria were: (1) males and females with a confirmed diagnosis of idiopathic PD by a neurologist (H&Y scale 1–3); (2) age between 40 and 85 years; (3) 0–10 years since diagnosis; (4) normal or corrected-to-normal vision with no ocular motor abnormalities such as double vision, eyelid opening apraxia, or blepharospasm; (5) no additional neurological conditions; (6) ability to provide informed consent; and (7) ability to follow verbal instructions.

Exclusion criteria were: (1) drug or alcohol abuse; (2) other neurological, movement, or eye movement disorders; (3) pregnancy or suspected pregnancy (self-declared); (4) history of epilepsy; and (5) inability to sit for 15 minutes.

A total of nine participants (4 females, 5 males) were recruited. The study was approved by the UCL Research Ethics Committee, and informed consent was obtained from all participants prior to testing.

7.3.2 Experimental Conditions

Each participant was evaluated twice during the levodopa challenge: once in the OFF state (Period A) and once in the ON state (Period B). Period A was defined as the OFF state, assessed after a minimum 12-hour withdrawal from all dopaminergic medications to ensure appropriate washout. This session was conducted in the early morning to minimise discomfort. Following ocular motor assessment, levodopa (200 mg dispersible) was administered according to the CAPSIT protocol, after a 12-hour medication washout and fasting period.

Period B (ON state) was defined as the time corresponding to peak levodopa effect, approximately 60 minutes after drug administration, based on levodopa's half-life of approximately 1.5 hours when taken with carbidopa. Participants also provided self-ratings of their perceived ON/OFF state using a Visual Rating Scale (VRS) from 0 to 10, where 0 indicated feeling completely OFF and 10 completely ON. This subjective self-assessment was recorded prior to each ocular motor assessment.

7.3.3 Ocular Motor Assessment

The experimental setup, including calibration and validation, was as described in Chapter 2: General Methods. An abridged version of the standard ocular motor battery was used due to clinical time constraints. The abridged protocol consisted of the following tasks:

1. **Central Fixation:** A central stationary target was displayed at the screen centre (960, 540) for 30 seconds. Participants were instructed to maintain focus on the target with minimal blinking. One trial (30 s total duration).
2. **Reflexive Saccades:** Saccades were elicited in both horizontal ($\pm 15^\circ$) and vertical ($\pm 10^\circ$) directions with 30 trials per direction, randomly ordered. Each trial lasted 60 seconds (total duration: 120 s).
3. **Volitional Saccades:** Two stationary targets were placed at $\pm 15^\circ$. Participants moved their eyes between them at their own pace. One trial (60 s duration).
4. **Memory-Guided Saccades:** A blank screen was shown after the volitional saccade task. Participants were instructed to recall and saccade between previously presented target locations. One trial (60 s duration).
5. **Antisaccades:** Participants were instructed to saccade in the opposite direction of a stimulus appearing at $\pm 15^\circ$ in randomised order (30 trials). Each trial lasted 2 seconds (total duration: 60 s).

7.3.4 Data Processing

Data were processed as described in Chapter 2: General Methods. All ocular motor metrics were extracted using standard procedures.

7.3.5 Statistical Analyses

Descriptive statistics were calculated for all metrics in ON and OFF states. Continuous variables were summarised using mean, standard deviation, and median values. As the data were paired and non-normally

distributed, Wilcoxon signed-rank tests were applied to assess ON vs. OFF differences. Multiple comparisons were corrected using the Bonferroni method with a 5% threshold.

Effect sizes were calculated using rank-biserial correlation, and 95% confidence intervals for these were obtained via bootstrapping. A LMM was also fitted for each ocular motor metric, with state (ON/OFF), age, sex, disease duration, and LEDD as fixed effects, and participant ID as a random effect to account for repeated measures. Model assumptions were assessed via residual diagnostics, and fixed effects' confidence intervals were computed using the Wald method. Statistical significance was set at $\alpha = 0.05$. Analyses were conducted in R (Version 2023.09.1+494, R Core Team, Vienna, Austria). Full tables of results are presented in the appendix.

7.4 Results

7.4.1 Participants

Eight participants were included in the final analysis (5 males, 3 females); one participant was excluded due to substantial eye-tracking data loss. The overall mean age was 57.50 ± 4.57 years. Males had a mean age of 55.20 ± 3.77 years, and females 61.33 ± 3.06 years. The mean disease duration was 2.80 ± 1.42 years, with males averaging 2.40 ± 1.66 years and females 3.49 ± 0.60 years.

Table 14: Demographic and clinical characteristics of the study cohort. Values are presented as mean \pm standard deviation (SD). Age and disease duration are reported for all participants. Data are stratified by group and sex. “-” indicates not applicable or unavailable.

Group	Age (Mean \pm SD)	Disease Duration (Mean \pm SD)
Overall (N = 8)	57.50 ± 4.57	2.80 ± 1.42
Males (N = 5)	55.20 ± 3.77	2.40 ± 1.66
Females (N = 3)	61.33 ± 3.06	3.49 ± 0.60

7.4.2 ON vs. OFF Comparisons

A significant decrease in average fixation duration was observed following levodopa administration, as indicated by the LMM analysis ($\beta = -553.265$, 95% CI [-955.094, -151.430], $p = 0.024$). This finding was corroborated by the Wilcoxon signed-rank test ($p = 0.023$). Additionally, fixation precision measured by standard deviation (SD) significantly decreased after medication, as shown by the Wilcoxon test ($p = 0.023$), suggesting a potential alteration in fixation stability post-levodopa.

No significant effects were observed for antisaccade performance following levodopa administration.

Levodopa significantly decreased saccade end time in the vertical reflexive saccade condition, as indicated by the LMM analysis ($\beta = -220.022$, 95% CI [-303.357, -131.892], $p = 0.014$), and further supported by the Wilcoxon test ($p = 0.016$). This finding suggests faster execution of vertical reflexive saccades post-medication. No significant effects were observed in the horizontal reflexive saccade condition.

Levodopa significantly influenced several metrics of volitional saccades, reflecting changes in temporal dynamics and clustering patterns. The total number of volitional saccades completed increased significantly post-medication (LMM: $\beta = 21.500$, 95% CI [5.652, 37.348], $p = 0.026$; Wilcoxon: $p = 0.039$), while the number of saccadic steps decreased significantly (LMM: $\beta = -0.132$, 95% CI [-0.228, -0.036], $p = 0.038$; Wilcoxon: $p = 0.039$).

Furthermore, both average saccade end time (LMM: $\beta = 1381.740$, 95% CI [514.990, 2248.489], $p = 0.013$; Wilcoxon: $p = 0.016$) and average saccade start time or latency (LMM: $\beta = 1363.712$, 95% CI [499.879, 2227.544], $p = 0.014$; Wilcoxon: $p = 0.023$) significantly increased post-medication. These findings indicate that levodopa affects both the spatial clustering and timing characteristics of volitional saccades.

No significant effects were found for memory-guided saccades following levodopa administration.

Levodopa Effect Central Fixation

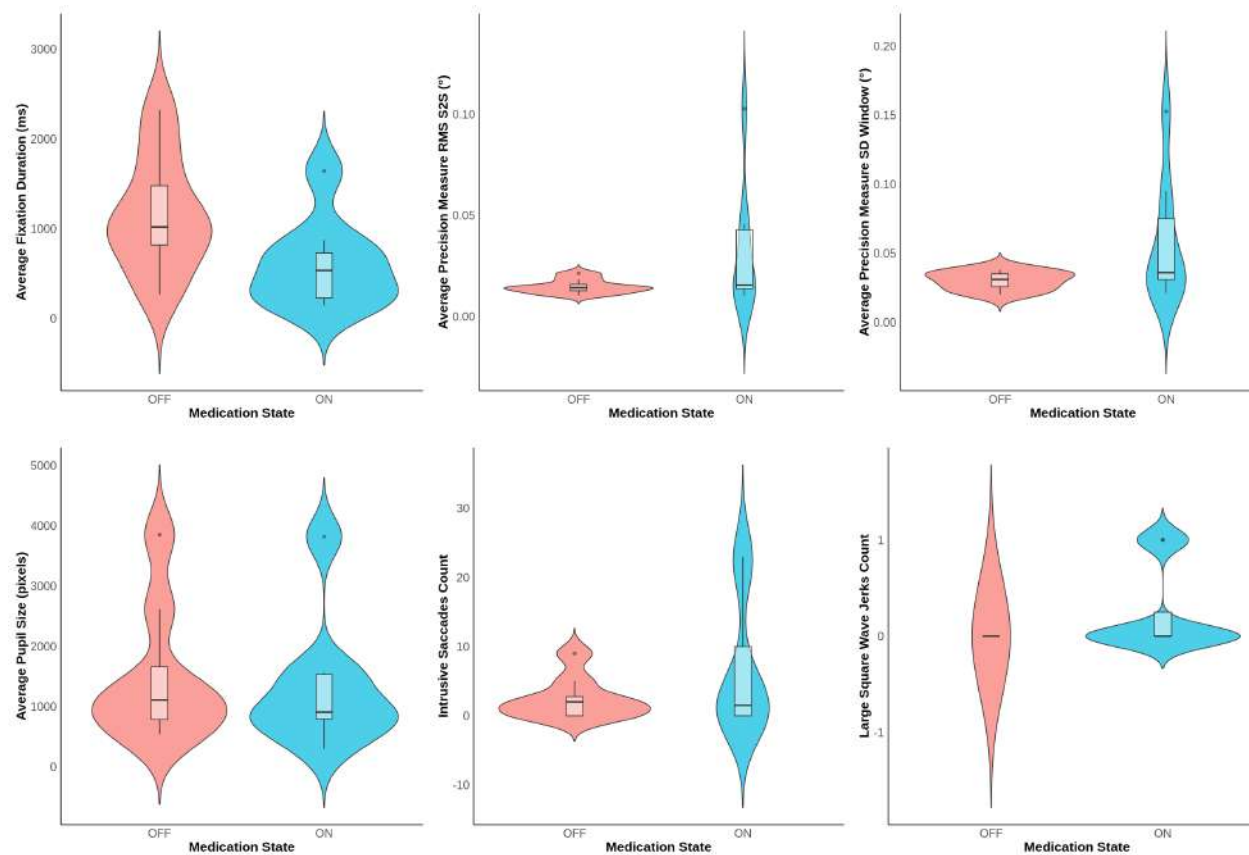


Figure 159: Central Fixation Metrics ON and OFF States. Within-subject differences were assessed using Wilcoxon signed-rank tests, with Bonferroni correction applied for multiple comparisons. Linear mixed-effects models were also fitted to evaluate the influence of state, age, sex, disease duration, and LEDD, with participant ID included as a random effect. Statistical significance was set at $p < 0.05$.

Levodopa Effect Central Fixation

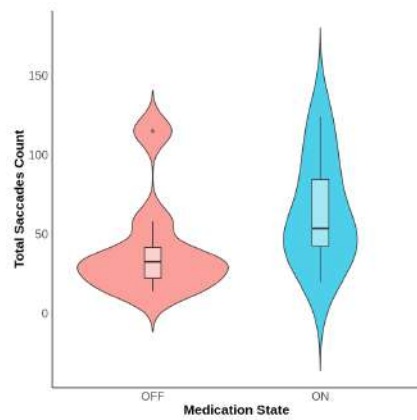


Figure 160: Central Fixation Metrics ON and OFF States. Within-subject differences were assessed using Wilcoxon signed-rank tests, with Bonferroni correction applied for multiple comparisons. Linear mixed-effects models were also fitted to evaluate the influence of state, age, sex, disease duration, and LEDD, with participant ID included as a random effect. Statistical significance was set at $p < 0.05$.

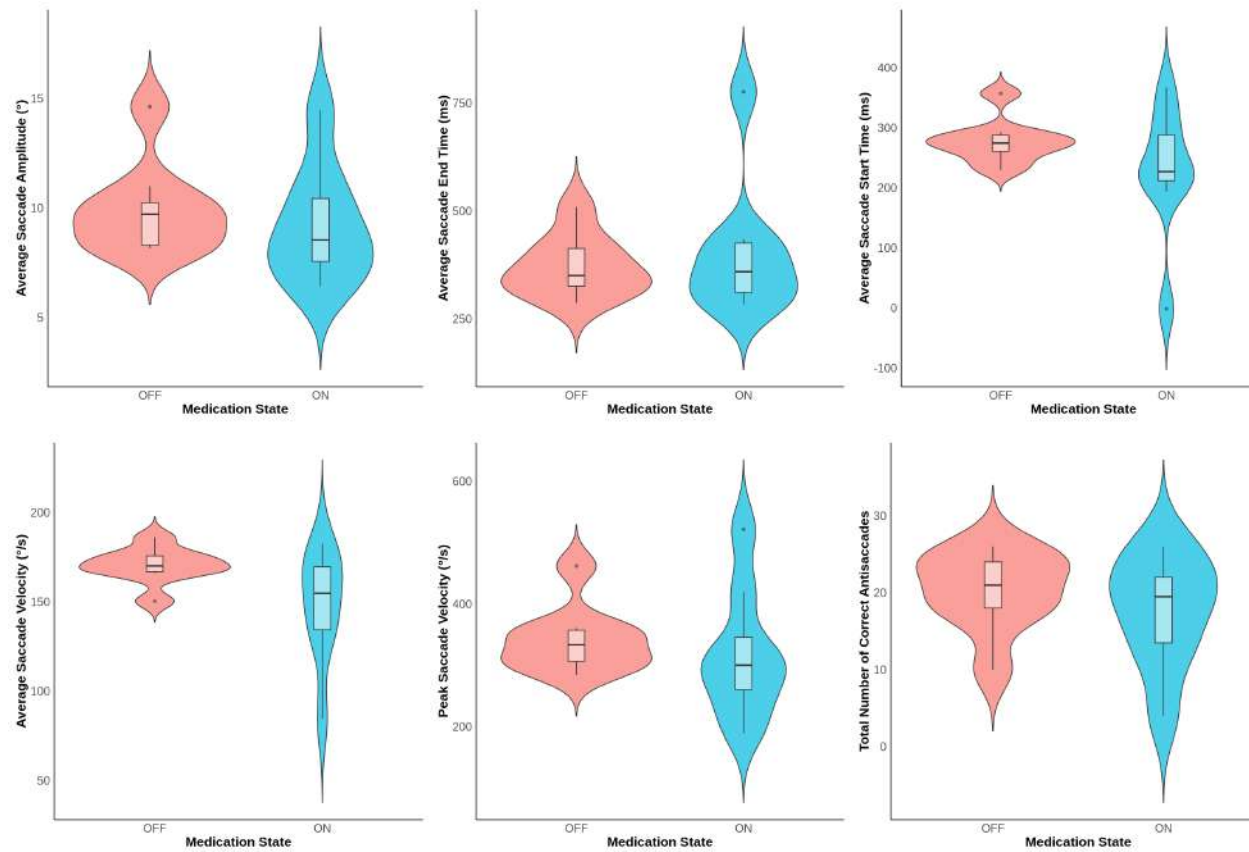


Figure 161: Antisaccades Metrics ON and OFF States. Within-subject differences were assessed using Wilcoxon signed-rank tests, with Bonferroni correction applied for multiple comparisons. Linear mixed-effects models were also fitted to evaluate the influence of state, age, sex, disease duration, and LEDD, with participant ID included as a random effect. Statistical significance was set at $p < 0.05$.

Levodopa Effect Antisaccades

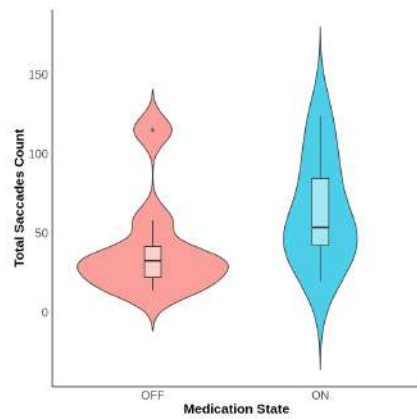


Figure 162: Antisaccades Metrics ON and OFF States. Within-subject differences were assessed using Wilcoxon signed-rank tests, with Bonferroni correction applied for multiple comparisons. Linear mixed-effects models were also fitted to evaluate the influence of state, age, sex, disease duration, and LEDD, with participant ID included as a random effect. Statistical significance was set at $p < 0.05$.

Levodopa Effect Reflexive Saccades Horizontal

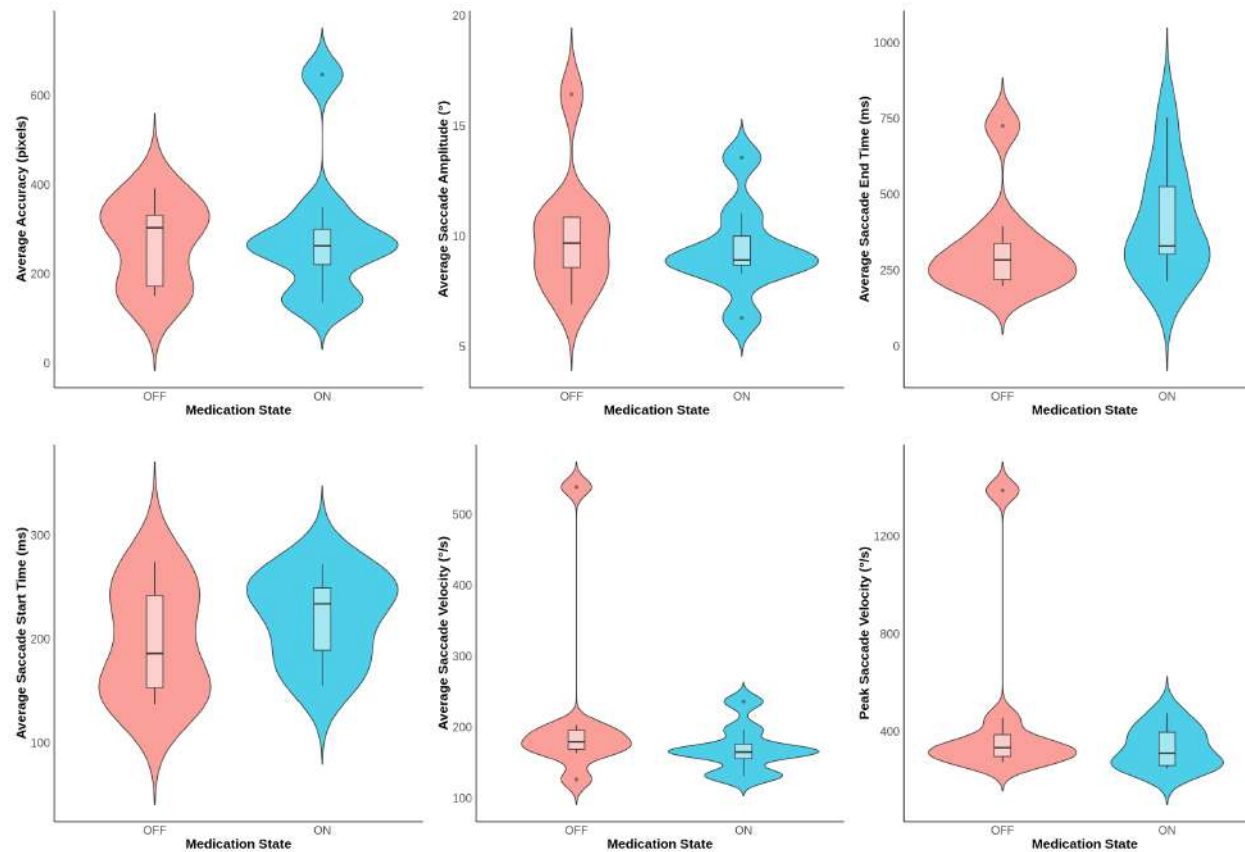


Figure 163: Reflexive Saccades Horizontal Metrics ON and OFF States. Within-subject differences were assessed using Wilcoxon signed-rank tests, with Bonferroni correction applied for multiple comparisons. Linear mixed-effects models were also fitted to evaluate the influence of state, age, sex, disease duration, and LEDD, with participant ID included as a random effect. Statistical significance was set at $p < 0.05$.

Levodopa Effect Reflexive Saccades Horizontal

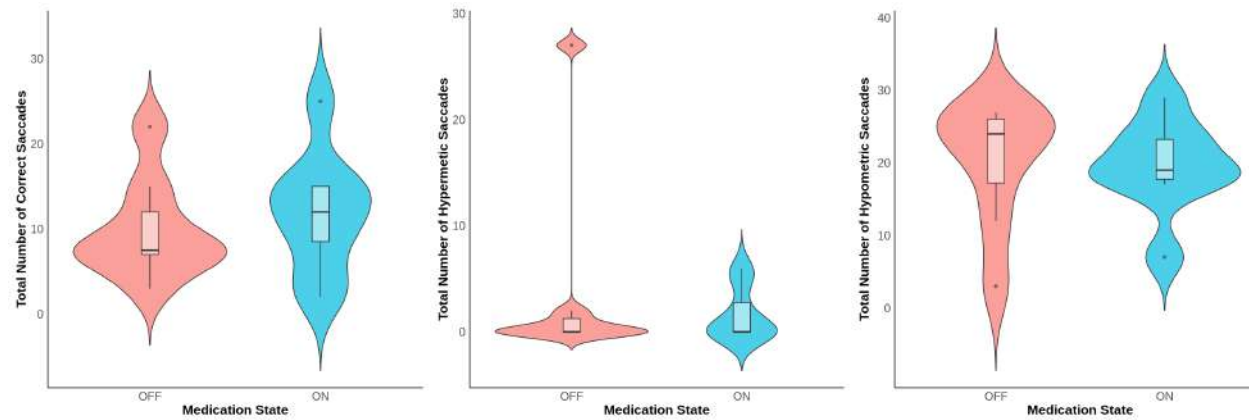


Figure 164: Reflexive Saccades Horizontal Metrics ON and OFF States. Within-subject differences were assessed using Wilcoxon signed-rank tests, with Bonferroni correction applied for multiple comparisons. Linear mixed-effects models were also fitted to evaluate the influence of state, age, sex, disease duration, and LEDD, with participant ID included as a random effect. Statistical significance was set at $p < 0.05$.

Levodopa Effect Reflexive Saccades Vertical

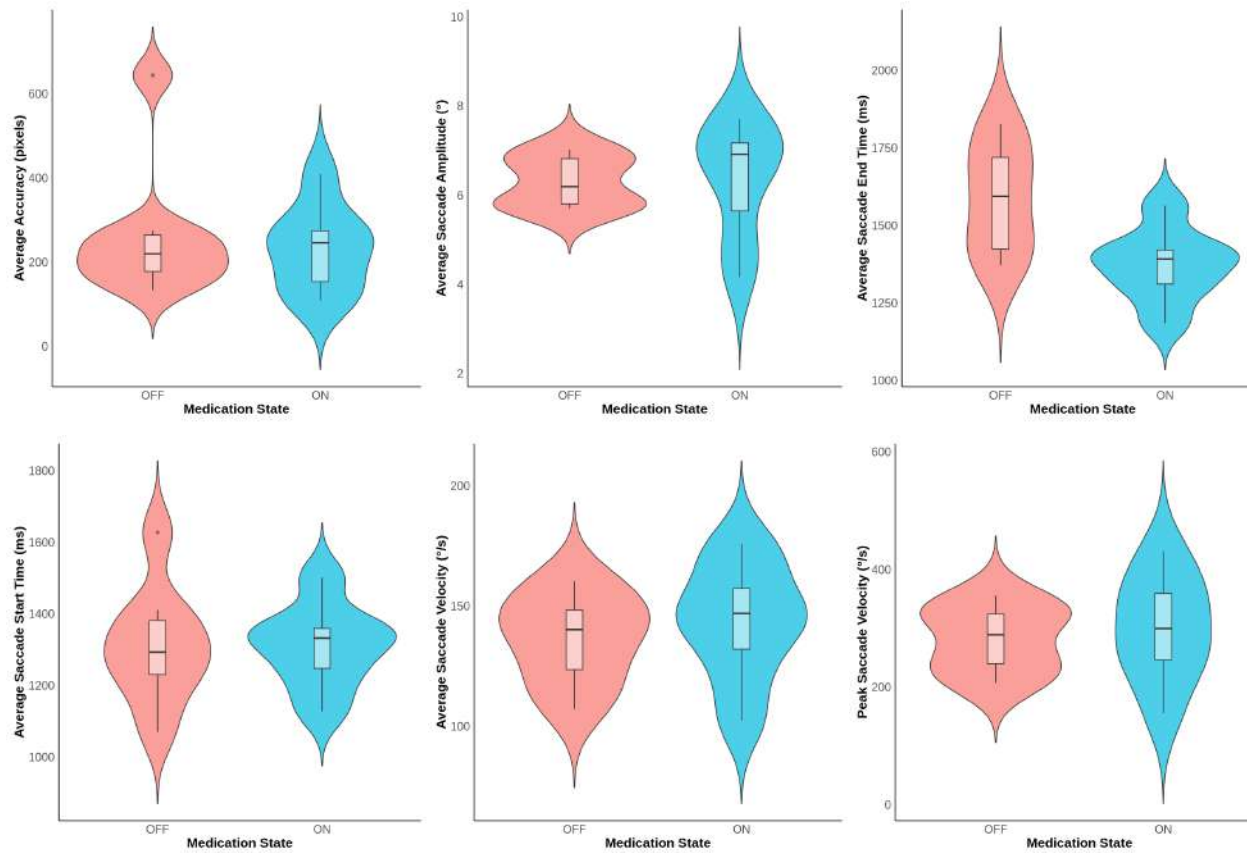


Figure 165: Reflexive Saccades Vertical Metrics ON and OFF States. Within-subject differences were assessed using Wilcoxon signed-rank tests, with Bonferroni correction applied for multiple comparisons. Linear mixed-effects models were also fitted to evaluate the influence of state, age, sex, disease duration, and LEDD, with participant ID included as a random effect. Statistical significance was set at $p < 0.05$.

Levodopa Effect Reflexive Saccades Vertical

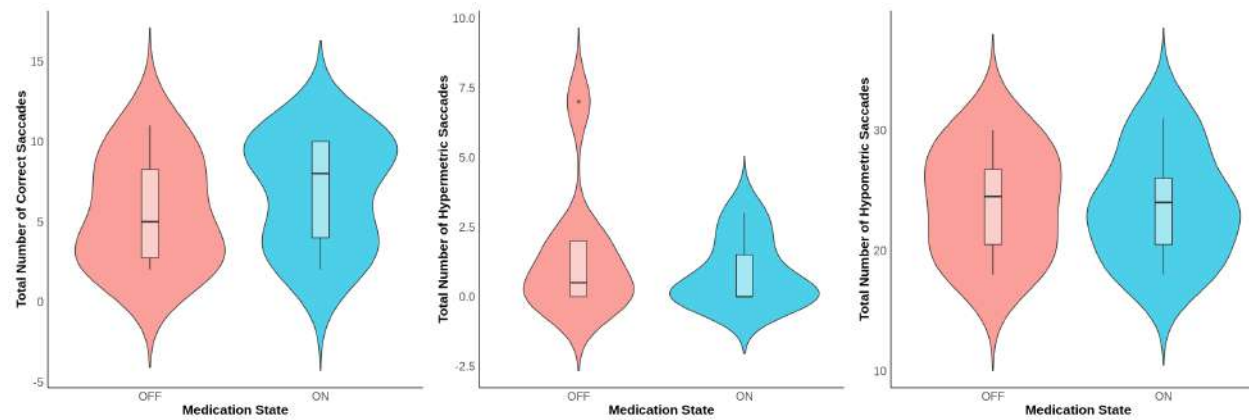


Figure 166: Reflexive Saccades Vertical Metrics ON and OFF States. Within-subject differences were assessed using Wilcoxon signed-rank tests, with Bonferroni correction applied for multiple comparisons. Linear mixed-effects models were also fitted to evaluate the influence of state, age, sex, disease duration, and LEDD, with participant ID included as a random effect. Statistical significance was set at $p < 0.05$.

Levodopa Effect Volitional Saccades

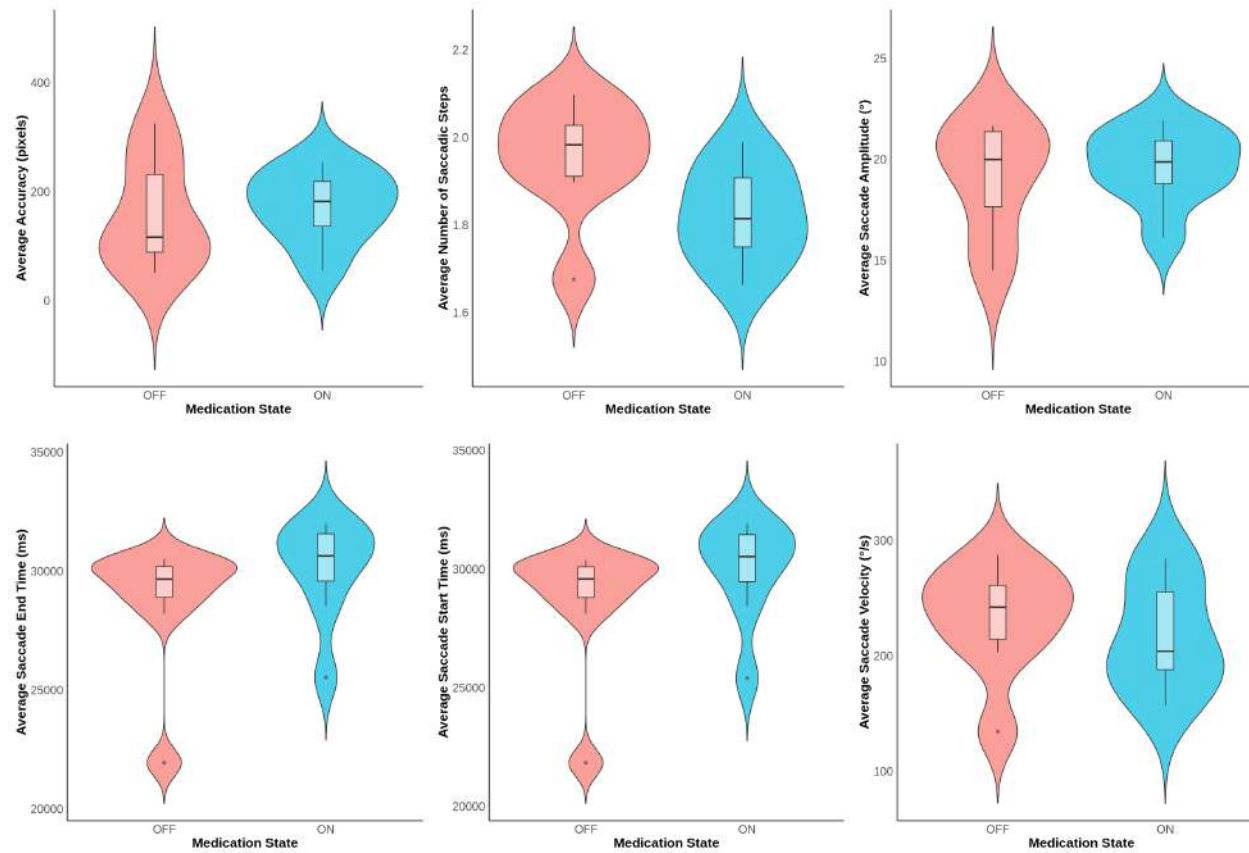


Figure 167: Volitional Saccades Metrics ON and OFF States. Within-subject differences were assessed using Wilcoxon signed-rank tests, with Bonferroni correction applied for multiple comparisons. Linear mixed-effects models were also fitted to evaluate the influence of state, age, sex, disease duration, and LEDD, with participant ID included as a random effect. Statistical significance was set at $p < 0.05$.

Levodopa Effect Volitional Saccades

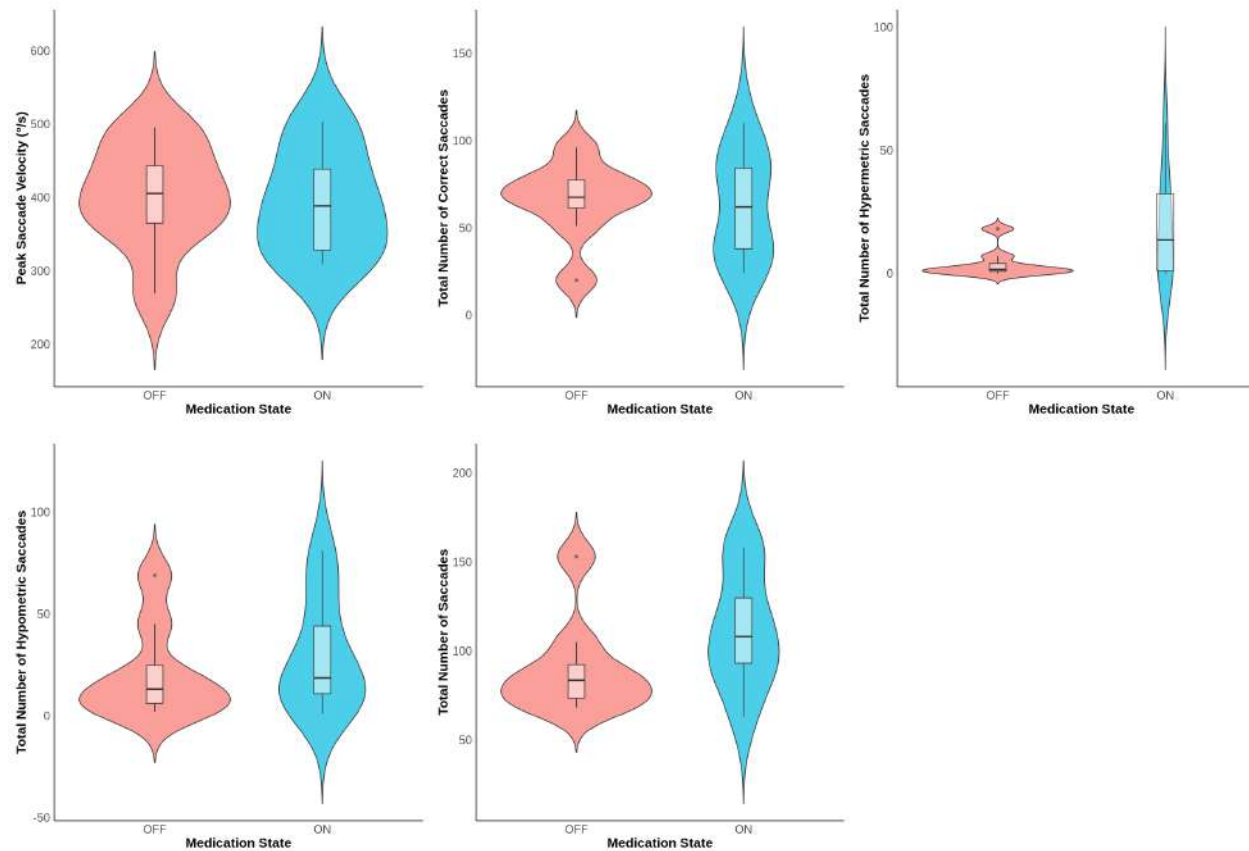


Figure 168: Volitional Saccades Metrics ON and OFF States. Within-subject differences were assessed using Wilcoxon signed-rank tests, with Bonferroni correction applied for multiple comparisons. Linear mixed-effects models were also fitted to evaluate the influence of state, age, sex, disease duration, and LEDD, with participant ID included as a random effect. Statistical significance was set at $p < 0.05$.

Levodopa Effect Memory Guided Saccades

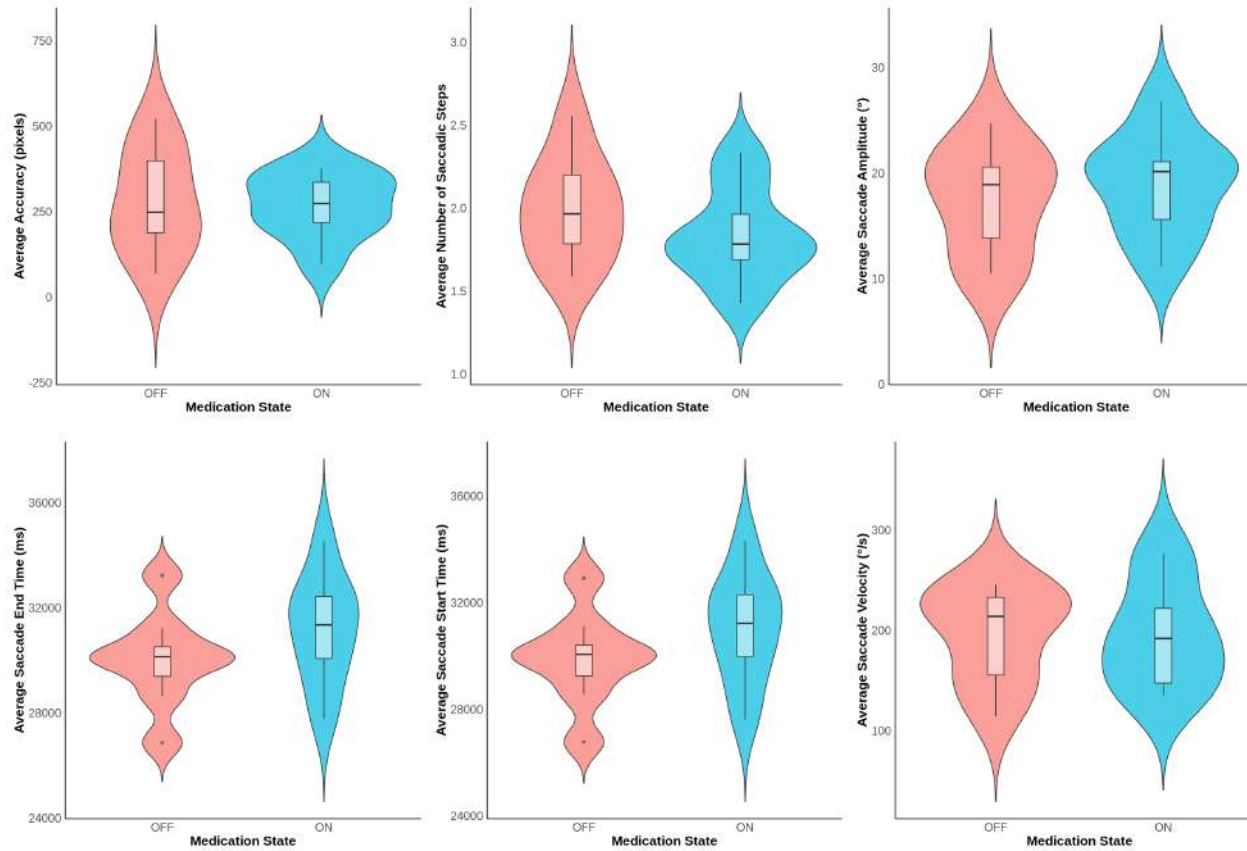


Figure 169: Memory Guided Saccades Metrics ON and OFF States. Within-subject differences were assessed using Wilcoxon signed-rank tests, with Bonferroni correction applied for multiple comparisons. Linear mixed-effects models were also fitted to evaluate the influence of state, age, sex, disease duration, and LEDD, with participant ID included as a random effect. Statistical significance was set at $p < 0.05$.

Levodopa Effect Memory Guided Saccades

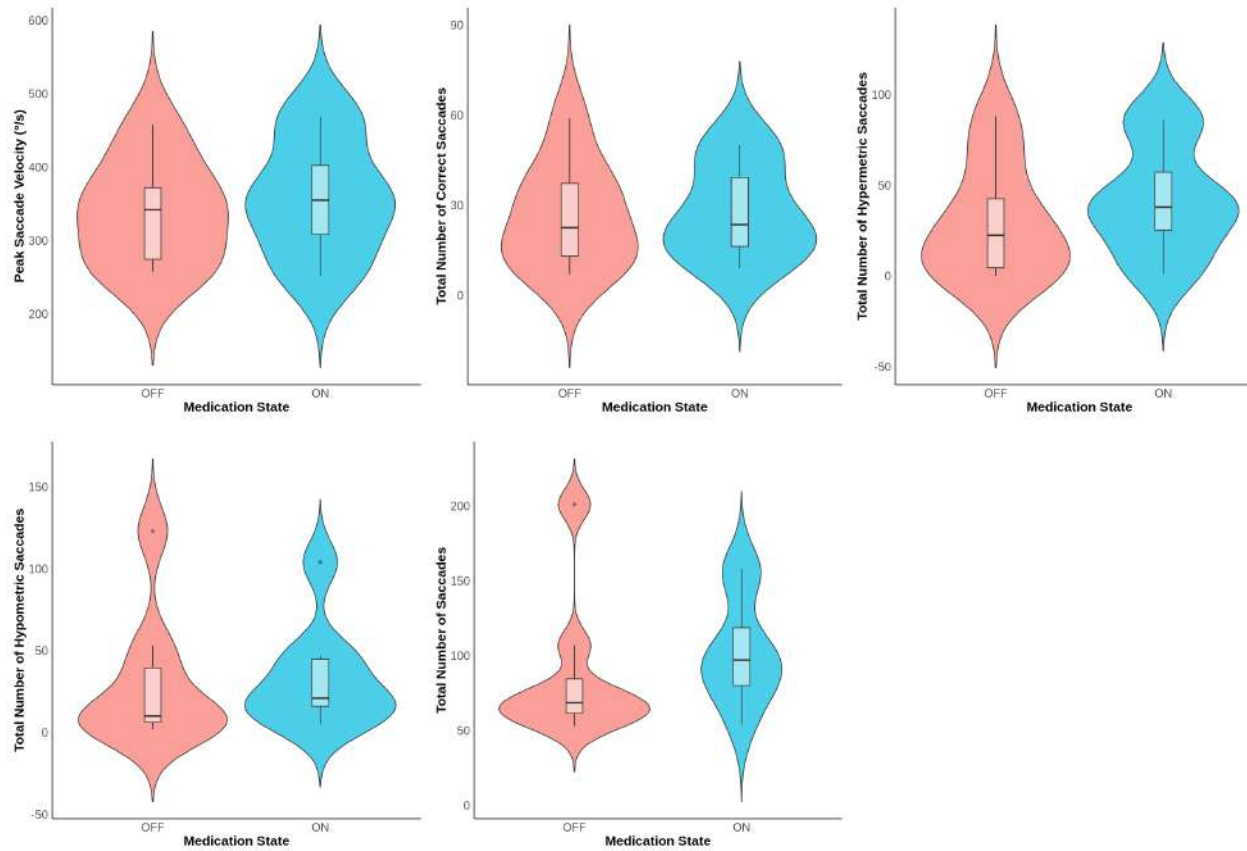


Figure 170: Memory Guided Saccades Metrics ON and OFF States. Within-subject differences were assessed using Wilcoxon signed-rank tests, with Bonferroni correction applied for multiple comparisons. Linear mixed-effects models were also fitted to evaluate the influence of state, age, sex, disease duration, and LEDD, with participant ID included as a random effect. Statistical significance was set at $p < 0.05$.

7.5 Discussion

This study found that levodopa administration had differential effects on specific aspects of ocular motor function in PD, particularly fixation stability, reflexive saccades, and volitional saccades. These results suggest that dopaminergic treatment, even in the short term, can influence ocular motor pathways. While previous studies have assessed the long-term effects of dopamine on ocular motor function and some have examined specific tasks such as fixation or antisaccades, the current findings provide novel insights into a broader range of eye movements, including volitional and memory-guided saccades, in both ON and OFF states. However, given the small sample size, these findings should be considered preliminary and warrant further investigation.

In the fixation task, levodopa administration led to a significant decrease in average fixation duration, confirmed by both the LMM analysis and the Wilcoxon signed-rank test. In addition, fixation precision—measured by the standard deviation of fixation position—also significantly decreased post-medication, suggesting increased variability in fixation stability. Previous studies examining motor symptoms during ON and OFF states report mixed findings, ranging from no improvement to decreased stability or enhanced speed of motor functioning (Corrà et al. 2021; Yin et al. 2022; Freitas, Hess and Fox 2017). The reduction in fixation duration and precision observed here may reflect dopamine overstimulation within the basal ganglia (H. Yu et al. 2007). Pulsatile stimulation from short-acting levodopa causes discontinuous activation of dopamine receptors, potentially destabilising motor circuits in the already dopamine-depleted basal ganglia (Olanow, Obeso and Stocchi 2006). Alternatively, excessive dopamine may induce hyperkinesia, resulting in the generation of intrusive saccades during fixation (Güttler et al. 2021). Variability in neural activity within other fixation-related regions such as the superior colliculus, FEFs, and SEFs could further contribute to erratic gaze behaviour (Lal and Truong 2019).

No significant changes were observed in antisaccade performance following levodopa administration. Antisaccades require top-down executive control, predominantly mediated by the dorsolateral prefrontal cortex. Since levodopa acts primarily on basal ganglia circuits, its effects on executive functioning may be limited (Kaufman et al. 2010). Although levodopa has been shown to improve frontal-subcortical and posterior cortical function in PD, it remains unclear whether these cognitive improvements translate to measurable changes in antisaccade performance (Gul and J. Yousaf 2019; Orcioli-Silva et al. 2020). Additionally, antisaccades are influenced by other neurotransmitter systems such as norepinephrine and acetylcholine, which may

explain the absence of significant effects (Aponte et al. 2020). Finally, if baseline antisaccade performance was already well-preserved, a ceiling effect may have masked potential improvements.

Levodopa administration significantly reduced saccade end time in the vertical reflexive saccade task, suggesting a possible enhancement in saccade execution speed or a reduction in planning delay. Vertical and horizontal saccades are controlled by overlapping but distinct brainstem circuits, and it is plausible that vertical saccades may benefit more from dopamine-driven facilitation in areas such as the superior colliculus or cortico-striatal loops (McDowell, Clementz and Sweeney 2012; Lal and Truong 2019). However, caution should be exercised in interpreting this finding, as saccade end time is not a widely validated metric for saccadic performance. It may instead reflect variability in execution, trajectory adjustments, or post-saccadic corrections. The absence of similar changes in horizontal saccades further complicates interpretation and raises concerns about the robustness of this effect.

Volitional saccade metrics were significantly influenced by levodopa, with an increase in the total number of saccades completed and a decrease in the number of saccadic steps per movement. These findings suggest improved saccadic execution and possibly greater movement precision. The observed increase in volitional saccades aligns with prior studies showing that these movements rely heavily on basal ganglia integrity, particularly the dopaminergic nigrostriatal pathway, which is disrupted in PD (Redgrave et al. 2010; Hodgson et al. 2013). Levodopa likely restored some of this function, enhancing the ability to generate goal-directed saccades. The reduced need for corrective steps may reflect improved accuracy, although an alternative explanation is that levodopa-induced impulsivity led to more committed but less refined movements. Clarifying this would require analysis of endpoint accuracy and variability.

Despite the increase in saccade number, both saccade start time (latency) and end time increased post-medication, indicating a paradoxical slowing in initiation and completion. This may result from levodopa's modulation of the balance between movement initiation and inhibition in the basal ganglia, particularly increased inhibition within the indirect pathway delaying saccade release (Lerner et al. 2017; Graybiel, Canales and Capper-Loup 2000; Biase et al. 2023). Given the executive demands of volitional saccades, effects on prefrontal cortex function and planning could also introduce timing variability (Cieslik et al. 2016; René M. Müri and Nyffeler 2008; Molloy et al. 2006; Kiani, Heidari Beni and Aghajan 2023). Additionally,

the pulsatile pharmacodynamics of short-acting levodopa may cause fluctuating motor timing and inconsistent initiation speeds (N. Hattori 2022). Rather than facilitating faster responses, levodopa may introduce greater variability, which in turn prolongs initiation and termination of saccades.

No significant effects were observed for memory-guided saccades. These saccades rely on working memory and sustained attention, involving prefrontal and hippocampal regions, which are more influenced by cholinergic and noradrenergic neurotransmission than dopaminergic function. Since levodopa primarily targets dopamine in the basal ganglia, its influence on memory-guided saccades may be limited. This result parallels the antisaccade findings and reinforces the idea that levodopa has more substantial effects on movement execution than cognitive control.

Levodopa's differential influence across ocular motor tasks observed in this study can be explained by its complex modulation of basal ganglia circuits, particularly via the direct, indirect, and hyperdirect pathways (Neumann et al. 2018; Gerfen and Surmeier 2011). Enhanced dopaminergic stimulation from levodopa predominantly activates the direct pathway, facilitating movement by decreasing inhibitory output from basal ganglia nuclei such as SNpr (Sonne, Reddy and Beato 2020; Lanciego, Luquin and Obeso 2012). Simultaneously, levodopa suppresses the indirect and hyperdirect pathways, thereby reducing basal ganglia-mediated movement inhibition (McGregor and Nelson 2019; Nambu et al. 2023). This dual action might paradoxically prolong saccade initiation in certain tasks (e.g., volitional and reflexive saccades) by disrupting the balance between facilitation and inhibition, causing heightened cortical decision thresholds and delayed triggering of ocular movements. Conversely, increased movement frequency (as seen in volitional saccades) could arise from reduced tonic inhibition, facilitating repeated but less precise movements (Heo et al. 2020). Tasks heavily dependent on internal planning or cognitive load (antisaccades, memory-guided saccades) involve frontal-basal ganglia loops, whose complexity may limit rapid normalization through acute dopaminergic intervention (Leisman, Braun-Benjamin and Melillo 2014).

At the receptor level, differences in the expression and distribution of dopamine receptor subtypes (D1 vs. D2) offer insights into the task-specific responses observed with levodopa administration (Gerfen 2023). Reflexive saccades and fixation tasks, largely mediated by subcortical and collicular pathways, predominantly involve inhibitory D2 receptor pathways within the basal ganglia, potentially explaining why excessive D2 stimulation

from acute levodopa administration may paradoxically slow reflexive saccade initiation or disrupt fixation stability (R. Walker and McSorley 2006; Gerfen 2023; Lanciego, Luquin and Obeso 2012). In contrast, volitional, antisaccade, and memory-guided saccade tasks heavily engage frontal-cortical basal ganglia loops enriched in both D1 and D2 receptors, but with significant reliance on cortical D1 receptors to mediate planning and decision thresholds (Liversedge, Gilchrist and Everling 2012; Volkow et al. 2002; Luft and Schwarz 2009; Gerfen and Surmeier 2011). Excessive acute D1 receptor activation through levodopa might heighten cortical decision thresholds, prolonging saccadic initiation times, yet permitting greater overall movement frequency by facilitating release from tonic inhibition (P. S. Goldman-Rakic, Muly and G. V. Williams 2000; Chris Muly, Szigeti and Patricia S. Goldman-Rakic 1998). Chronic receptor adaptations in PD, particularly within these cognitive-executive circuits, could further limit responsiveness of antisaccades and memory-guided saccades to short-term levodopa treatment (Yunqi Xu et al. 2012).

7.5.1 Clinical Implications

The differential effects of levodopa on ocular motor function in PD have important clinical implications, particularly in understanding how dopaminergic therapy influences movement control beyond limb motor function. The observed increase in volitional saccades suggests that levodopa may enhance the ability to generate self-initiated movements, which could translate to improvements in tasks requiring voluntary gaze shifts, such as reading or visual scanning. However, the increased fixation instability and prolonged saccade start and end times highlight potential side effects of dopaminergic overstimulation, which may contribute to visual disturbances in PD patients. The absence of improvement in antisaccades and memory-guided saccades suggests that cognitive aspects of eye movement control are not significantly influenced by levodopa, reinforcing the need for adjunct treatments targeting executive dysfunction. These findings emphasize that while levodopa remains the cornerstone of PD management, its effects on ocular motor function should be considered when addressing visual and attentional symptoms in clinical settings. Additionally, the results suggest that ocular motor assessments could be used as objective biomarkers to evaluate dopaminergic treatment efficacy in PD, offering a non-invasive tool to track disease progression and medication responsiveness.

7.5.2 Limitations

Several limitations should be acknowledged in interpreting these findings. The small sample size of nine participants restricts the ability to generalize results to the broader PD population, as individual differences in disease progression, baseline motor function, and medication response may have influenced the observed effects. Given the variability in how PD patients respond to levodopa, a larger sample would provide greater statistical power and reduce the influence of outliers. Given the limitations associated with small samples in clinical ocular motor studies, future research would benefit from adopting advanced statistical methodologies, such as Bayesian statistical analyses. Bayesian methods explicitly quantify uncertainty and strength of evidence, providing probabilistic interpretations that are particularly advantageous in small-sample studies. By using Bayesian approaches, it is possible to integrate prior knowledge from existing literature, directly estimate effect size uncertainty, and better quantify evidence for or against the efficacy of levodopa treatment across ocular motor paradigms, thus mitigating the limitations inherent in frequentist analyses of limited data sets.

Additionally, this study assessed only the short-term effects of levodopa, leaving uncertainty regarding whether these ocular motor changes persist, diminish, or evolve with chronic levodopa use. Long-term administration often leads to motor complications such as dyskinesias and fluctuating efficacy, which may further influence ocular motor control. Future research should include longitudinal studies to evaluate how ocular motor function changes over months or years of levodopa therapy, and whether compensatory neural adaptations develop over time.

Another limitation is the use of a single levodopa dose rather than individualized titration based on disease severity or patient-specific pharmacokinetics. Levodopa's effects vary based on absorption rates and metabolism, so some participants may have been under- or over-medicated relative to their optimal response window. Future studies should consider dosage adjustments based on individual responsiveness, potentially incorporating plasma drug levels to confirm efficacy at the time of testing.

Potential confounding factors such as fatigue, attentional fluctuations, or unmeasured cognitive effects may have influenced outcomes. PD patients often experience variability in alertness, which could affect saccadic performance independently of levodopa's motor effects. Moreover, while this study focused on dopaminergic

modulation, other neurotransmitter systems (e.g., cholinergic, noradrenergic) also contribute to ocular motor control and may account for observed variability. Future studies should pair ocular motor paradigms with cognitive assessments to evaluate whether levodopa-induced changes in eye movement are linked to broader cognitive fluctuations.

Finally, the absence of a placebo-controlled or double-blinded design introduces the potential for expectancy effects or subtle experimenter bias. Future research should incorporate placebo-controlled, double-blind testing with repeated measures to improve the reliability of findings. Investigating how different PD subtypes (e.g., tremor-dominant vs. akinetic-rigid) respond to levodopa may also offer deeper insight into subtype-specific ocular motor modulation.

7.5.3 Future Directions

Future research should focus on clarifying the mechanisms underlying levodopa's differential effects on ocular motor function and determining whether observed changes represent true functional improvement or compensatory movement strategies. Larger-scale studies are necessary to confirm these findings and examine individual variability related to disease severity, medication dosage, and long-term dopaminergic exposure. Greater emphasis should also be placed on understanding the roles of non-dopaminergic systems—particularly cholinergic and noradrenergic pathways—in memory-guided and antisaccadic performance.

Additionally, it would be valuable to explore the effects of continuous dopaminergic stimulation (e.g., dopamine agonists or deep brain stimulation) on ocular motor stability, especially given the potential destabilising effects of pulsatile levodopa dosing. Finally, integrating ocular motor assessments into routine clinical evaluations may offer an objective, non-invasive biomarker to monitor motor and cognitive dysfunction in PD, allowing for more precise and personalized therapeutic interventions.

7.6 Chapter Summary

This chapter demonstrates that levodopa influences specific aspects of ocular motor function in PD, including fixation stability, reflexive saccades, and volitional saccades. Levodopa was associated with enhanced saccade

execution in certain paradigms, but also introduced timing complexity and fixation instability. The findings provide novel insight into the role of dopamine in ocular motor regulation and suggest that ocular motor metrics may serve as sensitive markers for dopaminergic effects. Further research is needed to validate these results, investigate the underlying neurophysiological mechanisms, and assess their implications for clinical management and therapeutic monitoring in PD.

8 Machine Learning for the Prediction of Parkinson's Disease and Atypical Parkinsonian Syndromes

8.1 Introduction

Artificial intelligence in healthcare has gained traction over the past decade with its ability to leverage large datasets to generate patterns and therefore improve patient outcomes and care delivery. Machine learning is a subfield of artificial intelligence that focuses on the development of algorithms that can make predictions based on data. There are several techniques within machine learning including supervised learning, unsupervised learning, reinforcement learning, and semi-supervised learning (Belle and Papantonis 2021). Each technique employs different methodologies to tackle problems therefore the choice of model is critical to achieving high predictive value and maximum system performance.

Supervised learning is the most widely recognised methodology in machine learning wherein models are trained with labelled datasets. The association of each input with the corresponding output allows the model to learn the mapping from start to finish and hence make predictions on unseen and new data (Nasteski 2017). Common algorithms used in supervised learning are support vector machines, decision trees and convolutional neural networks (Z. Ren et al. 2023). These models work best for regression and classification tasks or where the goal is to predict categorical or continuous outcomes (Muddasar Abbas et al. 2022). On the other hand, unsupervised learning uses unlabelled data to identify patterns without any guidance on what the output should be. Unsupervised learning involves clustering techniques such as k-means and hierarchical clustering and dimensionality reduction for example principle component analysis (Zang et al. 2017). These methods are primarily used in exploratory data analysis and scenarios where the underlying structure of the data is unknown (Leng 2024). Semi-supervised learning combines elements of both supervised and unsupervised learning to mitigate the cost and impracticality of acquiring large data sets. In this case a small amount of labelled data is used along with a large amount of unlabelled data, allowing the model to utilise the structure of the unlabelled data to improve its (Al-Azzam and Shatnawi 2021).

Machine learning models need to be evaluated to ensure the models are reliable and capable of making accurate predictions on new, unseen data to ensure they can be translated into real world applications. Two

key pitfalls are either over fitting, when the model is very closely aligned with the training dataset that it is unable to handle new data or under fitting, when the model is unable to capture the underlying structure of the data (Chauhan 2020). There are various metrics that can be utilised to evaluate the performance of a model such as classification, regression, ranking and statistical metrics. Classification metrics are used when the data is categorical and are commonly used for classification problems. One classification metric is the F1 score which combines the precision score (a measure of accuracy of the model) and recall score (the true positive rate) of a model. This metric tells you how many times a model made a correct prediction on the entire dataset (Hamner and Frasco 2018). Another method of evaluation is using the receiver operating characteristic curve which provides a comprehensive view of the model's ability to differentiate between classes and the area under the curve gives a single value for summarising the overall performance of the model focusing on sensitivity and specificity (AUC-ROC) (Rainio, Teuvo and Klén 2024). Utilising these evaluation methods can help determine the performance of your model and how it can be further improved.

The integration of machine learning models into clinical datasets in Parkinson's Disease has presented a significant advancement in diagnosis. Models including deep learning and XGBoost have been effectively able to diagnose PD using voice signals suggesting that non-invasive methods can be effective for early diagnosis (Nissar et al. 2019; Neto 2023; Alshammri et al. 2023) when quantified appropriately. Furthermore, in a heterogeneous condition such as PD where movement and gait patterns are complex, machine learning has been successful not only in differentiating PD from healthy individuals at an early stage but also continuously monitoring the progression of symptoms (A. Li and C. Li 2022; Zhixu Zhao et al. 2023). A challenge that machine learning has been able to overcome, although in the nascent stages, is the differentiation between PD and atypical parkinsonian syndromes. Numerous studies have utilised neuroimaging data (Segovia, Illán et al. 2015; Archer et al. 2019; Y. S. Kim, J. H. Lee and Gahm 2022) and postural data (Song et al. 2022). These models have primarily focused on the differentiation between PD, PSP and MSA and show that training models with even small datasets can be useful to provide diagnostic value. However, no studies have incorporated genetic cases of PD, CBS and DLB cohorts within the classification or utilised eye movements for machine learning models. The incorporation of these further sub groups will possibly provide a more granular diagnosis and the integration of more clinical symptoms such as posture and neuroimaging will further increase the diagnostic value of these models.

8.2 Project Aims

1. To build and validate a machine learning model using ocular motor data to differentiate between PD, APS, and healthy controls.
2. To identify the most informative ocular motor features for accurate classification and diagnosis.

8.3 Methods

8.3.1 Data Source

A combined dataset was created with data from all twelve unique eye movement paradigms and the relevant metrics from each: fixation (average pupil size, RMS precision measure, SD precision measure, average fixation, average fixation duration, microsaccades count, number of small, large square wave jerks and saccadic intrusions); nystagmus (average pupil size, RMS precision measure, SD precision measure, average fixation, average fixation duration, microsaccades count, number of small, large square wave jerks and saccadic intrusions); pursuit in horizontal, vertical and elliptical directions at 0.2 Hz and 0.4 Hz (pursuit gain, saccade count, and RMS gaze); antisaccades in the horizontal and vertical direction (latency, average velocity, peak velocity, average amplitude, end time, number of errors and self-correcting errors); oblique saccades at 4°, 8°, and 10° (latency, average velocity, peak velocity, average amplitude, end time, accuracy, and the number of correct, hypometric, or hypermetric saccades); reflexive saccades in the horizontal and vertical direction (latency, average velocity, peak velocity, average amplitude, end time, accuracy, and the number of correct, hypometric, or hypermetric saccades); volitional saccades in the horizontal and vertical direction (total number of complete saccades, saccadic steps, latency, average velocity, peak velocity, average amplitude, end time, accuracy, and the number of correct, hypometric, or hypermetric saccades); memory-guided saccades in the horizontal and vertical direction (total number of complete saccades, saccadic steps, latency, average velocity, peak velocity, average amplitude, end time, accuracy, and the number of correct, hypometric, or hypermetric saccades).

A total of 208 participants were included in the model: 52 controls, 12 GBA-positive PD, 3 LRRK2-positive PD, 101 idiopathic PD, 9 unclassified atypical, 4 CBS, 2 DLB, 10 MSA, and 15 PSP. This provides a rich set of features for machine learning models to identify patterns relevant for classification. A multi-level

classification system with four hierarchical levels was constructed. At each level, a predictive model is trained, and its output is passed as input to the next level, along with the eye movement data. This process continues iteratively until the final classification at Level 4 is achieved. The hierarchical structure ensures a systematic breakdown of the disease into subcategories, improving model interpretability and predictive accuracy. A breakdown of the construction of the model is detailed below.

8.3.2 Data Preparation

The dataset was cleaned and organised before training the model, including data merging, handling missing values, and classification mapping. The initial step involved consolidating twelve separate data files, each containing participant-specific measurements, into a single comprehensive dataset. This merging process ensured that all relevant participant information was centralised, facilitating streamlined analysis and processing. The dataset was merged using the unique participant ID, with all identifiable participant data removed.

To address missing values in the dataset, the iterative imputer technique was employed. In the initial stage, missing values were replaced with simple estimates (e.g., mean or median). At each step, one feature with missing values was selected, and a regression model was trained using the other features as predictors. This model was used to predict the missing values, which were updated iteratively. The cycle was repeated for all features with missing values, refining the imputations at each iteration. The process continued until a convergence criterion was met (i.e., when imputations stabilised). The advantage of the iterative imputer is that it considers interdependencies between features, making it more suitable for complex datasets such as those containing eye movement metrics.

After handling missing values, each participant ID was assigned four levels of classification based on diagnosis: Level 1 distinguished healthy controls from all disease cases; Level 2 differentiated PD from atypical parkinsonism; Level 3 further divided PD into idiopathic and genetic subtypes, and atypical parkinsonism into PSP, MSA, CBS, and DLB; Level 4 classified genetic PD into GBA or LRRK2 subtypes. These classifications were mapped and integrated with the merged eye movement dataset using participant ID as the key.

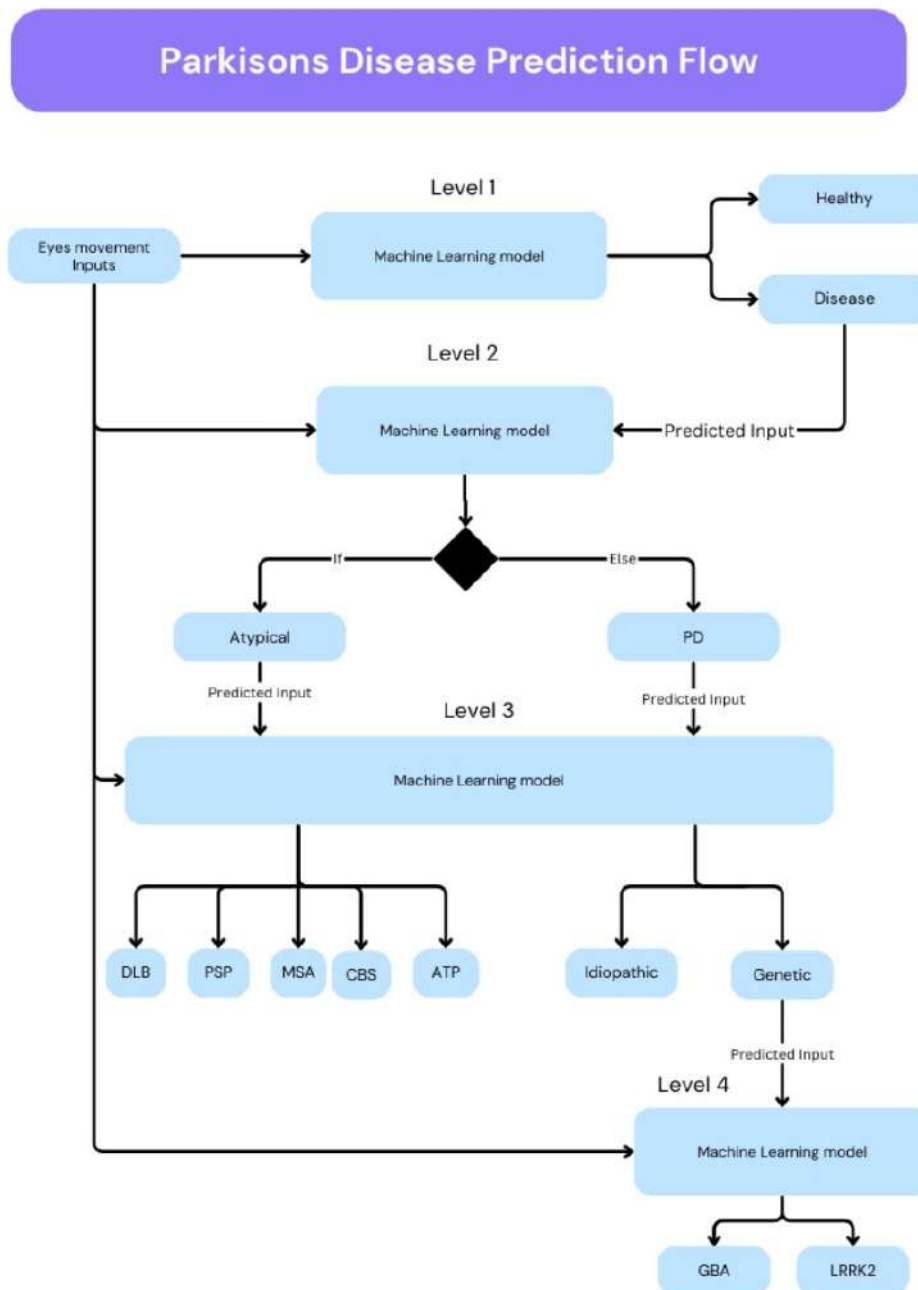


Figure 171: Machine Learning Pipeline for Classification. A hierarchical model classifying eye movement data into healthy, Parkinson’s Disease (PD), or atypical parkinsonian syndromes. Atypical cases are further classified into dementia with Lewy bodies (DLB), progressive supranuclear palsy (PSP), multiple system atrophy (MSA), corticobasal syndrome (CBS), and atypical parkinsonism (ATP). PD cases are subclassified into idiopathic and genetic forms, with genetic PD further divided into GBA- and LRRK2-associated subtypes.

8.3.3 Model Construction

For each classification level (Levels 1–4), depending on the classification task, six machine learning models were trained and evaluated. The following models were selected due to their individual strengths:

- **Random Forest:** Constructs a multitude of decision trees during training and outputs the mode of their

predictions. It handles high-dimensional data well and reduces the risk of overfitting through ensemble learning.

- **XGBoost:** Utilises gradient boosting algorithms to optimise performance by iteratively minimising errors. It has high computational efficiency, strong handling of missing values, and includes regularisation to prevent overfitting.
- **CatBoost:** Implements gradient boosting with native support for categorical features. It handles categorical data efficiently and reduces the need for extensive preprocessing.
- **LightGBM:** Employs a leaf-wise tree growth strategy for faster and more accurate results. It offers extremely fast training speed and is effective with large datasets.
- **AdaBoost:** Combines multiple weak classifiers to create a strong classifier by iteratively adjusting weights. It improves accuracy with minimal tuning and focuses on misclassified instances for better learning.
- **Gradient Boosting:** Builds trees sequentially to minimise prediction error by correcting prior tree errors. It is highly accurate, versatile, and robust against overfitting.

The performance of each model at every classification level was assessed using accuracy and confusion matrices. The best-performing model was selected, and its output was combined with the dataset for the subsequent level to train the next classification model. This hierarchical approach enabled the selection of the most appropriate model for each classification task based on data structure and sample size—particularly important when differentiating between binary classifications and multi-class subgroupings with varying sample sizes.

Study ID	Level 1 (Disease vs Healthy)	Level 2 (PD vs Atypical)	Level 3 IF PD = Idiopathic or Genetic, IF ATYPICAL = MSA, CBS, PSP, DLB, ATP	Level 4 IF GENETIC = GBA or LRRK2
0 OMS_PD001	Disease	PD	Genetic	GBA
1 OMS_PD002	Disease	PD	Idiopathic	NaN
2 OMS_PD003	Disease	PD	Idiopathic	NaN
3 OMS_PD004	Disease	PD	Genetic	LRRK2
4 OMS_PD005	Disease	PD	Idiopathic	NaN

Figure 172: Hierarchical Classification of Participants. Each participant was classified through four levels: (1) disease vs. healthy, (2) Parkinson’s Disease (PD) vs. atypical parkinsonism, (3) PD subtypes (idiopathic vs. genetic) or atypical syndromes (PSP, MSA, CBS, DLB, ATP), and (4) genetic PD subtypes (GBA vs. LRRK2). The classifications were mapped to the eye movement dataset by unique participant IDs.

8.3.4 Class Imbalance and Training Strategy

To address the imbalance between the classes, new data points were generated by shuffling the columns of existing data points for each class. This technique is broadly classified as data augmentation or synthetic data generation, specifically a column-shuffling augmentation strategy. For each data point, the values of its features (columns) were shuffled within the same class, i.e., rearranged randomly among instances of the same class. The shuffled versions were then used as synthetic data points to augment the dataset. This process created diverse rows for underrepresented classes without introducing bias. Because the new samples were derived entirely from existing data, no external noise was introduced, ensuring the synthetic data remained realistic representations of their respective classes.

- **Level 1:** 100 new rows were generated for healthy controls. Participants classified as healthy did not continue beyond Level 1.
- **Level 2:** 50 new rows were generated for PD and 120 for atypical parkinsonianism.
- **Level 3:** 90 rows were generated for genetic PD, 90 for PSP, 95 for MSA, 100 for CBS, and 100 for DLB. No new rows were generated for idiopathic PD.
- **Level 4:** 90 rows were generated for GBA and 100 for LRRK2.

The dataset's size, complexity, and number of classifications informed the training-test split ratio. For smaller, binary classification tasks, an 80/20 split was used (Levels 1 and 2). For more complex, multi-class classification tasks, a 70/30 split was adopted (Levels 3 and 4).

All code was written using Visual Studio Code (Version 1.95.2 Universal), and model development was conducted in Python (Version 3.13.1).

8.4 Results

Level 1: Binary classification of healthy controls vs. disease. The best-performing model was Random Forest with an accuracy of 84% and zero false negatives. Although it had 5 false positives, it outperformed other models including XGBoost (81%), CatBoost (77%), LightGBM (81%), AdaBoost (84%), and Gradient

Boosting (81%). Despite sharing the same accuracy as Random Forest, AdaBoost had more false negatives and four false positives.

Level 2: Binary classification of PD vs. atypical parkinsonism. AdaBoost achieved the highest accuracy at 97%, while XGBoost had the lowest at 85%. All models demonstrated high true positive rates for PD. However, some showed elevated false negatives (e.g., XGBoost) and false positives (e.g., XGBoost, CatBoost, Gradient Boosting). AdaBoost was selected due to its perfect classification (0 false positives and 0 false negatives) along with its high accuracy.

Level 3: Multi-class classification of idiopathic vs. genetic PD and PSP vs. MSA vs. CBS vs. DLB. CatBoost, LightGBM, and Gradient Boosting achieved the highest accuracy (99%), while AdaBoost performed poorest (40%). Despite XGBoost achieving slightly lower accuracy (97%), it was selected due to its training stability, a key consideration for machine learning models. Stable models avoid performance fluctuations across training epochs or data perturbations, making them more reliable and generalisable across datasets.

Level 4: Binary classification of GBA vs. LRRK2. Random Forest, XGBoost, CatBoost, AdaBoost, and Gradient Boosting all achieved 100% accuracy with perfect classification (0 false positives and false negatives). LightGBM lagged behind with 87%, misclassifying four samples. XGBoost was again selected due to its consistent stability across training, which is crucial for real-world applicability and reproducibility in collaborative research environments.

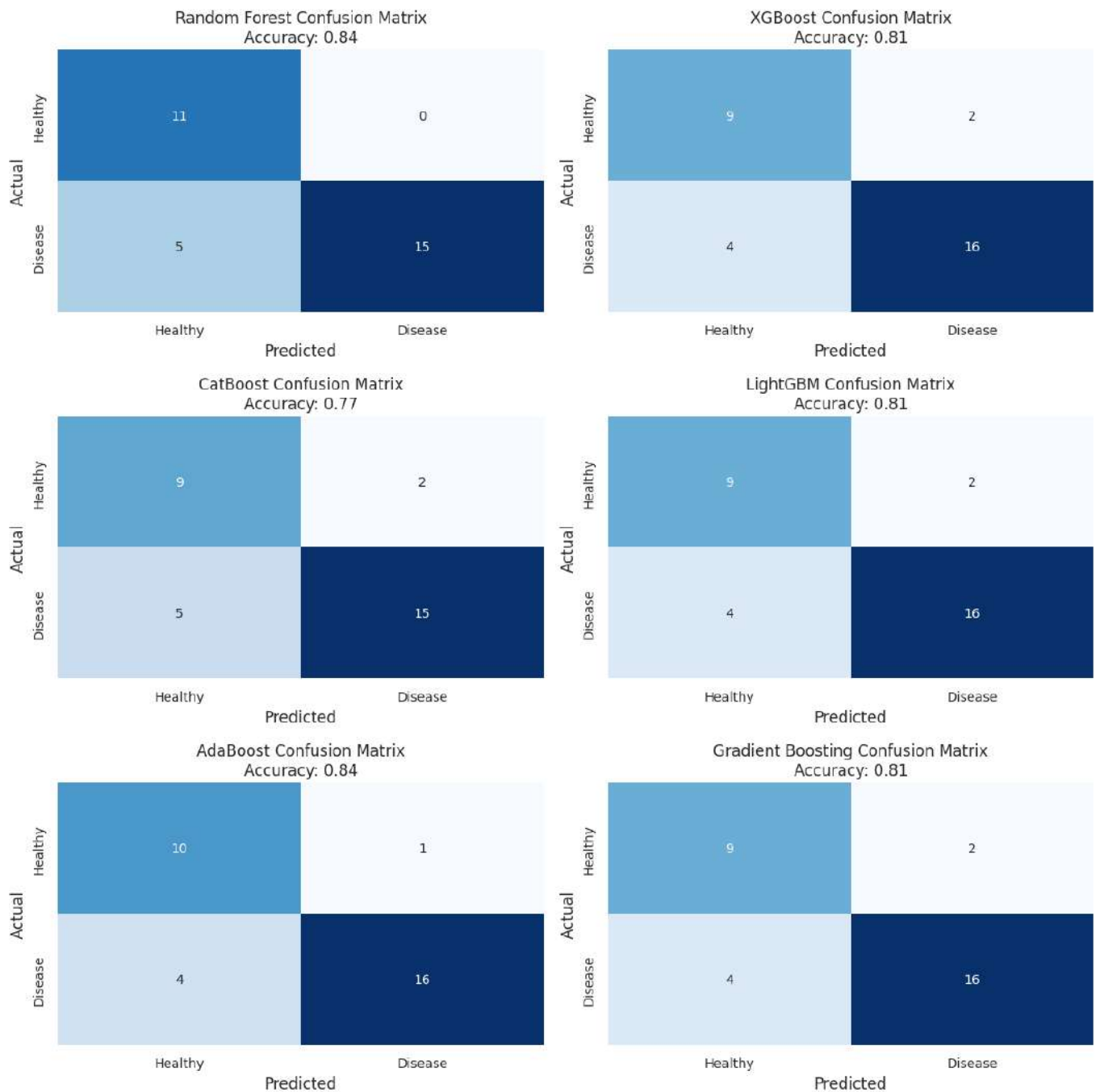


Figure 173: Confusion Matrices for Level 1 Classification (Disease vs. Healthy). Confusion matrices showing the performance of six machine learning models in distinguishing between healthy and diseased participants using eye movement data. Accuracy varies across models, with AdaBoost achieving the highest performance.

Model	True Positive (Healthy)	False Negative (Healthy)	False Positive (Disease)	True Negative (Disease)	Accuracy
Random Forest	11	0	5	15	0.84
XGBoost	9	2	4	16	0.81
CatBoost	9	2	5	15	0.77
LightGBM	9	2	4	16	0.81
AdaBoost	10	1	4	16	0.84
Gradient Boosting	9	2	4	16	0.81

Figure 174: Performance of Models in Level 1 Classification (Disease vs. Healthy). Comparison of machine learning models in classifying participants as healthy or diseased using eye movement data. AdaBoost and Random Forest achieved the highest accuracy (0.84), while CatBoost performed the lowest (0.77).

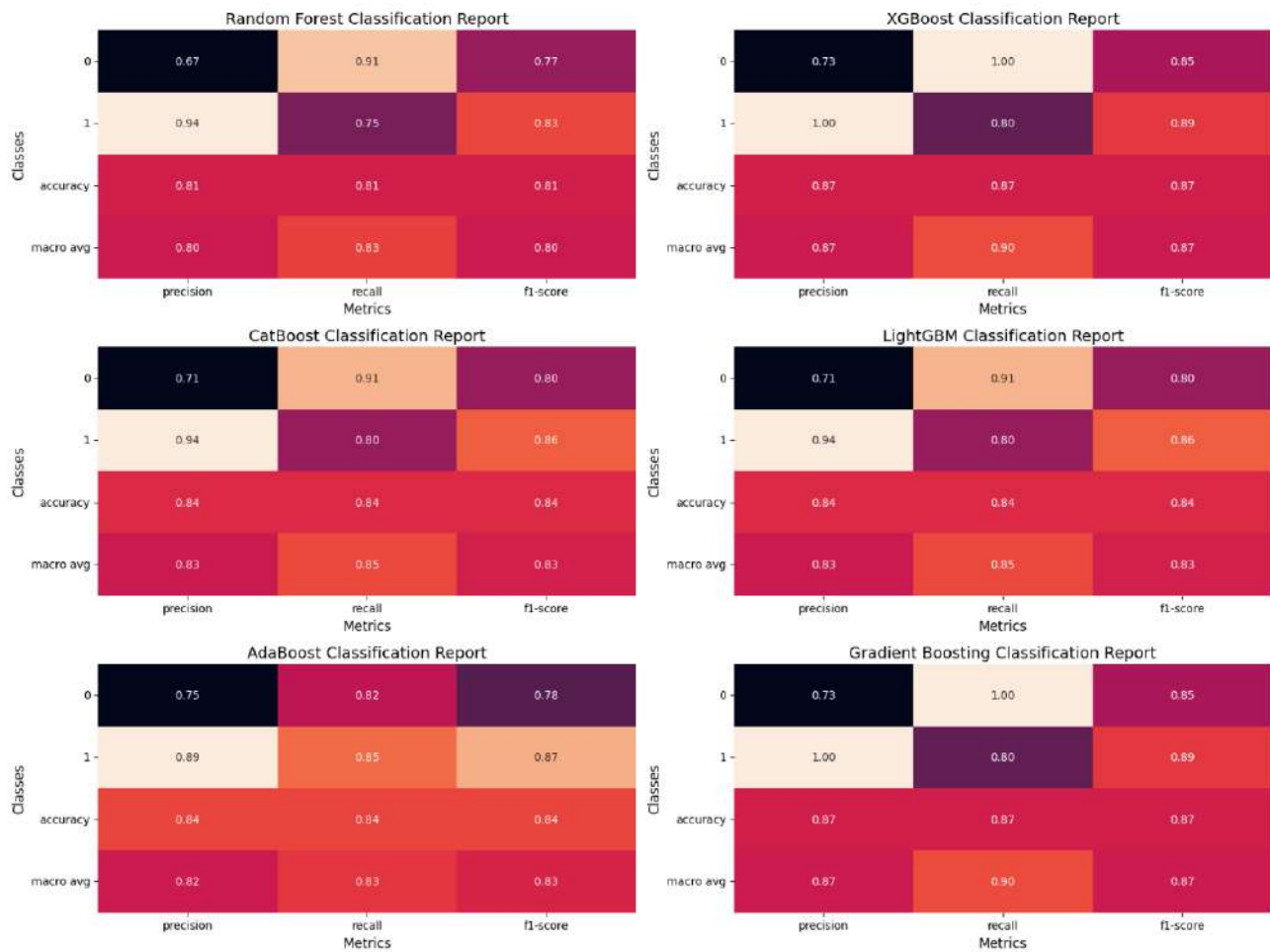


Figure 175: Classification Metrics for Level 1 (Disease vs. Healthy). Precision, recall, and F1-score for six models in classifying healthy vs. diseased participants. AdaBoost and Random Forest show the highest F1-scores, while CatBoost performs slightly lower.

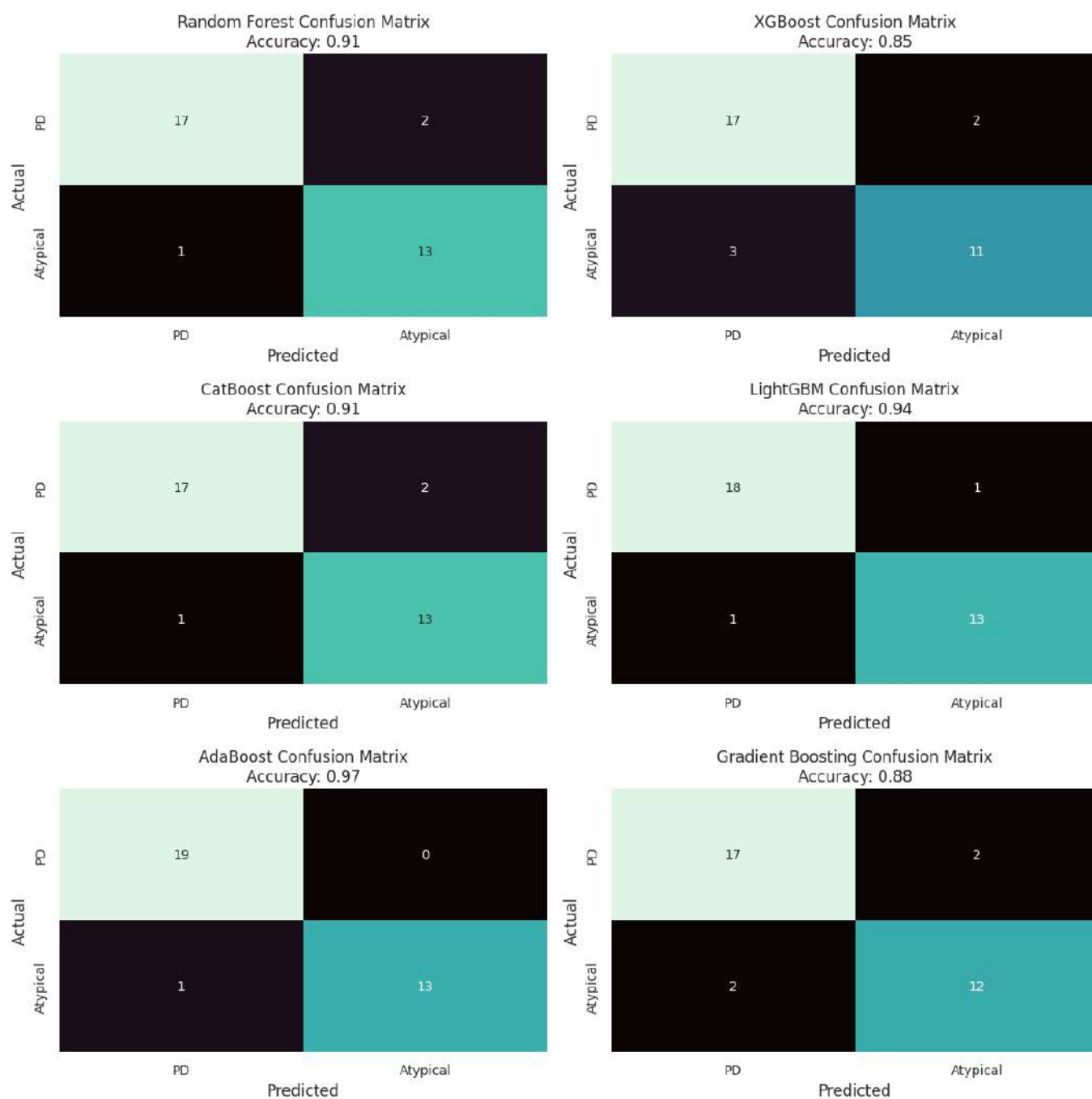


Figure 176: Confusion Matrices for Level 2 Classification (PD vs. Atypical Parkinsonian Syndromes.) Model performance in differentiating Parkinson’s Disease (PD) from atypical parkinsonian syndromes. AdaBoost achieves the highest accuracy, while XGBoost has the lowest.

Model	True Positive (PD)	False Negative (PD)	False Positive (Atypical)	True Negative (Atypical)	Accuracy
Random Forest	17	1	2	13	0.91
XGBoost	17	3	2	11	0.85
CatBoost	17	1	2	13	0.91
LightGBM	18	1	1	11	0.94
AdaBoost	19	0	0	11	0.97
Gradient Boosting	17	2	2	12	0.88

Figure 177: Performance of Models in Level 2 Classification (PD vs. Atypical Parkinsonian Syndromes.)
Evaluation of models in distinguishing Parkinson’s Disease (PD) from atypical parkinsonian syndromes. AdaBoost demonstrated the highest accuracy (0.97), while XGBoost had the lowest (0.85).

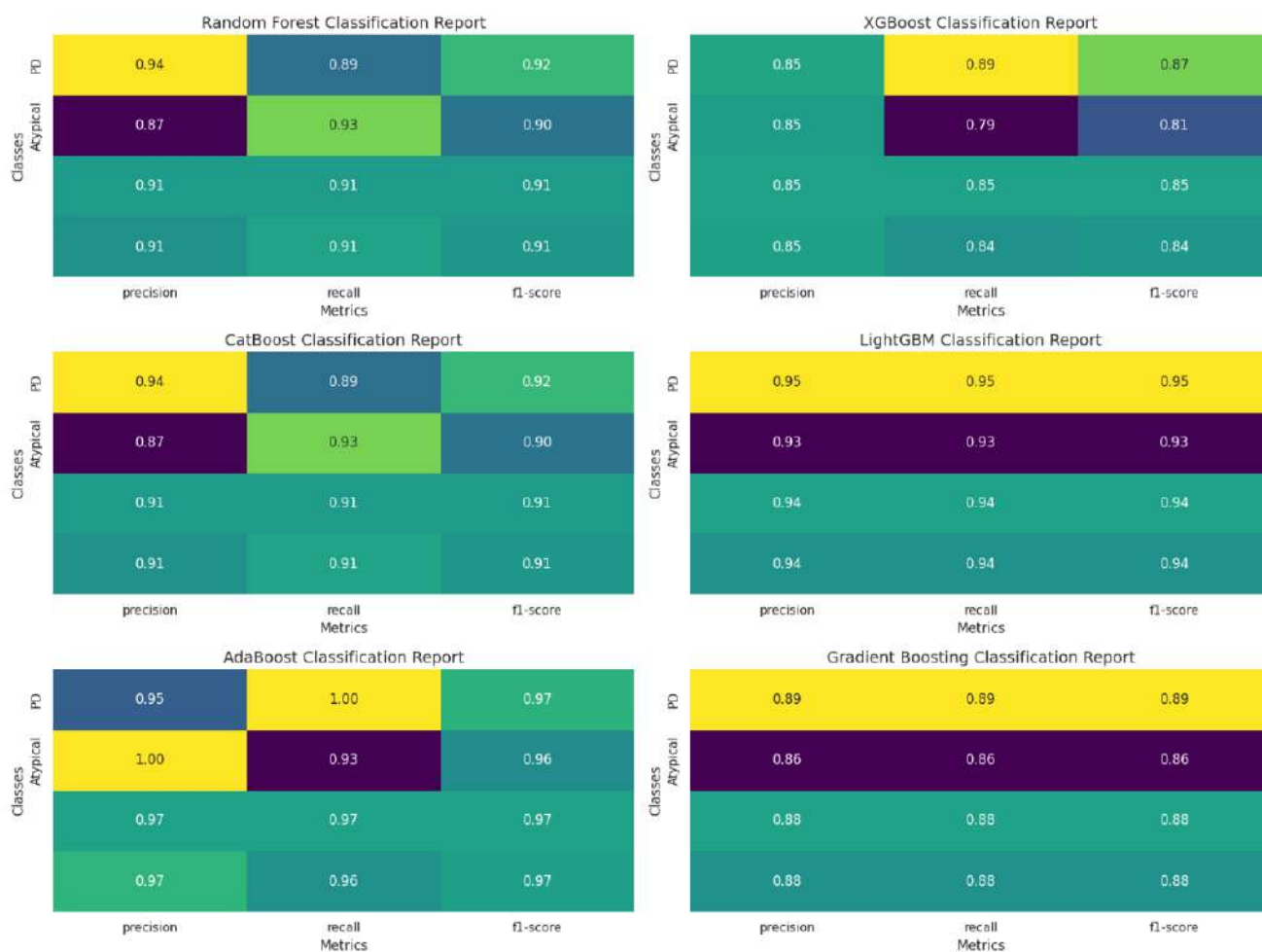


Figure 178: Classification Metrics for Level 2 (PD vs. Atypical Parkinsonian Syndromes). Evaluation of model performance in distinguishing PD from atypical parkinsonian syndromes. AdaBoost demonstrates the highest recall and F1-score, while XGBoost has reduced performance in recall for atypical cases.

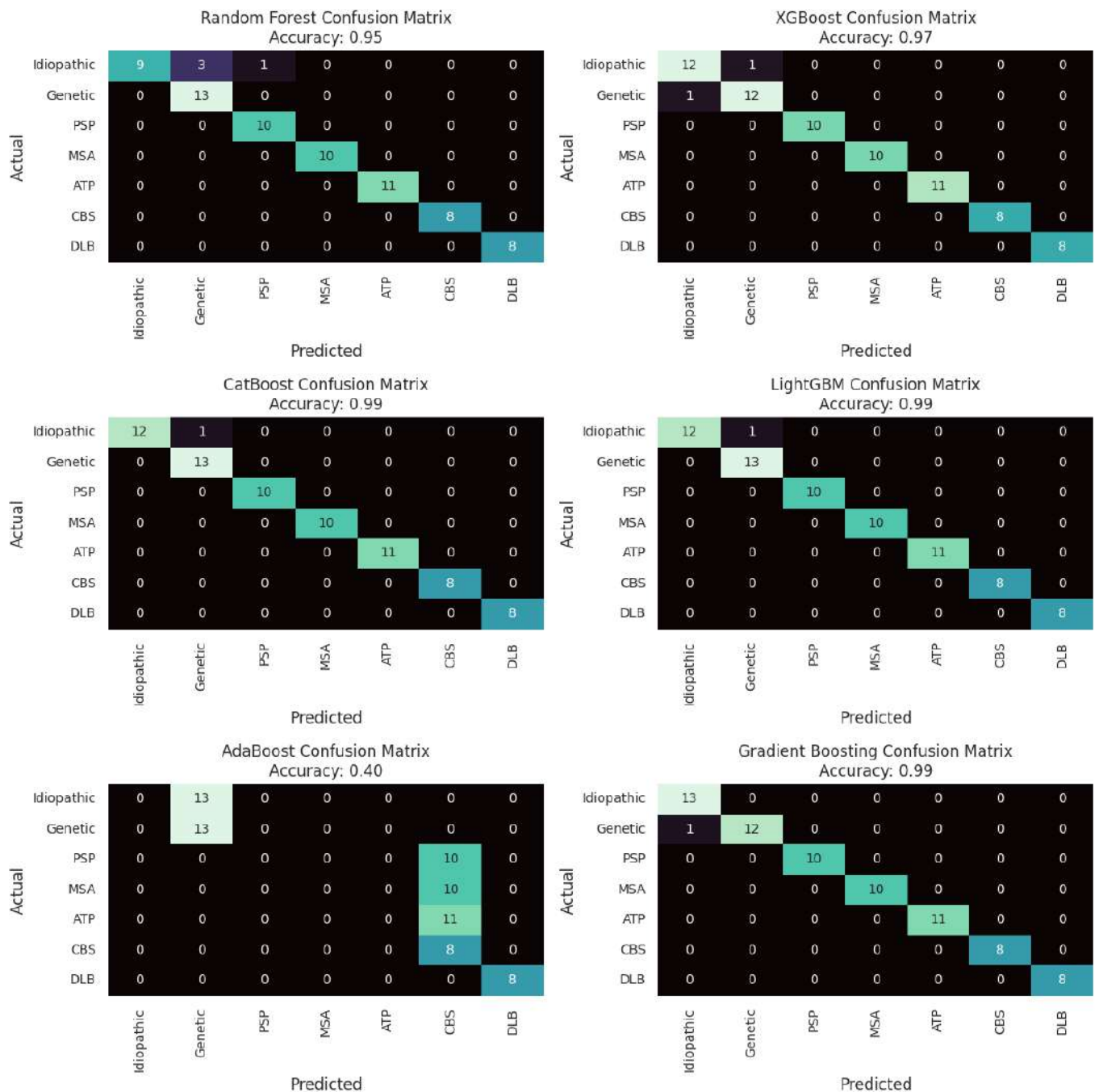


Figure 179: Confusion Matrices for Level 3 Classification (PD and Atypical Subtypes) Classification results for PD subtypes (idiopathic vs. genetic) and atypical syndromes (PSP, MSA, CBS, DLB, ATP). Models demonstrate high accuracy, with minor misclassifications.

Model	True Positive (Idiopathic)	False Negative (Idiopathic)	False Positive (Genetic)	True Negative (Genetic)	False Positive (PSP)	True Negative (PSP)	False Positive (ATP)	True Negative (ATP)	False Positive (CBS)	True Negative (CBS)	False Positive (DLB)	True Negative (DLB)	Accuracy
Random Forest	13	0	0	12	0	10	0	11	0	8	0	8	0.95
XGBoost	12	1	0	12	0	10	0	11	0	8	0	8	0.97
CatBoost	13	0	0	12	0	10	0	11	0	8	0	8	0.99
LightGBM	13	0	0	12	0	10	0	11	0	8	0	8	0.99
AdaBoost	13	0	0	12	0	10	0	11	0	8	0	8	0.40
Gradient Boosting	13	0	0	12	0	10	0	11	0	8	0	8	0.99

Figure 180: Performance of Models in Level 3 Classification (PD and Atypical Subtypes). Model classification results for idiopathic vs. genetic PD and atypical parkinsonian syndromes (PSP, MSA, CBS, DLB, ATP). LightGBM and CatBoost achieved near-perfect classification, while AdaBoost showed reduced performance.

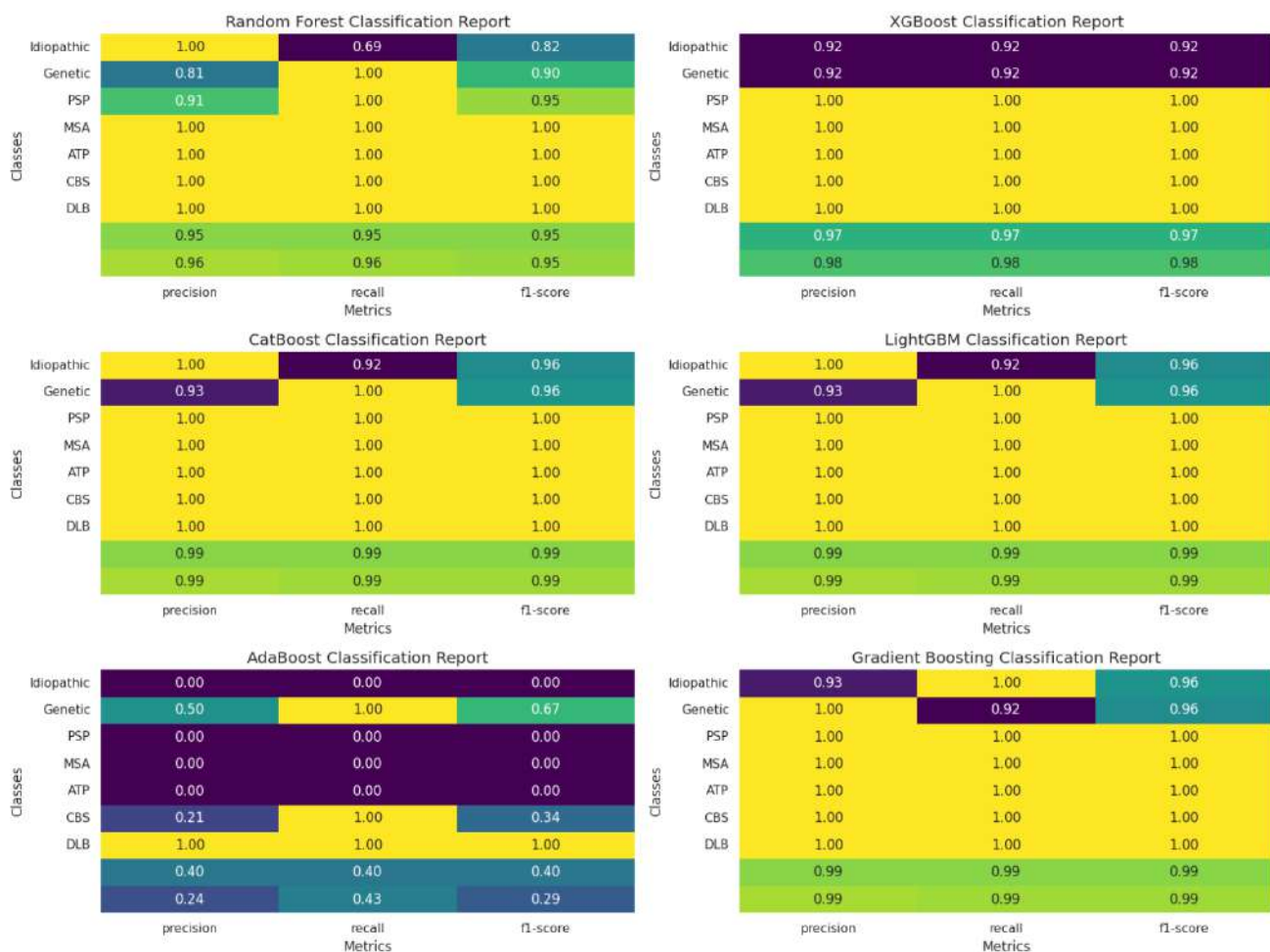


Figure 181: Classification Metrics for Level 3 (PD and Atypical Subtypes). Model performance for subclassifying PD into idiopathic vs. genetic and atypical parkinsonian syndromes into PSP, MSA, CBS, DLB, and ATP. Most models achieve high precision and recall, with AdaBoost showing reduced accuracy.

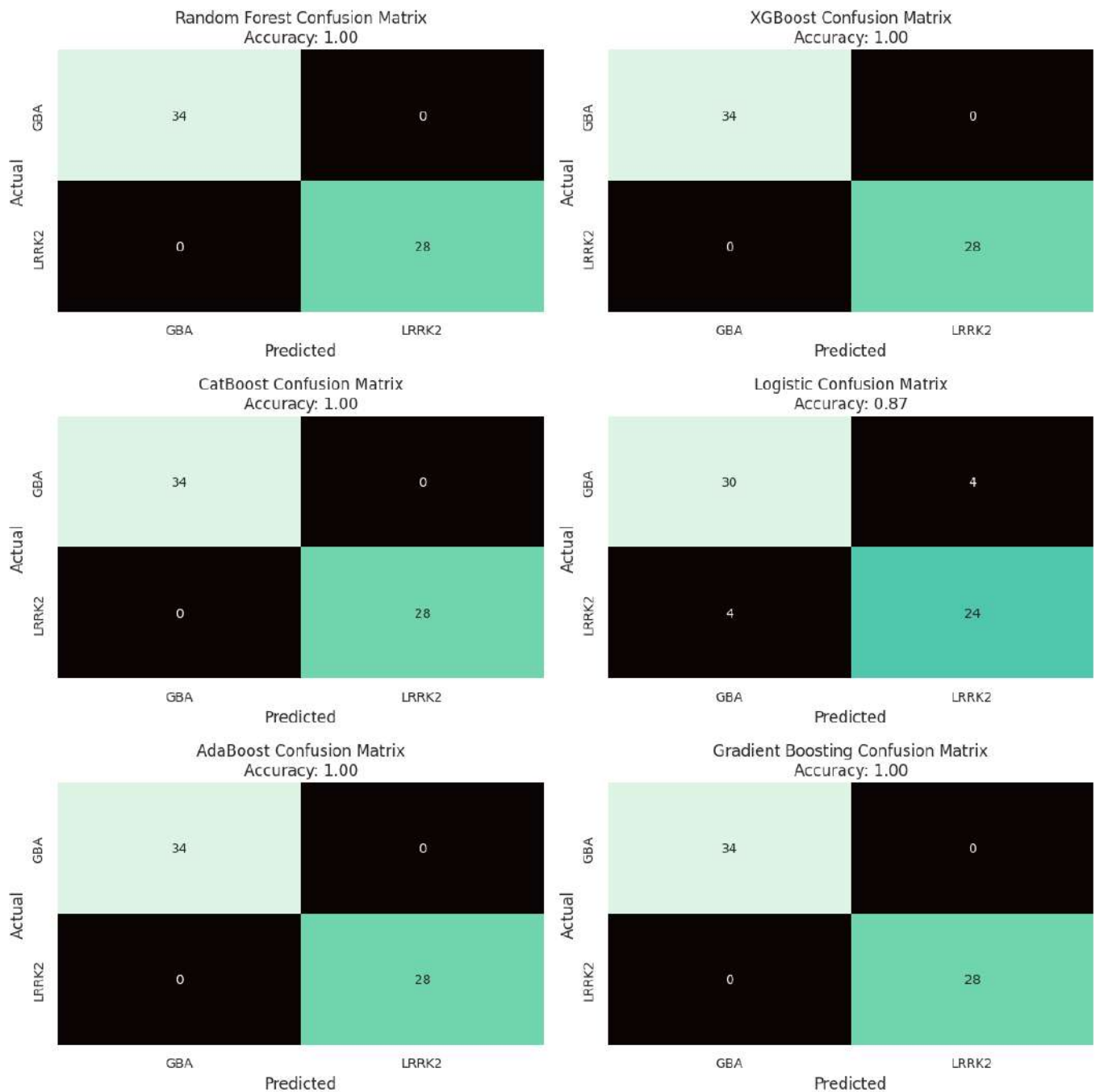


Figure 182: Confusion Matrices for Level 4 Classification (Genetic PD: GBA vs. LRRK2). Performance of machine learning models in subclassifying genetic PD cases into GBA or LRRK2-associated subtypes. Most models achieve perfect classification (accuracy = 1.0), except for logistic regression.

Model	True Positive (GBA)	False Negative (GBA)	False Positive (LRRK2)	True Negative (LRRK2)	Accuracy
Random Forest	34	0	0	28	1.00
XGBoost	34	0	0	28	1.00
CatBoost	34	0	0	28	1.00
Logistic	30	4	4	24	0.87
AdaBoost	34	0	0	28	1.00
Gradient Boosting	34	0	0	28	1.00

Figure 183: Performance of Models in Level 4 Classification (Genetic PD: GBA vs. LRRK2) Comparison of models in classifying genetic PD subtypes (GBA vs. LRRK2). Most models achieved perfect classification (accuracy = 1.0), except logistic regression (0.87).

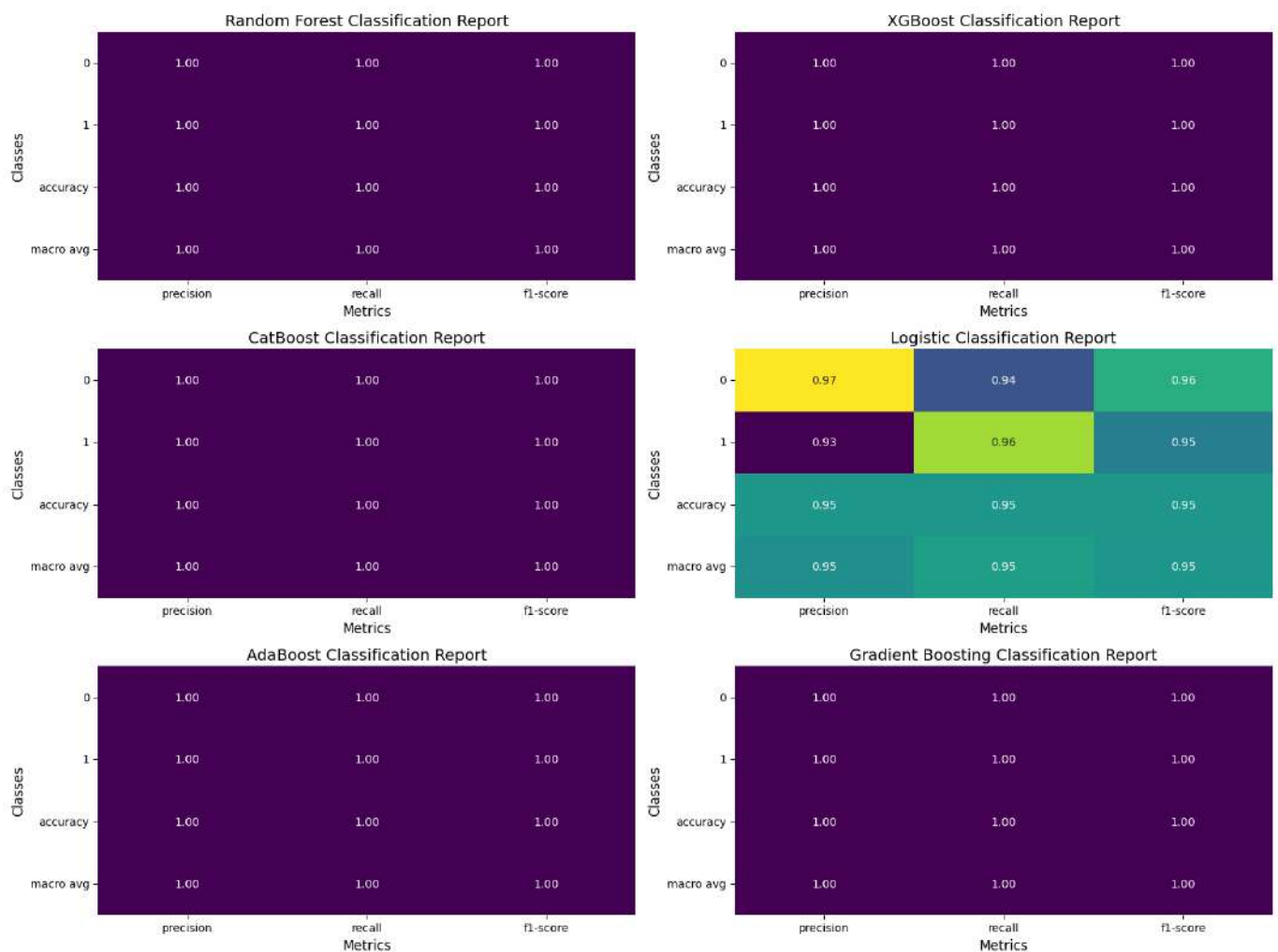


Figure 184: Classification Metrics for Level 4 (Genetic PD: GBA vs. LRRK2) Precision, recall, and F1-score for classifying genetic PD cases into GBA or LRRK2 subtypes. Most models achieve perfect classification, except logistic regression, which shows reduced recall.

8.5 Discussion

This project successfully utilised hierarchical machine learning models to systematically classify a complex dataset of different classes of eye movements into manageable levels, resulting in the accurate differential diagnosis of PD and atypical parkinsonian syndromes. Within these classes, it also accurately classified the subtypes of genetic (GBA and LRRK2 mutations) and idiopathic PD, as well as PSP, MSA, CBS, DLB, and ATP. The hierarchical structure enabled the stepwise classification of PD and atypical parkinsonian syndromes and their subtypes, ensuring that each layer provided a refined and focused diagnosis, significantly improving interpretability and predictive accuracy.

The inclusion of nuanced eye movement features such as fixation duration, pursuit gain, and antisaccadic errors was pivotal in enabling accurate classification. These metrics, being sensitive indicators of neurode-

generative processes, underscored their value as biomarkers. At Level 1, where individuals were classified as either disease or healthy controls, the Random Forest model achieved 84% accuracy, demonstrating the robustness of ensemble methods in handling diverse input features. Level 2 distinguished PD from atypical parkinsonian syndromes with 97% accuracy using AdaBoost, reflecting its strength in binary classification tasks. Level 3, a more complex task involving six subgroups, was managed using XGBoost, which yielded a high accuracy of 97% and offered greater stability during training. Lastly, Level 4 entailed the binary classification of GBA and LRRK2 subtypes, with both Random Forest and XGBoost achieving perfect accuracy (100%), highlighting the feasibility of classifying rare genetic subtypes with the right data and model selection.

This work builds on prior research into the diagnostic utility of motor and non-motor symptoms in combination with machine learning techniques to diagnose PD and differentiate between atypical parkinsonian syndromes. However, to date, no study has focused on the differential diagnosis between PD and atypical parkinsonian syndromes—including their subtypes—using eye movements and machine learning. Machine learning models have been applied to various data modalities in PD and atypical parkinsonian syndromes, including gait and movement data (Navita et al. 2025; Abbasi and Rezaee 2025; Hwang et al. 2025), neuroimaging (Cherubini et al. 2014; Choi et al. 2017; Segovia, Górriz et al. 2019), and less conventional methods such as voice (Sakar et al. 2013; H. Ma et al. 2017) and handwriting (Drotár et al. 2014; Pereira et al. 2017). Most studies used support vector machines, neural networks, or ensemble learning and achieved promising results. Given the variation in data type and classification tasks in this project, model selection was tailored at each level, improving overall accuracy and performance. Structuring tasks hierarchically enhanced generalisability and reduced overfitting.

The low performance of AdaBoost in Level 3 (accuracy: 40%) reflects its limitations when handling complex multi-class imbalances. AdaBoost's focus on misclassification penalties can overemphasise minority class errors, especially in highly imbalanced datasets (Chengsheng, Huacheng and Bing 2017). In such cases, gradient-boosting techniques like XGBoost are more effective (T. Chen and Guestrin 2016). Solutions include using ensemble strategies or employing SMOTE (Synthetic Minority Oversampling Technique), which interpolates between data points to generate synthetic samples (Chawla et al. 2002). A literature review of 448 machine learning studies applied to PD diagnosis found that few studies employed multiple models for one dataset, which can reduce robustness (Mei, Desrosiers and Frasnelli 2021). Ensemble methods, which

combine predictions from multiple models, offer more reliable performance.

Evaluating model performance using confusion matrices offers a comprehensive understanding of discrimination between groups. In Level 1, false positives (healthy classified as diseased) may reflect subclinical or age-related visuomotor changes (Dowiasch et al. 2015; Moschner and Baloh 1994). The selected metrics may require refinement or the addition of clinical variables to improve classification precision. False negatives in distinguishing APS from PD suggest difficulties capturing nuanced differences between these overlapping conditions (Stamelou, N. P. Quinn and Bhatia 2013). Limited representation of certain subtypes (e.g., MSA, PSP) may have further hindered the model's ability to learn these differences. Integrating ocular motor metrics with imaging data and hierarchical feature importance analysis could improve performance. Despite external influences like medication or comorbidities, eye movements offer diverse, multimodal inputs. However, overlapping pathways and compensatory mechanisms limit their independence from one another (Przybylszewski et al. 2023; Holland et al. 2020; Shaikh and David S. Zee 2018).

This research contributes significantly to the application of machine learning in healthcare. Hierarchical classification improved generalisability and reduced overfitting in multi-class environments. Ocular motor metrics, tied to basal ganglia and cerebellar circuits, offer diagnostic and prognostic utility. Clinically, the findings highlight the potential for more tailored treatment strategies and the use of portable, non-invasive eye-tracking tools for remote assessment—particularly valuable in underserved communities. The demonstrated feasibility of high-accuracy classification, even for rare genetic subtypes, supports early and accurate diagnosis and has the potential to improve patient outcomes while reducing healthcare disparities.

8.5.1 Clinical Implications

The findings from this study present significant clinical implications for the diagnosis and management of PD and atypical Parkinsonian syndromes. The successful implementation of hierarchical machine learning models to classify different classes of eye movements underscores the potential of eye-tracking technology as a non-invasive, objective biomarker for neurodegenerative diseases. Given the challenges in differentiating PD from atypical Parkinsonian syndromes based on clinical symptoms alone, these models offer a promising approach to improving diagnostic accuracy and reducing misdiagnosis, particularly in the early stages when

symptom overlap is highest.

The demonstrated high accuracy of classification, particularly in the differentiation between idiopathic and genetic PD, as well as among atypical Parkinsonian syndromes subtypes, suggests that these machine learning models could serve as valuable tools in clinical decision-making. Early and accurate classification of PD subtypes and atypical Parkinsonian syndromes can significantly impact treatment decisions, as different syndromes respond variably to dopaminergic therapy and disease-modifying interventions. For instance, the ability to distinguish between PSP and MSA using ocular motor metrics could guide more appropriate pharmacological and supportive interventions, ultimately improving patient outcomes.

Moreover, the hierarchical approach used in this study ensures that classification occurs in a stepwise manner, enhancing model interpretability and clinical applicability. The use of decision trees and ensemble learning methods, such as Random Forest and XGBoost, ensures robustness across different classification levels, making them suitable for real-world implementation. These models could be integrated into routine neurological assessments, complementing traditional clinical evaluations and neuroimaging findings.

Another critical clinical implication is the feasibility of using portable eye-tracking technology for remote monitoring of disease progression. Given that ocular motor impairments evolve over time, machine learning models trained on longitudinal eye movement data could provide a non-invasive means of tracking disease progression and evaluating treatment response. This could be particularly beneficial for patients in remote or underserved areas who may have limited access to specialized neurological care.

However, the presence of misclassifications, particularly false positives and false negatives, highlights the need for further refinement of feature selection and model training strategies. Incorporating additional clinical variables, such as cognitive test scores, imaging data, and genetic markers, could improve classification accuracy and reduce diagnostic uncertainty. Furthermore, addressing algorithmic biases and ensuring equitable model performance across diverse patient populations will be crucial for broader clinical adoption.

Overall, the integration of machine learning-based ocular motor assessments into clinical practice holds significant promise for enhancing diagnostic precision, enabling earlier intervention, and facilitating personalized

treatment strategies for neurodegenerative diseases.

8.5.2 Limitations

While the study leveraged a rich dataset with numerous ocular motor metrics, there are limitations which need to be acknowledged and addressed for increased diagnostic value. Some of the atypical groups, particularly DLB and CBS, had a small sample size. Although satisfactory diagnostic outcomes have been achieved with small datasets in machine learning (Belić et al. 2019), a larger sample size is necessary to better train a model, especially in extremely heterogeneous conditions with overlapping phenotypes such as atypical Parkinsonian syndromes (Deuschländer et al. 2018). Collecting large amounts of data is a challenge in clinical studies but could be overcome by combining data from various study locations or utilising local and publicly available repositories of data.

Another key limitation is that this study was not tested in clinical settings, leading to limited translatability into healthcare systems. This is also a significant problem with a number of machine learning studies in PD, as there is a need to refine technical approaches for specific clinical settings (Mei, Desrosiers and Frasnelli 2021). While ensemble models like XGBoost and Random Forest are powerful, their complexity limits interpretability. The study did not report efforts to enhance model explainability for clinicians. Techniques such as LIME or SHAP can bridge this gap (Zafar and N. Khan 2021; Y. C. Wang, T. C. T. Chen and Chiu 2023).

The study also did not report the use of feature selection techniques, which could dilute the model's focus on critical predictors, especially for small classes. Techniques such as Recursive Feature Elimination (RFE), Principal Component Analysis (PCA), and SHAP can reduce dimensionality and identify key metrics (Jeon and Sejong Oh 2020; Ding, Yang and F. Ma 2022; Bro and Smilde 2014; Lundberg 2019).

Additionally, the column-shuffling method for class imbalance may not sufficiently represent the distribution of rare classes. Techniques like SMOTE or adaptive weighting are more robust solutions (Gu, DeAngelis and Angelaki 2007; Gonzalez-Cuautle et al. 2020). Model selection was largely driven by accuracy, which is limited in imbalanced datasets. Metrics like F1-score and AUC-ROC provide a better understanding of model performance (Hamner and Frasco 2018). Cross-validation strategies, such as stratified k-fold, and

regularisation were also not reported and are critical to avoid overfitting (Liland, Skogholt and Indahl 2024; C. H. Yu, F. Gao and Q. Y. Wen 2021).

Iterative imputation may also introduce bias if missingness is not random. Alternative imputation methods like multiple imputation may reduce this bias (Woods et al. 2024). Finally, computational efficiency and fairness were not addressed. High computational costs can limit real-world implementation, and algorithmic bias can lead to inequitable outcomes across patient groups (Ngiam and Khor 2019; Ferrara 2024).

8.5.3 Future Directions

Future work should prioritise expanding datasets, especially for rare subtypes, such as PSP-RS vs. PSP-P, MSA-P vs. MSA-C, and tremor-dominant vs. akinetic-rigid PD (B. Chen et al. 2023; Gültekin 2020; M. C. Campbell et al. 2020). Integrating multimodal data—such as imaging and genetic profiles—and longitudinal tracking of motor and cognitive scores would enhance precision and provide insights into disease staging.

Transfer learning and external validation should be pursued to generalise findings across populations. Finally, model interpretability must be prioritised. Integrating SHAP or LIME into clinical dashboards will build trust and facilitate clinical adoption.

In conclusion, this work illustrates the successful application of hierarchical machine learning models to distinguish between PD, atypical Parkinsonian syndromes, and healthy controls using ocular motor data. It lays a strong foundation for developing scalable, explainable, and accurate diagnostic systems that could be deployed in real-world clinical environments for early diagnosis, personalised treatment, and remote monitoring.

8.6 Chapter Summary

This chapter examined the use of hierarchical machine learning models to classify PD and atypical Parkinsonian syndromes based on ocular motor metrics. The study successfully demonstrated that stepwise classification enhances predictive accuracy and interpretability, achieving high performance at different hier-

archical levels. Notably, the models achieved an accuracy of 84% in distinguishing diseased individuals from healthy controls, 97% in differentiating PD from atypical Parkinsonian syndromes, and 100% in classifying genetic subtypes of PD.

9 Pilot Test for the Comparison of EyeLink (Desktop-Based) and Tobii (Mobile) Eye Trackers as a Diagnostic Tool for Neurodegenerative Disorders

9.1 Introduction

Eye-tracking technology has a rich and evolving history that spans over a century, beginning with early explorations into the mechanics of eye movement and culminating in sophisticated applications across various fields today. The origins of eye-tracking can be traced back to the late 19th century when researchers first began to investigate the relationship between eye movements and cognitive processes. Early devices were rudimentary, often involving mechanical methods to record eye positions, but they laid the groundwork for future advancements in the field (Płużyczka 2018).

The development of eye-tracking technology can be categorized into three main phases: the early mechanical systems, the introduction of electronic devices, and the modern era characterized by mobile and unobtrusive tracking systems. In the early 20th century, researchers like Louis Émile Javal and later, Alfred L. Yarbus, made significant contributions by studying eye movements during reading and visual perception, establishing foundational theories about how gaze patterns reflect cognitive processes (Płużyczka 2018). These studies highlighted the importance of fixations and saccades—two fundamental components of eye movement that are still central to eye-tracking research today.

The second phase of development began in the mid-20th century with the advent of electronic eye trackers, which utilized infrared light to detect eye movements more accurately. This technological leap allowed for more precise measurements and opened new avenues for research in psychology, marketing, and human-computer interaction. For instance, the introduction of the first commercial eye trackers in the 1980s enabled researchers to explore visual attention in various contexts, from advertising to user interface design (Khachatryan and Rihn 2014).

As technology progressed into the 21st century, eye-tracking systems became increasingly sophisticated, incorporating features such as real-time data processing and mobile tracking capabilities. The integration

of eye-tracking technology into wearable devices, such as glasses, has allowed researchers to study gaze behaviour in naturalistic settings, providing insights into how people interact with their environments outside of controlled laboratory conditions (Hessels et al. 2020; Zhu et al. 2024). This shift has been particularly impactful in fields like sports science, where understanding gaze behaviour can inform training and performance strategies (Kredel et al. 2023).

The EyeLink 1000 Plus is a sophisticated eye-tracking system developed by SR Research, designed to provide high-precision measurements of eye movements for a variety of research applications. This system is particularly noted for its versatility, allowing for both remote and head-mounted configurations, which makes it suitable for diverse experimental settings, including cognitive psychology, neuroscience, and human-computer interaction studies (N. Stein et al. 2021; König et al. 2016). One of the standout features of the EyeLink 1000 Plus is its impressive sampling rate of 1000 Hz, which enables the system to capture eye movements with exceptional temporal resolution (Raju et al. 2021). This high sampling frequency is crucial for accurately recording rapid eye movements, such as saccades and fixations, which are fundamental to understanding visual attention and cognitive processes (Andersson, Nyström and Holmqvist 2010).

The system also boasts a spatial resolution of less than 0.01 degrees of visual angle (RMS), allowing for precise localization of gaze direction (Raju et al. 2021; Kirkby et al. 2013). This level of accuracy is particularly beneficial in studies where minute differences in gaze behavior can yield significant insights into cognitive functioning and visual processing. The EyeLink 1000 Plus is equipped with advanced calibration techniques that enhance its usability and accuracy. The calibration process can be performed using a variety of methods, including standard visual-target calibration and innovative approaches that do not require participants to view the screen directly (Harrar et al. 2018). This flexibility is particularly advantageous in studies involving populations with cognitive impairments or those who may have difficulty following traditional calibration protocols.

Furthermore, the system's ability to track one eye while maintaining high accuracy has been shown to yield comparable results to binocular tracking, making it a practical choice for many researchers (Hooge et al. 2019). In terms of hardware, the EyeLink 1000 Plus features a compact camera that can be mounted on a tabletop or used in a head-mounted configuration, depending on the experimental requirements. The camera utilizes infrared illumination to minimize interference from ambient light, ensuring reliable data collection

even in varied lighting conditions (Felßberg and Strazdas 2025). The system's design also accommodates head movements, which is critical for maintaining data integrity during dynamic tasks (Hooge et al. 2019).

The EyeLink 1000 Plus can be integrated with various stimulus presentation software, such as MATLAB and Psychophysics Toolbox, allowing researchers to create complex experimental designs while seamlessly collecting eye movement data (Hartmann and Weisz 2020). The data output from the EyeLink 1000 Plus includes detailed information on fixation duration, saccade metrics (such as velocity and amplitude), and pupil size, which can be analyzed to gain insights into cognitive processes and emotional responses (Koochaki and Najafizadeh 2021). The system's software provides robust tools for data visualization and analysis, enabling researchers to interpret their findings effectively. Additionally, the EyeLink 1000 Plus has been validated in numerous studies, demonstrating its reliability and accuracy across various research domains, including visual perception, attention, and cognitive neuroscience (Z. Huang et al. 2024; Iacobelli et al. 2023).

The Tobii Pro Nano is a compact, screen-based eye-tracking device developed by Tobii Technology, designed to facilitate high-quality gaze data collection across research domains such as psychology, marketing, and human-computer interaction (Limin Zhang and Cui 2022; Pauszek 2023). The device is particularly valued for its portability and ease of use, making it highly suitable for both laboratory-based and field studies (Convery et al. 2023; Saleem, Straus and Napolitano 2021). With a sampling rate of up to 60 Hz, the Tobii Pro Nano can reliably capture key eye movement behaviors such as fixations and saccades. It provides binocular data, enabling researchers to obtain a more comprehensive understanding of gaze behavior (Limin Zhang and Cui 2022; Reshetniak and Faure 2024; SR Labs 2024). The device offers spatial accuracy of approximately 0.4° , which is sufficient for many applications, though it does not match the spatial precision of higher-end systems like the EyeLink 1000 Plus (SR Labs 2024).

Unlike head-mounted systems, the Tobii Pro Nano employs a remote tracking methodology, typically mounted on a monitor, thus allowing participants to interact naturally with visual stimuli (SR Labs 2024; Thibeault et al. 2019). This is especially advantageous for studies emphasizing participant comfort or naturalistic behavior (Narcizo, De Queiroz and Gomes 2014). It compensates for moderate head movements, maintaining tracking fidelity within the system's range (Thibeault et al. 2019). Integrated with Tobii software (Tobii Pro Lab and Tobii Analyzer), the device supports sophisticated gaze data analysis tools, including gaze plots,

heat maps, and fixation metrics (Blascheck et al. 2017; Blascheck et al. 2014). Calibration is simple and user-friendly, typically requiring participants to follow an on-screen procedure, which is advantageous in studies involving children or individuals with cognitive impairments (Cho et al. 2022; Kooiker et al. 2016). The device also supports diverse stimuli types, from static images to interactive tasks (Niehorster, Andersson and Nyström 2020; Pentus et al. 2020).

Its lightweight and portable design further enhances its utility in field research, allowing high-quality gaze data collection beyond controlled laboratory environments (Limin Zhang and Cui 2022; Thibeault et al. 2019). Despite its mobility, the Tobii Pro Nano maintains robust data quality in variable conditions **Dilbeck2023**. It has been widely used to assess attentional biases in at-risk populations and individuals with cognitive disorders **Thibeault2019; Tsitsi2023**, providing insights into decision-making and consumer behavior **Jaeger2020; Weinberg2020**.

By contrast, the EyeLink 1000 Plus, with its 1000 Hz sampling rate and sub-0.01 degree spatial resolution, offers unmatched precision for eye movement research (SR Research n.d.). This makes it ideal for analyzing rapid eye movements such as saccades and fixations in cognitive neuroscience studies (S. B. Hutton 2019). While the EyeLink 1000 Plus supports both remote and head-mounted configurations, its laboratory-based setup and complex calibration may pose challenges for less experienced users or time-sensitive clinical environments (SR Research n.d.; S. B. Hutton 2019). However, this configuration offers unmatched data quality in controlled settings.

In terms of usability, the Tobii Pro Nano stands out for its user-friendly setup. It requires no head-mounted hardware and features a simplified calibration process, enhancing its appeal in clinical settings with cognitively impaired participants (Limin Zhang and Cui 2022). While its precision is lower, its ease of use and participant comfort make it suitable for outpatient clinics, home visits, and usability testing (Thibeault et al. 2019).

Clinically, the EyeLink 1000 Plus is preferred where high precision is required—such as detecting subtle ocular motor changes in neurodegenerative diseases like Alzheimer’s disease (Eraslan Boz et al. 2023; Seokjun Oh and J.-H. Lee 2024). However, its bulkier setup and sensitivity to head movements may limit its applicability in real-world or fast-paced clinical settings. The Tobii Pro Nano’s mobility and unobtrusive

design allow for more natural participant behavior, improving ecological validity in usability and marketing studies (Thibeault et al. 2019).

Despite their strengths, both systems have limitations. The EyeLink 1000 Plus demands a controlled environment and experienced operators, while the Tobii Pro Nano may underperform in high-precision applications due to its lower sampling rate and sensitivity to environmental factors such as ambient lighting. In summary, the EyeLink 1000 Plus is best suited for controlled laboratory-based research that requires high spatial and temporal resolution. The Tobii Pro Nano excels in studies prioritizing usability, participant comfort, and mobility. The choice between the two depends on the specific research goals, participant population, and environmental constraints.

9.2 Project Aims

1. To compare the performance of the Tobii portable eye tracker and the EyeLink 1000 Plus desktop-mounted eye tracker in capturing precise eye movement metrics.
2. To evaluate the feasibility of using portable eye trackers in clinical and research settings.

9.3 Methods

9.3.1 Participants

Participants were recruited for the Tobii study following the procedures outlined in Chapter 2: General Methods. Inclusion criteria were: (1) a confirmed diagnosis of iPD, verified via consultant letters prior to enrolment, (2) age between 40–80 years, (3) normal or corrected-to-normal vision, (4) ability to provide informed consent, (5) ability to follow verbal instructions, and (6) capacity to sit comfortably for the duration of testing. Exclusion criteria included: (1) history of other neurological conditions, head trauma, or stroke, (2) bilateral visual impairments or conditions impairing ocular motor function (e.g., diplopia), (3) severe psychiatric illness such as psychosis, (4) systemic health conditions affecting vision, such as diabetic retinopathy, (5) pregnancy or suspected pregnancy (self-declared), and (6) history of epilepsy.

Thirteen participants with iPD were included. The study received ethical approval from the UCL Research Ethics Committee, and informed consent was obtained from all participants prior to testing.

9.3.2 EyeLink 1000 Plus Experimental Procedure

The standard ocular motor battery described in Chapter 2: General Methods was administered to all participants using the EyeLink 1000 Plus, excluding the pursuit paradigm. The setup, calibration, and validation procedures were identical to those outlined previously.

9.3.3 Tobii Nano Pro Experimental Procedure

The Tobii Nano Pro is a portable, screen-based eye tracker with dimensions $17 \times 1.8 \times 1.3$ cm and a weight of 59g. It operates at a sampling frequency of 60 Hz and offers spatial accuracy of 0.3° under optimal conditions. The device includes an embedded camera that captures binocular eye data in 3D space to compute gaze coordinates, pupil diameter, and eye position. The tracker was attached via USB to a Microsoft Surface Pro 7 tablet (screen size: 26×17 cm; resolution: 1920×1080 pixels) and secured with magnetic brackets below the display. Participants were seated approximately 50 cm from the device to match the visual angles used in EyeLink testing. Calibration used a 9-point target and 3D eye model, with drift compensation. Calibration was conducted prior to each test.

A modified ocular motor battery (excluding pursuit) was administered using the Tobii Nano Pro:

Fixation: A central target was followed by four peripheral targets presented for 30 seconds each. Targets were positioned at 10° vertically at positions up and down of the screen, and 15° horizontally, to the right and the left of the screen. Participants were instructed to fixate steadily with minimal blinking.

Antisaccades: Horizontal ($\pm 15^\circ$) and vertical ($\pm 10^\circ$) antisaccade trials were presented in randomized blocks of 20 trials each. Participants were instructed to look in the opposite direction of the target. Each trial lasted 2 seconds.

Oblique Saccades: Targets were placed at 8° eccentricity from screen center in 30 randomized trials. Twelve target positions were evenly distributed along a circle's circumference. Participants were instructed to follow each target.

Reflexive Saccades: Participants made reflexive saccades to stimuli at $\pm 15^\circ$ horizontally and $\pm 10^\circ$ vertically in randomized 30-trial blocks. Participants were instructed to look directly at the appearing target.

9.3.4 Data Processing and Analysis

Data processing for EyeLink 1000 Plus followed procedures described in Chapter 2: General Methods. For Tobii Nano Pro, raw data files were exported, including fixation metrics (average fixation duration, saccade count, and pupil size), and saccadic metrics (average amplitude, peak velocity, latency, and velocity). Analysis proceeded in two stages: (1) comparing iPD vs. Control performance using Tobii, and (2) comparing metrics from EyeLink 1000 Plus vs. Tobii Nano Pro.

9.4 Statistical Analyses

Descriptive statistics (medians, interquartile ranges, and ranges) were calculated for all metrics across Control and iPD groups. Data normality was evaluated using the Shapiro-Wilk test, revealing non-normal distributions. Thus, non-parametric methods were employed. Between-group comparisons (iPD vs. Control using Tobii) were conducted using Mann–Whitney U tests with rank-biserial correlation effect sizes and p-values reported. Agreement between EyeLink and Tobii data was assessed using four analyses: (1) Spearman correlation, (2) Bland–Altman analysis for systematic bias and limits of agreement, (3) Intraclass Correlation Coefficients (ICC) to quantify reliability, and (4) Wilcoxon signed-rank tests to assess systematic paired differences. To test the effect of Tracker (EyeLink vs. Tobii) and Group (iPD vs. Control), a Friedman test was used as a non-parametric repeated-measures ANOVA alternative. All statistical analyses were conducted in R (Version 2023.09.1+494, R Core Team, Vienna, Austria), with significance set at $\alpha = 0.05$.

9.5 Results

9.5.1 Participants

The dataset included a total of 15 participants, comprising 3 Controls and 11 individuals with iPD. The mean age of all participants was 63.24 years, with Controls averaging 59.24 years and the iPD group 64.11 years. There were 9 male and 6 female participants overall. Among iPD participants, the mean Levodopa Equivalent Daily Dose (LEDD) was 580.45 mg, and the mean disease duration was 4.54 years. As expected, LEDD values were not applicable to the Control group.

9.5.2 Ocular Motor Metrics Using Tobii

Significant differences between iPD and control groups were observed in selected metrics using the Mann–Whitney U test. In the fixation paradigm, the iPD group exhibited a significantly greater number of total saccades ($U = 27.00$, $p = 0.0490$, effect size = -0.80) compared to controls. In the vertical reflexive saccades paradigm, saccadic amplitude was significantly reduced in the iPD group compared to controls ($U = 27.00$, $p = 0.0490$, effect size = -0.80). No other fixation or saccade metrics were significantly different between groups.

9.5.3 Tobii Versus EyeLink 1000 Plus

In the fixation paradigm, Spearman correlation analysis revealed weak associations between Tobii Nano Pro and EyeLink 1000 Plus for all fixation metrics. Average Fixation Duration showed a weak negative correlation ($\rho = -0.387$, $p = 0.191$), Pupil Size exhibited an extremely weak negative correlation ($\rho = -0.110$, $p = 0.721$), and Number of Saccades showed a weak positive correlation ($\rho = 0.283$, $p = 0.348$), indicating poor convergence between the two devices. Bland–Altman plots revealed wide limits of agreement across metrics, underscoring systematic variability in recorded values. Intraclass Correlation Coefficient (ICC) values were low across fixation parameters: Average Fixation Duration (ICC = 0.073), Pupil Size (ICC = 0.121), and Number of Saccades (ICC ≈ 0.000), confirming poor measurement agreement. Wilcoxon signed-rank tests revealed significant differences between Tobii and EyeLink on all fixation metrics: Average Fixation Duration ($p = 0.0002$), Pupil Size ($p = 0.0002$), and Number of Saccades ($p = 0.0017$), suggesting systematic discrepancies likely due to device differences in sampling rate, spatial resolution, and calibration.

For saccadic metrics across the antisaccade, reflexive, and oblique paradigms, Spearman correlations between devices ranged from weak to moderate: Peak Velocity ($\rho = 0.168$, $p = 0.602$), Saccade Amplitude ($\rho = 0.112$, $p = 0.729$), and Start Time ($\rho = 0.538$, $p = 0.071$), indicating inconsistent alignment. Bland–Altman analysis showed systematic bias and wide limits of agreement across all metrics. ICC values indicated poor reliability between devices: Peak Velocity (ICC = 0.136), Saccade Amplitude (ICC = 0.121), and Start Time (ICC = 0.0046). Wilcoxon signed-rank tests detected significant differences in Peak Velocity ($p = 0.0005$), Saccade Amplitude ($p = 0.0005$), and Start Time ($p = 0.0010$) between EyeLink and Tobii, confirming systematic divergence likely due to differences in tracking algorithms and hardware performance.

9.6 Discussion

This study compared the usability of the Tobii Nano Pro, a portable eye tracker, to the EyeLink 1000 Plus, a high-precision desktop-mounted tracker, in capturing ocular motor performance in individuals with iPD and healthy Controls. The results revealed significant discrepancies across several key eye movement metrics, reflecting both methodological and technical differences between the two systems.

The cross-device comparison demonstrated poor agreement between the Tobii and EyeLink trackers. Spearman correlation analyses indicated weak to moderate associations across metrics, while Bland–Altman analyses highlighted systematic biases and wide limits of agreement. These inconsistencies were further supported by low ICC values across fixation and saccadic parameters, suggesting unreliable measurement equivalence. Wilcoxon signed-rank tests confirmed statistically significant differences in nearly all parameters, particularly in fixation duration, pupil size, and saccadic velocity. Together, these results underscore substantial divergence between Tobii and EyeLink recordings, likely stemming from fundamental differences in hardware specifications, calibration procedures, and data preprocessing pipelines.

Device performance varied by paradigm. During fixation tasks, the Tobii system yielded greater variability in pupil size and saccade count, while EyeLink delivered more stable and precise metrics—an expected finding given its higher temporal resolution (1000 Hz vs. 60 Hz). In saccade-based paradigms, including antisaccades and reflexive saccades, Tobii consistently produced lower peak velocity and saccade amplitude estimates.

This may reflect Tobii's lower sampling frequency, which can attenuate detection of high-speed ocular events, and its simplified gaze-detection algorithms. While EyeLink reliably captured expected iPD-associated impairments in saccadic control, Tobii's ability to detect these differences was inconsistent, highlighting concerns about sensitivity for clinical research.

Preprocessing and calibration differences likely contributed to these discrepancies. EyeLink employs a robust multi-point calibration protocol, while Tobii relies on a shorter 9-point model, potentially increasing noise and reducing accuracy. Additionally, Tobii's lower signal-to-noise ratio and reduced pupil tracking precision in suboptimal lighting conditions may explain variability in pupil size and fixation data. These technical limitations undermine Tobii's capacity to capture subtle ocular motor deficits that are detectable using the EyeLink system.

Furthermore, EyeLink provides more granular outputs, including microsaccade detection and saccade velocity profiles, while Tobii offers a limited set of aggregated metrics. This restricts Tobii's ability to detect fine-grained impairments frequently observed in PD, such as memory-guided saccade errors or vertical antisaccade latency increases.

From a methodological perspective, the EyeLink 1000 Plus may be particularly advantageous for diagnostic and exploratory clinical research, given its superior spatial and temporal resolution, robust gaze position accuracy, and capability to capture subtle ocular motor abnormalities. In diagnostic research—where precise detection of subtle eye movement impairments is crucial—the EyeLink system's higher sampling rate and accuracy provide greater reliability in identifying disease-specific biomarkers. Additionally, in exploratory research investigating nuanced differences across clinical subpopulations or novel ocular motor paradigms, the EyeLink's sensitivity facilitates detailed analyses, enhancing the interpretability and reproducibility of findings. Conversely, while the Tobii Nano Pro offers practical benefits due to its portability, ease of setup, and user-friendly interface, its comparatively lower precision may limit its application in diagnostic contexts requiring fine-grained measurement. Future comparative research should carefully consider the balance between accuracy and practical usability, potentially integrating both systems in a complementary approach where EyeLink is utilized in exploratory or diagnostic phases and Tobii in larger-scale screening or longitudinal monitoring.

While the present study provides a comparison of Tobii Nano Pro and EyeLink 1000 Plus, it is important to acknowledge that direct comparison of these two fundamentally different eye trackers may not be the most effective strategy for evaluating their relative utility. These systems differ not only in hardware specifications—such as sampling rate, spatial resolution, and calibration protocols—but also in their core design philosophies: EyeLink is engineered for high-precision, lab-based neuroscience research, whereas Tobii prioritizes portability and ease of use for more naturalistic or field-based settings. As a result, attempting to draw equivalence across all metrics may overlook the strengths and intended applications of each device. More critically, the significant differences observed in raw output between the two systems raise concerns about measurement validity rather than simply measurement precision. In this context, rather than comparing identical metrics across devices, a more constructive approach would involve analysing data collected from each device separately, identifying the metrics most sensitive to disease-related changes within each system, and then evaluating their respective diagnostic performance.

Future research should consider using each eye tracker independently to develop device-specific models of ocular motor impairment, particularly in clinical populations such as iPD. These models could then be compared on the basis of diagnostic sensitivity, specificity, or predictive value, offering a more ecologically valid and clinically relevant assessment of each device's utility. This paradigm shift—from attempting to equate raw measurements to assessing diagnostic performance within each system's constraints—may yield more actionable insights, particularly when considering the translation of eye-tracking technology into clinical screening or monitoring tools. Moreover, incorporating machine learning or multivariate classification techniques could help optimize each system's strengths and accommodate their limitations, ultimately providing a more nuanced understanding of how mobile and lab-based eye-tracking systems can be best utilized in neurodegenerative disease research.

9.6.1 Clinical Implications

Although the Tobii Nano Pro provides an accessible and portable eye-tracking option, its reduced temporal resolution and limited precision diminish its utility for detecting subtle ocular motor changes in iPD. These findings suggest that Tobii may be more suitable for large-scale field studies or screening tools, whereas EyeLink remains the preferred system for high-resolution, laboratory-based research. Future studies should

explore methods to harmonize data outputs between devices, such as through standardized calibration corrections or cross-device transformation models.

9.6.2 Limitations

This study had several limitations. Most notably, the sample size was substantially smaller for the Tobii dataset (13 iPD, 3 Controls) compared to the EyeLink dataset, potentially limiting statistical power and generalizability. Additionally, Tobii's lower sampling frequency and simpler calibration procedures likely contributed to systematic measurement differences. Environmental factors such as lighting and head movement tolerance also differ between the two systems, affecting measurement consistency. Future studies should prioritize larger Tobii datasets and aim to standardize preprocessing methods to enhance inter-device comparability.

9.6.3 Future Directions

Further research should investigate methods to enhance Tobii's measurement accuracy and alignment with high-precision systems like EyeLink. Machine learning models trained on both datasets may enable correction of Tobii-derived outputs, improving metric comparability. Developing adaptive preprocessing pipelines that address differences in sampling, calibration drift, and noise levels could enhance Tobii's clinical research utility. Additionally, larger-scale validation studies with diverse participant groups are needed to evaluate Tobii's sensitivity to disease-related ocular motor changes. Multimodal approaches integrating eye-tracking with imaging or motion sensors may offer a more comprehensive view of ocular motor deficits in neurodegenerative disorders.

9.7 Chapter Summary

In summary, while both Tobii and EyeLink successfully captured ocular motor data, substantial differences in measurement precision, calibration, and data output limit their interchangeability. EyeLink 1000 Plus remains the gold standard for high-resolution ocular motor research, particularly in clinical populations like iPD. Tobii Nano Pro provides a promising alternative for portable applications but requires further refinement to match the precision of lab-based systems. Researchers must account for these device-specific characteristics when

designing studies or interpreting eye-tracking results in neurodegenerative disease research.

10 Detection of Eye Movements in Parkinson's Disease in Laptop/Tablet/Smartphone Application – Proof of Concept

10.1 Introduction

Eye movement measurement has significantly evolved, transitioning from invasive traditional methods to modern, non-invasive technologies that improve accuracy, feasibility, and cost-effectiveness in clinical settings. Early foundational techniques, such as search coils and infrared systems, provided high accuracy but were often impractical and uncomfortable, limiting their clinical applicability. Search coils embedded in contact lenses or surgically implanted offered precise data but were invasive and unsuitable for routine assessments. Similarly, infrared-based systems like the Dual Purkinje Tracker, while non-invasive, exhibited limitations due to positional sensitivity and calibration dependency (Murray, Hunfalvay and Bolte 2017). These shortcomings have hindered broader adoption in clinical practice (Niehorster, Santini et al. 2020).

Recent advancements have introduced video-based and wearable eye-tracking systems that allow accurate and unobtrusive gaze recording in naturalistic environments. Devices like the Tobii Pro Glasses have demonstrated robust performance even under dynamic conditions (J. Y. Lee et al. 2009; Onkhar, Dodou and Winter 2024), expanding their use in contexts like paediatric ADHD assessment and real-world behavioural studies (Kasneci, Black and Wood 2017). Accuracy remains a critical benchmark for clinical applicability, and studies show that calibration procedures, individual physiology, and target size significantly affect measurement precision (Novák et al. 2024).

Cost is another determinant in the clinical deployment of eye-tracking technologies. Traditional systems are often prohibitively expensive, whereas modern video-based alternatives have become increasingly affordable. Open-source platforms like GazeParser (Sogo 2013) democratize access, supporting widespread adoption across varied clinical and research settings.

From a practicality standpoint, modern systems—especially wearable models—have been designed for seamless integration into clinical workflows (Junaid et al. 2022; Dwivedi, Mehrotra and Chandra 2022), enabling eye care professionals to obtain objective metrics with minimal disruption. Their ecological validity,

derived from assessments in real-world settings, enhances the clinical relevance of collected data **Evans2012**. These tools are increasingly employed in applications ranging from glaucoma assessment to multimodal investigations in ADHD and depression (Kasneci, Black and Wood 2017; D. Y. Lee et al. 2023). However, standardization in calibration protocols and evaluation metrics remains necessary for improving reproducibility.

Despite progress, several challenges remain in applying eye-tracking to PD. Off-the-shelf systems, such as the Tobii EyeX, often lack the spatial and temporal resolution required for detecting the subtle visual and cognitive impairments characteristic of PD (Morgante, Zolfaghari and Johnson 2012; Pauszek 2023). Moreover, affordability often comes at the cost of reduced accuracy, limiting meaningful data acquisition in economically constrained settings. Additionally, current devices rarely allow integration with other physiological measures like EEG, resulting in fragmented insights (Gong et al. 2021).

PD-specific applications must account for the unique eye movement strategies and cognitive changes associated with the disorders (X. Liao et al. 2024). Without this sensitivity, generalized systems may fail to provide actionable data. Machine learning and artificial intelligence integration holds promise for overcoming these challenges, allowing for the development of adaptive models that enhance diagnostic specificity and tailor interventions (D. Li et al. 2024). However, clinician familiarity with these systems remains limited, highlighting the need for awareness and education to support adoption (Tahri Sqalli et al. 2023).

Medical application development must prioritize usability, diagnostic accuracy, and workflow integration. User-friendly design increases clinical uptake, as shown in trials evaluating digital medication reconciliation and history-taking tools (Gionfriddo et al. 2022; Kripalani et al. 2019; Noack et al. 2023). Precision is equally critical—studies employing AI-driven models have demonstrated high diagnostic accuracy in radiology and lesion detection (Khalifa and Albadawy 2024; Pinto-Coelho 2023; Harry 2023). Integration into existing clinical systems, as demonstrated by applications in ICU management (De Backere et al. 2015), ensures minimal workflow disruption. Case studies also underscore the role of mobile tools in improving dosage accuracy and diagnosis via gaze detection (Khaleel, Abbas and Ibrahim 2024; Harpaz et al. 2024). AI-driven triaging and diagnostic support applications further reinforce the value of intelligent tools in enhancing patient outcomes (Khosravi et al. 2024). The continued evolution of healthcare will require such synergistic

collaborations between technology developers and medical professionals.

In summary, modern eye-tracking technologies offer significant advantages over traditional methods but still face limitations in the context of PD. These include low specificity, lack of integration with other diagnostic modalities, and inadequate sensitivity to PD-specific ocular signatures. By prioritizing user-centered design, integrating AI, standardizing metrics, and enabling multimodal analysis, the proposed mobile-based application aims to bridge these gaps. The ultimate goal is to improve diagnostic precision, personalize interventions, and enhance the quality of life for individuals with PD.

10.2 Project Aims

1. To develop and test a proof-of-concept app for automated detection and analysis of saccades and antisaccades.
2. To evaluate the app's accuracy and usability as a portable tool for ocular motor assessment.

10.3 Methods

10.3.1 Experimental Design

The initial application was designed for reflexive and antisaccades in the horizontal direction. Each paradigm ran for one minute and total of thirty saccades each. In the reflexive saccades the participants were instructed to follow the target and in the antisaccades paradigm the participants were instructed to look in the opposite direction. The paradigms were designed to emulate the specifications of an eye tracker. A one degree green dot was used as the target, adjusted for the dimensions of the screen used.

10.3.2 Hardware and Software Requirements

The application was designed for laptops, tablets and phones with an integrated webcam and can be used either on MacOS or Windows. For the development of the application MacOS was used with a dynamically adjustable, baseline screen resolution of 640×480 px. Visual Studio Code 1.95.2 (Universal) was used to

code and Python 3.13.1 was used to run the application.

10.3.3 Software Development

To run the application successfully a series of packages in python were utilised: cv2 - captures live video and displays the experimental screen; dlib - provides robust facial landmark detection for eye-tracking; numpy - handles array-based operations and numerical computations; scipy.spatial.distance - calculates distances, essential for eye metrics like velocity and amplitude; PyQt5 (QApplication, QWidget, QVBoxLayout, QLabel, PyQt5.QtWidgets, PyQt5.QtCore) - used to create a graphical user interface (GUI) for displaying post-experiment results and sys: allows clean exits of the PyQt application. These imports allow for modular development and simplification of tasks like video processing, numerical analysis, and GUI creation.

The face predictor and the landmark predictor were incorporated next. A face detector is to identify facial regions in the video feed and a facial landmark predictor to locate sixty eight specific points on the face, such as the eyes, nose, and mouth. Facial landmarks are foundational for accurately identifying and tracking eye regions. The try-except block ensures the predictor file is loaded correctly and provides error handling if the file is missing or invalid. Within the sixty eight point facial model, the eye landmark indices were set as 36-42 for the right eye and 42-48 for the left eye. These indices help isolate the eye regions for calculating metrics like the eye aspect ratio. The eye aspect ratio is a metric to measure eye openness. It uses vertical distances and horizontal distance between landmarks. This is commonly used in eye-tracking studies to detect blinks or prolonged closures, aiding in understanding eye activity during the task.

After the configurations for the detection of eye are set, the webcam is initialised. The target and the timing of the paradigms were configured. Targets were defined based on screen resolution and angular displacement, fifteen degrees horizontally converted to pixel distances. Dynamic adjustments allowed for customized experiments, including grid-like arrangements: right, left, top, bottom, and centre targets were calculated relative to the screen centre. Custom setups included grid-based or corner-aligned positions for varied saccade patterns. Targets' positions were adjusted by modifying the angular offsets and a uniform grid of targets was created using specified horizontal and vertical spacing. For instance, an 8-target grid surrounding the centre position was implemented, with dynamic adjustments based on experimental requirements. Positions

were calculated as fractions of the screen width and height, ensuring dynamic adaptability to varying screen resolutions. Target positions alternated every 2 seconds. Custom timing configurations were introduced to extend durations if required for experimental variation. A real time processing loop was created wherein a black frame was configured for displaying targets and frames from the webcam are captured and converted to greyscale for faster processing.

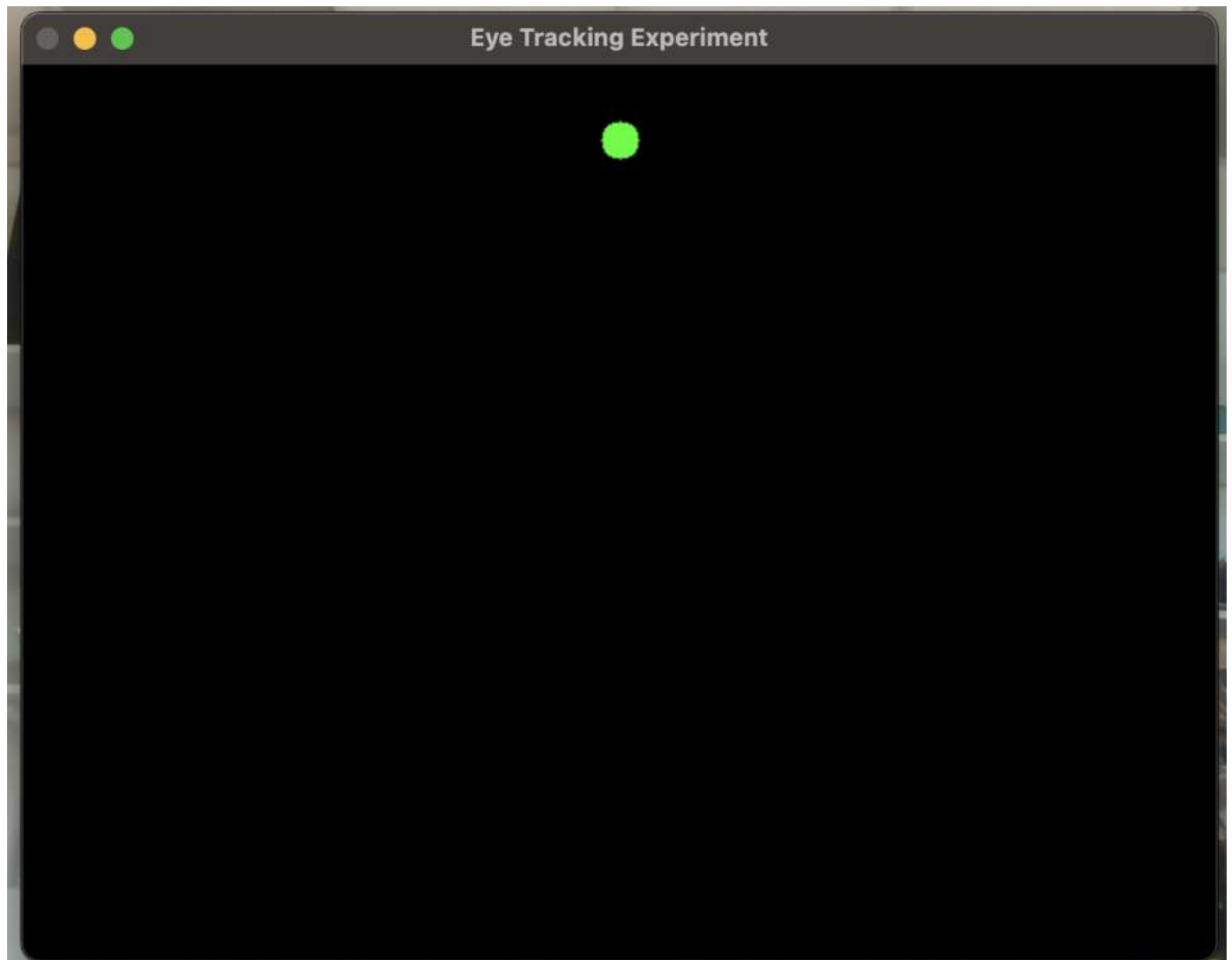


Figure 185: Targets Displayed on Laptop Screen. Based on screen resolution and angular displacement.

Real-time processing is critical for dynamic experiments, allowing continuous eye-tracking and target adjustments. OpenCV captured real-time video streams from the webcam and Dlib's facial landmark detector isolated eye regions for subsequent tracking. Algorithms extracted gaze direction and eye-centre positions, enabling dynamic calculation of saccade metrics. State machine managed phase transitions and dynamically adjusted target switching mechanisms.

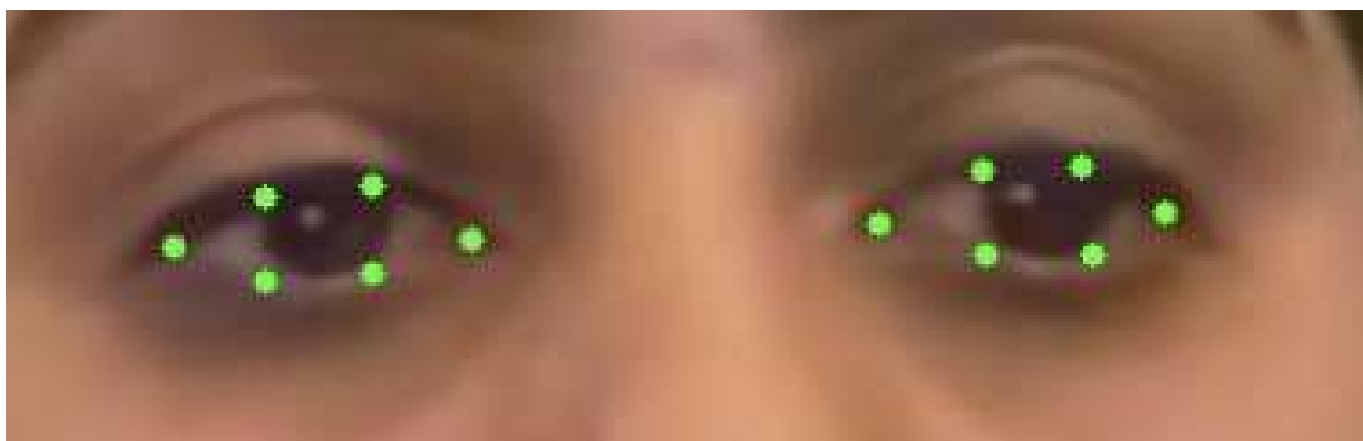


Figure 186: Isolated Eye Regions for Tracking.Using packages from python.

The captured frames are used to output metrics for the paradigms in real time. The following metrics were calculated: velocity - calculated as the Euclidean distance between successive positions over elapsed time, velocity data were updated for each frame, ensuring accurate temporal resolution; amplitude - measured as the displacement between initial and final positions within a phase, the largest displacement values for each phase were recorded to evaluate participant response; deviation or accuracy - quantified as the Euclidean distance from the gaze position to the target, deviation data were logged over time to assess consistency and target adherence and error detection - counted erroneous movements towards targets during the antisaccade phase.

The PyQt5 framework was used to create a graphical interface for post-experiment analysis. The GUI displayed the metrics of mean and peak velocity, amplitude, deviation or accuracy and error rate (for antisaccade paradigm). The GUI provided real-time experiment feedback and summarized participant performance. Metrics were displayed in an organized format for immediate interpretation by experimenters.

Metrics after 120.05 seconds:

First Minute - Avg Velocity: 1.55 pixels/s

First Minute - Peak Velocity: 8.32 pixels/s

First Minute - Avg Amplitude: 21.06 pixels

First Minute - Avg Deviation: 676.51 pixels

First Minute - Accuracy: 676.51 pixels

First Minute - Errors: 0

Second Minute - Avg Velocity: 0.02 pixels/s

Second Minute - Peak Velocity: 0.37 pixels/s

Second Minute - Avg Amplitude: 44.09 pixels

Second Minute - Avg Deviation: 676.89 pixels

Second Minute - Accuracy: 676.89 pixels

Second Minute - Errors: 0

Figure 187: Sample Results from Application. Results displayed and stored for the first minute (reflexive saccades) and second minute (antisaccades).

10.3.4 Ethical Considerations

Data were anonymized using session-specific labels, with no identifiable visual data stored. Ensured compliance with relevant data protection laws, particularly in managing video streams and participant information, therefore, data was processed in real time rather than retrospective video analysis. No video recordings were stored after the completion of the paradigms.

10.3.5 Pilot Testing

For the pilot testing an M1 16 inch MacBook Pro was used. Fifteen participants, three controls and twelve idiopathic PD, were briefed about the project and the instructions of how to use the application. The participants were recruited through the methods detailed in Chapter 2: General Methods. They were instructed to complete the task with independence and only seek help if absolutely necessary. The participants were left in the testing room for the task.

As the aim was also to test the usability of the application, participants were asked to record their eye movements independently after the instructions were completed. First they were asked to position themselves at 30 cm from the screen and check if both their eyes are being captured. Once this was confirmed, they were asked to commence the first paradigm. An instruction screen for the reflexive saccade task was displayed and then upon pressing enter the paradigm commenced and lasted for one minute. Once reflexive saccades were complete the instructions for the antisaccade task were displayed and upon pressing enter the paradigm commenced and also lasted for one minute. After the completion of both tasks, the results were stored under a unique participant ID.

The participants were asked two questions about the ease of use and the applicability of the application: 1) On a scale of 1-10, how would the ease of setup for this application, with 1 being it was extremely easy and 10 being it was extremely difficult? 2) On a scale of 1-10, would you be able to replicate the same procedure at home, with 1 being I would be able to do it very comfortably and 10 being I will not be able to do it very comfortably? Their scores were recorded along with their unique participant ID.

10.3.6 Statistical Analyses

Descriptive statistics were calculated for saccadic measures, demographic variables, and questionnaire scores. Continuous variables were summarized using mean, standard deviation (SD), and median. Normality was assessed using the Shapiro-Wilk test. Since most variables did not meet the assumption of normality, Mann-Whitney U tests were used to compare PD and control groups for all saccadic measures. To correct for multiple comparisons, Bonferroni correction was applied. The significance level for all analyses was set at $\alpha=0.05$. All analyses were done using R (Version 2023.09.1494, R Core Team, Vienna, Austria).

10.4 Results

10.4.1 Application Development

The development of the eye-tracking application was successful and demonstrated feasibility for conducting reflexive and antisaccade paradigms. The application was functional across multiple devices, including laptops, tablets, and phones with an integrated webcam, supporting both MacOS and Windows operating systems. The software accurately captured and processed real-time eye-tracking data, successfully computing saccadic metrics such as velocity, amplitude, accuracy, and error rate.

However, the application remains in its preliminary stages, with pilot testing highlighting areas for improvement in usability, robustness, and optimization for diverse screen resolutions and lighting conditions. While initial results indicate that the system can track saccades and provide real-time feedback, further refinements are required to enhance stability, increase accuracy in detecting eye landmarks, and streamline the user interface for improved participant accessibility.

10.4.2 Participants

A total of 15 participants were included in the study, comprising 10 males and 5 females. The mean age of participants in the control group was 61.33 ± 3.06 years, while the PD group had a mean age of 63.33 ± 8.34 years. Within the control group, the mean age for males was 61.00 ± 4.24 years, and for females, it was 62.00 . In the PD group, the mean age for males was 62.38 ± 9.01 years, while females had a mean age of 65.25 ± 7.63 years.

Table 15: Demographic and clinical characteristics of the study cohort. Values are presented as mean \pm standard deviation (SD). Age and disease duration are reported for all participants. Data are stratified by group and sex. “-” indicates not applicable or unavailable.

Group	Age (Mean \pm SD)	Ease of Use Score (Mean \pm SD)	Ability of Home Use (Mean \pm SD)
Control (N = 3)	61.33 \pm 3.06	4.67 \pm 0.58	5.00 \pm 1.00
Females (N = 1)	62.00 \pm -	5.00 \pm -	4.00 \pm -
Males (N = 2)	61.00 \pm 4.24	4.50 \pm 0.71	5.50 \pm 0.71
PD (N = 12)	63.33 \pm 8.34	3.33 \pm 1.30	4.67 \pm 1.61
Females (N = 4)	65.25 \pm 7.63	3.75 \pm 2.06	5.00 \pm 1.41
Males (N = 8)	62.38 \pm 9.01	3.12 \pm 0.83	4.50 \pm 1.77

10.4.3 Application Function

The analysis revealed notable differences between the control and PD groups in several saccadic measures. Reflexive average velocity was lower in PD (8.12 ± 7.03) compared to controls (13.23 ± 18.54), showing a 47.86% difference; however, the Mann-Whitney U test indicated no significant difference ($W = 16.5$, $p = 0.885$). Similarly, reflexive amplitude was markedly reduced in PD (22.80 ± 17.19) compared to controls (48.28 ± 49.52), a 71.71% difference, but this was not statistically significant ($W = 16$, $p = 0.840$). Reflexive accuracy was higher in PD (1767.08 ± 1913.63) compared to controls (1135.48 ± 794.62), with a 43.52% difference, though again, statistical testing did not show significance ($W = 20$, $p = 0.840$).

For antisaccade measures, peak velocity was higher in controls (2.14 ± 2.93) than in PD (1.32 ± 2.06), a 47.27% difference, but this difference was not statistically significant ($W = 10.5$, $p = 0.312$). Antisaccade amplitude was also larger in controls (456.64 ± 561.79) compared to PD (236.10 ± 272.13), reflecting a 63.67% difference, though this difference was not significant ($W = 14.5$, $p = 0.665$). Other measures, including antisaccade average velocity, latency, and error rate, did not show major differences between groups, with all p-values exceeding 0.05.

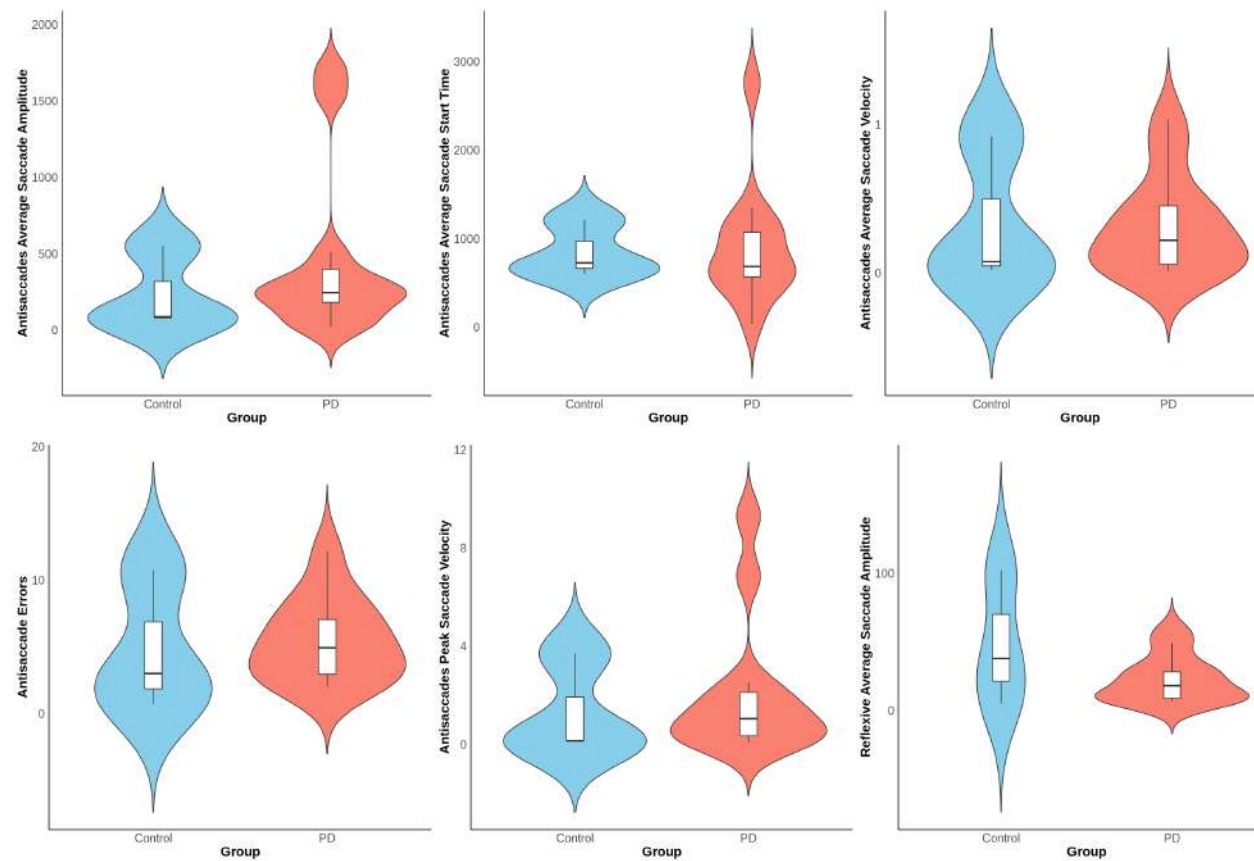


Figure 188: Application Results for Saccadic Metrics. Between-group comparisons were performed using Mann–Whitney U tests, with Bonferroni correction applied for multiple comparisons. Statistical significance was defined as $p < 0.05$.

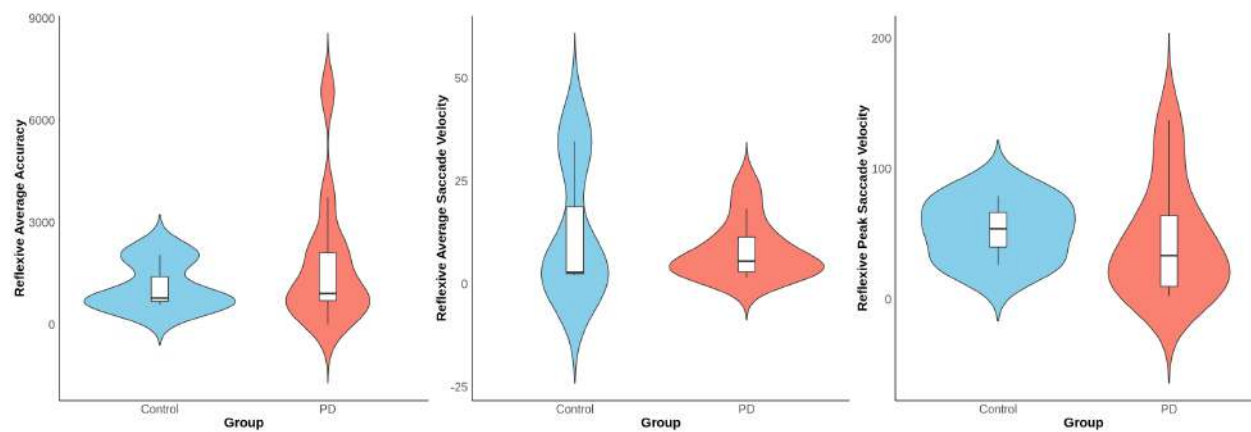


Figure 189: Application Results for Saccadic Metrics. Between-group comparisons were performed using Mann–Whitney U tests, with Bonferroni correction applied for multiple comparisons. Statistical significance was defined as $p < 0.05$.

10.4.4 Application Usability

The usability of the application was assessed based on participant responses to two questions: ease of setup and the likelihood of replicating the procedure at home. On a scale from 1 (extremely easy) to 10 (extremely difficult), control participants rated the ease of setup at an average of 4.67 ± 0.58 , while PD participants provided an average rating of 3.33 ± 1.30 . For home-based usability, where 1 indicated high confidence in replicating the procedure and 10 indicated significant difficulty, controls reported an average score of 5.00 ± 1.00 , whereas PD participants rated their confidence lower at 4.67 ± 1.61 .

10.5 Discussion

The results of this study highlight both the feasibility and limitations of the developed webcam-based eye-tracking application in assessing reflexive and antisaccadic eye movements. The application successfully computed key saccadic measures such as velocity, amplitude, accuracy, and error rate while maintaining compatibility across multiple devices. However, pilot testing revealed areas requiring refinement, particularly in optimizing the system's robustness across varying lighting conditions and screen resolutions.

Although the descriptive statistics suggested meaningful differences between the control and PD groups, particularly in reflexive and antisaccade measures, these differences did not reach statistical significance. Reflexive amplitude was markedly lower in PD participants compared to controls, reflecting the well-documented impairment in saccadic control in PD (C. A. Antoniadou and Sperling 2024; Lal and Truong 2019). Similarly, reflexive accuracy was higher in PD participants, which may be attributed to compensatory mechanisms or differences in fixation stability (Otero-Millan, R. Schneider et al. 2013). Notably, antisaccade amplitude and peak velocity were also higher in PD, though these differences were not statistically significant. Given the variability in the dataset, these trends warrant further investigation with a larger sample size to better understand their clinical significance.

The trends observed in this study align with established ocular motor profiles of PD. Previous research has consistently shown that PD is associated with hypometric reflexive saccades, which is consistent with the reduced reflexive amplitude observed in this study (Sekar, T N Panouillères and Kaski n.d.). This finding

likely reflects deficits in the basal ganglia circuitry responsible for initiating and executing saccadic movements (Enderle 2002). The increased reflexive accuracy in PD participants may be due to prolonged fixation durations or a compensatory strategy to maintain visual stability (Briand et al. 1999). Similarly, the observed differences in antisaccade measures are in line with known deficits in voluntary eye movement control in PD, where patients often exhibit prolonged latencies and increased error rates due to impaired prefrontal cortical regulation (C. A. Antoniadou, Demeyere et al. 2015). However, the lack of statistical significance suggests that the small sample size may have limited the ability to detect meaningful group differences, reducing the effect sizes and increasing the likelihood of type II errors.

From a technical perspective, several hardware and software improvements are necessary to enhance the accuracy and usability of the application. One notable issue was the accuracy of eye-tracking under suboptimal lighting conditions. Variability in lighting can affect the ability of the facial landmark detector to reliably identify eye regions, leading to fluctuations in tracking accuracy. Implementing adaptive contrast adjustments or infrared-based tracking could mitigate these issues and improve overall reliability. Hardware compatibility and performance optimization are necessary to enhance the application's reliability. Since webcam quality varies across different consumer and medical devices, further testing is required to ensure consistency across multiple platforms. Optimizing the software for mobile devices could improve portability, allowing for broader use in home-based assessments and in low-resource settings where traditional eye-tracking systems are unavailable. Addressing these compatibility concerns will be key to expanding the application's reach.

User experience and accessibility are critical factors for the widespread adoption of this application. While participants generally found the software easy to use, those with more advanced PD may experience difficulties due to motor impairments and cognitive deficits. Incorporating features such as voice-guided instructions, an adaptive interface, and a multi-language option could significantly improve usability. Ensuring that the application remains accessible to individuals with varying levels of disease severity will be essential for its practical implementation.

Cognitive impairment is a significant factor in PD that may influence eye movement performance. Beyond motor deficits, PD is associated with executive dysfunction, which could impact the ability to perform antisaccadic tasks correctly. Integrating cognitive screening elements alongside saccadic assessments may

provide a more comprehensive neurological evaluation. Given the established link between eye movement abnormalities and cognitive function, this application has the potential to expand its use beyond PD to include conditions such as mild cognitive impairment and dementia.

Data security and ethical considerations must also be addressed before large-scale deployment. Since the application processes live video feeds, ensuring that data privacy is protected is paramount. Although the current design avoids storing raw video data, additional encryption measures and secure cloud storage solutions should be explored to meet the requirements of GDPR, HIPAA, and other data protection regulations. Future versions of the application must ensure compliance with legal and ethical standards to enable clinical use.

Another challenge identified was the issue of head movement stability. Participants, particularly those with PD, may struggle to maintain a steady head position during the task, leading to tracking inconsistencies. Implementing real-time head position correction or a guided feedback mechanism to encourage minimal movement could help address this issue. Additionally, using a more sophisticated gaze-tracking algorithm with predictive filtering could compensate for small head displacements and improve tracking precision.

Lastly, a key technical issue identified in this study is the challenge of calibration and ensuring data quality. Accurate eye-tracking relies on a robust calibration process to correctly map gaze positions across different screen resolutions and user environments. Inconsistent calibration can lead to erroneous gaze estimations, particularly in participants with PD who may struggle to maintain a steady fixation during the calibration process. Implementing an automated and adaptive calibration method that adjusts in real-time based on gaze stability could help mitigate these challenges. Additionally, incorporating quality assurance checks, such as periodic recalibration prompts and real-time validation of gaze consistency, would enhance the reliability of the collected data.

10.5.1 Clinical Implications

The clinical implications of this study lie in the potential for a portable and cost-effective eye-tracking solution for PD assessment. Traditional eye-tracking systems are expensive and require specialized equipment, limiting accessibility. This application, leveraging readily available webcams, presents an opportunity for scalable, remote monitoring of saccadic function in neurological conditions. The ability to detect subtle differences in

saccadic parameters in PD suggests potential applications in disease monitoring and early diagnosis. Further refinements to the algorithm to enhance precision, along with validation against gold-standard eye-tracking devices, will be necessary to strengthen clinical utility.

10.5.2 Limitations

Several limitations must be acknowledged. First, the small sample size reduces the statistical power of the study, increasing the likelihood of type II errors and impacted the ability to achieve statistical significance despite observable trends. Small samples are inherently more susceptible to variability, making it difficult to distinguish true differences from noise. Future studies should aim to recruit a larger and more diverse participant pool to increase statistical power and enhance the generalizability of findings. Increasing the number of participants would also allow for more robust subgroup analyses, potentially revealing differential effects based on disease severity or cognitive status. Additionally, variability in lighting conditions and device specifications may have influenced the accuracy of eye-tracking measurements. The application also relies on webcam-based tracking, which may not achieve the same level of precision as infrared-based eye trackers. Lastly, usability assessments relied on subjective ratings, which may introduce bias in participant responses.

10.5.3 Future Directions

Future research should focus on expanding the sample size to improve the statistical power of the study. Efforts should also be made to refine the tracking algorithm to improve landmark detection and minimize environmental influences on tracking accuracy. Incorporating additional features such as real-time calibration and automated quality control checks would enhance reliability. Further validation studies comparing the webcam-based system to traditional eye-tracking methods are necessary to establish its validity in clinical and research settings. Additionally, improving the robustness of the GUI to guide users through setup, ensuring proper calibration and minimizing errors, will be crucial for increasing adoption and usability in real-world applications.

Another critical direction for future development is expanding the application to support a broader range of eye movements beyond reflexive and antisaccades. Incorporating paradigms for smooth pursuit, memory-guided

saccades, and fixation stability assessments would provide a more comprehensive evaluation of ocular motor function in PD and other neurological conditions. Moreover, integrating machine learning algorithms to analyse eye-tracking data and generate automated diagnostic predictions with a likelihood percentage could significantly enhance the clinical utility of the application. Such an approach would allow for more precise, data-driven assessments, reducing the reliance on manual interpretation. Finally, efforts should be made to explore the feasibility of deploying this system into healthcare settings for routine screenings and telemedicine applications, ensuring that the technology can be seamlessly integrated into existing clinical workflows.

10.6 Chapter Summary

In summary, this study demonstrates the feasibility of using a webcam-based eye-tracking application for assessing reflexive and antisaccadic eye movements. While the application showed promise, further improvements are needed to enhance accuracy and robustness. The findings provide a foundation for future developments aimed at creating an accessible and scalable tool for remote eye movement assessments in PD and other neurological conditions. Continued refinements in tracking accuracy, usability, and validation against standard clinical tools will be necessary to ensure the application's efficacy and reliability in practical settings.

11 General Discussion

The overarching aim of this thesis was to investigate the utility of eye movements as biomarkers for PD and atypical Parkinsonian syndromes through a series of complementary studies. This research examined how distinct eye movement paradigms—including fixation, saccades, pursuit, and saccadic adaptation—can aid in disease characterization, progression monitoring, and the differentiation of neurodegenerative conditions. In addition, the effect of levodopa on eye movements was assessed to evaluate the potential of ocular motor metrics as indicators of treatment response. The usability of two eye-tracking systems, the Eyelink and Tobii, was also evaluated to determine their suitability for both research and clinical applications. Finally, machine learning approaches were integrated to enhance the diagnostic and predictive potential of ocular motor data in distinguishing PD and atypical Parkinsonian syndromes.

PD is associated with a range of eye movement abnormalities that reflect underlying BG dysfunction. Across studies, consistent findings showed that individuals with PD exhibit fixation instability, increased SWJs, hypometric saccades, and prolonged saccadic latency. Antisaccade tasks, in particular, revealed significantly elevated error rates and delayed responses, reflecting impairments in volitional saccade control and inhibitory processes. While reflexive saccades were relatively preserved, they showed increased latency and reduced gain as the disease progressed.

The atypical Parkinsonian syndromes-focused study identified distinct ocular motor signatures across MSA, PSP, and CBS. PSP was marked by severely impaired vertical saccades, disrupted smooth pursuit, and frequent SWJs, clearly differentiating it from PD. MSA presented with mild supranuclear gaze palsy, increased SWJs, and gaze-evoked nystagmus, while CBS was characterized by asymmetric saccadic deficits. These findings reinforce the diagnostic utility of eye movement analysis, particularly in the early stages of atypical Parkinsonian syndromes when clinical presentations often overlap.

























































	Eye Movement and Associated Diagnostic Value							
Neurodegenerative Disease	Central Fixation	Positional Fixation/ Nystagmus	Smooth Pursuit	Antisaccades	Oblique Saccades	Reflexive Saccades	Volitional Saccades	Memory Guided Saccades
Idiopathic Parkinson's Disease								
GBA Mutation Parkinson's Disease								
LRRK2 Mutation Parkinson's Disease								
Progressive Supranuclear Palsy								
Multiple System Atrophy								
Corticobasal Syndrome								
Dementia with Lewy Bodies								

Figure 190: Ocular Motor Features of Parkinson's Disease and Atypical Parkinsonian Syndromes. Red: low diagnostic value, yellow: medium diagnostic value and green: high diagnostic value. Figure by author.

Given that atypical Parkinsonian syndromes often present with more pronounced ocular motor impairments compared to PD, eye movement assessments hold particular promise for differential diagnosis. These findings underscore the value of ocular motor analysis in distinguishing atypical Parkinsonian subtypes, especially during early disease stages when clinical presentations commonly overlap.

The one-year follow-up study evaluated disease progression in PD using ocular motor metrics. Participants exhibited worsening fixation instability, increased SWJs, greater saccadic latency, and reduced pursuit gain over time. Notably, these changes correlated with both disease severity and cognitive decline, reinforcing the potential of eye-tracking as a longitudinal tool for monitoring neurodegeneration. Additionally, increased hypometric saccades and higher antisaccade error rates were associated with faster progression, suggesting these metrics may serve as early indicators of disease worsening. Given that levodopa can influence eye movements over time, its long-term impact should be carefully considered during study design. Stratifying PD participants by their LEDD may improve the interpretation of ocular motor findings by distinguishing medication effects from disease-related changes.

The levodopa challenge study revealed selective improvements in ocular motor function following dopaminergic administration. Antisaccade error rates significantly improved, while reflexive saccadic latencies and peak velocities showed modest enhancements. However, fixation instability and pursuit deficits remained largely unaffected, suggesting that dopaminergic modulation primarily influences volitional rather than reflexive eye movement control. These results indicate that specific ocular motor tasks may serve as biomarkers for levodopa responsiveness, supporting more tailored treatment strategies. Given the measurable effects of levodopa on eye movements, it is crucial that future studies and clinical evaluations account for patients' on and off medication states when designing protocols and interpreting findings.

Saccadic adaptation, a form of motor learning, was investigated in PD and MSA. The results indicated that individuals with PD exhibited impaired memory-guided saccadic adaptation, whereas those with MSA showed more pronounced deficits in visually guided adaptation. These findings suggest that distinct neural circuits underlie adaptation impairments in PD and MSA, offering a potential means of differentiating these conditions. Furthermore, the reduced adaptation observed in PD highlights diminished neuroplasticity, which may have broader implications for rehabilitation approaches and adaptive motor learning strategies.

A machine learning model was developed using ocular motor data to classify PD, atypical Parkinsonian syndromes, and healthy controls. Feature selection identified antisaccade error rates, fixation instability, and smooth pursuit gain as the most informative ocular motor biomarkers. The model achieved high classification accuracy, supporting the feasibility of automating PD diagnosis through eye-tracking metrics. This study underscores the potential of machine learning-assisted diagnostic tools to enhance early detection and differential diagnosis of neurodegenerative diseases.

While clinical assessments of eye movements can offer preliminary insights into ocular motor abnormalities during the diagnostic phase, more concrete and objective differentiation—particularly in PD, where ocular motor deviations from controls may be subtle—necessitates the integration of advanced machine learning models. These computational approaches can detect nuanced patterns and assess performance across multiple paradigms simultaneously, rather than in isolation. For eye movements to serve as a reliable diagnostic biomarker in PD, their analysis must be complemented by data-driven techniques that enhance sensitivity and diagnostic precision.

In the context of atypical Parkinsonian syndromes, initial differential diagnosis can be informed by clinical evaluation of hallmark ocular motor features—such as vertical saccade slowing in PSP, gaze-evoked nystagmus in MSA, and asymmetric saccadic impairments in CBS. Standard statistical analyses can aid in detecting group-level differences across specific metrics; however, due to clinical overlap and phenotypic heterogeneity within atypical Parkinsonian subtypes, these methods often fall short in enabling precise individual-level classification. To overcome this limitation, the application of machine learning is equally critical for atypical Parkinsonian syndromes. By integrating data across diverse ocular motor paradigms and leveraging non-linear feature interactions, machine learning models provide a more robust and scalable framework for accurate subtype differentiation and early diagnosis.

Together, these findings underscore that while specific eye movement paradigms—such as fixation, saccades, and pursuit—are clinically relevant and can reveal important disease-specific abnormalities, their diagnostic value is limited when evaluated in isolation. Conventional clinical assessments and statistical analyses offer a useful starting point for identifying group-level trends and informing preliminary differential diagnoses.

However, the complexity and subtlety of ocular motor changes, particularly in early PD and across atypical Parkinsonian subtypes, necessitate a more holistic approach. Integrating data across multiple paradigms using advanced machine learning models enhances the sensitivity and specificity of diagnostic classification, enabling the discovery of latent patterns that may not be visible through traditional methods. For eye movements to serve as robust, clinically actionable biomarkers, they must therefore be analysed in unison, within a framework that combines rich behavioural data with computational precision.

The comparative analysis between the Eyelink 1000 Plus (desktop-based) and Tobii Nano Pro (portable eye tracker) revealed notable discrepancies in measurement accuracy and reliability. While the Eyelink system provided superior temporal resolution and spatial accuracy, the Tobii device exhibited greater variability and reduced precision across fixation and saccadic metrics. Intraclass correlation coefficient (ICC) values were low, and Bland-Altman analyses indicated systematic biases, suggesting that the two systems are not interchangeable. Nevertheless, the portability of the Tobii Nano Pro makes it a viable tool for field-based studies, provided that calibration protocols and preprocessing pipelines are rigorously optimized.

The feasibility of using smartphone cameras for eye movement detection was also explored as a low-cost diagnostic alternative. Preliminary findings indicated reliable detection of saccadic onset; however, the accuracy of fine-grained metrics such as pursuit gain and microsaccade detection was limited. Future advances in image processing and AI-based gaze estimation could significantly enhance the accessibility and scalability of eye-tracking technology in clinical contexts.

Collectively, these studies underscore the utility of eye-tracking as an objective and non-invasive method for characterizing neurodegenerative disorders, tracking disease progression, and evaluating treatment effects. The consistent association between ocular motor impairments and symptom severity in PD reinforces the potential of eye movement metrics as viable clinical biomarkers. Additionally, the presence of distinct ocular motor profiles in atypical Parkinsonian subtypes supports the role of eye-tracking in differential diagnosis—particularly in early disease stages where motor symptoms may overlap.

Technology selection emerged as a critical factor in eye-tracking research. The observed discrepancies between Eyelink and Tobii systems demonstrate that while high-precision devices offer more reliable data, portable systems can still serve as practical tools for large-scale screening or field-based applications if paired

with appropriate preprocessing strategies. Moreover, the integration of machine learning algorithms into eye-tracking workflows enhances diagnostic capabilities by automating classification and prediction, laying the groundwork for more accessible and scalable diagnostic tools.

The incorporation of eye-tracking into clinical practice holds substantial promise for improving diagnostic precision, enabling earlier detection of neurodegenerative diseases, and facilitating real-time monitoring of disease progression in PD and atypical Parkinsonian syndromes. The strong correlation between ocular motor abnormalities and disease severity suggests that eye movement assessments could be integrated into routine neurological evaluations, guiding timely intervention and personalized treatment planning. Eye-tracking is a non-invasive, cost-effective, and objective modality that could complement existing diagnostic tools. Notably, its ability to differentiate PD from atypical Parkinsonian syndromes—including subtypes such as PSP and MSA—could help reduce diagnostic uncertainty in early stages. Longitudinal ocular motor assessments may also enable more granular monitoring of disease progression, further supporting individualized management strategies.

Machine learning enhances the clinical utility of eye-tracking by enabling high-accuracy, automated classification models. These tools could assist neurologists in real-time decision-making and potentially be integrated into wearable technology and telemedicine platforms to facilitate remote patient monitoring. Such advancements would be particularly valuable in underserved settings with limited access to specialist care. However, for widespread clinical adoption, further validation across larger, diverse cohorts is necessary, along with standardization of protocols and regulatory approval. Future work should prioritize the development of affordable, smartphone-based eye-tracking solutions to ensure accessibility across varied healthcare settings.

Several methodological considerations must be addressed when interpreting these findings. Differences in device characteristics—such as sampling rate, spatial resolution, and calibration techniques—can significantly influence data reliability. Variability in sample sizes across studies may also affect statistical power, with larger datasets providing more robust conclusions. Preprocessing steps, including noise filtering, fixation detection algorithms, and data smoothing, further impact cross-study comparability. Additionally, environmental factors such as lighting conditions, screen size, and participant head movement tolerance may introduce variability, particularly when comparing results across eye-tracking platforms. Addressing these

methodological limitations is essential to improve reproducibility and enhance the clinical reliability of eye-tracking metrics.

Future studies should aim to standardize eye-tracking protocols across research centres and clinical applications. Integrating multimodal data—including gait analysis, neuroimaging, and electrophysiological recordings—may yield a more comprehensive understanding of neurodegenerative disease mechanisms. Further refinement of machine learning approaches, particularly through the use of longitudinal data, could enhance predictive accuracy and improve forecasting of disease trajectories. Development of cost-effective, smartphone-compatible eye-tracking solutions should also be prioritized to expand global access to these tools. Finally, larger-scale longitudinal studies are needed to validate eye movement metrics as robust clinical biomarkers for use in trials and routine diagnostics.

This thesis emphasizes the pivotal role of eye-tracking in the clinical and research domains of PD and atypical Parkinsonian syndromes. The findings highlight the diagnostic, monitoring, and treatment evaluation potential of ocular motor assessments. While machine learning significantly advances diagnostic precision, future efforts must focus on validation, standardization, and technological innovation to fully realize the clinical potential of eye movement analysis.

References

- Abbasi, Sara and Khosro Rezaee (Jan. 2025). 'Deep Learning–Based Prediction of Freezing of Gait in Parkinson's Disease With the Ensemble Channel Selection Approach'. In: *Brain and Behavior* 15.1. ISSN: 2162-3279. DOI: 10.1002/brb3.70206.
- Abrahão, Agessandro et al. (2011). 'Cognitive impairment in multiple system atrophy: Changing concepts'. In: *Dementia & Neuropsychologia* 5.4. DOI: 10.1590/s1980-57642011dn05040008.
- Adams, Jamie L. et al. (2023). 'Using a smartwatch and smartphone to assess early Parkinson's disease in the WATCH-PD study'. In: *npj Parkinson's Disease* 9.1. ISSN: 23738057. DOI: 10.1038/s41531-023-00497-x.
- Aiba, Ikuko et al. (2023). 'Clinical course of pathologically confirmed corticobasal degeneration and corticobasal syndrome'. In: *Brain Communications* 5.6. ISSN: 26321297. DOI: 10.1093/braincomms/fcad296.
- Alahyane, N. et al. (2008). 'Separate neural substrates in the human cerebellum for sensory-motor adaptation of reactive and of scanning voluntary saccades'. In: *Cerebellum* 7.4. ISSN: 14734230. DOI: 10.1007/s12311-008-0065-5.
- Alexander, G. E., M. R. DeLong and P. L. Strick (1986). 'Parallel organization of functionally segregated circuits linking basal ganglia and cortex'. In: *Annual Review of Neuroscience* VOL. 9. ISSN: 0147006X. DOI: 10.1146/annurev.ne.09.030186.002041.
- Alexander, Robert G., Stephen L. Macknik and Susana Martinez-Conde (2018). *Microsaccade characteristics in neurological and ophthalmic disease*. DOI: 10.3389/fneur.2018.00144.
- Ali, Farwa, Hugo Botha et al. (2019). 'Utility of the Movement Disorders Society Criteria for Progressive Supranuclear Palsy in Clinical Practice'. In: *Movement Disorders Clinical Practice* 6.6. ISSN: 23301619. DOI: 10.1002/mdc3.12807.
- Ali, Farwa, Peter R. Martin et al. (2019). 'Sensitivity and Specificity of Diagnostic Criteria for Progressive Supranuclear Palsy'. In: *Movement Disorders* 34.8. ISSN: 15318257. DOI: 10.1002/mds.27619.
- Alkan, Yelda et al. (2011). 'Segregation of frontoparietal and cerebellar components within saccade and vergence networks using hierarchical independent component analysis of fMRI'. In: *Visual Neuroscience* 28.3. ISSN: 09525238. DOI: 10.1017/S0952523811000125.
- Alshammri, Raya et al. (2023). 'Machine learning approaches to identify Parkinson's disease using voice signal features'. In: *Frontiers in Artificial Intelligence* 6. ISSN: 26248212. DOI: 10.3389/frai.2023.1084001.

- Alvarez, Tara L. et al. (2014). 'Functional activity within the frontal eye fields, posterior parietal cortex, and cerebellar vermis significantly correlates to symmetrical vergence peak velocity: An ROI-based, fMRI study of vergence training'. In: *Frontiers in Integrative Neuroscience* 8.JUNE. ISSN: 16625145. DOI: 10.3389/fnint.2014.00050.
- Anagnostou, Evangelos et al. (2020). 'A cortical substrate for square-wave jerks in progressive supranuclear palsy'. In: *Journal of Clinical Neurology (Korea)* 16.1. ISSN: 20055013. DOI: 10.3988/jcn.2020.16.1.37.
- Anders, Silke et al. (2004). 'Infrared oculography - Validation of a new method to monitor startle eyeblink amplitudes during fMRI'. In: *NeuroImage* 22.2. ISSN: 10538119. DOI: 10.1016/j.neuroimage.2004.01.024.
- Anderson, Clare et al. (2013). 'Assessment of drowsiness based on ocular parameters detected by infrared reflectance oculography'. In: *Journal of Clinical Sleep Medicine* 9.9. ISSN: 15509389. DOI: 10.5664/jcsm.2992.
- Anderson, Tim et al. (2008). 'Oculomotor function in multiple system atrophy: Clinical and laboratory features in 30 patients'. In: *Movement Disorders* 23.7. ISSN: 08853185. DOI: 10.1002/mds.21999.
- Anderson, Tim J. and Michael R. MacAskill (2013). *Eye movements in patients with neurodegenerative disorders*. DOI: 10.1038/nrneuro1.2012.273.
- Andersson, Richard, Marcus Nyström and Kenneth Holmqvist (2010). 'Sampling frequency and eye-tracking measures: how speed affects durations, latencies, and more'. In: *Journal of Eye Movement Research* 3.3. DOI: 10.16910/jemr.3.3.6.
- Angelova, Plamena R., Noemi Esteras and Andrey Y. Abramov (2021). *Mitochondria and lipid peroxidation in the mechanism of neurodegeneration: Finding ways for prevention*. DOI: 10.1002/med.21712.
- Antoniades, Chrystalina A., Nele Demeyere et al. (2015). 'Antisaccades and executive dysfunction in early drug-naïve Parkinson's disease: The discovery study'. In: *Movement Disorders* 30.6. ISSN: 15318257. DOI: 10.1002/mds.26134.
- Antoniades, Chrystalina A. and Miriam Spering (2024). *Eye movements in Parkinson's disease: from neurophysiological mechanisms to diagnostic tools*. DOI: 10.1016/j.tins.2023.11.001.
- Antonini, Angelo, Valentina D'Onofrio and Andrea Guerra (2023). *Current and novel infusion therapies for patients with Parkinson's disease*. DOI: 10.1007/s00702-023-02693-8.

- Antonini, Angelo, Heinz Reichmann et al. (2023). 'Toward objective monitoring of Parkinson's disease motor symptoms using a wearable device: wearability and performance evaluation of PDMonitor®'. In: *Frontiers in Neurology* 14. ISSN: 16642295. DOI: 10.3389/fneur.2023.1080752.
- Aponte, Eduardo A. et al. (2020). 'Computational Dissociation of Dopaminergic and Cholinergic Effects on Action Selection and Inhibitory Control'. In: *Biological Psychiatry: Cognitive Neuroscience and Neuroimaging* 5.3. ISSN: 24519030. DOI: 10.1016/j.bpsc.2019.10.011.
- Archer, Derek B. et al. (2019). 'Development and validation of the automated imaging differentiation in parkinsonism (AID-P): a multicentre machine learning study'. In: *The Lancet Digital Health* 1.5. ISSN: 25897500. DOI: 10.1016/S2589-7500(19)30105-0.
- Armstrong, Melissa J. (2015). 'Armstrong MJ, Litvan I, Lang AE, et al. Criteria for the diagnosis of corticobasal degeneration. *Neurology*. 2013;80(5):496-503. doi:10.1212/WNL.0b013e31827f0fd1.' In: *Brain and nerve = Shinkei kenkyū no shinpo* 67.4. ISSN: 1881-6096.
- Averbuch-Heller, Lea et al. (1999). 'Square-wave jerks induced by pallidotomy in parkinsonian patients'. In: *Neurology* 52.1. ISSN: 00283878. DOI: 10.1212/wnl.52.1.185.
- Awat, Holger et al. (2005). 'Effect of saccadic adaptation on localization of visual targets'. In: *Journal of Neurophysiology* 93.6. ISSN: 00223077. DOI: 10.1152/jn.01013.2003.
- Al-Azzam, Nosayba and Ibrahim Shatnawi (2021). 'Comparing supervised and semi-supervised Machine Learning Models on Diagnosing Breast Cancer'. In: *Annals of Medicine and Surgery* 62. ISSN: 20490801. DOI: 10.1016/j.amsu.2020.12.043.
- Baik, Mokryun et al. (2013). 'Investigation of eye-catching colors using eye tracking'. In: *Human Vision and Electronic Imaging XVIII*. Vol. 8651. DOI: 10.1117/12.2001141.
- Baltaretu, Bianca R. et al. (2020). *Parietal cortex integrates saccade and object orientation signals to update grasp plans*. DOI: 10.1523/JNEUROSCI.0300-20.2020.
- Banta, Conor W et al. (2023). 'Drug-Resistant Parkinson's Disease in a Patient With Hereditary Hemochromatosis: A Case Report'. In: *Cureus*. DOI: 10.7759/cureus.44530.
- Barbosa, Pedro et al. (2019). 'Saccadic Direction Errors are Associated with Impulsive Compulsive Behaviours in Parkinson's Disease Patients'. In: *Journal of Parkinson's Disease* 9.3. ISSN: 1877718X. DOI: 10.3233/JPD-181460.
- Barnes, G. R. (2008). 'Cognitive processes involved in smooth pursuit eye movements'. In: *Brain and Cognition* 68.3. ISSN: 02782626. DOI: 10.1016/j.bandc.2008.08.020.

- Batla, Amit et al. (2013). 'Markedly asymmetric presentation in multiple system atrophy'. In: *Parkinsonism and Related Disorders* 19.10. ISSN: 13538020. DOI: 10.1016/j.parkreldis.2013.05.004.
- Becker, Wolfgang et al. (2023). 'Patterns of small involuntary fixation saccades (SIFs) in different neurodegenerative diseases: the role of noise'. In: *Experimental Brain Research* 241.7. ISSN: 14321106. DOI: 10.1007/s00221-023-06633-6.
- Beigi, M. et al. (2016). 'Levodopa medication improves incidental sequence learning in Parkinson's disease'. In: *Neuropsychologia* 93. ISSN: 18733514. DOI: 10.1016/j.neuropsychologia.2016.09.019.
- Belić, Minja et al. (Sept. 2019). 'Artificial intelligence for assisting diagnostics and assessment of Parkinson's disease—A review'. In: *Clinical Neurology and Neurosurgery* 184, p. 105442. ISSN: 03038467. DOI: 10.1016/j.clineuro.2019.105442.
- Belle, Vaishak and Ioannis Papantonis (2021). *Principles and Practice of Explainable Machine Learning*. DOI: 10.3389/fdata.2021.688969.
- Benarroch, Eduardo (2023). 'What Are the Functions of the Superior Colliculus and Its Involvement in Neurologic Disorders?' In: *Neurology* 100.16. ISSN: 1526632X. DOI: 10.1212/WNL.0000000000207254.
- Benarroch, Eduardo E. (2003). *Brainstem in multiple system atrophy: Clinicopathological correlations*. DOI: 10.1023/A:1025067912199.
- Berardelli, Alfredo et al. (2001). *Pathophysiology of bradykinesia in parkinson's disease*. DOI: 10.1093/brain/124.11.2131.
- Berman, R. A. et al. (1999). 'Cortical networks subserving pursuit and saccadic eye movements in humans: An FMRI study'. In: *Human Brain Mapping* 8.4. ISSN: 10659471. DOI: 10.1002/(SICI)1097-0193(1999)8:4<209::AID-HBM5>3.0.CO;2-0.
- Beylergil, Sinem B. et al. (2022). 'Eye movements in Parkinson's disease during visual search'. In: *Journal of the Neurological Sciences* 440. ISSN: 18785883. DOI: 10.1016/j.jns.2022.120299.
- Biagioni, Francesca et al. (2019). 'Degeneration of cholinergic basal forebrain nuclei after focally evoked status epilepticus'. In: *Neurobiology of Disease* 121. ISSN: 1095953X. DOI: 10.1016/j.nbd.2018.09.019.
- Biase, Lazzaro di et al. (2023). *Levodopa-Induced Dyskinesias in Parkinson's Disease: An Overview on Pathophysiology, Clinical Manifestations, Therapy Management Strategies and Future Directions*. DOI: 10.3390/jcm12134427.
- Blandini, Fabio et al. (2000). *Functional changes of the basal ganglia circuitry in Parkinson's disease*. DOI: 10.1016/S0301-0082(99)00067-2.

- Blascheck, T. et al. (2014). 'State-of-the-Art of Visualization for Eye Tracking Data'. In: *16th Eurographics Conference on Visualization - State of the Art Reports, EuroVis-STAR 2014*. DOI: 10.2312/eurovisstar.20141173.
- (2017). 'Visualization of Eye Tracking Data: A Taxonomy and Survey'. In: *Computer Graphics Forum* 36.8. ISSN: 14678659. DOI: 10.1111/cgf.13079.
- Blesa, Javier, Sudarshan Phani et al. (2012). *Classic and new animal models of Parkinson's disease*. DOI: 10.1155/2012/845618.
- Blesa, Javier and Serge Przedborski (2014). 'Parkinson's disease: Animal models and dopaminergic cell vulnerability'. In: *Frontiers in Neuroanatomy* 8.DEC. ISSN: 16625129. DOI: 10.3389/fnana.2014.00155.
- Blochberger, Annett and Shelley Jones (2011). 'Parkinson's disease clinical features and diagnosis'. In: *Clinical Pharmacist* 3.11. ISSN: 17589061.
- Block, Hannah and Pablo Celnik (2013). 'Stimulating the cerebellum affects visuomotor adaptation but not intermanual transfer of learning'. In: *Cerebellum* 12.6. ISSN: 14734222. DOI: 10.1007/s12311-013-0486-7.
- Blohm, Gunnar, Marcus Missal and Philippe Lefèvre (2003). 'Interaction between smooth anticipation and saccades during ocular orientation in darkness'. In: *Journal of Neurophysiology* 89.3. ISSN: 00223077. DOI: 10.1152/jn.00675.2002.
- Blurton, Steven P., Markus Raabe and Mark W. Greenlee (2012). 'Differential cortical activation during saccadic adaptation'. In: *Journal of Neurophysiology* 107.6. ISSN: 00223077. DOI: 10.1152/jn.00682.2011.
- Boeve, Bradley F. (2011). 'The multiple phenotypes of corticobasal syndrome and corticobasal degeneration: Implications for further study'. In: *Journal of Molecular Neuroscience*. Vol. 45. 3. DOI: 10.1007/s12031-011-9624-1.
- Bose, Anindita and M. Flint Beal (2016). *Mitochondrial dysfunction in Parkinson's disease*. DOI: 10.1111/jnc.13731.
- Bosman, J. et al. (2002). 'The influence of eye muscle surgery on shape and relative orientation of displacement planes: Indirect evidence for neural control of 3D eye movements'. In: *Strabismus* 10.3. ISSN: 09273972. DOI: 10.1076/stra.10.3.199.8124.

- Boxer, Adam L. et al. (2006). *Patterns of brain atrophy that differentiate corticobasal degeneration syndrome from progressive supranuclear palsy*. DOI: 10.1001/archneur.63.1.81.
- Bradshaw, J. M. et al. (2006). 'Higher cortical deficits influence attentional processing in dementia with Lewy bodies, relative to patients with dementia of the Alzheimer's type and controls'. In: *Journal of Neurology, Neurosurgery and Psychiatry* 77.10. ISSN: 1468330X. DOI: 10.1136/jnnp.2006.090183.
- Brainard, Michael S. and Allison J. Doupe (2000). 'Interruption of a basal ganglia-forebrain circuit prevents plasticity of learned vocalizations'. In: *Nature* 404.6779. ISSN: 00280836. DOI: 10.1038/35008083.
- Brandt, Thomas et al. (1998). 'Reciprocal inhibitory visual-vestibular interaction. Visual motion stimulation deactivates the parieto-insular vestibular cortex'. In: *Brain* 121.9. ISSN: 00068950. DOI: 10.1093/brain/121.9.1749.
- Brett, Francesca M., Craig Henson and Hugh Staunton (2002). 'Familial diffuse Lewy body disease, eye movement abnormalities, and distribution of pathology'. In: *Archives of Neurology* 59.3. ISSN: 00039942. DOI: 10.1001/archneur.59.3.464.
- Briand, Kevin A. et al. (1999). 'Control of voluntary and reflexive saccades in Parkinson's disease'. In: *Experimental Brain Research* 129.1. ISSN: 00144819. DOI: 10.1007/s002210050934.
- Bro, Rasmus and Age K. Smilde (2014). *Principal component analysis*. DOI: 10.1039/c3ay41907j.
- Brockington, Alice et al. (2013). 'Unravelling the enigma of selective vulnerability in neurodegeneration: Motor neurons resistant to degeneration in ALS show distinct gene expression characteristics and decreased susceptibility to excitotoxicity'. In: *Acta Neuropathologica* 125.1. ISSN: 00016322. DOI: 10.1007/s00401-012-1058-5.
- Brooks, Sarah H. et al. (2017). 'Slowed prosaccades and increased antisaccade errors as a potential behavioral biomarker of multiple system atrophy'. In: *Frontiers in Neurology* 8.JUN. ISSN: 16642295. DOI: 10.3389/fneur.2017.00261.
- Bruce, C. J. and M. E. Goldberg (1985). 'Primate frontal eye fields. I. Single neurons discharging before saccades'. In: *Journal of Neurophysiology* 53.3. ISSN: 00223077. DOI: 10.1152/jn.1985.53.3.603.
- Bryan, S and Damask Direct Access Magnetic Reso (2008). 'Cost-effectiveness of magnetic resonance imaging of the knee for patients presenting in primary care DAMASK (Direct Access to Magnetic Resonance Imaging: Assessment for Suspect Knees) Trial Team'. In: *British Journal of General Practice* 58.556. ISSN: 0960-1643.

- Buch, Karen A. et al. (2022). 'Clinical Correlation Between Vertical Gaze Palsy and Midbrain Volume in Progressive Supranuclear Palsy'. In: *Journal of Neuro-Ophthalmology* 42.2. ISSN: 15365166. DOI: 10.1097/WNO.0000000000001393.
- Bucher, Meghan L. et al. (2020). 'Acquired dysregulation of dopamine homeostasis reproduces features of Parkinson's disease'. In: *npj Parkinson's Disease* 6.1. ISSN: 23738057. DOI: 10.1038/s41531-020-00134-x.
- Bueno, A. P.A., J. R. Sato and M. Hornberger (2019). *Eye tracking – The overlooked method to measure cognition in neurodegeneration?* DOI: 10.1016/j.neuropsychologia.2019.107191.
- Burr, David C. and John Ross (1982). 'Contrast sensitivity at high velocities'. In: *Vision Research* 22.4. ISSN: 00426989. DOI: 10.1016/0042-6989(82)90196-1.
- Burrell, James R. et al. (2014). 'Apraxia and motor dysfunction in corticobasal syndrome'. In: *PLoS ONE* 9.3. ISSN: 19326203. DOI: 10.1371/journal.pone.0092944.
- Bylsma, Frederick W. et al. (Feb. 1995). 'Changes in visual fixation and saccadic eye movements in Alzheimer's disease'. In: *International Journal of Psychophysiology* 19.1, pp. 33–40. ISSN: 01678760. DOI: 10.1016/0167-8760(94)00060-R.
- Cameron, Ian G.M., Justin M. Riddle and Mark D'Esposito (2015). 'Dissociable roles of dorsolateral prefrontal cortex and frontal eye fields during saccadic eye movements'. In: *Frontiers in Human Neuroscience* 9.NOVEMBER. ISSN: 16625161. DOI: 10.3389/fnhum.2015.00613.
- Campbell, Ian G. (2009). *EEG recording and analysis for sleep research*. DOI: 10.1002/0471142301.ns1002s49.
- Campbell, Meghan C. et al. (2020). 'Parkinson disease clinical subtypes: key features & clinical milestones'. In: *Annals of Clinical and Translational Neurology* 7.8. ISSN: 23289503. DOI: 10.1002/acn3.51102.
- Campos-Acuña, Javier, Daniela Elgueta and Rodrigo Pacheco (2019). *T-cell-driven inflammation as a mediator of the gut-brain axis involved in Parkinson's disease*. DOI: 10.3389/fimmu.2019.00239.
- Cao, Hengyi et al. (2018). 'Cerebello-thalamo-cortical hyperconnectivity as a state-independent functional neural signature for psychosis prediction and characterization'. In: *Nature Communications* 9.1. ISSN: 20411723. DOI: 10.1038/s41467-018-06350-7.
- Cassanello, Carlos R., Sven Ohl and Martin Rolfs (2016). 'Saccadic adaptation to a systematically varying disturbance'. In: *Journal of Neurophysiology* 116.2. ISSN: 15221598. DOI: 10.1152/jn.00206.2016.

- Catalan, Mauro et al. (2021). '123I-Metaiodobenzylguanidine Myocardial Scintigraphy in Discriminating Degenerative Parkinsonisms'. In: *Movement Disorders Clinical Practice* 8.5. ISSN: 23301619. DOI: 10.1002/mdc3.13227.
- Catz, N. and P. Thier (2007). *Neural control of saccadic eye movements*. DOI: 10.1159/000100349.
- Chai, Chou and Kah-Leong Lim (2014). 'Genetic Insights into Sporadic Parkinson's Disease Pathogenesis'. In: *Current Genomics* 14.8. ISSN: 13892029. DOI: 10.2174/1389202914666131210195808.
- Chan, Florence et al. (2005). 'Deficits in saccadic eye-movement control in Parkinson's disease'. In: *Neuropsychologia* 43.5. ISSN: 00283932. DOI: 10.1016/j.neuropsychologia.2004.06.026.
- Chang, Kuo Hsuan and Chiung Mei Chen (2020). *The role of oxidative stress in Parkinson's disease*. DOI: 10.3390/antiox9070597.
- Chauhan, Nagesh Singh (2020). 'Model Evaluation metrics in Machine learning'. In: *Kdnuggets*.
- Chawla, Nitesh V. et al. (2002). 'SMOTE: Synthetic minority over-sampling technique'. In: *Journal of Artificial Intelligence Research* 16. ISSN: 10769757. DOI: 10.1613/jair.953.
- Chen, Athena L. et al. (2010). 'The disturbance of gaze in progressive supranuclear palsy: Implications for pathogenesis'. In: *Frontiers in Neurology* DEC. ISSN: 16642295. DOI: 10.3389/fneur.2010.00147.
- Chen, Boyu et al. (2023). 'Automatic classification of MSA subtypes using Whole-brain gray matter function and Structure-Based radiomics approach'. In: *European Journal of Radiology* 161. ISSN: 18727727. DOI: 10.1016/j.ejrad.2023.110735.
- Chen, Chuyu et al. (2020). 'Pathway-specific dysregulation of striatal excitatory synapses by LRRK2 mutations'. In: *eLife* 9. ISSN: 2050084X. DOI: 10.7554/eLife.58997.
- Chen, K. J. et al. (2005). 'Initial ocular following in humans depends critically on the fourier components of the motion stimulus'. In: *Annals of the New York Academy of Sciences*. Vol. 1039. DOI: 10.1196/annals.1325.025.
- Chen, Tianqi and Carlos Guestrin (2016). 'XGBoost: A scalable tree boosting system'. In: *Proceedings of the ACM SIGKDD International Conference on Knowledge Discovery and Data Mining*. Vol. 13-17-August-2016. DOI: 10.1145/2939672.2939785.
- Chengsheng, Tu, Liu Huacheng and Xu Bing (Dec. 2017). 'AdaBoost typical Algorithm and its application research'. In: *MATEC Web of Conferences* 139, p. 00222. ISSN: 2261-236X. DOI: 10.1051/mateconf/201713900222.

- Cherici, Claudia et al. (2012). 'Precision of sustained fixation in trained and untrained observers'. In: *Journal of Vision* 12.6. ISSN: 15347362. DOI: 10.1167/12.6.31.
- Cherubini, Andrea et al. (2014). 'Magnetic resonance support vector machine discriminates between Parkinson disease and progressive supranuclear palsy'. In: *Movement Disorders* 29.2. ISSN: 08853185. DOI: 10.1002/mds.25737.
- Cheviet, Alexis, Laure Pisella and Denis Pélisson (2021). 'The posterior parietal cortex processes visuo-spatial and extra-retinal information for saccadic remapping: A case study'. In: *Cortex* 139. ISSN: 19738102. DOI: 10.1016/j.cortex.2021.02.026.
- Cho, Vanessa Y. et al. (2022). 'Understanding Children's Attention to Dental Caries through Eye-Tracking'. In: *Caries Research* 56.2. ISSN: 1421976X. DOI: 10.1159/000524458.
- Choi, Hongyoon et al. (2017). 'Refining diagnosis of Parkinson's disease with deep learning-based interpretation of dopamine transporter imaging'. In: *NeuroImage: Clinical* 16. ISSN: 22131582. DOI: 10.1016/j.nicl.2017.09.010.
- Chris Muly, E., Klara Szigeti and Patricia S. Goldman-Rakic (1998). 'D1 receptor in interneurons of macaque prefrontal cortex: Distribution and subcellular localization'. In: *Journal of Neuroscience* 18.24. ISSN: 02706474. DOI: 10.1523/jneurosci.18-24-10553.1998.
- Chubb, M. C. and A. F. Fuchs (1982). 'Contribution of y group of vestibular nuclei and dentate nucleus of cerebellum to generation of vertical smooth eye movements'. In: *Journal of Neurophysiology* 48.1. ISSN: 00223077. DOI: 10.1152/jn.1982.48.1.75.
- Churchland, Anne K. and Stephen G. Lisberger (2002). 'Gain control in human smooth-pursuit eye movements'. In: *Journal of Neurophysiology* 87.6. ISSN: 00223077. DOI: 10.1152/jn.2002.87.6.2936.
- Cieslik, Edna C. et al. (2016). *Different involvement of subregions within dorsal premotor and medial frontal cortex for pro- and antisaccades*. DOI: 10.1016/j.neubiorev.2016.05.012.
- Coakeley, Sarah and Antonio P. Strafella (2015). *Imaging pathological tau in atypical parkinsonian disorders*. DOI: 10.1097/WCD.0000000000000210.
- Compta, Yaroslau et al. (2011). 'Lewy- and Alzheimer-type pathologies in Parkinson's disease dementia: Which is more important?' In: *Brain* 134.5. ISSN: 14602156. DOI: 10.1093/brain/awr031.
- Constantinides, Vasilios C. et al. (2019). *Corticobasal degeneration and corticobasal syndrome: A review*. DOI: 10.1016/j.prdoa.2019.08.005.

- Convery, Rhian S et al. (2023). 'A portable eye tracking experiment for the assessment of cognitive impairment in presymptomatic frontotemporal dementia'. In: *Alzheimer's & Dementia* 19.S15. ISSN: 1552-5260. DOI: 10.1002/alz.079622.
- Corrà, Marta Francisca et al. (2021). 'Comparison of laboratory and daily-life gait speed assessment during on and off states in parkinson's disease'. In: *Sensors* 21.12. ISSN: 14248220. DOI: 10.3390/s21123974.
- Costela, Francisco M. et al. (2013). 'Microsaccades restore the visibility of minute foveal targets'. In: *PeerJ* 2013.1. ISSN: 21678359. DOI: 10.7717/peerj.119.
- Creel, Donnell J. (2019). 'The electrooculogram'. In: *Handbook of Clinical Neurology*. Vol. 160. DOI: 10.1016/B978-0-444-64032-1.00033-3.
- Culham, Jody C., Cristiana Cavina-Pratesi and Anthony Singhal (2006). 'The role of parietal cortex in visuomotor control: What have we learned from neuroimaging?' In: *Neuropsychologia* 44.13. ISSN: 00283932. DOI: 10.1016/j.neuropsychologia.2005.11.003.
- Cyclops Medtech Pvt Ltd (n.d.). *Cyclops Medtech*.
- Dai, Weiwei et al. (2017). 'A nonlinear generalization of the Savitzky-Golay filter and the quantitative analysis of saccades'. In: *Journal of Vision* 17.9. ISSN: 15347362. DOI: 10.1167/17.9.10.
- Dalmaso, Mario et al. (2017). 'Working memory load modulates microsaccadic rate'. In: *Journal of Vision* 17.3. ISSN: 15347362. DOI: 10.1167/17.3.6.
- De Backere, Femke et al. (2015). 'Platform for efficient switching between multiple devices in the intensive care unit'. In: *Methods of Information in Medicine* 54.1. ISSN: 00261270. DOI: 10.3414/ME13-02-0021.
- De Hemptinne, C., G. R. Barnes and M. Missal (2010). 'Influence of previous target motion on anticipatory pursuit deceleration'. In: *Experimental Brain Research* 207.3-4. ISSN: 00144819. DOI: 10.1007/s00221-010-2437-6.
- Delaville, Claire, Philippe de Deurwaerdère and Abdelhamid Benazzouz (2011). *Noradrenaline and Parkinson's disease*. DOI: 10.3389/fnsys.2011.00031.
- Dell'Osso, L. F. and Z. I. Wang (2008). 'Extraocular proprioception and new treatments for infantile nystagmus syndrome'. In: *Progress in Brain Research*. Vol. 171. DOI: 10.1016/S0079-6123(08)00610-9.
- DeLong, Mahlon and Thomas Wichmann (2009). 'Update on models of basal ganglia function and dysfunction'. In: *Parkinsonism and Related Disorders* 15.SUPPL. 3. ISSN: 13538020. DOI: 10.1016/S1353-8020(09)70822-3.

- Demer, J. L. and F. Amjadi (1993). 'Dynamic visual acuity of normal subjects during vertical optotype and head motion'. In: *Investigative Ophthalmology and Visual Science* 34.6. ISSN: 01460404.
- Deng, Xiao et al. (2020). 'Four-Year Longitudinal Study of Motor and Non-motor Symptoms in LRRK2-Related Parkinson's Disease'. In: *Frontiers in Neurology* 10. ISSN: 16642295. DOI: 10.3389/fneur.2019.01379.
- Desmurget, M. et al. (2000). 'Functional adaptation of reactive saccades in humans: A PET study'. In: *Experimental Brain Research* 132.2. ISSN: 00144819. DOI: 10.1007/s002210000342.
- Deubel, Heiner (1999). 'Separate mechanisms for the adaptive control of reactive, volitional, and memory-guided saccadic eye movements'. In: *Attention and Performance* 17. ISSN: 10470387. DOI: 10.7551/mitpress/1480.003.0034.
- Deutschländer, A. B. et al. (2018). *Atypical parkinsonian syndromes: a general neurologist's perspective*. DOI: 10.1111/ene.13412.
- Deyaert, Egon et al. (2017). 'A homologue of the Parkinson's disease-associated protein LRRK2 undergoes a monomer-dimer transition during GTP turnover'. In: *Nature Communications* 8.1. ISSN: 20411723. DOI: 10.1038/s41467-017-01103-4.
- Dias, Vera, Eunsung Junn and M. Maral Mouradian (2013). *The role of oxidative stress in parkinson's disease*. DOI: 10.3233/JPD-130230.
- Dickson, Dennis W. (2018). 'Neuropathology of Parkinson disease'. In: *Parkinsonism and Related Disorders* 46. ISSN: 18735126. DOI: 10.1016/j.parkreldis.2017.07.033.
- Dickson, Dennis W., Heiko Braak et al. (2009). *Neuropathological assessment of Parkinson's disease: refining the diagnostic criteria*. DOI: 10.1016/S1474-4422(09)70238-8.
- Dickson, Dennis W., Rosa Rademakers and Michael L. Hutton (2007). 'Progressive supranuclear palsy: Pathology and genetics'. In: *Brain Pathology*. Vol. 17. 1. DOI: 10.1111/j.1750-3639.2007.00054.x.
- Ding, Xiaojian, Fan Yang and Fuming Ma (2022). 'An efficient model selection for linear discriminant function-based recursive feature elimination'. In: *Journal of Biomedical Informatics* 129. ISSN: 15320464. DOI: 10.1016/j.jbi.2022.104070.
- DiScenna, Alfred O. et al. (1995). 'Evaluation of a video tracking device for measurement of horizontal and vertical eye rotations during locomotion'. In: *Journal of Neuroscience Methods* 58.1-2. ISSN: 01650270. DOI: 10.1016/0165-0270(94)00162-A.

- Do, Jenny et al. (2019). *Glucocerebrosidase and its relevance to Parkinson disease*. DOI: 10.1186/s13024-019-0336-2.
- Dodge, Raymond (1903). 'FIVE TYPES OF EYE MOVEMENT IN THE HORIZONTAL MERIDIAN PLANE OF THE FIELD OF REGARD'. In: *American Journal of Physiology-Legacy Content* 8.4. ISSN: 0002-9513. DOI: 10.1152/ajplegacy.1903.8.4.307.
- Dopper, Elise G.P. et al. (2011). 'Symmetrical corticobasal syndrome caused by a novel c.314dup progranulin mutation'. In: *Journal of Molecular Neuroscience*. Vol. 45. 3. DOI: 10.1007/s12031-011-9626-z.
- Dorr, Michael et al. (2010). 'Variability of eye movements when viewing dynamic natural scenes'. In: *Journal of Vision* 10.10. ISSN: 15347362. DOI: 10.1167/10.10.28.
- Dowiasch, Stefan et al. (2015). 'Effects of aging on eye movements in the real world'. In: *Frontiers in Human Neuroscience* 9.FEB. ISSN: 16625161. DOI: 10.3389/fnhum.2015.00046.
- Drotár, Peter et al. (2014). 'Analysis of in-air movement in handwriting: A novel marker for Parkinson's disease'. In: *Computer Methods and Programs in Biomedicine* 117.3. ISSN: 18727565. DOI: 10.1016/j.cmpb.2014.08.007.
- Dwivedi, Ruby, Divya Mehrotra and Shaleen Chandra (2022). 'Potential of Internet of Medical Things (IoMT) applications in building a smart healthcare system: A systematic review'. In: *Journal of Oral Biology and Craniofacial Research* 12.2. ISSN: 22124268. DOI: 10.1016/j.jobcr.2021.11.010.
- Eggert, T. (2007). *Eye movement recordings: Methods*. DOI: 10.1159/000100347.
- Eimeren, Thilo van et al. (2019). 'Neuroimaging biomarkers for clinical trials in atypical parkinsonian disorders: Proposal for a Neuroimaging Biomarker Utility System'. In: *Alzheimer's and Dementia: Diagnosis, Assessment and Disease Monitoring* 11. ISSN: 23528729. DOI: 10.1016/j.dadm.2019.01.011.
- Elgueta, Daniela et al. (2022). 'Analyzing the Parkinson's Disease Mouse Model Induced by Adeno-associated Viral Vectors Encoding Human α -Synuclein'. In: *Journal of Visualized Experiments* 2022.185. ISSN: 1940087X. DOI: 10.3791/63313.
- Enderle, John D. (2002). 'Neural control of saccades'. In: *Progress in Brain Research*. Vol. 140. DOI: 10.1016/S0079-6123(02)40040-4.
- Engbert, Ralf and Reinhold Kliegl (2003). 'Microsaccades uncover the orientation of covert attention'. In: *Vision Research* 43.9. ISSN: 00426989. DOI: 10.1016/S0042-6989(03)00084-1.

- Engbert, Ralf, Hans A. Trukenbrod et al. (2015). 'Spatial statistics and attentional dynamics in scene viewing'. In: *Journal of Vision* 15.1. ISSN: 15347362. DOI: 10.1167/15.1.14.
- Eraslan Boz, Hatice et al. (2023). 'Eye movement patterns during viewing face images with neutral expressions in patients with early-stage Alzheimer's disease and amnesic mild cognitive impairment'. In: *Brain and Behavior* 13.11. ISSN: 21623279. DOI: 10.1002/brb3.3232.
- Erkelens, C. J. and J. Hulleman (1993). 'Selective adaptation of internally triggered saccades made to visual targets'. In: *Experimental Brain Research* 93.1. ISSN: 00144819. DOI: 10.1007/BF00227790.
- Espay, Alberto J., Peter A. Lewitt and Horacio Kaufmann (2014). 'Norepinephrine deficiency in Parkinson's disease: The case for noradrenergic enhancement'. In: *Movement Disorders* 29.14. ISSN: 15318257. DOI: 10.1002/mds.26048.
- Esposito, Matteo et al. (2021). 'A subcortical network for implicit visuo-spatial attention: Implications for Parkinson's Disease'. In: *Cortex* 141. ISSN: 19738102. DOI: 10.1016/j.cortex.2021.05.003.
- Evans, Karen M. et al. (2012). 'Collecting and analyzing eye-tracking data in outdoor environments'. In: *Journal of Eye Movement Research* 5.2. ISSN: 19958692. DOI: 10.16910/jemr.5.2.6.
- Everling, Stefan and Burkhardt Fischer (1998). 'The antisaccade: A review of basic research and clinical studies'. In: *Neuropsychologia* 36.9. ISSN: 00283932. DOI: 10.1016/S0028-3932(98)00020-7.
- Fanciulli, Alessandra et al. (2022). 'A multiplex pedigree with pathologically confirmed multiple system atrophy and Parkinson's disease with dementia'. In: *Brain Communications* 4.4. ISSN: 26321297. DOI: 10.1093/braincomms/fcac175.
- Fang, Yu et al. (2018). 'Monocular microsaccades: Do they really occur?' In: *Journal of Vision* 18.3. ISSN: 15347362. DOI: 10.1167/18.3.18.
- Fearon, Conor et al. (2020). *The "round the houses" sign and "zig-zag" sign in progressive supranuclear palsy and other conditions*. DOI: 10.1016/j.parkreldis.2020.10.030.
- Fekete, R. et al. (2012). 'Familial Corticobasal Syndrome Associated with Basal Ganglia Hypointensities (P06.081)'. In: *Neurology* 78.Meeting Abstracts 1. ISSN: 0028-3878. DOI: 10.1212/wnl.78.1{_}meetingabstracts.p06.081.
- Felßberg, Anna-Maria and Dominykas Strazdas (Mar. 2025). 'RELAY: Robotic EyeLink AnalYsis of the Eye-Link 1000 Using an Artificial Eye'. In: *Vision* 9.1, p. 18. ISSN: 2411-5150. DOI: 10.3390/vision9010018.
- Fernandes, Hugo L. et al. (2014). 'Saliency and saccade encoding in the frontal eye field during natural scene search'. In: *Cerebral Cortex* 24.12. ISSN: 14602199. DOI: 10.1093/cercor/bht179.

- Fernández-Botrán, Rafael et al. (2011). 'Cytokine expression and microglial activation in progressive supranuclear palsy'. In: *Parkinsonism and Related Disorders* 17.9. ISSN: 13538020. DOI: 10.1016/j.parkreldis.2011.06.007.
- Fernández-Vidal, Joan Miquel et al. (Nov. 2024). 'Cognitive phenotyping of GBA1-Parkinson's disease: A study on deep brain stimulation outcomes'. In: *Parkinsonism & Related Disorders* 128, p. 107127. ISSN: 13538020. DOI: 10.1016/j.parkreldis.2024.107127.
- Ferrara, Emilio (2024). *Fairness and Bias in Artificial Intelligence: A Brief Survey of Sources, Impacts, and Mitigation Strategies*. DOI: 10.3390/sci6010003.
- Freeman, Tom C.A., Rebecca A. Champion and Paul A. Warren (2010). 'A Bayesian Model of Perceived Head-Centered Velocity during Smooth Pursuit Eye Movement'. In: *Current Biology* 20.8. ISSN: 09609822. DOI: 10.1016/j.cub.2010.02.059.
- Frei, Karen (2021). *Abnormalities of smooth pursuit in Parkinson's disease: A systematic review*. DOI: 10.1016/j.prdoa.2020.100085.
- Freitas, Maria Eliza, Christopher W. Hess and Susan H. Fox (2017). 'Motor Complications of Dopaminergic Medications in Parkinson's Disease'. In: *Seminars in Neurology* 37.2. ISSN: 10989021. DOI: 10.1055/s-0037-1602423.
- Fridley, Jared et al. (2013). 'Effect of subthalamic nucleus or globus pallidus interna stimulation on oculomotor function in patients with parkinson's disease'. In: *Stereotactic and Functional Neurosurgery* 91.2. ISSN: 10116125. DOI: 10.1159/000343200.
- Friedman, Lee et al. (2023). 'Factors affecting inter-rater agreement in human classification of eye movements: a comparison of three datasets'. In: *Behavior Research Methods* 55.1. ISSN: 15543528. DOI: 10.3758/s13428-021-01782-4.
- Fukushima, Kikuro et al. (2013). *Cognitive processes involved in smooth pursuit eye movements: Behavioral evidence, neural substrate and clinical correlation*. DOI: 10.3389/fnsys.2013.00004.
- Furman, Joseph M. and Floris L. Wuyts (2012). 'Vestibular Laboratory Testing'. In: *Aminoff's Electrodiagnosis in Clinical Neurology*. DOI: 10.1016/B978-1-4557-0308-1.00032-7.
- Gaki, Georgia S. and Athanasios G. Papavassiliou (2014). 'Oxidative stress-induced signaling pathways implicated in the pathogenesis of Parkinson's disease'. In: *NeuroMolecular Medicine* 16.2. ISSN: 15591174. DOI: 10.1007/s12017-014-8294-x.

- Gamlin, Paul D.R. (2002). 'Neural mechanisms for the control of vergence eye movements'. In: *Annals of the New York Academy of Sciences*. Vol. 956. DOI: 10.1111/j.1749-6632.2002.tb02825.x.
- Garbutt, S., M. R. Harwood and C. M. Harris (2001). 'Comparison of the main sequence of reflexive saccades and the quick phases of optokinetic nystagmus'. In: *British Journal of Ophthalmology* 85.12. ISSN: 00071161. DOI: 10.1136/bjo.85.12.1477.
- Garbutt, Siobhan et al. (2008). 'Oculomotor function in frontotemporal lobar degeneration, related disorders and Alzheimer's disease'. In: *Brain* 131.5. ISSN: 14602156. DOI: 10.1093/brain/awn047.
- Garcia-Esparcia, Paula et al. (2017). 'Dementia with lewy bodies: Molecular pathology in the frontal cortex in typical and rapidly progressive forms'. In: *Frontiers in Neurology* 8.MAR. ISSN: 16642295. DOI: 10.3389/fneur.2017.00089.
- Gate, David et al. (2021). 'CD4+ T cells contribute to neurodegeneration in Lewy body dementia'. In: *Science* 374.6569. ISSN: 10959203. DOI: 10.1126/science.abf7266.
- Gauthier, Gabriel M., Jean Louis Vercher and David S. Zee (1994). 'Changes in ocular alignment and pointing accuracy after sustained passive rotation of one eye'. In: *Vision Research* 34.19. ISSN: 00426989. DOI: 10.1016/0042-6989(94)90247-X.
- Gerardin, Peggy et al. (2012). 'Functional activation of the cerebral cortex related to sensorimotor adaptation of reactive and voluntary saccades'. In: *NeuroImage* 61.4. ISSN: 10538119. DOI: 10.1016/j.neuroimage.2012.03.037.
- Gerfen, Charles R. (2023). *Segregation of D1 and D2 dopamine receptors in the striatal direct and indirect pathways: An historical perspective*. DOI: 10.3389/fnsyn.2022.1002960.
- Gerfen, Charles R. and D. James Surmeier (2011). 'Modulation of striatal projection systems by dopamine'. In: *Annual Review of Neuroscience* 34. ISSN: 0147006X. DOI: 10.1146/annurev-neuro-061010-113641.
- Giachino, Carmela et al. (2022). 'LRRK2-G2019S Synergizes with Ageing and Low-Grade Inflammation to Promote Gut and Peripheral Immune Cell Activation that Precede Nigrostriatal Degeneration'. In: *bioRxiv*.
- Gilman, S. et al. (2008). 'Second consensus statement on the diagnosis of multiple system atrophy'. In: *Neurology* 71.9. ISSN: 1526632X. DOI: 10.1212/01.wnl.0000324625.00404.15.
- Gionfriddo, Michael R. et al. (2022). 'Evaluation of a Web-Based Medication Reconciliation Application Within a Primary Care Setting: Cluster-Randomized Controlled Trial'. In: *JMIR Formative Research* 6.3. ISSN: 2561326X. DOI: 10.2196/33488.

- Goetz, Christopher G. et al. (2008). 'Movement Disorder Society-Sponsored Revision of the Unified Parkinson's Disease Rating Scale (MDS-UPDRS): Scale presentation and clinimetric testing results'. In: *Movement Disorders* 23.15. ISSN: 15318257. DOI: 10.1002/mds.22340.
- Goldman-Rakic, P. S., E. C. Muly and G. V. Williams (2000). 'D1 receptors in prefrontal cells and circuits'. In: *Brain Research Reviews* 31.2-3. ISSN: 01650173. DOI: 10.1016/S0165-0173(99)00045-4.
- Golla, Heidrun et al. (2008). 'Reduced saccadic resilience and impaired saccadic adaptation due to cerebellar disease'. In: *European Journal of Neuroscience* 27.1. ISSN: 14609568. DOI: 10.1111/j.1460-9568.2007.05996.x.
- Gong, Jinnan et al. (2021). 'Distinct effects of the basal ganglia and cerebellum on the thalamocortical pathway in idiopathic generalized epilepsy'. In: *Human Brain Mapping* 42.11. ISSN: 10970193. DOI: 10.1002/hbm.25444.
- Gonzalez-Cuautle, David et al. (2020). 'Synthetic minority oversampling technique for optimizing classification tasks in botnet and intrusion-detection-system datasets'. In: *Applied Sciences (Switzerland)* 10.3. ISSN: 20763417. DOI: 10.3390/app10030794.
- Gorges, Martin, Hans Peter Müller et al. (2016). 'The association between alterations of eye movement control and cerebral intrinsic functional connectivity in Parkinson's disease'. In: *Brain Imaging and Behavior* 10.1. ISSN: 19317565. DOI: 10.1007/s11682-015-9367-7.
- Gorges, Martin, Elmar H. Pinkhardt and Jan Kassubek (2014). *Alterations of eye movement control in neurodegenerative movement disorders*. DOI: 10.1155/2014/658243.
- Graybiel, Ann M., Juan J. Canales and Christine Capper-Loup (2000). *Levodopa-induced dyskinesias and dopamine-dependent stereotypies: A new hypothesis*. DOI: 10.1016/S1471-1931(00)00027-6.
- Grossman, G. E. et al. (1988). 'Frequency and velocity of rotational head perturbations during locomotion'. In: *Experimental Brain Research* 70.3. ISSN: 00144819. DOI: 10.1007/BF00247595.
- Gu, Yong, Gregory C. DeAngelis and Dora E. Angelaki (2007). 'A functional link between area MSTd and heading perception based on vestibular signals'. In: *Nature Neuroscience* 10.8. ISSN: 10976256. DOI: 10.1038/nn1935.
- Guerrasio, Lorenzo et al. (2010). 'Fastigial oculomotor region and the control of foveation during fixation'. In: *Journal of Neurophysiology* 103.4. ISSN: 00223077. DOI: 10.1152/jn.00771.2009.
- Guillaume, Alain et al. (2018). 'Cortico-cerebellar network involved in saccade adaptation'. In: *Journal of Neurophysiology* 120.5. ISSN: 15221598. DOI: 10.1152/jn.00392.2018.

- Gul, Amara and Javed Yousaf (2019). 'Effect of levodopa on frontal-subcortical and posterior cortical functioning in patients with Parkinson's disease'. In: *Singapore Medical Journal* 60.8. ISSN: 00375675. DOI: 10.11622/SMEDJ.2018116.
- Gültekin, Murat (2020). 'Phenotypic variants of patients with progressive supranuclear palsy'. In: *Noropsikiyatri Arsivi* 57.1. ISSN: 13000667. DOI: 10.5152/npa.2017.22771.
- Guo, Yanxia et al. (2018). 'Immune checkpoint inhibitor PD-1 pathway is down-regulated in synovium at various stages of rheumatoid arthritis disease progression'. In: *PLoS ONE* 13.2. ISSN: 19326203. DOI: 10.1371/journal.pone.0192704.
- Güttler, Christopher et al. (2021). 'Levodopa-Induced Dyskinesia Are Mediated by Cortical Gamma Oscillations in Experimental Parkinsonism'. In: *Movement Disorders* 36.4. ISSN: 15318257. DOI: 10.1002/mds.28403.
- Hafed, Ziad M. and Richard J. Krauzlis (2010). 'Microsaccadic suppression of visual bursts in the primate superior colliculus'. In: *Journal of Neuroscience* 30.28. ISSN: 02706474. DOI: 10.1523/JNEUROSCI.1137-10.2010.
- Hafed, Ziad M., Masatoshi Yoshida et al. (2021). *Dissociable Cortical and Subcortical Mechanisms for Mediating the Influences of Visual Cues on Microsaccadic Eye Movements*. DOI: 10.3389/fncir.2021.638429.
- Hamner, Ben and Michael Frasco (2018). *Metrics: Evaluation metrics for machine learning*.
- Hanes, Doug P. and Robert H. Wurtz (2001). 'Interaction of the frontal eye field and superior colliculus for saccade generation'. In: *Journal of Neurophysiology* 85.2. ISSN: 00223077. DOI: 10.1152/jn.2001.85.2.804.
- Hansen, D. et al. (2019). *Review: Clinical, neuropathological and genetic features of Lewy body dementias*. DOI: 10.1111/nan.12554.
- Harpaz, Eran et al. (2024). 'Video-Based Gaze Detection for Oculomotor Abnormality Measurements'. In: *Applied Sciences (Switzerland)* 14.4. ISSN: 20763417. DOI: 10.3390/app14041519.
- Harrar, Vanessa et al. (2018). 'A nonvisual eye tracker calibration method for video-based tracking'. In: *Journal of Vision* 18.9. ISSN: 15347362. DOI: 10.1167/18.9.13.
- Harry, Alexandra (2023). 'The Future of Medicine: Harnessing the Power of AI for Revolutionizing Healthcare'. In: *International Journal of Multidisciplinary Sciences and Arts* 2.1. DOI: 10.47709/ijmdsa.v2i1.2395.

- Hartmann, Thomas and Nathan Weisz (2020). 'An Introduction to the Objective Psychophysics Toolbox'. In: *Frontiers in Psychology* 11. ISSN: 16641078. DOI: 10.3389/fpsyg.2020.585437.
- Hashiba, Motoyuki et al. (1995). 'Quantitative analysis of smooth pursuit eye movement'. In: *Nippon Jibiinkoka Gakkai Kaiho* 98.4. ISSN: 00306622. DOI: 10.3950/jibiinkoka.98.681.
- Hattori, Nobutaka (2022). 'Levodopa Therapy for the Treatment of Parkinson's Disease'. In: *NeuroPsycho-pharmacotherapy*. DOI: 10.1007/978-3-030-62059-2{_}225.
- Havermann, Katharina, Robert Volcic and Markus Lappe (2012). 'Saccadic adaptation to moving targets'. In: *PLoS ONE* 7.6. ISSN: 19326203. DOI: 10.1371/journal.pone.0039708.
- Hayakawa, Yuuki et al. (2002). 'Human cerebellar activation in relation to saccadic eye movements: A functional magnetic resonance imaging study'. In: *Ophthalmologica* 216.6. ISSN: 00303755. DOI: 10.1159/000067551.
- Healy, Daniel G. et al. (2008). 'Phenotype, genotype, and worldwide genetic penetrance of LRRK2-associated Parkinson's disease: a case-control study'. In: *The Lancet Neurology* 7.7. ISSN: 14744422. DOI: 10.1016/S1474-4422(08)70117-0.
- Heide, Wolfgang, Klaus Kurzidim and Detlef Kömpf (1996). 'Deficits of smooth pursuit eye movements after frontal and parietal lesions'. In: *Brain* 119.6. ISSN: 00068950. DOI: 10.1093/brain/119.6.1951.
- Heiman, Myriam et al. (2014). 'Molecular adaptations of striatal spiny projection neurons during levodopa-induced dyskinesia'. In: *Proceedings of the National Academy of Sciences of the United States of America* 111.12. ISSN: 10916490. DOI: 10.1073/pnas.1401819111.
- Helmchen, Christoph, Björn Machner et al. (2022). 'Bilateral lesion of the cerebellar fastigial nucleus: Effects on smooth pursuit acceleration and non-reflexive visually-guided saccades'. In: *Frontiers in Neurology* 13. ISSN: 16642295. DOI: 10.3389/fneur.2022.883213.
- Helmchen, Christoph, Jonas Pohlmann et al. (2012). 'Role of anticipation and prediction in smooth pursuit eye movement control in Parkinson's disease'. In: *Movement Disorders* 27.8. ISSN: 08853185. DOI: 10.1002/mds.25042.
- Helo, Andrea et al. (2014). 'The maturation of eye movement behavior: Scene viewing characteristics in children and adults'. In: *Vision Research* 103. ISSN: 18785646. DOI: 10.1016/j.visres.2014.08.006.
- Heo, Jun Young et al. (2020). 'Aberrant Tonic Inhibition of Dopaminergic Neuronal Activity Causes Motor Symptoms in Animal Models of Parkinson's Disease'. In: *Current Biology* 30.2. ISSN: 09609822. DOI: 10.1016/j.cub.2019.11.079.

- Hessels, Roy S. et al. (2020). *Wearable Technology for “Real-World Research”: Realistic or Not?* DOI: 10.1177/0301006620928324.
- Hikosaka, Okihide, Yoriko Takikawa and Reiko Kawagoe (2000). *Role of the basal ganglia in the control of purposive saccadic eye movements*. DOI: 10.1152/physrev.2000.80.3.953.
- Hinkley, Leighton B.N. et al. (2009). ‘Visual-manual exploration and posterior parietal cortex in humans’. In: *Journal of Neurophysiology* 102.6. ISSN: 00223077. DOI: 10.1152/jn.90785.2008.
- Hodgson, Timothy L. et al. (2013). ‘Learning and switching between stimulus-saccade associations in Parkinson’s disease’. In: *Neuropsychologia* 51.7. ISSN: 18733514. DOI: 10.1016/j.neuropsychologia.2013.03.026.
- Hoffman-Zacharska, Dorota et al. (2013). ‘Novel A18T and pA29S substitutions in α -synuclein may be associated with sporadic Parkinson’s disease’. In: *Parkinsonism and Related Disorders* 19.11. ISSN: 13538020. DOI: 10.1016/j.parkreldis.2013.07.011.
- Hoglinger, G et al. (2017). ‘Movement Disorder Society - Clinical Diagnostic Criteria for Progressive Supranuclear Palsy’. In: *Movement Disorders* 32.Supplement 2. ISSN: 1531-8257.
- Höglinger, Günter U. et al. (2017). ‘Clinical diagnosis of progressive supranuclear palsy: The movement disorder society criteria’. In: *Movement Disorders* 32.6. ISSN: 15318257. DOI: 10.1002/mds.26987.
- Holland, Peter J. et al. (2020). ‘A Neuroanatomically Grounded Optimal Control Model of the Compensatory Eye Movement System in Mice’. In: *Frontiers in Systems Neuroscience* 14. ISSN: 16625137. DOI: 10.3389/fnsys.2020.00013.
- Hong, Charles Chong Hwa et al. (2009). ‘fMRI evidence for multisensory recruitment associated with rapid eye movements during sleep’. In: *Human Brain Mapping* 30.5. ISSN: 10659471. DOI: 10.1002/hbm.20635.
- Hood, Ashley J. et al. (2007). ‘Levodopa slows prosaccades and improves antisaccades: An eye movement study in Parkinson’s disease’. In: *Journal of Neurology, Neurosurgery and Psychiatry* 78.6. ISSN: 00223050. DOI: 10.1136/jnnp.2006.099754.
- Hooge, Ignace T.C. et al. (2019). ‘Gaze tracking accuracy in humans: One eye is sometimes better than two’. In: *Behavior Research Methods* 51.6. ISSN: 15543528. DOI: 10.3758/s13428-018-1135-3.
- Huang, Jeff et al. (2020). ‘Altered Pupil Dynamics in Patients with Neurodegenerative Diseases (1641)’. In: *Neurology* 94.15_supplement. ISSN: 0028-3878. DOI: 10.1212/wnl.94.15{_}supplement.1641.

- Huang, Zehao et al. (2024). 'Assessing the data quality of AdHawk MindLink eye-tracking glasses'. In: *Behavior Research Methods* 56.6. ISSN: 15543528. DOI: 10.3758/s13428-023-02310-2.
- Hutton, S. B. (2019). 'Eye Tracking Methodology'. In: pp. 277–308. DOI: 10.1007/978-3-030-20085-5{_}8.
- Hwang, Juseon et al. (Jan. 2025). 'Machine learning for early detection and severity classification in people with Parkinson's disease'. In: *Scientific Reports* 15.1, p. 234. ISSN: 2045-2322. DOI: 10.1038/s41598-024-83975-3.
- Iacobelli, Emanuele et al. (2023). 'Eye-Tracking System with Low-End Hardware: Development and Evaluation'. In: *Information (Switzerland)* 14.12. ISSN: 20782489. DOI: 10.3390/info14120644.
- Iakovakis, Dimitrios et al. (2018). 'Touchscreen typing-pattern analysis for detecting fine motor skills decline in early-stage Parkinson's disease'. In: *Scientific Reports* 8.1. ISSN: 20452322. DOI: 10.1038/s41598-018-25999-0.
- Ilg, Uwe J. (1997). *Slow eye movements*. DOI: 10.1016/S0301-0082(97)00039-7.
- Inagaki, Keiichiro et al. (2020). 'Effect of fixational eye movement on signal processing of retinal photoreceptor: A computational study'. In: *IEICE Transactions on Information and Systems* E103D.7. ISSN: 17451361. DOI: 10.1587/TRANSINF.2019EDP7225.
- Inomata-Terada, Satomi et al. (2023). 'Abnormal saccade profiles in hereditary spinocerebellar degeneration reveal cerebellar contribution to visually guided saccades'. In: *Clinical Neurophysiology* 154. ISSN: 18728952. DOI: 10.1016/j.clinph.2023.07.006.
- Ipata, Anna E. et al. (2006). 'Activity in the lateral intraparietal area predicts the goal and latency of saccades in a free-viewing visual search task'. In: *Journal of Neuroscience* 26.14. ISSN: 02706474. DOI: 10.1523/JNEUROSCI.5074-05.2006.
- Isella, V. et al. (2018). 'Cognitive reserve maps the core loci of neurodegeneration in corticobasal degeneration'. In: *European Journal of Neurology* 25.11. ISSN: 14681331. DOI: 10.1111/ene.13729.
- Issa, Mohamed F. and Zoltan Juhasz (2019). 'Improved EOG artifact removal using wavelet enhanced independent component analysis'. In: *Brain Sciences* 9.12. ISSN: 20763425. DOI: 10.3390/brainsci9120355.
- Ivanchenko, Daria et al. (2021). 'A low-cost, high-performance video-based binocular eye tracker for psychophysical research'. In: *Journal of Eye Movement Research* 14.3. ISSN: 19958692. DOI: 10.16910/JEMR.14.3.3.

- Jacobs, R. J. (1979). 'Visual resolution and contour interaction in the fovea and periphery'. In: *Vision Research* 19.11. ISSN: 00426989. DOI: 10.1016/0042-6989(79)90183-4.
- Jankovic, J. (2008). *Parkinson's disease: Clinical features and diagnosis*. DOI: 10.1136/jnnp.2007.131045.
- Jensen, Kelsey, Sinem Balta Beylergil and Aasef G. Shaikh (2019). *Slow saccades in cerebellar disease*. DOI: 10.1186/s40673-018-0095-9.
- Jeon, Hyelynn and Sejong Oh (2020). 'Hybrid-recursive feature elimination for efficient feature selection'. In: *Applied Sciences (Switzerland)* 10.9. ISSN: 20763417. DOI: 10.3390/app10093211.
- Jeong, Ga Ram and Byoung Dae Lee (2020). *Pathological functions of lrrk2 in parkinson's disease*. DOI: 10.3390/cells9122565.
- Johansson, Fredrik, Germund Hesslow and Javier F. Medina (2016). *Mechanisms for motor timing in the cerebellar cortex*. DOI: 10.1016/j.cobeha.2016.01.013.
- Junaid, Sahalu Balarabe et al. (2022). *Recent Advancements in Emerging Technologies for Healthcare Management Systems: A Survey*. DOI: 10.3390/healthcare10101940.
- Jung, Ileok and Ji Soo Kim (2019). *Abnormal Eye Movements in Parkinsonism and Movement Disorders*. DOI: 10.14802/jmd.18034.
- Kadodwala, Viren H. et al. (2019). 'Is 1H-MR spectroscopy useful as a diagnostic aid in MSA-C?' In: *Cerebellum and Ataxias* 6.1. ISSN: 20538871. DOI: 10.1186/s40673-019-0099-0.
- Kakei, Shinji et al. (2019). 'Contribution of the cerebellum to predictive motor control and its evaluation in ataxic patients'. In: *Frontiers in Human Neuroscience* 13. ISSN: 16625161. DOI: 10.3389/fnhum.2019.00216.
- Kanai, R., J. N. Van Der Geest and M. A. Frens (2003). 'Inhibition of saccade initiation by preceding smooth pursuit'. In: *Experimental Brain Research* 148.3. ISSN: 00144819. DOI: 10.1007/s00221-002-1281-8.
- Kapoula, Zoi et al. (2010). 'Spread deficits in initiation, speed and accuracy of horizontal and vertical automatic saccades in dementia with Lewy bodies'. In: *Frontiers in Neurology* NOV. ISSN: 16642295. DOI: 10.3389/fneur.2010.00138.
- Karantinos, Thomas et al. (2014). 'Increased intra-subject reaction time variability in the volitional control of movement in schizophrenia'. In: *Psychiatry Research* 215.1. ISSN: 01651781. DOI: 10.1016/j.psychres.2013.10.031.
- Kasai, Takashi et al. (2016). 'Serum levels of coenzyme Q10 in patients with multiple system atrophy'. In: *PLoS ONE* 11.1. ISSN: 19326203. DOI: 10.1371/journal.pone.0147574.

- Kasneci, Enkelejda, Alex A. Black and Joanne M. Wood (2017). *Eye-Tracking as a Tool to Evaluate Functional Ability in Everyday Tasks in Glaucoma*. DOI: 10.1155/2017/6425913.
- Kato, Naoko, Kimihito Arai and Takamichi Hattori (2003). 'Study of the rostral midbrain atrophy in progressive supranuclear palsy'. In: *Journal of the Neurological Sciences* 210.1-2. ISSN: 0022510X. DOI: 10.1016/S0022-510X(03)00014-5.
- Kaufman, Liam D. et al. (2010). *Antisaccades: A probe into the dorsolateral prefrontal cortex in Alzheimer's disease. A critical review*. DOI: 10.3233/JAD-2010-1275.
- Keiflin, Ronald and Patricia H. Janak (2015). *Dopamine Prediction Errors in Reward Learning and Addiction: From Theory to Neural Circuitry*. DOI: 10.1016/j.neuron.2015.08.037.
- Khachatryan, Hayk and Alicia L. Rihn (2014). 'Eye-Tracking Methodology and Applications in Consumer Research'. In: *EDIS* 2014.7. DOI: 10.32473/edis-fe947-2014.
- Khaleel, Amal Hameed, Thekra H. Abbas and Abdul Wahab Sami Ibrahim (2024). 'Best low-cost methods for real-time detection of the eye and gaze tracking'. In: *i-com* 23.1. ISSN: 21966826. DOI: 10.1515/i-com-2023-0026.
- Khalifa, Mohamed and Mona Albadawy (2024). *AI in diagnostic imaging: Revolutionising accuracy and efficiency*. DOI: 10.1016/j.cmpbup.2024.100146.
- Khan, Aarlenne Z., Stephen J. Heinen and Robert M. McPeck (2010). 'Attentional cueing at the saccade goal, not at the target location, facilitates saccades'. In: *Journal of Neuroscience* 30.16. ISSN: 02706474. DOI: 10.1523/JNEUROSCI.4437-09.2010.
- Kheradmand, A., A. I. Colpak and D. S. Zee (2016). 'Eye movements in vestibular disorders'. In: *Handbook of Clinical Neurology*. Vol. 137. DOI: 10.1016/B978-0-444-63437-5.00008-X.
- Kheradmand, Amir and David S. Zee (2011). 'Cerebellum and ocular motor control'. In: *Frontiers in Neurology* SEP. ISSN: 16642295. DOI: 10.3389/fneur.2011.00053.
- Khosravi, Mohsen et al. (2024). *Artificial Intelligence and Decision-Making in Healthcare: A Thematic Analysis of a Systematic Review of Reviews*. DOI: 10.1177/23333928241234863.
- Kiani, Mohammad Mahdi, Mohammad Hossein Heidari Beni and Hamid Aghajan (2023). 'Aberrations in temporal dynamics of cognitive processing induced by Parkinson's disease and Levodopa'. In: *Scientific Reports* 13.1. ISSN: 20452322. DOI: 10.1038/s41598-023-47410-3.
- Kim, Jeongjin et al. (2017). 'Inhibitory Basal Ganglia Inputs Induce Excitatory Motor Signals in the Thalamus'. In: *Neuron* 95.5. ISSN: 10974199. DOI: 10.1016/j.neuron.2017.08.028.

- Kim, Soo Chan et al. (2006). 'A new method for accurate and fast measurement of 3D eye movements'. In: *Medical Engineering and Physics*. Vol. 28. 1 SPEC. ISS. DOI: 10.1016/j.medengphy.2005.04.002.
- Kim, Yun Soo, Jae Hyeok Lee and Jin Kyu Gahm (2022). 'Automated Differentiation of Atypical Parkinsonian Syndromes Using Brain Iron Patterns in Susceptibility Weighted Imaging'. In: *Diagnostics* 12.3. ISSN: 20754418. DOI: 10.3390/diagnostics12030637.
- Kirkby, J. A. et al. (2013). 'Investigating eye movement acquisition and analysis technologies as a causal factor in differential prevalence of crossed and uncrossed fixation disparity during reading and dot scanning'. In: *Behavior Research Methods* 45.3. ISSN: 1554351X. DOI: 10.3758/s13428-012-0301-2.
- Koga, Shunsuke et al. (2015). 'When DLB, PD, and PSP masquerade as MSA: an autopsy study of 134 patients.' In: *Neurology* 85.5. ISSN: 1526-632X.
- Kojima, Yoshiko, Daisuke Koketsu and Paul J. May (2023). 'Activity of the Substantia Nigra Pars Reticulata during Saccade Adaptation'. In: *eNeuro* 10.9. ISSN: 23732822. DOI: 10.1523/ENEURO.0092-23.2023.
- Kojima, Yoshiko, Robijanto Soetedjo and Albert F. Fuchs (2010). 'Behavior of the oculomotor vermis for five different types of saccade'. In: *Journal of Neurophysiology* 104.6. ISSN: 00223077. DOI: 10.1152/jn.00558.2010.
- (2011). 'Effect of inactivation and disinhibition of the oculomotor vermis on saccade adaptation'. In: *Brain Research* 1401. ISSN: 00068993. DOI: 10.1016/j.brainres.2011.05.027.
- Komogortsev, Oleg V. and Alex Karpov (2013). 'Automated classification and scoring of smooth pursuit eye movements in the presence of fixations and saccades'. In: *Behavior Research Methods* 45.1. ISSN: 1554351X. DOI: 10.3758/s13428-012-0234-9.
- Konen, Christina S. et al. (2005). 'An fMRI study of optokinetic nystagmus and smooth-pursuit eye movements in humans'. In: *Experimental Brain Research* 165.2. ISSN: 00144819. DOI: 10.1007/s00221-005-2289-7.
- König, Peter et al. (2016). 'Eye movements as a window to cognitive processes'. In: *Journal of Eye Movement Research* 9.5. ISSN: 19958692. DOI: 10.16910/jemr.9.5.3.
- Koochaki, Fatemeh and Laleh Najafizadeh (2021). 'A Data-Driven Framework for Intention Prediction via Eye Movement with Applications to Assistive Systems'. In: *IEEE Transactions on Neural Systems and Rehabilitation Engineering* 29. ISSN: 15580210. DOI: 10.1109/TNSRE.2021.3083815.
- Koohi, Nehzat et al. (2021). *Saccadic Bradykinesia in Parkinson's Disease: Preliminary Observations*. DOI: 10.1002/mds.28609.

- Kooiker, Marlou J.G. et al. (2016). 'A method to quantify visual information processing in children using eye tracking'. In: *Journal of Visualized Experiments* 2016.113. ISSN: 1940087X. DOI: 10.3791/54031.
- Kovacs, Gabor G. (2015). *Invited review: Neuropathology of tauopathies: Principles and practice*. DOI: 10.1111/nan.12208.
- Koziol, Leonard F. et al. (2014). *Consensus paper: The cerebellum's role in movement and cognition*. DOI: 10.1007/s12311-013-0511-x.
- Kraus, Marilyn F. et al. (2010). 'Procedural learning impairments identified via predictive saccades in chronic traumatic brain injury'. In: *Cognitive and Behavioral Neurology* 23.4. ISSN: 15433633. DOI: 10.1097/WNN.0b013e3181cefe2e.
- Krauzlis, Richard J. (2004). *Recasting the Smooth Pursuit Eye Movement System*. DOI: 10.1152/jn.00801.2003.
- Kredel, Ralf et al. (2023). *Eye-tracking technology and the dynamics of natural gaze behavior in sports: an update 2016–2022*. DOI: 10.3389/fpsyg.2023.1130051.
- Kripalani, Sunil et al. (2019). 'Use of a tablet computer application to engage patients in updating their medication list'. In: *American Journal of Health-System Pharmacy* 76.5. ISSN: 15352900. DOI: 10.1093/ajhp/zxy047.
- Kuang, Xutao et al. (2012). 'Temporal encoding of spatial information during active visual fixation'. In: *Current Biology* 22.6. ISSN: 09609822. DOI: 10.1016/j.cub.2012.01.050.
- Kumar, Arun N. et al. (2005). 'Evaluating large saccades in patients with brain-stem or cerebellar disorders'. In: *Annals of the New York Academy of Sciences*. Vol. 1039. DOI: 10.1196/annals.1325.038.
- Kumar, Arvind and Glenn Krol (1992). 'Binocular infrared oculography'. In: *Laryngoscope* 102.4. ISSN: 15314995. DOI: 10.1288/00005537-199204000-00002.
- Ladd, Mark E. et al. (2018). *Pros and cons of ultra-high-field MRI/MRS for human application*. DOI: 10.1016/j.pnmrs.2018.06.001.
- Lage, Carmen et al. (June 2024). 'Oculomotor Dysfunction in Idiopathic and *LRRK2* -Parkinson's Disease and At-Risk Individuals'. In: *Journal of Parkinson's Disease* 14.4, pp. 797–808. ISSN: 1877-7171. DOI: 10.3233/JPD-230416.
- Lahlou, Adnane et al. (2019). 'Accidental Modopar® Poisoning in a Two-Year-Old Child: A Case Report'. In: *Journal of Critical Care Medicine* 5.4. ISSN: 23931809. DOI: 10.2478/jccm-2019-0024.

- Lai, Joel Weijia et al. (2021). *Schizophrenia: A survey of artificial intelligence techniques applied to detection and classification*. DOI: 10.3390/ijerph18116099.
- Lal, Vivek and Daniel Truong (2019). *Eye movement abnormalities in movement disorders*. DOI: 10.1016/j.prdoa.2019.08.004.
- Lanciego, José L., Natasha Luquin and José A. Obeso (2012). 'Functional neuroanatomy of the basal ganglia'. In: *Cold Spring Harbor Perspectives in Medicine* 2.12. ISSN: 21571422. DOI: 10.1101/cshperspect.a009621.
- Landes, Reid D. et al. (2022). 'Levodopa ONOFF-state freezing of gait: Defining the gait and non-motor phenotype'. In: *PLoS ONE* 17.6 June. ISSN: 19326203. DOI: 10.1371/journal.pone.0269227.
- Lanfranchi, Silvia, Olga Jerman and Renzo Vianello (2009). 'Working memory and cognitive skills in individuals with down syndrome'. In: *Child Neuropsychology* 15.4. ISSN: 09297049. DOI: 10.1080/09297040902740652.
- Lang, A E and A M Lozano (1998). 'Parkinson's disease. First of two parts.' In: *The New England journal of medicine* 339.15. ISSN: 0028-4793. DOI: 10.1056/NEJM199810083391506.
- Larrazabal, A. J., C. E. García Cena and C. E. Martínez (2019). *Video-oculography eye tracking towards clinical applications: A review*. DOI: 10.1016/j.combiomed.2019.03.025.
- Larsen, Rylan S. and Jack Waters (2018). *Neuromodulatory correlates of pupil dilation*. DOI: 10.3389/fncir.2018.00021.
- Lawrence, Andrew D. (2000). *Error correction and the basal ganglia: Similar computations for action, cognition and emotion?* DOI: 10.1016/S1364-6613(00)01535-7.
- Lebedev, S., P. Van Gelder and Wai Hon Tsui (1996). 'Square-root relations between main saccadic parameters'. In: *Investigative Ophthalmology and Visual Science* 37.13. ISSN: 01460404.
- Lee, Dong Yun et al. (2023). 'Use of eye tracking to improve the identification of attention-deficit/hyperactivity disorder in children'. In: *Scientific Reports* 13.1. ISSN: 20452322. DOI: 10.1038/s41598-023-41654-9.
- Lee, Jee Young et al. (2009). 'Perverted head-shaking and positional downbeat nystagmus in patients with multiple system atrophy'. In: *Movement Disorders* 24.9. ISSN: 08853185. DOI: 10.1002/mds.22559.
- Lee, Yujeong et al. (2019). *Significant roles of neuroinflammation in Parkinson's disease: therapeutic targets for PD prevention*. DOI: 10.1007/s12272-019-01133-0.
- Leigh, R. John and David S. Zee (2015a). *The Neurology of Eye Movements*. DOI: 10.1093/med/9780199969289.001.0001.

- Leigh, R. John and David S. Zee (June 2015b). *The Neurology of Eye Movements*. Oxford University Press. ISBN: 9780199969289. DOI: 10.1093/med/9780199969289.001.0001.
- Leisman, Gerry, Orit Braun-Benjamin and Robert Melillo (2014). ‘Cognitive-motor interactions of the basal ganglia in development’. In: *Frontiers in Systems Neuroscience* 8.FEB. ISSN: 16625137. DOI: 10.3389/fnsys.2014.00016.
- Lemos, J. et al. (2017). ‘Cortical control of vertical and horizontal saccades in progressive supranuclear palsy: An exploratory fMRI study’. In: *Journal of the Neurological Sciences* 373. ISSN: 18785883. DOI: 10.1016/j.jns.2016.12.049.
- Lemos, João and Eric Eggenberger (2013). *Saccadic intrusions: Review and update*. DOI: 10.1097/WCO.0b013e32835c5e1d.
- Leng, Zimeng (2024). ‘Using data resampling and category weight adjustment to solve sample imbalance’. In: *Applied and Computational Engineering* 39.1. ISSN: 2755-2721. DOI: 10.54254/2755-2721/39/20230574.
- Lerner, Renata P. et al. (2017). ‘Levodopa-induced abnormal involuntary movements correlate with altered permeability of the blood-brain-barrier in the basal ganglia’. In: *Scientific Reports* 7.1. ISSN: 20452322. DOI: 10.1038/s41598-017-16228-1.
- Lewis, Mechelle M. et al. (2013). *The role of the cerebellum in the pathophysiology of Parkinson’s disease*. DOI: 10.1017/S0317167100014232.
- Li, Alex and Chenyu Li (2022). ‘Detecting Parkinson’s Disease through Gait Measures Using Machine Learning’. In: *Diagnostics* 12.10. ISSN: 20754418. DOI: 10.3390/diagnostics12102404.
- Li, Deming et al. (2024). ‘Automating the analysis of eye movement for different neurodegenerative disorders’. In: *Computers in Biology and Medicine* 170. ISSN: 18790534. DOI: 10.1016/j.combiomed.2024.107951.
- Li, Han et al. (2023). *Abnormal eye movements in Parkinson’s disease: From experimental study to clinical application*. DOI: 10.1016/j.parkreldis.2023.105791.
- Li, Hsin Hung and Clayton E. Curtis (2023). ‘Neural population dynamics of human working memory’. In: *Current Biology* 33.17. ISSN: 18790445. DOI: 10.1016/j.cub.2023.07.067.
- Li, Hyung Chul O. et al. (2002). ‘Systematic distortion of perceived 2D shape during smooth pursuit eye movements’. In: *Vision Research* 42.23. ISSN: 00426989. DOI: 10.1016/S0042-6989(02)00295-X.

- Li, Jing Shuang et al. (2023). 'Internal feedback in the cortical perception–action loop enables fast and accurate behavior'. In: *Proceedings of the National Academy of Sciences of the United States of America* 120.39. ISSN: 10916490. DOI: 10.1073/pnas.2300445120.
- Li, Xianting et al. (2010). 'Enhanced striatal dopamine transmission and motor performance with LRRK2 overexpression in mice is eliminated by familial Parkinson's disease mutation G2019S'. In: *Journal of Neuroscience* 30.5. ISSN: 02706474. DOI: 10.1523/JNEUROSCI.5604-09.2010.
- Liang, Yajie et al. (2008). 'Intrastriatal injection of colchicine induces striatonigral degeneration in mice'. In: *Journal of Neurochemistry* 106.4. ISSN: 00223042. DOI: 10.1111/j.1471-4159.2008.05526.x.
- Liao, Xianglian et al. (Jan. 2024). 'Deciphering Parkinson's Disease through Eye Movements: A Promising Tool for Early Diagnosis in the Face of Cognitive Impairment'. In: *International Journal of Clinical Practice* 2024.1. ISSN: 1368-5031. DOI: 10.1155/2024/5579238.
- Likitgorn, Techawit, Yan Yan and Yaping Joyce Liao (2021). 'Freezing of saccades in dopa-responsive parkinsonian syndrome'. In: *American Journal of Ophthalmology Case Reports* 23. ISSN: 24519936. DOI: 10.1016/j.ajoc.2021.101124.
- Liland, Kristian Hovde, Joakim Skogholt and Ulf Geir Indahl (2024). 'A New Formula for Faster Computation of the K-Fold Cross-Validation and Good Regularisation Parameter Values in Ridge Regression'. In: *IEEE Access* 12. ISSN: 21693536. DOI: 10.1109/ACCESS.2024.3357097.
- Limphaibool, Nattakarn et al. (2019). *Infectious etiologies of Parkinsonism: Pathomechanisms and clinical implications*. DOI: 10.3389/fneur.2019.00652.
- Linder, Jan et al. (2012). 'Impaired oculomotor function in a community-based patient population with newly diagnosed idiopathic parkinsonism'. In: *Journal of Neurology* 259.6. ISSN: 03405354. DOI: 10.1007/s00415-011-6338-9.
- Ling, H. et al. (2014). 'Characteristics of progressive supranuclear palsy presenting with corticobasal syndrome: A cortical variant'. In: *Neuropathology and Applied Neurobiology* 40.2. ISSN: 03051846. DOI: 10.1111/nan.12037.
- Ling, Xia et al. (2023). 'Loss of torsional quick eye movements during head roll in progressive supranuclear palsy: a new diagnostic marker'. In: *Journal of Neurology* 270.4. ISSN: 14321459. DOI: 10.1007/s00415-023-11578-5.
- Liu, Ganqiang et al. (2016). 'Specifically neuropathic Gaucher's mutations accelerate cognitive decline in Parkinson's'. In: *Annals of Neurology* 80.5. ISSN: 15318249. DOI: 10.1002/ana.24781.

- Liu, Yaping et al. (2021). 'Longitudinal Changes in Parkinson's Disease Symptoms with and Without Rapid Eye Movement Sleep Behavior Disorder: The Oxford Discovery Cohort Study'. In: *Movement Disorders* 36.12. ISSN: 15318257. DOI: 10.1002/mds.28763.
- Liversedge, Simon P., Iain D. Gilchrist and Stefan Everling (2012). *The Oxford Handbook of Eye Movements*. DOI: 10.1093/oxfordhb/9780199539789.001.0001.
- Low, Phillip A. et al. (2015). 'Natural history of multiple system atrophy in the USA: A prospective cohort study'. In: *The Lancet Neurology* 14.7. ISSN: 14744465. DOI: 10.1016/S1474-4422(15)00058-7.
- Luft, Andreas R. and Stefanie Schwarz (Aug. 2009). 'Dopaminergic signals in primary motor cortex'. In: *International Journal of Developmental Neuroscience* 27.5, pp. 415–421. ISSN: 0736-5748. DOI: 10.1016/j.ijdevneu.2009.05.004.
- Lundberg, Scott (2019). *SHAP (SHapley Additive exPlanations)*.
- Ma, Hengbo et al. (2017). 'Support Vector Machine-recursive feature elimination for the diagnosis of Parkinson disease based on speech analysis'. In: *7th International Conference on Intelligent Control and Information Processing, ICICIP 2016 - Proceedings*. DOI: 10.1109/ICICIP.2016.7885912.
- Ma, Wenbo et al. (2022). 'Multiple step saccades in simply reactive saccades could serve as a complementary biomarker for the early diagnosis of Parkinson's disease'. In: *Frontiers in Aging Neuroscience* 14. ISSN: 16634365. DOI: 10.3389/fnagi.2022.912967.
- MacAskill, Michael R. and Tim J. Anderson (2016). *Eye movements in neurodegenerative diseases*. DOI: 10.1097/WCD.0000000000000274.
- MacAskill, Michael R., Tim J. Anderson and Richard D. Jones (2002). 'Saccadic adaptation in neurological disorders'. In: *Progress in Brain Research*. Vol. 140. DOI: 10.1016/S0079-6123(02)40066-0.
- MacAskill, Michael R., Charlotte F. Graham et al. (2012). 'The influence of motor and cognitive impairment upon visually-guided saccades in Parkinson's disease'. In: *Neuropsychologia* 50.14. ISSN: 00283932. DOI: 10.1016/j.neuropsychologia.2012.09.025.
- MacLean, Gregory H., Raymond M. Klein and Matthew D. Hilchey (2015). 'Does oculomotor readiness mediate exogenous capture of visual attention?' In: *Journal of Experimental Psychology: Human Perception and Performance* 41.5. ISSN: 19391277. DOI: 10.1037/xhp0000064.
- Madetko-Alster, Natalia et al. (2024). 'Glucose Metabolism and Cognitive Decline in Progressive Supranuclear Palsy and Corticobasal Syndrome: A Preliminary Study'. In: *Journal of Clinical Medicine* 13.2. ISSN: 20770383. DOI: 10.3390/jcm13020465.

- Mandler, Markus et al. (2015). 'Active immunization against alpha-synuclein ameliorates the degenerative pathology and prevents demyelination in a model of multiple system atrophy'. In: *Molecular Neurodegeneration* 10.1. ISSN: 17501326. DOI: 10.1186/s13024-015-0008-9.
- Manto, Mario et al. (2012). 'Consensus paper: Roles of the cerebellum in motor control-the diversity of ideas on cerebellar involvement in movement'. In: *Cerebellum*. Vol. 11. 2. DOI: 10.1007/s12311-011-0331-9.
- Mantokoudis, Georgios, Jorge Otero-Millan and Daniel R. Gold (2022). *Current concepts in acute vestibular syndrome and video-oculography*. DOI: 10.1097/WCO.0000000000001017.
- Marandi, Ramtin Z. and Parisa Gazerani (2019). *Aging and eye tracking: In the quest for objective biomarkers*. DOI: 10.2217/fnl-2019-0012.
- Martinez-Conde, Susana and Stephen L. Macknik (2008). *Fixational eye movements across vertebrates: Comparative dynamics, physiology, and perception*. DOI: 10.1167/8.14.28.
- Martinez-Conde, Susana, Stephen L. Macknik and David H. Hubel (2004). *The role of fixational eye movements in visual perception*. DOI: 10.1038/nrn1348.
- Martinez-Conde, Susana, Stephen L. Macknik, Xoana G. Troncoso et al. (2006). 'Microsaccades counteract visual fading during fixation'. In: *Neuron* 49.2. ISSN: 08966273. DOI: 10.1016/j.neuron.2005.11.033.
- Martinez-Conde, Susana, Jorge Otero-Millan and Stephen L. MacKnik (2013). *The impact of microsaccades on vision: Towards a unified theory of saccadic function*. DOI: 10.1038/nrn3405.
- Martinez-Martin, Pablo et al. (2018). *Validation study of the hoehn and yahr scale included in the MDS-UPDRS*. DOI: 10.1002/mds.27242.
- Masselink, Jana and Markus Lappe (2021). 'Visuomotor learning from postdictive motor error'. In: *eLife* 10. ISSN: 2050084X. DOI: 10.7554/eLife.64278.
- Massey, Luke A. et al. (2013). 'The midbrain to pons ratio'. In: *Neurology* 80.20. ISSN: 0028-3878. DOI: 10.1212/wnl.0b013e318292a2d2.
- Matsumoto, Hideyuki et al. (2012). 'Basal ganglia dysfunction reduces saccade amplitude during visual scanning in Parkinson's disease'. In: *Basal Ganglia* 2.2. ISSN: 22105336. DOI: 10.1016/j.baga.2012.01.005.
- Mayà, Gerard et al. (Dec. 2024). 'Post-mortem neuropathology of idiopathic rapid eye movement sleep behaviour disorder: a case series'. In: *The Lancet Neurology* 23.12, pp. 1238–1251. ISSN: 14744422. DOI: 10.1016/S1474-4422(24)00402-2.

- McCamy, Michael B., Jorge Otero-Millan, Leandro Luigi Di Stasi et al. (2014). 'Highly informative natural scene regions increase microsaccade production during visual scanning'. In: *Journal of Neuroscience* 34.8. ISSN: 02706474. DOI: 10.1523/JNEUROSCI.4448-13.2014.
- McCamy, Michael B., Jorge Otero-Millan, Stephen L. Macknik et al. (2012). 'Microsaccadic efficacy and contribution to foveal and peripheral vision'. In: *Journal of Neuroscience* 32.27. ISSN: 02706474. DOI: 10.1523/JNEUROSCI.0515-12.2012.
- McDowell, Jennifer E., Brett A. Clementz and John A. Sweeney (2012). 'Eye movements in psychiatric patients'. In: *The Oxford Handbook of Eye Movements*. DOI: 10.1093/oxfordhb/9780199539789.013.0038.
- McDowell, Jennifer E., Kara A. Dyckman et al. (2008). 'Neurophysiology and neuroanatomy of reflexive and volitional saccades: Evidence from studies of humans'. In: *Brain and Cognition* 68.3. ISSN: 02782626. DOI: 10.1016/j.bandc.2008.08.016.
- Mcfarland, Nikolaus R. (2016). *Diagnostic Approach to Atypical Parkinsonian Syndromes*. DOI: 10.1212/CON.0000000000000348.
- McGregor, Matthew M. and Alexandra B. Nelson (2019). *Circuit Mechanisms of Parkinson's Disease*. DOI: 10.1016/j.neuron.2019.03.004.
- McNeill, Alisdair et al. (2014). 'Ambroxol improves lysosomal biochemistry in glucocerebrosidase mutation-linked Parkinson disease cells'. In: *Brain* 137.5. ISSN: 14602156. DOI: 10.1093/brain/awu020.
- Meeter, Martijn, Stefan Van Der Stigchel and Jan Theeuwes (2010). 'A competitive integration model of exogenous and endogenous eye movements'. In: *Biological Cybernetics* 102.4. ISSN: 03401200. DOI: 10.1007/s00422-010-0365-y.
- Mei, Jie, Christian Desrosiers and Johannes Frasnelli (2021). *Machine Learning for the Diagnosis of Parkinson's Disease: A Review of Literature*. DOI: 10.3389/fnagi.2021.633752.
- Mendez, Alicia Viviana et al. (2024). 'PROGRESSIVE SUPRANUCLEAR PALSY AND DEMENTIA – LITERATURE REVIEW'. In: *International Journal of Health Science* 4.8. DOI: 10.22533/at.ed.159482417018.
- Meng, Meng et al. (2023). 'Characteristics of Anal Sphincter Electromyography in Patients with Multiple System Atrophy'. In: *BIO Web of Conferences*. Vol. 60. DOI: 10.1051/bioconf/20236002019.
- Merriam, Elisha P., Christopher R. Genovese and Carol L. Colby (2003). 'Spatial updating in human parietal cortex'. In: *Neuron* 39.2. ISSN: 08966273. DOI: 10.1016/S0896-6273(03)00393-3.

- Métais, Camille et al. (2022). 'Neural substrates of saccadic adaptation: Plastic changes versus error processing and forward versus backward learning'. In: *NeuroImage* 262. ISSN: 10959572. DOI: 10.1016/j.neuroimage.2022.119556.
- Micieli, Giuseppe et al. (1991). 'Disordered pupil reactivity in Parkinson's disease'. In: *Clinical Autonomic Research* 1.1. ISSN: 09599851. DOI: 10.1007/BF01826058.
- Miki, Yasuo et al. (2022). 'Pathological substrate of memory impairment in multiple system atrophy'. In: *Neuropathology and Applied Neurobiology* 48.7. ISSN: 13652990. DOI: 10.1111/nan.12844.
- Milstein, David M. and Michael C. Dorris (2011). 'The relationship between saccadic choice and reaction times with manipulations of target value'. In: *Frontiers in Neuroscience* OCT. ISSN: 16624548. DOI: 10.3389/fnins.2011.00122.
- Mitoma, H. et al. (2020). 'Consensus Paper. Cerebellar Reserve: From Cerebellar Physiology to Cerebellar Disorders'. In: *Cerebellum* 19.1. ISSN: 14734230. DOI: 10.1007/s12311-019-01091-9.
- Miura, Kenichiro et al. (2019). 'Model of optokinetic responses involving two different visual motion processing pathways'. In: *Progress in Brain Research*. Vol. 248. DOI: 10.1016/bs.pbr.2019.02.005.
- Miyasaki, Janis M. (2010). 'Evidence-based initiation of dopaminergic therapy in Parkinson's disease'. In: *Journal of Neurology*. Vol. 257. SUPPL. 2. DOI: 10.1007/s00415-010-5718-x.
- Molloy, S. A. et al. (2006). 'Effect of levodopa on cognitive function in Parkinson's disease with and without dementia and dementia with Lewy bodies'. In: *Journal of Neurology, Neurosurgery and Psychiatry* 77.12. ISSN: 00223050. DOI: 10.1136/jnnp.2006.098079.
- Moran, Eileen E. et al. (2021). 'Cognitive Functioning of Glucocerebrosidase (GBA) Non-manifesting Carriers'. In: *Frontiers in Neurology* 12. ISSN: 16642295. DOI: 10.3389/fneur.2021.635958.
- Morawski, Markus et al. (2010). 'Distinct glutaminy cyclase expression in Edinger-Westphal nucleus, locus coeruleus and nucleus basalis Meynert contributes to pGlu-A β pathology in Alzheimer's disease'. In: *Acta Neuropathologica* 120.2. ISSN: 00016322. DOI: 10.1007/s00401-010-0685-y.
- Morgante, James D., Rahman Zolfaghari and Scott P. Johnson (2012). 'A critical test of temporal and spatial accuracy of the Tobii T60XL eye tracker'. In: *Infancy* 17.1. ISSN: 15250008. DOI: 10.1111/j.1532-7078.2011.00089.x.
- Moschner, C. and R. W. Baloh (1994). 'Age-related changes in visual tracking'. In: *Journals of Gerontology* 49.5. ISSN: 00221422. DOI: 10.1093/geronj/49.5.M235.

- Mosimann, Urs P. et al. (2005). 'Saccadic eye movement changes in Parkinson's disease dementia and dementia with Lewy bodies'. In: *Brain* 128.6. ISSN: 00068950. DOI: 10.1093/brain/awh484.
- Muddasar Abbas et al. (2022). 'Skin Diseases Diagnosis System Based on Machine Learning'. In: *Journal of Computing & Biomedical Informatics* 4.01. ISSN: 2710-1606. DOI: 10.56979/401/2022/53.
- Munoz, Douglas P. and Stefan Everling (2004). *Look away: The anti-saccade task and the voluntary control of eye movement*. DOI: 10.1038/nrn1345.
- Munoz, Miranda J., Rishabh Arora et al. (2023). 'Medication only improves limb movements while deep brain stimulation improves eye and limb movements during visually-guided reaching in Parkinson's disease'. In: *Frontiers in Human Neuroscience* 17. ISSN: 16625161. DOI: 10.3389/fnhum.2023.1224611.
- Munoz, Miranda J., James L. Reilly et al. (2022). 'Medication adversely impacts visually-guided eye movements in Parkinson's disease'. In: *Clinical Neurophysiology* 143. ISSN: 18728952. DOI: 10.1016/j.clinph.2022.07.505.
- Müri, René M. and Thomas Nyffeler (2008). 'Neurophysiology and neuroanatomy of reflexive and volitional saccades as revealed by lesion studies with neurological patients and transcranial magnetic stimulation (TMS)'. In: *Brain and Cognition* 68.3. ISSN: 02782626. DOI: 10.1016/j.bandc.2008.08.018.
- Murray, Nicholas P., Melissa Hunfalvay and Takumi Bolte (2017). 'The Reliability, Validity, and Normative Data of Interpupillary Distance and Pupil Diameter Using Eye-Tracking Technology'. In: *Translational Vision Science & Technology* 6.4. ISSN: 2164-2591. DOI: 10.1167/tvst.6.4.2.
- Mustari, Michael J. and Seiji Ono (2011). 'Neural mechanisms for smooth pursuit in strabismus'. In: *Annals of the New York Academy of Sciences* 1233.1. ISSN: 17496632. DOI: 10.1111/j.1749-6632.2011.06117.x.
- Nakashima, Hanae et al. (2003). 'An autopsied case of dementia with Lewy bodies with supranuclear gaze palsy'. In: *Neurological Research* 25.5. ISSN: 01616412. DOI: 10.1179/016164103101201788.
- Nambu, Atsushi et al. (2023). 'Dynamic Activity Model of Movement Disorders: The Fundamental Role of the Hyperdirect Pathway'. In: *Movement Disorders* 38.12. ISSN: 15318257. DOI: 10.1002/mds.29646.
- Narcizo, Fabricio Batista, José Eustáquio Rangel De Queiroz and Herman Martins Gomes (2014). 'Remote eye tracking systems: Technologies and applications'. In: *Proceedings - 26th SIBGRAPI - Conference on Graphics, Patterns and Images Tutoriais, SIBGRAPI-T 2013*. DOI: 10.1109/SIBGRAPI-T.2013.8.
- Narendra, Derek P. et al. (2010). 'PINK1 is selectively stabilized on impaired mitochondria to activate Parkin'. In: *PLoS Biology* 8.1. ISSN: 15449173. DOI: 10.1371/journal.pbio.1000298.

- Nasteski, Vladimir (2017). 'An overview of the supervised machine learning methods'. In: *HORIZONS.B* 4. ISSN: 18578578. DOI: 10.20544/horizons.b.04.1.17.p05.
- Navita et al. (Jan. 2025). 'Gait-based Parkinson's disease diagnosis and severity classification using force sensors and machine learning'. In: *Scientific Reports* 15.1, p. 328. ISSN: 2045-2322. DOI: 10.1038/s41598-024-83357-9.
- Neggers, S. F.W. et al. (2005). 'Cortical and subcortical contributions to saccade latency in the human brain'. In: *European Journal of Neuroscience* 21.10. ISSN: 0953816X. DOI: 10.1111/j.1460-9568.2005.04129.x.
- Neto, Osmar Pinto (2023). 'Harnessing Voice Analysis and Machine Learning for Early Diagnosis of Parkinson's Disease: A Comprehensive Study Across Diverse Datasets'. In: *SSRN Electronic Journal*. DOI: 10.2139/ssrn.4617895.
- Neumann, Wolf Julian et al. (2018). 'Functional segregation of basal ganglia pathways in Parkinson's disease'. In: *Brain* 141.9. ISSN: 14602156. DOI: 10.1093/brain/awy206.
- Newman, Jacob L., John S. Phillips and Stephen J. Cox (2022). 'Reconstructing animated eye movements from electrooculography data to aid the diagnosis of vestibular disorders'. In: *International Journal of Audiology* 61.1. ISSN: 17088186. DOI: 10.1080/14992027.2021.1883196.
- Newsome, W. T., R. H. Wurtz and H. Komatsu (1988). 'Relation of cortical areas MT and MST to pursuit eye movements. II. Differentiation of retinal from extraretinal inputs'. In: *Journal of Neurophysiology* 60.2. ISSN: 00223077. DOI: 10.1152/jn.1988.60.2.604.
- Ngiam, Kee Yuan and Ing Wei Khor (2019). *Big data and machine learning algorithms for health-care delivery*. DOI: 10.1016/S1470-2045(19)30149-4.
- Nieboer, Ward et al. (2023). *Eye Tracking to Assess the Functional Consequences of Vision Impairment: A Systematic Review*. DOI: 10.1097/OPX.0000000000002088.
- Niehorster, Diederick C., Richard Andersson and Marcus Nyström (2020). 'Titta: A toolbox for creating PsychToolbox and Psychopy experiments with Tobii eye trackers'. In: *Behavior Research Methods* 52.5. ISSN: 15543528. DOI: 10.3758/s13428-020-01358-8.
- Niehorster, Diederick C., Thiago Santini et al. (2020). 'The impact of slippage on the data quality of head-worn eye trackers'. In: *Behavior Research Methods* 52.3. ISSN: 15543528. DOI: 10.3758/s13428-019-01307-0.

- Nimmo, Jacqui T. et al. (2020). 'Novel antibodies detect additional α -synuclein pathology in synucleinopathies: potential development for immunotherapy'. In: *Alzheimer's Research and Therapy* 12.1. ISSN: 17589193. DOI: 10.1186/s13195-020-00727-x.
- Nissar, Iqra et al. (2019). 'Voice-based detection of parkinson's disease through ensemble machine learning approach: A performance study'. In: *EAI Endorsed Transactions on Pervasive Health and Technology* 5.19. ISSN: 24117145. DOI: 10.4108/eai.13-7-2018.162806.
- Nitschke, Matthias F. et al. (2004). 'Activation of cerebellar hemispheres in spatial memorization of saccadic eye movements: An fMRI study'. In: *Human Brain Mapping* 22.2. ISSN: 10659471. DOI: 10.1002/hbm.20025.
- Noack, Eva Maria et al. (2023). 'Evaluating an app for digital medical history taking in urgent care practices: study protocol of the cluster-randomized interventional trial 'DASI''. In: *BMC Primary Care* 24.1. ISSN: 27314553. DOI: 10.1186/s12875-023-02065-x.
- Novák, Jakub Štěpán et al. (2024). 'Eye Tracking, Usability, and User Experience: A Systematic Review'. In: *International Journal of Human-Computer Interaction* 40.17. ISSN: 15327590. DOI: 10.1080/10447318.2023.2221600.
- Nussbaum, Robert L. (2017). *The Identification of Alpha-Synuclein as the First Parkinson Disease Gene*. DOI: 10.3233/JPD-179003.
- O'Driscoll, Gillian A. et al. (2000). 'Functional neuroanatomy of smooth pursuit and predictive saccades'. In: *NeuroReport* 11.6. ISSN: 09594965. DOI: 10.1097/00001756-200004270-00037.
- O'Regan, Grace et al. (2017). *Glucocerebrosidase Mutations in Parkinson Disease*. DOI: 10.3233/JPD-171092.
- O'Sullivan, John D. et al. (2003). 'Unilateral pallidotomy for Parkinson's disease disrupts ocular fixation'. In: *Journal of Clinical Neuroscience* 10.2. ISSN: 09675868. DOI: 10.1016/S0967-5868(02)00125-X.
- Oh, Seokjun and Jong-Ha Lee (July 2024). 'The Development of an Alzheimer's Diagnostic Sensor and Algorithm using Microsaccades Biomarkers'. In: *2024 46th Annual International Conference of the IEEE Engineering in Medicine and Biology Society (EMBC)*. IEEE, pp. 1–4. ISBN: 979-8-3503-7149-9. DOI: 10.1109/EMBC53108.2024.10781816.
- Okkels, Niels et al. (2024). *Cholinergic changes in Lewy body disease: implications for presentation, progression and subtypes*. DOI: 10.1093/brain/awae069.

- Olanow, C. Warren, José A. Obeso and Fabrizio Stocchi (2006). *Drug insight: Continuous dopaminergic stimulation in the treatment of Parkinson's disease*. DOI: 10.1038/ncpneuro0222.
- Onkhar, V., D. Dodou and J. C.F. de Winter (2024). 'Evaluating the Tobii Pro Glasses 2 and 3 in static and dynamic conditions'. In: *Behavior Research Methods* 56.5. ISSN: 15543528. DOI: 10.3758/s13428-023-02173-7.
- Optican, Lance M. and David S. Zee (1984). 'A hypothetical explanation of congenital nystagmus'. In: *Biological Cybernetics* 50.2. ISSN: 03401200. DOI: 10.1007/BF00337159.
- Orcioli-Silva, Diego et al. (2020). 'Levodopa Facilitates Prefrontal Cortex Activation During Dual Task Walking in Parkinson Disease'. In: *Neurorehabilitation and Neural Repair* 34.7. ISSN: 15526844. DOI: 10.1177/1545968320924430.
- Ortiz, Juan Fernando et al. (2020). 'Multiple System Atrophy – Cerebellar Type: Clinical Picture and Treatment of an Often-Overlooked Disorder'. In: *Cureus*. DOI: 10.7759/cureus.10741.
- Otero-Millan, Jorge, Stephen L. Macknik, Rachel E. Langston et al. (2013). 'An oculomotor continuum from exploration to fixation'. In: *Proceedings of the National Academy of Sciences of the United States of America* 110.15. ISSN: 00278424. DOI: 10.1073/pnas.1222715110.
- Otero-Millan, Jorge, Stephen L. Macknik, Alessandro Serra et al. (2011). 'Triggering mechanisms in microsaccades and saccade generation: A novel proposal'. In: *Annals of the New York Academy of Sciences* 1233.1. ISSN: 17496632. DOI: 10.1111/j.1749-6632.2011.06177.x.
- Otero-Millan, Jorge, Rosalyn Schneider et al. (2013). 'Saccades during Attempted Fixation in Parkinsonian Disorders and Recessive Ataxia: From Microsaccades to Square-Wave Jerks'. In: *PLoS ONE* 8.3. ISSN: 19326203. DOI: 10.1371/journal.pone.0058535.
- Otero-Millan, Jorge, Alessandro Serra et al. (2011). 'Distinctive features of saccadic intrusions and microsaccades in progressive supranuclear palsy'. In: *Journal of Neuroscience* 31.12. ISSN: 02706474. DOI: 10.1523/JNEUROSCI.2600-10.2011.
- Palermo, Giovanni et al. (2022). *Early Compensatory Mechanisms in LRRK2 Mutation Carriers*. DOI: 10.1002/mds.28908.
- Pallus, Adam C., Mark M.G. Walton and Michael J. Mustari (2018). 'Response of supraoculomotor area neurons during combined saccade-vergence movements'. In: *Journal of Neurophysiology* 119.2. ISSN: 15221598. DOI: 10.1152/jn.00193.2017.

- Pang, Shirley Yin Yu et al. (2019). *The interplay of aging, genetics and environmental factors in the pathogenesis of Parkinson's disease*. DOI: 10.1186/s40035-019-0165-9.
- Panouillères, Muriel, Sebastiaan F.W. Neggers et al. (2012). 'Transcranial magnetic stimulation and motor plasticity in human lateral cerebellum: Dual effect on saccadic adaptation'. In: *Human Brain Mapping* 33.7. ISSN: 10659471. DOI: 10.1002/hbm.21301.
- Panouillères, Muriel, Christian Urquizar et al. (2011). 'Sensory processing of motor inaccuracy depends on previously performed movement and on subsequent motor corrections: A study of the saccadic system'. In: *PLoS ONE* 6.2. ISSN: 19326203. DOI: 10.1371/journal.pone.0017329.
- Pansell, T. et al. (2011). 'Slow oscillatory eye movement during visual fixation'. In: *Experimental Brain Research* 209.1. ISSN: 00144819. DOI: 10.1007/s00221-010-2457-2.
- Parmera, Jacy Bezerra et al. (2016). 'Corticobasal syndrome: A diagnostic conundrum'. In: *Dementia & Neuropsychologia* 10.4. DOI: 10.1590/s1980-5764-2016dn1004003.
- Pattadkal, Jagruti J., Carrie Barr and Nicholas J. Priebe (2024). 'Interactions between Saccades and Smooth Pursuit Eye Movements in Marmosets'. In: *eNeuro* 11.6. ISSN: 23732822. DOI: 10.1523/ENEURO.0027-24.2024.
- Paus, Tomáš (1996). *Location and function of the human frontal eye-field: A selective review*. DOI: 10.1016/0028-3932(95)00134-4.
- Pauszek, Joseph R. (2023). 'An introduction to eye tracking in human factors healthcare research and medical device testing'. In: *Human Factors in Healthcare* 3. ISSN: 27725014. DOI: 10.1016/j.hfh.2022.100031.
- Pentus, Kristian et al. (2020). 'Mobile and stationary eye tracking comparison – package design and in-store results'. In: *Journal of Consumer Marketing* 37.3. ISSN: 07363761. DOI: 10.1108/JCM-04-2019-3190.
- Pereira, Clayton R. et al. (2017). 'Deep learning-aided Parkinson's disease diagnosis from handwritten dynamics'. In: *Proceedings - 2016 29th SIBGRAPI Conference on Graphics, Patterns and Images, SIBGRAPI 2016*. DOI: 10.1109/SIBGRAPI.2016.054.
- Petit, Laurent and James V. Haxby (1999). 'Functional anatomy of pursuit eye movements in humans as revealed by fMRI'. In: *Journal of Neurophysiology* 82.1. ISSN: 00223077. DOI: 10.1152/jn.1999.82.1.463.
- Pierrot-Deseilligny, C., R. M. Müri, C. J. Ploner, B. Gaymard, S. Demeret et al. (2003). 'Decisional role of the dorsolateral prefrontal cortex in ocular motor behaviour'. In: *Brain* 126.6. ISSN: 00068950. DOI: 10.1093/brain/awg148.

- Pierrot-Deseilligny, C., R. M. Müri, C. J. Ploner, B. Gaymard and S. Rivaud-Péchoux (2003). 'Cortical control of ocular saccades in humans: A model for motricity'. In: *Progress in Brain Research*. Vol. 142. DOI: 10.1016/S0079-6123(03)42003-7.
- Pierrot-Deseilligny, C., S. Rivaud et al. (1991). 'Cortical control of memory-guided saccades in man'. In: *Experimental Brain Research* 83.3. ISSN: 00144819. DOI: 10.1007/BF00229839.
- Pin, G. et al. (2023). 'Brain FDG-PET correlates of saccadic disorders in early PSP'. In: *Journal of Neurology* 270.10. ISSN: 14321459. DOI: 10.1007/s00415-023-11824-w.
- Pinkhardt, Elmar H., Reinhart Jürgens et al. (2012). 'Eye movement impairments in Parkinson's disease: Possible role of extradopaminergic mechanisms'. In: *BMC Neurology* 12. ISSN: 14712377. DOI: 10.1186/1471-2377-12-5.
- Pinkhardt, Elmar H., Jan Kassubek et al. (2009). 'Comparison of smooth pursuit eye movement deficits in multiple system atrophy and Parkinson's disease'. In: *Journal of Neurology* 256.9. ISSN: 03405354. DOI: 10.1007/s00415-009-5131-5.
- Pinto-Coelho, Luís (2023). *How Artificial Intelligence Is Shaping Medical Imaging Technology: A Survey of Innovations and Applications*. DOI: 10.3390/bioengineering10121435.
- Plużyczka, Monika (Dec. 2018). 'The First Hundred Years: a History of Eye Tracking as a Research Method'. In: *Applied Linguistics Papers* 4/2018.25, pp. 101–116. ISSN: 25449354. DOI: 10.32612/uw.25449354. 2018.4. pp. 101–116.
- Poewe, Werner (2009). 'Clinical measures of progression in Parkinson's disease'. In: *Movement Disorders* 24.SUPPL. 2. ISSN: 08853185. DOI: 10.1002/mds.22600.
- Pouget, P. (2015). 'The cortex is in overall control of 'voluntary' eye movement'. In: *Eye (Basingstoke)*. Vol. 29. 2. DOI: 10.1038/eye.2014.284.
- Pozzo, T., A. Berthoz and L. Lefort (1990). 'Head stabilization during various locomotor tasks in humans - I. Normal subjects'. In: *Experimental Brain Research* 82.1. ISSN: 00144819. DOI: 10.1007/BF00230842.
- Prasuhn, Jannik et al. (2022). 'Assessment of Bioenergetic Deficits in Patients With Parkinson Disease and Progressive Supranuclear Palsy Using 31P-MRSI'. In: *Neurology* 99.24. ISSN: 1526632X. DOI: 10.1212/WNL.0000000000201288.
- Pretegitani, Elena and Lance M. Optican (2017). *Eye movements in Parkinson's disease and inherited parkinsonian syndromes*. DOI: 10.3389/fneur.2017.00592.

- Przewodowska, Dominika, Weronika Marzec and Natalia Madetko (2021). *Novel Therapies for Parkinsonian Syndromes—Recent Progress and Future Perspectives*. DOI: 10.3389/fnmol.2021.720220.
- Przybyszewski, Andrzej W. et al. (2023). *Machine Learning and Eye Movements Give Insights into Neurodegenerative Disease Mechanisms*. DOI: 10.3390/s23042145.
- Quessy, Stephan, Julie Quinet and Edward G. Freedman (2010). ‘The locus of motor activity in the superior colliculus of the rhesus monkey is unaltered during saccadic adaptation’. In: *Journal of Neuroscience* 30.42. ISSN: 02706474. DOI: 10.1523/JNEUROSCI.3111-10.2010.
- Quinet, Julie et al. (2020). ‘Neural control of rapid binocular eye movements: Saccade-vergence burst neurons’. In: *Proceedings of the National Academy of Sciences of the United States of America* 117.46. ISSN: 10916490. DOI: 10.1073/pnas.2015318117.
- Quinn, N. and R. J. Leigh (1996). *The ‘round the houses’ sign in progressive supranuclear palsy [5]*. DOI: 10.1002/ana.410400630.
- Rafal, Robert D. et al. (1984). ‘Cognition and the basal ganglia: Separating mental and motor components of performance in parkinson’s disease’. In: *Brain* 107.4. ISSN: 00068950. DOI: 10.1093/brain/107.4.1083.
- Raffi, Milena et al. (2021). ‘Sensory input modulates microsaccades during heading perception’. In: *International Journal of Environmental Research and Public Health* 18.6. ISSN: 16604601. DOI: 10.3390/ijerph18062865.
- Rainio, Oona, Jarmo Teuho and Riku Klén (2024). ‘Evaluation metrics and statistical tests for machine learning’. In: *Scientific Reports* 14.1. ISSN: 20452322. DOI: 10.1038/s41598-024-56706-x.
- Raju, Mehedi H. et al. (2021). ‘Filtering Eye-Tracking Data From an EyeLink 1000: Comparing Heuristic, Savitzky-Golay, IIR and FIR Digital Filters’. In: *Journal of Eye Movement Research* 14.3. ISSN: 19958692. DOI: 10.16910/JEMR.14.3.6.
- Ramat, Stefano et al. (2007). *What clinical disorders tell us about the neural control of saccadic eye movements*. DOI: 10.1093/brain/awl309.
- Rambold, Holger, Ieman El Baz and Christoph Helmchen (2005). ‘Blink effects on ongoing smooth pursuit eye movements in humans’. In: *Experimental Brain Research* 161.1. ISSN: 00144819. DOI: 10.1007/s00221-004-2040-9.

- Rascol, O. et al. (1995). 'Abnormal vestibuloocular reflex cancellation in multiple system atrophy and progressive supranuclear palsy but not in Parkinson's disease'. In: *Movement Disorders* 10.2. ISSN: 15318257. DOI: 10.1002/mds.870100206.
- Redgrave, Peter et al. (2010). *Goal-directed and habitual control in the basal ganglia: Implications for Parkinson's disease*. DOI: 10.1038/nrn2915.
- Reilly, James L. et al. (2008). 'Pharmacological treatment effects on eye movement control'. In: *Brain and Cognition* 68.3. ISSN: 02782626. DOI: 10.1016/j.bandc.2008.08.026.
- Ren, Jingru et al. (2023). 'Association of GBA genotype with motor and cognitive decline in Chinese Parkinson's disease patients'. In: *Frontiers in Aging Neuroscience* 15. ISSN: 16634365. DOI: 10.3389/fnagi.2023.1091919.
- Ren, Shan et al. (2019). 'Altered functional connectivity of cerebello-cortical circuit in multiple system atrophy (cerebellar-type)'. In: *Frontiers in Neuroscience* 13.JAN. ISSN: 1662453X. DOI: 10.3389/fnins.2018.00996.
- Ren, Zhonglian et al. (2023). *The value of machine learning in preoperative identification of lymph node metastasis status in endometrial cancer: a systematic review and meta-analysis*. DOI: 10.3389/fonc.2023.1289050.
- Reshetniak, V. and E. Faure (June 2024). 'Eye-tracking as a tool for researching user behavior'. In: *COMPUTER-INTEGRATED TECHNOLOGIES: EDUCATION, SCIENCE, PRODUCTION* 55, pp. 181–190. ISSN: 2524-0560. DOI: 10.36910/6775-2524-0560-2024-55-23.
- Rey, Fabian et al. (Mar. 2025). 'Reflexive and voluntary saccades as a proxy for bradykinesia and apathy in Parkinson's disease'. In: *Journal of Neurology* 272.3, p. 236. ISSN: 0340-5354. DOI: 10.1007/s00415-025-12973-w.
- Riek, Heidi C et al. (Mar. 2023). 'Cognitive correlates of antisaccade behaviour across multiple neurodegenerative diseases'. In: *Brain Communications* 5.2. ISSN: 2632-1297. DOI: 10.1093/braincomms/fcad049.
- Riek, Heidi C. et al. (Dec. 2024). 'Multimodal oculomotor assessment reveals prodromal markers of Parkinson's disease in non-manifesting LRRK2 G2019S mutation carriers'. In: *npj Parkinson's Disease* 10.1, p. 234. ISSN: 2373-8057. DOI: 10.1038/s41531-024-00840-w.
- Righini, Andrea et al. (2004). 'MR imaging of the superior profile of the midbrain: Differential diagnosis between progressive supranuclear palsy and Parkinson disease'. In: *American Journal of Neuroradiology* 25.6. ISSN: 01956108.

- Rinne, J. O. et al. (1994). 'Corticobasal degeneration: A clinical study of 36 cases'. In: *Brain* 117.5. ISSN: 00068950. DOI: 10.1093/brain/117.5.1183.
- Rivaud-Péchoux, S. et al. (2007). 'Mixing pro- and antisaccades in patients with parkinsonian syndromes'. In: *Brain* 130.1. ISSN: 14602156. DOI: 10.1093/brain/awl315.
- Rivaud-Péchoux, Sophie et al. (2000). 'Longitudinal ocular motor study in corticobasal degeneration and progressive supranuclear palsy'. In: *Neurology* 54.5. ISSN: 00283878. DOI: 10.1212/WNL.54.5.1029.
- Robinson, David A. (1963). 'A Method of Measuring Eye Movement Using a Scleral Search Coil in a Magnetic Field'. In: *IEEE Transactions on Bio-medical Electronics* 10.4. ISSN: 21681600. DOI: 10.1109/TBMEL.1963.4322822.
- Rocha, Emily M. et al. (2022). *LRRK2 and idiopathic Parkinson's disease*. DOI: 10.1016/j.tins.2021.12.002.
- Rolfs, Martin and Sven Ohl (2011). *Visual suppression in the superior colliculus around the time of microsaccades*. DOI: 10.1152/jn.00862.2010.
- Rottach, Klaus G. et al. (1997). 'Evidence for independent feedback control of horizontal and vertical saccades from Niemann-Pick type C disease'. In: *Vision Research* 37.24. ISSN: 00426989. DOI: 10.1016/S0042-6989(96)00066-1.
- Rucker, Janet C. (2014). 'Eye Movement Disorders in Clinical Practice'. In: *Journal of Neuro-Ophthalmology* 34.4. ISSN: 1070-8022. DOI: 10.1097/wno.0000000000000176.
- Ryan, Michael B., Chloe Bair-Marshall and Alexandra B. Nelson (2018). 'Aberrant Striatal Activity in Parkinsonism and Levodopa-Induced Dyskinesia'. In: *Cell Reports* 23.12. ISSN: 22111247. DOI: 10.1016/j.celrep.2018.05.059.
- Sackner-Bernstein, Jonathan (2021). *Estimates of Intracellular Dopamine in Parkinson's Disease: A Systematic Review and Meta-Analysis*. DOI: 10.3233/JPD-212715.
- Sakar, Betul Erdogan et al. (2013). 'Collection and analysis of a Parkinson speech dataset with multiple types of sound recordings'. In: *IEEE Journal of Biomedical and Health Informatics* 17.4. ISSN: 21682194. DOI: 10.1109/JBHI.2013.2245674.
- Saleem, M. R., A. Straus and R. Napolitano (2021). 'Interpretation of historic structure for non-invasive assessment using eye tracking'. In: *International Archives of the Photogrammetry, Remote Sensing and Spatial Information Sciences - ISPRS Archives*. Vol. 46. M-1-2021. DOI: 10.5194/isprs-Archives-XLVI-M-1-2021-653-2021.

- Salman, Michael S. et al. (2006). 'Saccadic adaptation in children'. In: *Journal of Child Neurology* 21.12. ISSN: 08830738. DOI: 10.1177/7010.2006.00238.
- Santaella, Anna et al. (2020). 'Cerebrospinal fluid myelin basic protein is elevated in multiple system atrophy'. In: *Parkinsonism and Related Disorders* 76. ISSN: 18735126. DOI: 10.1016/j.parkreldis.2020.06.004.
- Sarter, Martin, Ben Givens and John P. Bruno (2001). *The cognitive neuroscience of sustained attention: Where top-down meets bottom-up*. DOI: 10.1016/S0165-0173(01)00044-3.
- Schmid, R. and S. Ron (1986). 'A model of eye tracking of periodic square wave target motion'. In: *Biological Cybernetics* 54.3. ISSN: 03401200. DOI: 10.1007/BF00356856.
- Schneider, Andrea et al. (2020). 'The interplay between task difficulty and microsaccade rate: Evidence for the critical role of visual load'. In: *Journal of Eye Movement Research* 13.5. ISSN: 19958692. DOI: 10.16910/JEMR.13.5.6.
- Schneider, Rosalyn et al. (2011). 'Influence of orbital eye position on vertical saccades in progressive supranuclear palsy'. In: *Annals of the New York Academy of Sciences* 1233.1. ISSN: 17496632. DOI: 10.1111/j.1749-6632.2011.06120.x.
- Schneider, Rosalyn M. et al. (2013). 'Neurological Basis for Eye Movements of the Blind'. In: *PLoS ONE* 8.2. ISSN: 19326203. DOI: 10.1371/journal.pone.0056556.
- Schrag, Anette et al. (2010). 'A comparison of depression, anxiety, and health status in patients with progressive supranuclear palsy and multiple system atrophy'. In: *Movement Disorders* 25.8. ISSN: 15318257. DOI: 10.1002/mds.22794.
- Schulz-Schaeffer, Walter J. (2010). *The synaptic pathology of α -synuclein aggregation in dementia with Lewy bodies, Parkinson's disease and Parkinson's disease dementia*. DOI: 10.1007/s00401-010-0711-0.
- Schumacher, Julia et al. (2019). 'Dynamic functional connectivity changes in dementia with Lewy bodies and Alzheimer's disease'. In: *NeuroImage: Clinical* 22. ISSN: 22131582. DOI: 10.1016/j.nicl.2019.101812.
- Schütz, Alexander C., Dirk Kerzel and David Souto (2014). 'Saccadic adaptation induced by a perceptual task'. In: *Journal of Vision* 14.5. ISSN: 15347362. DOI: 10.1167/14.5.4.
- Segovia, Fermín, Juan M. Górriz et al. (2019). 'Assisted diagnosis of parkinsonism based on the striatal morphology'. In: *International Journal of Neural Systems* 29.9. ISSN: 17936462. DOI: 10.1142/S0129065719500114.

- Segovia, Fermín, Ignacio A. Illán et al. (2015). 'Distinguishing Parkinson's disease from atypical parkinsonian syndromes using PET data and a computer system based on support vector machines and Bayesian networks'. In: *Frontiers in Computational Neuroscience* 9.November. ISSN: 16625188. DOI: 10.3389/fncom.2015.00137.
- Segura-Aguilar, Juan et al. (2014). *Protective and toxic roles of dopamine in Parkinson's disease*. DOI: 10.1111/jnc.12686.
- Seidel, Kay et al. (2015). 'The brainstem pathologies of Parkinson's disease and dementia with lewy bodies'. In: *Brain Pathology* 25.2. ISSN: 17503639. DOI: 10.1111/bpa.12168.
- Sekar, Akila, Muriel T N Panouillères and Diego Kaski (n.d.). 'Detecting Abnormal Eye Movements in Patients with Neurodegenerative Diseases - Current Insights'. In: *Eye Brain* ().
- Sekiya, Hiroaki et al. (2019). 'Wide distribution of alpha-synuclein oligomers in multiple system atrophy brain detected by proximity ligation'. In: *Acta Neuropathologica* 137.3. ISSN: 14320533. DOI: 10.1007/s00401-019-01961-w.
- Sequeira, Alexandra Lloyd Smith, John Ross Rizzo and Janet C. Rucker (2017). 'Clinical approach to supranuclear brainstem saccadic gaze palsies'. In: *Frontiers in Neurology* 8.AUG. ISSN: 16642295. DOI: 10.3389/fneur.2017.00429.
- Sereno, A. B. et al. (2009). 'Executive Functions: Eye Movements and Neuropsychiatric Disorders'. In: *Encyclopedia of Neuroscience*. DOI: 10.1016/B978-008045046-9.00420-4.
- Sereno, Anne B. (1992). 'Programming Saccades: The Role of Attention'. In: DOI: 10.1007/978-1-4612-2852-3{_}6.
- Shaikh, Aasef G., Chrystalina Antoniadou et al. (2018). *Effects of deep brain stimulation on eye movements and vestibular function*. DOI: 10.3389/fneur.2018.00444.
- Shaikh, Aasef G., Stewart A. Factor and Jorge L. Juncos (2017). 'Saccades in Progressive Supranuclear Palsy—Maladapted, Irregular, Curved, and Slow'. In: *Movement Disorders Clinical Practice* 4.5. ISSN: 23301619. DOI: 10.1002/mdc3.12491.
- Shaikh, Aasef G. and Fatema F. Ghasia (2019). 'Saccades in Parkinson's disease: Hypometric, slow, and maladaptive'. In: *Progress in Brain Research*. Vol. 249. DOI: 10.1016/bs.pbr.2019.05.001.
- Shaikh, Aasef G., Minnan Xu-Wilson et al. (2011). "'Staircase' square-wave jerks in early Parkinson's disease'. In: *British Journal of Ophthalmology* 95.5. ISSN: 00071161. DOI: 10.1136/bjo.2010.179630.

- Shaikh, Aasef G. and David S. Zee (2018). *Eye Movement Research in the Twenty-First Century—a Window to the Brain, Mind, and More*. DOI: 10.1007/s12311-017-0910-5.
- Shakespeare, Timothy J. et al. (2015). ‘Abnormalities of fixation, saccade and pursuit in posterior cortical atrophy’. In: *Brain* 138.7. ISSN: 14602156. DOI: 10.1093/brain/awv103.
- Shalash, Ali et al. (2022). ‘A 6-month longitudinal study on worsening of Parkinson’s disease during the COVID-19 pandemic’. In: *npj Parkinson’s Disease* 8.1. ISSN: 23738057. DOI: 10.1038/s41531-022-00376-x.
- Shelhamer, Mark and Wilsaan M. Joiner (2003). ‘Saccades exhibit abrupt transition between reactive and predictive, predictive saccade sequences have long-term correlations’. In: *Journal of Neurophysiology* 90.4. ISSN: 00223077. DOI: 10.1152/jn.00478.2003.
- Shibata, Tomohiro et al. (2005). ‘A model of smooth pursuit in primates based on learning the target dynamics’. In: *Neural Networks* 18.3. ISSN: 08936080. DOI: 10.1016/j.neunet.2005.01.001.
- Siegenthaler, Eva et al. (2014). ‘Task difficulty in mental arithmetic affects microsaccadic rates and magnitudes’. In: *European Journal of Neuroscience* 39.2. ISSN: 0953816X. DOI: 10.1111/ejn.12395.
- Skelton, Patrick D., Valerie Tokars and Loukia Parisiadou (2022). *LRRK2 at Striatal Synapses: Cell-Type Specificity and Mechanistic Insights*. DOI: 10.3390/cells11010169.
- Skoglund, Martin A. et al. (2022). ‘Comparing In-ear EOG for Eye-Movement Estimation With Eye-Tracking: Accuracy, Calibration, and Speech Comprehension’. In: *Frontiers in Neuroscience* 16. ISSN: 1662453X. DOI: 10.3389/fnins.2022.873201.
- Slingerland, Sofie et al. (2024). ‘Cholinergic innervation topography in GBA-associated de novo Parkinson’s disease patients’. In: *Brain* 147.3. ISSN: 14602156. DOI: 10.1093/brain/awad323.
- Soetedjo, Robijanto and Albert F. Fuchs (2006). ‘Complex spike activity of Purkinje cells in the oculomotor vermis during behavioral adaptation of monkey saccades’. In: *Journal of Neuroscience* 26.29. ISSN: 02706474. DOI: 10.1523/JNEUROSCI.4658-05.2006.
- Sogo, Hiroyuki (2013). ‘GazeParser: An open-source and multiplatform library for low-cost eye tracking and analysis’. In: *Behavior Research Methods* 45.3. ISSN: 1554351X. DOI: 10.3758/s13428-012-0286-x.
- Sommer, Marc A. and Robert H. Wurtz (2004). ‘What the Brain Stem Tells the Frontal Cortex. II. Role of the SC-MD-FEF Pathway in Corollary Discharge’. In: *Journal of Neurophysiology* 91.3. ISSN: 00223077. DOI: 10.1152/jn.00740.2003.

- Song, Joomee et al. (2022). 'Differential diagnosis between Parkinson's disease and atypical parkinsonism based on gait and postural instability: Artificial intelligence using an enhanced weight voting ensemble model'. In: *Parkinsonism and Related Disorders* 98. ISSN: 18735126. DOI: 10.1016/j.parkreldis.2022.04.003.
- Sonne, James, Vamsi Reddy and Morris R. Beato (2020). *Neuroanatomy, Substantia Nigra*. December 2018.
- Spauschus, Alexander et al. (1999). 'The origin of ocular microtremor in man'. In: *Experimental Brain Research* 126.4. ISSN: 00144819. DOI: 10.1007/s002210050764.
- Spering, Miriam et al. (2013). 'Efference copy failure during smooth pursuit eye movements in schizophrenia'. In: *Journal of Neuroscience* 33.29. ISSN: 02706474. DOI: 10.1523/JNEUROSCI.0578-13.2013.
- SR Labs (2024). *TOBII PRO NANO*.
- SR Research (n.d.). *EyeLink 1000 Plus*.
- Srivastava, Anshul, Ratna Sharma, Vinay Goyal et al. (2020). 'Saccadic Eye Movements in Young-Onset Parkinson's Disease - A BOLD fMRI Study'. In: *Neuro-Ophthalmology* 44.2. ISSN: 1744506X. DOI: 10.1080/01658107.2019.1652656.
- Srivastava, Anshul, Ratna Sharma, Sanjay K. Sood et al. (2014). *Saccadic eye movements in Parkinson's disease*. DOI: 10.4103/0301-4738.133482.
- Stahl, J. S., A. M. Van Alphen and C. I. De Zeeuw (2000). 'A comparison of video and magnetic search coil recordings of mouse eye movements'. In: *Journal of Neuroscience Methods* 99.1-2. ISSN: 01650270. DOI: 10.1016/S0165-0270(00)00218-1.
- Stamelou, Maria and Kailash P. Bhatia (2015). *A typical Parkinsonism diagnosis and treatment*. DOI: 10.1016/j.ncl.2014.09.012.
- Stamelou, Maria, Niall P. Quinn and Kailash P. Bhatia (2013). '"Atypical" atypical parkinsonism: New genetic conditions presenting with features of progressive supranuclear palsy, corticobasal degeneration, or multiple system atrophy-A diagnostic guide'. In: *Movement Disorders* 28.9. ISSN: 08853185. DOI: 10.1002/mds.25509.
- Stein, J F (2023). 'Space and the parietal association areas'. In: *Brain And Space*. DOI: 10.1093/oso/9780198542841.003.0011.
- Stein, Niklas et al. (2021). 'A Comparison of Eye Tracking Latencies Among Several Commercial Head-Mounted Displays'. In: *i-Perception* 12.1. ISSN: 20416695. DOI: 10.1177/2041669520983338.

- Stern, Yaakov et al. (2019). 'Brain reserve, cognitive reserve, compensation, and maintenance: operationalization, validity, and mechanisms of cognitive resilience'. In: *Neurobiology of Aging* 83. ISSN: 15581497. DOI: 10.1016/j.neurobiolaging.2019.03.022.
- Strassman, A., S. M. Highstein and R. A. McCrea (1986). 'Anatomy and physiology of saccadic burst neurons in the alert squirrel monkey. I. Excitatory burst neurons'. In: *Journal of Comparative Neurology* 249.3. ISSN: 10969861. DOI: 10.1002/cne.902490303.
- Straube, Andreas and Heiner Deubel (1995). 'Rapid gain adaptation affects the dynamics of saccadic eye movements in humans'. In: *Vision Research* 35.23-24. ISSN: 00426989. DOI: 10.1016/0042-6989(95)00076-Q.
- Straube, Andreas, Heiner Deubel et al. (1995). 'Differential effect of a bilateral deep cerebellar nuclei lesion on externally and internally triggered saccades in humans'. In: *Neuro-Ophthalmology* 15.2. ISSN: 01658107. DOI: 10.3109/01658109509009645.
- Street, Duncan et al. (2023). 'Progression of atypical parkinsonian syndromes: PROSPECT-M-UK study implications for clinical trials'. In: *Brain* 146.8. ISSN: 14602156. DOI: 10.1093/brain/awad105.
- Stuart, Samuel et al. (2019). 'Pro-Saccades Predict Cognitive Decline in Parkinson's Disease: ICICLE-PD'. In: *Movement Disorders* 34.11. ISSN: 15318257. DOI: 10.1002/mds.27813.
- Stuphorn, Veit (2015). *The role of supplementary eye field in goal-directed behavior*. DOI: 10.1016/j.jphysparis.2015.02.002.
- Sturm, Edith et al. (2016). 'Neuroprotection by Epigenetic Modulation in a Transgenic Model of Multiple System Atrophy'. In: *Neurotherapeutics* 13.4. ISSN: 18787479. DOI: 10.1007/s13311-016-0447-1.
- Sugiyama, Atsuhiko et al. (2020). 'Vertical pons hyperintensity and hot cross bun sign in cerebellar-type multiple system atrophy and spinocerebellar ataxia type 3'. In: *BMC Neurology* 20.1. ISSN: 14712377. DOI: 10.1186/s12883-020-01738-9.
- Sugiyama, Tetsuya and Takashi Utsumi (1990). 'Pupillary dynamics in parkinson's disease'. In: *Neuro-Ophthalmology* 10.1. ISSN: 01658107. DOI: 10.3109/01658109008997254.
- Surendranathan, Ajenthan, James B. Rowe and John T. O'Brien (2015). *Neuroinflammation in Lewy body dementia*. DOI: 10.1016/j.parkreldis.2015.10.009.
- Suricog (n.d.). *EyeBrain T2*.
- Sweeney, John A. et al. (2007). *fMRI studies of eye movement control: Investigating the interaction of cognitive and sensorimotor brain systems*. DOI: 10.1016/j.neuroimage.2007.03.018.

- Tahri Sqalli, Mohammed et al. (2023). 'Eye tracking technology in medical practice: a perspective on its diverse applications'. In: *Frontiers in Medical Technology* 5. ISSN: 26733129. DOI: 10.3389/fmedt.2023.1253001.
- Takagi, Mineo, David S. Zee and Rafael J. Tamargo (1998). 'Effects of lesions of the oculomotor vermis on eye movements in primate: Saccades'. In: *Journal of Neurophysiology* 80.4. ISSN: 00223077. DOI: 10.1152/jn.1998.80.4.1911.
- Takahashi, M., Y. Sugiuchi and Y. Shinoda (2024). 'Brainstem neural circuits triggering vertical saccades and fixation'. In: *Journal of Neuroscience* 44.1. ISSN: 15292401. DOI: 10.1523/JNEUROSCI.1657-23.2023.
- Takahashi, Mayu et al. (2022). 'Brainstem Circuits Triggering Saccades and Fixation'. In: *Journal of Neuroscience* 42.5. ISSN: 15292401. DOI: 10.1523/JNEUROSCI.1731-21.2021.
- Takeichi, Norihito, Chris R.S. Kaneko and Albert F. Fuchs (2007). 'Activity changes in monkey superior colliculus during saccade adaptation'. In: *Journal of Neurophysiology* 97.6. ISSN: 00223077. DOI: 10.1152/jn.01278.2006.
- Tanabe, Jody et al. (2002). 'Brain activation during smooth-pursuit eye movements'. In: *NeuroImage* 17.3. ISSN: 10538119. DOI: 10.1006/nimg.2002.1263.
- Tang, Jiawei, Patrick Luk and Yuyang Zhou (2023). 'Wearable and Invisible Sensor Design for Eye-Motion Monitoring Based on Ferrofluid and Electromagnetic Sensing Technologies'. In: *Bioengineering* 10.5. ISSN: 23065354. DOI: 10.3390/bioengineering10050514.
- Taylor, John Paul et al. (2012). 'Visual cortex in dementia with Lewy bodies: Magnetic resonance imaging study'. In: *British Journal of Psychiatry* 200.6. ISSN: 00071250. DOI: 10.1192/bjp.bp.111.099432.
- Taymans, Jean Marc et al. (2023). 'Perspective on the current state of the LRRK2 field'. In: *npj Parkinson's Disease* 9.1. ISSN: 23738057. DOI: 10.1038/s41531-023-00544-7.
- Temel, Yasin, Veerle Visser-Vandewalle and Roger H.S. Carpenter (2009). 'Saccadometry: A novel clinical tool for quantification of the motor effects of subthalamic nucleus stimulation in Parkinson's disease'. In: *Experimental Neurology* 216.2. ISSN: 00144886. DOI: 10.1016/j.expneurol.2009.01.007.
- Terao, Yasuo (2022). *Making saccades, fast and slow: The voluntary versus reflexive saccade systems in Parkinson's disease*. DOI: 10.1016/j.clinph.2022.08.012.
- Terao, Yasuo, Hideki Fukuda, Yoshikazu Ugawa et al. (2013). *New perspectives on the pathophysiology of Parkinson's disease as assessed by saccade performance: A clinical review*. DOI: 10.1016/j.clinph.2013.01.021.

- Terao, Yasuo, Hideki Fukuda, Akihiro Yugeta et al. (2011). 'Initiation and inhibitory control of saccades with the progression of Parkinson's disease - Changes in three major drives converging on the superior colliculus'. In: *Neuropsychologia* 49.7. ISSN: 00283932. DOI: 10.1016/j.neuropsychologia.2011.03.002.
- Terao, Yasuo, Shin ichi Tokushige et al. (2019). 'Differentiating early Parkinson's disease and multiple system atrophy with parkinsonism by saccade velocity profiles'. In: *Clinical Neurophysiology* 130.12. ISSN: 18728952. DOI: 10.1016/j.clinph.2019.09.004.
- (2022). 'Deciphering the saccade velocity profile of progressive supranuclear palsy: A sign of latent cerebellar/brainstem dysfunction?' In: *Clinical Neurophysiology* 141. ISSN: 18728952. DOI: 10.1016/j.clinph.2020.12.023.
- Termsarasab, Pichet et al. (2015). 'The diagnostic value of saccades in movement disorder patients: a practical guide and review'. In: *Journal of Clinical Movement Disorders* 2.1. DOI: 10.1186/s40734-015-0025-4.
- Thibeault, Mark et al. (2019). 'Improved Accuracy Test Method for Mobile Eye Tracking in Usability Scenarios'. In: *Proceedings of the Human Factors and Ergonomics Society*. Vol. 63. 1. DOI: 10.1177/1071181319631083.
- Timothy, C. Hain (2024). *Eye Movement Recording Devices*. tobii (n.d.). *Tobii Pro Nano*.
- Toffoli, Marco et al. (2023). 'Phenotypic effect of GBA1 variants in individuals with and without Parkinson's disease: The RAPSODI study'. In: *Neurobiology of Disease* 188. ISSN: 1095953X. DOI: 10.1016/j.nbd.2023.106343.
- Torres, Elizabeth B., Jonathan Cole and Howard Poizner (2014). 'Motor output variability, deafferentation, and putative deficits in kinesthetic reafference in Parkinson's disease'. In: *Frontiers in Human Neuroscience* 8.OCT. ISSN: 16625161. DOI: 10.3389/fnhum.2014.00823.
- Troost, B. Todd and Robert B. Daroff (1977). 'The ocular motor defects in progressive supranuclear palsy'. In: *Annals of Neurology* 2.5. ISSN: 15318249. DOI: 10.1002/ana.410020509.
- Tsitsi, Panagiota, Mattias Nilsson Benfatto et al. (2021). 'Fixation Duration and Pupil Size as Diagnostic Tools in Parkinson's Disease'. In: *Journal of Parkinson's Disease* 11.2. ISSN: 1877718X. DOI: 10.3233/JPD-202427.
- Tsitsi, Panagiota, Mattias Nilsson et al. (2023). 'Pupil light reflex dynamics in Parkinson's disease'. In: *Frontiers in Integrative Neuroscience* 17. ISSN: 16625145. DOI: 10.3389/fnint.2023.1249554.

- Tu, P. C. et al. (2006). 'Neural correlates of antisaccade deficits in schizophrenia, an fMRI study'. In: *Journal of Psychiatric Research* 40.7. ISSN: 00223956. DOI: 10.1016/j.jpsychires.2006.05.012.
- Tyralla, Sandra, Antonella Pomè and Eckart Zimmermann (2023). 'Motor recalibration of visual and saccadic maps'. In: *Proceedings of the Royal Society B: Biological Sciences* 290.1994. ISSN: 14712954. DOI: 10.1098/rspb.2022.2566.
- Ubhi, Kiren, Phillip Low and Eliezer Masliah (2011). *Multiple system atrophy: A clinical and neuropathological perspective*. DOI: 10.1016/j.tins.2011.08.003.
- Upadhyaya, Suraj and Vallabh E. Das (2019). 'Response properties of cells within the rostral superior colliculus of strabismic monkeys'. In: *Investigative Ophthalmology and Visual Science* 60.13. ISSN: 15525783. DOI: 10.1167/iov.19-27786.
- Vabalas, Andrius et al. (2020). 'Applying Machine Learning to Kinematic and Eye Movement Features of a Movement Imitation Task to Predict Autism Diagnosis'. In: *Scientific Reports* 10.1. ISSN: 20452322. DOI: 10.1038/s41598-020-65384-4.
- Valliappan, Nachiappan et al. (2020). 'Accelerating eye movement research via accurate and affordable smartphone eye tracking'. In: *Nature Communications* 11.1. ISSN: 20411723. DOI: 10.1038/s41467-020-18360-5.
- Van der Stigchel, S. et al. (2012). 'The role of the frontal eye fields in the oculomotor inhibition of reflexive saccades: Evidence from lesion patients'. In: *Neuropsychologia* 50.1. ISSN: 00283932. DOI: 10.1016/j.neuropsychologia.2011.11.020.
- Van der Stigchel, Stefan et al. (2020). 'Transsaccadic perception is affected by saccade landing point deviations after saccadic adaptation'. In: *Journal of Vision* 20.9. ISSN: 15347362. DOI: 10.1167/JOV.20.9.8.
- Van Leeuwen, Anna F., Han Collewyn and Casper J. Erkelens (1998). 'Dynamics of horizontal vergence movements: Interaction with horizontal and vertical saccades and relation with monocular preferences'. In: *Vision Research* 38.24. ISSN: 00426989. DOI: 10.1016/S0042-6989(98)00092-3.
- Van Opstal, A. J. and J. A.M. Van Gisbergen (1987). 'Skewness of saccadic velocity profiles: A unifying parameter for normal and slow saccades'. In: *Vision Research* 27.5. ISSN: 00426989. DOI: 10.1016/0042-6989(87)90071-X.
- Vermersch, Anne-Isabelle -I et al. (1994). 'Sequences of memory-guided saccades in Parkinson's disease'. In: *Annals of Neurology* 35.4. ISSN: 15318249. DOI: 10.1002/ana.410350419.

- Vieira, Sophia R.L. and Anthony H.V. Schapira (2022). *Glucocerebrosidase mutations and Parkinson disease*. DOI: 10.1007/s00702-022-02531-3.
- Vinny, Pulikottil Wilson and Vivek Lal (2016). *Gaze disorders: A clinical approach*. DOI: 10.4103/0028-3886.173627.
- Vintonyak, Olga et al. (2017). 'Patterns of Eye Movement Impairment Correlate with Regional Brain Atrophy in Neurodegenerative Parkinsonism'. In: *Neurodegenerative Diseases* 17.4-5. ISSN: 16602862. DOI: 10.1159/000454880.
- Vokoun, Corinne R. et al. (2014). 'Response normalization in the superficial layers of the superior colliculus as a possible mechanism for saccadic averaging'. In: *Journal of Neuroscience* 34.23. ISSN: 15292401. DOI: 10.1523/JNEUROSCI.3022-13.2014.
- Volkow, Nora D. et al. (2002). *Role of dopamine, the frontal cortex and memory circuits in drug addiction: Insight from imaging studies*. DOI: 10.1006/nlme.2002.4099.
- Waespe, Walter and Ralf Baumgartner (1992). 'Enduring dysmetria and impaired gain adaptivity of saccadic eye movements in wallenberg's lateral medullary syndrome'. In: *Brain* 115.4. ISSN: 00068950. DOI: 10.1093/brain/115.4.1125.
- Wagner, Ilja, Christian Wolf and Alexander C. Schütz (2021). 'Motor learning by selection in visual working memory'. In: *Scientific Reports* 11.1. ISSN: 20452322. DOI: 10.1038/s41598-021-87572-6.
- Waldthaler, Josefine, Panagiota Tsitsi and Per Svenningsson (2019). 'Vertical saccades and antisaccades: complementary markers for motor and cognitive impairment in Parkinson's disease'. In: *npj Parkinson's Disease* 5.1. ISSN: 23738057. DOI: 10.1038/s41531-019-0083-7.
- Walker, Robin, Heiner Deubel et al. (1997). 'Effect of remote distractors on saccade programming: Evidence for an extended fixation zone'. In: *Journal of Neurophysiology* 78.2. ISSN: 00223077. DOI: 10.1152/jn.1997.78.2.1108.
- Walker, Robin and Eugene McSorley (2006). 'The parallel programming of voluntary and reflexive saccades'. In: *Vision Research* 46.13. ISSN: 00426989. DOI: 10.1016/j.visres.2005.12.009.
- Walker, Robin, David G. Walker et al. (2000). 'Control of voluntary and reflexive saccades'. In: *Experimental Brain Research* 130.4. ISSN: 00144819. DOI: 10.1007/s002219900285.
- Walton, Mark M.G. and Edward G. Freedman (2014). 'Activity of long-lead burst neurons in pontine reticular formation during head-unrestrained gaze shifts'. In: *Journal of Neurophysiology* 111.2. ISSN: 00223077. DOI: 10.1152/jn.00841.2012.

- Wan, Yu et al. (2020). 'Evaluation of eye movements and visual performance in patients with cataract'. In: *Scientific Reports* 10.1. ISSN: 20452322. DOI: 10.1038/s41598-020-66817-w.
- Wang, Yu Cheng, Tin Chih Toly Chen and Min Chi Chiu (2023). 'A systematic approach to enhance the explainability of artificial intelligence in healthcare with application to diagnosis of diabetes'. In: *Healthcare Analytics* 3. ISSN: 27724425. DOI: 10.1016/j.health.2023.100183.
- Warren, N. M. et al. (2007). 'The basal ganglia cholinergic neurochemistry of progressive supranuclear palsy and other neurodegenerative diseases'. In: *Journal of Neurology, Neurosurgery and Psychiatry* 78.6. ISSN: 1468330X. DOI: 10.1136/jnnp.2006.099937.
- Warren Olanow, C. et al. (2013). 'Factors predictive of the development of Levodopa-induced dyskinesia and wearing-off in Parkinson's disease'. In: *Movement Disorders* 28.8. ISSN: 08853185. DOI: 10.1002/mds.25364.
- Watanabe, Hirohisa et al. (2023). *Multiple System Atrophy: Advances in Diagnosis and Therapy*. DOI: 10.14802/jmd.22082.
- Watanabe, Yasuhiro et al. (2023). 'Clinical availability of eye movement during reading'. In: *Neuroscience Research* 195. ISSN: 18728111. DOI: 10.1016/j.neures.2023.05.004.
- Weil, Rimona S. et al. (2016). *Visual dysfunction in Parkinson's disease*. DOI: 10.1093/brain/aww175.
- Wen, Min et al. (2022). *Depression and Cognitive Impairment: Current Understanding of Its Neurobiology and Diagnosis*. DOI: 10.2147/NDT.S383093.
- Wenning, G. K. et al. (1997). 'Multiple system atrophy: A review of 203 pathologically proven cases'. In: *Movement Disorders* 12.2. ISSN: 08853185. DOI: 10.1002/mds.870120203.
- White, Owen B. et al. (1983). 'Ocular motor deficits in parkinson's disease: II. Control of the saccadic and smooth pursuit systems'. In: *Brain* 106.3. ISSN: 00068950. DOI: 10.1093/brain/106.3.571.
- Whitwell, J. L. et al. (2013). 'Midbrain atrophy is not a biomarker of progressive supranuclear palsy pathology'. In: *European Journal of Neurology* 20.10. ISSN: 13515101. DOI: 10.1111/ene.12212.
- Whitwell, Jennifer L., Jonathan Graff-Radford et al. (2017). '18F-FDG PET in posterior cortical atrophy and dementia with lewy bodies'. In: *Journal of Nuclear Medicine* 58.4. ISSN: 2159662X. DOI: 10.2967/jnumed.116.179903.
- Whitwell, Jennifer L., Val J. Lowe et al. (2017). '[18F]AV-1451 tau positron emission tomography in progressive supranuclear palsy'. In: *Movement Disorders* 32.1. ISSN: 15318257. DOI: 10.1002/mds.26834.

- Wiegel, Patrick et al. (2022). 'Trial-to-trial Variability and Cortical Processing Depend on Recent Outcomes During Human Reinforcement Motor Learning'. In: *Neuroscience* 501. ISSN: 18737544. DOI: 10.1016/j.neuroscience.2022.08.012.
- Williams, David R., Rohan De Silva et al. (2005). 'Characteristics of two distinct clinical phenotypes in pathologically proven progressive supranuclear palsy: Richardson's syndrome and PSP-parkinsonism'. In: *Brain* 128.6. ISSN: 00068950. DOI: 10.1093/brain/awh488.
- Williams, David R., Janice L. Holton et al. (2007). 'Pure akinesia with gait freezing: A third clinical phenotype of progressive supranuclear palsy'. In: *Movement Disorders* 22.15. ISSN: 08853185. DOI: 10.1002/mds.21698.
- Williams, David R. and Andrew J. Lees (2009). *Progressive supranuclear palsy: clinicopathological concepts and diagnostic challenges*. DOI: 10.1016/S1474-4422(09)70042-0.
- Wolf, Andrew B. et al. (2015). *An integrative role for the superior colliculus in selecting targets for movements*. DOI: 10.1152/jn.00262.2015.
- Wolfe, Jeremy M., Evan M. Palmer and Todd S. Horowitz (2010). 'Reaction time distributions constrain models of visual search'. In: *Vision Research* 50.14. ISSN: 00426989. DOI: 10.1016/j.visres.2009.11.002.
- Wolpert, Daniel M., Zoubin Ghahramani and Michael I. Jordan (1995). 'An internal model for sensorimotor integration'. In: *Science* 269.5232. ISSN: 00368075. DOI: 10.1126/science.7569931.
- Wong, Aaron L. and Mark Shelhamer (2011). 'Sensorimotor adaptation error signals are derived from realistic predictions of movement outcomes'. In: *Journal of Neurophysiology* 105.3. ISSN: 00223077. DOI: 10.1152/jn.00394.2010.
- Wong, Oscar WH et al. (2018). 'Eye movement parameters and cognitive functions in Parkinson's disease patients without dementia'. In: *Parkinsonism and Related Disorders* 52. ISSN: 18735126. DOI: 10.1016/j.parkreldis.2018.03.013.
- Woods, Adrienne D. et al. (2024). 'Best practices for addressing missing data through multiple imputation'. In: *Infant and Child Development* 33.1. ISSN: 15227219. DOI: 10.1002/icd.2407.
- Wright, Isaac Hempstead et al. (2022). 'Reflexive and volitional saccadic eye movements and their changes in age and progressive supranuclear palsy'. In: *Journal of the Neurological Sciences* 443. ISSN: 18785883. DOI: 10.1016/j.jns.2022.120482.
- Wu, Tao and Mark Hallett (2013). *The cerebellum in Parkinson's disease*. DOI: 10.1093/brain/aws360.

- Wunderlich, Jessica et al. (2021). 'Diagnostic value of video-oculography in progressive supranuclear palsy: a controlled study in 100 patients'. In: *Journal of Neurology* 268.9. ISSN: 14321459. DOI: 10.1007/s00415-021-10522-9.
- Wurtz, Robert H. (2008). 'Neuronal mechanisms of visual stability'. In: *Vision Research* 48.20. ISSN: 00426989. DOI: 10.1016/j.visres.2008.03.021.
- Wyatt, Harry J. (1998). 'Detecting saccades with jerk'. In: *Vision Research* 38.14. ISSN: 00426989. DOI: 10.1016/S0042-6989(97)00410-0.
- Xing, Bo, Yan Chun Li and Wen Jun Gao (2016). *Norepinephrine versus dopamine and their interaction in modulating synaptic function in the prefrontal cortex*. DOI: 10.1016/j.brainres.2016.01.005.
- Xu, Yaoda (2018). *The Posterior Parietal Cortex in Adaptive Visual Processing*. DOI: 10.1016/j.tins.2018.07.012.
- Xu, Yunqi et al. (Apr. 2012). 'Neurotransmitter receptors and cognitive dysfunction in Alzheimer's disease and Parkinson's disease'. In: *Progress in Neurobiology* 97.1, pp. 1–13. ISSN: 03010082. DOI: 10.1016/j.pneurobio.2012.02.002.
- Xu, Zheyu, Kirstie N. Anderson and Nicola Pavese (2022). *Longitudinal Studies of Sleep Disturbances in Parkinson's Disease*. DOI: 10.1007/s11910-022-01223-5.
- Xue, Cheng et al. (2020). 'Sustained spatial attention accounts for the direction bias of human microsaccades'. In: *Scientific Reports* 10.1. ISSN: 20452322. DOI: 10.1038/s41598-020-77455-7.
- Yamada, Jinzo and Hiroharu Noda (1987). 'Afferent and efferent connections of the oculomotor cerebellar vermis in the macaque monkey'. In: *Journal of Comparative Neurology* 265.2. ISSN: 10969861. DOI: 10.1002/cne.902650207.
- Yamada, Masahito et al. (2020). *Diagnostic criteria for dementia with lewy bodies: Updates and future directions*. DOI: 10.14802/jmd.19052.
- Yamada, Yasunori and Masatomo Kobayashi (2018). 'Detecting mental fatigue from eye-tracking data gathered while watching video: Evaluation in younger and older adults'. In: *Artificial Intelligence in Medicine* 91. ISSN: 18732860. DOI: 10.1016/j.artmed.2018.06.005.
- Yamamoto, K. et al. (1992). 'Multiple system atrophy with macro square wave jerks and pendular nystagmus'. In: *Clinical Neurology* 32.11. ISSN: 0009918X.
- Yarbus, Alfred L. (1967). *Eye Movements and Vision*. DOI: 10.1007/978-1-4899-5379-7.

- Yin, Chunyu et al. (2022). 'Comparison of Motor Scores between OFF and ON States in Tremor-Dominant Parkinson's Disease after MRgFUS Treatment'. In: *Journal of Clinical Medicine* 11.15. ISSN: 20770383. DOI: 10.3390/jcm11154502.
- Yousaf, Tayyabah et al. (2019). *Neuroimaging in Lewy body dementia*. DOI: 10.1007/s00415-018-8892-x.
- Yu, Chao Hua, Fei Gao and Qiao Yan Wen (2021). 'An Improved Quantum Algorithm for Ridge Regression'. In: *IEEE Transactions on Knowledge and Data Engineering* 33.3. ISSN: 15582191. DOI: 10.1109/TKDE.2019.2937491.
- Yu, Fang et al. (2015). 'Patterns of gray matter atrophy in atypical parkinsonism syndromes: A VBM meta-analysis'. In: *Brain and Behavior* 5.6. ISSN: 21623279. DOI: 10.1002/brb3.329.
- Yu, Hong et al. (2007). 'Role of hyperactive cerebellum and motor cortex in Parkinson's disease'. In: *NeuroImage* 35.1. ISSN: 10538119. DOI: 10.1016/j.neuroimage.2006.11.047.
- Yu, Megan and Shu-Min Wang (2020). *Neuroanatomy, Nucleus Fastigial*.
- Yu, Yaqin et al. (2024). 'Smooth Pursuit and Reflexive Saccade in Discriminating Multiple-System Atrophy With Predominant Parkinsonism From Parkinson's Disease'. In: *Journal of Clinical Neurology (Korea)* 20.2. ISSN: 20055013. DOI: 10.3988/jcn.2022.0413.
- Zach, Heidemarie, Michiel F. Dirx, Jaco W. Pasman et al. (2017). 'Cognitive Stress Reduces the Effect of Levodopa on Parkinson's Resting Tremor'. In: *CNS Neuroscience and Therapeutics* 23.3. ISSN: 17555949. DOI: 10.1111/cns.12670.
- Zach, Heidemarie, Michiel F. Dirx, Dominik Roth et al. (2020). 'Dopamine-responsive and dopamine-resistant resting tremor in Parkinson disease'. In: *Neurology* 95.11. ISSN: 1526632X. DOI: 10.1212/WNL.0000000000010316.
- Zafar, Muhammad Rehman and Naimul Khan (2021). 'Deterministic Local Interpretable Model-Agnostic Explanations for Stable Explainability'. In: *Machine Learning and Knowledge Extraction* 3.3. ISSN: 25044990. DOI: 10.3390/make3030027.
- Zang, Qingda et al. (2017). 'Prediction of skin sensitization potency using machine learning approaches'. In: *Journal of Applied Toxicology* 37.7. ISSN: 10991263. DOI: 10.1002/jat.3424.
- Zargari Marandi, Ramtin et al. (2018). 'Eye movement characteristics reflected fatigue development in both young and elderly individuals'. In: *Scientific Reports* 8.1. ISSN: 20452322. DOI: 10.1038/s41598-018-31577-1.

- Zee, David S. (2012). *What the future holds for the study of saccades*. DOI: 10.1016/s0208-5216(12)70037-2.
- Zee, David S. et al. (1976). 'Ocular motor abnormalities in hereditary cerebellar ataxia'. In: *Brain* 99.2. ISSN: 00068950. DOI: 10.1093/brain/99.2.207.
- Zhai, Shenyu et al. (2023). *Distributed dopaminergic signaling in the basal ganglia and its relationship to motor disability in Parkinson's disease*. DOI: 10.1016/j.conb.2023.102798.
- Zhang, Jian Yuan et al. (2021). 'Eye movement especially vertical oculomotor impairment as an aid to assess Parkinson's disease'. In: *Neurological Sciences* 42.6. ISSN: 15903478. DOI: 10.1007/s10072-020-04796-6.
- Zhang, Limin and Hong Cui (2022). 'Reliability of MUSE 2 and Tobii Pro Nano at capturing mobile application users' real-time cognitive workload changes'. In: *Frontiers in Neuroscience* 16. ISSN: 1662453X. DOI: 10.3389/fnins.2022.1011475.
- Zhang, Lingyu et al. (2022). 'Fatigue in Patients with Multiple System Atrophy: A Prospective Cohort Study'. In: *Neurology* 98.1. ISSN: 1526632X. DOI: 10.1212/WNL.00000000000012968.
- Zhang, Yu et al. (2018). 'Oculomotor performances are associated with motor and non-motor symptoms in Parkinson's disease'. In: *Frontiers in Neurology* 9.NOV. ISSN: 16642295. DOI: 10.3389/fneur.2018.00960.
- Zhao, Zhe et al. (2021). 'Fecal microbiota transplantation protects rotenone-induced Parkinson's disease mice via suppressing inflammation mediated by the lipopolysaccharide-TLR4 signaling pathway through the microbiota-gut-brain axis'. In: *Microbiome* 9.1. ISSN: 20492618. DOI: 10.1186/s40168-021-01107-9.
- Zhao, Zhixu et al. (2023). 'Early detection of Parkinson's disease based on IMU and machine learning'. In: DOI: 10.1117/12.2674576.
- Zhong, Yuke et al. (2022). *A review on pathology, mechanism, and therapy for cerebellum and tremor in Parkinson's disease*. DOI: 10.1038/s41531-022-00347-2.
- Zhou, Hong et al. (2022). 'Quantitative assessment of oculomotor function by videonystagmography in multiple system atrophy'. In: *Clinical Neurophysiology* 141. ISSN: 18728952. DOI: 10.1016/j.clinph.2022.05.019.
- Zhou, Zhi Dong et al. (2023). *Role of dopamine in the pathophysiology of Parkinson's disease*. DOI: 10.1186/s40035-023-00378-6.

- Zhu, Lisen et al. (July 2024). 'Wearable Near-Eye Tracking Technologies for Health: A Review'. In: *Bioengineering* 11.7, p. 738. ISSN: 2306-5354. DOI: 10.3390/bioengineering11070738.
- Zimmermann, Eckart, David Burr and Maria Concetta Morrone (2011). 'Spatiotopic visual maps revealed by saccadic adaptation in humans'. In: *Current Biology* 21.16. ISSN: 09609822. DOI: 10.1016/j.cub.2011.06.014.
- Zingale, Carolina M. and Eileen Kowler (1987). 'Planning sequences of saccades'. In: *Vision Research* 27.8. ISSN: 00426989. DOI: 10.1016/0042-6989(87)90210-0.
- Zirra, Alexandra and Brook Huxford (2022). 'CD4+ T Cells Contribute to Neurodegeneration in Lewy Body Dementia'. In: *Movement Disorders* 37.2. ISSN: 15318257. DOI: 10.1002/mds.28881.

Appendices

A Ocular Motor Function in Parkinson's Disease

Metric	Estimate	Pr(> t)	CI 0.025	CI 0.975	AIC	BIC
Saccade Amplitude	-1.725502	0.012832	-3.068823	-0.382182	692.612906	720.456658
Saccade Average Velocity	-23.403952	0.022285	-43.273247	-3.534656	1570.867030	1598.710782
Saccade End Time	-9.269553	0.803259	-82.069945	63.530840	1994.192941	2022.036693
Saccade Peak Velocity	-55.167015	0.045053	-108.681029	-1.653000	1893.857387	1921.701138
Saccade Latency	-3.265369	0.885988	-47.827977	41.297240	1834.183592	1862.027343
Number of Errors	0.378227	0.817647	-2.831401	3.587854	976.562253	1004.406005
Number of Correct Saccades	-0.357602	0.829288	-3.602758	2.887555	980.151105	1007.994857
Number of Self Corrected Errors	0.347796	0.810030	-2.483071	3.178663	935.625833	963.469585

Table 16: GBA-PD Generalised Linear Model Results for Antisaccades Horizontal

Metric	Estimate	Pr(> t)	CI 0.025	CI 0.975	AIC	BIC
Saccade Amplitude	-1.644265	0.007303	-2.829684	-0.458846	651.847205	679.690957
Saccade Average Velocity	-30.982368	0.000761	-48.660923	-13.303812	1532.782649	1560.626400
Saccade End Time	2.489433	0.945124	-68.281919	73.260785	1984.977878	2012.821630
Saccade Peak Velocity	-86.757550	0.009239	-151.262119	-22.252981	1954.751737	1982.595489
Saccade Latency	29.374594	0.205485	-15.908122	74.657310	1839.409465	1867.253217
Number of Errors	-0.702674	0.606137	-3.368337	1.962989	916.023389	943.867141
Number of Correct Saccades	0.688284	0.616751	-2.001821	3.378389	918.998907	946.842659
Number of Self Corrected Errors	0.396074	0.730371	-1.852381	2.644529	860.535158	888.378910

Table 17: GBA-PD Generalised Linear Model Results for Antisaccades Vertical

Metric	Estimate	Pr(> t)	CI 0.025	CI 0.975	AIC	BIC
Average Pupil Size	595.517106	0.040412	30.795247	1160.238965	2662.040445	2689.884196
Fixation Precision RMS	-0.005470	0.261041	-0.014973	0.004034	-921.489731	-893.645979
Fixation Precision SD	-0.004343	0.580777	-0.019723	0.011037	-764.549602	-736.705850
Large SWJ Count	0.576400	0.016656	0.109664	1.043137	347.986788	375.830540
Intrusive Saccade Count	0.378990	0.908619	-6.082008	6.839988	1204.641291	1232.485042
Microsaccade Count	2.210830	0.881496	-26.808613	31.230273	1694.352715	1722.196466
Small SWJ Count	5.168029	0.776112	-30.387161	40.723220	1760.569863	1788.413615
Fixation Duration	33.778198	0.913419	-574.131340	641.687737	2686.064284	2713.908036
Saccade Count	7.425158	0.405325	-10.015616	24.865932	1528.368100	1556.211852

Table 18: GBA-PD Generalised Linear Model Results for Central Fixation

Metric	Estimate	Pr(> t)	CI 0.025	CI 0.975	AIC	BIC
Total Number of Saccades	-4.703083	0.539274	-19.684752	10.278587	1478.821525	1506.665276
Saccadic Steps	0.171389	0.573651	-0.424334	0.767111	427.534038	455.377790
Accuracy	-90.613190	0.090490	-194.871914	13.645535	2111.277210	2139.120961
Number of Correct Saccades	7.435526	0.155124	-2.765438	17.636491	1353.524991	1381.368743
Number of Hypometric Saccades	-2.254186	0.711627	-14.183771	9.675399	1404.556767	1432.400519
Number of Hypermetric Saccades	-8.967641	0.217784	-23.171013	5.235731	1461.430067	1489.273819
Saccade Amplitude	0.188460	0.918110	-3.398312	3.775231	1012.780078	1040.623830
Saccade Average Velocity	-7.972680	0.640142	-41.331994	25.386635	1739.787656	1767.631408
Saccade End Time	297.710944	0.614191	-857.462917	1452.884805	2895.349783	2923.193534
Saccade Peak Velocity	-42.954215	0.262781	-117.859929	31.951498	2003.486816	2031.330567
Saccade Latency	300.652991	0.610762	-854.728584	1456.034565	2895.408396	2923.252148

Table 19: GBA-PD Generalised Linear Model Results for Memory Guided Saccades Horizontal

Metric	Estimate	Pr(> t)	CI 0.025	CI 0.975	AIC	BIC
Total Number of Saccades	-0.993069	0.894662	-15.668924	13.682786	1472.098163	1499.941915
Saccadic Steps	0.139287	0.597186	-0.376247	0.654821	380.403799	408.247550
Accuracy	-10.982539	0.748218	-77.922740	55.957662	1966.834481	1994.678233
Number of Correct Saccades	-5.146812	0.225494	-13.436414	3.142790	1285.886425	1313.730177
Number of Hypometric Saccades	12.677394	0.049677	0.116958	25.237830	1421.355696	1449.199448
Number of Hypermetric Saccades	-7.450006	0.107678	-16.474102	1.574091	1313.562645	1341.406397
Saccade Amplitude	-1.388485	0.320009	-4.116306	1.339335	923.537688	951.381440
Saccade Average Velocity	-20.935220	0.149703	-49.277095	7.406655	1686.650752	1714.494504
Saccade End Time	499.075481	0.529049	-1051.413059	2049.564021	2991.297844	3019.141596
Saccade Peak Velocity	-80.842150	0.044574	-159.084469	-2.599831	2017.694057	2045.537809
Saccade Latency	547.333449	0.494483	-1019.152121	2113.819019	2994.644088	3022.487840

Table 20: GBA-PD Generalised Linear Model Results for Memory Guided Saccades Vertical

Metric	Estimate	Pr(> t)	CI 0.025	CI 0.975	AIC	BIC
Microsaccade Count Up	4.044316	0.581484	-10.305821	18.394452	1464.781366	1492.625118
Microsaccade Count Down	-17.377039	0.401417	-57.854952	23.100875	1802.842391	1830.686143
Microsaccade Count Right	6.041244	0.677860	-22.410003	34.492491	1687.906374	1715.750126
Microsaccade Count Left	-2.800852	0.773039	-21.802021	16.200317	1556.302944	1584.146696
Small SWJ Count Up	4.639282	0.413022	-6.438743	15.717308	1380.413869	1408.257621
Small SWJ Count Down	-21.623764	0.440044	-76.372692	33.125163	1901.294816	1929.138568
Small SWJ Count Right	15.646990	0.287204	-13.069277	44.363258	1690.928973	1718.772725
Small SWJ Count Left	-9.117390	0.526403	-37.261371	19.026590	1684.366503	1712.210255
Large SWJ Count Up	0.186197	0.354878	-0.207079	0.579473	292.158284	320.002036
Large SWJ Count Down	0.170953	0.427113	-0.249854	0.591759	314.216123	342.059875
Large SWJ Count Right	0.073836	0.788156	-0.463803	0.611476	394.091112	421.934864
Large SWJ Count Left	-0.060078	0.766717	-0.456284	0.336129	294.578401	322.422153
Intrusive Saccade Count Up	-0.647517	0.767158	-4.926177	3.631143	1070.282384	1098.126135
Intrusive Saccade Count Down	0.463695	0.872932	-5.209351	6.136741	1162.242512	1190.086264
Intrusive Saccade Count Right	4.445762	0.225569	-2.715873	11.607396	1238.204433	1266.048185
Intrusive Saccade Count Left	0.813917	0.786680	-5.070590	6.698425	1174.173087	1202.016839
Average Fixation Duration Up	470.925609	0.081793	-55.971466	997.822685	2639.439485	2667.283237
Average Fixation Duration Down	753.231918	0.012170	171.313943	1335.149894	2671.819198	2699.662950
Average Fixation Duration Right	579.691880	0.037820	37.299287	1122.084474	2648.888547	2676.732299
Average Fixation Duration Left	499.465180	0.086995	-68.895916	1067.826277	2664.134546	2691.978298
Fixation Precision RMS Up	-0.004509	0.318438	-0.013337	0.004320	-945.499854	-917.656102
Fixation Precision RMS Down	-0.004158	0.491828	-0.015984	0.007669	-850.201329	-822.357578
Fixation Precision RMS Right	-0.002283	0.696936	-0.013752	0.009186	-860.216371	-832.372619
Fixation Precision RMS Left	-0.005686	0.295634	-0.016306	0.004934	-885.289345	-857.445593
Fixation Precision SD Up	-0.007599	0.319082	-0.022498	0.007301	-774.895129	-747.051377
Fixation Precision SD Down	-0.003608	0.669017	-0.020116	0.012901	-741.469447	-713.625695
Fixation Precision SD Right	-0.001441	0.876070	-0.019521	0.016639	-711.825909	-683.982157
Fixation Precision SD Left	-0.006207	0.448052	-0.022201	0.009787	-751.792039	-723.948288
Average Pupil Size Up	-224.747500	0.315799	-662.450308	212.955309	2578.977873	2606.821625
Average Pupil Size Down	-174.596128	0.474077	-651.459067	302.266810	2606.912470	2634.756222
Average Pupil Size Right	-98.242410	0.626574	-493.198837	296.714017	2545.476577	2573.320328
Average Pupil Size Left	-41.260760	0.849430	-466.523639	384.002120	2569.578431	2597.422183
Saccade Count Up	5.755489	0.543547	-12.773593	24.284572	1548.101113	1575.944864
Saccade Count Down	-3.421430	0.725941	-22.517508	15.674647	1557.927222	1585.770974
Saccade Count Right	2.485825	0.787544	-15.561194	20.532844	1539.507431	1567.351183
Saccade Count Left	-4.362932	0.656501	-23.552795	14.826931	1559.524368	1587.368119

Table 21: GBA-PD Generalised Linear Model Results for Nystagmus/ Positional Fixation

Metric	Estimate	Pr(> t)	CI 0.025	CI 0.975	AIC	BIC
Saccade Amplitude - 4 Degrees	-0.273194	0.292065	-0.779674	0.233285	374.627257	402.471009
Saccade Amplitude - 8 Degrees	-0.762035	0.081778	-1.614598	0.090528	544.396230	572.239981
Saccade Amplitude - 10 Degrees	-1.097199	0.027524	-2.063693	-0.130706	585.285428	613.129179
Saccade Average Velocity - 4 Degrees	-5.639104	0.334781	-17.062325	5.784118	1390.417104	1418.260855
Saccade Average Velocity - 8 Degrees	-12.701729	0.134474	-29.248134	3.844676	1511.206822	1539.050574
Saccade Average Velocity - 10 Degrees	-19.272839	0.044792	-37.945135	-0.600542	1550.611128	1578.454880
Saccade End Time - 4 Degrees	2.679327	0.908942	-43.160285	48.518939	1843.394230	1871.237981
Saccade End Time - 8 Degrees	16.944212	0.544531	-37.739206	71.627631	1900.904515	1928.748267
Saccade End Time - 10 Degrees	35.760522	0.184244	-16.790240	88.311284	1887.935931	1915.779682
Saccade Peak Velocity - 4 Degrees	-22.305695	0.268920	-61.708288	17.096898	1794.064891	1821.908643
Saccade Peak Velocity - 8 Degrees	-40.538145	0.125065	-92.057721	10.981431	1881.475345	1909.319097
Saccade Peak Velocity - 10 Degrees	-55.139109	0.045352	-108.701515	-1.576702	1894.152050	1921.995801
Saccade Latency - 4 Degrees	12.310673	0.392484	-15.827012	40.448359	1684.293575	1712.137327
Saccade Latency - 8 Degrees	16.663553	0.323310	-16.298474	49.625580	1735.881902	1763.725654
Saccade Latency - 10 Degrees	28.495506	0.056539	-0.574660	57.565673	1694.922035	1722.765786
X Accuracy - 4 Degrees	12.877934	0.447417	-20.260378	46.016246	1737.620749	1765.464501
X Accuracy - 8 Degrees	26.291749	0.262328	-19.513431	72.096930	1843.149268	1870.993020
X Accuracy - 10 Degrees	55.192570	0.025038	7.386304	102.998837	1857.088874	1884.932626
Y Accuracy - 4 Degrees	11.303242	0.669501	-40.500975	63.107459	1883.271507	1911.115259
Y Accuracy - 8 Degrees	44.949604	0.118926	-11.237223	101.136430	1909.746219	1937.589971
Y Accuracy - 10 Degrees	92.725785	0.006144	27.306451	158.145119	1959.342397	1987.186149
Correct Saccade Count - 4 Degrees	-1.258395	0.068997	-2.605308	0.088518	693.483526	721.327277
Correct Saccade Count - 8 Degrees	-2.594418	0.058805	-5.265535	0.076699	916.689720	944.533472
Correct Saccade Count - 10 Degrees	-3.671454	0.014370	-6.577967	-0.764940	944.222820	972.066572
Hypometric Saccade Count - 4 Degrees	-1.481996	0.522950	-6.018694	3.054703	1089.372825	1117.216577
Hypometric Saccade Count - 8 Degrees	-2.101307	0.372542	-6.706516	2.503901	1094.259030	1122.102782
Hypometric Saccade Count - 10 Degrees	-3.058308	0.182245	-7.531970	1.415354	1084.811366	1112.655118
Hypermetric Saccade Count - 4 Degrees	2.386480	0.322775	-2.328966	7.101926	1101.970774	1129.814526
Hypermetric Saccade Count - 8 Degrees	4.078239	0.069655	-0.297307	8.453784	1077.581950	1105.425701
Hypermetric Saccade Count - 10 Degrees	6.561568	0.002691	2.345253	10.777884	1065.497252	1093.341003

Table 22: GBA-PD Generalised Linear Model Results for Oblique Saccades

Metric	Estimate	Pr(> t)	CI 0.025	CI 0.975	AIC	BIC
RMSE Gaze Horizontal 0.2Hz	-0.421514	0.378423	-1.356779	0.513751	574.578120	602.421872
RMSE Gaze Horizontal 0.4Hz	-0.200525	0.719674	-1.293623	0.892573	625.414934	653.258686
RMSE Gaze Vertical 0.2Hz	-0.609314	0.244041	-1.630558	0.411929	603.248722	631.092474
RMSE Gaze Vertical 0.4Hz	0.335037	0.471616	-0.574946	1.245020	565.644425	593.488177
RMSE Gaze Anticlockwise 0.2Hz	0.109441	0.853899	-1.053460	1.272342	645.594940	673.438691
RMSE Gaze Anticlockwise 0.4Hz	0.256256	0.687830	-0.991405	1.503918	668.530155	696.373907
RMSE Gaze Clockwise 0.2Hz	0.529646	0.403773	-0.710315	1.769607	666.511812	694.355564
RMSE Gaze Clockwise 0.4Hz	0.074275	0.909719	-1.207462	1.356013	677.314315	705.158067
Pursuit Gain Horizontal 0.2Hz	3.005834	0.005545	0.911469	5.100200	837.391491	865.235243
Pursuit Gain Horizontal 0.4Hz	0.081460	0.876986	-0.948286	1.111206	605.951538	633.795290
Pursuit Gain Vertical 0.2Hz	0.543213	0.375371	-0.654375	1.740801	655.176643	683.020395
Pursuit Gain Vertical 0.4Hz	-0.082903	0.802047	-0.729927	0.564121	454.464705	482.308457
Pursuit Gain Anticlockwise 0.2Hz	0.063871	0.534003	-0.136971	0.264712	73.087512	100.931264
Pursuit Gain Anticlockwise 0.4Hz	-0.008566	0.865308	-0.107383	0.090251	-158.126637	-130.282885
Pursuit Gain Clockwise 0.2Hz	0.029466	0.779067	-0.176042	0.234974	80.575591	108.419343
Pursuit Gain Clockwise 0.4Hz	-0.002857	0.960783	-0.116574	0.110859	-112.343904	-84.500152

Table 23: GBA-PD Generalised Linear Model Results for Pursuit

Metric	Estimate	Pr(> t)	CI 0.025	CI 0.975	AIC	BIC
Accuracy	51.241076	0.330097	-51.554969	154.037120	2106.671262	2134.515014
Saccade Average Velocity	-21.198368	0.026047	-39.688134	-2.708602	1547.408649	1575.252401
Saccade End Time	-19.987456	0.809341	-182.075053	142.100140	2255.128413	2282.972165
Saccade Peak Velocity	-73.047788	0.022702	-135.258552	-10.837025	1942.947918	1970.791670
Saccade Latency	1.425259	0.985920	-156.606280	159.456799	2246.866830	2274.710582
Saccade Amplitude	-1.357749	0.012388	-2.409386	-0.306112	612.809141	640.652893
Number of Correct Saccades	-4.787668	0.029928	-9.070049	-0.505287	1070.565755	1098.409507
Number of Hypometric Saccades	4.090843	0.053508	-0.030139	8.211825	1058.041573	1085.885325
Number of Hypermetric Saccades	4.090843	0.033508	0.030139	8.211825	1058.041573	1085.885325

Table 24: Generalised Linear Model Results for Reflexive Saccades Horizontal

Metric	Estimate	Pr(> t)	CI 0.025	CI 0.975	AIC	BIC
Accuracy	51.144012	0.155373	-19.064193	121.352216	1982.373430	2010.217182
Saccade Average Velocity	-25.492556	0.013044	-45.386404	-5.598709	1571.269605	1599.113357
Saccade End Time	11.280265	0.791508	-72.209430	94.769960	2038.855547	2066.699299
Saccade Peak Velocity	-73.761202	0.030883	-140.124520	-7.397884	1964.012876	1991.856628
Saccade Latency	40.551165	0.053534	-0.303244	81.405575	1805.860592	1833.704344
Saccade Amplitude	-1.386879	0.027673	-2.609738	-0.164021	661.984089	689.827840
Number of Correct Saccades	-4.768116	0.022790	-8.831533	-0.704700	1053.455665	1081.299416
Number of Hypometric Saccades	6.335645	0.006994	1.793005	10.878285	1089.799512	1117.643263
Number of Hypermetric Saccades	-1.714055	0.263712	-4.708968	1.280858	953.990144	981.833896

Table 25: GBA-PD Generalised Linear Model Results for Reflexive Saccades Vertical

Metric	Estimate	Pr(> t)	CI 0.025	CI 0.975	AIC	BIC
Total Number of Saccades	-0.158177	0.985117	-16.751205	16.434851	1512.124112	1539.967864
Saccadic Steps	0.044317	0.821273	-0.339526	0.428161	284.244135	312.087887
Accuracy	-67.785901	0.175983	-165.516121	29.944319	2090.196511	2118.040263
Number of Correct Saccades	-5.199585	0.441689	-18.411915	8.012744	1437.850824	1465.694576
Number of Hypometric Saccades	3.364383	0.531084	-7.139725	13.868491	1363.071625	1390.915377
Number of Hypermetric Saccades	4.373714	0.342222	-4.624151	13.371578	1312.613638	1340.457390
Saccade Amplitude	1.509809	0.374745	-1.814407	4.834025	987.998017	1015.841769
Saccade Average Velocity	5.101787	0.778867	-30.446861	40.650435	1760.509872	1788.353624
Saccade End Time	-515.745039	0.526585	-2108.472013	1076.981935	3000.059927	3027.903679
Saccade Peak Velocity	-27.603226	0.483123	-104.563298	49.356847	2012.307262	2040.151013
Saccade Latency	-520.274279	0.530263	-2141.402596	1100.854037	3005.821904	3033.665655

Table 26: GBA-PD Generalised Linear Model Results for Volitional Saccades Horizontal

Metric	Estimate	Pr(> t)	CI 0.025	CI 0.975	AIC	BIC
Total Number of Saccades	3.513043	0.641339	-11.239062	18.265148	1473.787556	1501.631307
Saccadic Steps	-0.041401	0.846543	-0.459979	0.377178	312.485542	340.329294
Accuracy	-16.189147	0.644099	-84.738493	52.360199	1974.578341	2002.422092
Number of Correct Saccades	-3.356593	0.559601	-14.608229	7.895043	1385.483193	1413.326945
Number of Hypometric Saccades	15.564045	0.014382	3.241198	27.886892	1415.130117	1442.973869
Number of Hypermetric Saccades	-7.677173	0.152539	-18.143277	2.788932	1361.890043	1389.733795
Saccade Amplitude	-0.396957	0.758352	-2.921448	2.127534	898.284655	926.128407
Saccade Average Velocity	-10.240360	0.476512	-38.364145	17.883425	1684.132486	1711.976237
Saccade End Time	569.474842	0.553314	-1309.263121	2448.212805	3053.899685	3081.743437
Saccade Peak Velocity	-62.079600	0.121488	-140.221237	16.062036	2017.274291	2045.118043
Saccade Latency	587.437004	0.541331	-1293.381490	2468.255498	3054.260500	3082.104252

Table 27: GBA-PD Generalised Linear Model Results for Volitional Saccades Vertical

Table 28: Composite Scores for iPD, GBA-PD, LRRK2-PD

Paradigm	GBA Weighted Z	iPD Weighted Z	LRRK2 Weighted Z
Antisaccades Horizontal	31.971774744429904	1.2269597367314422	0.2104448708127101
Antisaccades Vertical	62.81707826	6.2417830496607065	0.3352666185605462
Central Fixation	0.012343471	0.2406766227101482	5.427186678307486
Memory Guided Saccades Horizontal	0.058742456	0.057633408	0.008844454
Memory Guided Saccades Vertical	0.029644893	0.068386545	0.0282616793459376
Nystagmus/ Positional Fixation	0.008395331	0.1573770656709374	0.0240582765990732
Oblique Saccades	3.446786312828965	0.1095234367445423	0.5788340895306906
Pursuit	0.1860802915320841	0.9712654321867285	0.6165419881039349
Reflexive Saccades Horizontal	0.008259874	0.032444519	0.003351059
Reflexive Saccades Vertical	0.048010802	0.003005667	0.00370069
Volitional Saccades Horizontal	0.033429549	0.0210926418831605	0.020592257
Volitional Saccades Vertical	0.0304846305308607	0.06266768	0.013472925

B Ocular Motor Function in Atypical Parkinsonian Syndromes

Table 29: Atypical Parkinsonian Syndromes Generalised Linear Model Results Memory Guided Saccades Vertical

Metric	Estimate	Pr(> t)	CI 0.025	CI 0.975	AIC	BIC
Total Number of Saccades	-7.706886	0.274886	-21.445053	6.031280	769.183648	791.376821
Total Number of Saccades	5.670241	0.577720	-14.209561	25.550043	769.183648	791.376821
Total Number of Saccades	-37.110443	0.011017	-65.047336	-9.173549	769.183648	791.376821
Total Number of Saccades	2.302021	0.731146	-10.782702	15.386744	769.183648	791.376821
Total Number of Saccades	-6.539372	0.279490	-18.309457	5.230713	769.183648	791.376821
Average Number of Saccadic Steps	0.586623	0.000787	0.257419	0.915828	119.945254	142.138427
Average Number of Saccadic Steps	-0.068821	0.777800	-0.545196	0.407553	119.945254	142.138427
Average Number of Saccadic Steps	0.135238	0.693214	-0.534206	0.804683	119.945254	142.138427
Average Number of Saccadic Steps	0.214561	0.183694	-0.098984	0.528107	119.945254	142.138427
Average Number of Saccadic Steps	0.308278	0.035251	0.026234	0.590321	119.945254	142.138427
Average Accuracy (pixels)	119.250381	0.000463	55.286263	183.214500	1036.820777	1059.013950
Average Accuracy (pixels)	40.548211	0.393149	-52.011009	133.107430	1036.820777	1059.013950
Average Accuracy (pixels)	190.323231	0.005297	60.250654	320.395809	1036.820777	1059.013950
Average Accuracy (pixels)	51.250790	0.103153	-9.670932	112.172512	1036.820777	1059.013950
Average Accuracy (pixels)	163.045268	0.000000	108.244428	217.846108	1036.820777	1059.013950
Total Number of Correct Saccades	-13.521364	0.001958	-21.793956	-5.248773	680.925623	703.118796
Total Number of Correct Saccades	0.751041	0.902446	-11.219805	12.721887	680.925623	703.118796
Total Number of Correct Saccades	-15.912710	0.067477	-32.735225	0.909804	680.925623	703.118796
Total Number of Correct Saccades	-7.101550	0.081168	-14.980663	0.777563	680.925623	703.118796
Total Number of Correct Saccades	-14.203297	0.000182	-21.290786	-7.115808	680.925623	703.118796
Total Number of Hypometric Saccades	20.098022	0.002220	7.642013	32.554031	752.136055	774.329228
Total Number of Hypometric Saccades	9.574353	0.030100	8.450104	27.598811	752.136055	774.329228
Total Number of Hypometric Saccades	-4.486494	0.729396	-29.816089	20.843102	752.136055	774.329228
Total Number of Hypometric Saccades	9.571298	0.117813	-2.292252	21.434849	752.136055	774.329228
Total Number of Hypometric Saccades	17.377854	0.002031	6.706250	28.049459	752.136055	774.329228
Total Number of Hypermetric Saccades	-14.075211	0.002940	-23.063324	-5.087099	695.359795	717.552968
Total Number of Hypermetric Saccades	-6.722729	0.314117	-19.728969	6.283511	695.359795	717.552968
Total Number of Hypermetric Saccades	-14.934796	0.113256	-33.212339	3.342747	695.359795	717.552968
Total Number of Hypermetric Saccades	-1.477723	0.736014	-10.038323	7.082878	695.359795	717.552968
Total Number of Hypermetric Saccades	-9.860087	0.014130	-17.560593	-2.159580	695.359795	717.552968
Average Saccade Amplitude	-7.775884	0.000000	-10.182042	-5.369725	466.050168	488.243341
Average Saccade Amplitude	-2.575443	0.151087	-6.057272	0.906387	466.050168	488.243341
Average Saccade Amplitude	-4.370869	0.083858	-9.263850	0.522112	466.050168	488.243341
Average Saccade Amplitude	-2.770667	0.020248	-5.062379	-0.478956	466.050168	488.243341
Average Saccade Amplitude	-7.092393	0.000000	-9.153854	-5.030933	466.050168	488.243341
Average Saccade Velocity	-72.949359	0.000002	-100.693101	-45.205617	891.476495	913.669668
Average Saccade Velocity	-9.263072	0.652346	-49.409629	30.883486	891.476495	913.669668
Average Saccade Velocity	-74.301310	0.011694	-130.718879	-17.883741	891.476495	913.669668
Average Saccade Velocity	-20.736855	0.128015	-47.160990	5.687281	891.476495	913.669668
Average Saccade Velocity	-64.905569	0.000001	-88.674838	-41.136299	891.476495	913.669668
Average Saccade End Time (ms)	1780.152223	0.021980	287.119716	3273.184729	1584.962936	1607.156109
Average Saccade End Time (ms)	-504.756198	0.648276	-2665.247540	1655.735143	1584.962936	1607.156109
Average Saccade End Time (ms)	-734.941104	0.636494	-3771.058721	2301.176513	1584.962936	1607.156109
Average Saccade End Time (ms)	-504.927791	0.488508	-1926.945528	917.089945	1584.962936	1607.156109
Average Saccade End Time (ms)	193.426384	0.767720	-1085.719456	1472.572224	1584.962936	1607.156109
Peak Saccade Velocity	-161.405054	0.000367	-246.371088	-76.439019	1086.224476	1108.417649
Peak Saccade Velocity	5.069978	0.935789	-117.880045	128.020002	1086.224476	1108.417649
Peak Saccade Velocity	-177.378347	0.047616	-350.158828	-4.597866	1086.224476	1108.417649
Peak Saccade Velocity	-59.114036	0.156169	-140.038736	21.810665	1086.224476	1108.417649
Peak Saccade Velocity	-169.903924	0.000017	-242.698019	-97.109830	1086.224476	1108.417649

Table 30: Atypical Parkinsonian Syndromes Generalised Linear Model Results Memory Guided Saccades Horizontal

Metric	Estimate	Pr(> t)	CI 0.025	CI 0.975	AIC	BIC
Total Number of Saccades	-20.384553	0.007432	-34.925001	-5.844105	779.059268	801.252441
Total Number of Saccades	-2.375957	0.825412	-23.416699	18.664786	779.059268	801.252441
Total Number of Saccades	-27.347394	0.043670	-56.915746	-2.220958	779.059268	801.252441
Total Number of Saccades	-4.567743	0.519860	-18.416587	9.281102	779.059268	801.252441
Total Number of Saccades	-9.738892	0.129456	-22.196326	2.718542	779.059268	801.252441
Average Number of Saccadic Steps	1.596417	0.000000	1.088524	2.104309	195.390233	217.583406
Average Number of Saccadic Steps	-0.210986	0.575260	-0.945931	0.523960	195.390233	217.583406
Average Number of Saccadic Steps	-0.407782	0.441331	-1.440593	0.625030	195.390233	217.583406
Average Number of Saccadic Steps	0.262988	0.289871	-0.220747	0.746723	195.390233	217.583406
Average Number of Saccadic Steps	0.697798	0.002355	0.262664	1.132931	195.390233	217.583406
Average Accuracy (pixels)	1.501651	0.980803	-120.427751	123.431053	1149.071644	1171.264817
Average Accuracy (pixels)	141.718845	0.119418	-34.718987	318.156676	1149.071644	1171.264817
Average Accuracy (pixels)	306.018343	0.017862	58.071962	553.964723	1149.071644	1171.264817
Average Accuracy (pixels)	163.192055	0.007298	47.062118	279.321993	1149.071644	1171.264817
Average Accuracy (pixels)	153.457887	0.005127	48.995669	257.920105	1149.071644	1171.264817
Total Number of Correct Saccades	-6.587521	0.194356	-16.451598	3.276556	711.541225	733.734398
Total Number of Correct Saccades	-9.566658	0.192777	-23.840462	4.707145	711.541225	733.734398
Total Number of Correct Saccades	-14.061044	0.173354	-34.119882	5.997795	711.541225	733.734398
Total Number of Correct Saccades	-7.139393	0.140358	-16.534294	2.255508	711.541225	733.734398
Total Number of Correct Saccades	-8.961162	0.040930	-17.412146	-0.510179	711.541225	733.734398
Total Number of Hypometric Saccades	-2.427269	0.759091	-17.886386	13.031848	789.719316	811.912489
Total Number of Hypometric Saccades	26.555364	0.022547	4.185263	48.925466	789.719316	811.912489
Total Number of Hypometric Saccades	12.526033	0.437161	-18.910455	43.962521	789.719316	811.912489
Total Number of Hypometric Saccades	4.039998	0.592237	-10.683820	18.763816	789.719316	811.912489
Total Number of Hypometric Saccades	9.462289	0.165351	-3.782209	22.706786	789.719316	811.912489
Total Number of Hypermetric Saccades	-11.454984	0.082218	-24.208850	1.298882	756.247895	778.441068
Total Number of Hypermetric Saccades	-19.066899	0.046256	-37.522370	-0.611429	756.247895	778.441068
Total Number of Hypermetric Saccades	-26.700591	0.047007	-52.635885	-0.765297	756.247895	778.441068
Total Number of Hypermetric Saccades	-1.715431	0.782668	-13.862670	10.431809	756.247895	778.441068
Total Number of Hypermetric Saccades	-10.662992	0.059418	-21.589783	0.263800	756.247895	778.441068
Average Saccade Amplitude	-6.229699	0.001765	-10.001517	-2.457880	544.267678	566.460851
Average Saccade Amplitude	-7.152074	0.012104	-12.610081	-1.694066	544.267678	566.460851
Average Saccade Amplitude	-12.090524	0.002767	-19.760608	-4.420439	544.267678	566.460851
Average Saccade Amplitude	-2.458824	0.183604	-6.051240	1.133592	544.267678	566.460851
Average Saccade Amplitude	-8.893078	0.000001	-12.124559	-5.661597	544.267678	566.460851
Average Saccade Velocity	-49.981426	0.002956	-81.917387	-18.045465	915.962186	938.155359
Average Saccade Velocity	-34.847023	0.143406	-81.059927	11.365880	915.962186	938.155359
Average Saccade Velocity	-95.287690	0.005178	-160.230237	-30.345144	915.962186	938.155359
Average Saccade Velocity	-10.882077	0.485236	-41.299032	19.534878	915.962186	938.155359
Average Saccade Velocity	-74.795463	0.000001	-102.156389	-47.434537	915.962186	938.155359
Average Saccade End Time (ms)	-245.341619	0.752853	-1767.162083	1276.478844	1588.285988	1610.479161
Average Saccade End Time (ms)	3296.901952	0.004375	1094.753000	5499.050881	1588.285988	1610.479161
Average Saccade End Time (ms)	950.213941	0.549026	-2144.444681	4044.872563	1588.285988	1610.479161
Average Saccade End Time (ms)	-241.194333	0.745174	-1690.630752	1208.242087	1588.285988	1610.479161
Average Saccade End Time (ms)	27.819335	0.966748	-1275.990399	1331.629069	1588.285988	1610.479161
Peak Saccade Velocity	-96.265889	0.007344	-164.825891	-27.705888	1048.894118	1071.087291
Peak Saccade Velocity	1.729216	0.972834	-97.480472	100.938905	1048.894118	1071.087291
Peak Saccade Velocity	-169.607782	0.019506	-309.026199	-30.189365	1048.894118	1071.087291
Peak Saccade Velocity	4.432426	0.894500	-60.866580	69.731432	1048.894118	1071.087291
Peak Saccade Velocity	-171.861168	0.000000	-230.599501	-113.122835	1048.894118	1071.087291
Average Saccade Start Time (ms)	-223.340450	0.778383	-1773.464010	1326.783109	1591.492347	1613.685520
Average Saccade Start Time (ms)	3514.543493	0.002926	1271.438594	5757.648392	1591.492347	1613.685520
Average Saccade Start Time (ms)	609.410339	0.705767	-2542.803312	3761.623991	1591.492347	1613.685520
Average Saccade Start Time (ms)	-254.673542	0.736194	-1731.066847	1221.719762	1591.492347	1613.685520
Average Saccade Start Time (ms)	44.364235	0.947963	-1283.693992	1372.422461	1591.492347	1613.685520

Table 31: Atypical Parkinsonian Syndromes Generalised Linear Model Results Volitional Saccades Vertical

Metric	Estimate	Pr(> t)	CI 0.025	CI 0.975	AIC	BIC
Total Number of Saccades	-18.485028	0.010370	-32.281305	-4.688752	769.918086	792.111259
Total Number of Saccades	6.987819	0.494701	-12.976071	26.951709	769.918086	792.111259
Total Number of Saccades	-41.082876	0.005263	-69.137938	-13.027814	769.918086	792.111259
Total Number of Saccades	3.753599	0.577142	-9.386470	16.893668	769.918086	792.111259
Total Number of Saccades	-6.982828	0.250398	-18.802698	4.837042	769.918086	792.111259
Average Number of Saccadic Steps	0.790689	0.000015	0.454720	1.126659	123.484846	145.678019
Average Number of Saccadic Steps	-0.078844	0.751431	-0.565008	0.407321	123.484846	145.678019
Average Number of Saccadic Steps	-0.296818	0.397061	-0.980020	0.386384	123.484846	145.678019
Average Number of Saccadic Steps	0.198938	0.226655	-0.121051	0.518928	123.484846	145.678019
Average Number of Saccadic Steps	0.228185	0.012424	0.059654	0.516025	123.484846	145.678019
Average Accuracy (pixels)	79.050699	0.027256	10.178562	147.922836	1049.684497	1071.877670
Average Accuracy (pixels)	7.604221	0.881504	-92.057143	107.265585	1049.684497	1071.877670
Average Accuracy (pixels)	116.584513	0.010676	23.468639	256.637666	1049.684497	1071.877670
Average Accuracy (pixels)	13.701281	0.683366	-51.895014	79.297576	1049.684497	1071.877670
Average Accuracy (pixels)	168.039663	0.000000	109.033910	227.045416	1049.684497	1071.877670
Total Number of Correct Saccades	-16.784743	0.006141	-28.467926	-5.101561	740.990872	763.184045
Total Number of Correct Saccades	4.288200	0.620471	-12.617939	21.194338	740.990872	763.184045
Total Number of Correct Saccades	-19.931507	0.010409	-43.689540	-3.826526	740.990872	763.184045
Total Number of Correct Saccades	-3.099364	0.586664	-14.226847	8.028118	740.990872	763.184045
Total Number of Correct Saccades	-17.056554	0.001281	-27.066045	-7.047064	740.990872	763.184045
Total Number of Hypometric Saccades	10.882090	0.089461	-1.522655	23.286835	751.418454	773.611627
Total Number of Hypometric Saccades	-0.314921	0.972656	-18.265196	17.635353	751.418454	773.611627
Total Number of Hypometric Saccades	-4.404047	0.733119	-29.629395	20.821301	751.418454	773.611627
Total Number of Hypometric Saccades	10.164900	0.095689	-1.649824	21.979624	751.418454	773.611627
Total Number of Hypometric Saccades	12.270453	0.026386	1.642769	22.898137	751.418454	773.611627
Total Number of Hypermetric Saccades	-11.219276	0.039203	-21.705988	-0.732564	722.191653	744.384826
Total Number of Hypermetric Saccades	2.134631	0.783493	-13.040156	17.309418	722.191653	744.384826
Total Number of Hypermetric Saccades	-14.059934	0.200042	-35.384916	7.265048	722.191653	744.384826
Total Number of Hypermetric Saccades	-2.639587	0.605923	-12.627508	7.348334	722.191653	744.384826
Total Number of Hypermetric Saccades	-5.017468	0.277032	-14.001890	3.966954	722.191653	744.384826
Average Saccade Amplitude	-6.869514	0.000004	-9.577212	-4.161817	486.593863	508.787036
Average Saccade Amplitude	0.507067	0.800427	-3.411104	4.425239	486.593863	508.787036
Average Saccade Amplitude	-4.864011	0.047287	-10.370179	-0.642158	486.593863	508.787036
Average Saccade Amplitude	-1.754570	0.186210	-4.333478	0.824338	486.593863	508.787036
Average Saccade Amplitude	-6.086338	0.000002	-8.406140	-3.766536	486.593863	508.787036
Average Saccade Velocity	-71.840811	0.000007	-101.097102	-42.584520	900.713164	922.906337
Average Saccade Velocity	7.910630	0.715171	-34.424659	50.245919	900.713164	922.906337
Average Saccade Velocity	-51.334660	0.094744	-110.828033	8.158713	900.713164	922.906337
Average Saccade Velocity	-15.954570	0.265168	-43.819311	11.910171	900.713164	922.906337
Average Saccade Velocity	-65.004162	0.000002	-90.069298	-39.939026	900.713164	922.906337
Average Saccade End Time (ms)	192.005519	0.797449	-1269.347831	1653.358869	1581.231274	1603.424447
Average Saccade End Time (ms)	-643.650594	0.552502	-2758.300641	1470.999453	1581.231274	1603.424447
Average Saccade End Time (ms)	-510.537879	0.737219	-3482.235168	2461.159409	1581.231274	1603.424447
Average Saccade End Time (ms)	-651.859611	0.361448	-2043.704982	739.985760	1581.231274	1603.424447
Average Saccade End Time (ms)	20.115067	0.974959	-1231.889863	1272.119997	1581.231274	1603.424447
Peak Saccade Velocity	-154.810677	0.001008	-243.650650	-65.970703	1093.982286	1116.175459
Peak Saccade Velocity	47.353032	0.472460	-81.202771	175.908835	1093.982286	1116.175459
Peak Saccade Velocity	-151.502020	0.104223	-332.160249	29.156209	1093.982286	1116.175459
Peak Saccade Velocity	-50.047634	0.249835	-134.662012	34.566745	1093.982286	1116.175459
Peak Saccade Velocity	-165.444985	0.000056	-241.558052	-89.331919	1093.982286	1116.175459
Average Saccade Start Time (ms)	239.347558	0.749113	-1222.392177	1701.087293	1581.277274	1603.470447
Average Saccade Start Time (ms)	-640.111196	0.554788	-2755.320361	1475.097968	1581.277274	1603.470447
Average Saccade Start Time (ms)	-926.051029	0.543211	-3898.534041	2046.431982	1581.277274	1603.470447
Average Saccade Start Time (ms)	-616.047194	0.388419	-2008.260572	776.166183	1581.277274	1603.470447
Average Saccade Start Time (ms)	58.789211	0.926925	-1193.546751	1311.125174	1581.277274	1603.470447

Table 32: Atypical Parkinsonian Syndromes Generalised Linear Model Results Volitional Saccades Horizontal

Metric	Estimate	Pr(> t)	CI 0.025	CI 0.975	AIC	BIC
Total Number of Saccades	-20.581352	0.010608	-35.991817	-5.170887	789.170845	811.364018
Total Number of Saccades	-1.339799	0.906559	-23.639498	20.959900	789.170845	811.364018
Total Number of Saccades	-31.765688	0.040418	-63.103240	-0.428136	789.170845	811.364018
Total Number of Saccades	-3.437569	0.647468	-18.115049	11.239910	789.170845	811.364018
Total Number of Saccades	-6.165782	0.362813	-19.368597	7.037033	789.170845	811.364018
Average Number of Saccadic Steps	1.227629	0.000002	0.758473	1.696785	181.585956	203.779129
Average Number of Saccadic Steps	0.081639	0.814281	-0.597252	0.760531	181.585956	203.779129
Average Number of Saccadic Steps	-0.358856	0.463167	-1.312896	0.595183	181.585956	203.779129
Average Number of Saccadic Steps	0.314878	0.171130	-0.131963	0.761719	181.585956	203.779129
Average Number of Saccadic Steps	0.753302	0.000434	0.351356	1.155248	181.585956	203.779129
Average Accuracy (pixels)	-39.269571	0.501436	-153.238358	74.699215	1137.323583	1159.516756
Average Accuracy (pixels)	-6.713188	0.936612	-171.631618	158.205242	1137.323583	1159.516756
Average Accuracy (pixels)	277.744119	0.021331	45.985842	509.502396	1137.323583	1159.516756
Average Accuracy (pixels)	53.149000	0.340150	-55.398962	161.696962	1137.323583	1159.516756
Average Accuracy (pixels)	89.042136	0.077718	-8.599877	186.684149	1137.323583	1159.516756
Total Number of Correct Saccades	-10.809056	0.115176	-24.108909	2.490798	763.541732	785.734905
Total Number of Correct Saccades	-5.673384	0.565058	-24.918926	13.572157	763.541732	785.734905
Total Number of Correct Saccades	-37.836894	0.007551	-64.882468	-10.791321	763.541732	785.734905
Total Number of Correct Saccades	-9.710662	0.136955	-22.377920	2.956596	763.541732	785.734905
Total Number of Correct Saccades	-14.607254	0.014022	-26.001816	-3.212691	763.541732	785.734905
Total Number of Hypometric Saccades	-8.745750	0.202490	-22.083621	4.592121	764.038394	786.231567
Total Number of Hypometric Saccades	3.014135	0.760346	-16.286419	22.314690	764.038394	786.231567
Total Number of Hypometric Saccades	8.922035	0.520972	-18.200848	36.044917	764.038394	786.231567
Total Number of Hypometric Saccades	-3.052587	0.638960	-15.756054	9.650879	764.038394	786.231567
Total Number of Hypometric Saccades	6.211856	0.289919	-5.215278	17.638990	764.038394	786.231567
Total Number of Hypermetric Saccades	1.725662	0.761426	-9.375974	12.827298	732.106792	754.299965
Total Number of Hypermetric Saccades	3.244339	0.693301	-12.820273	19.308952	732.106792	754.299965
Total Number of Hypermetric Saccades	4.381566	0.704669	-18.193879	26.957010	732.106792	754.299965
Total Number of Hypermetric Saccades	11.621553	0.034271	1.047956	22.195149	732.106792	754.299965
Total Number of Hypermetric Saccades	3.766593	0.439964	-5.744661	13.277847	732.106792	754.299965
Average Saccade Amplitude	-3.418959	0.051191	-6.803405	-0.034513	525.411779	547.604952
Average Saccade Amplitude	1.129219	0.652569	-3.768239	6.026678	525.411779	547.604952
Average Saccade Amplitude	-8.096673	0.023746	-14.979024	-1.214321	525.411779	547.604952
Average Saccade Amplitude	0.114797	0.944529	-3.108671	3.338264	525.411779	547.604952
Average Saccade Amplitude	-6.604920	0.000026	-9.504521	-3.705318	525.411779	547.604952
Average Saccade Velocity	-34.578827	0.050039	-68.633903	-0.523750	927.141068	949.334241
Average Saccade Velocity	13.218730	0.600540	-36.060639	62.498098	927.141068	949.334241
Average Saccade Velocity	-42.827238	0.229088	-112.079059	26.424582	927.141068	949.334241
Average Saccade Velocity	6.610708	0.690629	-25.824569	39.045985	927.141068	949.334241
Average Saccade Velocity	-65.223274	0.000036	-94.399739	-36.046810	927.141068	949.334241
Average Saccade End Time (ms)	-527.373148	0.530090	-2166.369124	1111.622827	1601.192708	1623.385881
Average Saccade End Time (ms)	-1925.466966	0.115560	-4297.174614	446.240682	1601.192708	1623.385881
Average Saccade End Time (ms)	1739.424238	0.309485	-1593.513615	5072.362091	1601.192708	1623.385881
Average Saccade End Time (ms)	-1400.316575	0.082592	-2961.355157	160.722008	1601.192708	1623.385881
Average Saccade End Time (ms)	-394.339515	0.583588	-1798.538603	1009.859573	1601.192708	1623.385881
Peak Saccade Velocity	-75.952013	0.047970	-150.055980	-1.848045	1062.424320	1084.617493
Peak Saccade Velocity	56.855539	0.301885	-50.376541	164.087619	1062.424320	1084.617493
Peak Saccade Velocity	-59.492500	0.441368	-210.184706	91.199706	1062.424320	1084.617493
Peak Saccade Velocity	33.869152	0.349810	-36.710126	104.448430	1062.424320	1084.617493
Peak Saccade Velocity	-157.951195	0.000005	-221.439285	-94.463105	1062.424320	1084.617493
Average Saccade Start Time (ms)	-520.903380	0.536350	-2164.797125	1122.990365	1601.711892	1623.905065
Average Saccade Start Time (ms)	-1985.886594	0.105769	-4364.681555	392.908367	1601.711892	1623.905065
Average Saccade Start Time (ms)	1492.709754	0.384126	-1850.187831	4835.607340	1601.711892	1623.905065
Average Saccade Start Time (ms)	-1395.212335	0.084604	-2960.915729	170.491059	1601.711892	1623.905065
Average Saccade Start Time (ms)	-370.010293	0.608049	-1778.405513	1038.384927	1601.711892	1623.905065

Table 33: Atypical Parkinsonian Syndromes Generalised Linear Model Results Reflexive Saccades Vertical

Metric	Estimate	Pr(> t)	CI 0.025	CI 0.975	AIC	BIC
Average Accuracy (pixels)	102.830555	0.013092	23.440981	182.220128	1074.412566	1096.605739
Average Accuracy (pixels)	97.265708	0.100992	-17.614903	212.146318	1074.412566	1096.605739
Average Accuracy (pixels)	169.147058	0.043331	7.706446	330.587670	1074.412566	1096.605739
Average Accuracy (pixels)	40.828127	0.293144	-34.785351	116.441606	1074.412566	1096.605739
Average Accuracy (pixels)	153.348875	0.000031	85.332377	221.365373	1074.412566	1096.605739
Average Saccade Velocity	-51.243709	0.000016	-73.120101	-29.367318	850.133698	872.326871
Average Saccade Velocity	-14.579951	0.369427	-46.236163	17.076261	850.133698	872.326871
Average Saccade Velocity	-67.586611	0.003855	-112.072780	-23.100441	850.133698	872.326871
Average Saccade Velocity	-21.672359	0.044830	-42.508219	-0.836499	850.133698	872.326871
Average Saccade Velocity	-59.421560	0.000000	-78.164015	-40.679104	850.133698	872.326871
Average Saccade End Time (ms)	112.612629	0.026353	15.098755	210.126503	1110.191772	1132.384946
Average Saccade End Time (ms)	53.336357	0.460990	-87.771007	194.443720	1110.191772	1132.384946
Average Saccade End Time (ms)	482.218933	0.000008	283.922118	680.515749	1110.191772	1132.384946
Average Saccade End Time (ms)	-32.207703	0.498693	-125.083416	60.668010	1110.191772	1132.384946
Average Saccade End Time (ms)	82.199354	0.057397	-1.345020	165.743729	1110.191772	1132.384946
Peak Saccade Velocity	-127.142594	0.002516	-206.984176	-47.301012	1075.400435	1097.593608
Peak Saccade Velocity	-38.062686	0.520341	-153.597375	77.472004	1075.400435	1097.593608
Peak Saccade Velocity	-187.803391	0.026117	-350.163174	-25.443607	1075.400435	1097.593608
Peak Saccade Velocity	-68.406225	0.081749	-144.450213	7.637763	1075.400435	1097.593608
Peak Saccade Velocity	-164.747946	0.000010	-233.151700	-96.344192	1075.400435	1097.593608
Average Saccade Start Time (ms)	151.073821	0.001574	60.636702	241.510940	1097.082634	1119.275807
Average Saccade Start Time (ms)	-9.354247	0.888940	-140.221199	121.512704	1097.082634	1119.275807
Average Saccade Start Time (ms)	2.608551	0.977891	-181.297512	186.514613	1097.082634	1119.275807
Average Saccade Start Time (ms)	-0.125334	0.997732	-86.260892	86.010223	1097.082634	1119.275807
Average Saccade Start Time (ms)	104.556931	0.009856	27.075521	182.038342	1097.082634	1119.275807
Average Saccade Amplitude	-3.451672	0.000003	-4.804107	-2.099236	365.804570	387.997743
Average Saccade Amplitude	-1.943547	0.055156	-3.900588	0.013494	365.804570	387.997743
Average Saccade Amplitude	-3.805208	0.008208	-6.555419	-1.054997	365.804570	387.997743
Average Saccade Amplitude	-1.652685	0.013944	-2.940793	-0.364577	365.804570	387.997743
Average Saccade Amplitude	-3.417589	0.000000	-4.576280	-2.258899	365.804570	387.997743
Total Number of Correct Saccades	-6.504652	0.004196	-10.828245	-2.181059	568.023794	590.216967
Total Number of Correct Saccades	-6.965064	0.032085	-13.221515	-0.708613	568.023794	590.216967
Total Number of Correct Saccades	-6.491844	0.151804	-15.283974	2.300287	568.023794	590.216967
Total Number of Correct Saccades	-4.335889	0.042330	-8.453834	-0.217944	568.023794	590.216967
Total Number of Correct Saccades	-7.184656	0.000282	-10.888866	-3.480446	568.023794	590.216967
Total Number of Hypometric Saccades	9.429529	0.000109	4.893582	13.965476	576.366599	598.559772
Total Number of Hypometric Saccades	7.948452	0.020052	1.384714	14.512190	576.366599	598.559772
Total Number of Hypometric Saccades	6.165755	0.193946	-3.058203	15.389713	576.366599	598.559772
Total Number of Hypometric Saccades	7.595579	0.000914	3.275380	11.915778	576.366599	598.559772
Total Number of Hypometric Saccades	9.161325	0.000015	5.275181	13.047468	576.366599	598.559772
Total Number of Hypermetric Saccades	-3.923300	0.017031	-7.077840	-0.768760	513.171319	535.364492
Total Number of Hypermetric Saccades	-0.966968	0.679132	-5.531742	3.597806	513.171319	535.364492
Total Number of Hypermetric Saccades	-3.466567	0.292754	-9.881399	2.948266	513.171319	535.364492
Total Number of Hypermetric Saccades	-2.702683	0.081754	-5.707180	0.301814	513.171319	535.364492
Total Number of Hypermetric Saccades	-2.390451	0.086896	-5.093082	0.312180	513.171319	535.364492

Table 34: Atypical Parkinsonian Syndromes Generalised Linear Model Results Reflexive Saccades Horizontal

Metric	Estimate	Pr(> t)	CI 0.025	CI 0.975	AIC	BIC
Average Accuracy (pixels)	37.587763	0.513821	-74.739483	149.915009	1134.799163	1156.992336
Average Accuracy (pixels)	58.001413	0.486364	-104.541627	220.544453	1134.799163	1156.992336
Average Accuracy (pixels)	306.446419	0.010275	78.026255	534.866584	1134.799163	1156.992336
Average Accuracy (pixels)	155.052429	0.005725	48.067929	262.036929	1134.799163	1156.992336
Average Accuracy (pixels)	127.392274	0.011287	31.156640	223.627907	1134.799163	1156.992336
Average Saccade Velocity	-24.509117	0.023559	-45.313618	-3.704617	841.392165	863.585338
Average Saccade Velocity	-16.044506	0.299412	-46.149640	14.060627	841.392165	863.585338
Average Saccade Velocity	-59.003939	0.007730	-101.310393	-16.697485	841.392165	863.585338
Average Saccade Velocity	-17.341220	0.090214	-37.156173	2.473733	841.392165	863.585338
Average Saccade Velocity	-47.036353	0.000002	-64.860473	-29.212233	841.392165	863.585338
Average Saccade End Time (ms)	-37.260253	0.622111	-184.851312	110.330806	1182.306189	1204.499362
Average Saccade End Time (ms)	-42.960228	0.694459	-256.531736	170.611281	1182.306189	1204.499362
Average Saccade End Time (ms)	463.282334	0.003350	163.152355	763.412312	1182.306189	1204.499362
Average Saccade End Time (ms)	251.288375	0.000759	110.717354	391.859396	1182.306189	1204.499362
Average Saccade End Time (ms)	-45.083013	0.486732	-171.530688	81.364662	1182.306189	1204.499362
Peak Saccade Velocity	-70.944638	0.069433	-146.489523	4.600247	1065.775196	1087.968369
Peak Saccade Velocity	-16.343155	0.770276	-125.660313	92.974003	1065.775196	1087.968369
Peak Saccade Velocity	-202.804260	0.011502	-356.426607	-49.181914	1065.775196	1087.968369
Peak Saccade Velocity	-37.796740	0.306347	-109.748400	34.154920	1065.775196	1087.968369
Peak Saccade Velocity	-140.426071	0.000058	-205.148657	-75.703484	1065.775196	1087.968369
Average Saccade Start Time (ms)	-23.507845	0.752160	-168.901977	121.886287	1179.696689	1201.889862
Average Saccade Start Time (ms)	-160.169745	0.139655	-370.562193	50.222702	1179.696689	1201.889862
Average Saccade Start Time (ms)	-457.793358	0.003259	-753.455833	-162.130883	1179.696689	1201.889862
Average Saccade Start Time (ms)	245.168895	0.000846	106.690306	383.647484	1179.696689	1201.889862
Average Saccade Start Time (ms)	-48.919658	0.443760	-173.485130	75.645814	1179.696689	1201.889862
Average Saccade Amplitude	-1.266564	0.041385	-2.463778	-0.069350	344.592210	366.785383
Average Saccade Amplitude	-0.852907	0.337526	-2.585334	0.879521	344.592210	366.785383
Average Saccade Amplitude	-3.730947	0.003572	-6.165511	-1.296384	344.592210	366.785383
Average Saccade Amplitude	-1.817724	0.002492	-2.957994	-0.677455	344.592210	366.785383
Average Saccade Amplitude	-2.710750	0.000002	-3.736455	-1.685045	344.592210	366.785383
Total Number of Correct Saccades	-7.745232	0.003427	-12.775687	-2.714777	594.371525	616.564698
Total Number of Correct Saccades	-3.026458	0.417592	-10.305774	4.252858	594.371525	616.564698
Total Number of Correct Saccades	-8.808318	0.095421	-19.037870	1.421234	594.371525	616.564698
Total Number of Correct Saccades	-7.636011	0.002497	-12.427197	-2.844825	594.371525	616.564698
Total Number of Correct Saccades	-8.748369	0.000153	-13.058178	-4.438559	594.371525	616.564698
Total Number of Hypometric Saccades	9.225674	0.000375	4.360522	14.090827	588.557766	610.750939
Total Number of Hypometric Saccades	2.679253	0.457940	-4.360861	9.719368	588.557766	610.750939
Total Number of Hypometric Saccades	1.203520	0.812167	-8.689885	11.096925	588.557766	610.750939
Total Number of Hypometric Saccades	7.766057	0.001523	3.132311	12.399803	588.557766	610.750939
Total Number of Hypometric Saccades	9.383146	0.000032	5.214958	13.551333	588.557766	610.750939
Total Number of Hypermetric Saccades	-1.132528	0.217676	-2.918814	0.653758	414.216823	436.409996
Total Number of Hypermetric Saccades	-0.519310	0.694813	-3.104153	2.065534	414.216823	436.409996
Total Number of Hypermetric Saccades	-0.653466	0.725334	-4.285922	2.978990	414.216823	436.409996
Total Number of Hypermetric Saccades	0.268433	0.757952	-1.432890	1.969756	414.216823	436.409996
Total Number of Hypermetric Saccades	-0.178830	0.819440	-1.709219	1.351559	414.216823	436.409996

Table 35: Atypical Parkinsonian Syndromes Generalised Linear Model Results Oblique Saccades

Metric	Estimate	Pr(> t)	CI 0.025	CI 0.975	AIC	BIC
4 Degrees Average Saccade Amplitude	-1.002205	0.000323	-1.524524	-0.479886	200.263812	222.456985
4 Degrees Average Saccade Amplitude	0.577803	0.138032	-0.178019	1.333624	200.263812	222.456985
4 Degrees Average Saccade Amplitude	-0.530508	0.330600	-1.592657	0.531641	200.263812	222.456985
4 Degrees Average Saccade Amplitude	-0.229885	0.367845	-0.727361	0.267590	200.263812	222.456985
4 Degrees Average Saccade Amplitude	-0.670251	0.004358	-1.117745	-0.222758	200.263812	222.456985
8 Degrees Average Saccade Amplitude	-2.341507	0.000002	-3.230775	-1.452238	292.852780	315.045953
8 Degrees Average Saccade Amplitude	-0.727287	0.271336	-2.014102	0.559528	292.852780	315.045953
8 Degrees Average Saccade Amplitude	-0.392911	0.671373	-2.201260	1.415438	292.852780	315.045953
8 Degrees Average Saccade Amplitude	-1.081689	0.014373	-1.928660	-0.234717	292.852780	315.045953
8 Degrees Average Saccade Amplitude	-2.101289	0.000001	-2.863164	-1.339414	292.852780	315.045953
10 Degrees Average Saccade Amplitude	-2.909323	0.000001	-4.003563	-1.815083	328.943180	351.136353
10 Degrees Average Saccade Amplitude	-1.367204	0.094523	-2.950623	0.216215	328.943180	351.136353
10 Degrees Average Saccade Amplitude	-0.079774	0.944159	-2.304938	2.145390	328.943180	351.136353
10 Degrees Average Saccade Amplitude	-1.245490	0.021685	-2.287683	-0.203296	328.943180	351.136353
10 Degrees Average Saccade Amplitude	-2.927916	0.000000	-3.865400	-1.990433	328.943180	351.136353
4 Degrees Average Saccade Velocity	-25.416234	0.000186	-38.119586	-12.712882	755.557362	777.750535
4 Degrees Average Saccade Velocity	-4.226136	0.653513	-22.608510	14.156237	755.557362	777.750535
4 Degrees Average Saccade Velocity	-18.020011	0.175437	-43.852583	7.812561	755.557362	777.750535
4 Degrees Average Saccade Velocity	-8.594787	0.167742	-20.693915	3.504341	755.557362	777.750535
4 Degrees Average Saccade Velocity	-23.861508	0.000049	-34.745022	-12.977995	755.557362	777.750535
8 Degrees Average Saccade Velocity	-36.396267	0.000095	-53.736781	-19.055753	809.702637	831.895810
8 Degrees Average Saccade Velocity	-22.516820	0.082488	-47.609395	2.575755	809.702637	831.895810
8 Degrees Average Saccade Velocity	-57.323996	0.002065	-92.586349	-22.061642	809.702637	831.895810
8 Degrees Average Saccade Velocity	-14.414661	0.091075	-30.930389	2.101067	809.702637	831.895810
8 Degrees Average Saccade Velocity	-39.095965	0.000002	-53.952337	-24.239593	809.702637	831.895810
10 Degrees Average Saccade Velocity	-45.661983	0.000014	-64.950196	-26.373770	828.224690	850.417863
10 Degrees Average Saccade Velocity	-23.414845	0.104101	-51.325837	4.496146	828.224690	850.417863
10 Degrees Average Saccade Velocity	-39.822525	0.050060	-79.045572	-0.599478	828.224690	850.417863
10 Degrees Average Saccade Velocity	-15.689921	0.098097	-34.060707	2.680866	828.224690	850.417863
10 Degrees Average Saccade Velocity	-49.226339	0.000000	-65.751389	-32.701288	828.224690	850.417863
4 Degrees Average Saccade End Time (ms)	43.636325	0.037420	3.234050	84.038600	956.878880	979.072053
4 Degrees Average Saccade End Time (ms)	16.186759	0.588899	-42.277317	74.650834	956.878880	979.072053
4 Degrees Average Saccade End Time (ms)	214.857143	0.000002	132.698143	297.016144	956.878880	979.072053
4 Degrees Average Saccade End Time (ms)	-1.237295	0.949910	-39.717871	37.243282	956.878880	979.072053
4 Degrees Average Saccade End Time (ms)	5.876298	0.740218	-28.738087	40.490683	956.878880	979.072053
8 Degrees Average Saccade End Time (ms)	14.807379	0.529865	-31.186485	60.801244	979.433095	1001.626268
8 Degrees Average Saccade End Time (ms)	30.407746	0.373258	-36.147634	96.963127	979.433095	1001.626268
8 Degrees Average Saccade End Time (ms)	570.684355	0.000000	477.154722	664.213989	979.433095	1001.626268
8 Degrees Average Saccade End Time (ms)	-8.610792	0.701079	-52.416999	35.195415	979.433095	1001.626268
8 Degrees Average Saccade End Time (ms)	5.199590	0.796599	-34.205352	44.604533	979.433095	1001.626268
10 Degrees Average Saccade End Time (ms)	46.992562	0.059970	-1.269388	95.254513	987.808666	1010.001839
10 Degrees Average Saccade End Time (ms)	29.354311	0.412523	-40.483102	99.191723	987.808666	1010.001839
10 Degrees Average Saccade End Time (ms)	207.365709	0.000086	109.223868	305.507550	987.808666	1010.001839
10 Degrees Average Saccade End Time (ms)	-6.634379	0.778006	-52.600792	39.332035	987.808666	1010.001839
10 Degrees Average Saccade End Time (ms)	32.230269	0.130565	-9.117842	73.578380	987.808666	1010.001839
4 Degrees Peak Saccade Velocity	-63.508378	0.007166	-108.594565	-18.422192	975.964909	998.158083
4 Degrees Peak Saccade Velocity	10.168511	0.760806	-55.073414	75.410437	975.964909	998.158083
4 Degrees Peak Saccade Velocity	-51.879700	0.270772	-143.563547	39.804148	975.964909	998.158083
4 Degrees Peak Saccade Velocity	-30.328717	0.170172	-73.270419	12.612985	975.964909	998.158083
4 Degrees Peak Saccade Velocity	-75.251864	0.000266	-113.879159	-36.624568	975.964909	998.158083
8 Degrees Peak Saccade Velocity	-99.045623	0.000568	-153.088984	-45.002262	1007.495587	1029.688760
8 Degrees Peak Saccade Velocity	-58.329551	0.147741	-136.532948	19.873845	1007.495587	1029.688760
8 Degrees Peak Saccade Velocity	-98.472034	0.082933	-208.370512	11.426444	1007.495587	1029.688760
8 Degrees Peak Saccade Velocity	-47.028366	0.077167	-98.501203	4.444470	1007.495587	1029.688760
8 Degrees Peak Saccade Velocity	-122.339196	0.000002	-168.640493	-76.037900	1007.495587	1029.688760
10 Degrees Peak Saccade Velocity	-105.679542	0.000450	-162.236552	-49.122532	1015.406054	1037.599227
10 Degrees Peak Saccade Velocity	-43.969441	0.295550	-125.810211	37.871330	1015.406054	1037.599227
10 Degrees Peak Saccade Velocity	-67.377428	0.254341	-182.387472	47.632617	1015.406054	1037.599227

Metric	Estimate	Pr(> t)	CI 0.025	CI 0.975	AIC	BIC
10 Degrees Peak Saccade Velocity	-37.749297	0.173476	-91.616223	16.117629	1015.406054	1037.599227
10 Degrees Peak Saccade Velocity	-138.298972	0.000000	-186.753821	-89.844123	1015.406054	1037.599227
4 Degrees Average Saccade Start Time (ms)	47.209986	0.005277	14.960497	79.459475	917.662083	939.855256
4 Degrees Average Saccade Start Time (ms)	-28.783154	0.230318	-75.449748	17.883440	917.662083	939.855256
4 Degrees Average Saccade Start Time (ms)	61.730413	0.048798	3.849701	127.310527	917.662083	939.855256
4 Degrees Average Saccade Start Time (ms)	11.064977	0.482229	-19.650593	41.780548	917.662083	939.855256
4 Degrees Average Saccade Start Time (ms)	13.603531	0.337491	-14.026008	41.233070	917.662083	939.855256
8 Degrees Average Saccade Start Time (ms)	49.112234	0.066809	-2.678640	100.903108	1000.087929	1022.281102
8 Degrees Average Saccade Start Time (ms)	-43.784788	0.255634	-118.728725	31.159150	1000.087929	1022.281102
8 Degrees Average Saccade Start Time (ms)	260.821769	0.000006	155.503777	366.139761	1000.087929	1022.281102
8 Degrees Average Saccade Start Time (ms)	12.793180	0.612645	-36.534307	62.120667	1000.087929	1022.281102
8 Degrees Average Saccade Start Time (ms)	36.176074	0.114045	-8.195419	80.547567	1000.087929	1022.281102
10 Degrees Average Saccade Start Time (ms)	54.479974	0.013833	12.069478	96.890471	965.319585	987.512758
10 Degrees Average Saccade Start Time (ms)	-12.586556	0.688788	-73.956626	48.783515	965.319585	987.512758
10 Degrees Average Saccade Start Time (ms)	54.039308	0.223054	-32.203459	140.282075	965.319585	987.512758
10 Degrees Average Saccade Start Time (ms)	13.141959	0.525529	-27.251319	53.535238	965.319585	987.512758
10 Degrees Average Saccade Start Time (ms)	27.554936	0.141165	-8.779979	63.889852	965.319585	987.512758
4 Degrees Average Accuracy X (pixels)	-2.876593	0.872047	-37.768932	32.015745	931.367208	953.560381
4 Degrees Average Accuracy X (pixels)	46.529206	0.074699	-3.961722	97.020133	931.367208	953.560381
4 Degrees Average Accuracy X (pixels)	88.810250	0.016362	17.855838	159.764663	931.367208	953.560381
4 Degrees Average Accuracy X (pixels)	-2.566556	0.880072	-35.799272	30.666160	931.367208	953.560381
4 Degrees Average Accuracy X (pixels)	44.399493	0.004680	14.505710	74.293277	931.367208	953.560381
8 Degrees Average Accuracy X (pixels)	20.292244	0.436728	-30.586779	71.171266	996.997123	1019.190297
8 Degrees Average Accuracy X (pixels)	48.616671	0.199357	-25.007773	122.241114	996.997123	1019.190297
8 Degrees Average Accuracy X (pixels)	65.853807	0.215899	-37.609912	169.317527	996.997123	1019.190297
8 Degrees Average Accuracy X (pixels)	-4.463840	0.857188	-52.922846	43.995167	996.997123	1019.190297
8 Degrees Average Accuracy X (pixels)	67.479432	0.003265	23.889162	111.069702	996.997123	1019.190297
10 Degrees Average Accuracy X (pixels)	33.815150	0.265699	-25.309319	92.939618	1023.130906	1045.324079
10 Degrees Average Accuracy X (pixels)	39.875881	0.363760	-45.680128	125.431890	1023.130906	1045.324079
10 Degrees Average Accuracy X (pixels)	49.887649	0.418519	-70.343384	170.118682	1023.130906	1045.324079
10 Degrees Average Accuracy X (pixels)	18.227346	0.527648	-38.084919	74.539612	1023.130906	1045.324079
10 Degrees Average Accuracy X (pixels)	108.708377	0.000068	58.053875	159.362879	1023.130906	1045.324079
4 Degrees Average Accuracy Y (pixels)	28.838207	0.135793	-8.667382	66.343796	943.933954	966.127127
4 Degrees Average Accuracy Y (pixels)	24.063056	0.387480	-30.209373	78.335484	943.933954	966.127127
4 Degrees Average Accuracy Y (pixels)	23.960951	0.539827	-52.307569	100.229471	943.933954	966.127127
4 Degrees Average Accuracy Y (pixels)	8.103646	0.657804	-27.618023	43.825314	943.933954	966.127127
4 Degrees Average Accuracy Y (pixels)	54.172493	0.001433	22.039825	86.305161	943.933954	966.127127
8 Degrees Average Accuracy Y (pixels)	102.421768	0.000405	48.083402	156.760134	1008.442813	1030.635987
8 Degrees Average Accuracy Y (pixels)	36.345813	0.367708	-42.284471	114.976096	1008.442813	1030.635987
8 Degrees Average Accuracy Y (pixels)	60.632006	0.285443	-49.866372	171.130384	1008.442813	1030.635987
8 Degrees Average Accuracy Y (pixels)	18.239668	0.491745	-33.514142	69.993478	1008.442813	1030.635987
8 Degrees Average Accuracy Y (pixels)	108.568449	0.000018	62.014409	155.122489	1008.442813	1030.635987
10 Degrees Average Accuracy Y (pixels)	137.741302	0.000056	74.397076	201.085528	1035.126274	1057.319447
10 Degrees Average Accuracy Y (pixels)	78.038854	0.099143	-13.623351	169.701059	1035.126274	1057.319447
10 Degrees Average Accuracy Y (pixels)	111.738140	0.093032	-17.073872	240.550151	1035.126274	1057.319447
10 Degrees Average Accuracy Y (pixels)	54.837635	0.078675	-5.493679	115.168949	1035.126274	1057.319447
10 Degrees Average Accuracy Y (pixels)	172.727566	0.000000	118.457814	226.997317	1035.126274	1057.319447
4 Degrees Total Number of Correct Saccades	-0.912849	0.229286	-2.389560	0.563863	381.100983	403.294156
4 Degrees Total Number of Correct Saccades	0.136448	0.900721	-2.000426	2.273322	381.100983	403.294156
4 Degrees Total Number of Correct Saccades	-0.674194	0.661113	-3.677123	2.328735	381.100983	403.294156
4 Degrees Total Number of Correct Saccades	0.985918	0.173356	-0.420555	2.392391	381.100983	403.294156
4 Degrees Total Number of Correct Saccades	-1.132046	0.083353	-2.397209	0.133117	381.100983	403.294156
8 Degrees Total Number of Correct Saccades	-2.800197	0.050688	-5.565967	-0.034427	490.286239	512.479412
8 Degrees Total Number of Correct Saccades	-2.244493	0.275030	-6.246698	1.757713	490.286239	512.479412
8 Degrees Total Number of Correct Saccades	-2.902359	0.314901	-8.526620	2.721901	490.286239	512.479412
8 Degrees Total Number of Correct Saccades	-1.414242	0.295892	-4.048461	1.219977	490.286239	512.479412
8 Degrees Total Number of Correct Saccades	-3.675775	0.003204	-6.045330	-1.306219	490.286239	512.479412
10 Degrees Total Number of Correct Saccades	-4.268347	0.012729	-7.549924	-0.986770	520.041086	542.234259
10 Degrees Total Number of Correct Saccades	-4.139146	0.091486	-8.887749	0.609457	520.041086	542.234259
10 Degrees Total Number of Correct Saccades	-3.723318	0.277467	-10.396483	2.949848	520.041086	542.234259

Metric	Estimate	Pr(> t)	CI 0.025	CI 0.975	AIC	BIC
10 Degrees Total Number of Correct Saccades	-2.988130	0.064652	-6.113622	0.137362	520.041086	542.234259
10 Degrees Total Number of Correct Saccades	-4.831300	0.001172	-7.642770	-2.019831	520.041086	542.234259
4 Degrees Total Number of Hypometric Saccades	-7.114891	0.006253	-12.078521	-2.151261	592.044596	614.237769
4 Degrees Total Number of Hypometric Saccades	-4.678102	0.205504	-11.860718	2.504515	592.044596	614.237769
4 Degrees Total Number of Hypometric Saccades	10.503776	0.044733	0.410114	20.597437	592.044596	614.237769
4 Degrees Total Number of Hypometric Saccades	-2.906373	0.231825	-7.633912	1.821167	592.044596	614.237769
4 Degrees Total Number of Hypometric Saccades	10.169473	0.000011	5.916915	14.422030	592.044596	614.237769
8 Degrees Total Number of Hypometric Saccades	-11.399881	0.000072	-16.731711	-6.068051	604.495539	626.688712
8 Degrees Total Number of Hypometric Saccades	-3.537388	0.371591	-11.252808	4.178031	604.495539	626.688712
8 Degrees Total Number of Hypometric Saccades	13.443029	0.017363	2.600624	24.285433	604.495539	626.688712
8 Degrees Total Number of Hypometric Saccades	-1.283144	0.621809	-6.361370	3.795082	604.495539	626.688712
8 Degrees Total Number of Hypometric Saccades	11.339595	0.000006	6.771585	15.907605	604.495539	626.688712
10 Degrees Total Number of Hypometric Saccades	-10.136836	0.000112	-15.022542	-5.251131	589.291298	611.484471
10 Degrees Total Number of Hypometric Saccades	-4.015977	0.268938	-11.085833	3.053880	589.291298	611.484471
10 Degrees Total Number of Hypometric Saccades	-3.654043	0.473129	-13.589244	6.281158	589.291298	611.484471
10 Degrees Total Number of Hypometric Saccades	-1.727674	0.468954	-6.380996	2.925647	589.291298	611.484471
10 Degrees Total Number of Hypometric Saccades	12.999277	0.000000	8.813481	17.185074	589.291298	611.484471
4 Degrees Total Number of Hypermetric Saccades	7.358109	0.004998	2.364787	12.351430	593.082324	615.275497
4 Degrees Total Number of Hypermetric Saccades	3.379824	0.362044	-3.845757	10.605405	593.082324	615.275497
4 Degrees Total Number of Hypermetric Saccades	9.699613	0.064873	-0.454426	19.853653	593.082324	615.275497
4 Degrees Total Number of Hypermetric Saccades	1.902335	0.435391	-2.853483	6.658153	593.082324	615.275497
4 Degrees Total Number of Hypermetric Saccades	11.216262	0.000002	6.938266	15.494257	593.082324	615.275497
8 Degrees Total Number of Hypermetric Saccades	13.655685	0.000005	8.196614	19.114757	608.599197	630.792370
8 Degrees Total Number of Hypermetric Saccades	4.931595	0.224747	-2.967949	12.831140	608.599197	630.792370
8 Degrees Total Number of Hypermetric Saccades	3.992873	0.482907	-7.108281	15.094026	608.599197	630.792370
8 Degrees Total Number of Hypermetric Saccades	2.317711	0.384940	-2.881705	7.517126	608.599197	630.792370
8 Degrees Total Number of Hypermetric Saccades	14.221450	0.000000	9.544426	18.898473	608.599197	630.792370
10 Degrees Total Number of Hypermetric Saccades	12.859140	0.000004	7.764570	17.953709	596.575190	618.768363
10 Degrees Total Number of Hypermetric Saccades	7.381302	0.053235	0.009209	14.753395	596.575190	618.768363
10 Degrees Total Number of Hypermetric Saccades	4.916907	0.355094	-5.443024	15.276837	596.575190	618.768363
10 Degrees Total Number of Hypermetric Saccades	4.819466	0.055123	-0.032786	9.671717	596.575190	618.768363
10 Degrees Total Number of Hypermetric Saccades	16.895725	0.000000	12.530986	21.260464	596.575190	618.768363

Table 36: Atypical Parkinsonian Syndromes Generalised Linear Model Results Antisaccades Vertical

Metric	Estimate	Pr(> t)	CI 0.025	CI 0.975	AIC	BIC
Average Saccade Amplitude	-3.797415	0.000000	-5.010981	-2.583850	346.952575	369.145748
Average Saccade Amplitude	-3.160496	0.000702	-4.916585	-1.404408	346.952575	369.145748
Average Saccade Amplitude	-2.377752	0.042638	-4.845566	-0.090062	346.952575	369.145748
Average Saccade Amplitude	-2.582440	0.000036	-3.738283	-1.426597	346.952575	369.145748
Average Saccade Amplitude	-4.347749	0.000000	-5.387463	-3.308035	346.952575	369.145748
Average Saccade Velocity	-59.018836	0.000000	-77.244067	-40.793606	818.361104	840.554277
Average Saccade Velocity	-47.531421	0.000691	-73.904224	-21.158618	818.361104	840.554277
Average Saccade Velocity	-40.398934	0.035737	-77.460380	-3.337489	818.361104	840.554277
Average Saccade Velocity	-32.595335	0.000424	-49.953698	-15.236971	818.361104	840.554277
Average Saccade Velocity	-72.653634	0.000000	-88.267981	-57.039287	818.361104	840.554277
Average Saccade End Time (ms)	117.492175	0.021625	19.223680	215.760669	1111.533105	1133.726278
Average Saccade End Time (ms)	28.543443	0.695069	-113.655893	170.742780	1111.533105	1133.726278
Average Saccade End Time (ms)	433.990014	0.000057	234.158660	633.821368	1111.533105	1133.726278
Average Saccade End Time (ms)	-44.382683	0.355503	-137.977123	49.211758	1111.533105	1133.726278
Average Saccade End Time (ms)	72.249656	0.096523	-11.941234	156.440547	1111.533105	1133.726278
Peak Saccade Velocity	-142.087729	0.000255	-214.798664	-69.376794	1059.122271	1081.315444
Peak Saccade Velocity	-118.730716	0.029876	-223.947008	-13.514423	1059.122271	1081.315444
Peak Saccade Velocity	-89.107964	0.241076	-236.967403	58.751476	1059.122271	1081.315444
Peak Saccade Velocity	-89.928318	0.012871	-159.180821	-20.675814	1059.122271	1081.315444
Peak Saccade Velocity	-191.856880	0.000000	-254.151499	-129.562262	1059.122271	1081.315444
Average Saccade Start Time (ms)	146.741333	0.001528	59.157569	234.325097	1091.504341	1113.697514
Average Saccade Start Time (ms)	-105.310631	0.107380	-232.048637	21.427376	1091.504341	1113.697514
Average Saccade Start Time (ms)	315.034347	0.000855	136.930651	493.138044	1091.504341	1113.697514
Average Saccade Start Time (ms)	-15.257938	0.720928	-98.675858	68.159981	1091.504341	1113.697514
Average Saccade Start Time (ms)	98.125670	0.012274	23.088852	173.162487	1091.504341	1113.697514
Total Number of Errors	1.708882	0.195159	-0.854638	4.272401	477.072990	499.266163
Total Number of Errors	3.387285	0.077334	-0.322253	7.096823	477.072990	499.266163
Total Number of Errors	2.139008	0.423684	-3.073970	7.351986	477.072990	499.266163
Total Number of Errors	6.685589	0.000001	4.244002	9.127177	477.072990	499.266163
Total Number of Errors	0.691402	0.539003	-1.504876	2.887680	477.072990	499.266163
Total Number of Correct Antisaccades	-2.309689	0.093415	-4.975473	0.356096	483.879404	506.072577
Total Number of Correct Antisaccades	-3.871559	0.052683	-7.729080	-0.014039	483.879404	506.072577
Total Number of Correct Antisaccades	-4.030781	0.148984	-9.451717	1.390156	483.879404	506.072577
Total Number of Correct Antisaccades	-6.649977	0.000002	-9.188966	-4.110989	483.879404	506.072577
Total Number of Correct Antisaccades	-1.066695	0.362766	-3.350588	1.217198	483.879404	506.072577
Total Number of Self Corrected Errors	0.010764	0.992761	-2.307017	2.328545	459.538913	481.732087
Total Number of Self Corrected Errors	-0.628041	0.714591	-3.981985	2.725902	459.538913	481.732087
Total Number of Self Corrected Errors	-3.534252	0.145619	-8.247517	1.179012	459.538913	481.732087
Total Number of Self Corrected Errors	2.873486	0.012665	0.665948	5.081024	459.538913	481.732087
Total Number of Self Corrected Errors	2.438417	0.018429	0.452673	4.424161	459.538913	481.732087

Table 37: Atypical Parkinsonian Syndromes Generalised Linear Model Results Antisaccades Horizontal

Metric	Estimate	Pr(> t)	CI 0.025	CI 0.975	AIC	BIC
Average Saccade Amplitude	-4.473198	0.000000	-5.884720	-3.061677	373.244994	395.438167
Average Saccade Amplitude	-1.629218	0.121967	-3.671759	0.413324	373.244994	395.438167
Average Saccade Amplitude	-2.413180	0.010337	-5.283543	-0.457184	373.244994	395.438167
Average Saccade Amplitude	-1.428283	0.040554	-2.772667	-0.083900	373.244994	395.438167
Average Saccade Amplitude	-6.320920	0.000000	-7.530232	-5.111608	373.244994	395.438167
Average Saccade Velocity	-50.865589	0.000006	-71.488325	-30.242853	839.865287	862.058460
Average Saccade Velocity	-20.409923	0.183932	-50.252035	9.432189	839.865287	862.058460
Average Saccade Velocity	-88.507456	0.000087	-130.444288	-46.570625	839.865287	862.058460
Average Saccade Velocity	-1.279191	0.898755	-20.921025	18.362644	839.865287	862.058460
Average Saccade Velocity	-71.977035	0.000000	-89.645430	-54.308640	839.865287	862.058460
Average Saccade End Time (ms)	-30.408114	0.308002	-88.494068	27.677839	1020.047454	1042.240627
Average Saccade End Time (ms)	-86.265587	0.047677	-170.318814	-2.212360	1020.047454	1042.240627
Average Saccade End Time (ms)	613.053215	0.000000	494.934027	731.172402	1020.047454	1042.240627
Average Saccade End Time (ms)	-53.494714	0.061726	-108.817860	1.828433	1020.047454	1042.240627
Average Saccade End Time (ms)	5.936505	0.815740	-43.828255	55.701266	1020.047454	1042.240627
Peak Saccade Velocity	-101.879740	0.000819	-159.254621	-44.504859	1017.904248	1040.097421
Peak Saccade Velocity	-25.713062	0.545584	-108.737332	57.311208	1017.904248	1040.097421
Peak Saccade Velocity	-114.407913	0.058223	-231.081117	2.265292	1017.904248	1040.097421
Peak Saccade Velocity	-12.945410	0.643704	-67.591305	41.700486	1017.904248	1040.097421
Peak Saccade Velocity	-172.802053	0.000000	-221.957608	-123.646499	1017.904248	1040.097421
Average Saccade Start Time (ms)	-18.803777	0.506872	-74.078687	36.471134	1011.416226	1033.609399
Average Saccade Start Time (ms)	-121.383999	0.003892	-201.369509	-41.398489	1011.416226	1033.609399
Average Saccade Start Time (ms)	325.197511	0.000000	212.794646	437.600375	1011.416226	1033.609399
Average Saccade Start Time (ms)	-48.232555	0.076372	-100.878363	4.413254	1011.416226	1033.609399
Average Saccade Start Time (ms)	-10.476916	0.665751	-57.833335	36.879502	1011.416226	1033.609399
Total Number of Errors	3.971947	0.017153	0.774645	7.169248	515.514162	537.707335
Total Number of Errors	7.439839	0.002294	2.813186	12.066491	515.514162	537.707335
Total Number of Errors	0.918683	0.782552	-5.583107	7.420473	515.514162	537.707335
Total Number of Errors	6.552032	0.000065	3.506807	9.597257	515.514162	537.707335
Total Number of Errors	4.766647	0.001024	2.027380	7.505915	515.514162	537.707335
Total Number of Correct Antisaccades	-4.002049	0.015211	-7.163139	-0.840959	513.532246	535.725419
Total Number of Correct Antisaccades	-7.524314	0.001839	-12.098567	-2.950062	513.532246	535.725419
Total Number of Correct Antisaccades	-4.984720	0.132539	-11.412873	1.443433	513.532246	535.725419
Total Number of Correct Antisaccades	-6.583630	0.000051	-9.594366	-3.572895	513.532246	535.725419
Total Number of Correct Antisaccades	-5.033970	0.000480	-7.742214	-2.325727	513.532246	535.725419
Total Number of Self Corrected Errors	-0.157781	0.907966	-2.824242	2.508680	483.923591	506.116764
Total Number of Self Corrected Errors	-2.669058	0.179034	-6.527559	1.189442	483.923591	506.116764
Total Number of Self Corrected Errors	-2.438941	0.380675	-7.861254	2.983373	483.923591	506.116764
Total Number of Self Corrected Errors	2.984722	0.023883	0.445089	5.524356	483.923591	506.116764
Total Number of Self Corrected Errors	-1.167423	0.319599	-3.451897	1.117050	483.923591	506.116764

Table 38: Atypical Parkinsonian Syndromes Generalised Linear Model Results Pursuit

Metric	Estimate	Pr(> t)	CI 0.025	CI 0.975	AIC	BIC
RMSE Horizontal 0.2Hz	0.342536	0.643447	-1.102275	1.787346	377.300869	399.494042
RMSE Horizontal 0.2Hz	4.336053	0.000113	2.245341	6.426764	377.300869	399.494042
RMSE Horizontal 0.2Hz	1.110238	0.461111	-1.827818	4.048295	377.300869	399.494042
RMSE Horizontal 0.2Hz	1.248990	0.079097	-0.127099	2.625079	377.300869	399.494042
RMSE Horizontal 0.2Hz	1.446300	0.024687	0.208469	2.684132	377.300869	399.494042
RMSE Horizontal 0.4Hz	-0.275065	0.737694	-1.879156	1.329025	395.497630	417.690803
RMSE Horizontal 0.4Hz	4.241338	0.000589	1.920139	6.562536	395.497630	417.690803
RMSE Horizontal 0.4Hz	5.471530	0.001510	2.209573	8.733487	395.497630	417.690803
RMSE Horizontal 0.4Hz	1.358038	0.085367	-0.169756	2.885831	395.497630	417.690803
RMSE Horizontal 0.4Hz	1.496671	0.035903	0.122377	2.870966	395.497630	417.690803
RMSE Vertical 0.2Hz	-0.638860	0.363679	-2.009339	0.731618	368.110516	390.303689
RMSE Vertical 0.2Hz	2.305367	0.025403	0.322217	4.288516	368.110516	390.303689
RMSE Vertical 0.2Hz	2.859719	0.047718	0.072818	5.646619	368.110516	390.303689
RMSE Vertical 0.2Hz	0.785689	0.241639	-0.519603	2.090982	368.110516	390.303689
RMSE Vertical 0.2Hz	0.980167	0.010578	0.193981	2.154315	368.110516	390.303689
RMSE Vertical 0.4Hz	0.164029	0.741860	-0.808569	1.136628	308.438263	330.631436
RMSE Vertical 0.4Hz	2.618517	0.000474	1.211120	4.025915	308.438263	330.631436
RMSE Vertical 0.4Hz	4.895150	0.000006	2.917348	6.872952	308.438263	330.631436
RMSE Vertical 0.4Hz	0.822514	0.085702	-0.103823	1.748852	308.438263	330.631436
RMSE Vertical 0.4Hz	1.284905	0.003381	0.451637	2.118172	308.438263	330.631436
RMSE Anticlockwise 0.2Hz	0.109518	0.882907	-1.343167	1.562203	378.246632	400.439805
RMSE Anticlockwise 0.2Hz	4.994236	0.000013	2.892129	7.096342	378.246632	400.439805
RMSE Anticlockwise 0.2Hz	2.991199	0.050661	0.037130	5.945269	378.246632	400.439805
RMSE Anticlockwise 0.2Hz	1.043518	0.143323	-0.340071	2.427107	378.246632	400.439805
RMSE Anticlockwise 0.2Hz	1.809781	0.005573	0.565203	3.054359	378.246632	400.439805
RMSE Anticlockwise 0.4Hz	0.603362	0.429455	-0.885630	2.092354	382.541983	404.735156
RMSE Anticlockwise 0.4Hz	4.348960	0.000165	2.194316	6.503604	382.541983	404.735156
RMSE Anticlockwise 0.4Hz	4.989416	0.001807	1.961515	8.017317	382.541983	404.735156
RMSE Anticlockwise 0.4Hz	2.045728	0.005945	0.627559	3.463897	382.541983	404.735156
RMSE Anticlockwise 0.4Hz	2.742976	0.000066	1.467292	4.018660	382.541983	404.735156
RMSE Clockwise 0.2Hz	0.908178	0.234568	-0.577849	2.394204	382.195120	404.388293
RMSE Clockwise 0.2Hz	4.385989	0.000143	2.235636	6.536343	382.195120	404.388293
RMSE Clockwise 0.2Hz	3.695138	0.018909	0.673267	6.717009	382.195120	404.388293
RMSE Clockwise 0.2Hz	1.367669	0.061893	-0.047676	2.783014	382.195120	404.388293
RMSE Clockwise 0.2Hz	2.118825	0.001635	0.845681	3.391968	382.195120	404.388293
RMSE Clockwise 0.4Hz	1.241934	0.133100	-0.361982	2.845850	395.478714	417.671887
RMSE Clockwise 0.4Hz	4.509772	0.000275	2.188826	6.830717	395.478714	417.671887
RMSE Clockwise 0.4Hz	2.431540	0.147937	-0.830063	5.693142	395.478714	417.671887
RMSE Clockwise 0.4Hz	2.416458	0.002679	0.888831	3.944086	395.478714	417.671887
RMSE Clockwise 0.4Hz	2.777225	0.000162	1.403080	4.151370	395.478714	417.671887
Gain Horizontal 0.2Hz	-0.210677	0.689786	-1.241392	0.820039	318.536755	340.729928
Gain Horizontal 0.2Hz	-0.283593	0.710394	-1.775089	1.207903	318.536755	340.729928
Gain Horizontal 0.2Hz	2.255935	0.038065	0.159950	4.351920	318.536755	340.729928
Gain Horizontal 0.2Hz	0.117042	0.815840	-0.864648	1.098732	318.536755	340.729928
Gain Horizontal 0.2Hz	0.636850	0.161437	-0.246209	1.519908	318.536755	340.729928
Gain Horizontal 0.4Hz	0.236031	0.372659	-0.279935	0.751998	198.134554	220.327727
Gain Horizontal 0.4Hz	-0.349567	0.361599	-1.096196	0.397062	198.134554	220.327727
Gain Horizontal 0.4Hz	-0.078499	0.883793	-1.127729	0.970732	198.134554	220.327727
Gain Horizontal 0.4Hz	-0.220613	0.381595	-0.712038	0.270812	198.134554	220.327727
Gain Horizontal 0.4Hz	0.213822	0.345998	-0.228228	0.655873	198.134554	220.327727
Gain Vertical 0.2Hz	0.184556	0.579005	-0.464690	0.833802	238.114513	260.307686
Gain Vertical 0.2Hz	-0.389437	0.418979	-1.328928	0.550054	238.114513	260.307686
Gain Vertical 0.2Hz	0.702584	0.300126	-0.617673	2.022841	238.114513	260.307686
Gain Vertical 0.2Hz	0.536767	0.092814	-0.081598	1.155132	238.114513	260.307686
Gain Vertical 0.2Hz	-0.626216	0.030250	-1.182453	-0.069979	238.114513	260.307686
Gain Vertical 0.4Hz	0.917905	0.017163	0.178949	1.656860	260.634645	282.827818
Gain Vertical 0.4Hz	0.240820	0.660125	-0.828485	1.310125	260.634645	282.827818
Gain Vertical 0.4Hz	-0.269747	0.725900	-1.772431	1.232936	260.634645	282.827818

Metric	Estimate	Pr(> t)	CI 0.025	CI 0.975	AIC	BIC
Gain Vertical 0.4Hz	-0.234876	0.514957	-0.938684	0.468931	260.634645	282.827818
Gain Vertical 0.4Hz	-0.147022	0.045024	-0.486073	0.780117	260.634645	282.827818
Gain Anticlockwise 0.2Hz	-0.063909	0.630795	-0.323522	0.195704	78.622741	100.815914
Gain Anticlockwise 0.2Hz	-0.229473	0.234805	-0.605146	0.146200	78.622741	100.815914
Gain Anticlockwise 0.2Hz	0.248026	0.359953	-0.279903	-0.077596	78.622741	100.815914
Gain Anticlockwise 0.2Hz	-0.141678	0.264830	-0.388943	0.105587	78.622741	100.815914
Gain Anticlockwise 0.2Hz	0.086753	0.446868	-0.135668	0.309175	78.622741	100.815914
Gain Anticlockwise 0.4Hz	-0.136239	0.147020	-0.318567	0.046089	17.133620	39.326793
Gain Anticlockwise 0.4Hz	-0.232300	0.088313	-0.496138	0.031537	17.133620	39.326793
Gain Anticlockwise 0.4Hz	-0.162856	0.391901	-0.533625	0.207912	17.133620	39.326793
Gain Anticlockwise 0.4Hz	-0.174645	0.042211	-0.348300	-0.000989	17.133620	39.326793
Gain Anticlockwise 0.4Hz	-0.120528	0.134454	-0.276736	0.035681	17.133620	39.326793
Gain Clockwise 0.2Hz	-0.034452	0.784773	-0.280859	0.211955	69.538571	91.731744
Gain Clockwise 0.2Hz	-0.281181	0.126197	-0.637744	0.075382	69.538571	91.731744
Gain Clockwise 0.2Hz	0.187630	0.465171	-0.313445	0.688704	69.538571	91.731744
Gain Clockwise 0.2Hz	-0.053215	0.657951	-0.287902	0.181471	69.538571	91.731744
Gain Clockwise 0.2Hz	0.039582	0.714241	-0.171526	0.250689	69.538571	91.731744
Gain Clockwise 0.4Hz	-0.107296	0.222055	-0.278160	0.063568	5.834315	28.027488
Gain Clockwise 0.4Hz	-0.267083	0.037390	-0.514331	-0.019834	5.834315	28.027488
Gain Clockwise 0.4Hz	-0.377419	0.036371	-0.724875	-0.029963	5.834315	28.027488
Gain Clockwise 0.4Hz	-0.202137	0.017168	-0.364874	-0.039400	5.834315	28.027488
Gain Clockwise 0.4Hz	-0.126162	0.095130	-0.272548	0.020225	5.834315	28.027488

Table 39: Composite Z-Scores for Atypical Parkinsonian Syndromes

Paradigm	ATP	CBS	DLB	MSA	PSP
Antisaccades Horizontal	0.580315862	0.2716800026475353	1.775881329050798	0.071784547	1.156390563320378
Antisaccades Vertical	0.6109522179634539	0.1157848597509247	1.5591434818815706	0.6990150796510181	1.3790069939430434
Central Fixation	0.5111207060927282	0.6916678850265089	1.442112504917125	0.9579437178291615	1.627688041
Memory Guided Saccades Horizontal	1.5096424433339652	0.055117793	1.3044521545941496	0.1751797671556333	0.5533418095157956
Memory Guided Saccades Vertical	1.1751987406291018	0.1757193405529925	0.5511587895131653	0.4462496873258625	0.7807367306589399
Nystagmus/ Positional Fixation	0.6227673783998526	0.9244442368470016	1.5188517228757217	0.8126168331206107	1.4195296794860135
Oblique Saccades	0.933781306748238	0.6494342381473672	1.7830886779412212	0.3734978914929122	0.0275629474962867
Pursuit	0.8972493360570332	1.4006295945221217	1.563971003293543	0.1409451330443632	0.063186538
Reflexive Saccades Horizontal	0.7149448094576741	0.6908101706962725	1.383736004852388	0.1935005313889839	0.5401452659920638
Reflexive Saccades Vertical	0.5889018247533642	0.2498446466308821	1.5061518554790507	0.0327411201085899	0.6183639441782101
Volitional Saccades Horizontal	1.3480221932976308	0.1806266756378341	1.327886976265497	0.2041123103546465	0.5388401936783861
Volitional Saccades Vertical	0.6344077929276265	0.2496767258488945	1.1878899398395932	0.1906926188250694	0.3417583365029142

C Longitudinal Study of Eye Movements in Parkinson’s Disease

Metric	Estimate	Std. Error	df	t value	Pr(> t)	CI 0.025	CI 0.975	AIC	BIC
Small SWJ Count	-19.465841	5.936162	34.000000	-3.279196	0.002407	-30.455215	-8.476466	348.687320	362.198356
Saccade Count	-14.824254	7.147843	21.807956	-2.073948	0.050100	-29.017139	-0.746119	373.906599	387.417634
Microsaccade Count	-7.389004	5.825099	20.809269	-1.268477	0.218635	-18.949347	4.210295	353.465186	366.976221
Large SWJ Count	-0.538264	0.324408	34.000000	-1.659217	0.106270	-1.138827	0.062300	151.023849	164.534885
Intrusive Saccade Count	-3.649208	1.897704	20.818966	-1.922960	0.068271	-7.403689	0.139674	277.843940	291.354975
Average Pupil Size	65.576897	159.219790	26.722859	0.411864	0.683724	-245.250810	370.522473	598.153141	611.664176
Fixation Precision SD	-0.007346	0.005432	21.601321	-1.352377	0.190244	-0.018380	0.003184	-111.792470	-98.281436
Fixation Precision RMS	0.000575	0.003442	20.348628	0.166920	0.869081	-0.006398	0.007336	-150.066650	-136.555610
Fixation Duration	46.328131	216.992876	21.067279	0.213501	0.832989	-381.289870	480.451689	602.774646	616.285682

Table 40: Longitudinal Study of Eye Movements in Parkinson’s Disease Fixation Generalised Linear Model Results

Metric	Estimate	Std. Error	df	t value	Pr(> t)	CI 0.025	CI 0.975	AIC	BIC
Average Fixation Duration Up	12.376859	16.235472	14.954492	0.762334	0.457717	-16.615796	41.340230	582.981827	596.492862
Average Fixation Duration Down	2.879638	16.057212	15.122707	0.179336	0.860055	-25.837134	31.576804	572.363965	585.875001
Average Fixation Duration Right	3.405993	14.242717	14.943180	0.239139	0.814246	-22.054927	28.852929	561.548738	575.059774
Average Fixation Duration Left	-0.653440	13.772202	15.139728	-0.047446	0.962778	-25.267231	23.954855	566.037058	579.548094
Fixation Precision RMS Up	-0.000457	0.000293	15.227061	-1.561972	0.138835	-0.000981	0.000066	-171.089751	-157.578715
Fixation Precision RMS Down	-0.000293	0.000388	34.000000	-0.753938	0.456077	-0.001011	0.000426	-129.156313	-115.645277
Fixation Precision RMS Right	-0.000337	0.000328	14.967876	-1.028005	0.320275	-0.000926	0.000250	-142.844404	-129.333368
Fixation Precision RMS Left	-0.000233	0.000489	15.025409	-0.476216	0.640771	-0.001105	0.000639	-117.840690	-104.329655
Fixation Precision SD Up	-0.000880	0.000557	15.264850	-1.581699	0.134213	-0.001878	0.000115	-130.614794	-117.103759
Fixation Precision SD Down	-0.000705	0.000707	14.932856	-0.997746	0.334297	-0.001992	0.000580	-89.586116	-76.075080
Fixation Precision SD Right	-0.000648	0.000681	14.636355	-0.951629	0.356737	-0.001894	0.000598	-91.759458	-78.248423
Fixation Precision SD Left	-0.000831	0.000840	15.127332	-0.988706	0.338359	-0.002334	0.000669	-89.276583	-75.765548
Average Pupil Size Up	-23.941572	28.534351	15.443709	-0.839044	0.414244	-75.164338	27.253073	596.509859	610.020894
Average Pupil Size Down	-17.943174	33.422963	15.561115	-0.536852	0.598963	-78.114949	42.173051	600.038471	613.549507
Average Pupil Size Right	-14.118829	30.692948	15.454457	-0.460002	0.651920	-69.235301	40.962530	600.483593	613.994629
Average Pupil Size Left	-16.598738	33.797906	15.445288	-0.491117	0.630249	-77.297133	44.051940	606.988906	620.499942
Saccade Count Up	-1.309235	0.934933	15.160106	-1.400351	0.181542	-2.979338	0.363889	381.249889	394.760925
Saccade Count Down	-1.142713	0.822912	15.125671	-1.388621	0.185059	-2.612190	0.328169	377.041352	390.552388
Saccade Count Right	-1.777453	0.792085	14.905419	-2.244019	0.040452	-3.190711	-0.362835	373.900720	387.411756
Saccade Count Left	-0.667217	0.944468	15.112286	-0.706447	0.490659	-2.353328	1.019394	392.321416	405.832451
Intrusive Saccade Count Up	-0.340295	0.090865	34.000000	-3.745079	0.000668	-0.508509	-0.172081	241.843056	255.354091
Intrusive Saccade Count Down	-0.058941	0.141180	15.104275	-0.417492	0.682192	-0.311207	0.193054	260.729391	274.240427
Intrusive Saccade Count Right	-0.230917	0.170313	15.052200	-1.355839	0.195144	-0.535199	0.073189	269.245755	282.756790
Intrusive Saccade Count Left	0.098716	0.255154	34.000000	0.386886	0.701252	-0.373641	0.571072	312.052956	325.563991
Large SWJ Count Up	-0.025393	0.016995	14.939856	-1.494138	0.155959	-0.055701	0.004975	115.844779	129.355814
Large SWJ Count Down	-0.001816	0.010803	15.090185	-0.168069	0.868761	-0.021098	0.017471	90.764754	104.275789
Large SWJ Count Right	-0.052514	0.012770	34.000000	-4.112356	0.000234	-0.076154	-0.028874	108.407700	121.918735
Large SWJ Count Left	-0.014062	0.012955	15.056011	-1.085472	0.294787	-0.037201	0.009048	102.651879	116.162915
Microsaccade Count Up	0.345742	0.584422	15.114415	0.591598	0.562865	-0.697323	1.389511	361.204232	374.715267
Microsaccade Count Down	1.549441	0.985432	14.844985	1.572347	0.136937	-0.207987	3.306716	397.365315	410.876351
Microsaccade Count Right	0.818371	0.850740	16.120085	0.961951	0.350283	-0.722088	2.365967	379.505815	392.814308
Microsaccade Count Left	1.294339	0.872740	16.240013	1.483075	0.157201	-0.265120	2.856240	373.052389	386.360882
Small SWJ Count Up	0.100724	0.445073	14.997715	0.226310	0.824016	-0.675228	0.879266	345.715385	359.226420
Small SWJ Count Down	3.642090	1.747323	34.000000	2.084383	0.044709	0.407343	6.876837	442.883058	456.394094
Small SWJ Count Right	0.356558	0.679962	16.017083	0.524379	0.607196	-0.831896	1.571376	362.971734	376.280227
Small SWJ Count Left	1.177320	0.751850	16.232965	1.565897	0.136657	-0.202666	2.558848	372.280825	385.589318

Table 41: Longitudinal Study of Eye Movements in Parkinson’s Disease Positional Fixation/ Nystagmus Generalised Linear Model Results

Metric	Estimate	Std. Error	df	t value	Pr(> t)	CI 0.025	CI 0.975	AIC	BIC
RMSE Gaze Horizontal 0.2Hz	0.080110	0.055833	15.097385	1.434810	0.171732	-0.019548	0.179781	203.074942	216.585978
RMSE Gaze Horizontal 0.4Hz	0.063254	0.055897	15.096712	1.131608	0.275455	-0.035136	0.161763	205.268084	218.779120
RMSE Gaze Vertical 0.2Hz	0.015130	0.031951	34.000000	0.473532	0.638860	-0.044020	0.074279	170.771627	184.282662
RMSE Gaze Vertical 0.4Hz	0.005094	0.038693	15.090403	0.131652	0.896999	-0.064409	0.074637	181.255313	194.766348
RMSE Gaze Anticlockwise 0.2Hz	0.052148	0.058965	15.080325	0.884389	0.390369	-0.053085	0.157427	205.661214	219.172249
RMSE Gaze Anticlockwise 0.4Hz	0.030724	0.069061	15.170342	0.444877	0.662690	-0.092651	0.154141	208.552635	222.063671
RMSE Gaze Clockwise 0.2Hz	0.006212	0.078643	15.014666	0.078991	0.938083	-0.134166	0.146644	219.540540	233.051575
RMSE Gaze Clockwise 0.4Hz	0.013580	0.074830	15.056354	0.181475	0.858415	-0.120078	0.147348	209.479362	222.990398
Pursuit Gain Horizontal 0.2Hz	-0.122743	0.151869	15.071329	-0.808218	0.431538	-0.397355	0.151912	275.145836	288.656872
Pursuit Gain Horizontal 0.4Hz	0.005565	0.014955	34.000000	0.372113	0.712118	-0.022121	0.033251	119.149253	132.660289
Pursuit Gain Vertical 0.2Hz	-0.021033	0.067328	34.000000	-0.312396	0.756647	-0.145675	0.103609	221.457442	234.968478
Pursuit Gain Vertical 0.4Hz	-0.037734	0.034833	15.112514	-1.083305	0.295655	-0.099952	0.024508	160.965478	174.476514
Pursuit Gain Anticlockwise 0.2Hz	-0.006291	0.007665	15.215494	-0.820737	0.424469	-0.020013	0.007447	43.170809	56.681845
Pursuit Gain Anticlockwise 0.4Hz	0.001961	0.005937	15.132941	0.330364	0.745654	-0.008647	0.012564	43.401634	56.912670
Pursuit Gain Clockwise 0.2Hz	-0.011186	0.008905	15.178976	-1.256147	0.228053	-0.027109	0.004743	61.138967	74.650003
Pursuit Gain Clockwise 0.4Hz	-0.001357	0.006368	15.230804	-0.213041	0.834120	-0.012742	0.010044	38.797001	52.308036

Table 42: Longitudinal Study of Eye Movements in Parkinson’s Disease Pursuit Generalised Linear Model Results

Metric	Estimate	Std. Error	df	t value	Pr(> t)	CI 0.025	CI 0.975	AIC	BIC
Correct Saccade Count - 10 Degrees	0.053402	0.068486	14.879347	0.779752	0.447763	-0.068704	0.175637	214.424154	227.935189
Hypermetric Saccade Count - 10 Degrees	-0.344773	0.163762	15.236251	-2.105336	0.052249	-0.637633	-0.051815	260.096388	273.607424
Hypometric Saccade Count - 10 Degrees	0.287390	0.139150	14.984573	2.065326	0.056641	0.038487	0.535895	248.687386	262.198421
X Accuracy - 10 Degrees	-2.469627	1.302855	15.138662	-1.895549	0.077276	-4.797757	-0.143332	410.657301	424.168337
Y Accuracy - 10 Degrees	-3.529715	2.008542	15.220468	-1.757352	0.098948	-7.121556	0.061602	432.171599	445.682635
Saccade Amplitude - 10 Degrees	0.069712	0.037328	15.159461	1.867540	0.081283	0.003017	0.136421	165.437471	178.948507
Saccade Average Velocity - 10 Degrees	1.486881	0.832722	15.109701	1.785566	0.094252	-0.001346	2.975104	373.263636	386.774672
Saccade End Time - 10 Degrees	-0.257509	1.568631	14.924756	-0.164162	0.871806	-3.057402	2.544119	418.581202	432.092238
Saccade Peak Velocity - 10 Degrees	1.833803	2.475475	15.213184	0.740789	0.470102	-2.600705	6.265267	436.702195	450.213231
Saccade Latency - 10 Degrees	1.652517	1.487613	14.990977	1.110851	0.284133	-1.009202	4.318048	399.475984	412.987020
Correct Saccade Count - 4 Degrees	-0.028375	0.046133	34.000000	-0.615073	0.542602	-0.113780	0.057030	195.750554	209.261590
Hypermetric Saccade Count - 4 Degrees	-0.226797	0.125112	15.112169	-1.812748	0.089781	-0.450135	-0.003417	256.859554	270.370589
Hypometric Saccade Count - 4 Degrees	0.367391	0.125539	15.058391	2.926508	0.010385	0.143273	0.591433	256.670042	270.181078
X Accuracy - 4 Degrees	-2.369501	1.196777	34.000000	-1.979902	0.055855	-4.585046	-0.153956	417.148294	430.659329
Y Accuracy - 4 Degrees	-3.005277	1.246037	34.000000	-2.411867	0.021418	-5.312015	-0.698539	419.891150	433.402186
Saccade Amplitude - 4 Degrees	-0.018340	0.023640	14.984898	-0.775802	0.449937	-0.059507	0.022835	145.909792	159.420828
Saccade Average Velocity - 4 Degrees	1.099614	0.440220	15.119893	2.497874	0.024503	0.311224	1.887339	319.367094	332.878129
Saccade End Time - 4 Degrees	-5.094505	1.602271	34.000000	-3.179553	0.003140	-8.060722	-2.128287	436.989972	450.501008
Saccade Peak Velocity - 4 Degrees	1.920004	1.338856	15.263564	1.434063	0.171723	-0.478095	4.315989	397.463630	410.974666
Saccade Latency - 4 Degrees	3.493066	2.088823	15.044902	1.672265	0.115134	-0.234575	7.221020	449.647012	463.158048
Correct Saccade Count - 8 Degrees	0.137143	0.085667	34.000000	1.600891	0.118653	-0.021448	0.295734	237.837501	251.348537
Hypermetric Saccade Count - 8 Degrees	-0.219003	0.129672	15.025084	-1.688891	0.111879	-0.450369	0.012490	258.887112	272.398148
Hypometric Saccade Count - 8 Degrees	0.186021	0.125053	14.232412	1.487537	0.158691	-0.036574	0.408428	253.645658	267.156693
X Accuracy - 8 Degrees	-0.889145	0.985752	34.000000	-0.901996	0.373405	-2.714028	0.935738	403.957478	417.468513
Y Accuracy - 8 Degrees	-3.197027	1.332795	15.086857	-2.398739	0.029815	-5.560639	-0.831359	421.471127	434.982162
Saccade Amplitude - 8 Degrees	0.033500	0.026667	15.112756	1.256247	0.228099	-0.014122	0.081111	149.221967	162.733003
Saccade Average Velocity - 8 Degrees	1.022146	0.736593	14.952051	1.387668	0.185573	-0.294389	2.337737	362.415368	375.926403
Saccade End Time - 8 Degrees	-2.805966	1.629718	14.801390	-1.721749	0.105940	-5.711050	0.101787	429.176837	442.687873
Saccade Peak Velocity - 8 Degrees	1.019141	2.118217	15.049261	0.481132	0.637343	-2.772658	4.806984	427.991531	441.502567
Saccade Latency - 8 Degrees	0.909621	1.695924	15.021920	0.536357	0.599565	-2.125417	3.949561	407.982088	421.493124

Table 43: Longitudinal Study of Eye Movements in Parkinson’s Disease Oblique Saccades Generalised Linear Model Results

Paradigm	Metric	Estimate	Std. Error	df	t value	Pr(> t)	CI 0.025	CI 0.975	AIC	BIC
Antisaccades Horizontal	Saccade Amplitude	0.006457	0.044270	14.922085	0.145851	0.885991	-0.074803	0.087710	192.363403	205.874438
	Saccade Average Velocity	0.943062	0.947757	14.682267	0.995046	0.335831	-0.750280	2.636924	371.525304	385.036339
	Saccade End Time	-2.634621	1.784867	14.948531	-1.476088	0.160673	-5.806187	0.537362	441.450081	454.961116
	Saccade Peak Velocity	-0.874708	2.309636	14.657585	-0.378721	0.710324	-5.023853	3.275751	412.427808	425.938843
	Saccade Latency	-0.048281	1.432227	14.997295	-0.033711	0.973552	-2.604241	2.508002	420.384639	433.895675
	Number of Correct Saccades	-0.042626	0.109854	15.158452	-0.388027	0.703391	-0.239015	0.153565	239.934624	253.445660
	Number of Erros	0.045233	0.110176	15.165603	0.410553	0.687142	-0.151540	0.242198	240.197293	253.708328
Antisaccades Vertical	Number of Self Corrected Errors	-0.109295	0.110126	14.840822	-0.992453	0.336883	-0.305706	0.087119	246.448125	259.959161
	Saccade Amplitude	0.030256	0.044280	14.885186	0.683289	0.504921	-0.048772	0.109243	181.642367	195.153402
	Saccade Average Velocity	1.577712	0.854623	14.935701	1.846092	0.084792	0.048445	3.105171	366.492923	380.003959
	Saccade End Time	-1.950581	1.650092	14.926769	-1.182105	0.255654	-4.894723	0.992410	432.935815	446.446851
	Saccade Peak Velocity	3.028855	2.188712	15.288862	1.383852	0.186275	-0.900228	6.951957	423.079931	436.590967
	Saccade Latency	1.390832	1.798410	15.014096	0.773368	0.451310	-1.823330	4.602959	425.155005	438.666040
	Number of Correct Saccades	-0.109589	0.107894	15.160265	-1.015715	0.325702	-0.302459	0.083136	237.933241	251.444277
	Number of Erros	0.141231	0.106229	15.180011	1.329498	0.203319	-0.048553	0.331167	235.707229	249.218265
	Number of Self Corrected Errors	-0.228286	0.087850	15.143276	-2.598582	0.020040	-0.385343	-0.071443	226.320368	239.831403

Table 44: Longitudinal Study of Eye Movements in Parkinson's Disease Antisaccades Generalised Linear Model Results with Paradigm

Paradigm	Metric	Estimate	Std. Error	df	t value	Pr(> t)	CI 0.025	CI 0.975	AIC	BIC
Reflexive Horizontal	Accuracy	0.630138	3.316420	14.992961	0.190005	0.851853	-5.297337	6.557321	463.208662	476.719698
	Saccade Amplitude	0.067675	0.045987	14.987596	1.471617	0.161809	-0.014521	0.149831	173.629868	187.140904
	Saccade Average Velocity	1.456409	0.708142	15.063146	2.056663	0.057470	0.191586	2.721084	366.820051	380.331086
	Saccade End Time	-9.651408	6.901324	15.092873	-1.398486	0.182178	-21.985901	2.667065	523.580908	537.091943
	Saccade Peak Velocity	1.834617	2.330448	14.548646	0.787238	0.443779	-2.322550	5.992375	439.659397	453.170432
	Saccade Latency	-0.809539	6.804700	15.165941	-0.118968	0.906863	-12.980506	11.343965	518.729561	532.240596
	Number of Correct Saccades	0.137474	0.151889	15.006409	0.905094	0.379718	-0.133648	0.408812	261.959700	275.470735
	Number of Hypermetric Saccades	-0.044217	0.041328	15.093524	-1.069910	0.301472	-0.118079	0.029520	179.366726	192.877761
	Number of Hypometric Saccades	-0.040712	0.155155	15.012663	-0.262395	0.796583	-0.317784	0.236310	263.855364	277.366399
Reflexive Vertical	Accuracy	-5.530334	2.237392	14.903064	-2.471776	0.025997	-9.521941	-1.538940	451.068938	464.579973
	Saccade Amplitude	0.094342	0.050493	15.295693	1.868429	0.080978	0.003983	0.184796	175.142581	188.653617
	Saccade Average Velocity	2.061645	0.802050	15.110324	2.570468	0.021223	0.627271	3.497768	362.530246	376.041282
	Saccade End Time	-6.456331	2.941003	14.966434	-2.195282	0.044330	-11.702636	-1.208771	473.110240	486.621275
	Saccade Peak Velocity	4.161184	2.586034	15.235921	1.609099	0.128115	-0.466304	8.792188	442.383512	455.894548
	Saccade Latency	3.073155	2.465876	15.226959	1.246273	0.231497	-1.337034	7.483396	444.730434	458.241470
	Number of Correct Saccades	0.251563	0.152918	14.919623	1.645081	0.120852	-0.021215	0.524619	264.972889	278.483925
	Number of Hypermetric Saccades	-0.090331	0.094051	34.000000	-0.960451	0.343609	-0.264443	0.083781	244.186615	257.697651
	Number of Hypometric Saccades	-0.108398	0.166052	15.161311	-0.652795	0.523664	-0.405494	0.188125	266.549895	280.060930

Table 45: Longitudinal Study of Eye Movements in Parkinson's Disease Reflexive Saccades Generalised Linear Model Results

Paradigm	Metric	Estimate	Std. Error	df	t value	Pr(> t)	CI 0.025	CI 0.975	AIC	BIC
Volitional Horizontal	Accuracy	-9.199353	4.405247	15.248064	-2.088272	0.053946	-17.077424	-1.309071	481.354109	494.865144
	Saccadic Steps	-0.003025	0.012634	14.726913	-0.239470	0.814042	-0.025601	0.019532	81.786869	95.297905
	Saccade Amplitude	0.315000	0.129124	15.185199	2.439511	0.027432	0.083974	0.545662	247.858877	261.369913
	Saccade Average Velocity	2.979414	1.387354	15.125037	2.147551	0.048356	0.500217	5.455825	416.482003	429.993039
	Saccade End Time	143.336864	62.207757	34.000000	2.304164	0.027452	28.174191	258.499537	685.805913	699.316948
	Saccade Peak Velocity	4.096104	3.889010	15.179666	1.053251	0.308704	-2.857453	11.044542	480.089244	493.600280
	Saccade Latency	156.922392	65.622094	34.000000	2.391304	0.022467	35.438895	278.405888	689.439339	702.950375
	Number of Correct Saccades	0.602150	0.410504	15.036101	1.466854	0.163019	-0.130075	1.335205	338.752143	352.263178
	Number of Hypermetric Saccades	-0.151424	0.278675	15.207181	-0.543372	0.594750	-0.649946	0.346569	299.125891	312.636927
	Number of Hypometric Saccades	0.168488	0.420407	15.104907	0.400773	0.694199	-0.582398	0.919437	332.210800	345.721836
Volitional Vertical	Total Number of Saccades	0.288491	0.597688	15.078305	0.482678	0.636257	-0.778164	1.356028	360.910958	374.421994
	Accuracy	-5.579848	2.873287	15.183422	-1.941974	0.070929	-10.721302	-0.440137	451.549735	465.060771
	Saccadic Steps	-0.003594	0.013495	15.102382	-0.266355	0.793568	-0.027689	0.020521	98.130803	111.641839
	Saccade Amplitude	0.169866	0.085143	15.154821	1.995067	0.064339	0.017704	0.322114	217.703820	231.214855
	Saccade Average Velocity	2.207124	1.312459	15.172846	1.681671	0.113095	-0.138098	4.553039	406.671646	420.182682
	Saccade End Time	55.719830	67.220346	14.972743	0.828913	0.420172	-63.302848	174.772423	687.942040	701.453076
	Saccade Peak Velocity	2.052569	4.323814	15.300799	0.474713	0.641696	-5.688682	9.794340	477.307792	490.818828
	Saccade Latency	68.104630	70.862673	14.973469	0.961079	0.351777	-56.871128	193.112288	691.238642	704.749677
	Number of Correct Saccades	0.319632	0.367623	15.139376	0.869457	0.398172	-0.337125	0.976076	325.512501	339.023537
	Number of Hypermetric Saccades	-0.186269	0.417086	15.189629	-0.446596	0.661468	-0.931832	0.559743	324.812418	338.323454
	Number of Hypometric Saccades	0.509073	0.430080	14.906852	1.183670	0.255076	-0.258154	1.276228	340.523556	354.034592
	Total Number of Saccades	0.430789	0.488913	34.000000	0.881117	0.384441	-0.474315	1.335893	356.274432	369.785468

Table 46: Longitudinal Study of Eye Movements in Parkinson’s Disease Volitional Saccades Generalised Linear Model Results

Paradigm	Metric	Estimate	Std. Error	df	t value	Pr(> t)	CI 0.025	CI 0.975	AIC	BIC
Memory Guided Horizontal	Accuracy	-8.095161	5.078428	15.188549	-1.594029	0.131523	-17.176285	0.990715	492.291180	505.802216
	Saccadic Steps	0.003961	0.019289	15.351361	0.205347	0.839999	-0.030601	0.038548	104.411606	117.922642
	Saccade Amplitude	0.214717	0.135173	15.020985	1.588463	0.133004	-0.026639	0.455961	258.242452	271.753488
	Saccade Average Velocity	1.699799	1.454450	15.128635	1.168689	0.260615	-0.899282	4.297809	415.010080	428.521116
	Saccade End Time	50.065161	58.655194	15.115259	0.853550	0.406678	-54.674952	154.768315	674.417387	687.928423
	Saccade Peak Velocity	-0.018874	3.979082	15.129345	-0.004743	0.996277	-7.124079	7.087015	489.331250	502.842285
	Saccade Latency	51.972767	58.351596	15.110027	0.890683	0.387062	-52.218850	156.127740	674.680289	688.191324
	Number of Correct Saccades	0.594557	0.246496	34.000000	2.412036	0.021409	0.138229	1.050884	309.705381	323.216416
	Number of Hypermetric Saccades	-0.561223	0.544744	15.033124	-1.030250	0.319184	-1.534459	0.411860	345.367162	358.878198
	Number of Hypometric Saccades	-0.375003	0.425049	14.569202	-0.882258	0.391961	-1.132197	0.382123	339.837202	353.348237
Memory Guided Vertical	Total Number of Saccades	-0.374116	0.425706	15.080860	-0.878812	0.393290	-1.133803	0.385855	341.892590	355.403625
	Accuracy	-5.451584	3.038435	15.090676	-1.794208	0.092836	-10.884367	-0.022209	459.600500	473.111535
	Saccadic Steps	-0.001721	0.015125	15.157156	-0.113782	0.910904	-0.028754	0.025307	102.853836	116.364872
	Saccade Amplitude	0.122454	0.104361	15.030731	1.173375	0.258904	-0.063889	0.308940	234.303529	247.814565
	Saccade Average Velocity	1.102020	1.522193	15.368368	0.723969	0.479961	-1.625759	3.831123	401.585982	415.097017
	Saccade End Time	83.268704	76.778414	15.097555	1.084533	0.295144	-53.806967	220.307693	693.994881	707.505917
	Saccade Peak Velocity	1.585588	4.590477	15.359066	0.345408	0.734473	-6.650686	9.824390	471.139536	484.650571
	Saccade Latency	86.256424	78.865201	15.096016	1.093720	0.291224	-54.541609	227.016736	696.100680	709.611716
	Number of Correct Saccades	-0.204650	0.294853	15.120787	-0.694073	0.498162	-0.730894	0.322162	312.832748	326.343783
	Number of Hypermetric Saccades	-0.521815	0.399601	14.757680	-1.305838	0.211597	-1.234435	0.190758	331.485497	344.996533
	Number of Hypometric Saccades	-0.141584	0.420668	34.000000	-0.336570	0.738510	-0.920349	0.637181	346.051305	359.562340
	Total Number of Saccades	-1.292247	0.533577	34.000000	-2.421858	0.020924	-2.280035	-0.304458	362.218902	375.729938

Table 47: Longitudinal Study of Eye Movements in Parkinson’s Disease Memory Guided Saccades Generalised Linear Model Results

D Effect of Levodopa on Eye Movements in Parkinson's Disease

Metric	Estimate	Std. Error	Pr(> t)	CI 0.025	CI 0.975	AIC	BIC
Large Square Wave Jerks Count	0.250000		0.170403	-0.046454	0.546454	33.722335	38.357867
Intrusive Saccades Count	4.250000		0.236516	-2.224008	10.724011	107.527414	112.162946
Average Pupil Size	-184.225751		0.485434	-703.875712	335.424014	219.937978	224.573510
Average Precision Measure RMS S2S	0.017518		0.132861	-0.003291	0.038327	-30.210746	-25.575214
Average Precision Measure SD Window	0.028184		0.101415	-0.002276	0.058643	-21.000183	-16.364651
Average Fixation Duration	-553.265000		0.024325	-955.093688	-151.430017	208.381673	213.017206
Total Saccades Count	22.625000		0.149057	-6.366760	51.616876	144.777008	149.412541

Table 48: Effect of Levodopa on Eye Movements in Parkinson's Disease Central Fixation Generalised Linear Model Results

Metric	Statistic	Pr(> W)
Large Square Wave Jerks Count	0.000000	0.345779
Intrusive Saccades Count	7.500000	0.599174
Average Pupil Size	20.000000	0.843750
Average Precision Measure RMS S2S	8.000000	0.195312
Average Precision Measure SD Window	2.000000	0.023438
Average Fixation Duration	34.000000	0.023438
Total Saccades Count	8.000000	0.195312

Table 49: Effect of Levodopa on Eye Movements in Parkinson's Disease Central Fixation Wilcoxon Signed-Rank Test Results

Metric	Estimate	Std. Error	Pr(> t)	CI 0.025	CI 0.975	AIC	BIC
Average Saccade Amplitude	-0.713208		0.286202	-1.996454	0.570038	72.756910	77.392443
Average Saccade Velocity	-22.088694		0.062340	-41.487130	-2.690257	134.068110	138.703643
Average Saccade End Time	33.548927		0.564240	-68.556127	135.653984	173.927545	178.563077
Peak Saccade Velocity	-23.860970		0.440631	-84.494114	36.771925	164.203871	168.839404
Average Saccade Start Time	-50.263087		0.203339	-124.563645	24.036533	166.711810	171.347342
Total Number of Errors	1.125000		0.293163	-0.931182	3.181181	89.757067	94.392599
Total Number of Correct Antisaccades	-2.625000		0.230629	-6.778174	1.528176	101.669800	106.305332
Total Number of Self Corrected Errors	-2.125000		0.380616	-6.681102	2.431094	99.095413	103.730945

Table 50: Effect of Levodopa on Eye Movements in Parkinson's Disease Antisaccades Generalised Linear Model Results

Metric	Statistic	Pr(> W)
Average Saccade Amplitude	25.000000	0.382812
Average Saccade Velocity	30.000000	0.109375
Average Saccade End Time	19.000000	0.945312
Peak Saccade Velocity	24.000000	0.460938
Average Saccade Start Time	29.000000	0.148438
Total Number of Errors	9.000000	0.229332
Total Number of Correct Antisaccades	27.000000	0.231073
Total Number of Self Corrected Errors	23.000000	0.527599

Table 51: Effect of Levodopa on Eye Movements in Parkinson's Disease Antisaccades Wilcoxon Signed-Rank Test Results

Metric	Estimate	Std. Error	Pr(> t)	CI 0.025	CI 0.975	AIC	BIC
Total Number of Saccades	16.625000		0.152689	-4.900420	38.150412	141.975530	146.611063
Average Number of Saccadic Steps	-0.158473		0.335413	-0.443438	0.126493	32.774208	37.409741
Average Accuracy	-12.852447		0.786862	-107.157331	81.453385	172.117953	176.753486
Total Number of Correct Saccades	1.250000		0.870154	-13.688539	16.188512	127.640352	132.275884
Total Number of Hypometric Saccades	3.000000		0.541509	-6.711021	12.711017	127.652957	132.288490
Total Number of Hypermetric Saccades	12.000000		0.311698	-10.862059	34.862051	141.712296	146.347828
Average Saccade Amplitude	1.522125		0.086882	-0.066603	3.110853	86.586301	91.221833
Average Saccade Velocity	-0.198605		0.989205	-29.622872	29.225651	149.529695	154.165227
Average Saccade End Time	1153.375893		0.071175	26.067588	2280.683764	238.472559	243.108091
Peak Saccade Velocity	19.960192		0.443719	-31.122510	71.042922	161.555171	166.190703
Average Saccade Start Time	1149.337701		0.072655	18.561583	2280.113344	238.311096	242.946628

Table 52: Effect of Levodopa on Eye Movements in Parkinson's Disease Reflexive Saccades Horizontal Generalised Linear Model Results

Metric	Statistic	Pr(> W)
Total Number of Saccades	8.000000	0.195312
Average Number of Saccadic Steps	25.000000	0.382812
Average Accuracy	23.000000	0.546875
Total Number of Correct Saccades	14.500000	0.674047
Total Number of Hypometric Saccades	10.500000	0.611453
Total Number of Hypermetric Saccades	10.000000	0.293029
Average Saccade Amplitude	6.000000	0.109375
Average Saccade Velocity	17.000000	0.945312
Average Saccade End Time	6.000000	0.109375
Peak Saccade Velocity	15.000000	0.742188
Average Saccade Start Time	6.000000	0.109375

Table 53: Effect of Levodopa on Eye Movements in Parkinson's Disease Reflexive Saccades Horizontal Wilcoxon Signed-Rank Test Results

Metric	Estimate	Std. Error	Pr(> t)	CI 0.025	CI 0.975	AIC	BIC
Total Number of Saccades	16.625000		0.152689	-4.900420	38.150412	141.975530	146.611063
Average Number of Saccadic Steps	-0.158473		0.335413	-0.443438	0.126493	32.774208	37.409741
Average Accuracy	-12.852447		0.786862	-107.157331	81.453385	172.117953	176.753486
Total Number of Correct Saccades	1.250000		0.870154	-13.688539	16.188512	127.640352	132.275884
Total Number of Hypometric Saccades	3.000000		0.541509	-6.711021	12.711017	127.652957	132.288490
Total Number of Hypermetric Saccades	12.000000		0.311698	-10.862059	34.862051	141.712296	146.347828
Average Saccade Amplitude	1.522125		0.086882	-0.066603	3.110853	86.586301	91.221833
Average Saccade Velocity	-0.198605		0.989205	-29.622872	29.225651	149.529695	154.165227
Average Saccade End Time	1153.375893		0.071175	26.067588	2280.683764	238.472559	243.108091
Peak Saccade Velocity	19.960192		0.443719	-31.122510	71.042922	161.555171	166.190703
Average Saccade Start Time	1149.337701		0.072655	18.561583	2280.113344	238.311096	242.946628

Table 54: Effect of Levodopa on Eye Movements in Parkinson's Disease Reflexive Saccades Vertical Generalised Linear Model Results

Metric	Statistic	Pr(> W)
Total Number of Saccades	8.000000	0.195312
Average Number of Saccadic Steps	25.000000	0.382812
Average Accuracy	23.000000	0.546875
Total Number of Correct Saccades	14.500000	0.674047
Total Number of Hypometric Saccades	10.500000	0.611453
Total Number of Hypermetric Saccades	10.000000	0.293029
Average Saccade Amplitude	6.000000	0.109375
Average Saccade Velocity	17.000000	0.945312
Average Saccade End Time	6.000000	0.109375
Peak Saccade Velocity	15.000000	0.742188
Average Saccade Start Time	6.000000	0.109375

Table 55: Effect of Levodopa on Eye Movements in Parkinson's Disease Reflexive Saccades Vertical Wilcoxon Signed-Rank Test Results

Metric	Estimate	Pr(> t)	CI 0.025	CI 0.975	AIC	BIC
Total Number of Saccades	16.625000	0.152689	-4.900420	38.150412	141.975530	146.611063
Average Number of Saccadic Steps	-0.158473	0.335413	-0.443438	0.126493	32.774208	37.409741
Average Accuracy	-12.852447	0.786862	-107.157331	81.453385	172.117953	176.753486
Total Number of Correct Saccades	1.250000	0.870154	-13.688539	16.188512	127.640352	132.275884
Total Number of Hypometric Saccades	3.000000	0.541509	-6.711021	12.711017	127.652957	132.288490
Total Number of Hypermetric Saccades	12.000000	0.311698	-10.862059	34.862051	141.712296	146.347828
Average Saccade Amplitude	1.522125	0.086882	-0.066603	3.110853	86.586301	91.221833
Average Saccade Velocity	-0.198605	0.989205	-29.622872	29.225651	149.529695	154.165227
Average Saccade End Time	1153.375893	0.071175	26.067588	2280.683764	238.472559	243.108091
Peak Saccade Velocity	19.960192	0.443719	-31.122510	71.042922	161.555171	166.190703
Average Saccade Start Time	1149.337701	0.072655	18.561583	2280.113344	238.311096	242.946628

Table 56: Effect of Levodopa on Eye Movements in Parkinson's Disease Volitional Saccades Generalised Linear Model Results

Metric	Statistic	Pr(> W)
Total Number of Saccades	8.000000	0.195312
Average Number of Saccadic Steps	25.000000	0.382812
Average Accuracy	23.000000	0.546875
Total Number of Correct Saccades	14.500000	0.674047
Total Number of Hypometric Saccades	10.500000	0.611453
Total Number of Hypermetric Saccades	10.000000	0.293029
Average Saccade Amplitude	6.000000	0.109375
Average Saccade Velocity	17.000000	0.945312
Average Saccade End Time	6.000000	0.109375
Peak Saccade Velocity	15.000000	0.742188
Average Saccade Start Time	6.000000	0.109375

Table 57: Effect of Levodopa on Eye Movements in Parkinson’s Disease Volitional Saccades Wilcoxon Signed-Rank Test Results

Metric	Estimate	Pr(> t)	CI 0.025	CI 0.975	AIC	BIC
Total Number of Saccades	16.625000	0.152689	-4.900420	38.150412	141.975530	146.611063
Average Number of Saccadic Steps	-0.158473	0.335413	-0.443438	0.126493	32.774208	37.409741
Average Accuracy	-12.852447	0.786862	-107.157331	81.453385	172.117953	176.753486
Total Number of Correct Saccades	1.250000	0.870154	-13.688539	16.188512	127.640352	132.275884
Total Number of Hypometric Saccades	3.000000	0.541509	-6.711021	12.711017	127.652957	132.288490
Total Number of Hypermetric Saccades	12.000000	0.311698	-10.862059	34.862051	141.712296	146.347828
Average Saccade Amplitude	1.522125	0.086882	-0.066603	3.110853	86.586301	91.221833
Average Saccade Velocity	-0.198605	0.989205	-29.622872	29.225651	149.529695	154.165227
Average Saccade End Time	1153.375893	0.071175	26.067588	2280.683764	238.472559	243.108091
Peak Saccade Velocity	19.960192	0.443719	-31.122510	71.042922	161.555171	166.190703
Average Saccade Start Time	1149.337701	0.072655	18.561583	2280.113344	238.311096	242.946628

Table 58: Effect of Levodopa on Eye Movements in Parkinson’s Disease Memory Guided Saccades Generalised Linear Model Results

Metric	Statistic	Pr(> W)
Total Number of Saccades	8.000000	0.195312
Average Number of Saccadic Steps	25.000000	0.382812
Average Accuracy	23.000000	0.546875
Total Number of Correct Saccades	14.500000	0.674047
Total Number of Hypometric Saccades	10.500000	0.611453
Total Number of Hypermetric Saccades	10.000000	0.293029
Average Saccade Amplitude	6.000000	0.109375
Average Saccade Velocity	17.000000	0.945312
Average Saccade End Time	6.000000	0.109375
Peak Saccade Velocity	15.000000	0.742188
Average Saccade Start Time	6.000000	0.109375

Table 59: Effect of Levodopa on Eye Movements in Parkinson's Disease Memory Guided Saccades Wilcoxon Signed-Rank Test Results

